KAZAN SCIENCE WEEK 2025

ABSTRACTS

KAZAN SCIENCE WEEK

ABSTRACTS OF THE INTERNATIONAL CONFERENCE "ADVANCED LASER TECHNOLOGIES"

KAZAN, SEPTEMBER 22–26, 2025

ORGANIZERS AND SPONSORS

Российская Академия Наук

Federal Research Center
"Kazan Scientific Center of
the Russian Academy of Sciences"

Ministry of Science
and Higher Education
of the Russian Federation

Academy of Sciences
of the Republic of Tatarstan

Government
of the Republic of Tatarstan

Ministry of Education and Science
of the Republic of Tatarstan

Prokhorov General Physics
Institute of RAS (GPI RAS)

Zavoisky Physical-Technical
Institute FRC KazanSC RAS

Lomonosov Moscow
State University

Kazan Federal University

MIPT
MOSCOW INSTITUTE OF PHYSICS AND TECHNOLOGY

MEPhI
National Research
Nuclear University MEPhI

ЭЛЕМЕНТ

AVESTA
LASERS AND OPTICAL SYSTEMS

special
systems
PHOTONICS

"НАУКА"
Центр Технического Сопровождения

SLS
PRIME TECHNOLOGY

Solar
Laser
Systems

LLS

LAOOPA

Solar Laser Systems

SOLAR LS Company has been working in the international photonics market for more than 30 years. We are experts in the design and manufacturing of solid-state laser systems and spectral analysis instruments for science, medicine and industry. Currently, the company comprises scientific research laboratories, a design department, a mechanical and assembly production facility, an optical department, and a group for adjustment and service maintenance. Therefore, we complete the entire cycle of work on creating laser and spectral analysis systems - from research and development to the supply of finished products and their service maintenance. Our instruments and systems successfully operate in more than 25 countries all over the world. Being one of the market leaders, we offer our customers the widest range of the cutting-edge solid-state lasers, laser systems and spectral instruments. Reliability and technical perfection of SOLAR LS products are ensured by more than 30 years of manufacturing experience while design and concept incorporates with the latest achievements of the photonics.

Our laser product line includes:

- Nanosecond lasers with lamp and diode pumping with pulse energy up to 2.5 J, pulse repetition rates up to 100 Hz;
- Lasers with kHz pulse repetition rates with average power up to 10 W, pulse repetition rates from 1 to 100 kHz;
- Picosecond and femtosecond lasers with average power up to 8 W, pulse energy up to 1 mJ, pulse duration from 150 fs to 30 ps;
- Tunable nanosecond laser systems with a tuning range from 200 nm to 20 μm.

All lasers are equipped with harmonic generators and nonlinear converters, providing the capability to operate in UV, visible and IR spectral ranges.

Typical spectral products of our company are:

- Monochromators/spectrographs with a focal length from 44 to 522 mm;
- Compact spectrometers in the spectral range from 190 to 2560 nm with high optical sensitivity, low level of stray light and high resolution;
- Tunable light sources based on xenon lamps in the spectral range from 190 to 2500 nm, with high resolution up to 0.1 nm;
- Wavelength meters for lasers and diodes in the spectral range from 190 to 1800 nm with high accuracy and extremely high resolution.

We offer a wide range of detectors and accessories to complete our spectral instrument registration systems, as well as to collect light and input/output it into a fiber or spectral instrument. In addition to standard models of lasers and spectral instruments, our specialists are ready to develop and manufacture absolutely unique systems for your specific requirements and tasks.

Why we are confident in excellent results:

- Extensive experience: over 30 years of designing and producing laser systems and spectral analysis instruments to meet the current User's needs;
- Rapid and high-quality development of custom instruments;
- Established small-scale production process;
- Our team is involved in optimizing optical schemes designs for experiments using our spectral analysis instruments and laser systems;
- We provide stable OEM-supplies of high-quality instruments and systems.

Фемтосекундные твердотельные лазеры





TiF
Ti:S лазер
- λ_{range}: 690-1040 нм
- τ_{pulse}: 6 фс - 30 пс
- P_{av}: до 4 Вт
- PRR: 40...125 МГц

TeMa
иттербиевый лазер
- λ: 1030...1054 / 525 нм
- τ_{pulse}: 15-150 фс
- P_{av}: >20 Вт / >8 Вт
- PRR: 10-80 МГц

CrF
Cr:F лазер
- λ_{range}: 1230-1270 нм
- τ_{pulse}: <70 фс
- P_{av}: до 1 Вт
- PRR: 75...125 МГц

Katyusha
многоканальная система
- λ: 525 / 740-860 / 1050 нм
- τ_{pulse}: <150/<50/<200 фс
- P_{av}: 1.5 Вт на 800 нм
- PRR: 80 МГц

TOPOL
ОПО с накачкой
- λ_{range}: 205-4750 нм
- τ_{pulse}: <150 фс
- P_{av}: >3 Вт
- PRR: 80 МГц

Фемтосекундные волоконные лазеры




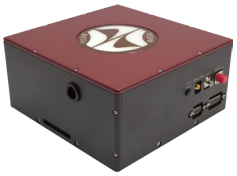


YFOA
иттербиевый лазер
- λ: 1030...1064 нм
- τ_{pulse}: <100 фс
- P_{av}: до 50 Вт
- PRR: 40-80 МГц

ANTAUS
микроджоульный
- λ: 1030...1053 нм
- τ_{pulse}: <250 фс
- E_{pulse}: до 60 мкДж
- P_{av}: до 50 Вт

PErL, EFO
эрбиевые лазеры
- λ: 1560 нм
- τ_{pulse}: 50...300 фс; 5 пс
- P_{av}: до 5 Вт
- PRR: 30...100 МГц

EFOA-SH/PErL-PM-SH
эрбиевый лазер
- λ: 1560/780 нм
- τ_{pulse}: <50 фс
- P_{av}: >2 Вт
- PRR: 30...100 МГц

EFO-COMB
комб-генератор
- λ: 200...3390 нм
- F_{rep}: 100-250 МГц
- Стаб.: $1*10^{-17}$ на 1 с

Усилители

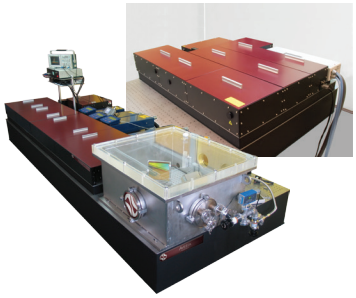


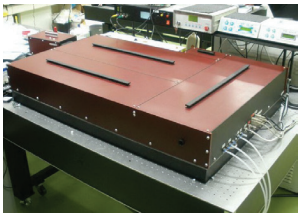


AVET и REUS
титан-сапфировые усилители
- λ: 740...950 нм
- τ_{pulse}: <35 фс (опция <8 фс)
- P_{peak}: до 20 ТВт
- E_{pulse}: >550 мДж@10 Гц

TETA иттербиевый усилитель
- λ: 1030/515/343/257 нм
- τ_{pulse}: <180 фс (опция <30 фс)
- P_{av}: до 30 Вт @ 2 МГц
- E_{pulse}: до 2 мДж

FREGAT хром-форстеритовый усилитель
- λ: 1240 нм
- τ_{pulse}: <100 фс
- E_{pulse}: до 100 мДж
- PRR: 10 Гц...1 кГц

PARUS
параметрический усилитель
- λ_{range}: 190 нм - 15 мкм
- τ_{pulse}: от <30 фс
- Eff. S+I: >10% от накачки

Непрерывные твердотельные лазеры

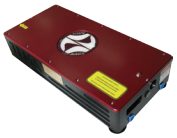

TiC Ti:S лазер
- λ: 690-1040 нм
- P_{av}: до 6 Вт
- <1 МГц ширина линии

TEMA-CW
- λ: 1010-1070 нм
- P_{av}: до 15 Вт
- USB

LF-100 Cr:F лазер
- λ: 1210-1290 нм
- P_{av}: до 1 Вт
- USB

DLS одночастотный диодный лазерный источник
- λ: 400...1670 нм
- P_{av}: до 10 Вт

АВЕСТА
ЛАЗЕРЫ И ОПТИЧЕСКИЕ СИСТЕМЫ

ООО «АВЕСТА», ул. Физическая, 11
Троицк, 108840, Москва, Россия
Тел.: +7 (495) 138-99-56

fs@avesta.ru
www.avesta.ru

Диагностическое оборудование

AA-DD и IRA
сканирующие автокорреляторы
- λ_{range}: 420 нм - 11 мкм
- τ_{pulse}: 10 фс - 250 пс
- Чувствительность: от 100 мВт^2
- USB и ПО для Windows

ASF, ASF-FROG
одноимпульсные автокорреляторы и FROG
- Диапазон длин волн: 400-2200 нм
- Диапазон длительности: 5 фс - 20 пс
- USB, ПО для Windows и LabView

SPIDER
измеритель спектральной фазы
- Input λ: 550-2200 нм
- Input $\tau_{pulse\ range}$: 5-320 фс
- USB и ПО для Windows

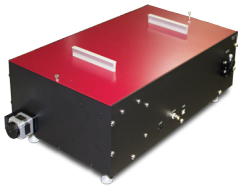

COMET измеритель контраста
- Диапазон длин волн: 700-1500 нм
- Динамический диапазон: 10^{10}
- Временной диапазон: до 10 нс
- USB и ПО для Windows

OD фотоприемники
- Диапазон длин волн: 200-2600 нм
- Полоса до 2500 МГц
- Время нарастания от 0.5 нс
- Со смещением, с усилителем, лавинные, волоконные

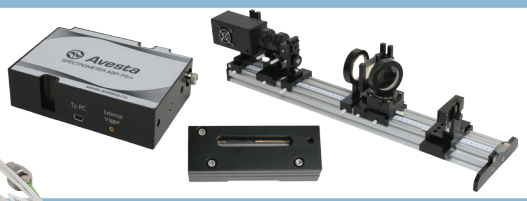

Спектрометры и сенсоры
- λ: 190-3450 нм
- Разрешение: от 0.01 нм
- Волоконный/free-space
- USB и ПО для Windows

Компоненты

OG ЭО и АО селекторы импульсов
- Длины волн: 210...2700 нм
- Выходная частота: до 40 МГц
- Пропускание >90%
- Контраст >2 000:1
- Блок генерации задержек
- USB, ПО для Windows и LabView

ALock. Блок ФАПЧ
- Входной сигнал до 3 ГГц
- Полоса ПИД до 2 МГц
- PZT до 50 Вт
- Синхронизация лазеров
- Стабилизация CEP
- ASOPS, THz-ASOPS

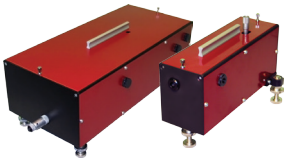

AG генераторы гармоник
- Выход: 195 нм - 5 мкм
- ЧГ на 800 нм = ТГ+основная
- Преобразование: до >50%

APC призменный компенсатор
GVD на 800 нм:
от +16500 фс^2 до -13800 фс^2

Compulse компрессор
- 6 фс, 500 мкДж на 800 нм
- 30 фс, 200 мкДж на 1030 нм

OA оптические аттенюаторы
- Динамический диапазон: 10^2
- λ: 250...2000 нм
- Модели с низкой дисперсией
- Порог пробоя: до 10 Дж/см^2

AF ротаторы и изоляторы
- λ: 400...1250 нм
- Изоляция: >38 dB; >60 dB
- Широкопол. и перестраив.
- Апертура: до 20 мм
- Порог пробоя: до 5 Дж/см^2

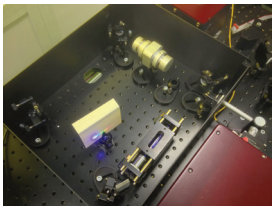

GECON генератор суперконтинуума
- Вх. λ: 800; 1030-1064 нм
- Вых. λ: 200-1200 нм
- Преобразование: >50%

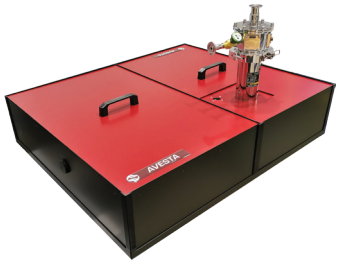

Tera-Ax ТГц генератор
- Центр. частота: 1 ТГц
- Длительность ТГц: <1 пс
- Энергия ТГц: >1 мДж
- ЭО детектор (опция)
- Версия с криостатом

• чопперы • шаттеры • USB контроллеры • оптомеханика • столики • оправы •

ООО «АВЕСТА», ул. Физическая, 11
Троицк, 108840, Москва, Россия
Тел.: +7 (495) 138-99-56

fs@avesta.ru
www.avesta.ru

rev 2507

LASERS & LASER SYSTEMS

PULSED Nd:YAG LASERS

- Pulse energy up to 2.5 J
- Flat top beam profile
- Pulse repetition rate up to 200 Hz
- All harmonics from 1064 to 213 nm
- Adjustable pulsewidth
- Adjustable pulse shape

FEMTO-, PICOSECOND LASERS

- Pulsewidth (FWHM) up to 110 fs
- Output power up to 7 W
- Output energy up to 1 mJ
- Harmonic generators
- Diode pumping
- Pulse selectors

TUNABLE LASERS

- Ti:Sapphire lasers, DFG converters
- Optical parametric oscillators
- Tuning range from 0.2 to 20 μm
- Linewidth up to 0.005 nm
- Pulse energy up to 100 mJ

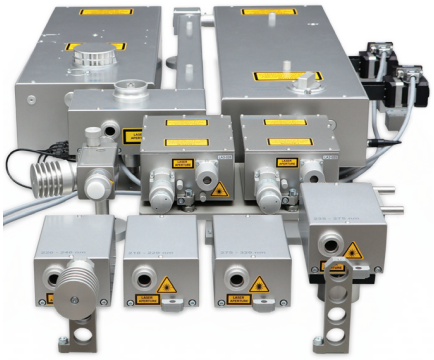

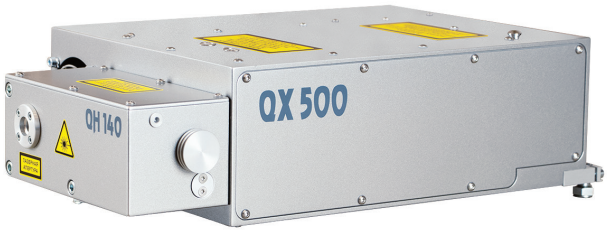

DIODE-PUMPED LASERS

- Compact industrial design
- Built-in or external harmonic generators
- up to 150 mJ per pulse at 20 Hz
- up to 3 W @ 355 nm at 30 kHz

SOLAR LS • +375 (17) 352 9490 • INFO@SOLARLS.EU • WWW.SOLAR-LASER.COM

Solar Laser Systems

SPECTRAL INSTRUMENTS

MONOCHROMATORS/ SPECTROGRAPHS

- Single and double
- Focal length from 44 to 522 mm
- Wide range of detectors

SPECTROMETERS

- Spectral range from 190 to 2560 nm
- High optical sensitivity
- Fiber input

WAVELENGTH METERS FOR LASERS AND DIODES

- Spectral range from 190 to 1800 nm
- High accuracy ± 3 pm
- FWHM and spectral line monitoring and analysis

TUNABLE LIGHT SOURCES

- Spectral range from 190 to 2500 nm
- Spectral resolution up to 0.1 nm

SOLAR LS • +375 (17) 352 9490 • INFO@SOLARLS.EU • WWW.SOLAR-LASER.COM

Solar Laser Systems

BUILT WITH ADVANCED TECHNOLOGIES

PULSED Nd:YAG LASERS

- Wavelength 1064, 532, 355, 266 and 213 nm
- Pulse energy up to 4 J
- Repetition rate up to 10 kHz
- Integrated energy meter
- Compact housing
- Manufactured in the Republic of Belarus

Convenient Operation · High Reliability · Guaranteed Service

SLS Prime Technology unites leading experts in lasers and laser systems development and production to bring innovative equipment to domestic markets.

We place special emphasis in engineering diode-pumped lasers, deliberately dissolving the boundaries of their applications between science and industry. We are determined that our products are designed to succeed in both domains.

AZURITE is our first and proven model of diode-pumped lasers generating nanosecond pulses. It delivers **up to 160 mJ** pulse energy at **up to 30 Hz** repetition rates in a completely **"dry" design**.

Its **extended service interval of over 1 billion pulses** makes AZURITE a robust solution not only for a wide range of R&D applications but also for integrating in industrial environments operating 24/7.

We use **exclusively domestically sourced components** for all critical parts, ensuring system maintainability and reliable long-term service support.

Please contact our specialists for more details by e-mail or phone:

SLS Prime Technology | +375 (17) 382-00-55 | sales@sls-prime.com | www.sls-prime.com

SLS
PRIME TECHNOLOGY

PULSED
Nd:YAG LASERS

AZURITE
Compact diode-pumped lasers

- Up to 160 mJ pulse energy at up to 30 Hz repetition rate
- >1 billion shots lifetime
- Completely dry cooling design
-

GRAPHITE
Compact lamp-pumped lasers

- 200 mJ - 750 mJ pulse energy at up to 100 Hz repetition rate
- >30 million shots lifetime
- Water-air cooling

CORUNDUM
Lamp-pumped Joule-class lasers

- Up to 1.5 J pulse energy at up to 20 Hz repetition rate
- >30 million shots lifetime
- Water-air cooling

OBSIDIAN
Picosecond lasers

- Up to 2 mJ pulse energy at up to 1 kHz repetition rate
- 300-500 ps pulse duration
- SLM operation mode

AMETHYST
Tunable laser systems

- Tunable output in the 0.2–20 μm range
- Up to 150 mJ pulse energy
- Customized configurations available

- *All Nd:YAG laser models incorporate replaceable harmonic generators for wavelength selection from IR to UV: 1064 nm, 532 nm, 355 nm, 266 nm, and 213 nm.*
- *Nd:YAG lasers are available with single longitude mode (TEM00) option.*
- *Lasers with pulse energies up to 4 J are available on a custom-order basis.*
- *Tunable wavelength systems are developed to individual specifications based on Nd:YAG lasers enhanced with OPOs and sum- and difference-frequency generators.*

SLS Prime Technology | +375 (17) 382-00-55 | sales@sls-prime.com | www.sls-prime.com

ЭЛЕМЕНТ

Сайт: https://element-msc.ru/

Компания «ЭЛЕМЕНТ» – надежный поставщик аналитического оборудования, запчастей и расходных материалов на российском рынке уже более 20 лет. Мы не только обеспечиваем лаборатории и научные центры передовой техникой, но и предлагаем полный спектр сервисных услуг, включая гарантийное обслуживание и ремонт приборов.

«ЭЛЕМЕНТ» является официальным дистрибьютором SHIMADZU в России, а также представляет ряд других ведущих производителей аналитического оборудования. Среди наших партнеров:

- **ZHONGTAI (CIQTEK)** – разработчик спектрометров ядерного магнитного резонанса (ЯМР) и электронного парамагнитного резонанса (ЭПР) X и W диапазона, а также уникального оборудования для измерения магнитных свойств веществ, включая NV-магнитометры и квантовые NV-микроскопы.
- **Zhenyi Scientific** – китайский производитель инновационных решений в области ЯМР-анализа, включая **бескриогенные низкопольные ЯМР-анализаторы** для пищевой науки, материаловедения и биомедицины.

ЭЛЕМЕНТ

СПЕКТРОМЕТРЫ ЯДЕРНОГО МАГНИТНОГО РЕЗОНАНСА (ЯМР)

ЯМР-спектрометры Zhenyi на постоянном магните серии HT-PNMR12 (60/90МГц)

Предназначены для проведения рутинных экспериментов. В зависимости от конфигурации они способны регистрировать ЯМР-спектры ядер: ^{1}H, ^{19}F, ^{13}C, ^{31}P. Уникальный постоянный магнит не требует охлаждения криогенными жидкостями. Для уменьшения влияния анизотропии магнитного поля используется система вращения. Все блоки прибора находятся в едином корпусе. Заводская гарантия 24 месяца с момента поставки.

- Две модификации: HT-PNMR12-6 на 60 МГц / HT-PNMR12-9 на 90 МГц
- Магнитное поле: 1,4 Тл / 2,1 Тл
- Разрешение: < 0,8 Гц / < 0,5 Гц
- Соотношение S/N (1% этилбензол): 100:1 / 120:1
- Температурная стабильность: 0,001 К/ч через 4 часа после запуска

Высокопольные ЯМР-спектрометры ZHONGTAI CAN400 и CAN600 (400/600 МГц)

Современные высокочувствительные ЯМР-спектрометры с интеллектуальным управлением и сверхпроводящим магнитом, обеспечивающим исключительную однородность поля. Приборы оснащены автоматизированным зондом и модульной системой, что позволяет проводить точные исследования молекулярной структуры с минимальным вмешательством оператора. ЯМР-спектрометры ZHONGTAI идеально подходят для современных лабораторий, сочетая высокое разрешение, надежность и удобство в эксплуатации.

- Две модели: CAN400 / CAN600
- Рабочая частота на ядрах 1H – 400 МГц / 600 МГц
- Магнитное поле: 9,39 Тл / 14,09 Тл
- Соотношение S/N (0,1% этилбензол): ≥ 500:1 / ≥ 850:1
- Наблюдаемые ядра: ^{1}H, ^{13}C, ^{15}N, ^{31}P, ^{19}F и другие
- Разрешение: < 0,0005 Гц
- Диаметр теплого отверстия: 54 мм
- Опции: температурная приставка (от -150 °C до +150 °C), автосамплер на 72 образца

СПЕКТРОМЕТРЫ ЭЛЕКТРОННОГО ПАРАМАГНИТНОГО РЕЗОНАНСА (ЭПР)

ЭПР -спектрометры X-, Q-, W- диапазона от ZHONGTAI

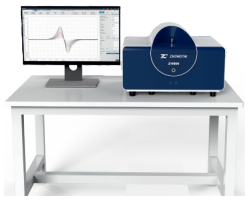
ZT6500

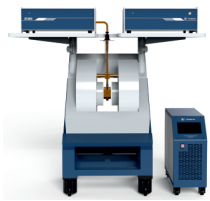
ZT15C


ZT15P


ZT60W

Линейка ЭПР спектрометоров ZHONGTAI включает :

- компактную настольную модель ZT6500
- две высокочувствительные модели ЭПР X-диапазона. Модель ZT15C для работы в CW-режиме и модель ZT15P с возможностью работы в импульсном +CW режиме. Обе модели можно модернизировать для работы в Q-диапазоне (с магнитом 1,8T).
- Вершина линейки - высокочастотный ЭПР-спектрометр W-диапазона ZT60W.

Кроме этого, производитель предлагает большой набор опций: резонаторы, азотные и гелиевые температурные приставки, системы облучения, ячейки для разных приложений, в том числе для модернизации ЭПР-спектрометров сторонних производителей.

8 (800) 250-34-64
element-msc.ru
info@element-msc.ru

ЭЛЕМЕНТ

"НАУКА"

Центр Технического Сопровождения

Адрес: 129626, Россия, Москва,
ул. Маломосковская, 22, стр. 1, «Технопарк»
Телефон: +7 (499) 322 06 62
Моб.: +7 915 404 65 97
E-mail: d.naberezhnyi@cts-nauka.ru

ЦЕНТР ТЕХНИЧЕСКОГО СОПРОВОЖДЕНИЯ «НАУКА» ЗАНИМАЕТСЯ ПОСТАВКОЙ И ОБСЛУЖИВАНИЕМ НАУЧНОГО ОБОРУДОВАНИЯ ДЛЯ ЛАБОРАТОРИЙ, РЕШАЯ СЛЕДУЮЩИЕ ЗАДАЧИ:

- разработка комплексного решения под задачи пользователя, в том числе поставка оборудования, разработанного по индивидуальным проектам
- поставка, запуск и обслуживание оборудования
- объединение приборов от разных производителей в единый комплекс
- поставка всех необходимых расходных материалов
- гарантийное и постгарантийное обслуживание

ЛАБОРАТОРНОЕ ОБОРУДОВАНИЕ | РАСХОДНЫЕ МАТЕРИАЛЫ | СЕРВИС

КОМПАНИЯ ОБРАЗОВАНА В 2013 ГОДУ И ЗАРЕКОМЕНДОВАЛА СЕБЯ КАК НАДЕЖНЫХ ПОСТАВЩИК ПРИБОРОВ ДЛЯ ИССЛЕДОВАНИЙ В ОБЛАСТИ ФИЗИКИ И ХИМИИ.

www.scientific-technology.ru | www.nauka-shop.ru | www.lgrinc.ru | www.cryoindustries.ru

ЦТС «НАУКА» ПРЕДЛАГАЕТ ШИРОКИЙ ПЕРЕЧЕНЬ УНИКАЛЬНОГО ОБОРУДОВАНИЯ ДЛЯ НАУЧНЫХ ИЗЫСКАНИЙ:

КРИОГЕННОЕ ОБОРУДОВАНИЕ:

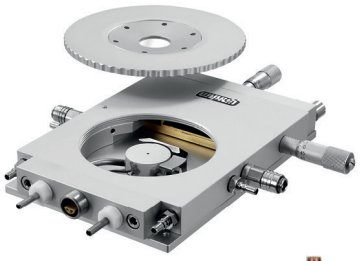

+ Столики для микроскопии с задаваемой температурой / давлением от **Linkam Scientific Instruments**.

+ **Advanced Research Systems:** оптические криостаты замкнутого цикла, проточные, сверхвысоковакуумные, исследовательские станции с зондом и иные аксессуары.

+ **Cryo Industries of America:** оптические безжидкостные криостаты, поточные гели евые криостаты, гелиевые и безжидкостные сверхпроводящие магниты, системы охлаждения газового потока, системы для криомикроскопии, генераторы жидкого азота, криостаты He-3, трансферные линии и сосуды Дьюара.

+ **SHI Cryogenic Group (Sumitomo):** криокулеры (криогенные рефрижераторы), крионасосы, гелиевые компрессоры.

+ **Quantum Design:** безжидкостные оптические криостаты, ожижители гелия, системы квантовой микроскопии, системы наноосаждения PVD/CVD, SQUID магнетометры, безжидкостные станции для исследования материалов и криомикроскопии.

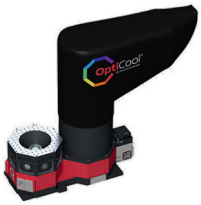

+ **Cryogenic Limited:** безжидкостные измерительные системы 18 Тл и криокулеры, криостаты замкнутого цикла, магниты высокого разрешения для ЯМР, SQUID магнетометры.

ВАКУУМНОЕ ОБОРУДОВАНИЕ:

PFEIFFER VACUUM

EDWARDS

Leybold

+ пластинчато-роторные насосы, спиральные насосы, турбомолекулярные насосы от **Pfeiffer Vacuum, Edwards Vacuum, Leybold GmbH.**

EVP®

+ вакуумные насосы и крионасосы от **EVP** и других производителей

YUNMU VAC TECH

+ вакуумные камеры, вакуумная арматура от **Yunmu** и иных производителей.

СОПУТСТВУЮЩИЕ АКСЕССУАРЫ:

SMC®

+ Чиллеры, сосуды Дьюара, трансферные линии и многое другое.

"НАУКА"

Центр Технического Сопровождения

Адрес: 129626, Россия, Москва,
ул. Маломосковская, 22, стр. 1, «Технопарк»
Телефон: +7 (499) 322 06 62
E-mail: info@nauka-shop.ru
www.nauka-shop.ru

ИЗМЕРИТЕЛЬНОЕ ОБОРУДОВАНИЕ:

Zurich Instruments

+ синхронные усилители от **Zurich instruments**

KEITHLEY
A Tektronix Company

+ генераторы и измерители электронных сигналов от **Keithley Instruments**

ABB

+ портативные газовые анализаторы от **ABB**

ThermoFisher SCIENTIFIC

+ спектрометры от **Thermo Fisher Scientific**

EDINBURGH INSTRUMENTS

+ спектрометры от **Edinburgh Instruments**

HORIBA

+ спектрометры от **Horiba**

[L G R]

+ изотопные анализаторы от **Los Gatos Research**

NETZSCH

+ термические анализаторы от **Netzsch.**

ЛАБОРАТОРНОЕ ОБОРУДОВАНИЕ | РАСХОДНЫЕ МАТЕРИАЛЫ | СЕРВИС

АО «ЛЛС» — ВАШ ПРОВОДНИК В МИРЕ ОПТИКИ И ФОТОНИКИ!

Нам доверяют эксперты отрасли, а мы обеспечиваем интеграцию оборудования под ключ — от поставки до пусконаладки

10 лет мы лидеры рынка оптики и фотоники — отбираем лучших производителей и предлагаем альтернативные решения без компромиссов по качеству.

Представим оборудование, доступное в АО «ЛЛС» (более 300 производителей):

- **Оптический анализ материалов: микроскопия, спектроскопия и терагерцовые технологии:**
  Apex Photon, Optosky, Oceanoptics, CIQTEK, YSL Photonics, B-THz,Toptica, CNI Laser
- **Производство и тестирование ФИС:**
  CUMEC, OMTools, Moji Nano, Santec, Quantifi photonics, Anritsu, Yokogawa, Toptica
- **Комплектующие и системы для микрообработки материалов:**
  NordLase, Grace Laser, Moji Nano, Huaray, ScanLab
- **Оптомеханика от ведущих мировых производителей:**
  LBTEK, OMTools, Thorlabs, Newport, Coremorrow, Luminous
- **Волоконно-оптические компоненты и оборудование для работы с волокном:**
  LightComm, Shinho, CSRazer, XLG, AFR, Optizone
- **Охлаждение атомов и квантовые технологии:**
  Faraday, CasColdAtom, Tuptek, Connet, KeyangPhotonics, Vision Datum, QUBIG, Zurich Instruments
- **Оборудование для измерения характеристик лазерного пучка:**
  Cai Huang Thermoelectricity, Ophir, Lightcomm, Dataray

+ многое другое оборудование на выставке

На стенде АО «ЛЛС» вас будут ждать подарки

ЛЛС
info@lenlasers.ru
+7 (812) 507 81 00
lenlasers.ru

специальные системы
ФОТОНИКА

О КОМПАНИИ

ООО «Специальные Системы. Фотоника» является специализированным поставщиком и интегратором лазерно-оптических и волоконно-оптических компонентов, измерительного, спектрального и технологического оборудования, источников излучения и лазерных систем различного назначения.

Специалисты компании обеспечивают высококвалифицированную техническую и информационную поддержку по продукции и оборудованию от ведущих мировых производителей для заказчиков из России и ЕАЭС.

Миссия компании - это внедрение передовых лазерно-оптических технологий и продукции в текущие и перспективные разработки российских научных и производственных центров. Активное участие в развитии фотоники в России, как наиболее перспективного направления науки и технологий.

НАПРАВЛЕНИЯ ДЕЯТЕЛЬНОСТИ И УСЛУГИ

- Дистрибуция лазерно-оптических и волоконно-оптических компонентов и оборудования.
- Комплексное оснащение лабораторий и производств.
- Разработка и производство волоконно-оптических модулей и систем (ВОЛС, радиофотоника).
- Собственная лаборатория с передовым измерительным и технологическим оборудованием.
- Технический консалтинг, инженерный сервис и обучение специалистов заказчика.
- Подготовка документации для закупочных процедур на электронных торговых площадках (ФЗ 223 и ФЗ 44).
- Логистические услуги, таможенное оформление лабораторного оборудования и лазерных компонентов.

ЛАКОПА
ПРОВОДНИК ИННОВАЦИЙ

Компания Лакопа – проводник инновационных решений, которая обеспечивает доступ к экспертным знаниям и перспективным технологиям, способствует повышению уровня научных исследований, подготовке квалифицированных кадров, способных работать с прорывными идеями и творчески мыслить.

Наша компания является официальным дистрибьютером Suzhou Niumag Analytical Instrument - ведущего производителя, специализирующееся на разработке и применении технологии «низкопольного ядерного магнитного резонанса». Компания отличается мощным научно-исследовательским потенциалом, осуществляет полный цикл производства. Благодаря постоянному накоплению технологий, новаторским решениям и разработкам в различных областях применения оборудования, Niumag быстро стало высокотехнологичным предприятием, ориентированным на привлечение в команду ведущих специалистов в отрасли, инновации и развитие.

纽迈 NIUMAG

НАСТОЛЬНЫЙ ТВЕРДОТЕЛЬНЫЙ ЯМР-СПЕКТРОМЕТР С ВРАЩЕНИЕМ ОБРАЗЦА ПОД МАГИЧЕСКИМ УГЛОМ (MAS)

Настольный твердотельный ЯМР-спектрометр MAS20 использует вращение под магическим углом для достижения высокоточного измерения химического сдвига в твердых телах или гетерогенных системах, что позволяет анализировать структурное и молекулярное движение, а также анализировать компонентный состав.

ТЕХНИЧЕСКИЕ ХАРАКТЕРИСТИКИ:

- Тип магнита: постоянный магнит, не требует охлаждения и обеспечивает крайне низкие затраты на обслуживание
- Индукция магнитного поля: 0,5 Тл
- Диаметр ротора: 3,5 мм
- Максимальная скорость: 20 кГц
- Детектируемые ядра: доступны в исполнениях 1H, 7Li, 19F и 31P
- Безопасность: магнитное поле <2 Гс на корпусе прибора
- Температура окружающей среды: 20–26 °C, температурный дрейф <2 °C/ч
- Влажность окружающей среды: менее 80%
- Питание: 220 В, 50/60 Гц
- Пользовательский интерфейс: английский

ОБЛАСТИ ПРИМЕНЕНИЯ:

MAS20 применяется для научных исследований, обучения, предварительного анализа образцов и рутинного контроля качества, особенно для изучения парамагнитных материалов. Прибор позволяет устранить значительные боковые полосы вращения (spinning sidebands) парамагнитных материалов в традиционных магнитно-резонансных системах с высоким полем, которые влияют на качественный и количественный анализ.

- Материалы для литиевых аккумуляторов: анализ дефектов, идентификация информации о связях Li-O-TM (TM = Co, Cr, Mn,Fe, Ni) и анализ искажений
- Фосфорсодержащие материалы: анализ распределения Fe^{2+}/Mn^{2+} в парамагнитных фосфатных соединениях и кислотности катализаторов
- Парамагнитные комплексы: определение структуры и дифференциация кристаллических и аморфных структур
- Фторсодержащие материалы: определение содержания фтора, участия фтора в реакциях и структурный анализ
- Анализ жидкостей: определение содержания масла, воды и каучука в сложных системах

Специалисты компании имеют большой опыт работы в области перспективных разработок и знают, как сложно прокладывать путь первопроходцам. Сотрудничая со многими ведущими экспертами, мы развиваем междисциплинарные коммуникации для обмена опытом, подбираем правильные технологии, адаптируем их для решения самых сложных задач.

НАШ САЙТ

ПОДПИСЫВАЙТЕСЬ НА НАШ ТЕЛЕГРАММ КАНАЛ

Дополнительную информацию о продуктах и решениях компании можно получить, отправив запросы на электронную почту **marketing@lacopa.group**

ADVANCED LASER TECHNOLOGIES

32nd INTERNATIONAL CONFERENCE
Advanced Laser Technologies
ALT'25

KAZAN, SEPTEMBER 22–26, 2025

COMMITTEE

Conference Chairman

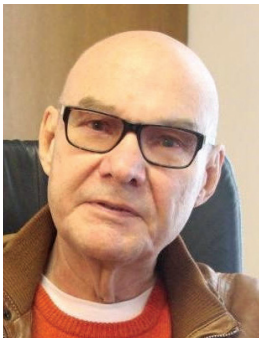

Ivan SHCHERBAKOV

Academician of RAS,
Scientific Director
of Prokhorov General
Physics Institute

Program-Committee Co-Chairs

Vitaly KONOV

Academician of RAS,
Director of Natural Sciences
Center of Prokhorov
General Physics Institute

Alexey KALACHEV

Corresponding member of
RAS, Director of FRC Kazan
Scientific Center of RAS

Organizing Committee Co-Chairs

Vladimir PUSTOVOY

Head of the Laser Physics
Department of the
Prokhorov General Physics
Institute

Sergey KHANTIMEROV

Director of Zavoisky
Physical-Technical Institute,
FRC Kazan Scientific Center
of RAS

INTERNATIONAL PROGRAM COMMITTEE

Mukhsin ASHUROV (Uzbekistan)
Ekaterina BARMINA (Russia)
Aladar CZITROVSKY (Hungary)
Boris DENKER (Russia)
Sergey GARNOV (Russia)
Mikhail GLYAVIN (Russia)
Leonid GOLOVAN (Russia)
Pavel KASHKAROV (Russia)
Nikolay KAZANSKIY (Russia)
Sergey KHARINTSEV (Russia)
Sergey KLIMENTOV (Russia)
Alexey KUCHERIK (Russia)
Aleksandr KUCHMIZHAK (Russia)
Yury KULCHIN (Russia)
Andrei LUGOVTSOV (Russia)
Vladimir MAKAROV (Russia)
Tofig MAMMADOV (Azerbaijan)
Andrei NAUMOV (Russia)
Kyung Hyun PARK (Korea)
Vladimir PAVELYEV (Russia)
Alexander PRIEZZHEV (Russia)
Vadim SEMASHKO (Russia)
Sergey SEMJONOV (Russia)
Alexander SHKURINOV (Russia)
Victor SOIFER (Russia)
Grigorii SOKOLOVSKII (Russia)
Nishant TRIPATHI (India)
Valery TUCHIN (Russia)
Vadim VEIKO (Russia)
Igor VLASOV (Russia)
Irina ZAVESTOVSKAYA (Russia)
Dan ZHU (China)

INTERNATIONAL ORGANIZING COMMITTEE

Natalia KHAKAMOVA (Moscow, Russia)
Anton SIZIKOV (Moscow, Russia)
Tatiana GAVRILOVA (Kazan, Russia)

LOCAL ORGANIZING COMMITTEE (IN KAZAN)

Tatiana GAVRILOVA
Kazan E.K. Zavoisky Physical-Technical Institute (KPhTI),
FRC Kazan Scientific Center,
Russian Academy of Sciences

t.gavrilova@knc.ru
Phone: +7 843 231 90 82
https://sci-kzn2025.knc.ru/

CONFERENCE SECRETARY (IN MOSCOW)

Natalia KHAKAMOVA
Prokhorov General Physics Institute of the Russian Academy of Sciences

khakamova@nsc.gpi.ru
Phone: +7 499 503-87-77, add 2-96

SECTIONS

- LASER-MATTER INTERACTION
  Co-chairs:
  Sergey KLIMENTOV (MEPHI University, Moscow)
  Ekaterina BARMINA (Prokhorov GPI RAS, Moscow)

- BIOMEDICAL PHOTONICS
  Co-chairs:
  Alexander PRIEZZHEV (Lomonosov MSU, Moscow)
  Andrey LUGOVTSOV (Lomonosov MSU, Moscow)

- LASER SYSTEMS AND MATERIALS
  Co-chairs:
  Boris DENKER (Prokhorov GPI RAS, Moscow)
  Grigorii SOKOLOVSKII (Ioffe Institute, Saint Petersburg)
  Alexey GLADYSHEV (Dianov Fiber Optics Research Center, Moscow)

- LASER DIAGNOSTICS AND SPECTROSCOPY
  Co-chairs:
  Leonid GOLOVAN (Lomonosov MSU, Moscow)
  Alexander MILEKHIN (Rzhanov Institute of Semiconductor Physics, Novosibisk)

- NONLINEAR AND TERAHERTZ PHOTONICS
  Co-chairs:
  Alexander SHKURINOV (Lomonosov MSU, Moscow)
  Vladimir MAKAROV (Lomonosov MSU, Moscow)

- PHOTONICS IN QUANTUM TECHNOLOGIES
  Co-chairs:
  Andrei NAUMOV (Lebedev Physical Institute, RAS, Moscow)
  Sergei KULIK (Lomonosov MSU, Moscow)

- NANOPHOTONICS
  Co-chairs:
  Igor VLASOV (Prokhorov GPI RAS, Moscow)
  Aleksander KUCHMIZHAK (FEFU, Vladivostok)

SECTION COLOR SCHEME

LASER-MATTER INTERACTION

BIOMEDICAL PHOTONICS

LASER SYSTEMS AND MATERIALS

LASER DIAGNOSTICS AND SPECTROSCOPY

NONLINEAR AND TERAHERTZ PHOTONICS

PHOTONICS IN QUANTUM TECHNOLOGIES

NANOPHOTONICS

TABLE OF CONTENTS

PLENARY LECTURES 1

LASER-MATTER INTERACTION 12

BIOMEDICAL PHOTONICS 60

LASER SYSTEMS AND MATERIALS 119

LASER DIAGNOSTICS AND SPECTROSCOPY 180

NONLINEAR AND TERAHERTZ PHOTONICS 227

PHOTONICS IN QUANTUM TECHNOLOGIES 271

NANOPHOTONICS 304

PLENARY LECTURES

Photoconductivity in HgCdTe-based topological insulators stimulated by terahertz laser pulses

Dmitry Khokhlov[1,2]

1- Lomonosov Moscow State University
2- Lebedev Physical Institute

e-mail: khokhlov@mig.phys.msu.ru

The paper reports on the observation and study of a new effect – chiral nonlocal terahertz photoconductivity. The effect is observed in thick epitaxial $Hg_{1-x}Cd_xTe$ films, which are topological insulators. The existence of a nonlocal component of terahertz photoconductivity in these structures in a magnetic field is demonstrated. The sign of the nonlocal photoresponse depends on the position of the potential probe and the direction of the magnetic field, which indicates the chirality of the induced nonequilibrium transport. The observed nontrivial features of photoconductivity can be interpreted as a manifestation of the formation of a chiral edge conducting channel in the topological phase of $Hg_{1-x}Cd_xTe$ alloys. It is important to note that the obtained result contradicts the apparent symmetry of the experiment. Possible origin of the symmetry breaking is discussed.

Linear carbon chains: properties, synthesis, prospective applications in photonics and optoelectronics

A. Kucherik[1], V. Samyshkin[1], A. Abramov[1], A. Lelekova[1], S. Arakelian[1], A. Povolotskiy[2], A. Osipov[1]

1- Department of Physics and Applied Mathematics, Stoletov Vladimir State University, Gorkii street, Vladimir, 600000 Russia
2- Institute of Chemistry, St. Petersburg State University, Ulianovskaya str. 5, St. Petersburg, 198504 Russia

e-mail: kucherik@vlsu.ru

After several decades of unsuccessful experimental attempts and controversies, the synthesis of long chains of carbon atoms, with alternating single and triple bonds between them, known as linear acetylenic carbon or carbyne, has now become a reality. Because of its ultimate one-dimensional (1D) nature, carbyne exhibits extremely anisotropic optical properties. In addition, unlike most carbon nanotubes, which suffer from poor quantum efficiency due to dark excitons arising from their multivalley band structure, carbyne is a direct band gap material characterized by strong photoluminescence in the visible range. A recent theoretical study has shown that individual carbyne chains should exhibit strong light absorption and emission when excited by light that is polarized along the chain . This motivates optical experiments with films of highly aligned carbynes excited by linearly polarized light with the ultimate goal of creating ultrathin polarization sensitive elements of optoelectronic devices. Carbyne is a highly reactive and unstable material, which makes its synthesis challenging. However, finite length carbyne chains can now be synthesized using a variety of techniques ranging from laser ablation [1, 2], to chemical vapor deposition, electrochemical reduction, and lowtemperature pyrolysis. While a true carbyne crystal is composed of an infinitely long chain of carbon atoms, finite length carbyne chains can still display distinctive optical and electronic properties that render them promising candidates for a diverse range of optoelectronic applications. Indeed, the length of the carbyne chain, and edge termination play an important role in determining its optical properties and behavior.

In this work, we synthesized and studied the optical properties of ultimately thin carbon chains. When these chains are terminated by gold clusters, they become highly aligned with absorption strongly dependent on the angle between the chains and the polarization plane of the excitation [3]. The luminescence from gold terminated chains is much stronger than that from the pure carbon structures which have quadratic dependence of photoluminescence intensity on the pumping power. When gold-terminated chains are illuminated by a laser with a frequency close to the plasma frequency of gold clusters, there is a weak blue-shifted luminescence observed. All these effects can be described by a model of finite-length chain interlevel transitions broadened by the exchange of carriers between the carbon chains and gold clusters. The presence of blue-shifted luminescence allows us to estimate the minimum length of the chains. The strong polarization dependence of the luminescence intensity of gold-terminated carbon chain arrays makes them promising candidates for nanoscale logic elements in emerging lightcontrolled quantum devices.

This work was supported by the framework of RSF-grant 23-12-20004 (https://rscf.ru/project/23-12-20004).

[1] S. Kutrovskaya, A. Osipov, S. Baryshev, A. Zasedatelev, V. Samyshkin, S. Demirchyan, O. Pulci, D. Grassano, L. Gontrani, R. R. Hartmann, M. E. Portnoi, A. Kucherik, P. G. Lagoudakis, and A. Kavokin, Nano Lett. 20, 6502 (2020).
[2] S. Kutrovskaya, I. Chestnov, A. Osipov, V. Samyshkin, I. Sapegina, A. Kavokin, and A. Kucherik, Sci. Rep. 10, 9709 (2020).
[3] A.Kucherik, A.Osipov, V. Samyshkin, R.R. Hartmann., A. Povolotskiy, M.E. Portnoi (2024) Polarization-sensitive photoluminescence from aligned carbon chains terminated by gold clusters, 2024, PRL 132, 056902 (2024).

Light as a factor in controlling plants growth and development

Yury N. Kulchin

Institute of Automation and Control Processes of the Far Eastern Branch of the Russian Academy of Sciences, Vladivostok, Russia

e-mail: kulchin@iacp.dvo.ru

Sunlight is an important adaptive stimulus, and many living organisms adapt their metabolism to the changing light conditions in their environment by sensing light signals and responding to them by changing their physiological functions. Light is a multifaceted factor characterized by qualitative (wavelength range) and quantitative (intensity, integral daily radiation, and photoperiod) parameters, as well as direction and polarization. Given that light controls the functioning of endogenous regulation systems (genetic, enzymatic, trophic, hormonal, etc.), the combined effect of which ensures an adequate response of plants to light conditions, it is possible to manipulate the characteristics of light in order to maximize the potential determined by the plant genome. Thus, by using different spectral components of light and their combination, it is possible to provide the plant with input data or "instructions" that will lead to predictable results.

In this case, the observed effects of plant morphogenesis control based on the use of different light spectra are somewhat similar to genetic modification, but they do not alter the plant's genetic makeup. The idea of using different spectral components of light to control plant development is not new. However, to understand why this approach is possible, it is crucial to understand how plant responses are influenced by the expression of different genes in response to light. These studies are highly relevant as they offer the potential to maximize the genetic potential of plant crops without resorting to genetic modification or increased use of chemicals. The purpose of this work is to address issues related to the photonic control of plant morphogenesis.

In order for light to affect plant organisms and, in particular, to be used in the process of photosynthesis, it must be absorbed by photosensitive proteins (antennas) called pigments, which selectively absorb light of a certain spectral composition. Pigments play an important and diverse role in the life of organisms, especially in the photobiological processes that occur in them.

As a result, light plays a key role in the control and regulation of intracellular processes in a plant organism throughout its life, performing two main functions in the cell: energy and information. The first function is realized through photosynthesis, where light energy is transformed into the chemical energy of organic compounds. The second function of light is to initiate various regulatory responses, with light quanta acting as a carrier of information. In the case of regulatory reactions, light is absorbed by specialized photoreceptors, which initiate signaling cascades in the cell that modulate enzyme activity, gene expression, and various physiological parameters.

In higher plants, several complex photoreceptor protein systems function to perceive light of different spectral composition: red/far-red (phytochromes), blue/UV-A (cryptochromes, phototropins, ZTL/FKF1/LKP2) and UV-B light (UVR8). Changes in the light regime of plant growth cause extensive reprogramming of the pattern of gene expression in plants through the transmission of signals from the photoreceptor through complex networks of secondary messengers to various effector systems. As a result, photoreceptor systems have a significant impact on the processes associated with plant growth and development, as well as on the formation of their biologically beneficial properties.

Photon sensors in photoreceptor proteins are chromophore molecules, whose photoconversion initiates structural changes in the photosensory domain, followed by signal transduction to the effector domains of photoreceptors or interacting proteins, causing modulation of their activity.

Thus, the basis of plant photomorphogenesis is the detection of light energy of a given intensity in a given wavelength range by special photosensitive structures, such as photoreceptor proteins (photoreceptors). It is assumed that the light signals received by the photoreceptors are transformed and then transmitted through photoregulatory systems, leading to gene expression and ultimately resulting in a physiological response. It has been demonstrated that plant hormones are also involved in the response to light through the photoreceptor system. As a result, when the light parameters are detected, the photoreceptor triggers a chain of biochemical processes that ultimately activate the desired response in the plant.

By changing the spectral composition of LED irradiation systems, it is possible to vary the useful characteristics of plant tissues, which are important for ensuring intensive growth and development of plants in greenhouses, as well as for improving the quality of future plant products (by increasing the content of nutrients or compounds with organoleptic and pharmacological properties).

The report discusses the light regulation of the plant genetic system and the light control of morphogenesis. It provides an overview of the mechanisms of light signal translation in the cell. The report also highlights the relationship between photoreceptor proteins and endogenous plant development programs. It describes the role of pigment proteins and phytohormones in regulating plant ontogenesis. The report presents experimental results that demonstrate the light control of plant morphogenesis.

Photon echo quantum memory: traditional and new approaches to implementation

Sergey A. Moiseev

Kazan Quantum Center, Kazan National Research Technical University named after A. N. Tupolev – KAI, Kazan, Russia

e-mail: s.a.moiseev@kazanqc.org

The creation of quantum memory devices is of great importance for the development of next-generation quantum communications and a universal quantum computer. At the same time, much attention is paid to quantum memory capable of storing a large number of photonic qubits. Such a quantum memory is created using photon echo protocols [1, 2], which was first experimentally demonstrated with the storage of more than 1,000 light pulses [3]. Since the appearance of the first photon echo quantum memory (PEQM) protocol [4], called the CRIB protocol, a number of protocols have been proposed based on it [2], which use various ways to implement inhomogeneous broadening of the resonant atomic transition and control the optical coherence of atoms excited by signal light pulses. In this work we discusses the main properties of existing PEQM protocols, their advantages, disadvantages, and implementation difficulties. New approaches and physical principles of PEQM implementation are also analyzed.

The basic principles that are inherent in the well-known (traditional) PEQM protocols include: 1) the use of an optically thick system of resonant atoms; 2) complete absorption of the signal pulse by resonant atoms, which is accompanied by dephasing of atoms; 3) retrieval (rephasing) of macroscopic atomic coherence at the right time, causing the appearance of a photon echo signal; 4) emission of the photon echo signal in the backward direction to the direction of propagation of the signal light pulse (with the exception of the CRIB/GEM protocol). The CRIB protocol implements a variant of photon echo emission under conditions of precise reversibility of the interaction of light with atoms compared to the absorption stage of a signal light pulse. Reversibility is realized by inversion the frequency offsets of atoms to the opposite at the time of the echo signal emission. The complexity of implementing the inversion of high-frequency detuning does not allow using the CRIB protocol for storing short light pulses. This problem is solved using the AFC protocol, in which the inhomogeneous broadening of the resonant atomic transition has the form of a periodic atomic frequency comb (AFC). The AFC protocol is actively being developed using crystals and other media doped with rare-earth ions [5]. Due to the loss of precise temporal reversibility in the AFC protocol, it becomes necessary to develop methods for controlling frequency dispersion [6, 7] and new ways to implement the AFC protocol. One of the ways of such implementation is based on the use of a system of coupled resonators [8], which demonstrates the possibility of achieving efficient quantum memory in the microwave frequency range [9]. Multi-resonator quantum memory also makes it possible to achieve ultra-high efficiency at points of spectral topological transition [10], which expands the understanding of impedance matching conditions.

The implementation of the CRIB- and AFC protocols on atomic systems is accompanied by a significant decrease in the optical thickness of the resonant transition. This problem can be solved by placing an atomic system in a resonator, which makes it possible to enhance the interaction of atoms with photons and achieve high efficiency of PEQM protocol at the impedance matching conditions of the resonator and a system of a small number of atoms [11, 12]. The great advantages of using a resonator are manifested with a high Q resonator, which, however, reduces the operating spectral width of quantum memory. Ways to solve this problem using resonator systems with atomic ensembles are being considered [13]. Large enhancement of interaction of atoms with photons can also be achieved by placing atoms on the surface of a dielectric/metal interface, or a metamaterial and graphene. In this case, there is a strong spatial localization of light near the interface, which opens up the possibility of implementing a nano-dimensional quantum memory [14].

An important approach to the implementation of PEQM protocol is based on the use of natural inhomogeneous broadening of the atomic resonant transition [15–17], a serious problem of which is the occurrence of optical quantum noise caused by spontaneous luminescence of atoms during their transfer by controlling atoms to excited atomic states. Recently, a new effective method for suppressing quantum noise has been proposed and experimentally implemented by using additional excited optical

energy levels [18]. This approach has so far demonstrated the low efficiency, which is the subject of further research.

A fundamentally new approach to the implementation of PEQM protocols [19] is interesting, which is based on the preliminary creation of a long-lived macroscopic spin coherence with specified parameters in a system of atoms. It is shown that this coherence can be used to program the retrieval time of the signal pulse, similar to the AFC protocol, and effectively suppress optical quantum noise. The physical principles of the implementation of this quantum memory, its properties and the possibility of using it for quantum frequency conversion are discussed.

This research was supported by the Ministry of Science and Higher Education of the Russian Federation (Reg. No. NIOKTR 121020400113-1).

[1] W. Tittel et al., Laser and Photonics Review, 4, No. 2, 244–267 (2010).
[2] S. A. Moiseev et al., Front. Phys. 20 (2025) 023301.
[3] M. Bonarota et al., New J. Phys. 13 (1), 013013 (2011).
[4] S. A. Moiseev and S. Kroll. Phys. Rev. Lett. 87, 173601 (2001).
[5] M. Guo et al., Front. Phys. 18(2), 21303 (2023).
[6] S. A. Moiseev and J. L. Le Gouët, J. Phys. At. Mol. Opt. Phys. 45(12), 124003 (2012).
[7] N. M. Arslanov and S. A. Moiseev, Optics and Spectroscopy 126(1), 29 (2019).
[8] S. A. Moiseev et al., Scientific Reports, 8, 3982 (2018).
[9] A. R. Matanin et al., Phys. Rev. Appl. 19, 034011 (2023).
[10] N. S. Perminov, S. A.Moiseev, Scientific Reports, 9, 1568 (2019).
[11] M. Sabooni et al., Phys. Rev. Lett. 110, 133604 (2013).
[12] M. M. Minnegaliev, et al., Phys. Rev. B 103, 174110 (2021).
[13] S.A. Moiseev, arXiv: 2507.04865
[14] A. A. Kamli, S. A. Moiseev, Plasmonics (2025) (in press).
[15] D. L. McAuslan et al., Phys. Rev. A 84(2), 022309 (2011).
[16] S. A. Moiseev, Phys. Rev. A 83(1), 012307 134 (2011).
[17] V. Damon et al., New J. Phys. 13, 093031 (2011).
[18] Y. Z. Ma et al., Nat. Commun. 12(1), 4378 (2021).
[19] S. A. Moiseev et al., Phys. Rev. Lett. 134, 070803 (2025).

Colloidal quantum dots as lasing material: optical gain vs nonradiative recombination

Anna V. Rodina

Ioffe Institute, St. Petersburg, Russia

e-mail: anna.rodina@mail.ioffe.ru

Chemically synthesized semiconductor nanocrystals are now widely used in a variety of applications, including in medicine and biology as sensors or labels, in photovoltaics for solar cells, and in optoelectronics for white light sources, LEDs, displays, and TVs. The growing importance of nanocrystal technology was acknowledged when the 2023 Nobel Prize in Chemistry was awarded for the 'discovery and synthesis of quantum dots'. The physics and technology of zero-dimensional structures, or quantum dots, started with the experimental observation and theoretical description of the quantum-size effect in semiconductor nanocrystals embedded in glass matrices (USSR, 1981–1982) and dispersed in aqueous solutions (USA, 1983). At the same time, the advantages of reducing dimensionality of epitaxatially grown heterostructures from 2D to 1D and 0D for lasing applications were predicted. The term 'quantum dots' and the first epitaxially grown quantum dots emerged shortly afterward in 1985–1986.

While epitaxial quantum dots have been successfully used in lasers, the use of colloidal nanocrystals for lasing has proven more challenging, progressing steadily but slowly. A major obstacle to achieving optical gain in colloidal quantum dots is their rapid nonradiative Auger recombination. This talk provides a concise review of the discovery of colloidal quantum dots and of research into their lasing applications, followed by an analysis of the state of the art. In particular, I will discuss the influence of spatial and dielectric confinement, as well as of nanocrystal surface properties, on electronic structure and radiative recombination efficiency.

The work was supported by the RFS grant No. 23-12-00300.

Infrared metrology based on quantum interferometry

A. S. Sabanin[1], L. A. Krivitsky[2], S. P. Kulik[1,3], A. V. Paterova[1,2]

1- Laboratory of Quantum Engineering of Light, South Ural State University, Chelyabinsk, Russia
2- Institute of Materials Research and Engineering, Singapore, Republic of Singapore
3- Quantum Technology Centre, Department of Physics, Lomonosov Moscow State University, Moscow, Russia

e-mail: paterovaav@susu.ru, paterova@physics.msu.ru

The infrared (IR) spectral range is highly attractive due to the presence of spectral "fingerprints" of materials. Spectral measurements in the IR range enable the identification of unique properties of the medium, making IR technologies essential in material composition analysis and sensing applications. However, modern IR metrology methods are based on the use of IR detectors, which face a number of limitations, including strong background noise and requirement for cryogenic cooling. These factors increase the cost of such systems and limit their sensitivity. As a result, existing IR metrology methods (both spectroscopy and microscopy) remain expensive and less efficient compared to their counterparts operating in the visible spectrum.

These limitations can be addressed by using the capabilities of quantum and nonlinear optics. An alternative to direct IR detection is the use of *induced coherence without induced emission* phenomenon, also known as quantum interferometry [1–3]. This approach allows one to study the IR properties of samples by analyzing visible light, thereby simplifying measurements and reducing costs.

In our research, we have demonstrated the effectiveness of the quantum interferometry method across several applications, including IR spectroscopy [3–5] and mid-IR imaging [6–8]. The obtained results open up possibilities for practical application of the developed method. In particular, in medical diagnostics, this approach can provide more accurate and non-invasive detection of diseases, and in chemical analysis, it can help determine the composition of complex substances and study their structural characteristics in detail. Thus, the proposed method shows significant potential for addressing a wide range of scientific and applied challenges.

[1] X. Y. Zou et al, "Induced coherence and indistinguishability in optical interference", Phys. Rev. Lett. 67, 318–321 (1991).
[2] G. B. Lemos et al, "Quantum imaging with undetected photons", Nature 512, 409–412 (2014).
[3] D. A. Kalashnikov et al, "Infrared spectroscopy with visible light", Nat. Photonics 10, 98–101 (2016).
[4] A. Sabanin et al, "Sensing of gas mixtures via nonlinear interferometry", Laser Physics Letters 22, 015203 (2024).
[5] A. V. Paterova et al, "Broadband Quantum Spectroscopy at the Fingerprint Mid-Infrared Region", ACS Photonics 9(6), 2151−2159 (2022).
[6] A. V. Paterova et al, "Quantum Imaging for the semiconductor industry", Appl. Phys. Lett. 117, 054004 (2020).
[7] A. V. Paterova et al, "Hyperspectral infrared microscopy with visible light", Science Advances 6(44), eabd0460 (2020).
[8] M. Suryana, et al., "Infrared imaging with visible light in microfluidic devices: the water absorption barrier", Analyst 150(2), 405–413 (2025).

Physics of extreme light fields

Alexander M. Sergeev

National Center of Physics and Mathematics

e-mail: almsergeev@rosatom.ru

In this report, development of a scientific field at the intersection of high-energy physics and physics of super-strong light fields is discussed. Currently, several laboratories around the world are building laser complexes with multi-petawatt and subexawatt power, which allow focusing laser pulses with a duration of about 10 femtoseconds to giant intensities exceeding 10^{23} W/cm^2. The states of matter and vacuum that arise in such fields are still the subject of theoretical studies that predict amazing properties and promise unique applications. The report will present the possibilities for obtaining super-dense electron-positron plasma, giant magnetic fields and powerful sources of highly directed gamma radiation in the laboratory, for studying the spatio-temporal structure of the quantum vacuum, and will discuss approaches for further moving along the intensity scale and approaching the level of Schwinger fields.

Benefits of optical imaging and phototherapy through tissue optical clearing

Valery V. Tuchin[1–3]

1- Institute of Physics and Science Medical Center, Saratov University
2- Institute of Precision Mechanics and Control,
FRS "Saratov Scientific Centre of the Russian Academy of Sciences"
3- Laboratory of Biophotonics, Tomsk University, Russia

e-mail: tuchinvv@mail.ru

Tissue optical clearing (TOC) is based on temporary and reversible suppression of light scattering in tissues using biocompatible immersion optical clearing agents (OCAs) [1–3]. Delivery of the appropriate OCA to living tissue ensures its temporal transparency over a wide spectral range from deep UV to THz, thereby providing higher image depth and contrast for optical techniques and better precision of phototherapy and laser surgery.

The lecture summarizes the advances in the development of the TOC method for solving problems of intravital optical imaging, diagnostics and laser therapy.

[1] L. Oliveira and V.V. Tuchin, The Optical Clearing Method: A New Tool for Clinical Practice and Biomedical Engineering, Basel: Springer Nature Switzerland AG, 2019.
[2] V.V. Tuchin, D. Zhu, E.A. Genina (Eds.), Handbook of Tissue Optical Clearing: New Prospects in Optical Imaging, CRC Press, Boca Raton, FL, 2022.
[3] D. Zhu, V.V. Tuchin, Tissue optical clearing imaging from ex vivo toward in vivo, BME Front. 5, 0058 (2024).

32nd INTERNATIONAL CONFERENCE
Advanced Laser Technologies
ALT'25

LASER-MATTER INTERACTION

Decoupling the intrinsic infrared response of melanin/polydopamine from hydration-driven spectral changes

P. A. Abramov[1], V. A. Brotsman[2], A. B. Mostert[3], K. A. Motovilov[1]

1- Moscow Institute of Physics and Technology, Moscow, Russia
2- Lomonosov Moscow State University, Leninskie Gory 1-3, Moscow, 119991 Russia
3- Swansea University, Faculty of Chemistry, Singleton Park, Wales, United Kingdom

e-mail: abramovpa33@gmail.com

Melanin and its synthetic analog polydopamine (PDA) have emerged as promising bioelectronic materials due to their unique mixed ionic-electronic conductivity, biocompatibility, and robust environmental stability [1, 2]. These materials show exceptional promise for applications in organic electronics, biosensors, and energy storage devices [3]. However, a fundamental challenge remains in interpreting their infrared spectra due to strong coupling between the polymer matrix and hydration water, which obscures their intrinsic vibrational signatures.

This study presents a comprehensive thermal-IR approach to resolve the intrinsic spectroscopic features of these materials. Using in situ vacuum-FTIR spectroscopy coupled with controlled thermal treatment, we systematically investigated the dehydration and thermal decomposition processes. Our DTGA-MS analysis revealed two distinct populations of confined water in natural melanin with different binding energies (desorbing at 50–80 °C, 100–140 °C and 160–170 °C), while PDA exhibited only one dominant water population.

Extending our thermal analysis to higher temperatures (up to 350 °C), we observed three distinct thermal regimes: water loss (30–150 °C), decarboxylation (100–200 °C), and (3) polymer decomposition (from 210 °C). The decarboxylation process in melanins was evidenced by CO_2 evolution (MS detection) and the progressive evolution of the 1720 cm^{-1} carbonyl band. Our thermal-IR approach enabled identification of persistent vibrational markers of the polymer backbone that remain unchanged by hydration. The thermal stability differences between melanins and PDA, particularly regarding carboxyl group retention, provide new insights into their distinct proton transport mechanisms.

These findings provide a framework for authenticating IR spectra of melanin materials, mechanistic insights into proton conduction pathways, and design principles for next-generation bioelectronic interfaces where controlled hydration is crucial.

The work was carried out with the financial support of the RNF grant No. 25-12-00134.

[1] d'Ischia M, Wakamatsu K, Cicoira F, Mauro E D, Garcia-Borron J C, Commo S, Galván I, Ghanem G, Kenzo K, Meredith P, Pezzella A, Santato C, Sarna T, Simon J D, Zecca L, Zucca F A, Napolitano A and Ito S 2015 Melanins and melanogenesis: from pigment cells to human health and technological applications Pigment Cell Melanoma Res. 28 520–44.
[2] Mostert A B 2021 Melanin, the What, the Why and the How: An Introductory Review for Materials Scientists Interested in Flexible and Versatile Polymers Polymers 13 1670.
[3] Mostert A B, Powell B J, Pratt F L, Hanson G R, Sarna T, Gentle I R and Meredith P 2012 Role of semiconductivity and ion transport in the electrical conduction of melanin Proc. Natl. Acad. Sci. U.S.A. 109 8943–7.

Evaluation of the photoresponse of Si:Au laser-assisted hyperdoped photodiode

A. Akhmatkhanov[1], V. Pryakhina[1], P. Paletskikh[1], D. Tkachuk[1], A. Sherstobitov[1], M. Kovalev[1,2], S. Kudryashov[1,2]

1- Ural Federal University, Yekaterinburg, Russia
2- Lebedev Physical Institute, Moscow, Russia

e-mail: andrey.akhmatkhanov@urfu.ru

Silicon (Si) has been established as one of the main materials of optoelectronics and photovoltaics leveraging the well-developed CMOS technologies and wide availability of high quality wafers. That's why it looks natural to find the ways of further enhancing its optical and electrical characteristics including the extension of the absorbance range thus enabling new near- and mid-IR Si applications. One of the possible approaches for this enhancement is silicon doping by appropriate impurities above the Mott limit to form the intermediate band in the bandgap. However, the potentially appropriate impurities like Au or Ag with acceptor and donor levels near the middle of silicon bandgap have solubility levels below the Mott limit. One of the solutions of this problem is impurity hyperdoping by pulsed laser irradiation of the thin film deposited on the sample [1, 2].

Pulsed laser with wavelength 1064 nm and pulse duration 100 ns (MiniMarker-2 M20, LTC, Russia) operating at 80 kHz pulse repetition rate was used. Au thin films with thickness 5–40 nm were deposited on 200-μm-thick Si wafers and processed by laser scanning over the sample surface. The extended absorbance range of the hyperdoped sample was confirmed by near-IR spectrometer and its photoresponse was analyzed during irradiation by CW 1550-nm laser (VPG Laser One, Russia).

Two photoresponse geometries were evaluated: the photodiode current response under the reverse bias obtained for Ohmic contacts deposited on the opposite sample surfaces, and the photoresistivity change obtained for the contacts deposited on the hyperdoped surface.

According to our results the optimal parameters [2] of laser hyperdoping allow to achieve the decrease of sample resistance (photoresistivity) to 2.5–5 times for 1 W irradiation as compared to non-irradiated sample depending on the doping type of the initial Si substrate. The photodiode current response of the samples increased linearly with irradiation power and reached the values of 100 μA for 0.1 V reverse bias.

The research funding from the Ministry of Science and Higher Education of the Russian Federation (Ural Federal University Program of Development within the Priority-2030 Program) is gratefully acknowledged. The equipment of the Ural Center for Share Used «Modern Nanotechnologies» Ural Federal University was used.

[1] M. Kovalev, et al. Au-hyperdoped Si nanolayer: Laser processing techniques and corresponding material properties, Materials, vol. 16, p. 4439, (2023).
[2] V. Pryakhina, et al. Spatial confinement in laser-induced gold-hyperdoping of Si wafers, Opt. Laser Technol., vol. 188, p. 112945, (2025).

Laser-induced highentropy surface nanostructures of specified topology with controlled functional optoelectronic characteristics

S. Arakelyan

Vladimir State University

Synthesis and modification of selenium nanoparticles during laser ablation and fragmentation in organic liquids

I. V. Baimler, A. V. Simakin, A. O. Dikovskaya, S. V. Gudkov

Prokhorov General Physics Institute of the Russian Academy of Sciences, Vavilova Street 38, Moscow, 119991 Russia

e-mail: ilyabaymler@yandex.ru

It is known that selenium has about 11 modifications, of which 7 are crystalline and 4 are non-crystalline [1]. Among the crystalline modifications of selenium, trigonal selenium (t-Se) forms nanocrystal rods with a thickness of several tens to hundreds of nanometers and a length of up to several microns, which has a number of unique optical, electrical and biological properties [2]. The synthesis of selenium nanoparticles by laser ablation and fragmentation in aqueous solutions has been well studied and is used to create spherical nanoparticles of various sizes [3]. However, the production of trigonal selenium nanoparticles using laser ablation techniques in liquids has not been previously reported. In this work, we demonstrated for the first time the possibility of obtaining trigonal crystalline selenium using laser ablation and fragmentation methods in various solvents without the use of additional substances and additional effects on the colloid of nanoparticles.

Laser ablation and subsequent laser fragmentation of some organic solvents, such as ethanol, propanol-2, isobutanol, polyethylene glycol, and diethanolamine, have been found to produce trigonal selenium in the form of elongated nanorods approximately 1 μm long and 200 nm thick, with a well-defined crystal structure (Fig. 1).

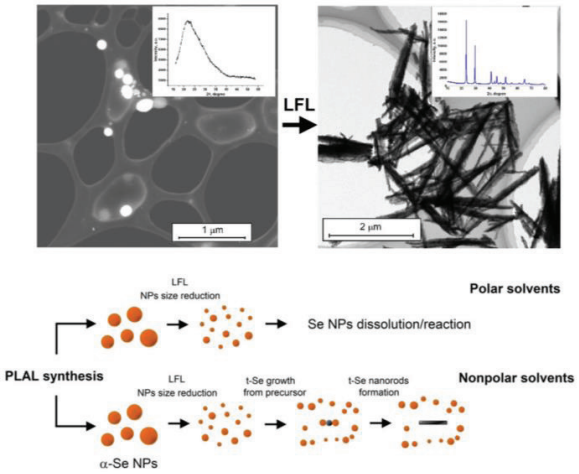

Fig. 1. TEM-images of Se NPs obtained by laser ablation in deionized water and by laser fragmentation in propanol (top); schematic representation of the formation of amorphous and trigonal selenium by laser fragmentation (bottom).

In contrast, the use of deionized water, acetone, glycerol, and benzene as solvents results in the formation of spherical amorphous nanoparticles approximately 100 nm in diameter. The polarity of the solvent molecules has been shown to influence the growth of crystalline selenium nanorods in solution during laser ablation and laser fragmentation. Generally, polar solvents hinder the growth of crystalline nanorods, due to interactions between selenium and solvent molecules. Nonpolar solvents, on the other hand, reduce particle size and initiate the epitaxial growth of elongated, crystalline selenium nanorods.

The research was supported by Russian Science Foundation (Project № 24-22-00363, https://rscf.ru/project/24-22-00363).

[1] V.S. Minaev, S.P. Timoshenkov, V.V. Kalugin, Structural and phase transformations in condensed selenium, Journal of Optoelectronics and Advanced Materials, 7(4), p. 1717, (2005).
[2] M.A. Ruiz-Fresneda, L.C. Staicu, G. Lazuén-López, M.L. Merroun, Allotropy of selenium nanoparticles: Colourful transition, synthesis, and biotechnological applications, Microbial Biotechnology, 16(5), 877–892, (2023).
[3] O. Van Overschelde, G. Guisbiers, R. Snyders, Green synthesis of selenium nanoparticles by excimer pulsed laser ablation in water. Apl Materials, Oct 1;1(4), (2013).

Ultrafast electron dynamics in HgTe quantum dots

D. Boschetto

Laboratoire d'Optique Appliquée, ENSTA, Ecole Polytechnique, CNRS, Institut Polytechnique de Paris, Palaiseau, France

e-mail: davide.boschetto@ensta.fr

Quantum confined systems, such as quantum dots and two-dimensional materials, have attracted growing attention over the past two decades due to their remarkable and tunable physical properties [1, 2]. Defined by their reduced dimensionality, these systems exhibit quantum confinement effects that alter their electronic structure, optical transitions, and mechanical behavior compared to bulk materials. Among them, semiconductor quantum dots have found a wide range of applications, particularly as sources and detectors of photons. In these nanostructures, the spatial confinement of electrons and holes in all three dimensions leads to discrete, atom-like energy levels, giving rise to size-dependent emission and absorption spectra and enabling their integration into a variety of photonic and quantum technologies. The dynamics of charge carriers in such confined systems play a critical role in determining the performance of associated optoelectronic devices. Ultrafast spectroscopy has emerged as a key technique for probing these carrier dynamics, offering direct access to the timescales and mechanisms of fundamental processes such as carrier relaxation, hot-carrier cooling, Auger recombination, and energy or charge transfer [3]. These processes, which span timescales from sub-picoseconds to several nanoseconds, are essential to understand in order to optimize the efficiency of devices. Time-resolved experiments have also revealed how environmental factors, such as ligand length and subsequent inter-dot coupling, influence carrier lifetimes and relaxation pathways.

In this talk, we will focus specifically on mercury telluride (HgTe) quantum dots, which are emerging as highly promising candidates for optoelectronic applications in the infrared spectral range [1–3]. Thanks to their narrow bandgap and strong quantum confinement, HgTe quantum dots exhibit a tunable photoresponse and photoluminescence that extend into the mid-infrared, a spectral region of key interest for telecommunications, sensing, and thermal imaging technologies. We will examine how the interplay between confinement effects and ligand length governs the available relaxation channels, and how this affects both carrier recombination dynamics and radiative efficiency. A particular emphasis will be placed on charge transfer mechanisms and their influence on non-radiative pathways. These mechanisms can either facilitate or suppress specific relaxation channels, thereby modulating the quantum efficiency and operational performance of photodetectors and light-emitting devices based on HgTe quantum dots. By combining insights from ultrafast pump-probe spectroscopy and device-level characterization, we aim to develop a comprehensive understanding of how to engineer and control these quantum dots for optimal performance in infrared optoelectronic applications.

[1] J. Qu et al., "Electroluminescence from Nanocrystals above 2 μm", Nature Photonics 16, 38 (2022).
[2] A. Khalili et al., "Guided-mode resonator coupled with nanocrystal intraband absorption", ACS Photonics 9, 985 (2022).
[3] S.G. Mizrahi et al., "Ultrafast Electron Dynamics in Coupled and Uncoupled HgTe Quantum Dots", The Journal of Physical Chemistry Letters 15, 12485 (2024).

Synthesis of composite nanomaterials based on iron and gold by laser ablation and assisted ultrasound

A. Chernikov, D. Kochuev, M. Dzus, E. Shingareva, K. Khorkov

Vladimir State University, Gorky Street 87, Vladimir, 600000 Russia

e-mail: khorkov@vlsu.ru

Recently, methods for synthesizing composite nanoparticles used in biomedical applications have been actively developing [1]. In this work, a three-stage process based on a combination of laser ablation and ultrasound techniques was used to produce composite nanoparticles (NPs) based on iron and gold. The first stage consisted in the laser ablative synthesis of gold NPs. The Yb:KGW femtosecond laser system (Avesta) was used as a radiation source in experiments on laser ablation synthesis. The radiation wavelength was 1030 nm, the maximum energy in a pulse was 150 μJ, the pulse duration was 280 fs, and the pulse repetition frequency was 10 kHz. Laser beam scanning on the target surface was performed using a galvanoscanner, the pulse energy was set at 30 μJ. The target was placed in a cuvette filled with 1 mmol of NaCl solution. The concentration of the resulting colloidal solution was 0.125 mg/ml. The gold NPs obtained at this stage had a characteristic size from 5 to 20 nm. The aim of the second stage was to obtain NPs with magnetic properties. A solution of α-Fe NPs was prepared by transferring α-Fe NPs synthesized by laser ablation of iron in argon stored in acetone to ethanol (95%). Polyvinylpyrrolidone K30 (PVP, M.W. 40000) was then added to a test tube with NPs, the PVP concentration in the solution was 10 mg/ml. This procedure was necessary to modify the surface of the NPs in order to protect against oxidation and increase the colloidal stability of the NPs. To select NPS with magnetic properties, the obtained colloidal solutions were subjected to a magnetic separation step [2]. The source of the ultrasonic effect in this experiment was an immersion dispersant UZTA-0,1/28-O (Center for Ultrasound Technologies), the maximum intensity of ultrasound exposure is 300 W/cm^2 with an ultrasonic vibration frequency of 28±2.5 kHz, the tip diameter is 4.5 mm. Ultrasonic exposure was carried out at an intensity of 240 W/cm^2. Upon completion of the process, a magnetic separation step was performed to separate the magneto-plasmon composite NPs from the gold ones. The NPs prepared in the second stage had an average size of 104 nm, and at the end of the third stage, the average size halved to 50 nm. The resulting magnetic NPs, together with gold NPs, were used at the final stage, the purpose of which was to form composite NPs with a "core-satellite" configuration as a result of ultrasonic exposure to a solution obtained by mixing two types of NPs. Before measuring the optical properties, the solutions were diluted 5 times. The optical density curves of solutions of gold NPs, PVP α-Fe NPs, composite NPs, and non-reacted gold NPs are shown in Fig. 1. The position of plasmon resonance for composite nanoparticles shifts to 548 nm.

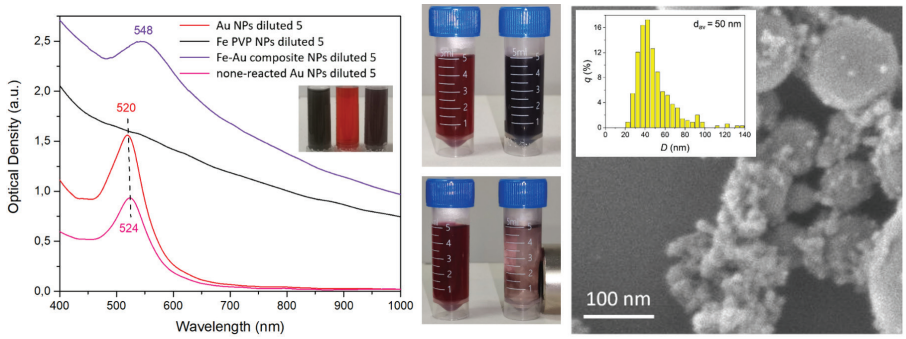

Fig. 1. Optical density curves of solutions of gold NPS (red curve), PVP α-Fe NPS (black curve), composite NPS (purple curve) and non-reacted gold NPs (pink curve); SEM-image of composite NPs.

This study was funded by the Russian Science Foundation (project no. 22-79-10348, https://rscf.ru/project/22-79-10348/).

[1] H.V. Tran et al, Multifunctional iron oxide magnetic nanoparticles for biomedical applications: a review, Materials, vol.15(2), p. 503, (2022).
[2] D.A. Kochuev et al, Magnetic selection of iron-based nanoparticles in pulsed laser synthesis, Pisma v Zhurnal Tekhnicheskoi Fiziki, vol. 50(12), pp. 28–31, (2024).
[3] A.S. Chernikov et al, Femtosecond laser synthesis of hybrid magnetic nanoparticles based on iron and gold with photothermal response, Fizika Tverdogo Tela, vol. 66(12), pp. 2210–2213, (2024).

Plasmon-induced radical polymerization: a route to chiral nanostructures

D. R. Dadadzhanov[1,2], D. Feferman[1], N. S. Petrov[2], V. S. Tuchin[2], I. A. Gladskikh[2], T. A. Vartanyan[2], G. Markovich[1]

1- School of Chemistry, Raymond and Beverly Sackler Faculty of Exact Sciences, Tel Aviv University, Tel Aviv, 6997801 Israel
2- International Research and Education Centre for Physics of Nanostructures, ITMO University, Kronverksky pr. 49, St. Petersburg, 197101 Russia

e-mail: daler.dadadzhanov@gmail.com

Design of functional plasmonic nanostructures based on unique chemical and surface physics phenomena, including plasmon-induced effects, is a rapidly advancing field in nanophotonics. These approaches holds significant promise for applications in analytical chemistry, photocatalysis, photovoltaics, sensing, and nanomedicine. Notably, site-selective deposition of target materials near metallic nanoparticles are of particular interest for inducing circular dichroism. This is because nanoparticles exhibit plasmon resonance, a collective excitation of free conduction electrons, which leads to distinctive phenomena at the metal-medium interface. These include non-uniform field distributions, where the field intensity can be significantly higher than the incident field, plasmon-resonant energy transfer, sharp temperature gradients, and the generation of hot charge carriers. Numerous materials have been used for site-selective deposition on nanoparticle surfaces, including salts (e.g., aryldiazonium, iodonium), oxides (e.g., PbO_2), metals (e.g., Ag, Au, Cu, Al), polymers (e.g., PETIA, PS, PVB), and biomolecules (e.g., proteins, DNA).

In this talk, I will provide an overview of the site-selective deposition approach on plasmonic nanoparticles based on plasmon-induced polymerization [1–3] and describe the reveal a relative role of various effects, including photochemical, optical, and thermodynamic factors for designing chiral nanostructures. In our work, chiral nanostructures were obtained using local photopolymerization of monomers (tetraphenylporphyrin) in the near-field of nanoparticles and irradiation by circularly polarized light. Two types of initially achiral structures were considered: self-organized Ag nanoparticles obtained by vacuum deposition and subsequent thermal treatment, as well as chemically synthesized bimetallic Ag@Au nanocuboids. Exposure to circularly polarized light leads to a disturbance in the racemate balance of enantiomers in the nanostructures, which is manifested in an increased circular dichroism absorption, primarily for the polarization state of the test beam that matches the polarization state of the laser used for polymerization. It was also shown that the resulting chiral nanostructures demonstrate high sensitivity to changes in the refractive index of the external environment, with an increase from 1 to 1.5 leading to a noticeable attenuation of the circular dichroism intensity. Special attention will be given to the potential use of plasmon-induced radical polymerization for visualizing the distribution of near-fields and training a deep neural network for prediction of the near-field distribution on initially unpolymerized plasmonic nanostructures.

This work was supported by ITMO University Research Projects in AI Initiative (RPAII), (Project 640098).

[1] Khitous, Amine, et al. "Plasmon-Induced Photopolymerization of Molecularly Imprinted Polymers for Nanosensor Applications." Advanced Materials Interfaces 10.7 (2023): 2201651.
[2] Deeb, Claire, et al. "Plasmon-based free-radical photopolymerization: effect of diffusion on nanolithography processes." Journal of the American Chemical Society 133.27 (2011): 10535–10542.
[3] Wang, Yunxia, et al. "Plasmon-directed polymerization: Regulating polymer growth with light." Nano Research 11 (2018): 6384–6390.

The concentration limit of stability gold nanoparticles colloid synthesized by laser ablation

A. O. Dikovskaya, I. V. Baimler, S. V. Gudkov, A. V. Simakin

Prokhorov General Physics Institute of the Russian Academy of Sciences, Vavilova Street 38, Moscow, 119991 Russia

e-mail: dikovskayaao@gmail.com

Aqueous gold nanoparticles colloids, synthesized by laser ablation due to their high purity, are vital in various applications. Understanding their stability at high concentrations is crucial [1]. This study investigates the concentration-dependent stability of 15 nm gold nanoparticles in water, revealing a critical threshold for spontaneous, irreversible aggregation.

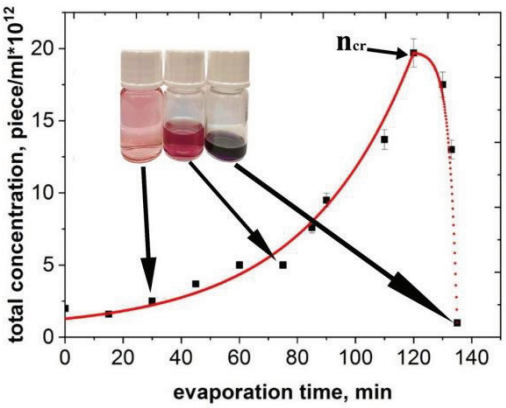

Fig. 1. Dependence of the concentration of Au NPs on evaporation time.

According to the DLFO theory, the properties of nanoparticles in a colloidal solution are largely determined by the surface layer of adsorbed components from the environment [2]. Gold nanoparticles, known for their significant stability, have a pronounced electric charge. When they approach, the role of the dipole-dipole potential increases, which increases the forces of attraction and can lead to aggregation [3]. However, this conceptual model does not provide an exhaustive explanation for cases of irreversible aggregate formation. Despite numerous studies of various aspects of aggregation, the fundamental physico-chemical mechanisms governing both reversible and irreversible aggregation of metal nanoparticles in liquid media remain poorly understood.

During the experiment, the concentration of gold nanoparticle colloidal solutions was gradually increased by evaporating water (Fig. 1). The aggregation process was monitored in real time using optical absorption spectroscopy. The aggregates morphology was characterized using transmission electron microscopy. Colloidal stability was assessed through measurements of ζ-potential. A clear stability limit of approximately 10^{13} nanoparticles/ml was established for gold nanoparticles with a size of 15 nm. When the concentration exceeds this critical value, irreversible aggregation occurs, forming linear nanochains such as dimers and trimers. It is worth noting that throughout this process, the ζ-potential of the colloid unchanged.

The research was supported by Russian Science Foundation (Project № 24-22-00363, https://rscf.ru/project/24-22-00363).

[1] G. Palazzo, G. Valenza, G., M. Dell'Aglio, A. De Giacomo, On the stability of gold nanoparticles synthesized by laser ablation in liquids. Journal of colloid and interface science, 489, 47–56, (2017).
[2] T. Kim, C.H. Lee, S.W. Joo, K. Lee,. Kinetics of gold nanoparticle aggregation: experiments and modeling. Journal of colloid and interface science, 318(2), 238–243, (2008).
[3] H. Zhang, D. Wang, D. (2008). Controlling the growth of charged-nanoparticle chains through interparticle electrostatic repulsion. Angewandte Chemie, 120(21), 4048-4051, (2008).

Laser synthesis of bismuth nanoparticles and its compounds for biomedicine

K. O. Fomin[1,2], A. V. Rudyy[2,3], E. I. Mavreshko[1,2], A. A. Fronya[1,2], I. N. Zavestovskaya[1–3]

1- Lebedev Physical Institute, Russian Academy of Sciences, Moscow, 119991 Russia
2- National Research Nuclear University MEPhI, Moscow, 115409 Russia
3- National Research Center "Kurchatov Institute", Moscow, 123182 Russia

e-mail: fronyaaa@lebedev.ru

In recent decades, there has been an intensive development of research with nanosized particles and their application in biomedicine: methods and technologies for obtaining, methods for monitoring, diagnosing, studying and stabilizing their properties are being developed.

Interest in bismuth nanoparticles in biomedicine is due to a number of properties. Bismuth and its compounds are currently used in medicine as part of drugs with antiseptic, healing, astringent, enveloping, antacid properties [1].

Nanosized bismuth has been studied quite recently and it is considered for potential use in diagnostics and therapy. The works [2, 3] presented the results of studying nanosized bismuth and its compounds as contrast agents in various visualization methods, such as X-ray, fluorescence and photoacoustic visualization. From the point of view of therapy, nanosized bismuth demonstrated good photothermal properties under the influence of infrared radiation [2, 4], as well as radiosensitizing properties under the influence of ionizing radiation [5]. Bismuth-based nanomaterials demonstrate significant potential for the creation of universal multifunctional theranostic drugs.

The unique properties of nanoparticles depend on the material, methods of production and processing, their resulting shape and size. When choosing a synthesis method for biomedical applications, the reproducibility of the results, stability in the size of the nanoparticles, and the exclusion of any changes in the chemical composition of the resulting nanoparticles are important. And here the most optimal is the synthesis of nanoparticles in the form of colloidal solutions by laser ablation methods in liquid.

The paper presents the results of an experimental study of laser-ablation synthesis of bismuth and bismuth germanate nanostructures under various conditions. For synthesis, a nanosecond laser system "SharpMark Fiber PRO 100F VAR" with an operating wavelength of 1064 nm was used. Laser system allow to vary the integral radiation power, the duration of the laser pulse, and the pulse repetition rate. Distilled water and isopropanol were used as liquid media for ablation. The size of the synthesized particles varied from tens to hundreds of nm. The use of distilled water led to the formation of bismuth oxide. Further use of bismuth-based nanomaterials requires detailed development of synthesis protocols, which will ensure the reproducibility of the synthesized materials in size and properties.

This work was supported by the Ministry of Science and Higher Education of the Russian Federation, project no. 075-15-2025-453.

[1] S.V. Okovity, D.Yu. Ivkin. Bismuth preparations - the pharmacological basis of the clinical effect. Attending doctor. Medical Scientific and Practical Journal. 2015. № 10. ISSN 2687-1181. [in Russian].
[2] C.Liu, L. Zhang, X. Chen, et al. Biomolecules-assisted synthesis of degradable bismuth nanoparticles for dual-modal imaging-guided chemo-photothermal therapy. Chemical Engineering Journal. 2020. V. 382, ISSN 1385-8947.
[3] H. Yu, H. Guo, Y. Wang, et al. Bismuth nanomaterials as contrast agents for radiography and computed tomography imaging and their quality/safety considerations. WIREs Nanomed Nanobiotechnol. 2022. V. 14. № 6, ISSN:1939-0041.
[3] H. Zhao, J. Wang, X. Li, et al. A biocompatible theranostic agent based on stable bismuth nanoparticles for X-ray computed tomography/magnetic resonance imaging-guided enhanced chemo/photothermal/chemodynamic therapy for tumours. Journal of Colloid and Interface Science. 2021, V. 604, P. 80–90, ISSN 0021-9797.
[3] C. Stewart, K. Konstantinov, S. McKinnon, et al. First proof of bismuth oxide nanoparticles as efficient radiosensitisers on highly radioresistant cancer cells. Phys. Med. 2016. V. 32, № 11. P. 1444–1452, ISSN 00942405.

Ultrafast laser-driven tunneling and ballistic free-carrier dynamics in nanostructures: a basis of sub-petahertz and peta-hertz electronics

V. Gruzdev

Department of Physics and Astronomy, University of New Mexico,
210 Yale Boulevard NE, Albuquerque, NM, 87106 USA

e-mail: gruzdevvitaly@hotmail.com

Recently emerged technologies of high critical importance, e. g., artificial intelligence (AI), big-data processing, and high-speed communications substantially rely of advancements in microelectronic circuits. The modern microelectronics is facing two fundamental challenges [1]: 1) a need to increase the switching speed of core semiconductor components – transistors and diodes; and 2) a need to reduce power consumption. Over the past two decades, the ultimate speed of microelectronic circuits has plateaued at a few gigahertz (GHz), limited by the basic properties of drift-based electron transport. The major parameter to characterize free-carrier drift in those materials – electron and hole mobility – is constrained by free-carrier scattering that results in picosecond-scale response times of the semiconductor devices. While past performance gains were achieved by reducing transistor dimensions towards few nanometers, this approach has reached its limits due to quantum effects and material instability at near-atomic scales. Other approaches, e. g., 3D stacking or switching electronic devices by femtosecond laser pulses [2, 3], suggest potential for operation at sub-terahertz and terahertz (THz) frequencies. However, these devices are experimental [3], require special conditions, e. g., near-zero temperatures [2] or suffer from significant thermal constraints [1]. As a result, a broad range of microelectronic systems – from smartphones to AI hardware – faces inherent barriers in both speed and energy efficiency.

In this talk, we overview the basic principles and recent progress of ultrafast electronic switching in nanoelectronic devices driven by few-cycle femtosecond laser pulses. The two major physical principles employed by those devices are ultrafast electron tunneling between metal nano-electrodes [4–6] and ballisitic (non-collision) dynamics of free electrons in metal-semiconductor nanostructures [6–8]. Being excited by few-cycle laser pulses, those nanostructures have demonstrated generation of electrical signals and switching within half-cycle of the electric field of driving laser pulse. Equivalent switching time of those devices can be easily adjusted around one femtosecond and below that suggests feasibility to drive those devices at sub-petahertz and petahertz (PHz) frequencies. Among reported devices, there are prototypes of diodes and PHz clocking units [4–6]. A characteristic feature of the devices is sensitivity of the electric signals they generate to magnitude of carrier-envelope phase (CEP) of driving few-cycle laser pulses. CEP scaling is frequently employed for verification and confirmation of the PHz capabilites of the nanodevices. Also, the CEP scaling suggests use of the nanodevices as unique sensors capable of detecting carrier-envelope phase of few-cycle laser pulses [5–8].

In spite of some 19 years of development in the field of laser-driven PHz nanodevices, there is still nearly zero progress in practical implementations of those research results. In this connection, we also review the major challenges in the field including low signla-to-nise ratio, huge back-ground signal, and lack of methods and technologies of device characterization [9].

[1] https://www.quora.com/Why-havent-CPU-clock-speeds-increased-in-the-last-5-years
[2] Chakraborty et al., "A 0.8 THz SiGe HBT Operating at 4.3 K," IEEE Electron Device Lett., 35 (2), 151−153 (2014).
[3] Mattes et al., "Femtosecond Electron Beam Probe of Ultrafast Electronics," Nature Comm. 15, 1743 (2024).
[4] Hommelhoff et al., "Field Emission Tip as a Nanometer Source of Free Electron Femtosecond Pulses," Phys. Rev. Lett. 96, 077401 (2006).
[5] Rybka et al., "Sub-cycle Optical Phase Control of Nanotunnelling in the Single-Electron Regime," Nature Photonics 10, 667–670 (2016).
[6] Zhou et al. "Ultrafast Electron Tunneling Devices – From Electric-Field Driven to Optical-Field Driven," Adv. Mater. 33, 21001449 (2021).
[7] A. Schiffrin, T. Paasch-Colberg, N. Karpowicz, V. Apalkov, et. al., "Optical-field-induced current in dielectrics" Nature, 493, 70–74 (2013).
[8] T. Paasch-Colberg, A. Schiffrin, N. Karpowicz, S. Kruchinin, et al., "Solid-state light-phase detector", Nature Photonics, 8, 214–218 (2014).
[9] L. A. Emmert, et al, "Characterization of Optoelectronic Response of Metal-Semiconductor-Metal Structures by Ultrafast Photocurrent Imaging", in Frontiers in Optics + Laser Science 2023 (FiO/LS), Technical Digest Series (Optica Publishing Group), paper JTu4A.40 (2023).

Combined photonics – hypersonic device based on thin structured nickel films

N. Inogamov[1–3]

1- Landau Institute for Theoretical Physics, RAS, Prosp. Akademika Semenova 1A, Chernogolovka, 142432 Russia
2- Dukhov All-Russia Research Institute of Automatics, Sushchevskaya 22, Moscow, 127055 Russia
3- Joint Institute for High Temperatures, RAS, Izhorskaya 13, Moscow, 125412 Russia

e-mail: nailinogamov@gmail.com

Structured optically thick films are considered for applications in telecommunications and nanosensing. Thanks to structure, these films transmit light [1, 2] thus acting as a photonic device. At the same time, the film remains an effective transducer of terahertz sound generators in the film and substrate [1]. Thus our device combines the properties of photonic and optoacoustic devices. The films are created by magnetron sputtering inside few Pa Argon atmosphere.

Sub-picosecond optical laser processing of metals is actively utilized for modification of a heated surface layer. But for deeper modification of different materials a laser in the hard x-ray range is required. Here, we demonstrate that a single 9-keV x-ray pulse from a free-electron laser can form a μm-diameter cylindrical cavity with length of ~1 mm in LiF surrounded by shock-transformed material [3]. The plasma-generated shock wave with TPa-level pressure results in damage, melting and polymorphic transformations of any material, including transparent and non-transparent to conventional optical lasers. Moreover, cylindrical shocks can be utilized to obtain a considerable amount of exotic high-pressure polymorphs. Pressure wave propagation in LiF, radial material flow, formation of cracks and voids are analyzed via continuum and atomistic simulations revealing a sequence of processes leading to the final structure with the long cavity. Similar results can be produced with semiconductors and ceramics, which opens a new pathway for development of laser material processing with hard x-ray pulses.

[1] Y. Petrov et al., Anomalous Light Transmission by Optically Thick Nickel Films Acting as Optoacoustic Transducers, ZhTEF, vol. 167, pp. 645–671, (2025). In Russian
[2] A. Dyshlyuk et al., Optical properties of the substrate-buried spherical dipole nanoantenna, Bulletin of the Russian Academy of Sciences: Physics, vol. 88(3), pp. S450–S456, (2024).
[3] S. Makarov et al., Formation of high-aspect-ratio nanocavity in LiF crystal using a femtosecond of x-ray FEL pulse, 2024 arXiv:2409.03625 [physics.plasm-ph].

Stimulated Raman scattering amplification under randomly distributed feedback

M. A. Karpov, A. D. Kudryavtseva, T. V. Mironova, M. A. Shevchenko, N. V. Tcherniega, S. F. Umanskaya

P. N. Lebedev Physical Institute of the Russian Academy of Sciences, Leninsky Prospekt, 53, Moscow, 119991 Russia

e-mail: akudr@lebedev.ru

We observe that ultrasound applied to water leads to a substantial enhancement of the Stimulated Raman scattering (SRS) intensity in both forward and backward directions. SRS energy returns to the initial level after the ultrasound is stopped. Quantitatively, the first Stokes component of SRS increases by approximately 4 and 2.5–3 times in the forward and backward directions, respectively, while the second Stokes component exhibits a 5-6-fold increase. This striking SRS enhancement is accompanied by a simultaneous decrease in the elastic scattering intensity, which suggests an energy redistribution between scattering mechanisms. In order to investigate the impact of ultrasound on SRS, the cells with the Raman-active liquids were placed into the ultrasonic bath with ultrasound frequency of 40 kHz and maximum ultrasound power of 200 W. Ultrasound waves were distributed randomly in the bath and created randomly distributed inhomogeneities in the liquids. Nd:YAG laser pulses at the wavelengths of 1064 nm (first harmonic) and of 532 nm (second harmonic) with the pulse duration of 30 ps and the frequency of 10 Hz were used. The peak pulse energy varied from 2 to 20 mJ. The laser beam was focused into a cell filled with liquid using a lens with a focal length of 11 cm. The beam diameter in the caustic waist was about 20 μm. We registered SRS both in the direction of the incoming laser beam (forward) and in the opposite (backward) direction. The experiments show that switching on ultrasound leads to a sharp rise of the SRS energy. The SRS energy jump in water exposed to ultrasound is shown in Fig. 1.

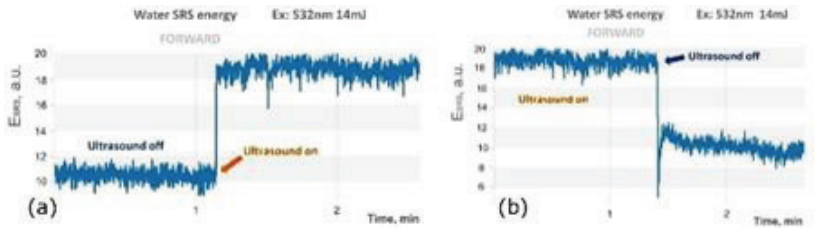

Fig. 1. Change in the SRS energy in water in the forward direction after switching ultrasound on (a) and off (b). The pump pulse energy was set at 14 mJ.

The effect is observed only at picosecond laser pumping: no increase is observed when nanosecond laser pulses are used. This points out to randomly distributed feedback caused by acoustic impact as an underlying physical mechanism [1]. Ultrasound generates a variety of dynamic processes in liquids, including sonoluminescence, cavitation (formation and violent collapse of microbubbles), shock wave propagation, and acoustic flow with associated eddy currents [2–5]. These phenomena create transient light reflecting phase inhomogeneities in liquids that propagate at the speed of sound. The mechanism certainly requires further careful and detailed study.

[1] V.N. Lugovoi. Raman laser with lumped feedback, JETP Letters, vol. 20 (9), pp. 625–627, (1974).
[2] M.A. Margulis, Sonochemistry and Cavitation. London: Gordon & Breach, 1996. 543 p.
[3] O.V. Abramov, High-intensity Ultrasonics: Theory and Industrial. Amsterdam: OPA, 1998. 692 p.
[4] M. Ashokkumar, The characterization of acoustic cavitation bubbles– An overview, Ultrasonics Sonochemistry, vol. 18 (20), pp. 864–872, (2011).
[5] A. Brotchie, F. Grieser, and M. Ashokkumar, Effect of Power and Frequency on Bubble-Size Distributions in Acoustic Cavitation, PRL, vol. 102, 084302, (2009).

Laser-assisted surface engineering by LIPSS for optoelectronic and photonic applications

A. Kuchmizhak[1,2]

1- Institute of Automation and Control Processes, Far Eastern Branch, Russian Academy of Science, Radio str. 5, Vladivostok, 690041 Russia
2- Far Eastern Federal University, Vladivostok, 690091 Russia

e-mail: alex.iacp.dvo@mail.ru

Pulsed laser irradiation of the material interfaces can drive self-organization phenomena yielding in periodically modulated energy deposition and formation of ripple-like surface morphologies also referred to as laser-induced induced periodic surface structures (LIPSS). LIPSS have appeared to be a universal phenomenon allowing to directly imprint nanoscale patterns over the surface of practically any type of material with a characteristic feature size reaching deep subwavelength scales. Such self-organization phenomena driven by short laser pulses can be created using distinctly large focal spots as compared to the created surface feature size justifying practical attractiveness of such technologies for diverse applications. Modulation of optical properties through laser imprinting of LIPSS representing naturally anisotropic grating-like morphologies is of particular interest. This report highlights our recent effort related to LIPSS formation over the surfaces of diverse materials including monocrystalline silicon, several types of promising nonlinear crystals, thin films of titanium and thermochromic vanadium dioxide (Fig. 1). We will discuss the origin of LIPSS formation as well as demonstrate applications of such grating-type morphologies for modulation of the optical properties of mentioned materials with the application area in structural coloration [1], anti-reflection [2], filtering [3] and optoelectronics [4].

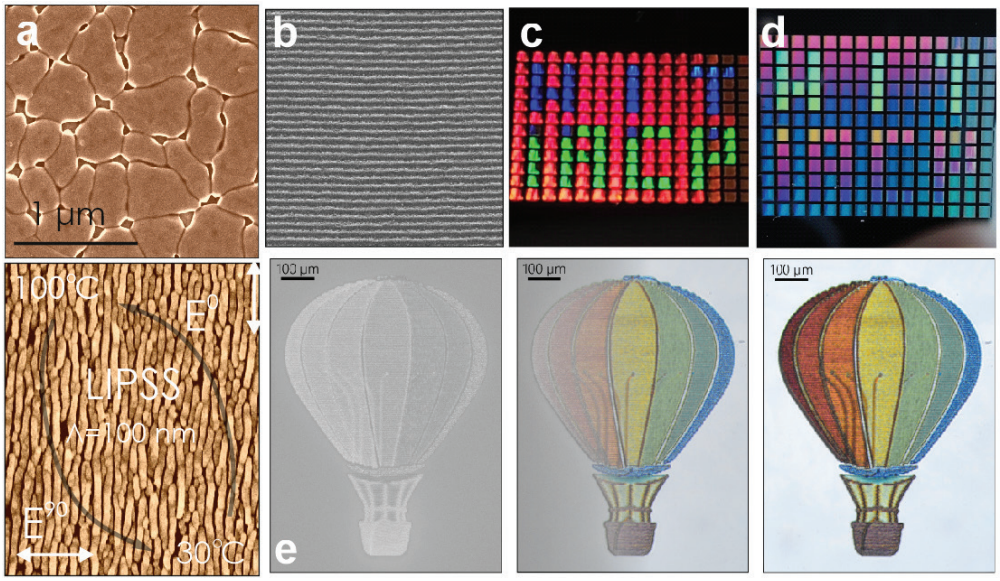

Fig. 1. (a) SEM image of the pristine VO_2 film surface before and after LIPSS patterning. (b) SEM image of the typical LIPSS with a period around 650 nm on stainless steel surface as well as (c, d) optical photographs of the LIPSS-patterned squares under collimated (c) and ambient (d) light visualization. The color modulation in different squares was achieved by controllably varying the LIPSS periodicity. (e) Correlated SEM and optical images of the Ti-TiO_2-Ti sandwich structure laser-patterned at different regimes to cause different surface nano-morphologies and surface color modulation.

[1] V. Lapidas, et.al., Structural Coloration on Titanium Films by Direct Femtosecond Laser Patterning Empowered by Neural Networks, ACS Applied Materials & Interfaces 17, 16122–16131 (2025).
[2] D.V. Pavlov, et.al. Anisotropic Vanadium Dioxide Nanogratings by Direct Laser-Induced Periodic Surface Structuring (LIPSS), The Journal of Physical Chemistry Letters 16, 4969–4974 (2025).
[3] Y. Borodaenko, et.al. Liquid-Assisted Laser Nanotexturing of Silicon: Onset of Hydrodynamic Processes Regulated by Laser-Induced Periodic Surface Structures. Advanced Materials Technologies 9 (8), 2301567 (2025).
[4] Y. Borodaenko, et.al. Polarized p-n junction Si photodetector enabled by direct laser-induced periodic surface structuring, Surfaces and Interfaces 56, 105568 (2025).

Laser-induced diagnostics and photodynamic therapy in oncology and inflammatory diseases

V. Loschenov[1,2], K. Efendiev[1], T. Savelieva[1,2]

1- Prokhorov General Physics Institute of the Russian Academy of Sciences, Vavilov 38, Moscow, 119991 Russia,
2- National Research Nuclear University MEPhI, Moscow, Russia

e-mail: loschenov@mail.ru

Cancer treatment with photodynamic therapy (PDT), in addition to direct damage to tumor cells or the tumor vascular system, allows for the impact on tumor-associated macrophages (TAM). The advantage of PDT is the ability to selectively destroy both resident and monocytic M2-like TAM due to their selective accumulation of photosensitizer and oxygen. A promising approach in the treatment of various tumor types is the ability to change the polarization of TAM to a proinflammatory M1-like phenotype upon exposure to light. Thus, PDT allows for the regulation of the body's immune response by stimulating or suppressing individual components of immunity. However, the conditions for triggering these processes depend on the optimal energy parameters of laser irradiation, the determination of which is a complex task due to dynamic changes in the blood flow and in the intra-tissue distribution of the photosensitizer, which requires intraoperative monitoring of the PDT process using fluorescence diagnostics. Due to the peculiarities of infiltrative growth of pathological tissues and their vascular system, it is also important to determine the exact boundaries of the tumor for further effective treatment. The presence of residual tumor areas after their surgical removal often leads to a high frequency of postoperative relapses. Fluorescence diagnostic methods allow for high-precision visualization of tumor tissues both in the "tumor bed" and in border areas, which can then be treated using PDT or surgical methods.

PDT methods have been significantly developed for the treatment of antibiotic-resistant wounds using photosensitizers in emulsion form. A positive effect is also exerted on aseptic inflammatory processes (osteoarthritis).

We have developed laser fiber-optic systems that allow simultaneous monitoring of fluorescent images and exposure to intense laser radiation. Clinical studies are being conducted jointly with a number of clinics (brain, cervix, bladder, peritoneum, liver, stomach, head and neck organs).

The study was funded by a state assignment for fundamental scientific research for state academies of sciences "Physical methods in medicine, agriculture and ecology" ("Life"), FFWF-2023-0005.

Optical phenomena with micrometer dielectric spheres

B. S. Luk'yanchuk

Lomonosov Moscow State University

e-mail: lukyanchukbs@my.msu.ru

In optical microscopy, two problems related to the magnification and resolution of optical images have historically emerged. The problem of magnification was basically solved in the works of Hooke and Leeuwenhoek. Hooke proposed using small spherical lenses formed by melting the end of a thin glass thread for microscopy. Leeuwenhoek improved this technique and created a microscope with 500x magnification using millimeter-sized lenses. In 1677, Leeuwenhoek gave the first description of unicellular bacteria in his letter to the Royal Academy, the size of which varied from 5 to 30 microns. Two hundred years later, Ernst Abbe formulated the diffraction limit criterion, which is actually due to the Heisenberg uncertainty principle for the momentum and coordinates of a photon. Overcoming the diffraction limit is one of the pressing problems in optics. There are about ten known methods for solving this problem: big-field optical microscopy, plasmonics, superoscillations, fluorescence microscopy, etc. [1–7]. I discuss a number of new optical phenomena with micrometer dielectric spheres.

[1] V. N. Astratov et al, Roadmap on Label-Free Super-Resolution Imaging, Laser Photonics Rev. 17(12), 2370055, (2023), doi: 10.1002/lpor.202200029.
[2] Z. B. Wang et al, Optical virtual imaging at 50 nm lateral resolution with a white light nanoscope, Nature Communications 2, 218 (2011), doi: 10.1038/ncomms1211 (2011).
[3] S. Lee, L. Li, Y. Ben-Aryeh, et al., Overcoming the diffraction limit induced by microsphere optical nanoscopy, J. Opt. 15(12), 125710 (2013).
[4] Y. Duan, G. Barbastathis, B. Zhang, Classical imaging theory of a microlens with super-resolution, Opt. Lett. 38(16), 2988–2990 (2013).
[5] A. Bekirov, B. Luk'yanchuk, and A. Fedyanin, Virtual image within a transparent dielectric sphere, JETP Lett. 112(6), 341–345 (2020).
[6] A. R. Bekirov, Z. B. Wang, B. S. Luk'yanchuk, and A. A. Fedyanin, Dielectric microparticles for enhanced optical imaging: an FDTD analysis of contrast and resolution, J. Opt. Soc. America A 42 (1), 45–50 (2024).
[7] C. Simovski, A. Linear, Direct Far-Field Subwavelength Imaging Method: Microparticle-Assisted Nanoscopy, Photonics 11(11), 1005 (2024).

Comparative analysis of the results of continuum and atomistic modeling of laser fragmentation of metal

V. I. Mazhukin, A. V. Shapranov, O. N. Koroleva, M. M. Demin, A. V. Mazhukin

Keldysh Institute of Applied Mathematics, Moscow, Russia

e-mail: koroleva.on@mail.ru

A mathematical model describing the ruptures of a homogeneous molten metal (Al) has been developed and applied for continuous modeling. The quality of the obtained results of continuous modeling is determined by their verification by the results of molecular dynamics (MD) modeling under completely identical conditions.

The laser action on the target was carried out by an ultrashort pulse with a Gaussian profile, a duration of 100 fs, a fluence of 0.3 J/cm^2 and an intensity of 3×10^{12} W/cm^2 on an Al film with a thickness of 200 nm. The surface reflection coefficient was assumed to be equal to 0.78.

The electron temperature on the surface reaches 2.2×10^4 K in a short time, while the crystal lattice remains relatively cold. During the electron-ion energy exchange, the crystal lattice heats up to temperatures exceeding the equilibrium melting temperature T_m by 1.2–1.4 times. As a result, the volumetric melting mechanism is triggered, causing the formation of a homogeneous liquid with a density close to the initial density of the solid phase in a 50 nm thick surface layer. The maximum pressure in the liquid reaches 15 GPa. The pressure wave begins to propagate deep into the target, forming a shock wave. Following the outgoing shock wave, the unloading stage begins in the liquid: during thermal expansion of the liquid, its density drops, and the pressure becomes negative.

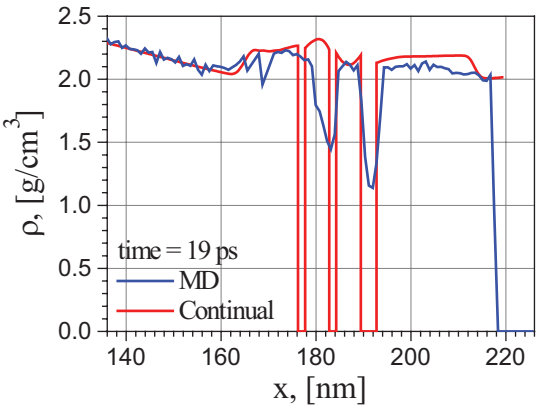

Fig. 1. Comparison of ruptures of the metal melt at a time of 19 ps.

Figure 1 shows the moment of time t ~19 ps, when the first discontinuities were formed. Comparison with the MD calculation demonstrates good agreement between the sizes and positions of the first two separating fragments of liquid. The third discontinuity from the right in the continuum model is located next to a wide density gap in the MD simulation. This is explained by the fact that the continuum model is deterministic in nature, while fluctuations play a large role in the formation of discontinuities in the MD process. In addition, the discontinuities in the continuum model are of zero thickness, while in the results of MD simulation the width of the fronts is determined by the viscosity in the atomic system of the liquid.

Insights of ultrafast carrier dynamics of light-harvesting nanomaterials

A. Patra

School of Materials Sciences, Indian Association for the Cultivation of Science, Jadavpur, Kolkata-700032, India

e-mail: amitavapatra.patra@gmail.com, msap@iacs.res.in

Nanomaterials-based light-harvesting systems have been the research subject because they can generate exciton after photoexcitation. A deep understanding of hot carrier (HC) dynamics is crucial to improving the performance of optoelectronic devices by reducing thermalization losses. Here, we investigate the carrier dynamics, energy transfer, and charge carrier dynamics of 2D CdSe nanoplatelets and perovskite nanocrystals [1–7]. Ultrafast spectroscopic investigations provide direct insight into the impacts of electron and hole transfer at the interface of hybrid materials for optoelectronic applications. The fundamental knowledge of these photophysical processes is crucial for developing efficient light-harvesting systems.

[1] Simanta Kundu and Amitava Patra, Chem. Rev., 2017, 117, 712−757.
[2] K. Marjit, G. Ghosh, S. Ghosh, S. Sain, A. Ghosh, and A. Patra, J. Phys. Chem. C 2021, 125, 12214−12223.
[3] G. Ghosh, R. K Biswas, K. Marjit, S. Ghosh, A. Ghosh, S. K Pati, and A. Patra, Adv. Optical Mater. 2022, 10, 2200030 (1-12).
[4] K. Marjit, G. Ghosh, R. K Biswas, S. Ghosh, S. K Pati and A. Patra, J. Phys. Chem. Lett. 2022, 13, 5431−5440.
[5] D. Ghosh, K. Marjit, G. Ghosh, S. Ghosh and A. Patra, J. Phys. Chem. C 2022, 126, 14590−14597.
[6] G. Ghosh, K.Marjit, S. Ghosh, and A. Patra, J. Phys. Chem. C 2023, 127, 8670−8679.
[7] A. Das, K. Marjit, S. Ghosh, D. Ghosh and A. Patra, J. Phys. Chem. C 2023, 127, 15385−15394.

Laser-induced structural dynamics and non-stationary processes in matter studied by X-ray optical methods

F. V. Potemkin[1,2], E. I. Mareev[1,2], A. G. Kulikov, Yu. V. Pisarevsky[2], A. E. Blagov[1], M. V. Kovalchuk[1]

1- National Research Center NRC Kurchatov Institute, Moscow, 123182 Russia
2- Faculty of Physics Lomonosov Moscow State University, Moscow, 119991 Russia

e-mail: potemkin@physics.msu.ru

The study of structural transformations in matter on natural spatial and temporal scales is the basis for the creation of nature-like technologies and the development of modern approaches in materials science, the creation of new materials with specified properties [1]. Pulsed laser radiation has the necessary characteristics for ultrafast excitation and diagnostics of matter, providing the opportunity to implement the conditions of reversible and irreversible structural rearrangement of matter due to flexibly changeable parameters in the experiment (duration, focusing conditions, energy density, intensity). The use of X-ray pulsed radiation provides access to direct observation of these processes in dynamics. The combination of these two channels, optical and X-ray, in the laser synchrotron center of the National Research Center Kurchatov Institute gave a completely new quality of pump-probe experiments with the ability to observe non-stationary processes in matter on an ultra-wide time interval from femtoseconds (characteristic times of ultra-fast movement of atoms) to microseconds (characteristic times of thermal diffusion processes).

In this work, measurements were carried out in the optical pumping – X-ray probing scheme. Laser radiation was synchronized with the period of electron bunches in the synchrotron ring storage ring. Silicon and lithium niobate were chosen as objects. As a result, it was possible to demonstrate for the first time that the relaxation of photoinduced excitation of the silicon crystal lattice occurs in three stages (Fig. 1). On a subnanosecond time scale, fast phase transitions to the b-Sn phase occur along the entire shock wave front. After the shock wave has passed, the lattice begins to return to its original state, but due to the melting process of silicon at a high temperature initiated by a laser pulse, the final rearrangement of the silicon crystal lattice after nanosecond laser exposure ends only after ~300 μs. It was found that the achievable temperatures of the silicon crystal lattice (~7000 K) significantly affect the newly formed phases (Si-III, Si-XI, Si-XII) that arise during the propagation of a laser-induced shock wave in the bulk of the material on a microsecond time scale [3].

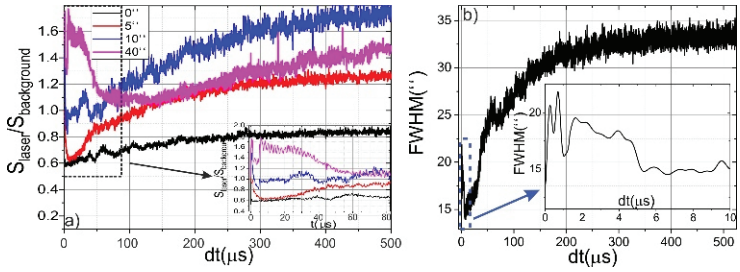

Fig. 1. a) Dynamics of changes in the DRC signal at different angles and b) dynamics of changes in the DRC width of silicon under intense nanosecond laser pulse excitation of silicon.

For lithium niobate crystals, an unusual time-delayed response of X-ray diffraction characteristics to optical excitation was recorded for the first time. The response of the crystals to the optical action consisted of a reversible change in the parameters of the diffraction reflection curve (DRC) – a shift in the position of the peak and a decrease in the integral intensity, observed for ~35 nanoseconds after the pulse action. The dynamics of the amplitude of deformations of the crystal lattice indicates the process of formation and subsequent disintegration of the double electric layer due to the directed migration of photoelectrons due to the bulk photovoltaic effect (BPE) [4, 5]. Registration of the DRC in other reflections (006, 0012 and 0018) made it possible to observe the dynamics of the piezophotovoltaic effect not only with temporal but also with spatial resolution (Fig. 2).

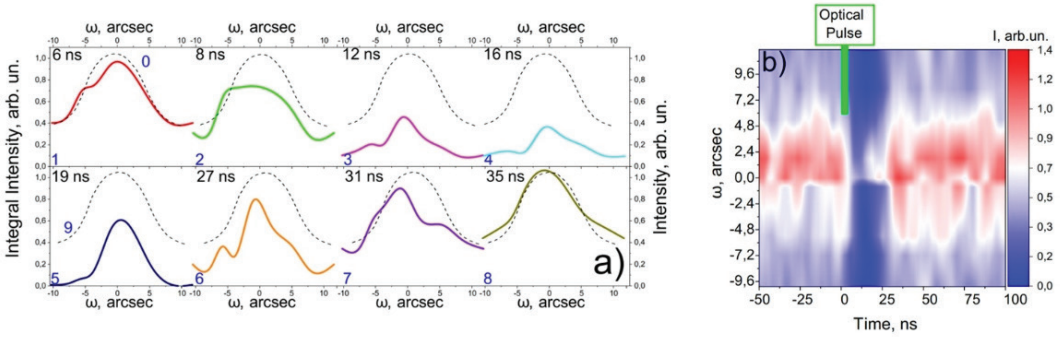

Fig. 2. a), b) Dynamics of changes in the DRC when lithium niobate doped with iron is exposed to an intense nanosecond laser pulse.

This work was supported by Russian Science Foundation (X-ray diagnostics – Project № 23-73-00039, optical diagnostics – Project № 25-22-00084).

[1] Ковальчук М.В. // Вестник РАН, 2019, Т. 89, С. 455–465
[2] Potemkin F. V. et al. // Rev. Sci. Instrum. AIP Publishing. 2021. Vol. 92, P. 053101
[3] Kovalchuk M. V. et al. // Crystallogr. Reports. 2022. Vol. 67. P. 717–728.
[4] Kovalchuk M.V. et al. // Crystallogr. Reports. - 2024. - Vol. 69. P. 221–229.
[5] F. S. Pilyak et al. // Phys. Rev. B – 2024. – Vol. 110, L100302

Laser-pumped hybrid nanoheaters with precise temperature measurement by luminescence thermometry

A. Povolotskiy[1], E. Chebanova[1], A. Del Carpio Rocha[1], D. Soldatova[2], D. Lukyanov[1], A. Konev[1]

1- St. Petersburg State University, St. Petersburg, Peterhof, Ulianovskaya str. 5, 198504 Russia
2- Peter the Great St. Petersburg Polytechnic University, St. Petersburg, 195251 Russia

e-mail: alexey.povolotskiy@spbu.ru

This research project aims to develop hybrid molecular-plasmonic nanostructures for precision-controlled optical heating in photomedicine, particularly for non-invasive photothermal therapy. Metal nanoparticles are used for cell hyperthermia, but the current approach to temperature measurement in therapy does not control the temperature of the nanoparticles themselves. This leads to significant overheating of the surrounding cells and tissue necrosis. This is because medical professionals currently lack the ability to measure the temperature of the nanoparticles themselves, only the average tissue temperature. Unlike modern nanoparticles used in photothermal therapy, the use of the developed nanoparticles will enable us to completely eliminate the necrotic mechanism of cell destruction. This will enable a qualitative leap in photomedicine. Furthermore, we can expect to gain new fundamental knowledge and practical results on improving photothermal therapy methods with the help of fundamentally new tools based on hybrid nanostructures.

The hybrid nanoparticles under development are based on plasmonic spherical cores made of silver, gold, copper or their alloys. In this study, we used the laser ablation in water method to obtain nanoparticles, which has a number of advantages over chemical synthesis methods [1]. The most significant of these are the ability to form nanoparticles from metal alloys with a specific elemental ratio and the high chemical purity of the resulting colloidal nanoparticle solutions. The absence of by-products characteristic of wet chemistry methods ensures chemical purity.

Hybrid nanostructures were formed based on gold, silver and copper nanoparticles, as well as their alloys, with a polymer or dielectric shell, and porphyrins or porphyrin dyads [2, 3]. The functional properties of porphyrins and porphyrin dyads for luminescence thermometry, which is based on a ratiometric approach, were investigated. In this approach, the temperature-sensitive parameter is the ratio of the fluorescence band intensities of one porphyrin, different independent porphyrins, or different porphyrins included in the molecular dyad. A model of luminescent thermometers using two types of emitting centres in a pair of porphyrins has been proposed. The influence of temperature on the fluorescence spectra of porphyrin dyads and porphyrins within hybrid nanostructures was investigated and calibration curves were obtained. The thermometric characteristics, such as relative thermal sensitivity and temperature resolution, were determined.

The proposed model structure of a hybrid molecular nanostructure allows luminophore molecules to be encapsulated inside a silicon dioxide shell. It has been demonstrated that this process increases the luminescence intensity of porphyrins. This is due to the organic phosphors being shielded from water molecules, which act as fluorescence quenchers. Furthermore, the creation of a 1.5 nm buffer layer between the metal core and the organic phosphor was found to enhance fluorescence by a factor of 16 compared to hybrid nanostructures in which the porphyrin is located directly on the metal core's surface [4]. This fluorescence enhancement is attributed to an increase in the extinction coefficient caused by plasmonic absorption.

[1] A.V. Povolotskiy, O.S. Smirnova, D.A. Soldatova, D.A. Lukyanov, A.V. Povolotckaia, High-Precision Optical Excited Heaters Based on Au Nanoparticles and Water-Soluble Porphyrin, Metals, vol. 13(11), 1851, (2023).
[2] A.V. Povolotskiy, O.S. Smirnova, D.A. Soldatova, D.A. Lukyanov, Fluorescent Ratiometric Thermometers Based on Dyads of Tetraphenylporphyrin and Zinc Metalated Tetraphenylporphyrin, Bulletin of the Russian Academy of Sciences Physics, vol. 87(11), pp. 1691–1696, (2023).
[3] D.A. Soldatova, E.S. Chebanova, A. Del Carpio Rocha, A.S. Konev, I.A. Sokolov, A.V. Povolotskiy, The Role of SiO_2 Shell in the Formation of Hybrid Molecular Plasmonic Core–Shell Nanoparticles, Glass Physics and Chemistry, vol. 50(5), pp. 546–552, (2024).
[4] A.V. Povolotskiy, D.A. Soldatova, A.A. Smirnov, A.V. Povolotckaia, D.A. Lukyanov, A.S. Konev, E.V. Solovyeva, Photophysical Properties of Hybrid Nanoparticles Based on Water-Soluble Porphyrin, Gold Core, and Polymer Shell, Russian Journal of General Chemistry, vol. 94(11), pp. 3023–3032, (2024).

Active components of flat optics based on high-index and anisotropic dielectric metastructures

A. V. Prokhorov[1,2]

1- Center for Photonics and 2D Materials, Moscow Institute of Physics and Technology, Institutskiy per. 9, Dolgoprudny, 141701 Russia
2- Department of Physics and Applied Mathematics, Vladimir State University named after A. G. and N. G. Stoletovs, Gorkogo str. 87, Vladimir, 600000 Russia

e-mail: alprokhorov33@gmail.com

In this work, we discuss the fundamental principles for the design of optical metasurfaces to control the amplitude-phase characteristics of light in a wide spectral range. General approaches for numerical simulation, design and fabrication of optical metasurfaces, as well as their functionalization for the observation of optical phenomena on their basis, are considered. The control of the near-field response of individual nanoresonators, i.e., the metasurface's building blocks, is based on the effects of optical (bi)- and anisotropy caused, among other reasons, by breaking the C2–C4 rotational symmetry [1] or by a new type of surrounding medium symmetry breaking [2]. Both the conventional Si and new class of optical materials such as strongly anisotropic layered van der Waals (vdW) materials are considered as materials for the fabrication. The basis for localization and strong concentration of near-field energy, accompanying the appearance of high-Q spectral features, is the excitation of so-called quasi-trapped modes (QTMs) in the plane of metasurfaces. The practical results are the development of a polarizing metamirror [3], see Fig. 1a, and metasurface-(energy concentrator) based on QTMs [4], see Fig. 1b. The firstly-discovered fundamental effect of high order multipole coupling (HOC) [2] allowed the excitation of QTM without symmetry breaking in metasurfaces based on transition metal dichalcogenides, see Fig. 1c. The design of HOC-supporting MoS_2 metasurface was the basis for the first experimental demonstration of this remarkable effect [5], see Fig. 1d. The preliminary simulation allowed us to precisely tune the QTM resonance in Si metasurface to the photoluminescence peak in thin $MoTe_2$ flake, which caused the laser generation and became the prototype for vdW-metalaser [6], see Fig. 1e. Finally, our look into the future is aimed on the realization of active elements of flat optics using both optomechanical effects [7], see Fig. 1f, and many other novel phenomena of modern nanophotonics.

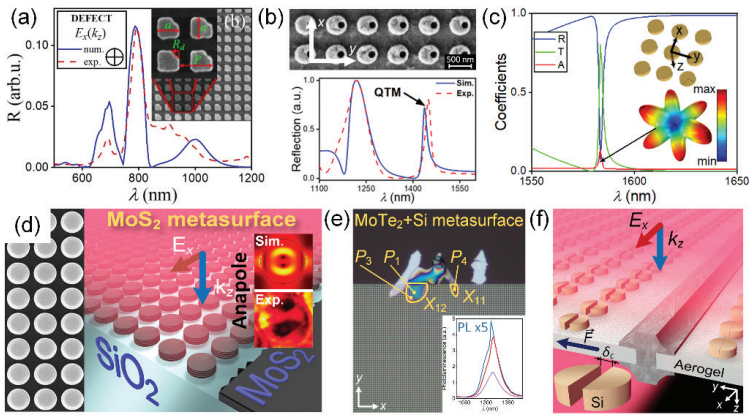

Fig. 1. Metasurface-assisted near-field and far-field light manipulation.

This work was supported by the Russian Science Foundation (Grants No. 25-12-00154, 24-12-20015).

[1] A. Evlyukhin et al., Laser Photonics Rev., 15, 2100206 (2021).
[2] A. Prokhorov et al., ACS Photonics, 9, 3869–3875 (2022).
[3] A. Prokhorov et al., ACS Appl. Nano Mater., 5, 14582−14590 (2022).
[4] A. Prokhorov et al., ACS Photonics, 10, 1110−1118 (2023).
[5] A. Prokhorov et al., Laser Photonics Rev., 19, 2401666 (2025).
[6] A. Prokhorov et al., Appl. Phys. Lett., 125, 041702 (2024).
[7] A. Prokhorov et al., ACS Appl. Nano Mater., 8, 2319–2327 (2025).

Laser hyperdoping of silicon with transition metals: specifics of using fs- and ns- pulses

V. Pryakhina[1], P. Paletskikh[1], D. Tkachuk[1], A. Akhmatkhanov[1], S. Kudryashov[1,2]

1- Ural Federal University, Yekaterinburg, Russia
2- Lebedev Physical Institute, Moscow, Russia

e-mail: viktoria.pryahina@urfu.ru

In silicon-based optoelectronics, expanding silicon's photosensitivity into the infrared spectrum is crucial to avoid expensive hybrid integration methods. A promising solution involves hyperdoping: introducing impurities at concentrations exceeding their solubility limits in silicon. This results in either shallow or deep-level defects that allow sub-bandgap photon absorption. While transition metals show promise as dopants for enhancing Si-based near-infrared photodetector performance [1], further investigation is required to overcome challenges related to their incorporation through pulsed laser melting.

Pulsed laser melting enables hyperdoping with pulse durations from femtoseconds to nanoseconds. Longer pulses yield deeper molten layers, whereas shorter ones facilitate rapid recrystallization. Pulse length, along with power density, beam focus, etc., substantially affect dopant distribution. Laser-induced hyperdoping combined with annealing improves crystalline structure without losing dopants. Optimizing these parameters results in adjustable dopant profiles, layer thicknesses, and improved impurity absorption [2–4], making silicon suitable for various applications.

We studied the hyperdoping of silicon with selected transition metals (Ti, Cr, Zn, Ag, Au) using fs- and ns- laser pulses. We used Si (100) substrates (either nominally undoped or doped as p- or n-type) with pre-deposited metal film varying in thickness from 5 to 100 nm. The sample surface was irradiated with either 100-ns laser pulses at 1064-nm wavelength (Yb pulsed fiber laser within MiniMarker2-M20 laser marking system, equipped with galvanoscanner) or with 240-fs laser pulsed at 1030-nm wavelength (TETA-10, Avesta Project, combined with motorized tables).

To investigate the elemental composition and chemical state within the hyperdoped silicon surface layer, we employed cross-sectional X-ray photoelectron spectroscopy (XPS) along with scanning electron microscopy (SEM). Changes in surface morphology were examined via SEM imaging, while confocal Raman microspectroscopy was used to evaluate modifications in crystalline structure. Visible-near infrared (vis-NIR) optical and photoresponse measurements provided insights into light absorption properties.

The laser-hyperdoped Si samples, after removing residual metal, have shown reduced transmittance in the intra-gap spectral region (> 1.1 μm) which indicates impurity absorption effects. We optimized laser-processing parameters and metal-film thicknesses to determine appropriate fluence levels for incorporating impurities into silicon. Thickness variations had a significant impact on doping efficiency and should be carefully selected during process design. Enhanced doping efficiency was confirmed through measurements showing increased near-infrared photoresponse.

The research funding from the Ministry of Science and Higher Education of the Russian Federation (Ural Federal University Program of Development within the Priority-2030 Program) is gratefully acknowledged. The equipment of the Ural Center for Share Used «Modern Nanotechnologies» Ural Federal University was used.

[1] S.Q. Lim and J.S. Williams, Electrical and optical doping of silicon by pulsed-laser melting, Micro, vol. 2, pp. 1–22, (2022).
[2] V. Pryakhina, et al. Spatial confinement in laser-induced gold-hyperdoping of Si wafers, Opt. Laser Technol., vol. 188, p. 112945, (2025).
[3] M. Kovalev, et al. Au-hyperdoped Si nanolayer: Laser processing techniques and corresponding material properties, Materials, vol. 16, p. 4439, (2023).
[4] S. Kudryashov, et al. Double gold/nitrogen nanosecond-laser-doping of gold-coated silicon wafer surfaces in liquid nitrogen, Technologies, vol. 12, p. 224, (2024).

Laser modification of a metal surfaces to improve their chemical and biological stability

G. Romanova, V. Veiko

ITMO University, Birzhevaya liniya 14-16, St. Petersburg, 199034 Russia

e-mail: gvromanova@itmo.ru

Corrosion and surface contamination, including mineral and biological fouling, are serious problems in many industries, causing damage to materials, equipment and infrastructure. These processes not only impair the aesthetic and functional properties of materials but also increase the risk of critical failures. This highlights the need for advanced methods protection methods.

Existing methods of post-processing (mechanical and chemical cleaning from contaminants) and preventive actions (anti-corrosion coatings, alloy building) are multi-stage and require consumables. In this context, laser treatment emerges as a promising alternative due to its non-impacted, lack of consumables, and ability to target influence local areas, creating surfaces with mixed wetting (for example, to remove liquid from the surface of the material).

This study explores the principles and strategies behind developing a laser microstructuring method aimed at enhancing the environmental resistance of steel surfaces. The laser processing was carried out under ambient conditions using a technological setup based on a pulsed ytterbium fiber laser operating at a central wavelength of 1064 nm.

By controlling the geometry, chemical composition and wetting state, it becomes possible to increase the time until the first pitting or biofouling occurs. This effect is attributed to the reduction in contact area between the metal and the liquid environment, the lowered surface energy of the substrate, and the formation of protective oxide layers. Surface energy reduction can be achieved through as a result of the use of a hydrophobic coating (e.g. stearic acid) or prolonged exposure to air. These findings form the foundation for developing a laser-based metal protection method, resulting in up to a 1.5-fold decrease in surface contamination compared to untreated steel.

Nonlinear optical and photoelectric properties of GaSe thin films

M. A. Samsonov[1], S. R. Saitov[1], A. Hasan[1], D. M. Zhigunov[2], V. N. Mantsevich[1], A. M. Smirnov[1,3]

1- Faculty of Physics, Lomonosov Moscow State University, Leninskie Gory 1-2, Moscow, 119991 Russia
2- Skolkovo Institute of Science and Technology, Bolshoy Boulevard, 30, bld. 1, Moscow, 121205 Russia
3- Kotelnikov Institute of Radioengineering and Electronics of RAS, Mokhovaya 11-7, Moscow, 125009 Russia

e-mail: alsmir1988@mail.ru

Layered materials with a strong interaction between the atoms within the layers and weak Van der Waals interactions between the layers attract a great attention due to their unique physical properties, which are promising for opto-electronic applications. Weak van der Waals interaction between the layers allows splitting of bulk crystals into two- or quasi-two-dimensional structures, which demonstrate intriguing optical and transport properties. Selenide based A_3B_6 materials are widely used for such devices as single photons sources, field transistors, photodetectors, memristors, gas sensors, light emitting devices and *etc*.

We present the analysis of linear and nonlinear optical properties of gallium selenide (GaSe) films measured by means of pump and probe technique. GaSe films with different thickness were obtained by mechanical exfoliation. The exciton transition bleaching was observed under excitation of 10 ns pulses centered at 360 nm and 540 nm, which was explained by the exciton phase space filling effect. The main mechanisms of recombination of excited charge carriers at room temperature were established and their kinetic properties were studied. Three bands were identified within the measured photoluminescence (PL) spectra of GaSe films. The detuning of the maxima of these PL bands was shown to be stable across different samples, different excitation energies, and different excitation wavelengths (Fig. 1a) [1]. This consistency of relative peak positions indicates their physical nature. We were able to identify the contribution to PL signal from direct excitons, indirect excitons and electron-hole pairs with the participation of optical phonons. The theoretical model was proposed, which allowed to analyze electron, hole and exciton kinetics measured by time-resolved PL.

Also, photoconductivity spectral dependences of GaSe thin film obtained by mechanical exfoliation have been determined (Fig. 1b). The dependences were measured at different excitation powers. The coincidence of the spectra shapes and the difference in the conductivity values indicate that a stable photoresponse was obtained from the GaSe film sample. It is also worth noting the presence of impurity photoconductivity.

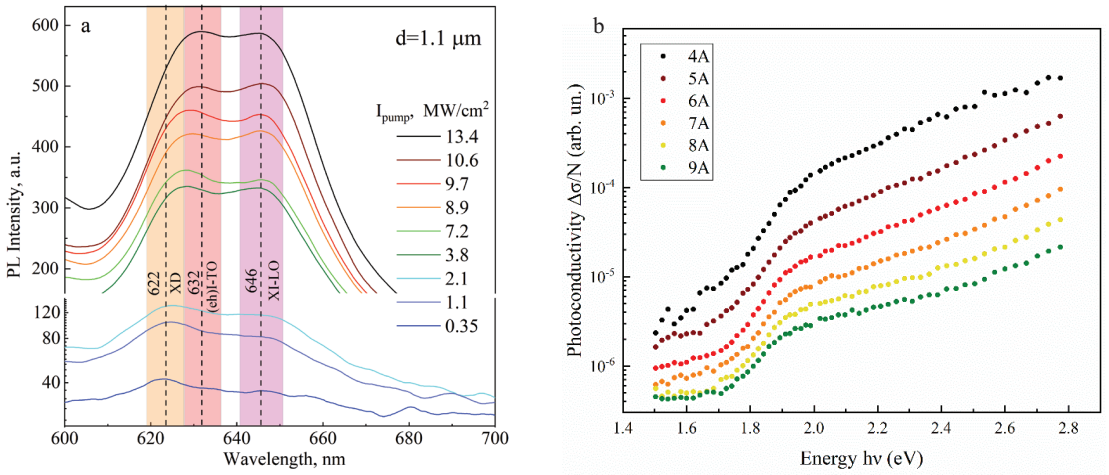

Fig. 1. a) PL spectra at different excitation intensities of the GaSe films with 1.1 μm (XD for direct excitons PL process, XI-LO for indirect excitons PL process with LO-phonons emission, (eh)I-TO for free electron and hole radiative recombination at the indirect transition with emission of the TO-phonon. b) Spectral dependences of GaSe film photoconductivity obtained at different excitation powers, which are given in the values of currents supplied to the light source (halogen lamp).

The research was funded by the Russian Science Foundation grant № 23-72-10008.

[1] M.A. Samsonov, A. Hasan, D.M. Zhigunov, V.N. Mantsevich, A.M. Smirnov, Photoluminescence and nonlinear transmission of GaSe thin films, Journal of Luminescence, 284, 121293 (2025).

Photostability and lasing in mixed-halide perovskite microcrystals

E. Sapozhnikova[1,2], A. Pushkarev[1]

1- Skolkovo Institute of Science and Technology, Bolshoy Boulevard 30, bld. 1, Moscow, 121205, Russia
2- ITMO University, Kronverksky pr. 49, bldg. A, St. Petersburg, 197101 Russia

e-mail: e.sapozhnikova@metalab.ifmo.ru

Over the last decade, metal halide perovskites (MHP) have been intensively studied as promising semiconductor material for advanced photonics and optoelectronics [1]. Perovskite crystals demonstrate outstanding structural and optoelectronic properties, such as low lattice defect concentration, high carrier mobility and high optical absorption coefficient. Moreover, resonant perovskite structures can be synthesized in various forms (wires, platelets, cubes, disks etc.) by cheap and easy solution methods [2]. Such crystals demonstrate outstanding laser generation and high quantum yield of luminescence at room temperature and emission can be tuned in all visible range by substitution of halide (X) in perovskite crystal lattice $CsPbX_3$ (X = Br, Cl, I).

However, the main drawback of MHPs that prevents their commercialization is the limited device stability. Due to the dynamic ionic nature of metal halide perovskites the crystal structure can change in response to electrical current or light irradiation [3].

In this work, perovskite microcrystals $CsPbBr_3$ were synthesized by novel colloidal method at high-temperature in a nitrogen atmosphere and the form of crystals was controlled by precursor concentration. The wavelength was tuned by partial substitution of Br^- in crystal lattice with I^- and Cl^- using YI_3 and YCl_3 dissolved in diphenyl ether. Synthesized structures demonstrated laser emission under UV femtosecond laser excitation. The mixed chloride and pure bromine crystals showed rather high photostability and low lasing threshold compared to mixed-iodide structures.

The work was supported by the Russian Science Foundation (Project No. 24-73-10072, https://rscf.ru/project/24-73-10072/).

[1] Dey, A., Ye, J., De, A., Debroye, E., Ha, S. K., Bladt, E., ... & Polavarapu, L., State of the art and prospects for halide perovskite nanocrystals, ACS nano, 15 (7), 10775–10981, (2021).
[2] Li, J., Han, Z., Gu, Y., Yu, D., Liu, J., Hu, D., ... & Zeng, H., Perovskite single crystals: synthesis, optoelectronic properties, and application, Advanced Functional Materials, 31(11), 2008684, (2021).
[3] Zhu, H., Teale, S., Lintangpradipto, M. N., Mahesh, S., Chen, B., McGehee, M. D., ... & Bakr, O. M., Long-term operating stability in perovskite photovoltaics, Nature Reviews Materials, 8(9), 569–586, (2023).

Method of *in situ* assessment of optical properties of biological tissues for personalized planning of laser-induced therapy

T. Savelieva[1,2], A. Krivetskaya[1,2], D. Kustov[1], V. Loschenov[1,2]

1- Prokhorov General Physics Institute of the Russian Academy of Sciences, Vavilov 38, Moscow, 119991 Russia,
2- National Research Nuclear University MEPhI, Moscow, Russia

e-mail: savelevat@gmail.com

Laser-induced therapy encompasses several types of medical treatments that use laser energy to target and treat diseased tissues, particularly tumors and abnormal growths. The most widely used methods in clinical practice include laser-induced photodynamic therapy (PDT) and laser hyperthermia. The personalized planning in laser-induced therapy integrates patient-specific anatomical data, computational modeling, and real-time imaging feedback to optimize treatment delivery. Advanced computational frameworks use patient-specific data to simulate and predict laser-induced effect zones before treatment. These models optimize laser parameters such as probe location, power, and frequency to match the desired absorbed light profile and treatment goals. The optical properties of tissue (primarily absorption (μ_a) and scattering (μ_s') coefficients) directly influence how light penetrates and distributes within the tissue during laser-induced therapy. Accurate measurement of these properties allows for precise calculation of the energy flow rate required to efficiently activate the photosensitizer during PDT or to achieve the therapeutic temperature threshold during hyperthermia, which determines optimal treatment outcomes. We propose a method for intraoperative determination of optical properties of tissues of the walls of gastrointestinal organs based on measuring both diffusely reflected and diffusely transmitted light. To implement the method, an intraluminal illumination scheme is used with a fiber-optic diffuser placed in a balloon filled with a scattering medium to ensure a uniform scattering indicatrix. Restoration of optical properties is carried out using a two-stage technique. At the first stage, a modified Kubelka-Munk model is used to estimate the initial values of optical properties, and at the second stage, the inverse adding-doubling method is used. Method was validated on the optical phantoms and biological specimens.

This work was funded by the Russian Science Foundation, grant No. 25-25-00516.

Optical method for the study of the pyroelectric phenomena

S. Shandarov[1], K. Mambetova[1], A. Aksenov[1], L. Orlikov[1], N. Burimov[1], K. Melnik[1], E. Savchenkov[1], M. Bryushinin[2], I. Sokolov[2]

1- Tomsk State University of Control Systems and Radioelectronics, Lenin Avenue 40, Tomsk, 634050, Russia
2- Ioffe Institute, Polytechnical Street 26, Saint Petersburg, 194021 Russia

e-mail: stanislavshandarov@gmail.com

Pyroelectric $LiNbO_3$ and $LiTaO_3$ crystals are the base materials for realisation of solid-state devices generating fluxes of charged particles, X-rays and neutrons during the heating/cooling cycles [1–5]. The generation of X-rays and neutrons are observed in the vacuum condition only [1–3], whereas the pyroelectric ion source [4] meant for mass spectrometry operated at atmospheric pressure. The electron pulses generated at a thermocycling of pyroelectric crystals have a sporadic character with weakly studied time parameters. In ref. [5] it was obtained that for assembly with coaxial geometry and for cylindrical lithium niobate sample, in the conditions of atmospheric pressure, the pyroelectrically generated sporadic discharge pulses having current in maximum from 45 mA to 600 mA, duration about 15 ns, and rise time from 1 to 1.9 ns are registered.

We have studied the dynamics of an electric field in case of pyroelectric discharge generation in a cylindrical lithium niobate crystal with parallel faces Z+ and Z− by using the reflection from it's of a laser beam with a wavelength of 532 nm. That crystal represented optical Fabry-Perot cavity having the reflectance, which is determined by its refractive index depending on the electric field strength due to the linear electro-optic effect. All experiments were realized at atmospheric pressure for temperature range of up to 110 ºC by using the accommodation of crystal in the cylindrical copper cup jointly with a grounded semitransparent conductive anode. The heating of this crystal was performed by resistive heater with rate of 10 K/min whereas in the cooling cycle a free decrease of temperature has been used. The time dependences of variation in the intensity of the reflected light beam have been registered by using a pin photodiode BWP34, which was connected via an emitter repeater to the input of digital oscilloscope Keysight DSO-X 3102T (1 GHz). A differentiating link and a transistor amplifier were used to implement a standby scanning mode relating to the beginning of sharp changes in the intensity of the laser beam reflected from the crystal.

At the variations of a temperature, we observed as the slowly changes in the intensity of reflection beam connected with thermo-optic effect and pyroelectric generation of electric field in the crystal as well as the abrupt jumps of such field on the values $\Delta E(t)$. We believe that these abrupt jumps of electric field $\Delta E(t)$ in the lithium niobate crystal caused by the electric discharges between one and a semitransparent anode. The described optical technique for recording the dynamics of the electric field in a lithium niobate crystal with parallel Z-faces in case of pyroelectric generation of electric discharges made it possible to display its time dependences during the interval from ~90 s to ~9 μs.

By using the known relationship for reflection coefficient from Fabry-Perot cavity and for linear electrooptic effect in lithium niobate we have estimated from the mass of experimental data that the magnitudes of the abrupt jumps ΔE may be taken the values from 0.6 kV/cm to 4 kV/cm, demonstrate the behavior characteristic of electric discharges. Also, it has been established that time duration of abrupt jumps not exceed the value of 1 μs.

This study was funded by the Ministry of Science and Higher Education of the Russian Federation in the framework of the state assignment for 2023-2025 (job-order FEWM-2023-0012).

[1] G. Rosenman, D. Shur, Y.F. Krasik, A. Dunaevsky, Electron emission from ferroelectrics, J. Appl. Phys., vol. 88, pp. 6109–6161 (2000).
[2] J.A. Geuther, Y. Danon, Enhanced neutron production from pyroelectric fusion, Appl. Phys. Lett., vol. 90, p.174103 (2007).
[3] M. Ali, P. Karataev, A. Kubankin, A. Oleinik, Stability of electrons and X-rays generated in a pyroelectric accelerator, Nucl. Instr. and Methods in Phys. Research A, vol. 1061, p. 169134 (2024).
[4] E.L. Neidholdt, J.L. Beauchamp, Compact ambient pressure pyroelectric ion source for mass spectrometry, Anal. Chem., vol. 79, pp. 3945–3948 (2007).
[5] K.M. Mambetova, S.M. Shandarov, S.I Arestov, L.N. Orlikov, A.A. Elchaninov, N.I. Burimov, A.I Aksenov, Registration of a pulsed generation of electron beam in the nanosecond range under heating and cooling cycles of a lithium niobate crystal at atmospheric pressure, Journal of Instrumentation, vol. 17, p. 04008 (2022).

Nonlinear photonic crystals based on periodically poled ferroelectrics

V. Shur, A. Akhmatkhanov, M. Chuvakova, B. Lisjikh, M. Kosobokov

School of Natural Sciences and Mathematics, Ural Federal University, Ekaterinburg, 620002 Russia

e-mail: vladimir.shur@urfu.ru

The achievements and recent progress in fabrication of effective nonlinear light frequency converters based on quasi-phase matching effect realized by creation of the stable periodic domain structure with nanoscale reproducibility of micron period will be presented. The second harmonic generation, optical parametric oscillation and spontaneous parametric down conversion for generating of entangled photon pairs have been realized in periodically poled uniaxial lithium niobate and lithium tantalate crystals [1]. The promising abilities of all-optical domain switching at the polar surface and in the crystal bulk by IR pulse laser irradiation for creation of the three-dimensional nonlinear photonic crystals will be demonstrated [2–6].

All obtained achievements are based on complex study of the domain structure evolution in uniaxial ferroelectric crystals by complimentary domain imaging methods with high spatial and temporal resolution by example of MgO doped lithium niobate and lithium tantalate. The methods of domain engineering are based on application of the nonuniform electric field using: (1) periodical stripe electrodes [1], (2) biased tip of scanning probe microscope [7, 8], (3) focused electron and ion beams [9]. The tightly focused irradiation by femtosecond near-IR laser allowed us to realize the domain nucleation in the crystal bulk and subsequent in-bulk domain growth under the action of the pyroelectric field [3–6]. The produced stable tailored domain structures allowed us to realize the out-of-cavity second harmonics generation with record efficiency and mid-infrared optical parametric amplifier (OPA) [10]. It was shown that the fan-out periodical domain structures allowed us to obtain super-wide OPA tuning range from 2.5 to 4.5 μm in one element [10].

The creation of the three-dimensional nonlinear photonic crystals and tailored domain structures in the crystal bulk was demonstrated in the single-domain plates of MgO doped lithium niobate and lithium tantalate as a result of tightly focused irradiation created by femtosecond laser emitting at the 1030 nm wavelength [4–6].

The research was made possible by Russian Science Foundation (Grant No. 24-12-00302). The equipment of the Ural Center for Shared Use "Modern nanotechnology" Ural Federal University (Reg. № 2968) was used.

[1] V.Ya. Shur, A.R. Akhmatkhanov, and I.S. Baturin, Micro- and nano-domain engineering in lithium niobate, Appl. Phys. Rev., vol. 2, p. 040604 (2015).
[2] V.Ya. Shur, M.S. Kosobokov, A.V. Makaev, D.K. Kuznetsov, M.S. Nebogatikov, D.S. Chezganov, E.A. Mingaliev, Dimensionality increase of ferroelectric domain shape by pulse laser irradiation, Acta Materialia, vol. 219, p. 117270 (2021).
[3] S. Kudryashov, A. Rupasov, M. Kosobokov, A. Akhmatkhanov, G. Krasin, P. Danilov, B. Lisjikh, A. Turygin, E. Greshnyakov, M. Kovalev, A. Efimov, V. Shur, Ferroelectric nanodomain engineering in bulk lithium niobate crystals in ultrashort-pulse laser nanopatterning regime, Nanomaterials, vol. 12, p. 4147 (2022).
[4] B. Lisjikh, M. Kosobokov, A. Turygin A. Efimov, V. Shur, Creation of a periodic domain structure in MgOLN by femtosecond laser irradiation, Photonics, vol. 10, p. 1211 (2023).
[5] B.I. Lisjikh, M.S. Kosobokov, A.V. Efimov, D.K. Kuznetsov, V.Ya. Shur, Thermally assisted growth of bulk domains created by femtosecond laser in magnesium doped lithium niobate, Ferroelectrics, vol. 604, pp. 47–52 (2023).
[6] B. Lisjikh, M. Kosobokov, V. Shur, Photonics, The creation of a domain structure by using ultrashort pulse NIR laser irradiation in the bulk of MgO-doped lithium tantalate, vol. 11, p. 928, (2024)
[7] B.N. Slautin, A.P. Turygin, E.D. Greshnyakov, A.R. Akhmatkhanov, H. Zhu, V.Ya. Shur, Domain structure formation by local switching in the ion sliced lithium niobate thin films, Appl. Phys. Lett., vol. 116, p. 152904 (2020).
[8] B.N. Slautin, H. Zhu, V.Ya. Shur, Submicron periodical poling by local switching in the ion sliced lithium niobate thin films with dielectric layer, Ceramics International, vol. 47, pp. 32900–32904 (2021).
[9] D.S. Chezganov, E.O. Vlasov, E.A. Pashnina, M.A. Chuvakova, A.A. Esin, E.D. Greshnyakov, V.Ya. Shur, Domain structure formation by electron beam irradiation in lithium niobate crystals at elevated temperatures, Appl. Phys. Lett., vol. 115, p. 092903 (2019).
[10] E. Erushin, B. Nyushkov, A. Ivanenko, A. Akhmathanov, V. Shur, A. Boyko, N. Kostyukova, D. Kolker, Tunable injection-seeded fan-out-PPLN optical parametric oscillator for high-sensitivity gas detection, Laser Phys. Lett. vol. 18, p. 116201 (2021).

Fabrication of silicon-based nanoheterostructures by laser scanning processing of thin film multilayers

N. Tarasenka[1,2], V. Kornev[1], M. Nedelko, N. Tarasenko[1]

1- B. I. Stepanov Institute of Physics, National Academy of Sciences of Belarus, Nezalezhnasti ave. 68-2, Minsk, 220072 Belarus
2- University of Strathclyde, Glasgow, UK

e-mail n.tarasenko@ifanbel.bas-net.by

In the past decades, direct bandgap materials based on silicon have received great attention because a progress in such fields as opto- and microelectronics, photovoltaics and thermoelectric applications is connected with a use of silicon. But pure silicon material with an indirect bandgap has some disadvantages for effective application in the above-mentioned fields. Particularly, pure silicon possess low absorption coefficient in the solar spectrum, emits light poorly and has a high thermal conductivity that hinders its application in photovoltaic devices and thermoelectric convertors, respectively. Therefore, a special attention is paid to a development of the methods for the fabrication of doped and hybrid silicon structures. In particular, the use of group IV elements for doping and formation of binary or ternary alloys (GeSn [1], SiSn [2], SiGeSn [3]) is one of the ways for band gap engineering and structural modification of silicon-based devices. However, preparation of such nanostructures with attaining a composition control poses a persistent challenge.

In this work, we have adopted laser ablation method for the formation of $Si_{1-x}Sn_x$ nanostructures by scanning of a laser beam in the ablation mode over the surface of a Si substrate coated with a tin film and submerged under ethanol. The focused radiation from a Nd:YAG laser (1064 nm) was used. The laser operated in a double-pulse mode with a duration of individual pulses of 10 ns, a time delay between pulses of 10 μs, and a pulse repetition rate of 10 Hz. It has been demonstrated that the formation of nanocrystalline $Si_{1-x}Sn_x$ layers can be achieved with optimized laser parameters (laser fluence, spatial structure of the applied laser beam, irradiation duration). The laser beam profile (Bessel, Gauss, annular) has been shown to be an important factor that significantly affects not only the ablation efficiency, but also the morphology of the resulting nanostructures. The formed $Si_{1-x}Sn_x$ thin layers were characterized by different methods to investigate their structural and optical properties. The optical characterization of the films was performed using Raman and optical absorption spectroscopy. The X-ray diffraction (XRD) was used to study the alloy crystallinity. Energy-dispersive X-ray spectrometry (EDX) performed during scanning electron microscopy (SEM) studies verified uniform incorporation of Sn atoms in the Si substrate surface. The electrophysical properties of the prepared $Si_{1-x}Sn_x$ heterostructures were tested to estimate their potential as components of photovoltaic (photodetector) devices.

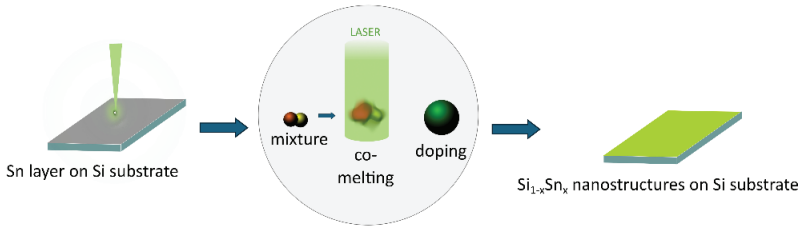

Fig. 1. A principal scheme of laser scanning processing of a Si-Sn bilayer under ethanol for fabrication of $Si_{1-x}Sn_x$ film on silicon plate.

The work was supported by the Belarusian Foundation for Fundamental Researches under Grant F23RNF-156.

[1] N.N. Tarasenka, N.V. Tarasenko, V.V. Pankov, Preparation of Germanium-Tin Alloy Nanoparticles by Laser-Assisted Techniques in Liquid, Intern. J. of Nanoscience, vol. 18, p. 1940049 (2019).
[2] S. Banihashemian, J. M. Grant, A. Sabbar, H. Tran, O. Olorunsola, S. Ojo, S. Amoah, M. Mehboudi, Shui-Qing Yu, A. Mosleh, H. A. Naseem. Growth and characterization of low-temperature $Si_{1-x}Sn_x$ on Si using plasma enhanced chemical vapor deposition // Optical Materials Express, vol. 10, p. 2242 (2020).
[3] J. Vanjaria, A. C. Arjunan, T. Salagaj, G. S. Tompa, and H. Yu, "PECVD Growth of Composition Graded SiGeSn Thin Films as Novel Approach to Limit Tin Segregation," ECS J. Solid State Sci. Technol. 9(3), 034009 (2020).

Self-powered NIR polarization photodetector based on TMD-SiNW hybrid heterostructures

N. Tripathi

Samara National Research University, Moskovskoye Shosse 34, Samara, 443086 Russia

e-mail: nishant.tripathi.11@gmail.com

Achieving self-powered and polarization-sensitive detection in the near-infrared (NIR) range is essential for the development of compact and energy-efficient optoelectronic devices. In this study, we report a novel NIR photodetector based on a vertical heterostructure integrating transition metal dichalcogenides (TMDs) with silicon nanowires (SiNWs), combining energy autonomy with polarization selectivity. The layered TMDs offer strong in-plane optical anisotropy and broadband NIR absorption, while the SiNWs provide enhanced light trapping and efficient charge transport due to their high aspect ratio and large surface area. The TMD-SiNW interface naturally generates a built-in electric field, enabling photocurrent generation without external power. The device demonstrates notable polarization sensitivity, with a high extinction ratio and consistent responsivity in the 800–1300 nm spectral range. Additionally, it exhibits rapid photoresponse and low dark current, making it suitable for use in areas such as optical communications, biomedical diagnostics, remote sensing, and wearable technologies. These results establish TMD-SiNW heterostructures as promising candidates for multifunctional, self-powered NIR photodetectors.

The study was supported by the grant of the Russian Science Foundation No. 25-23-00494, https://rscf.ru/project/25-23-00494).

PLAL of porous and thin-film targets: fabrication of composite nanoparticles for biophotonics and biosensorics

S. Zabotnov[1], I. Dzhun[1,2], D. Shuleiko[1], V. Nesterov[1], D. Presnov[1], I. Romashkina[2], M. Kozin[2], N. Chechenin[1,2], S. Gurbatov[3], A. Kuchmizhak[3]

1- Faculty of Physics, Lomonosov Moscow State University, Leninskie Gory 1/2, Moscow, 119991 Russia
2- Skobeltsyn Institute of Nuclear Physics, Lomonosov Moscow State University, Leninskie Gory 1/2, Moscow, 119991 Russia
3- Institute of Automation and Control Processes, Far Eastern Branch of RAS, Vladivostok, 690041 Russia

e-mail: zabotnovav@my.msu.ru

Pulsed laser ablation in liquid (PLAL) allows to fabricate various nanoparticles (NPs) with desirable sizes and functionalities. In particular, such NPs can be used in biomedical applications [1, 2]. Functional properties of the NPs might be improved when we fabricate nanocomposites, for example, decorated particles, metal-oxide alloys, and core-shell structures.

In our work, to achieve better size distributions of the NPs, we additionally proposed to carry out PLAL of porous or thin-film targets.

In the first case, we used porous silicon layers. This technology made it possible to produce nanocrystalline silicon cores with a reduced average diameter of ~200 nm and a rather narrow monomodal size distribution as compared to the nanomaterial produced by similar ablation of monocrystalline Si wafers [3]. By adding a certain controlled amount of an acid metal precursor $HAuCl_4$, one can create core-satellites NPs. As compared to pure Si NPs, Au-Si nanocomposites were found to demonstrate superior laser heating performance. This makes them suitable for effective light-to-heat conversion that might be promising in photohyperthermia.

In the second case, we studied fabrication of magnetic NPs via PLAL of thin cobalt (5–500 nm) and iron films (250 nm). Similar magnetic NPs can be applied as labels in magnetic biosensorics [4].

The cobalt-based particles predominantly consist of Co_3O_4 and pure Co in the form of a disordered alloy according to a transmission electron microscopy analysis and Raman spectroscopy. The average size of MNPs obtained using Co targets non-monotonically depends on the film thickness and varies in the range of 70–1000 nm according to scanning electron microscopy and dynamic light scattering data [5]. The minimum relative standard deviation of the size distribution obtained is about 20% for the films with the thickness of 5–35 nm used in PLAL. The ablation threshold value and ablation craters profile were found to be dependent on the thickness of the Co film too. These characteristics for thicknesses less than 35 nm are typical for the phase explosion. At larger thicknesses the spallative ablation most likely occurs. These peculiarities are connected to changing the ablation mechanism near the skin layer depth that was estimated as 38 nm.

PLAL of the iron films also made it possible to fabricate colloids of MNPs (~90 nm) with an iron core with an oxide shell in the form of FeO according to Raman and Mössbauer spectroscopy data [6].

Thus, we demonstrated that PLAL of porous silicon layers, cobalt and iron thin films makes it possible to fabricate NPs with rather small sizes and narrow size distributions. These NPs are promising for biophotonics and biosensorics as photothermal agents and magnetic labels, respectively.

This investigation was supported by the Russian Science Foundation (projects #25-79-20016 and #25-29-00176).

[1] V. Amendola, P. Riello, M. Meneghetti, Magnetic nanoparticles of iron carbide, iron oxide, iron@iron oxide, and metal iron synthesized by laser ablation in organic solvents, J. Phys. Chem. C, 115, 5140–5146, (2011).
[2] S.V. Zabotnov, A.V. Skobelkina, E.A. Sergeeva, et al., Nanoparticles produced via laser ablation of porous silicon and silicon nanowires for optical bioimaging, Sensors, 20, 4874, (2020).
[3] S.O. Gurbatov, A.Yu. Zhizhchenko, V.Yu. Nesterov, et al., Au−Si nanocomposites with high near-IR light-to-heat conversion efficiency via single-step reactive laser ablation of porous silicon for theranostic applications, ACS Appl. Nano Mater., 7, 10779–10786, (2024).
[4] H.T. Huang, P. Garu, C.H. Li, et al., Magnetoresistive biosensors for direct detection of magnetic nanoparticle conjugated biomarkers on a Chip, SPIN, 91940002, (2019).
[5] I.O. Dzhun, V.Yu. Nesterov, D.V. Shuleiko, et al., Magnetic nanoparticles produced by pulsed laser ablation of thin cobalt films in water, Bull. Russ. Acad. Sci.: Phys., 88(4), 540–548, (2024).
[6] I.O. Dzhun, D.V. Shuleiko, A.V. Nazarov, et al, Laser-assisted nanomaterials fabrication from thin films for magnetic biosensors, Bull. Russ. Acad. Sci.: Phys., 88(Suppl. 2), S166–S173, (2024).

Advanced laser and nano technologies for nuclear medicine

I. Zavestovskaya[1,2]

1- National Research Center "Kurchatov Institute", Kurchatov Square 1, Moscow, Russia
2- Lebedev Physics Institute of the Russian Academy of Sciences, Leninsky pr. 53, Moscow, Russia

e-mail: zavestovskayain@lebedev.ru

Recent data which we have in realization of the joint project with LPI, MEPHI and Tsyb Radiological Center show that the field of nuclear medicine can be significantly expanded by integrating with nanomedicine, which utilizes nanoparticles (NPs) as carriers of radionuclides or as radiosensitizers for radiation therapy and/or active agents for imaging (radiopharmaceutical medicines in situ). The synergy of laser nanotechnology with nuclear medicine opens up a new direction of cancer imaging and therapy - nuclear nanotheranostics.

We propose different types of NPs synthesized by promising laser-based approaches as a NPs for nanotheranostics. One can use these methods to make stable colloidal dispersions of nanoparticles in both organic and aqueous media, which are suitable for a multitude of applications across the important fields of health care. For example, size tailoring allows production of Si*NPs with efficient photoluminescence that can be tuned across a broad spectral range from the visible to near-IR by varying particle size and surface functionalization. These applications encompass several types of bioimaging and various therapies, including phototherapy, RF thermal therapy, and radiotherapy. Laser-synthesized NPs have ideal round shape, controllable size with low size dispersion, and are free of any toxic impurities, which promises a better transport in vivo and the absence of side effects.

We demonstrate the possibility for fast PEGylization and conjugation of laser-synthesized Si*NPs with Rhenium-188 (188Re) radionuclide, which is one of most promising generator-type therapeutic beta-emitters. Our tests on rat survival demonstrate excellent therapeutic effect. Combined with a series of imaging and therapeutic functionalities based on unique intrinsic properties of Si*NPs, the proposed biodegradable complex promises a major advancement of nuclear nanomedicine.

Technologies of targeted proton therapy using promising nanoparticles and systems based on them as therapy sensitizers and active agents for diagnostics are considered. The introduction of non-radioactive materials that can be activated from the outside using various external sources of nuclear particles to produce radioactivity in situ is one of the new directions of activation of nano-drugs at the site of a cancerous tumor, which can be considered as in situ production of radiopharmaceuticals. Such binary radiotherapy technologies become especially efficient when one can achieve a high tumor/non-tumor action contrast, which enables to minimize side effects related to the irradiation of healthy issues.

The study is supported by the Ministry of Science and Higher Education of RF (project No 075-15-2025-453), RSF (project No 24-62-00018).

Laser-assisted production of silicon microparticles with Fano resonance

K. O. Aiyyzhy[1], E. V. Barmina[1], N. N. Melnik[2], D. S. Kostsov[2], V. V. Tregulov[3], A. I. Ivanov[3]

1- Prokhorov General Physics Institute of the Russian Academy of Sciences, Vavilova str. 38, Moscow, 119991 Russia
2- P. N. Lebedev Physical Institute of the Russian Academy of Sciences, Leninsky Prospekt, 53, Moscow, 119991 Russia
3- Esenin Ryazan State University, ul. Svobody 46, Ryazan, 390000 Russia

e-mail: aiyyzhy@phystech.edu

Silicon (Si) microparticles (MPs) are promising for biomedicine, including cancer theranostics. They can be considered as photosensitizers for photodynamic therapy [1]. Thus tumor cells destroy due to occurrence of hyperthermia effect under the influence of electromagnetic or optical radiation to Si particles [2]. It can be promising to use for photodynamic therapy particles with field enhancing and variable optical properties. For example, Fano resonance objects can be candiates for such request [3]. Fano resonance as asymmetric non-Lorentz resonance occurs during interference between a wide continuous state and a narrow discrete state [4]. There is currently no data in the literature about the production of Si particles with Fano resonance. Therefore the aim of this work is to synthesis Si MPs with Fano resonance by laser ablation a por-Si film doped with boron in liquid.

An Ytterbium fiber laser with a wavelength of 1060–1070 nm, pulse duration of 200 ns, pulse repetition rate of 20 kHz, and pulse energy of 1 mJ was used as a source of laser radiation. The time of the ablation process was 20 min. Isopropanol was used as a working liquid; the thickness of the isopropanol layer above the por-Si film was 4 mm. The morphology of Si MPs deposited on the surface of an aluminum mirror was studied using a scanning electron microscope. Typical MPs image is shown in Fig. 1a. Si MPs are spherical in shape and their sizes range from 0.13 to 6.71 μm.

Laser-generated Si MPs were investigated using Raman spectroscopy. Due to the spatial resolution of the Raman spectrometer (inVia Renishaw, excitation wavelength of 785 nm) is 0.8 μm, Si MPs with a minimum size of 1 μm were studied. According to the Raman spectrum (Fig. 1b), Si MPs demonstrate a Fano resonance (Fano resonance parameters are presented in the table in Fig. 1c).

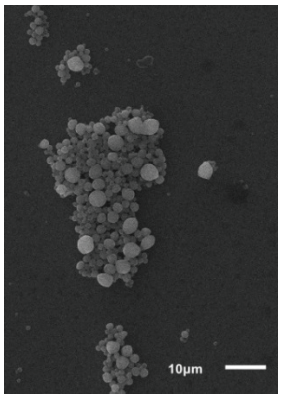

a)

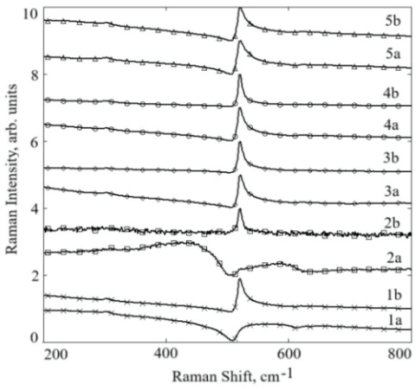

b)

spectrum number	*d*, μm	ν_0, cm^{-1}	Γ, cm^{-1}	*q*
1a	1	509.0	13.0	0.19
1b		515.7	5.5	2.6
2a	2	506.0	15.0	0.02
2b		519.0	3.8	4.9
3a	3	517.5	5.4	2.1
3b		518.5	4.5	3.2
4a	4	516.5	5.1	2.6
4b		518.5	4.0	3.8
5a	6	516.3	6.7	1.6
5b		518.0	6.0	2.0

c)

Fig. 1. SEM image of silicon microparticles (a), Raman spectra of silicon microparticles (b), Fano resonance parameters of the first-order silicon spectral line for microparticles (c): d – diameter of silicon particles, q – parameter Fano, ν_0, Γ – position and width of the spectral line of the Fano resonance, respectively.

Thus, this work demonstrates for the first time the synthesis of Si MPs with Fano resonance by laser ablation in isopropanol.

[1] C. Lee, H. Kim, Y.J. Cho, W.I. Lee, The properties of porous silicon as a therapeutic agent via the new photodynamic therapy, J. Mater. Chem., 17, 2648–2653 (2007).
[2] K. Tamarov et al., Temperature responsive porous silicon nanoparticles for cancer therapy – spatiotemporal triggering through infrared and radiofrequency electromagnetic heating, Journal of Controlled Release, 241, 220–228 (2016).
[3] E.Y. Tiguntseva et al., Tunable hybrid Fano resonances in halide perovskite nanoparticles, Nano letters, 18, 5522–5529 (2018).
[4] M.F. Limonov, Fano resonance for applications. Advances in Optics and Photonics, 13, 703–771 (2021).

Formation of broadband terahertz absorbers by laser microstructuring

D. A. Antipov, E. V. Barmina, D. I. Borovikov, E. D. Shevelkina

Prokhorov General Physics Institute of the Russian Academy of Sciences, 38, Vavilova street, 119991 Moscow, Russia

e-mail: antipov.dima.99@mail.ru, e.shevelkina@yandex.ru

Laser ablation of solid targets is well-established as a method that leads to significant modifications of their optical properties [1, 2]. In particular, laser-induced periodic surface structures (LIPSS) have been shown to drastically reduce material reflectivity, thus holding promise for the creation of broadband, highly absorptive surfaces [3]. This work focuses on demonstrating the capabilities and potential of nanosecond pulsed laser ablation in air, for creating a quasi-periodic array of microstructures on glassy carbon. This material exhibits high strength and thermal stability and is widely utilized in industrial and aerospace applications for the creation of wear-resistant and heat-resistant protective coatings [4]. One prospective application of this microstructured material is its use as a broadband, highly absorptive material within the 0.2–2 THz spectral range, thereby enabling the development of highly sensitive radiation detectors and thermal receivers.

The reduction in specular reflectance (MCR) to below 4% on the laser-treated surfaces is attributed to the formation of microstructures during laser ablation, which effectively trap and absorb incident radiation. A special microstructure with micro-perforated blocks (Fig. 1a) facilitates a low reflection coefficient. As a result, microholes and fractures acting as light traps may reduce the surface reflection through internal multireflection process. These internal reflections enhance light-matter interaction, ultimately leading to light absorption between the microstructures.

In this study, laser ablation regimes were optimized to control the depth and periodicity of the structure. Fig. 1b shows that the structured surface achieves near-complete absorption of incident radiation through multiple reflections and absorption within the material. This absorption mechanism renders the material an effective broadband absorber. Furthermore, the creation of broadband radiation sources with a flat spectral response represents another promising application for terahertz spectroscopy and communications. Future research will be directed toward a detailed investigation of the mechanisms governing microstructure and oxide layer formation, alongside optimization of laser ablation parameters to achieve maximum absorption within the target spectral range.

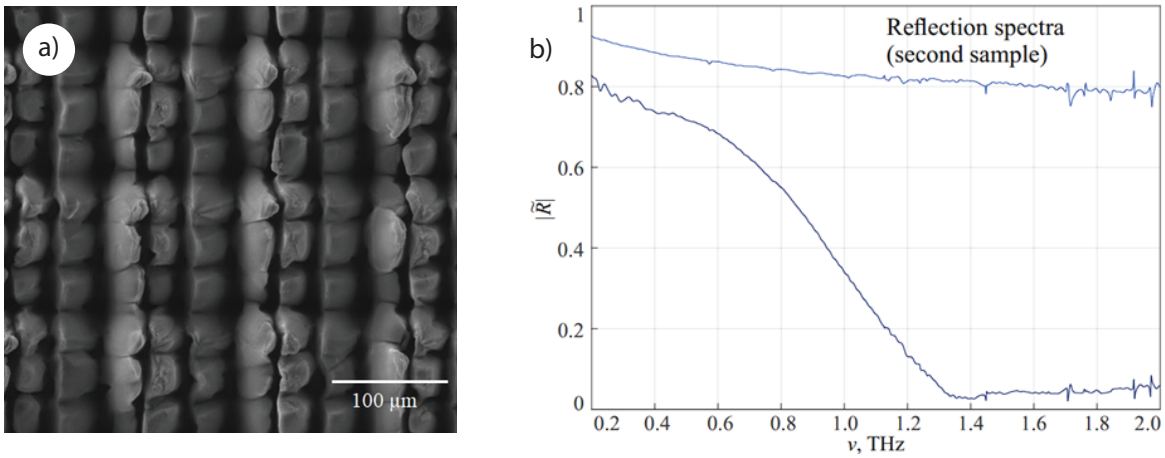

Fig. 1. (a) SEM images of the modified glassy carbon surface. (b) Measured specular reflectance spectra of the initial (light blue line) and modified (dark blue line) glassy carbon surfaces.

[1] A. Y. Vorobyev and C. Guo Colorizing metals with femtosecond laser pulses, Appl. Phys. Lett. vol. 92, p. 041914, (2008).
[2] E. V. Barmina, E. Stratakis, C. Fotakis, G. A. Shafeev Laser-assisted micro- and nanostructuring of solids, in Ultrafast Laser Micro- and Nanoprocessing, ed. K. Sugioka, Singapore: Pan Stanford Publishing, (2013).
[3] Bonse, J., J. Kruger, S. Hohm, A. Rosenfeld Femtosecond laser-induced periodic surface structures, J. of Laser Applications, (2012).
[4] K. Holmberg, A. Matthews, Coatings tribology: properties, techniques and applications in surfaceengineering, Elsevier Science, Amsterdam, (1994).

The influence of gas pressure on spatial and spectral parameters of a high-power femtosecond laser pulse during filamentation in argon

D. V. Apeksimov, P. A. Babushkin, Yu. E. Geints, A. M. Kabanov, E. E. Khoroshaeva, V. K. Oshlakov, A. V. Petrov, A. A. Udalov

V. E. Zuev Institute of Atmospheric Optics SB RAS, Tomsk, Russia

e-mail: bpa@iao.ru

The filamentation of high-power femtosecond laser pulses in gases is of significant theoretical and practical interest for beam profile structuring along the propagation path or for extending the propagation distance. These challenges are directly relevant to cutting-edge developments in novel environmental monitoring techniques and greenhouse gas tracking [1, 2].

One striking manifestation of beam structuring effects is the enhancement of fluorescence signals from aerosol-contained impurities, correlated with the number of postfilamentation channels (PFCs) in the beam cross-section [3]. This approach can be used to increase the detection range of atmospheric aerosol impurities through controlled beam structuring.

In this work, we studied the influence of gas pressure (argon) on the variation of PFCs in the beam cross-section and the spectral-angular properties during nonlinear propagation. The experiments were conducted using the 2-meter high-pressure cell, which simulates conditions relevant to extended atmospheric paths or planetary atmospheres. Figure 1 demonstrates the change of spectral width of the laser beam and number of PFCs is depend on argon pressure. The measures were carried out for pressure range from 1 to 50 bar.

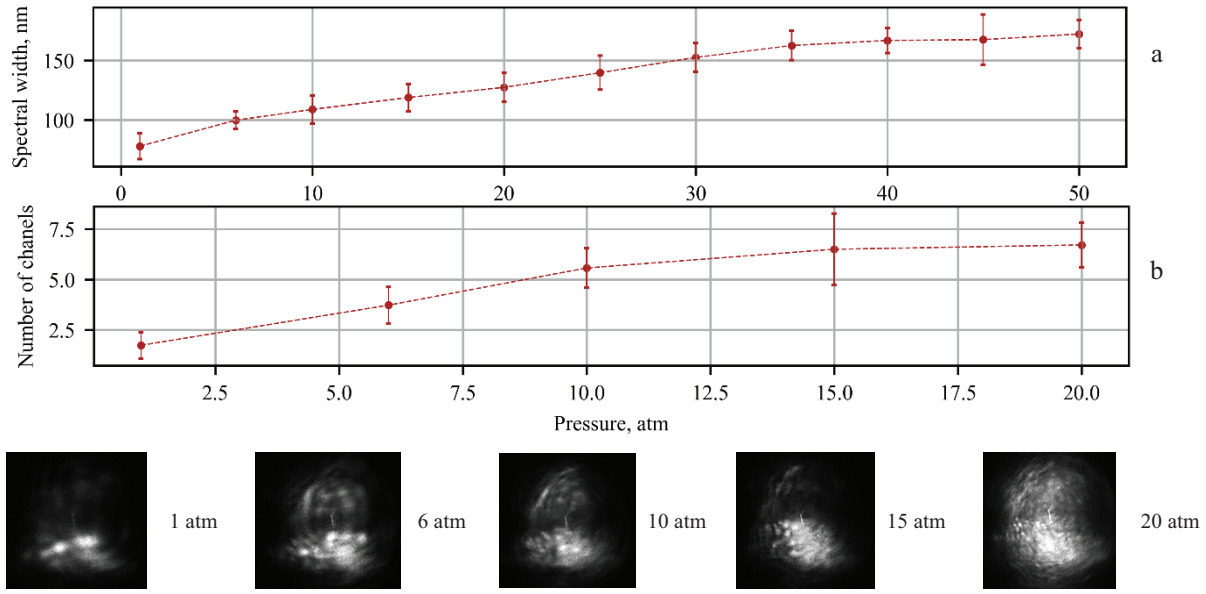

Fig. 1. (a) Spectral width and (b) number of PFC in the dependence on argon pressure in optical cell.

The data presented in Fig. 1 demonstrate an efficient way to control the spatial and spectral characteristics of femtosecond radiation during filamentation by changing the gas pressure in the optical cell.

The work was financially supported by the Russian Science Foundation (agreement no. 24-12-00056).

[1] Kasparian J., Wolf J. P. Physics and applications of atmospheric nonlinear optics and filamentation // Optics express. 2008. V. 16. N. 1. pp. 466–493.
[2] Qi P., Qian W., Guo L., Xue J., Zhang N., Wang Y., Liu W. Sensing with femtosecond laser filamentation // Sensors. 2022. V. 22. N. 18. p. 7076.
[3] Apeksimov D.V., Babushkin P.A., Zemlyanov A.A., Kabanov A.M., Kochetov D.I., Oshlakov V.K., Petrov A.V., Khoroshaeva E.E. The Effect of Turbulence on Generation of High-Intensity Light Channels during Femtosecond Laser Pulse Propagation along a 100-Meter Air Path // Atmospheric and Oceanic Optics, 2024, V. 37. N. 01. pp. 1–6.

Laser synthesis of nanoparticles of nonstoichiometric molybdenum oxide with the addition of BSA

A. Chernikov, D. Kochuev, M. Dzus, E. Shingareva, K. Khorkov

Vladimir State University, Gorky Street, 87, Vladimir, 600000 Russia

e-mail: khorkov@vlsu.ru

The synthesis of nanoparticles (NPs) of nonstoichiometric molybdenum oxide (MoO_{3-x}) was carried out by femtosecond laser fragmentation in a liquid medium. Ethanol (95%) was used as the liquid medium, and suspensions prepared from commercial MoS_2 powder were used as the irradiation object. Suspensions with a concentration of 0.2 mg/ml were prepared for experiments on laser fragmentation. The Yb:KGW femtosecond laser system (Avesta) was used as a radiation source in experiments on laser ablation synthesis. The radiation wavelength was 1030 nm, the maximum energy in a pulse was 150 μJ, the pulse duration was 280 fs, and the pulse repetition frequency was 10 kHz. The duration of the laser fragmentation process was 60 minutes, and the pulse energy was 100 μJ. 5 minutes after the start of the laser fragmentation process, the solution acquired a dark brown hue. Then the color of the solution changed to brown-green after about 30–40 minutes, and at the end of the laser fragmentation process (60 minutes) it acquired a green-blue hue. Such a color usually indicates high absorption in the visible and near-infrared regions of the spectrum [1]. Laser exposure to a suspension in ethanol for 10 minutes leads to the transformation of the initial powder into NPs of a near-spherical shape, the average size of NPs is 38 nm, while a number of submicron particles of random shape can be observed. An increase in the duration of laser fragmentation (60 minutes) leads to a decrease in the size of NPs, so the average size of NPs is about 26 nm. In the Raman spectra for NPs obtained by laser fragmentation in ethanol for 60 minutes, peaks characteristic of MoS_2 are not observed, peaks are present at 196, 222, 348, 485, 726, 850, 962 cm^{-1}. This set of peaks is typical for nonstoichiometric molybdenum oxide. BSA was used for further functionalization and stabilization of NPs [2]. The effect of BSA concentration on the optical and photothermal properties of colloidal systems was evaluated. The prepared solution of MoO_{3-x} NPs in deionized water was poured into test tubes (required volume of 1 ml), in which the required amount of BSA (0, 1.25, 2.5, 5 mg) was added in advance. The tubes were placed in an ultrasound bath for 30 minutes at a temperature of 37 °C. Fig. 1a shows the optical density curves of solutions of MoO_{3-x} NPs in deionized water with different concentrations of BSA, and Fig. 1b shows graphs of temperature versus time when irradiating colloidal solutions with continuous radiation at a wavelength of 805 nm. Based on the experimental data obtained, colloidal solutions of MoO_{3-x} NPs in deionized water with a concentration of BSA 1.25 mg/ml and without the addition of BSA demonstrated the best result in terms of photothermal properties and stability.

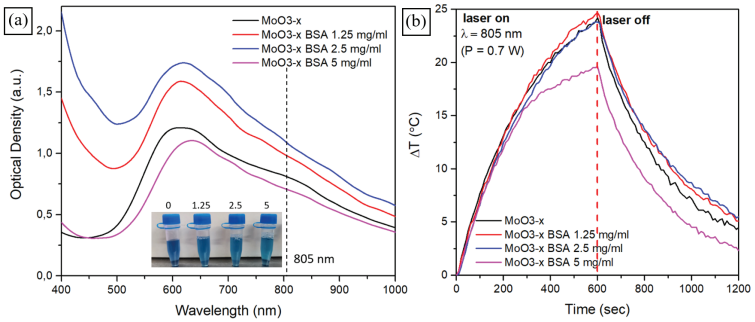

Fig. 1. Optical density curves of solutions of MoO_{3-x} nanoparticles in deionized water with different concentrations of BSA (a); graphs of temperature versus time dependence when irradiating colloidal solutions with continuous radiation at a wavelength of 805 nm (b).

This study was funded by the Russian Science Foundation (project no. 22-79-10348, https://rscf.ru/project/22-79-10348/).

[1] A.S. Chernikov, et al, Tunable optical properties of transition metal dichalcogenide nanoparticles synthesized by femtosecond laser ablation and fragmentation, Journal of Materials Chemistry C, vol. 11(10), pp. 3493–3503, (2023).
[2] U.E. Kurilova, et al, Studies of the morphology and cytotoxicity of photosensitized metal chalcogenide nanoparticles, Biomedical Engineering, vol. 58(2), pp. 106–109, (2024).

Glass marking by combining laser-induced backward transfer (LIBT) and laser-induced periodic surface structures (LIPSS) via nanosecond IR laser

V. Domakova[1], A. Ramos-Velazquez[1,2], K. Arbuzova[1], D. Sinev[1]

1- ITMO University, St. Petersburg, Russia
2- Laser Center, St. Petersburg, Russia

e-mail: veradomakova@itmo.ru

The marking of optically transparent products is a critical technological process widely employed for identification and anti-counterfeiting purposes, particularly in medical ampoules, excise-labeled bottles, and specialty glassware. Current demands necessitate the development of novel marking techniques that ensure high durability, resolution, and non-replicable properties. This study presents an advanced laser-based approach combining laser-induced backward transfer (LIBT). and laser-induced periodic surface structures (LIPSS), enabling two-step glass marking only using a nanosecond IR laser system. The proposed method involves the transfer of a metallic coating onto the glass substrate followed by laser structuring under LIPSS generation conditions, resulting in thin-film coatings exhibiting rainbow hologram-like optical effects. The fabricated periodic nanostructures demonstrate a characteristic spatial period of approximately 730 nm. Beyond static marking, this technique allows for dynamic visual effects, expanding its potential applications in laser art and high-security product labeling.

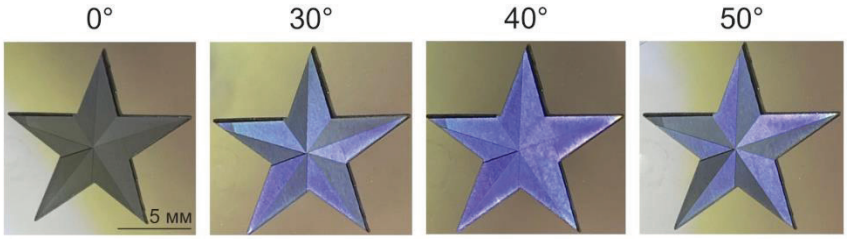

Fig. 1. Demonstration of the effects of the dynamics of the image created on the glass surface, the angles indicate the angle of illumination of the sample.

Research was financially supported by Russian science foundation, project #24-79-10230, https://rscf.ru/en/project/24-79-10230/.

Laser modification of titanium surfaces using absorbing layers in confined conditions

X. Egorova, A. Sidorova, F. Gorensky, D. Sinev

Institute Laser Technology, University ITMO, Kronverksky avenue 49, St. Petersburg, 197101 Russia

e-mail: x_egorova@itmo.ru

Laser treatment of metal parts with variation of laser parameters makes it possible to achieve desired surface layer properties. A promising direction is laser treatment in confined conditions, where the absorbing layer is placed between the metal sample and a plate transparent to the laser wavelength [1, 2]. This configuration localized energy absorption and more precise structure formation. The use of nanosecond a commercially available setup, allows intense thermomechanical effects, which lead to the formation of amorphous structures and a significant increase in the hardness of the treated layer [3].

This work presents experimental and analytical results on the optimization of laser treatment parameters to control the mechanical properties of the surface layer of titanium samples. The treatment was performed in a "metal–absorbing layer–glass" configuration. Three types of absorbing layers were used: graphite powder [3], a laser-induced graphene layer on a polymer base [4], and a mixture of SrO and TiO powders [5]. Under nanosecond laser pulses (λ = 1.06 μm), a localized flame was formed, resulting in intensive heating and surface modification. Depending on the configuration, it was possible to obtain an amorphous layer with increased hardness or with piezoelectric properties.

Thus, the results show the potential of laser treatment in confined conditions for precision surface modification of metals with controllable property enhancement. The presented methods demonstrated new opportunities for integration of this technology in mass production in the fields of mechanical engineering.

Research was financially supported by Russian science foundation, project #24-79-10230, https://rscf.ru/en/project/24-79-10230/.

[1] S. Bovid, et al. Pressure amplification and modelization in laser shock peening of Ti-6Al-4V and AA7085 with adhesive-backed opaque overlays, J. Mater. Process. Technol. vol. 299, 117381, (2022).
[2] D. Weiwei, et al. Progressive developments, challenges and future trends in laser shock peening of metallic materials and alloys: A comprehensive review. International Journal of Machine Tools and Manufacture, vol.191, 104061, (2023).
[3] X. Egorova, et al. Hardness enhancement by laser modification of titanium under an auxiliary graphite layer. Applied Physics A vol. 129, p. 855, (2023).
[4] Y. Zhengwei, et al. Laser-induced graphene assisting self-conversion reaction for sulfur-free aqueous Cu-S battery. Advanced Functional Materials vol. 31, 2103893, (2021).
[5] W. Cong, et al. A novel structure design of barium strontium titanate piezoelectric coating on titanium surface enhanced its response to low-intensity pulsed ultrasound. Surface and Coatings Technology vol. 479, 130497, (2024).

Prediction of residual stress distribution based on finite element modeling of laser hardening

D. D. Fedotov[1], I. A. Antoshin[1], S. I. Yaresko[2]

1- Samara State Technical University, Molodogvardeyskaya str. 244, Samara, 443100 Russia
2- Samara Branch of P. N. Lebedev Physical Institute of the Russian Academy of Sciences, Novo-Sadovaya str. 221, Samara, 443011 Russia

e-mail: dnsfdtv62@gmail.com

The finite element (FE) method was used to determine the temperature field and residual stresses (RS) during strengthening laser heat treatment (LHT) and laser shock peening (LSP).

The LSP analysis was performed in the SIMULIA ABAQUS software. The calculation was carried out using experimental data obtained during the processing of the Ti-6Al-4V alloy [1]. The model was a parallelepiped with a square cross-section of 20×20 mm, divided into FEs of 0.1 mm in size with specified boundary conditions. A single laser pulse was simulated with a pulse duration of 10 ns and a load of P_{max} = 5.5 GPa (laser power density of 5.6 GW/cm^2) uniformly distributed over the impact spot area.

The analysis of continuous LHT of a two-layer structure (substrate + coating) was performed in ANSYS Workbench software using the Moving Heat Source V4.1 module. AISI 4140 steel was chosen as the substrate, the gas-thermal HVOF coating WC-10Co-4Cr had a thickness of 300 μm. The model is presented in the form of two combined parallelepipeds of rectangular cross-section with dimensions of 20×10×5 and 20×10×0.3 mm, respectively. The element size did not exceed 0.05 mm in the treatment area. As in the modeling of the LSP process, the conditions for the symmetry of the model were specified. The load is specified as a heat flow with a power of P = 900 W, distributed over the circle area with a radius of R = 0.48 mm. The heat source moved along the plane of symmetry at a speed of V = 20 mm/s. Under these conditions, LHT with melting of the coating leads to an increase in its microhardness and homogeneity due to the formation of compact structures and carbides W_2C and WC_{cube} in the melt zone [2].

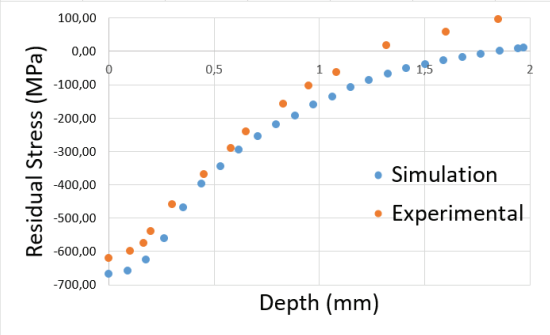

Fig. 1. Distribution of residual stresses along the depth of the plate after LSP.

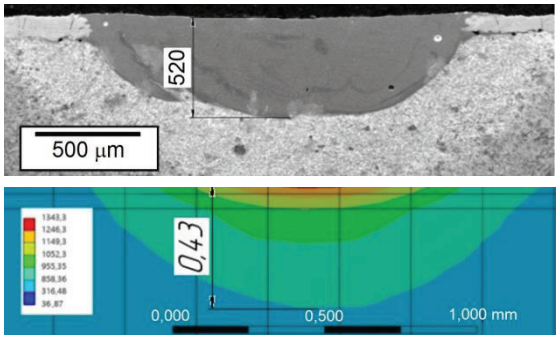

Fig. 2. Comparison of the depth of the hardening zone according to metallography and FE-calculation data for LHT.

According to the results of FE modeling, the discrepancy between the experimental and calculated values of RS for LSP does not exceed 10% (Fig. 1). When modeling continuous hardening LHT at the first stage, the temperature field in the processing zone was determined and it was found that the depth of the hardening zone differs from the experimental values by no more than 17.3% (Fig. 2). At the second stage of modeling, it is assumed that the distribution of RS is determined and the deviation of their values from the experimental values is minimized by correcting the FE model.

[1] Nakhodchi S., Poormir M.A., Gharibdosti M.S. A finite element study of thermal residual stress relaxation in multiple laser shock peened Ti-6Al-4V // Modares Mechanical Engineering 2018; 18 (3):38-44. 20.1001.1.10275940.1397.18.3.12.3
[2] Yaresko, S.I., Antoshin, I.A. Laser Modification of Thermal Spray Coatings Obtained by HVOF Spraying. AReview // GlassCeram (2025). V. 82. Nos. 1-2. https://doi.org/10.1007/s10717-025-00745-x

Phase transformations in liquid water under the influence of a laser in an ultrasonic wave field

M. A. Karpov, A. D. Kudryavtseva, T. V. Mironova, M. A. Shevchenko, N. V. Tcherniega, S. F. Umanskaya

P. N. Lebedev Physical Institute of the Russian Academy of Sciences. Leninsky Prospekt 53, Moscow, 119991 Russia

e-mail: tchera@lebedev.ru

A picosecond YAG: Nd^{3+} laser (532 nm and 1064 nm, 30 ps duration) was used for SRS excitation in liquid water exposed to ultrasound fields (40 kHz, 200 W). The peak pulse energy varied from 2 to 20 mJ. The laser beam was focused into a cell filled with liquid using a lens with a focal length of 11 cm. The beam diameter in the caustic waist was about 20 μm. Raman spectra were recorded using an Ocean Optics HDX fiber spectrometer, providing a resolution of 0.6 nm in the spectral range of 200–1100 nm and connected to a PC. The SRS power was measured by a power meter Ophir. We recorded SRS both in the direction of the incoming laser beam (forward) and in the opposite (backward) direction. SRS thresholds, conversion efficiency and spectrum were measured and influence of ultrasound on scattered wave features was estimated.

It was shown that the presence of ultrasound, which leads to the appearance of randomly distributed phase inhomogeneities in the active medium, ensures the appearance of feedback. Which in turn leads not only to a strong increase in the efficiency of the SRS conversion but also to the phase transformation of water, which is demonstrated in Fig. 1. Figure 1 presents SRS spectrum in water excited by the first harmonic of Nd:YAG laser with wavelength of 1064 nm.

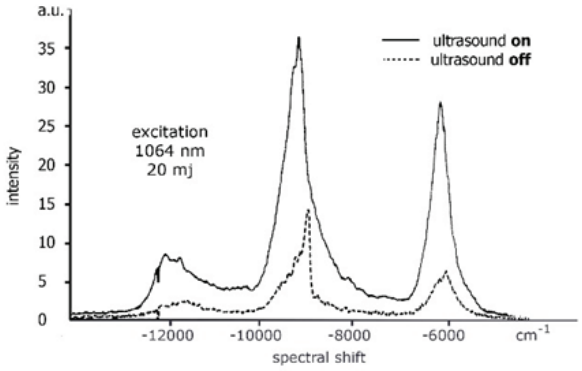

Fig. 1. The SRS spectrum in water excited by the first harmonic of Nd:YAG laser (1064 nm) at a pulse energy of 20 mJ.

As shown in Fig. 1, in this case the anti-Stokes components up to the fourth order were observed in the forward SRS spectrum. The intensity of the first anti-Stokes component was very weak due to the strong absorption at this wavelength. The frequency shift in the case of the SRS anti-Stokes components in water excited by the first laser harmonic was in the region of 3000 cm^{-1}. As it was shown in [1], this component corresponds to the stretching vibrational mode of the OH bond for ice VII. The structure of ice VII is formed by high pressure (~10 GPa) caused by the shock wave because of optical breakdown and formation of high-density plasma. Switching on the ultrasound leads to increasing the spectral shift of anti-Stokes components.

[1] V. Rakesh Kumar and P. Prem Kiran, Transformation of liquid water to ice VII during propagation of picosecond laser pulses: effects of wavelength and polarization, JOSA B, vol. 33(6), pp. 1157–1168, (2016).

Atomistic modeling of ultrafast dynamics of laser melting/crystallization interface of metals considering deeply superheated/supercooled phases in sequential pressure measurements

V. I. Mazhukin, A. V. Shapranov, O. N. Koroleva, M. M. Demin, A. V. Mazhukin

Keldysh Institute of Applied Mathematics, Moscow, Russia

e-mail: vim@modhef.ru

When a substance is exposed to ultra-short, ultra-powerful laser radiation, sufficiently high degrees of overheating during melting and supercooling during crystallization of the substance are achieved, and, as a consequence, high velocities of the melting/crystallization of fronts are achieved. Such exposure is also accompanied by a powerful transfer of the substance, which leads to pressure surges at the melting/crystallization front.

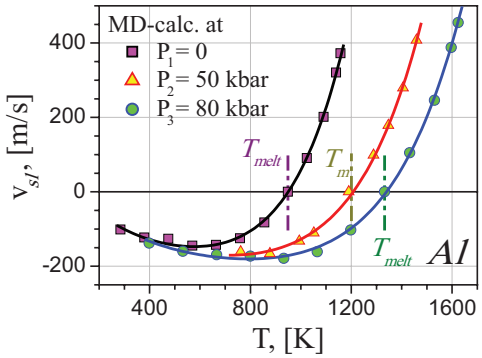

Fig. 1. Phase front velocity depending on temperature at three pressure values. Markers show the results of MD calculations, solid lines are approximations of the analytical expression $\upsilon_{s\ell}(T,P)$. The standard deviation for all three pressure values does not exceed 7.6 m/s.

The dependence of the velocity of the melting/crystallization front $\upsilon_{s\ell}$ on the magnitude of superheating/supercooling and pressure plays an important role in crystallization/melting processes and is one of the fundamental concepts of materials science.

Based on the new algorithm for constructing the temperature dependence of the steady-state velocity $\upsilon_{s\ell}(T)$ of propagation of the interphase boundary of crystallization/melting in metals at constant pressure, obtained earlier [1] within the framework of the kinetic-atomistic [2–4] approach, an analytical expression for the dependence of the velocity $\upsilon_{s\ell}(T,P)$ in a wide range of pressures containing a number of parameters to be determined was obtained.

Using the EAM interaction potential for Al [5] and the molecular dynamics method, atomistic modeling of the melting/crystallization processes of metal (Al) under conditions of deep superheating/supercooling was performed, which made it possible to obtain unknown parameters of the analytical expression for the velocity $\upsilon_{s\ell}(T,P)$ in a wide range of pressures (Fig. 1).

[1] Mazhukin V.I., Shapranov A.V., Koroleva O.N., Mazhukin A.V. Modification of the Wilson-Frankel kinetic model and atomistic simulation of the rate of melting/crystallization of metals // Mathematical Models and Computer Simulations, 2024, Vol. 16, No. 2, pp. 223–234.
[2] Jackson K.A., Chalmers B. Kinetics of solidification // Can. J. Phys., 1956, v. 34, 473–490.
[3] Wilson H.A. On the velocity of solidification and viscosity of supercooled liquids // Philos. Mag., 1900, v. 50, 238–250.
[4] Frenkel Ja.I. Note on the relation between the speed of crystallization and viscosity // Phys. Z. Sowjet Union, 1932, v. 1, 498–499.
[5] V.V. Zhakhovskii, N.A. Inogamov, Yu.V. Petrov, S.I. Ashitkov, K. Nishihara. Molecular dynamics simulation of femtosecond ablation and spallation with different interatomic potentials // Appl. Surf. Sci., 2009, v. 255, No. 24, pp. 9592–9596.

Phase-matching curves dynamics in $\chi^{(2)}$ grating formation during fiber poling

A. Ostapiv[1], K. Zotov[1], N, Tereshchenko[1], A. Konyashkin[2]

1- LaserOne LLC, Vvedenskogo Square 3, Building 5, Fryazino, Moscow Region, 141190 Russia
2- Fryazino Branch of the V. A. Kotelnikov Institute of Radio Engineering and Electronics, Russian Academy of Sciences, Vvedenskogo Square 1, Fryazino, Moscow Region, 141190 Russia

e-mail: ostapiv.ayu@phystech.su

Second-harmonic generation (SHG) is a nonlinear optical process requiring a non-zero quadratic nonlinear susceptibility in the material. Despite the inherent centrosymmetry of fused silica, SHG in optical fibers has been observed since 1986 [1]. The direct cause of SHG is the formation of a spatially periodic grating of nonlinear susceptibility, whose period satisfies the phase-matching condition. However, the microscopic origin of this grating formation remains a subject of scientific debate.

A key parameter characterizing SHG is the phase mismatch between interacting waves. The dependence of SHG efficiency on phase mismatch – i.e., the phase-matching curve – can provide insights into the nature of SHG and validate or refute theoretical models. Although phase-matching curves in optical fibers have been measured previously [2, 3], the evolution of these curves during the grating inscription process has not been investigated.

This work presents experimental measurements of temperature- and wavelength-dependent phase-matching curves in optical fibers during SHG. The obtained curves are compared with predictions from the model [1]. It is shown that the model [1] predicts asymmetry and a shift in the optimal phase-matching wavelength during grating formation. The observed direction and shape of asymmetry align with theoretical expectations.

[1] B. P. Antonyuk and V. B. Antonyuk, Self-organization of excitations in Ge-doped silica fibers and its role in second harmonic generation, UFN, vol. 171, pp. 61–68, (2001).
[2] M. Farries, P. Russell, M. Rogers and D. Payne, Second-harmonic generation in an optical fibre by self-written x(2) grating, Electronics Letters, vol. 23, pp. 322–324, (1987).
[3] S. Bardal and P. Wells, Intensity-dependent shift of phasematched wavelength in second-harmonic generation in optical fibres, Electronics Letters, vol. 27, pp. 896–897, (1991).

The electrocapillary acceleration of metal melt in deep penetration by powerful laser radiation

R. D. Seidgazov, F. Kh. Mirzade

NRC «Kurchatov Institute», Academician Kurchatov sq. 1, Moscow, 123182 Russia

e-mail: seidgazov@mail.ru, fmirzade@rambler.ru

The deep penetration (keyhole) mode is used in a number of modern laser and electron beam metal melting technologies to create welding joints and assemble products through additive moulding of metal powders. This mode is characterized by a high aspect ratio (the depth of the molten bath to its width) and requires exceeding a threshold value of radiation power, which depends on the focus spot size. The thermocapillary mechanism provides adequate coupling between the parameters of the laser beam and the hydrodynamic flow [1]. This is confirmed by experiment [2], numerical calculation [3], comparison of calculated and experimental threshold conditions of deep penetration [4], analysis in [5, 6]. Along with this, the thermocapillary mechanism does not reveal the synergetic effect nature in hybrid laser-arc action [7], does not reflect the reason for the empirically observed correlations of keyhole depth with characteristics of near-surface plasma, emission current signal [8], and parameters of external electric field [9].

To address this issue, we propose a physical mechanism that explains how electrodynamic processes can accelerate thermocapillary flow in a melt layer during the process of deep penetration of a metal by intense laser radiation. This mechanism takes into account the acceleration of thermocapillary flow by the action of electrocapillary forces, which are caused by the dependence of surface tension on electric potential and its non-uniform distribution over the surface. The mechanism clarifies the relationship between hydrodynamic processes, thermionic and electrocapillary effects, and qualitatively explains the patterns observed experimentally. In order to better understand hydrodynamic processes during deep penetration, it is important to take into account not only the dependence of surface tension on temperature, but also its electrical potential dependency. This includes knowledge of the distribution of potential on the surface of the melt.

The work was carried out within the framework of the state assignment of NRC «Kurchatov Institute».

[1] R.D. Seidgazov, Thermocapillary mechanism of melt displacement during keyhole formation by the laser beam, J Physics D: Appl Phys, 42 No 17, 175501, (2009).
[2] R.D. Seidgazov, F.Kh. Mirzade Features of the keyhole evolution during deep penetration of metals by laser radiation, Technical Physics Letters, Vol. 48, No. 14 pp. 12–14 (2022).
[3] S. Ly, G. Guss, A.M. Rubenchik, et al. Resonance excitation of surface capillary waves to enhance material removal for laser material processing, Scientific Reports, 9:8152 (2019).
[4] R.D. Seidgazov, F.Kh. Mirzade, Threshold conditions for thermocapillary transition to deep penetration mode in selective laser melting of metal powder bed, IOP Conf. Ser.: Mater. Sci. Eng. 759, 012023 (2020).
[5] R. D. Seidgazov "Analysis of the Main Hydrodynamic Mechanisms in Laser Induced Keyhole Welding," IEEE 8th Int. Conf. on Advanced Optoelectronics and Lasers (CAOL), Bulgaria, (2019); 216–219. DOI: 10.1109/CAOL46282.2019.9019431
[6] R.D. Seidgazov, F.Kh. Mirzade, Physical substantiation of discretization scheme in modeling of keyhole mode melting of metals in laser and related technologies. Matematicheskoe modelirovanie, Vol. 36, № 5, 41–54 (2024). DOI: 10.20948/mm-2024-05-04
[7] I.V. Krivtsun et al. Analysis of the main mechanisms and regularities of the synergistic effect in hybrid laser-arc processes. Technical science /«Colloquium-journal», #18 (42), 10–20 (2019).
[8] P.J. DePond, et al. Laser-metal interaction dynamics during additive manufacturing resolved by detection of thermallyinduced electron emission. Communications materials (2020) 1:92 DOI:10.1038/s43246-020-00094-y
[9] Salah A. H. Fawzi, Influence of electrical Field on Pulsed Laser beam welding of Stainless Steel (304) Raz N. Arif. Tr. J. Physics, Vol. 23, pp. 959–967 (1999).

Deep penetration of metals by powerful laser radiation: physical nature, dependence on scan speed and strategy for pore-free process

R. D. Seidgazov[1], F. Kh. Mirzade[1], G. G. Gladush[1,2]

1- NRC «Kurchatov Institute», Academician Kurchatov sq. 1, Moscow, 123182 Russia
2- JSC «SSC RF TRINITI» SC «Rosatom», Pushkovykh str. 12, Troitsk, Moscow, 108840 Russia

e-mail: seidgazov@mail.ru, fmirzade@rambler.ru

The phenomenon of deep penetration in laser technologies (including additive ones) manifests itself when the threshold beam power is reached as an elongation of melting zone due to a hollow channel formation (so called "keyhole") and the beam propagation deep into the metal. This opens up the possibility of processing large-thickness parts with increased efficiency and with minimal thermal deformation. Classical idea about the phenomenon nature were formed at the initial stage of technology development under the influence of need to use computational formalism of ablative mechanism of melt displacement by vapor recoil pressure for numerical modeling of technological processes. This approach makes it possible to simulate the keyhole formation for determining temperature fields in a wide range of engineering tasks without precise knowledge of deep penetration nature. On the other hand, such a computational formalism does not allow to predict the formation of pores of hydrodynamic origin, which is very much in demand when creating technologies for responsible products. Solving such problems requires adequate reproduction in calculations of hydrodynamic fields based on a clear understanding of the physical picture of keyhole formation in deep penetration.

The current state of research on various aspects of deep penetration phenomenon is discussed. Investigations [1–7] confirm that the keyhole formation and its dynamic behavior in technological range of laser power occurs with a minor role of evaporation and mainly under the influence of a number of capillary effects (thermocapillary, electrocapillary, excitation of capillary-wave oscillations). Each of the effects can determine the specifics of technological processes in different conditions and stages. A new view of hydrodynamic processes, different from that adopted in engineering, provides tools for solving engineering problems in the form of ratios to determine the conditions for the threshold transition to deep penetration mode, for the cessation of pore formation (to determine the process window), for obtaine physically justified requirements for discretization in computational models, etc. Modern knowledge and developed recommendations open up previously unknown opportunities for technologies development and indicate the directions of further research.

The work was carried out within the state assignment of NRC «Kurchatov Institute».

[1] R.D. Seidgazov, Thermocapillary mechanism of melt displacement during keyhole formation by the laser beam, J Physics D: Appl Phys, 42 No 17, 175501, (2009).
[2] S. Ly, G. Guss, A.M. Rubenchik, et al. Resonance excitation of surface capillary waves to enhance material removal for laser material processing, Scientific Reports, 9:8152 (2019).
[3] R.D. Seidgazov, F.Kh Mirzade, Threshold conditions for thermocapillary transition to deep penetration mode in selective laser melting of metal powder bed, IOP Conf. Ser.: Mater. Sci. Eng. 759, 012023 (2020).
[4] R.D. Seidgazov, F.Kh Mirzade, On the initial stage of the evolution of hydrodynamic parameters during deep penetration of metals by high-power laser radiation, Technical Physics Letters, 48(9):57, (2022).
[5] R.D. Seidgazov, F.Kh Mirzade, Excitation of a capillary wave as a mechanism for the formation of pores in the process of deep penetration by laser radiation, Technical Physics Letters, т. 49, № 6, с. 65 (2023).
[6] R.D. Seidgazov, F.Kh. Mirzade, Keyhole–induced porosity in laser manufacturing processes: formation mechanism and dependence on scan speed, Ch. J. of Mechanical Eng.: Add. Manuf. Frontiers, V.1. N3 (2022).
[7] R.D. Seidgazov, F.Kh Mirzade, Electrocapillary acceleration of molten metal flows during the formation of a deep penetration cavity by powerful laser radiation, Technical Physics Letters, (2025) – in press

Domain structure formation by femtosecond IR laser irradiation in the bulk of strontium barium niobate single crystals

V. Shikhova[1], B. Lisjikh[1], M. Kholodenko[1], A. Akhmatkhanov[1], A. Javakrisna[1], V. Shalunov[1], L. Ivleva[2], V. Shur[1]

1- School of Natural Sciences and Mathematics, Ural Federal University, Ekaterinburg, 620002 Russia
2- Prokhorov General Physics Institute, Russian Academy of Sciences, Moscow, 119991 Russia

e-mail: vera@urfu.ru

At the present time the light-only methods are used for creation of the ferroelectric domain structures with a given geometry by pulse laser irradiation without application of electric field. The most interesting achievement is the ability of the domain switching in the bulk of the crystals using focused NIR femtosecond laser irradiation [1, 2].

The domain structures were created by femtosecond pulse laser irradiation in single crystals of relaxor ferroelectric strontium barium niobate ($Sr_{0.61}Ba_{0.39}Nb_2O_6$) pure and doped by Ni (0.05 wt.% Ni_2O_3). The samples were cut perpendicular to the polar axis. The domain structure of the crystals before irradiation was: 1) polydomain, created during zero-field cooling; 2) single-domain, created by electron beam irradiation or by switching in uniform electric field.

Yb-solid state femtosecond laser TETA-10 (Avesta Project, Russia) with 1030 nm wavelength and 250 fs pulse duration was used for irradiation using 50x objective with NA = 0.65. The focusing was at 200–300 μm from polar surface of the crystals. The energy from 0.07 to 2,1 μJ and number of pulses from 1 to 1000 were used. Irradiation was carried out in matrices (5*5, 8*8 and 10*10) with a distance between domains from 1 to 30 μm. Cherenkov-type second harmonic generation microscopy (SHGM) was used for 3D domain imaging after femtosecond laser irradiation.

It was found that in polydomain crystals at the point of femtosecond laser irradiation the spindle-shaped domains are formed. The length of created domains was up to 100 μm, diameter was about 1.5 μm. The length of domains increases with pulse energy and is almost independent on the number of pulses (N) for N above 25. The distance between adjacent domains does not affect the length of domains, but affects their size: as the distance increases, the radius of the domains decreases.

In single-domain SBN crystals the formation of additional spindle-shaped domains was detected at low irradiation energies, which expand with increasing energy until they merge. The total length of domain structure increased to 250 μm with an increase of the energy and the number of pulses. The radius of the spindle-shaped domains in polydomain crystal is larger than in single-domain crystal.

The obtained results can be used for the creating of 3D nonlinear photonic crystals based on SBN single crystals and in-bulk waveguides with periodical domain structures.

The work was supported by Russian Science Foundation (project 25-22-00231). The equipment of the Ural Center for Share Used «Modern Nanotechnologies» Ural Federal University (Reg. 2968) was used.

[1] Y. Sheng, X. Chen, T. Xu, S. Liu, R. Zhao, W. Krolikowski, Research progress on femtosecond laser poling of ferroelectrics, Photonics 2024, vol. 11 (5), 447 (2024).
[2] S. Wang, S. Liu, D. Liu, N. Wang, R. Zhao, Y. Liu, Z. Li, G. Mao, F. Chen, Y. Sheng, T. Xu, W. Krolikowski, Ferroelectric domain engineering with femtosecond pulses of different wavelengths, Optics Express, vol. 31 (4), 5843–5852, (2023).

Femtosecond laser pulses for investigation of photoluminescence spectra and temporal response of γ-rays scintillators

V. Simonova[1,2], A. Savvin[1], V. Mitrokhin[1], A. Dormidonov[1]

1- Dukhov Automatics Research Institute, Federal State Unitary Enterprise, Suschevskaya st. 22, Moscow, 127055 Russia
2- Prokhorov General Physics Institute of the Russian Academy of Sciences, Vavilova st. 38, GSP-1, Moscow, 119991 Russia

e-mail: vas@optoacoustics.ru

For registration of ultrafast γ-pulses efficient detectors with subnanosecond response time are needed. So, the development of efficient, fast, and robust scintillators for ionizing radiation detection is an important problem of modern high-energy particle physics. Typically, it is difficult to achieve optimal performance and high-speed operation of the scintillator at the same time. A new class of scintillator based on quantum shells opens a way to solve this problem.

In this work we performed a comparative analysis of photoluminescence and radioluminescence properties of traditional plastic, inorganic, and colloidal quantum shells scintillators. Photoluminescence data was collected using a pump generated by a femtosecond Ti:sapphire laser, with emission collected by fiber and directed onto a visible-range spectrometer. Time-resolved emission was registered by a streak camera with 5 ps resolution. Radioluminescence spectra and temporal response of scintillators were investigated under excitation by X-ray pulses with picosecond duration.

Delayed effects in pulsed laser-metal ablation

I. A. Stutchebruhov, A. A.Samokhin, P. A. Pivovarov, S. A. Abrosimov

Prokhorov General Physics Institute of the Russian Academy of Sciences, Vavilova str. 38, Moscow, 119991 Russia

e-mail: st777@kapella.gpi.ru

Delayed effects in pulsed laser ablation can be due to some relaxation processes, e.g., electron-lattice energy relaxation with characteristic time in picoseconds region or mean lifetime for superheated liquids with the minimum value of the same order near spinodal line and very strong temperature dependence. However, the papers [1–3] reported on such delayed effects in laser-metal ablation which cannot be explained with these processes and remaining poorly understood and investigated up to now. We observe many-microseconds delay in material ejection after 70 ps laser pulse (λ = 527 nm) action on metals (an irradiance 10^{13}–10^{14} Wcm^{-2}) using time-of-flight method. Two probe CW laser beams (λ = 655 nm) separated by l_{12} ~ 100 μm distance between their centers at normal direction to the target surface are used. The distance from the surface to the center of the nearest beam is equal to the double beam radius $2R$ ~ 100 μm. Fig. 1 shows that the probe signals for aluminum target after the initial drop (t > 10 μs) almost return to its initial transparent levels (displaced for convenience). However, this behavior is disturbed later with somewhat irregular drops which are supposed to be due to the ejected materials, crossing the beams. Material velocity can be estimated as $v \sim l_{12}/(t_2 - t_1) \sim 10$ m/s. For such velocity values the time t_1 or t_2 seem to be too large because vt_1 exceeds considerably all relevant distances including the crater depth (about 100 μm) if no delayed ejection time is supposed. Taking this into account one obtains for the delay of ejection development from the irradiated zone ~45 μs (a) and ~130 μs (b).

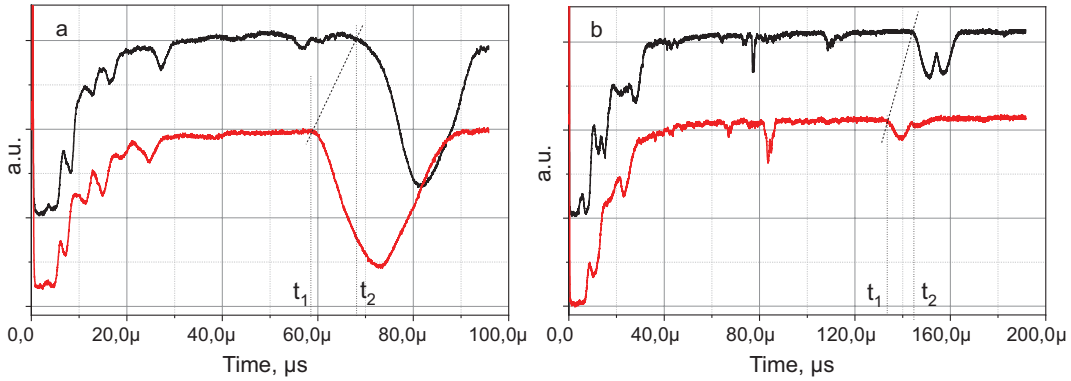

Fig. 1. Probe transmittance signals for Al target at laser intensities $4 \cdot 10^{13}$ W/cm^2 and different (a) and (b) monitoring durations. Lower curves are for the probe beam closer to the target, in case (a) laser strikes to the previously formed crater.

We believe that such long delays are determined not with straightforward manifestation of explosive boiling processes but with subsequent cavitation effect as supposed in [4]. The delayed cavitation pressure pulse is observed recently in theoretical calculation [5]. In any case the delayed effects in laser ablation needs more detailed experimental and theoretical investigations.

[1] A.V. Pakhomov, M.S. Thompson, D.A. Gregory, Laser-induced phase explosions in lead, tin and other elements: microsecond regime and UV-emission, J. Phys. D: Appl. Phys. 36 (2003) 2067
[2] Q. Lu, S.S. Mao, X. Mao, and R.E. Russo, Theory analysis of wavelength dependence of laser-induced phase explosion of silicon, Journal of Applied Physics 104, 083301 (2008); doi: 10.1063/1.2978369
[3] S.I. Kudryashov, S. Paul, K. Lyon, S.D. Allen, Dynamics of laser-induced surface phase explosion in silicon, Appl. Phys. Lett. 98 254102 (2011)
[4] V.I. Vovchenko, S.M. Klimentov, P.A. Pivovarov, A.A. Samokhin, Effect of submillisecond radiation of the erbium laser on absorbing liquid. Bull. Lebedev Phys. Inst. 34 325–328 (2007).
[5] D.S.Ivanov, P.A. Pivovarov , A.A.Samokhin, Pressure generation mechanisms in picosecond laser – metal interaction Mathematica Montesnigri 62, 78-88 (2025).

32nd INTERNATIONAL CONFERENCE
Advanced Laser Technologies
ALT'25

BIOMEDICAL PHOTONICS

Optical response of tetrapyrrolic compounds in the taxonomic analysis of microorganisms

U. Bagrianskaia, B. Yakimov, A. Rubekina, E. Shirshin

Faculty of Physics, M. V. Lomonosov Moscow State University, Moscow, 119991 Russia

e-mail: bagrianskayauy@my.msu.ru

Bacterial infections pose a significant challenge to medicine and public health, accounting for high rates of morbidity and mortality [1]. Rapid and accurate diagnosis of bacterial infections is a priority in modern microbiology and clinical diagnostics. Optical techniques based on the detection and analysis of spectral signatures from endogenous molecular markers of microorganisms represent a promising tool for their analysis [2–4].

In this study, we explore the potential for microbial analysis using endogenous optical response of bacteria with a particular emphasis on the optical properties of porphyrins present in microorganisms. Porphyrins are tetrapyrrolic compounds whose fluorescence emission spectra lie in the 550–750 nm range [5]. In biological systems, porphyrins play a pivotal role in respiratory processes and redox reactions, participating in the biosynthesis of heme and other metalloporphyrins. In microorganisms, porphyrins may serve both as intermediates in the heme biosynthetic pathway and as end products accumulating within cells as a consequence of specific metabolic characteristics.

Endogenous fluorescence of microorganisms, driven by the accumulation of porphyrins and their derivatives (such as protoporphyrin IX, coproporphyrin, and others), is potentially highly specific and may be leveraged for the taxonomic analysis of microbes. In this work, we demonstrate the distinct patterns of porphyrin derivative accumulation in bacteria and assess the feasibility of species- and genus-level diagnostics based on endogenous tetrapyrrole fluorescence and resonance Raman scattering spectra.

[1] Ikuta, Kevin S et al., Global mortality associated with 33 bacterial pathogens in 2019: a systematic analysis for the Global Burden of Disease Study, The Lancet, vol. 400, issue 10369, pp. 2221–2248, (2022).
[2] Anandh Sundaramoorthy, Ganesan Bharanidharan, Aruna Prakasarao, Singaravelu Ganesan. Characterization and classification of pathogenic bacteria using native fluorescence and spectral deconvolution. Journal of Biophotonics, vol. 17, issue 7, (2024).
[3] Du, R.; Yang, D.; Yin, X. Rapid Detection of Three Common Bacteria Based on Fluorescence Spectroscopy. Sensors, vol. 22, issue 3, p. 1168, (2022).
[4] Ho, CS., Jean, N., Hogan, C.A. et al. Rapid identification of pathogenic bacteria using Raman spectroscopy and deep learning. Nat Commun vol. 10, p. 4927, (2019).
[5] Fernanda Ricchelli, Photophysical properties of porphyrins in biological membranes, Journal of Photochemistry and Photobiology B: Biology, vol. 29, issues 2-3, (1995).

Laser-induced changes in reflection, absorption and transmission spectra of blood-containing tissues

A. V. Belikov[1], V. Yu. Chuchin[1,2], A. A. Masharskaya[1,2]

1- ITMO University, Kronverksky Pr. 49, Saint Petersburg, 197101 Russia
2- NPP VOLO LLC, 17th line V.O. 4-6, Saint Petersburg, 199034 Russia

e-mail: avbelikov@gmail.com

The possibilities of modern laser medicine can be significantly expanded through the use of laser multi-wave technologies, which involve the use of laser radiation with one wavelength to create optimal conditions for the effect of radiation with another wavelength on biological tissue. The optimal result in this case can be achieved by monitoring the optical properties of the biotissue during laser exposure with one wavelength and controlling the parameters of laser radiation with another wavelength when any optical characteristic of the biotissue reaches the optimal value for laser action at this wavelength, that is, when used in a laser feedback system. In some cases, for example in the treatment of vascular diseases of the skin, the treatment of blood-containing tissues is of particular interest. It is obvious that in the context of creating such technologies and systems, the study of laser-induced changes in reflection, absorption and transmission spectrum of blood-containing tissues is relevant.

In the theoretical part of the report, we will present an original optical numerical model of human blood and skin. In particular, the results of numerical modeling using the Monte Carlo method will be considered of the effect of human blood oxygenation and methemoglobin content on the spectra of its reflection, absorption and transmission of light in the wavelength range of 400–1100 nm. The motivation for using lasers with wavelengths of 450 and 980 nm to affect blood-filled biological tissues will be explained. In the context of single- or dual-wave exposure of blood-filled tissue to radiation from these lasers, the dynamics of reflection, absorption, and transmission of light by blood at wavelengths of 450 and 980 nm will be considered, depending on its oxygenation and methemoglobin content.

In the experimental part of the report changes in the reflectance spectrum of human blood in vitro when exposed by laser radiation with a wavelength of 450 or 980 nm will be demonstrated and, within the framework of the developed optical numerical model of human blood, substantiated [1]. These changes have characteristic features that can be associated with changes in blood oxygen saturation. It has been demonstrated that the greatest specific change in blood oxygen saturation occurs when exposed to laser radiation with a wavelength of 450 nm and not with a wavelength of 980 nm, which is a consequence of higher absorption of blue spectral range radiation by hemoglobin. The relationship between the reflection coefficient of human skin at a wavelength of 980 nm and its temperature during exposure to laser radiation of the same wavelength has been measured in an in vivo experiment [2]. Association of the observed alteration in the reflection coefficient at the wavelength of 980 nm to the conversion of skin blood hemoglobin into methemoglobin is demonstrated.

In vivo experiments measuring the reflection spectra of animal's skin (rabbit ear) before and after laser exposure at 450 nm and 980 nm demonstrated that immediately after laser exposure, the reflection of the animal's skin in the 400–800 nm range increases but drop on 600±10 nm. The most significant change of reflection at 600±10 nm was recorded under dual-wavelength laser exposure first with 980 nm radiation, followed immediately by 450 nm radiation.

The results of this research may find application in the development of novel laser systems with feedback mechanisms and technologies for treating dermatological conditions, including telangiectasias.

[1] Chuchin V.Y., Masharskaya A.A., Belikov A.V. Investigation of Changes in the Reflection Spectrum of Human Blood When Exposed to Laser Radiation With Wavelengths of 450 or 980 nm, Journal of Biophotonics, e20240025 (2024).
[2] Belikov A.V., Chuchin V.Y. Investigation of the Influence of Thermally Induced Methemoglobin on the Human Skin Optical Reflection, Journal of Biomedical Photonics & Engineering, Vol. 10, No. 2, p. 020303 (2024).

Optimization of ICG fluorescence imaging

Y. Belozerov, I. Turchin

A. V. Gaponov-Grekhov Institute of Applied Physics of the Russian Academy of Sciences,
Ul'yanov Street 46, Nizhny Novgorod, 603950 Russia

e-mail: u.belozerov@ipfran.ru

Fluorescence imaging with indocyanine green (ICG) is a powerful tool for evaluating blood supply in tissues and organs, identifying tumor boundaries, and detecting sentinel lymph nodes [1]. ICG is particularly valuable due to its spectral properties, with excitation and emission peaks within the biological tissue transparency window, combined with low toxicity and clinical versatility.

While numerous commercial and experimental ICG imaging systems exist, their performance varies significantly in terms of size, cost, and image quality [2]. The key performance parameter is contrast, defined as the ratio of fluorescence signal to background signal originating from optical system imperfections and tissue autofluorescence [3]. Despite widespread use of ICG imaging, systematic approaches to contrast optimization remain limited, and existing research findings lack comprehensive studies [4–6].

This work presents an experimental and numerical evaluation of ICG visualization contrast as a function of optical component parameters, including excitation source spectra, excitation and emission filters spectral properties, tissue autofluorescence, and lens numerical aperture.

The results demonstrate that an optimal optical imaging system configuration combines specifically arranged interference and absorption emission filters with an interference excitation filter. The autofluorescence background shows a monotonic decrease as the excitation wavelength is increased from 650 nm to 790 nm. In the proposed configuration, backscattered excitation light propagating through detection optics becomes negligible, while autofluorescence remains the dominant background contribution. Maximum contrast is achieved at 780 nm excitation wavelength, optimally balancing autofluorescence, stray light, and ICG fluorescence signal.

The study provides a high-contrast ICG imaging solution and establishes a modeling framework adaptable for optimizing fluorescence imaging with other contrast agents.

[1] K. Kim, J.-H. Park, H.-J. Kim, and S.-Y. Jeong, Identification of metastatic lymph nodes using indocyanine green fluorescence imaging, Cancers, vol. 15, no. 7, p. 1964, (2023).
[2] A. V. DSouza, H. Lin, E. R. Henderson, K. S. Samkoe, and B. W. Pogue, Review of fluorescence guided surgery systems: identification of key performance capabilities beyond indocyanine green imaging, Journal of Biomedical Optics, vol. 21, no. 8, p. 080901, (2016).
[3] Y. A. Khristoforova, I. A. Bratchenko, D. N. Artemyev, O. O. Myakinin, A. A. Moryatov, S. V. Kozlov, and V. P. Zakharov, Method of autofluorescence diagnostics of skin neoplasms in the near infrared region, Journal of Biomedical Photonics & Engineering, vol. 1, no. 3, pp. 186–192, (2015).
[4] B. Zhu, H. B. Manning, M. J. Miller, and E. M. Sevick-Muraca, Reduction of excitation light leakage to improve near-infrared fluorescence imaging for tissue surface and deep tissue imaging, Medical Physics, vol. 37, no. 11, pp. 5961–5970, (2010).
[5] K. Sasagawa, A. Kiyose, M. Haruta, T. Noda, T. Tokuda, and J. Ohta, Highly sensitive lens-free fluorescence imaging device enabled by a complementary combination of interference and absorption filters, Biomedical Optics Express, vol. 9, no. 9, pp. 4329–4344, (2018).
[6] B. Zhu and E. M. Sevick-Muraca, Minimizing excitation light leakage and maximizing measurement sensitivity for molecular imaging with near-infrared fluorescence, Journal of Innovative Optical Health Sciences, vol. 4, no. 3, pp. 301–307, (2011).

Multifunctional nanostructures with laser-switchable properties and tunable bioactivity window for photopharmacology

G. Bikbaeva[1], A. Pilip[2], A. Egorova[3], I. Kolesnikov[4], D. Pankin[4], K. Laptinskiy[5,6], A. Vervald[6], T. Dolenko[6], A. Manshina[1]

1- Institute of Chemistry, St. Petersburg State University, St. Petersburg, 198504 Russia
2- St. Petersburg Federal Research Center of the Russian Academy of Sciences (SPC RAS), Scientific Research Centre for Ecological Safety of the Russian Academy of Sciences, St. Petersburg, 197110 Russia
3- St. Petersburg State Technological Institute (Technical University), St. Petersburg, 190013 Russia
4- Center for Optical and Laser Materials Research, St. Petersburg State University, St. Petersburg, 198504 Russia
5- Faculty of Physics, M. V. Lomonosov Moscow State University, Moscow, 119991 Russia
6- Skobeltsyn Institute of Nuclear Physics, M.V. Lomonosov Moscow State University (SINP MSU), Moscow, 119991 Russia

e-mail: bikbaevagi@yandex.ru

The design of hybrid nanostructures through the combination of various components represents a promising strategy for creating next-generation functional materials [1]. In particular, incorporating photoactive fragments into nanomaterials enables remote control of their properties using laser irradiation, which is especially valuable for photopharmacology.

This study presents unique nanohybrides based on carbon quantum dots with various functional groups on the surface and photoactive molecules with an inhibitory effect on the enzyme butyrylcholinesterase.

The study of the obtained hybrids with luminescent spectroscopy, IR spectroscopy and IPC–micro analysis of neurotoxins revealed a pronounced effect of laser radiation on the optical and biological properties of new objects. Hybrids demonstrate not only properties of initial components – luminescence and photo-switchable butyrylcholinesterase inhibition, but also strong effect of carrier nature on bioactivity, and photo-switchable effect on luminescence properties [2].

Thus, nanohybrid materials demonstrate combination of important functions for photopharmacology: biological activity and its strong changes as a result of laser irradiation, luminescence as an indicator of the state of bioactivity and the possibility of spatial localization on the surface.

This work was supported by RSF project 22-13-00082-P. Authors are grateful to "Centre for optical and laser materials research", Research park of Saint Petersburg State University for technical support. Authors are grateful to Interdisciplinary scientific and educational school of Lomonosov Moscow state university "Photonic and quantum technologies. Digital medicine".

[1] F. Cardano, M. Frasconi, S. Giordani, Photo-Responsive Graphene and Carbon Nanotubes to Control and Tackle Biological Systems, Front. Chem. 6, (2018).
[2] G. Bikbaeva, et al, All-in-One Photoactivated Inhibition of Butyrylcholinesterase Combined with Luminescence as an Activation and Localization Indicator: Carbon Quantum Dots@Phosphonate Hybrids, Nanomaterials 13, 2409 (2023).

Quantitative measurements of concentration and counting of foreign objects in blood using photoacoustic methods

D. Bratashov[1,2]

1- Saratov State University, Astrakhanskaya 83, Saratov, Russia
2- MIPT, Institutsky per. 9, Dolgoprudny, Russia

e-mail: bratashovdn@info.sgu.ru

Biomedical photoacoustics is a relatively new imaging technique for biomedical research and diagnostics that provides deep imaging with strong natural contrast based on optical adsorption. It typically has two modalities – linear with a signal nearly proportional to the optical adsorption of the chromophore and the chromophore concentration, and nonlinear with a very strong signal associated with phase transformations that provide strong signals. Modern photoacoustic measurement techniques allow direct detection of very rare objects in the bloodstream that are difficult to detect using conventional flow cytometry methods. It also allows spectral measurements, distinguishing objects by variations in optical spectra and even directly measuring the concentration of natural chromophores of interest. In this presentation, we discuss the required laser parameters that allow reliable detection of foreign objects in deep large vessels using *in vivo* photoacoustic flow cytometry. We also discuss the problems and some results of spectral measurements of metabolites in blood *in vivo*, the parameters of the processes taking place and data processing to obtain correct concentrations from a relatively small number of measurements, which allows for direct non-invasive measurements of the concentration of the metabolite of interest, and we also discuss some of the complexities of these processes.

The study was partially supported by the grant of the Russian Science Foundation No. 25-19-00828, https://rscf.ru/project/25-19-00828/.

Optical navigation in endoscopic surgery

G. S. Budylin[1], N. R. Rovnyagina[1], E. E. Nikonova[1], P. V. Dyakonov[1], V. A. Petrov[1], D. A. Davydov[1], A. S. Kochmareva[2], A. Yu. Turkina[2], E. B. Kalinskiy[3], K. M. Azarkin[3], B. D. Raikov[3], A. V. Lychagin[3], P. S. Timashev[4], E. A. Shirshin[1,5]

1- Laboratory of Clinical Biophotonics, Sechenov First Moscow State Medical University, Moscow, Russia
2- Therapeutic dentistry department, Sechenov First Moscow State Medical University Moscow, Russia
3- Department of Trauma, Orthopedics and Disaster Surgery, Sechenov First Moscow State Medical University, Moscow, Russia
4- Institute for Regenerative Medicine, Sechenov First Moscow State Medical University, Moscow, Russia
5- Faculty of Physics, M. V. Lomonosov Moscow State University, Moscow, Russia

e-mail: budylin_g_s@staff.sechenov.ru

An urgent challenge in the field of biophotonics is the development of reliable, real-time methods for objectively assessing tissue conditions during surgery. Optical technologies are increasingly used to address this need, with successful applications in various medical fields including identification of cancerous tumor margins, guiding tissue resection, and improving diagnostic accuracy [1]. This study focuses on practical problems in orthopedics and dentistry: evaluating the condition of knee joint tissues during arthroscopy and distinguishing between affected and infected dentin during the treatment of dental caries.

Early diagnosis of osteoarthritis (OA) is essential to prevent permanent joint damage, especially since cartilage has a limited ability to heal [2]. Traditional imaging methods often fail to detect the early biochemical and structural changes that occur in OA. In contrast, optical spectroscopy techniques – infrared (IR) and Raman spectroscopy – offer powerful tools for real-time assessment of cartilage during arthroscopy. Our research demonstrates that diffuse reflectance spectroscopy (DRS) in NIR (810–1050 nm) and MIR (1100–1800 nm) spectral ranges effectively discriminates between late-stage (ICRS grade IV) and intermediate (grades II-III) degeneration. Raman spectroscopy provides complementary diagnostic value, distinguishing advanced degeneration (ICRS IV) from earlier stages, and also identifies initial degradation (ICRS II). Crucially, we have established correlations between optical parameters and mechanical properties that underscores water content's fundamental role in their formation.

Our studies also explored fluorescence spectra of dentin excited at visible wavelength range to identify characteristic spectral features distinguishing healthy, altered, and caries-infected zones determined using dentist evaluation and further histology. Fluorescence response strongly depends on the excitation wavelength, with red shift in emission spectra observed across all carious dentin types. Spectral differences were especially pronounced between CAD (caries-affected dentin) and CID (caries-infected dentin), with widening and red-shifting of fluorescence peaks, suggesting matrix alterations. While traditional diagnostic devices focus on porphyrin peaks from bacterial activity [3], our results indicate that structural changes alone can also enhance red fluorescence, even in the absence of bacteria. These findings support the development of optical tools to enhance navigation and decision-making in minimally invasive dental procedures, potentially adaptable to endoscopic surgical environments.

This research work was supported by the Academic leadership program Priority 2030 proposed by Federal State Autonomous Educational Institution of Higher Education I. M. Sechenov First Moscow State Medical University of the Ministry of Health of the Russian Federation (Sechenov University).

[1] Shirshin, E. A., B. P. Yakimov, G. S. Budylin, N. V. Zlobina, D. A. Davydov, A. G. Armaganov, V. V. Fadeev, N. N. Sysoev, and A. A. Kamalov. Biomedical photonics for intraoperative diagnostics: review of capabilities and clinical applications. Moscow University Physics Bulletin 77, no. 6 (2022): 777-800.
[2] Mahmoudian, A., Lohmander, L. S., Mobasheri, A., Englund, M., & Luyten, F. P. (2021). Early-stage symptomatic osteoarthritis of the knee – time for action. Nature Reviews Rheumatology, 17(10), 621–632.
[3] Lennon, Á. M., Brune, L., Techert, S., & Buchalla, W. (2023). Fluorescence spectroscopy shows porphyrins produced by cultured oral bacteria differ depending on composition of growth media. Caries research, 57(1), 74–86.

Multiphoton tools for quantitative imaging of reactive oxygen species (ROS) in vivo

A. S. Chebotarev[1], G. P. Linovsky[1,3], A. B. Fedotov[1–3], A. G. Shokhina[4,5], E. S. Potekhina[4,5], D. S. Bilan[6], V. V. Belousov[3–6], A. A. Lanin[1–3]

1- Physics Department, M. V. Lomonosov Moscow State University, Russia
2- Russian Quantum Center (RQC), Skolkovo, Russia
3- Life Improvement by Future Technologies (LIFT) Center, Skolkovo, Russia
4- Federal Center of Brain Research and Neurotechnologies, Federal Medical-Biological Agency, Russia
5- Pirogov Russian National Research Medical University, Russia
6- M. M. Shemyakin and Yu. A. Ovchinnikov Institute of Bioorganic Chemistry, Russian Academy of Science, Russia

e-mail: lanin@physics.msu.ru, a.lanin@lift.center

Redox reactions in living animals, proposed by a plentiful number of biological molecules, contribute greatly to intra- and inter-cell signaling processes. To real-time monitoring of the specific regulators in organisms, genetically encoded fluorescent indicators (GEFIs), which fused to proteins of interest, have provided significant advances [1]. Two- and three-photon excitation fluorescence (2PEF and 3PEF) microscopy grant the high contrast imaging with subcellular resolution of fluorescent agents from the deep layers of scattering tissue, but its realization faces difficulties with continuous ratiometric readout. To increase the depth of visualization, temporal and spatial resolution, brightness and contrast of the image it is necessary to investigate nonlinear optical processes leading to signal generation.

We present a laser optical toolbox integrated with a dual-channel 2PEF microscopy for the investigation of nonlinear optical properties of fluorescent indicators and its potential for ratiometric two-photon imaging. We provided accurate nonlinear transformation of low power pulses in a photonic crystal fiber (PCF) to an ultrashort sub-octave-spanning supercontinuum (SC) generation and its amplitude and phase tuning to produce an appropriate source for both TPA spectra measurements and ratiometric dual-channel 2PEF imaging [2, 3]. Such a laser source was exploited for quantitative TPA spectra measurements of the palette of redox and metabolism cell status sensors including indicators of H_2O_2, HyPer3, HyPer7 and HyPerFLEX-family, the ratios of the oxidized and reduced forms of NAD+/NADH and GSSH/GSH, RexYFP and Grx1-roGFP2, hypohalous acids and intracellular pH-level, Hypocrates https://www.zotero.org/google-docs/?qaPy7t and SypHer3s [2–4]. Developed alternating interrogation of the reduced and oxidized forms by a pair of laser pulses synchronized with the microscope imaging build up allowed the recording of H_2O_2 dynamics at up to one frame per second. We visualized the HyPer7-expressing neurons at depths up to 600 μm below the mouse brain surface by two-photon excitation microscopy in vivo in an anesthetized mouse [5, 6].

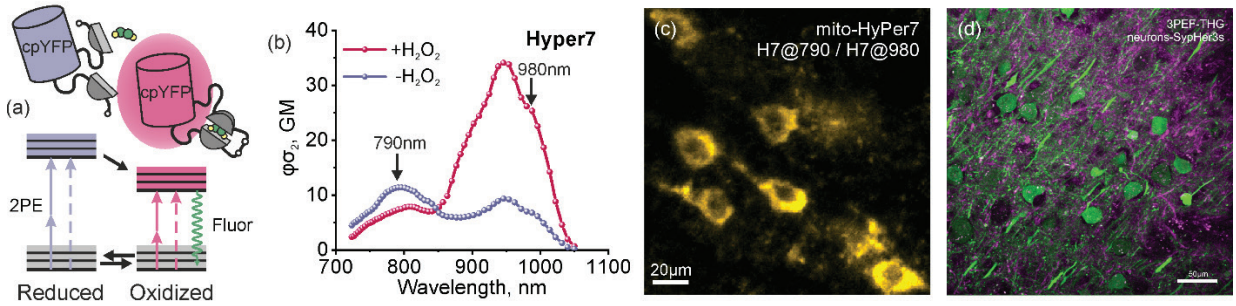

Fig. 1. (a) The concept of GEFIs based on cpFP. (b) TPA spectrum of HyPer7 protein, a sensor of hydrogen peroxide. (c) Dual-channel HyPer7 imaging in neurons ex vivo. (d) 3PEF imaging pyramidal neurons with SypHer3s.

[1] A. I. Kostyuk et al, Int. Journ. Mol. Sci. 21, 8164 (2020).
[2] A. S. Chebotarev et al, Journ Ram. Spec. 52(9), 1552–1560 (2021).
[3] A. S. Chebotarev et al, Appl. Phys. Lett., 124, 24 (2024).
[4] E. S. Potekhina et al, Nat. Chem. Biol, (2025) accepted
[5] A. S. Chebotarev et al, Journ. Biophot. 14, e202000301 (2021).
[6] A. S. Chebotarev et al, Sens. Act.: B. Chem 410, 135646 (2024).

Terahertz spectroscopy of blood serum for traumatic brain injury diagnosis

O. P. Cherkasova[1,2], D. A. Vrazhnov[3], Yu. V. Kistenev[3], N. A. Nikolaev[1]

1- Institute of Automation and Electrometry, Siberian Branch of the Russian Academy of Sciences, Academician Koptyug Ave. 1, Novosibirsk, 630090 Russia
2- Novosibirsk State Technical University, K. Marks Ave. 20, Novosibirsk, 630073 Russia
3- Laboratory of Laser Molecular Imaging and Machine Learning, Tomsk State University, Lenin Ave. 36, Tomsk, 634050 Russia

e-mail: o.p.cherkasova@gmail.com

Traumatic brain injury (TBI) has a global annual incidence of more than 10 million new cases [1]. Accurate recognition of mild to moderate TBI is a bottleneck for current diagnostic technologies in neurosurgery. Widely used neuroimaging techniques are less effective in detecting mild TBI, and there are still some technical challenges regarding scanning protocols, analysis techniques, and the use of different contrast agents [2]. Analyzing biomarkers that may be altered in brain injury using omics technologies is time-consuming and expensive [3]. Also, there is a suggestion that traumatic brain injury may promote the development of glioblastoma multiforme, one of the most aggressive types of cancer with a poor prognosis [4]. Because TBI has long-term effects, early diagnosis is crucial for treatment and prognosis.

In this work, we demonstrate an approach to TBI diagnosis through blood serum analysis by terahertz time-domain spectroscopy and machine learning algorithms. At first, we developed and tested algorithms during the experiments on mice, and then we applied them to analyze the blood plasma of human patients with TBI. The blood was measured in 3D-printed single-use cuvettes in the range of 0.3–1.7 THz using the T-SPEC spectrometer by TeraVil Ltd. [5–7].

Spectral analysis included two dimensionality reduction algorithms (principal component analysis and t-distributed stochastic neighbor embedding) and three classification algorithms (support vector machine, random forest, and extreme gradient boosting machine). Constructed prediction data models were verified using 10-fold cross-validation, the receiver operational characteristic curve combined with area under the curve analysis, and quality metrics like sensitivity, specificity, and accuracy. The proposed machine learning pipeline allowed for distinguishing the TBI group with quality metrics values above 95%. Therefore, the suggested method, which involves terahertz time-domain spectroscopy of blood serum and subsequent machine learning analysis, can aid in the differentiation of traumatic brain injury.

The work was partially carried out within the state assignment of IA&E SB RAS (FWNG-2024-0025) and was partially funded by the Ministry of Science and Higher Education of the Russian Federation grant # 075-15-2024-557 dated 04/25/2024 (data analysis by D.V. and Yu.K.).

[1] J. Ghajar, Traumatic brain injury, Lancet, vol. 356, pp. 923–929 (2000).
[2] M. F. Mendez, E. M. Owens, G. R. Berenji et al., Mild traumatic brain injury from primary blast vs. blunt forces: Post-concussion consequences and functional neuroimaging, NeuroRehabilitation, vol. 32(2), pp. 397–407 (2013).
[3] X. Dai, L. Shen, Advances and Trends in Omics Technology Development, Front. Med., vol. 9, p. 911861 (2022).
[4] Y. L. Lan, Y. Zhu, G. Chen et al., The Promoting Effect of Traumatic Brain Injury on the Incidence and Progression of Glioma: A Review of Clinical and Experimental Research, J. Inflamm. Res., vol. 14, pp. 3707–3720 (2021).
[5] D. Vrazhnov, A. Knyazkova et al, Analysis of Mouse Blood Serum in the Dynamics of U87 Glioblastoma by Terahertz Spectroscopy and Machine Learning, Appl. Sci., vol. 12, 10533 (2022).
[6] D. Vrazhnov, D.A. Ovchinnikova et al, Terahertz Time-Domain Spectroscopy of Blood Serum for Differentiation of Glioblastoma and Traumatic Brain Injury, Appl. Sci., vol. 14, 2872 (2024).
[7] O. Cherkasova, D. Vrazhnov et al, Terahertz Time-Domain Spectroscopy of Glioma Patient Blood Plasma: Diagnosis and Treatment, Appl. Sci., vol. 13, 5434 (2023).

Luminescent Au-atomic nanoclusters for detection, imaging, and photodynamic inactivation of planktonic bacteria and biofilms

D. Chumakov[1], S. Evstigneeva[1], N. Khlebtsov[1,2]

1- Institute of Biochemistry and Physiology of Plants and Microorganisms, "Saratov Scientific Centre of the Russian Academy of Sciences", Prospekt Entuziastov 13, Saratov, 410049 Russia
2- Saratov State University, Ulitsa Astrakhanskaya 83, Saratov, 410012 Russia

e-mail: khlebtsov@ibppm.ru

Gold nanoclusters (NCs) consist of a small number of atoms and exhibit strong fluorescence due to intraband transitions between discrete, size-dependent energy levels. In a sense, NCs are artificial multi-electron atoms, occupying an intermediate position between gold atoms and plasmonic nanoparticles. Thanks to protein or biocompatible stabilizers, these NCs are water-soluble and promising for various biomedical applications. Here, we discuss two types of NCs. First, we consider highly fluorescent AuNCs stabilized by bovine serum albumin (BSA) and conjugated with human antistaphylococcal immunoglobulin (antiSAIgG) and the photodynamic (PD) synthesizer Photosens™ (PS) to form Au–BSA–antiSAIgG–PS complexes. Along with fluorescence, these complexes are capable of selectively binding to S. aureus and photodynamically killing them even in mixed bacterial cultures [1].

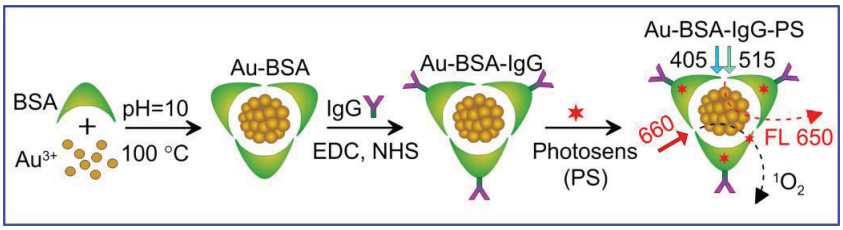

Fig. 1. Scheme for the preparation of Au–BSA–IgG–PS complexes and their fluorescent and PD properties under (405, 515 nm) and 660 nm excitation, respectively [1]. Note that 405 and 515 nm correspond to the excitation spectrum maxima.

Next, we discuss the problem of fluorescent detection of biofilms that colonize chronic wounds or surfaces of medical devices. It is worth noting that bacteria naturally exist in the form of biofilms, rather than in laboratory suspensions. We have found that fluorescent glutathione-stabilized gold nanoclusters (GSH-AuNCs) are capable of selectively binding to the components of the extracellular matrix of Gram-negative and Gram-positive bacterial biofilms [2]. Importantly, GSH-AuNCs do not contain targeting molecules and do not stain planktonic bacteria. According to molecular docking, GSH-AuNCs show a high affinity to amyloid proteins of the biofilm matrix. The fluorescent limit of biofilm detection is 1.7×10^5 CFU/mL – one order lower than with crystal violet assay.

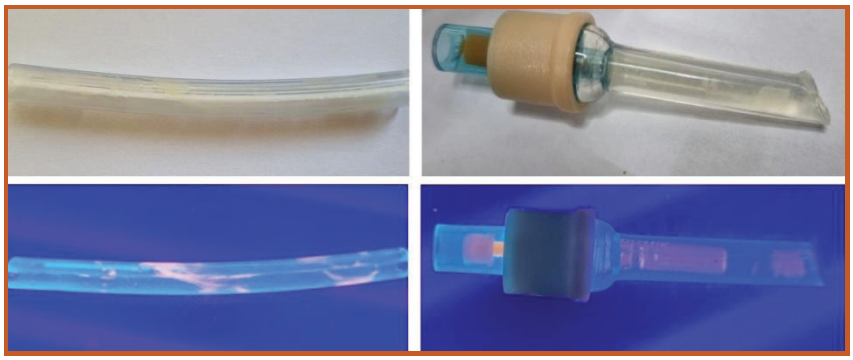

Fig. 2. Detection of biofilm formation on urinary catheter surfaces [2].

[1] B. Khlebtsov, E. Tuchina, V. Tuchin, N. Khlebtsov. Multifunctional Au nanoclusters for targeted bioimaging and enhanced photodynamic inactivation of Staphylococcus aureus, RSC Advances, vol. 5, pp. 61639–61649 (2015).
[2] S. Evstigneeva, D. Chumakov, R. Tumskiy, B. Khlebtsov, N. Khlebtsov, Detection and imaging of bacterial biofilms with glutathione-stabilized gold nanoclusters, Talanta, vol. 264, p. 124773 (1–13) (2023).

Time-frequency analysis of microcirculation: from single capillary blood flow to tissue perfusion

V. Dremin[1,2]

1- Research & Development Center of Biomedical Photonics, Orel State University, Orel, 302026 Russia
2- Aston Institute of Photonic Technologies, Aston University, Birmingham B4 7ET, UK

e-mail: viktor.dremin@bmecenter.ru

The precise evaluation of blood microcirculation is fundamental for understanding tissue metabolism, diagnosing vascular disorders, and assessing therapeutic efficacy. Over recent decades, a spectrum of optical techniques has emerged to study microvascular blood flow across spatial and temporal scales. This work traces the evolution of time-frequency analysis (in particular, wavelet analysis) in microcirculation monitoring, from high-resolution videocapillaroscopy (VCS) to laser Doppler flowmetry (LDF) and laser speckle contrast imaging (LSCI), highlighting their complementary capabilities in advancing microcirculatory diagnostics.

Videocapillaroscopy represents a pivotal method for visualizing individual capillaries *in vivo*, allowing direct observation and measurement of red blood cell (RBC) velocity within distinct segments of the capillary loop. Recent high-speed VCS studies have demonstrated that the blood flow velocity in the arterial portion of the capillary is approximately twice that in the venous portion, with both exhibiting coherent oscillations. Time-frequency analysis, particularly wavelet coherence, reveals synchronization in these oscillations, suggesting systemic regulatory mechanisms of perfusion at the micro-level [1]. Moreover, VCS and corresponding time-frequency analysis have been employed to validate the physiological basis of complex LDF signals and uncover phenomena such as reverse capillary flow during occlusion tests [2].

Building on these micro-level insights, LDF has become a cornerstone in assessing perfusion at the tissue level. The technique is based on the Doppler shift of laser light scattered by moving RBCs and offers high temporal resolution. However, LDF signals often integrate responses from various vascular beds, making signal interpretation challenging. Time-frequency decomposition, using wavelet transforms, enables the identification of distinct frequency bands associated with physiological regulatory mechanisms: cardiac (0.6–2 Hz), respiratory (0.145–0.6 Hz), myogenic (0.05–0.15 Hz), neurogenic (0.02–0.05 Hz), and endothelial (0.005–0.02 Hz) activities. This decomposition has proven valuable in detecting angiospastic disorders and diabetic microvascular complications, particularly when used with functional tests [3, 4].

Further advancing spatial coverage and diagnostic power, LSCI provides full-field, non-scanning imaging of perfusion with high spatial and temporal resolutions. While rooted in the same optical principles as LDF, LSCI allows visualization of dynamic blood flow patterns across wide tissue areas. Recent studies demonstrate that temporal LSCI signals contain the same physiological oscillations as LDF, making them amenable to similar time-frequency analysis frameworks [5]. Moreover, LSCI's capability to map regional variations in oscillatory patterns is particularly valuable in cerebral and skin microcirculation research, providing new opportunities for spatially resolved diagnostics [6].

Together, the synergy of VCS, LDF, and LSCI, interpreted through time-frequency analyses, offers a comprehensive view of microcirculatory dynamics: from individual capillaries to entire tissue beds.

This work was supported by the grant of the Russian Federation Government (075-15-2025-011).

[1] V. Dremin et al., Blood flow dynamics in the arterial and venous parts of the capillary, J. Biomech. 179, 112482 (2025).
[2] V. Dremin et al., Dynamic evaluation of blood flow microcirculation by combined use of the laser Doppler flowmetry and high-speed videocapillaroscopy methods, J. Biophotonics 12(6), e201800317 (2019).
[3] I. Makovik et al., Detection of angiospastic disorders in the microcirculatory bed using laser diagnostics technologies, J. Innov. Opt. Health Sci. 11(1), 1750016 (2018).
[4] I. Mizeva et al., Spectral analysis of the blood flow in the foot microvascular bed during thermal testing in patients with diabetes mellitus, Microvasc. Res. 120, 13–20 (2018).
[5] I. Mizeva et al., Wavelet analysis of the temporal dynamics of the laser speckle contrast in human skin, IEEE Trans. Biomed. Eng. 67(7), 1882–1889 (2019).
[6] N. Golubova et al., Time-frequency analysis of laser speckle contrast for transcranial assessment of cerebral blood flow, Biomed. Signal Process. Control. 85, 104969 (2023).

Wearable optical analyzers in clinical and space medicine

A. Dunaev, Y. Loktionova, V. Yanushin, E. Zharkikh

Research & Development Center of Biomedical Photonics, Orel State University, Orel, 302026 Russia

e-mail: dunaev@bmecenter.ru

Researchers have focused on the microcirculatory-tissue system (MTS) for many decades due to its involvement in vital bodily processes. Two main methods of studying the MTS are laser Doppler flowmetry (LDF) and fluorescence spectroscopy (FS). However, a number of factors prevent the wider implementation of these technologies in the clinic, the main ones being the size of the equipment and the use of optical fibers, which makes them highly sensitive to motion artifacts. One of the first developments of wearable optical device is the «LAZMA PF» analyzer (LAZMA Ltd, Russia), which enables the study of the microvasculature and oxidative metabolism of biological tissues [1]. The design features of these devices allow to record index of microcirculation (perfusion) and NADH fluorescence intensity with less sensitivity to motion artifacts, larger diagnostic volume and approximately the same variability of measurement results compared to stationary devices [2]. The purpose of this work is to demonstrate the successful use of these devices in clinical and space medicine.

Analyzers were used in the form of distributed system (of 2 or 4 devices) in upper and lower extremities in various fields of medicine – endocrinology, cardiology (arterial hypertension), rehabilitation (long covid), physiotherapy (hatha yoga breathing exercises, interval hypoxic training), sports and space [1–4] medicine. The time of the MTS parameters registration (I_m – index of microcirculation, A_{NADH} – normalized amplitude of the biotissue coenzyme NADH) averaged for 10 min.

Studies in patients with diabetes mellitus have shown a decrease in I_m and nutritive blood flow in the lower extremities and an increase in the upper extremities. The results indicate the body's attempts to compensate for microcirculation disorders in the upper extremities. Studies of women with pregestational diabetes revealed a decrease in the oscillatory activity of MTS in patients and an increase in A_{NADH}. Patients with post-COVID syndrome had reduced values of I_m and nutritive blood flow, as well as increased oscillatory activity of blood flow. In the study of the effect of hypo- and hyperventilation yoga breathing exercises on the parameters of peripheral blood flow, a correlation was found between the parameters of blood microcirculation and gas analysis during free breathing and hypoventilation. The technique has shown promise in studying various processes associated with centralised circulation, such as cardiac surgery and extreme breath-holding. Also, the use of wearable devices during the year-long isolation experiment showed a deterioration in the oscillatory activity of microvessels in the legs with a decrease in nutritive blood flow as a result of hypodynamics. For the first time a technique was developed to measure the microcirculatory bed and oxidative metabolism of biotissues of cosmonauts' limbs during the period of acute adaptation to microgravity conditions and readaptation after completion of a long-term space flight. The results of this study confirmed the redistribution of circulating blood volume to the upper part of the body during the first days of space flight and the normalization of blood flow on the 6th day of space flight. These technologies make it possible to evaluate different adaptation mechanisms in cosmonauts during a long flight (to evaluate the ratio of the nutritional and shunt parts of the microcirculatory bed).

Thus, the data on the state of the microcirculatory bed and the oxidative metabolism of biotissues, obtained using wearable multimodal optical analyzers, allow a more comprehensive and reliable assessment of the relationship and dynamics of oxygen utilization by tissues.

The study was supported by the grant of the Russian Federation Government no. 075-15-2025-011.

[1] A.V. Dunaev. Wearable devices for multimodal optical diagnostics of microcirculatory-tissue systems: application experience in the clinic and space, Journal of Biomedical Photonics & Engineering, 9(2), (2023).
[2] Y.I. Loktionova, E.V. Zharkikh, V.E. Parshakova, V.V. Sidorov, A.V. Dunaev. Wearable Multimodal Optical Analyzers: Physiological Variability and Reproducibility of Measurements, Journal of Biophotonics, 18(4), (2025).
[3] E.A. Zherebtsov, E.V. Zharkikh, Y.I. Loktionova, A.I. Zherebtsova, V.V. Sidorov, E.U. Rafailov, A.V. Dunaev. Wireless dynamic light scattering sensors detect microvascular changes associated with ageing and diabetes, IEEE Transactions on Biomedical Engineering, 70(11), (2023).
[4] A.V. Dunaev, Y.I. Loktionova, E.V. Zharkikh, A.A. Fedorovich, V.V. Sidorov, A.V. Vasin, V.I. Dubinin. Investigation of blood microcirculation in microgravity with the use of portable laser doppler flowmeters, Aerospace and environmental medicine, 58(1), (2024).

Cells' targets and mediators of various PDT regimen

V. Elagin[1], A. Komarova[1], P. Bureev[1,2], L. Shimolina[1], P. Morozov[3]

1- Institute of Experimental Oncology and Biomedical Technologies, Privolzhsky Research Medical University, Nizhny Novgorod, Russia
2- Institute of Biology and Biomedicine, Lobachevsky State University of Nizhny Novgorod, Nizhny Novgorod, Russia
3- LLC "Superconducting Nanotechnology" (SCONTEL), Moscow, Russia

e-mail: elagin.vadim@gmail.com

Photodynamic therapy (PDT) is a promising approach that used as treatment for various kinds of cancers and microbial infection. PDT consists of three components: the non-toxic dyes, known as photosensitizers (PS), the light of the appropriate wavelength to excite the PS molecule and ambient molecular oxygen. The excited state of PS may undergo intersystem crossing to the triplet state, which can then react with molecular oxygen to produce singlet oxygen or with other substrates to produce reactive species (superoxide, hydroxyl and lipid-derived radicals). The type of reaction depends on the nature and concentration of the PS, oxygen content, substrate reactivity and etc. It supposed that in bacterial and eukaryotic cells both reactions can proceed in parallel. Due to the high reactivity and short half-life of ROS, the targets within a cell strongly depend on the photosensitizer localization. First of all, membrane lipids undergo to oxidation due to the presence of unsaturated fatty acid. Another cellular target for ROS may be DNA. The aim of this study was to investigate the effect of PDT on the main biological macromolecules.

The work was performed on HeLa Kyoto cells and Escherichia coli bacteria. Photoditazine was used as a PS. To measure phosphorescence lifetime of singlet oxygen in cells and in various solutions, a system based on time-correlated single photon counting and a superconducting single-photon detector was used. Moreover, the rate of singlet oxygen production during PDT was assessed. The level of lipid oxidation was determined by concentration of malondialdehyde, diene and triene conjugates and Schiff bases. The comet assay and gel electrophoresis of DNA was used to detection of DNA damage.

It was found that the phosphorescence lifetime of singlet oxygen in aqueous solutions of PS to be about 3.1–3.5 μs, which correlates well with published data. In the case of singlet oxygen generation inside eukaryotic cells, shorter phosphorescence lifetime was observed (1–1.1 μs), which is due to its interaction with the micro-environment. The rate of generation of singlet oxygen depends on the concentration of the PS and the power density of the radiation used. Increasing the photosensitizer concentration from 5 μM to 10 μM resulted in an approximately 2-fold rise in the registered phosphorescence photons (1550 and 3330 counts/second, respectively). The laser radiation with a power density of 14 mW/cm^2 was accompanied by the lowest rate of singlet oxygen production (213 counts per second). Increasing the power density to 29 mW/cm^2 led to an increase in the rate of generation of singlet oxygen phosphorescence photons to 2200 counts per second.

PDT treatment of eukaryotic cells resulted in a time-dependent increase in the concentration of triene conjugates and Schiff bases in neutral lipids and phospholipids. The maximal change was noted 1 hour after the procedure. Comet analysis showed that increasing the power density of the laser radiation used for PDT led to an increase in the degree of DNA damage.

PDI of bacteria led to an increase in the MDA content, which indicates an intensification of the lipid oxidation. Addition of Triton X-100 simultaneously with PS led to a decrease in the MDA content due to the penetration of PS into cells. Evaluation of DNA condition showed that the degree of damage increased with the laser radiation power density. In addition, the presence of Triton X-100 caused even greater DNA damage, which was associated with an increase in the concentration of PS in the bacteria cells. Thus, the nature of the targets in cells and their damage degree during PDT depend on the localization of the PS and the illumination regimen.

This work was supported by the Russian Science Foundation, project № 23-65-10005.

Optical clearing as an assisted technology for optical diagnostics and phototherapy of cancer

E. A. Genina[1], Yu. I. Surkov[1], I. A. Serebryakova[1], V. D. Genin[1], M. Yu. Kirillin[2], D. Kurakina[2], A. B. Bucharskaya[3], V. Tuchin[1,4,5]

1- Optics and Biophotonics Department, Saratov State University, Astrakhanskaya str. 83, Saratov, 410012 Russia
2- Biophotonics Laboratory, FRC "A. V. Gaponov-Grekhov Institute of Applied Physics of the Russian Academy of Sciences", Ul'anov str. 46, Nizhny Novgorod, 603950 Russia
3- Department of Faculty Surgery and Oncology, Saratov State Medical University, Bolshaya Kazachya str. 112, Saratov, 410012 Russia
4- Laboratory of Laser Molecular Imaging and Machine Learning, National Research Tomsk State University, Lenin Ave. 36, Tomsk, 634050 Russia
5- Institute of Precision Mechanics and Control, FRC "Saratov Scientific Centre of the RAS", Rabochaya str. 24, Saratov, 410028 Russia

e-mail: eagenina@yandex.ru

Multimodal optical approaches to diagnostics and early detection of cancer are a rapidly developing area of modern oncology. In particular, combinations of diffuse reflectance spectroscopy, optical coherence tomography (OCT), Raman spectroscopy and other optical methods are used for improvement of classification of skin cancer clinical forms and benign neoplasms [1]. The effectiveness of antitumor plasmon photothermal therapy (PPT) is also confirmed by numerous studies [2]. However, the use of light as a diagnostic and therapeutic tool is limited by the depth of light penetration into biological tissue due to scattering. Tissue optical clearing (OC) is a method that uses biocompatible optical clearing agents (OCAs) to make tissue more transparent through the refractive index matching effect [3]. Thus, skin OC can improve the diagnostic accuracy of skin lesions. In photothermal and photodynamic therapy of subcutaneous tumors, the assistance of OC can provide more targeted tumor treatment and reduce damage to healthy tissue.

We used biocompatible OCA in multimodal study of human skin benign neoplasms *in vivo*. Fig. 1 (a, b) shows OCT images of a benign neoplasm before OC and after 10-min exposure to OCA.

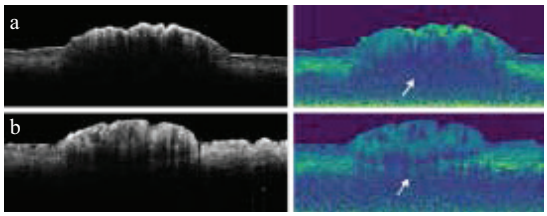

Fig. 1. Typical OCT images and their corresponding reconstructed scattering coefficient images: a) intact skin with keratoma, b) after OC. White arrows point to image fragments containing structural information that is absent in intact skin images and appears after 10 min of exposure.

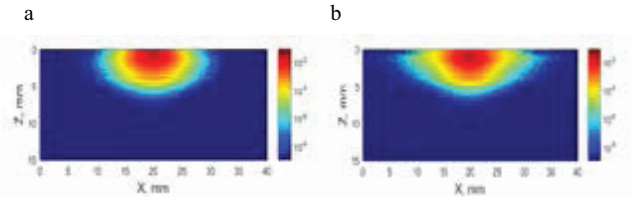

Fig. 2. Absorption maps calculated with MC technique normalized for the total delivered dose: a) a subcutaneous tumor model with GNRs in the central part of the tumor, b) after OC of epidermis. The wavelength of laser irradiation was 808 nm.

We also present the results of Monte Carlo (MC) simulations of light propagation changes induced by skin OC in a multilayered tumor model with intratumorally embedded gold nanorods (GNRs) (Fig. 2 a, b) and *in vivo* PPT of transplanted cholangiocarcinoma in rats.

The work was supported by the RSF grant no. 23-14-00287.

[1] V.V. Tuchin, J. Popp, V. Zakharov (Eds.), Multimodal Optical Diagnostics of Cancer (Springer Nature, Cham, Switzerland), (2020).
[2] A. Bucharskaya, N. Khlebtsov, B. Khlebtsov, G. Maslyakova, N. Navolokin, V. Genin, E. Genina, V. Tuchin, Photothermal and photodynamic therapy of tumors with plasmonic nanoparticles: challenges and prospects, Materials, vol. 15(4), 1606, (2022).
[3] V. Tuchin, D. Zhu, E.A. Genina, Handbook of tissue optical clearing: new prospects in optical imaging (CRC Press, Boca Raton, USA), (2022).

Multimodal and multifunctional contrast agents: preparation and in vitro and in vivo testing

D. A. Gorin

Skolkovo Institute of Science and Technology, Bolshoy Boulevard 30, bld. 1, Moscow 121205 Russia

e-mail: d.gorin@skoltech.ru

Visualization of the normal/pathological tissue boundary, as well as angiography, are priority tasks of modern biophotonics. Solutions to such problems are associated with the use of multimodal contrast agents. Multimodality means the ability to provide contrast when using various methods that are used in clinical practice, such as MRI, ultrasound, optoacoustic and fluorescence visualization. Various types of contrast agents and methods for their production are considered.

Advanced contrast agent will combine the ability to deploy drugs in a controllable manner with physical triggering, multimodal detection, and visualization as well as sensing of important biological markers. It is required to apply a new bottom-up method as layer by layer assembly [1] and freezing induced loading [2] and their combination [3]. It can be allowed us to vary the volume fraction of components and their chemical composition led to the control of the optical and thermal properties of multifunctional carriers [4]. Raman spectroscopy is perspective method for in situ monitoring of freezing induced loading method [5]. Physical targeting of carriers was realized by the magnetic field gradient [6]. Acoustics tweezers has a good perspective for the same purpose. The carrier sensitivity to external influences such as laser irradiation, ultrasound (US) treatment can be changed by variation of volume fraction and chemical composition of inorganic nanoparticles and/or organic dyes in the carrier shells.

As results, there are some trends of modern biophotonics can be formulated: 1) combination of OA, US, MRI, FI, OCT; 2) transfer to mid-IR; 3) preparation of multimodal contrast agents, that can be provided the contrast by some clinical methods including OA, MRI, USI etc. [7]; 4) using minimally invasive OA [8] by developing PIC based US transducers [9] using biomimetic approach for preparation a sensitive part (membrane) of such type of sensors [10,11]; 5) using optical clearing approach [12]; 6) realization of theranostic approach by the submicron polymer shells containing dyes and nanozymes [13].

Thus, the developed technology allows to create a new generation of contrast agents combining such functionalities as multimodal visualization and remotely triggered therapeutic action by laser irradiation or/and ultrasound.

[1] M.V. Novoselova et al, *J. Biophotonics*, 12 (4), e201800265, (2019).
[2] S.V. German et al, *Scientific Reports*, 8, 17763, (2018).
[3] M.V. Novoselova et al, *Colloids and Surfaces B*, 2021, 111576, (2021).
[4] R. E. Noskov et al, *Adv. Mater*, 2008484, (2021).
[5] S.V. German et al, *Langmuir*, 37,4, 1365, (2021).
[6] E.S. Vavaev et al, *ACS Applied Nano Materials*, 5 (2), 2994, (2022).
[7] E.A. Maksimova et al, *Laser & Photonics Reviews*, 2300137, (2023).
[8] N. Kaydanov et al, *ACS Photonics*, 8, 11, 3346, (2021).
[9] W. J. Westerveld et al, *Nature Photonics*, 15, 202, 341, (2021).
[10] J. Cvjetinovic et al., *Scientific Reports*, 13, 5518, (2023).
[11] J. Cvjetinovic et al, *Applied Physics Letters*, 123 (18), 184101, (2023).
[12] M.V. Novoselova et al, *Photoacoustics*, 100186, (2020).
[13] I.S. Sergeev et al, *Particle & Particle Systems Characterization*, 2300149, (2024).

Picosecond laser induced inactivation of tobacco mosaic virus

M. Yr. Grishin[1], O. V. Karpova[2], M. V. Arkhipenko[2], S. M. Pershin[1], E. V. Shashkov[1], G. A. Boldin[1]

1- Prokhorov General Physics Institute of the Russian Academy of Sciences, Moscow, 119991 Russia
2- Faculty of Biology, Lomonosov Moscow State University, Moscow, 119234 Russia

e-mail: pershin@kapella.gpi.ru

For the first time, to the best of our knowledge, the tobacco mosaic virus (TMV) was inactivated by biharmonic picosecond laser pulses impact due to RNA destruction as revealed by electrophoresis. Conventional development of the vaccine for virus requires a lot of time as we recently observed during COVID-19 pandemic. However, the developed vaccine became low efficient after a few weeks due to ongoing virus mutation. A new instrumental technique for virus inactivation is of a high demand in modern medicine especially for new modification of viruses. Biharmonic generating of picosecond pulses was suggested to damage virus species. The resultant electro-magnetic field oscillations are in the GHz range which corresponded to the virus capsid mechanical oscillations. These vibrations are in the GHz range and quite high compared to that of human cells oscillations. The tobacco mosaic virus (TMV) is a well described so it was chosen for our experiments. TMV [1] is a single-stranded RNA – virus in the form of a hollow tube 300 nm long, 18 nm in diameter with an opening of ~2 nm with helical structure arranged from coat protein with the molecular weight 17 kDa. TMV infects a wide range of plants. Virus suspension samples were provided by the Department of Virology of the Biological Faculty of Lomonosov Moscow State University [2].

First, we have demonstrated that resonant action in the microwave (2–100 GHz) frequency range resulted in TMV activity inactivation by 15–40% when irradiating the suspension at a frequency of 9 GHz (0.3 cm^{-1}) with non-thermal intensity (100 $\mu W/cm^2$) [3]. The possibility of suppressing TMV activity in the field of picosecond (30 ps) pulses of the Nd^{3+}:YAG laser remained unclear. A 10 mm long cuvette with a TMV suspension (concentration 1.2 μg/μl) was placed inside the resonator and irradiated for 30 minutes at a frequency of 0.3 Hz. Control samples with a TMV suspension of the same concentration were stored in the laboratory (2 pcs) of virologists and one sample near the laser. Then, four samples of the aqueous TMV suspension (three control and one irradiated in a picosecond laser resonator) were analyzed twice sequentially using electrophoresis in 1% agarose gel. In order to isolate RNA, the TMV samples were heated for 10 minutes at 56 °C before being applied to agarose. The results of the first (a) and repeated (b) analysis are presented in Fig. 1. According to Fig. 1 the RNA signal is absent on the 3rd track so the tobacco mosaic virus RNA has been destroyed by laser pulses.

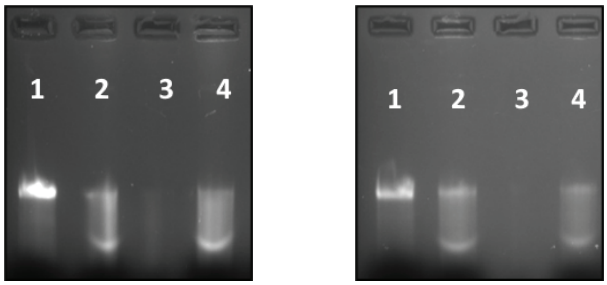

Fig. 1. Two parallel analysis of TMV by the gel electrophoresis: 1, 2 – control samples, 3 – sample alternated by biharmonic picosecond laser pulses pumping, 4 – control sample stored near laser.

Note that the approach discussed above was not mentioned in a recent review of physical influence on viruses [4]. This work was supported by the Russian Science Foundation (project No. RSF-23-42-10019).

[1] M. Zaitlin, "The Discovery of the Causal Agent of the Tobacco Mosaic Disease." In Discoveries in Plant Biology. S.D. Kung and S.F. Yang eds, (World Publishing Co. Hong Kong,), pp.105–110 (1998).
[2] Evtushenko E.A., Ryabchevskaya E.M., Nikitin N.A., Atabekov J.G., Karpova O.V. (2020) Plant virus particles with various shapes as potential adjuvants. Scientific Reports 10, 10365. DOI:10.1038/s41598-020-67023-4. PMID: 32587281.
[3] V.I. Kovalev, S.M. Pershin, M.V. Arkhipenko, A.N. Fedorov, O.V. Karpova, V.B. Oshurko, "On the Origin of a Low Intensity Microwave Irradiation Effect on Tobacco Mosaic Virus Activity", Proc. Of Frontiers in Optics / Laser Science © OSA (2019) www.osa-opn.org/bio-quantum..
[4] M. Sadraeian, I. Kabakova, J. Zhou, and D. Jin, Virus inactivation by matching the vibrational resonance Appl. Phys. Rev. 11, 021324 (2024); doi: 10.1063/5.0183276

Control over nonspecific binding of single molecules in a zero-mode-waveguide

A. Gritchenko[1], A. Safonova[1,2], M. Markov[1,2], A. Kalmykov[1], V. Balykin[1,2], P. Melentiev[1,2], A. Bukatin[3], Y. Alekseev[3,4], A. Evstrapov[3]

1- Institute of Spectroscopy RAS, Troitsk, Moscow, Russia
2- Higher School of Economics, National Research University, Moscow, Russia
3- Institute for Analytical Instrumentation RAS, St. Petersburg, Russia
4- Syntol LLC, Moscow, Russia

e-mail: gritchenkoant@gmail.com

Non-specific molecular binding plays one of the key roles in the formation of basic biological elements that are essential for living organisms, such as DNA, RNA, proteins and others. Non-specific binding is a necessary prerequisite for the formation of another important bond between two molecules - specific binding [1]. The establishment of specific molecular interactions is a prerequisite for the entire range of biosensors being developed for the diagnosis and study of various diseases. One of the most important requirements in the development of sensors is a high specificity for a target substance, which also means that non-specific binding, which can lead to falls-true signals during detection, must be minimized.

Approaches based on the detection of single molecules offer the highest sensitivity. One such approach is the use of zero-mode waveguides (ZMWs) [2]. A ZMW is a nanoscale aperture with a diameter of 50–200 nm that is produced in a thin, approximately 100 nm thick metal film on a dielectric substrate. The use of ZMWs enables a significant improvement in the signal-to-noise ratio in the detection and spectroscopy of individual molecules [3]. However, when studying specific biological processes in ZMWs – such as enzymatic reactions, receptor–ligand binding and others – the problem of non-specific molecular interactions with the structural elements of the ZMW becomes particularly apparent. This manifests itself in the occurrence of "false" signals that require complex filtering or are completely indistinguishable from "real" signals.

This work investigates the physical and chemical mechanisms underlying non-specific binding in ZMWs and outlines strategies to mitigate this undesirable effect. It is shown how non-specific binding directly affects the achievable accuracy of single-molecule detection in ZMW arrays as well as single-molecule sequencing of long DNA fragments. Importantly, non-specific binding is not always a purely parasitic effect. In some cases, specific binding can be regulated by controlling non-specific interactions so that it can be switched on» or «off». In addition, the report discusses the potential benefits of utilizing non-specific binding for the development of highly sensitive biosensors.

The study was supported by a grant Russian Science Foundation No. 23-42-00049, https://rscf.ru/project/23-42-00049/.

[1] Frutiger A. et al. Nonspecific binding – fundamental concepts and consequences for biosensing applications, Chemical reviews. vol. 121. №. 13. pp. 8095–8160 (2021).
[2] Foquet M. et al. Improved fabrication of zero-mode waveguides for single-molecule detection, Journal of Applied Physics. Vol. 103. №. 3 (2008).
[3] Melentiev P. N. et al. Optical methods for detection of single biomolecules: visualization, sensorics, sequencing of DNA molecules, Uspekhi Fizicheskikh Nauk. vol. 194. №. 11. pp. 1130–1145 (2024).

In vivo laser speckle blood apparent viscosity imaging

J. Hong[1], W. Zhu[1], M. Huang[1], A. V. Priezzhev[4], A. Lugovtsov[4], J. Lu[1], P. Li[1–3]

1- MOE Key Laboratory for Biomedical Photonics, Wuhan National Laboratory for Optoelectronics, Huazhong University of Science and Technology, Wuhan, 430074 China
2- Advanced Biomedical Imaging Facility, Huazhong University of Science and Technology, Wuhan, 430074 China
3- State Key Laboratory of Digital Medical Engineering, Key Laboratory of Biomedical Engineering of Hainan Province, School of Biomedical Engineering, Hainan University, Sanya, 572025 China
4- Department of Physics, M.V. Lomonosov Moscow State University, Moscow, Russia

e-mail: pengchengli@mail.hust.edu.cn

Blood viscosity is a vital regulator of microvascular flow. Changes in microcirculatory blood viscosity and vascular morphology can offer insights into the compensatory mechanisms of vascular resistance, especially in limited myogenic or metabolic regulation of blood flow in microcirculation. However, in vivo real-time monitoring hemorgeology remains challenge in microcirculation. We developed laser speckle apparent viscosity imaging (LSAVI) to measure blood rheology in vivo and investigated its impact on local vascular resistance. Moreover, we validated the Fåhræus-Lindqvist effect in microcirculation with LSAVI. The difference of hemorgeology changes induced by glucose between diabetic and control mice demonstrated that local vascular resistance are primarily influenced by blood viscosity rather than vessel diameter. This underscores the importance of precise monitoring and individualized therapeutic strategies for managing vascular complications. LSAVI may be a valuable tool for understanding the regulatory mechanisms of vascular health.

Development of resistance of *Staphylococcus aureus* to violet LED (405 nm) radiation during antimicrobial photodynamic therapy

M. V. Kanevsky, T. V. Sharabarina, Yu. I. Surkov, I. A. Serebryakova, E. S. Tuchina, V. V. Tuchin

Saratov State University, Astrakhanskaya 83, Saratov, 410012 Russia

e-mail: matvejkanev@mail.ru

The development of antimicrobial photodynamic therapy (APDT) as a promising method for treating infectious diseases has led to a comprehensive study of intracellular effects in response to exposure. At the same time, some authors have shown that bacteria are able to acquire tolerance to the occurrence of APDT after 10–15 cycles of irradiation.

The aim of this study is to investigate the effect of enhancing the photodynamic action of violet (405 nm) LED radiation on the replication of cells of *Staphylococcus aureus* 209 P with repeated use. The light-emitting diode with a maximum radiation intensity of $\lambda = 405\pm15$ nm, radiation power of 70 mW/cm^2 served as a radiation source. One (1) irradiation cycle was considered to be a single irradiation of the bacterial suspension for 15 min. Control (non-irradiated) and irradiated bacterial suspensions were seeded on the surface of dense medium. After 24 hours, the number of grown colonies (CFU) was counted. At 0 (control), 15 and 30 cycles of irradiation of the experimental resistance of the culture to the action of H_2O_2 in the minimum inhibitory concentration. For spectrophotometric study of the carotenoid composition of pigments in *S. aureus* 209 P cells, cultures were grown in Petrovich medium for 3–5 days at 37 °C, then collected and extracted with a mixture of ethyl acetate and 1.7 M aqueous NaCl (1:1). To evaluate the transmission spectra of the obtained extracts, spectrophotometric analysis was performed using USB4000-UV-VIS (Ocean Optics, USA) and QR400-7-VIS-NIR fiber-optic probes (Ocean Optics, USA) in the wavelength range of 345–800 nm in a 1 mm thick cuvette.

It was shown that the number of *S. aureus* 209 P decreased with repeated irradiation. From the 1st to the 10th cycle, the number of CFU of the *S. aureus* 209 P decreased by 15–18%, from the 10th to the 15th cycle, the decrease in the number of cells became more pronounced – by 18–33%, then, from the 15th to the 20th cycle, the number was restored (a decrease in CFU relative to the control by 28%), from the 20th to the 30th cycle, the survival values after irradiation remained at the same level (a decrease in CFU relative to the control by 20%). Since hydrogen peroxide is formed in cells during type I photoreactions under the action of radiation, the ability of bacterial cells to adapt to this compound as an oxidative stress factor was assessed. It was found that *S. aureus* 209 P had the highest resistance to 20 and 25 irradiation cycles, the MIC of H_2O_2 for which was 176 and 264 μM, respectively.

In order to assess the contribution of carotenoids to the neutralization of the photodynamic effect, the following were used: the initial (control) culture – not exposed to violet (405 nm, 70 mW/cm^2) radiation, and *S. aureus* 209 P strain 30 – exposed to radiation for 30 cycles.

It was found that the colonies of strain 30 on Petrovich medium had a more pronounced golden color. To assess the content of carotenoids in the cells, an analysis of the transmission spectra of extracts obtained from samples of the control strain and strain 30 cultures of equal biomass was performed.

The obtained spectra had differences within 10–15%. At the same time, the transmission coefficient values for strain 30 were lower than for control strain which indicates a higher content of substances in this sample. A characteristic minimum is noted at wavelengths of 450–470 nm, which corresponds to the maximum absorption of staphyloxanthin.

The results obtained during the work showed that the use of the photodynamic therapy method in practice should be approached with caution, since the formation of tolerance to the effect in the target microorganism occurs by the 15th cycle of irradiation and can significantly worsen the treatment results. Nevertheless, the study can become the basis for the implementation of a comprehensive approach to solving the problem of tolerance/resistance of microorganisms to the action of optical radiation, designed to ensure both the effective destruction of bacteria and the absence of their resistance to the method.

The work of was supported by grant program of the Russian Science Foundation № 25-24-00370 dated 12/28/2024.

Plasmonic gold nanorods: from SERS spectroscopy to controlled drug delivery

V. A. Khanadeev[1,2], A. V. Simonenko[1,3], A. M. Burov[1], B. N. Khlebtsov[1], N. G. Khlebtsov[1,3]

1- Institute of Biochemistry and Physiology of Plants and Microorganisms, Saratov Scientific Centre of the Russian Academy of Sciences (IBPPM RAS), Prospect Entuziastov 13, Saratov, 410049 Russia
2- Saratov State University of Genetics, Biotechnology and Engineering Named after N. I. Vavilov, Teatralnaya pl. 1, Saratov, 410012 Russia
3- Saratov State University, Ulitsa Astrakhanskaya 83, Saratov, 410012 Russia

e-mail: khanadeev@gmail.com

Gold nanorods are widely used in biomedical research due to their pronounced plasmon properties and the capability to tune the plasmon resonance to a given wavelength, including the first transparency window of biological tissues in the near-IR region [1]. The use of gold nanorods in biomedicine is often accompanied by laser exposure. One of the promising diagnostic areas of using gold nanorods is SERS spectroscopy [2]. As is known, the efficiency of using SERS spectroscopy depends on the plasmon properties of nanorods and the details of their shape [3]. We report on an experimental study of the dependence of the SERS signal of gold nanorods on the morphology and spectral position of their plasmon resonance relative to the wavelength of the irradiating laser. It was found that the shape of the nanorods ("cigar" or "dumbbell") affects the magnitude of the SERS signal to a greater extent than the spectral tuning of the plasmon resonance.

Gold nanorods can also be effectively utilized in therapeutic applications. Alone or as part of composite nanoparticles, they can be used for photothermal therapy, as well as for laser-induced release of a loaded drug. In this work, we studied nanocomposites based on gold nanorods coated with a hollow silica shell and loaded with the drug doxorubicin, which was retained inside due to the use of a thermosensitive molecular gate – tetradecanol. Gold nanorods acted as a sensitive transducer capable of heating under the action of laser radiation and causing the drug to release. The use of drug-loaded nanocomposites was studied *in vitro* on the HeLa cell line. It was found that unloaded nanocomposites combined with laser irradiation exhibited significant photothermal effect, and drug-loaded nanocomposites exhibited combined drug and photothermal effect, which is a more effective strategy for suppressing tumor cell activity.

The work was supported by a grant from the Russian Science Foundation No. 24-65-00015.

[1] S.E. Lohse and C.J. Murphy, The quest for shape control: a history of gold nanorod synthesis, Chem. Mater., vol. 25, pp. 1250–1261, (2013).
[2] K.-Q. Lin, J. Yi, S. Hu et al., Size effect on SERS of gold nanorods demonstrated via single nanoparticle spectroscopy, J. Phys. Chem. C, vol. 120, pp. 20806–20813, (2016).
[3] B.N. Khlebtsov, V.A. Khanadeev, A.M. Burov, E.C. Le Ru, N.G. Khlebtsov, Reexamination of surface-enhanced Raman scattering from gold nanorods as a function of aspect ratio and shape, J. Phys. Chem. C, vol. 124, pp. 10647–10658, (2020).

Photophysical properties of in vivo imaging sensors based on colored fluorescent proteins

M. Khrenova, A. Gavshina, N. Marynich, I. Soloviev, S. Kasatkina, G. Demina, M. Shleeva, A. Savitsky

FRC Biotechnology of the RAS, Leninsky prospect 33, Moscow, 117091 Russia

e-mail: apsavitsky@inbi.ras.ru

The dynamic properties of the protein globule play an important role in the manifestation of photophysical properties of colored fluorescent proteins. Photoswitching from the fluorescent state to the non-fluorescent state is associated mainly with the processes of cis-trans isomerization and subsequent proton transfer. Due to this, the biphotochromic protein SAASoti, which is rapidly switchable in the green and red states, can be used to develop various variants of kinetic subdiffraction microscopy, allowing one to study the fast processes of movement of protein molecules and nanostructures in living cells. The key process in the presence of two photoswitching processes at once in both the green and red forms is the correlated motion of substituents in the chromophore structure: they must belong to the same community of correlated motions. Using Dynamic Network Analysis methods, it was shown that the replacement of a single amino acid residue near the chromophore critically affects both of these processes [1]. The dynamics of the protein globule determines the intraprotein change in the pK of chromophore [2], which is manifested in a change in the excitation spectra of new sensors for hypochlorite, which is a key compound in the manifestation of the bactericidal properties of macrophages. Two-laser excitation in the picosecond time range allows us to study the intracellular localization of hypochlorite generation during photodynamic exposure and during the development of an immune response.

[1] A.V. Gavshina, I.D. Solovyev, M.G. Khrenova, K.M. Boyko, L.A. Varfolomeeva, M.E. Minyaev, V.O. Popov, A.P. Savitsky. The role of the correlated motion (s) of the chromophore in photoswitching of green and red forms of the photoconvertible fluorescent protein mSAASoti. Scientific Reports 14 (1), 8754 (2024).
[2] N. Marynich, M. Khrenova, A. Gavshina, I. Solovyev, A. Savitsky. First Biphotochromic Fluorescent Protein moxSAASoti Stabilized for Oxidizing Environment. Scientific Reports, 12 (1) 1–10, doi.org/10.1038/s41598-022-11249-x (2022).

Optical diagnostics modalities for photoaging studies and photodynamic therapy assistance

M. Kirillin[1], M. Shakhova[1,2], V. Fokeev[1,2], D. Kurakina[1], V. Perekatova[1], V. Prokopenko[1], D. Pshenitsyna[3], A. Getmanskaya[1,3], A. Saveliev[1,3], A. Mironycheva[1,2], S. Gamayunov[1,4], I. Turchin[1], E. A. Sergeeva[1]

1- Institute of Applied Physics RAS, Nizhny Novgorod, Russia
2- Privolzhsky Research Medical University, Nizhny Novgorod, Russia
3- Lobachevsky State University of Nizhny Novgorod, Nizhny Novgorod, Russia
4- Nizhny Novgorod Regional Clinical Oncology Center, Nizhny Novgorod, Russia

e-mail: kirillin@ipfran.ru

Optical diagnostics techniques have high potential in noninvasive monitoring of tissue reactions to light exposure, both natural and artificial. In this paper we give an overview of complementary application of different optical diagnostic modalities for detection changes in skin induced by photoaging and monitoring the procedure and the follow-up in photodynamic therapy (PDT).

In photoaging studies, we inspected skin of volunteers with different stages of photodamage in accordance with Glogau scale by optical coherence tomography (OCT) and diffuse reflectance spectroscopy (DRS). OCT allowed to reveal differences in morphological features of skin, such as epidermis thickness and dermis structure, while DRS provided information about skin chromophores content. OCT data was analyzed using machine learning approach (Fig. 1) based on U-Net architecture [1], while DRS signals were processed using a refined analytical model [2].

In PDT studies, we focused on dual-wavelength fluorescence monitoring of the procedure and its follow-up. We developed a Monte-Carlo model [3] that allowed to simulate absorbed dose distribution when performing treatment with chlorin-based photosensitizers (PSs) as well as to assess the depth distribution of fluorescence photons that contribute to the signal when monitoring a PDT procedure. Monte Carlo simulations also allowed to verify the analytical model that was further employed to assess PS localization depth from the results of dual-wavelength fluorescence monitoring [4].

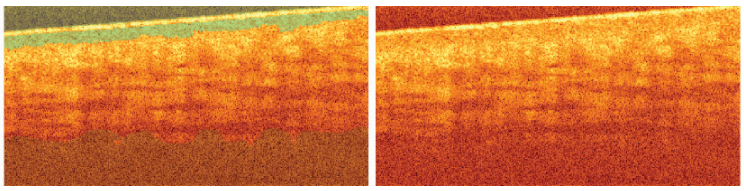

Fig. 1. Segmentation of OCT images of skin: segmented image (left), initial image (right).

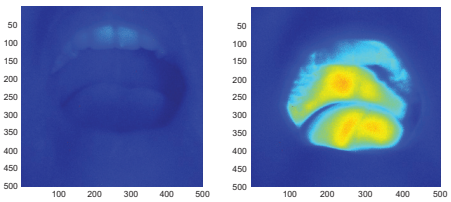

Fig. 2. Fluorescence images of oral cavity before (left) and after (right) administration of PS.

Clinical studies included development of novel protocols of PDT treatment of ENT pathologies and retrospective analysis of fluorescence monitoring of skin cancer treatment. In treatment of chronic pharyngitis, protocols of intranasal an oral application of PS were compared using fluorescence control of PS accumulation (Fig. 2). In skin cancer PDT treatment, PS fluorescence monitoring demonstrated alterations of signal associated with PS accumulation, photobleaching and blood flow activity.

The study is supported by the Russian Science Foundation (project 24-15-00175).

[1] V.A. Shishkova, N.V. Gromov, A.M. Mironycheva, M.Y. Kirillin "Segmentation of 3D OCT Images of Human Skin Using Neural Networks with U-Net Architecture" CTM, 17 (1), 6–17 (2025).
[2] E. Sergeeva, D. Kurakina, I. Turchin, M. Kirillin, "A refined analytical model for reconstruction problems in diffuse reflectance spectroscopy," Journal of Innovative Optical Health Sciences, 2342002 (2024).
[3] D. Kurakina, E. Sergeeva, A. Khilov, M. Kirillin, "Light Dose and Fluorescence Imaging Depth in Dual-Wavelength PDT: a Numerical Study for Various Photosensitizer Distributions in a Layered Biotissue", Journal of Biomedical Photonics & Engineering 10 (4), 040318 (2024).
[4] M. Kirillin, A. Khilov, D. Kurakina, A. Orlova, V. Perekatova, V. Shishkova, A. Malygina, A. Mironycheva, I. Shlivko, S. Gamayunov, I. Turchin, E. Sergeeva. "Dual-wavelength fluorescence monitoring of photodynamic therapy: from analytical models to clinical studies". Cancers, 13(22), 5807 (2021).

Quantitative and qualitative analysis of IR spectroscopy data for medical and ecological applications

Yu. Kistenev, D. Vrazhnov, V. Skiba, V. Nikolaev, G. Rasponin, D. Makashev, A. Borisov

LMIML Laboratory, Tomsk State University, Tomsk, Russia

e-mail: yuk@iao.ru

IR spectra of gas samples of natural origin contain information about volatile biomarkers of patient conditions or atmosphere industrial pollutions. Qualitative and quantitative analysis of such spectra means an estimation of the sample chemical composition and concentration of its components. Methods like Multivariate Curve Resolution [1], Univariate Calibration [2] are very popular in this field. The major problem of in this field is that the composition of gas samples of natural origin is unknown. This problem is closely related to the field of so cold gray systems analysis.

The problem of presence of unaccounted (latent) components requires more sophistical methods, including machine learning (ML), first of all, aimed on extracting new informative variables (features) of minimum quantity, which describe peculiarities in data analogously to initial variables. Original chemometrics and ML methods suitable for gray systems analysis will be presented including examples of their medical and ecological applications.

The work was conducted with the financial support of the Ministry of Science and Higher Education of Russia (Agreement No. 075-15-2024-557 dated 04/25/2024).

[1] A.de Juan, R. Tauler "Multivariate Curve Resolution: 50 years addressing the mixture analysis problem–A review". Analytica Chimica Acta. V. 1145, 59–78 (2021).
[2] P. Kościelniak, M. Wieczorek "Univariate analytical calibration methods and procedures. A review". Analytica chimica acta. V. 944, 14–28 (2016).

Multi-wavelength refractometry in studies of protein glycation

E. Lazareva[1], V. Tuchin[1–3]

1- Saratov State University, Saratov, 410012 Russia
2- Tomsk State University, Tomsk, 634050 Russia
3- Laboratory of Laser Diagnostics of Technical and Living Systems, Institute of Precision Mechanics and Control RAS, Saratov, Russia

e-mail: lazarevaen@sgu.ru

Modern methods of diagnosing diabetes mellitus and monitoring the degree of its compensation are associated with determining the level of glucose in the blood on an empty stomach. While measurements of glucose in the blood, plasma or serum are short-term and reflect the diabetic status over a 24-hour period, the level of glycated protein is a long-term glycemic indicator. The main glycated proteins in the blood are glycated hemoglobin (HbA1c) and glycated albumin (GA). The HbA1c test measures the average blood glucose level over the past 2–3 months depending on the concentration of hemoglobin molecules (Hb) to which a glucose molecule is attached [1, 2]. GA has been proposed as an additional marker for monitoring glycemic status in people with type II diabetes. In vivo, the proportion of GA in healthy people ranges from 1% to 10%, and in diabetes mellitus this proportion can increase two to three times [3].

Optical research methods occupy a special place and are widely used in the field of medical diagnostics and therapy [4]. Many studies have shown the possibility of using optical methods to determine glycated proteins [5]. The widespread use of refractometric methods in biomedicine is based on the dependence of the refractive properties of biological tissues on their structure and chemical composition, since the structure and composition of biological tissues change with the development of pathology. Measuring the refractive index has been used by several scientific groups to assess changes in the optical properties of blood during the development of hyperglycemia and diabetes mellitus. [5, 6]. An increase in the refractive index occurs due to the interaction of glucose and hemoglobin molecules with the formation of various forms of glycated hemoglobin with new molecular structures and, accordingly, optical properties. For example, since hyperglycemia changes the molecular structure of hemoglobin, as glucose is attached to the protein R-group, Mazarevica et al. proposed measuring the refractive index of hemoglobin and red blood cell mass in patients with diabetes mellitus to determine the degree of glycation [7].

The present work presents data on measuring the refractive index (RI) of glycated hemoglobin and glycated albumin in the spectral range of 480–1550 nm at room, physiological and high temperatures. Graphs of dispersion and temperature dependences are given, a comparison with data for non-glycated forms of hemoglobin and albumin. Based on the obtained results, an increase in the modulus of temperature increment for the glycated form of proteins was established. As is known, the full derivative of RI with respect to temperature is associated with the effect of thermal expansion and the temperature dependence of molecular polarizability. In this case, the full polarizability is considered equal to the sum of the polarizability of each of the molecules. Thus, the molecular complex of protein with glucose has a high molecular polarizability, and RI depends on the content of charged amino acids in the molecule.

The work was supported by the grant of the Russian Science Foundation No. 23-14-00287.

[1] J. Wen, F. Hu, Q. Yang, "Comparison of hemoglobin alc, glycated albumin and fasting plasma glucose for prediction of arterial stiffness in chinese adults, " Diabetes Metab Syndr Obes, 10(13), pp. 65–70, (2020).
[2] C. Weykamp, "HbA1c: A Review of Analytical and Clinical Aspects," Ann Lab Med., 33(6), pp. 393–400 (2013).
[3] Ph. Rondeau, E. Bourdon, "The glycation of albumin: Structural and functional impacts," Biochimie, vol. 93 (2011).
[4] V. V. Tuchin, Tissue Optics: Light Scattering Methods and Instruments for Medical Diagnostics, 3rd ed., PM 254, p. 988, SPIE Press, Bellingham, Washington (2015).
[5] O.A. Smolyanskaya et al., "Multimodal Optical Diagnostics of Glycated Biological Tissues," Biochemistry (Moscow), vol. 84 (1), pp. 124–143 (2019).
[6] E.N. Lazareva et al., "Optical Properties of Glycated and Non-Glycated Hemoglobin–Raman/Fluorescence Spectroscopy and Refractometry," Journal of Biomedical Photonics & Eng. 8(2), pp. 020303(1–9), (2022).
[7] G. Mazarevica et al., "Properties of erythrocyte light refraction in diabetic patients," Journal of Biomedical Optics 7(2), 244–247 (2002).

Erythrocyte size and deformability in laser diffractometry

M. Lebedeva[1], E. Tsybrov[2], S. Nikitin[1]

1- Faculty of Physics, Lomonosov Moscow State University, Moscow, Russia
2- Faculty of Computational Mathematics and Cybernetics, Lomonosov Moscow State University, Moscow, Russia

e-mail: 2mary.lebedeva@gmail.com

Today, various methods of assessing the size of red blood cells are used, for example, microscopy, flow cytometry. Laser diffractometry is often used to assess the deformability of red blood cells (commercial devices such as Lorrca and Rheoscan work on this principle). Our goal is to develop the method of laser diffractometry, starting from the theory and ending with the experimental methodology, as a universal method for measuring the moments of red blood cell distributions in size-shape and deformability.

In this work, venous blood of young healthy donors (22–28 years old) was studied. We used wet blood smears for size measurements of erythrocytes. In such smears, which are a highly diluted cell suspension between a slide and a cover glass, erythrocytes retain their natural forms. Measurements of the first two moments of cell size-shape distribution were carried out in two ways – by laser diffractometry and microscopy using the algorithm described in the article [1]. We examined 9 blood samples with 2–3 wet smears for each sample. The data obtained by the two methods showed a need to introduce a correction, hardware number that affects the accuracy of measurements by laser diffractometry. This number is defined as the ratio of an experimentally calculated visibility of the diffraction pattern to its theoretical value. At the moment, the specific value of the hardware number is determined empirically.

Measurements of the deformability of red blood cells were carried out using a disk laser ectacytometer assembled in our laboratory. In this work, the methodological aspects of measurements on an ectacytometer were considered, the results of measurements on 3 donors obtained using the algorithms developed by us [2] were presented.

The study was conducted with the financial support of the scholarship grant of the "BASIS" foundation № 23-2-2-36-1.

[1] S. Nikitin, V. Ustinov, E. Tsybrov, M. Lebedeva, Scattering of a Laser Beam on an Ensemble of Asymmetrical Erythrocytes, Optics and Spectroscopy (English translation of Optika i Spektroskopiya), vol. 129, № 7, pp. 1064–1074, (2021).
[2] S. Nikitin, E. Tsybrov, M. Lebedeva, Calibration Problem in Laser Ektacytometry of Erythrocytes, Journal of Biomedical Photonics & Engineering, vol. 8, № 4, pp. 040503 1–9, (2022).

Copolymer-based materials for biomedical applications: in vitro and in vivo degradation monitoring using MRI and fluorescence imaging

A. Likhov[1], V. Tuchin[2], V. Zherdeva[1]

1- Research Center of Biotechnology RAN, A. N. Bach Institute of Biochemistry, Moscow, Russia
2- Institute of Physics and Science Medical Center, Saratov State University, Saratov, Russia

e-mail: vjerdeva@inbi.ras.ru

Copolymer-based materials are extensively used in medicine and biotechnology for the fabrication of implants, prostheses, drug delivery systems, and biosensors. Combining optical fluorescence imaging and magnetic resonance imaging (MRI) offers a powerful tool for in vivo evaluation of tissue responses and quantitative or semi-quantitative assessment of the degradation of implantable copolymer-based composites [1].

Polyester-based copolymers were labeled with Indocyanine Green (ICG) and gadolinium citrate (Gd^{3+}). In vitro degradation, both enzymatic and non-enzymatic, was assessed using gravimetric analysis, fluorescence spectroscopy, and MRI. These degradation studies, along with cell viability tests, represent essential approaches for evaluating biodegradable materials.

For in vivo analysis, the copolymer samples were implanted subcutaneously in BALB/c mice. Post-implantation monitoring was performed using planar fluorescence imaging and MRI. To enhance visualization, tissue optical clearing (TOC) with 70% glycerol was applied. The efficiency of optical clearing (Q) was calculated using the following formula:

$$Q = \frac{\int_a^b F_{\text{after}}\,dx - \int_a^b F_{\text{before}}\,dx}{\int_a^b F_{\text{after}}\,dx + \int_a^b F_{\text{before}}\,dx},$$

where F_{after} and F_{before} are the fluorescence densities after and before TOC application, respectively.

In vitro degradation experiments showed distinct differences between non-enzymatic hydrolysis and enzyme-mediated degradation. Complete enzymatic degradation was observed within 24–28 days, accompanied by consistent release of both Gd^{3+} and ICG. In contrast, degradation in enzyme-free serum extended up to 56–60 days. In vivo resorption dynamics of the copolymer implants based on MRI with Gd^{3+} and imaging with ICG showed variability in the terminal phases, particularly in the effects observed from tissue response, volumetric changes, and interpretation of optical clearing effects.

Wound healing and individual immune responses significantly influenced implant resorption. Three primary types of healing responses were identified based on Q-values and MRI data: (a) Negative Q-values associated with non-healing wounds; (b) Biphasic Q-value peaks related to changes in peri-implant tissue viscosity; (c) Progressive increase in Q-values corresponding to dye retention within fibrous tissue. MRI further confirmed that inflammation, fibrosis, or impaired healing impacted TOC effectiveness, with Q-values ranging from –30% to +70%.

Understanding individual degradation profiles is critical for the development of temporary co-polymer-based implants, including bioengineered scaffolds and medical device components. In vivo methods such as MRI and fluorescence imaging provide valuable insights into the degradation behavior of copolymers and associated tissue responses. Moreover, tissue optical clearing (TOC) has emerged as an indirect marker of biointegration efficiency, reflecting the nature of healing, inflammation, or fibrotic encapsulation around the implant.

[1] Zherdeva VV, Likhov AR, Saidvaliev UA, Fixler D, Demin D, Volodina VN, Apukhtina UA, Pawar S, Atuar B, Tuchin VV. Enhanced Fluorescence Imaging of Implants Based on Polyester Copolymers in Combination With MRI. J Biophotonics. 2025 (online)

Laser-optical study of alterations in blood cells under chronic heart failure

A. E. Lugovtsov[1], Ia. A. Orlova[2], A. N. Sveshnikova[1], L. I. Dyachuk[2], N. A. Mironov[2], N. A. Karanadze[2], S. Yu. Nikitin[1], M. S. Lebedeva[1], M. K. Maksimov[1], D. A. Umerenkov[1], A. V. Priezzhev[1]

1- Physics Department and 2- Medical Research and Educational Institute, M. V. Lomonosov Moscow State University, Leninskie Gory 1, Moscow, 119991 Russia

e-mail: anlug@biomedphotonics.ru

Chronic heart failure (CHF) is one of the most common causes of death worldwide. More than 6 % of deaths in the world are caused by this disease, and the prevalence of the disease, for example in Russia, is approaching to 9 %. This disease is characterized by a decrease in the contractile function of the heart and systemic hypoxia associated with inadequate perfusion of organs and tissues at rest or under physical activity. CHF is accompanied by fluid retention in the body and its accumulation in soft tissues that lead to a decrease in resistance to physical activity, the appearance of edema and shortness of breath. The severity of CHF is determined by the functional class (FC) from I to IV, showing how limited the patient's physical activity is [1]. The state of human organism essentially depends on the aggregation properties of red blood cells (RBC) and platelets as well as RBC deformability, distribution of the cells in sizes and deformability [2]. The importance of monitoring these properties is determined by the need to correct them using various drugs and to estimate the effectiveness of therapy. So far there is no information about the alterations of blood cells properties for different FC of CHF [1].

The goal of this paper is to demonstrate the efficiency of laser-optical methods for estimating the relation of CHF in different FC and blood microrheological properties: RBC aggregation and deformability, platelets aggregation, distribution of RBC in sizes and ability to deform in shear flow. Particular attention is paid to verifying the hypothesis about the interrelation of the width of the distribution of RBC in size and deformability with the decrease in physical activity tolerance [1].

For assessing the blood properties, a comprehensive study was performed for 69 patients suffering from CHF and 18 practically healthy volunteers. All patients were subjected to the test with 6-minute walk to determine the FC of CHF. All participants of the study underwent standard clinical tests and measurements of blood microrheological properties. Blood microrheology was measured *in vitro* using diffuse light scattering [2], diffractometry, turbidimetry, evaluation of RBC size and deformability distribution parameters using laser ektacytometry on wet blood smears and microscopy of RBC suspensions in microfluidic channels using the algorithms of machine learning [3].

A comprehensive study of microrheological parameters alterations in CHF depending on FC were performed. As a result of this work the microrheological profiles of patients suffering from CHF was obtained. CHF leads to changes in the microrheological properties of the blood: increased aggregation of erythrocytes and platelets, as well as a decrease in the deformability of erythrocytes. The degree of changes in microrheological parameters is associated with the FC of CHF. The used set of laser-optical methods are an effective tool for *in vitro* monitoring disorders of blood properties in CHF.

This work was supported by the grant of Interdisciplinary Scientific and Educational School of MSU «Photonic and Quantum technologies. Digital medicine» (grant No. 23-Ш06-03).

[1] N.A. Mironov, A.V. Priezzhev, A.N. Sveshnikova, A.E. Lugovtsov, N.A. Karanadze, L.I. Dyachuk, Yu.I. Begrambekova, S.A. Zakharchuk, Ia.A. Orlova, Correlation between blood rheology, hemostasis and functional status in patients with chronic heart failure: rationale and study protocol, Russian Cardiology Bulletin, vol. 19(1), pp. 79–83 (2024). (In Russian)
[2] A. E. Lugovtsov, Y. I. Gurfinkel, P. B. Ermolinskiy, A. I. Maslyanitsina, L. I. Dyachuk, A. V. Priezzhev, Optical assessment of alterations of microrheologic and microcirculation parameters in cardiovascular diseases, Biomedical Optics Express, vol. 10(8), pp. 3974–3986 (2019).
[3] A.I. Ladynin, Kinetics of aggregation and deformability of human red blood cells in the flow: study using machine learning methods in vitro. Master's thesis, MSU, Moscow (2025).

Zebrafish as an emerging model for cardiovascular research using biophotonics techniques

A. Machikhin

Scientific and Technological Center of Unique Instrumentation of the Russian Academy of Sciences, Butlerova street 15, Moscow, 117342 Russia

e-mail: machikhin@ntcup.ru

Studying the cardiovascular system of fish is very important in biology and medicine. The cardiovascular system of fish and humans has common features related to its basic functions (presence of the heart, arteries and veins, a closed circulatory system, the transport function of the blood, formed elements of the blood: erythrocytes, leukocytes and platelets), and significant differences due to different living conditions and evolutionary adaptation (heart structure, type of blood circulation, blood temperature). This allows to solve many fundamental and applied problems, including: identifying the mechanisms of formation and development of the heart and blood vessels, evolutionary studies of the heart and blood circulation, genetic studies of the regulation of the development and function of the heart, modeling of cardiovascular diseases (cardiomyopathy, arrhythmia, heart failure, atherosclerosis, etc.) and determining the effectiveness of methods for their treatment, testing drugs aimed at treating cardiovascular diseases, understanding the cardiotoxicity of chemicals, drugs and environmental pollutants.

One of the most effective model biological objects used to study the cardiovascular system is the aquarium fish *Danio rerio* (zebrafish) [1]. Small size, ease of maintenance, high reproduction rate with the production of many (up to several hundred) embryos, short period of embryonic development (3 days) and the possibility of studying a few generations make *Danio rerio* a very convenient object for conducting comparative experiments on the offspring obtained from one pair. Due to the transparency of the body in the visible and near infrared ranges [2], studies at the embryonic and larval stages can be carried out *in vivo* using biophotonics techniques: fluorescence imaging, confocal microscopy, light sheet microscopy, optical coherence tomography, photoacoustic microscopy, etc.

Almost all conventional optical methods for analyzing the state of the cardiovascular system and hemodynamic parameters of zebrafish are invasive, since they involve the introduction of contrast agents, anesthesia, lighting, heating and other stressors that affect the physiological state. The development and introduction into experimental practice of new non-invasive methods for monitoring the state of the cardiovascular system of fish, free from all or at least most of these effects will contribute to acquisition of a more objective data and conducting more physiologically significant experiments.

This study is dedicated to the analysis of photopletysmography and video capillaroscopy for *in vivo* assessment of hemodynamics, vascular morphology and cardiac rhythm. With this techniques, we developed hardware and software for absolutely non-invasive and real-time measurement of the heart rate of free-swimming zebrafish based on image acquisition in the short-wave infrared range and machine learning algorithms [3].

[1] C. Nguyen, Q. Lu, Y. Wang, J.Chen, Zebrafish as a model for cardiovascular development and disease, Drug Discovery Today: Disease Models, vol. 5(3), 135–140 (2008).
[2] M. Volkov, A. Machikhin, V. Bukova, D. Khokhlov, A. Burlakov, V. Krylov, Optical transparency and label-free vessel imaging of zebrafish larvae in shortwave infrared range as a tool for prolonged studying of cardiovascular system development, Scientific reports, vol. 12, № 20884 (2022).
[3] A. Machikhin, A. Slavin, A. Guryleva, V. Krylov, Anesthesia-free Heartbeat Measurements in Freely Moving Zebrafish, Journal of Visualized Experiments, vol. 218, e68145 (2025).

SERS identification of the infection of food crops by fungi of the genus *Fusarium*, highly pathogenic for human

M. N. Moskovsky[1], S. M. Kuznetsov[1,2], M. O. Kulpina[1], A. S. Sibirev[1], V. S. Novikov[1,2]

1- Federal Scientific Agronomic and Engineering Center VIM, 1st Institutsky proezd 5, Moscow, 109428 Russia
2- Prokhorov General Physics Institute of the Russian Academy of Sciences, Vavilov str. 38, Moscow, 119991 Russia

e-mail: maxmoskovsky74@yandex.ru

Fusarium is one of the most widespread type of phytopathogenic fungi. It produces various mycotoxins, and their collective impact is much more than that of any other toxin. Such mycotoxins, as well as *Fusarium* fungi, not only cause agricultural crop diseases all around the world, but also can enter the human body and cause significant harm to health [1].

In this contribution, we present a simple and fast technique based on SERS spectroscopy that results in the detection of fungi growth on agricultural plants. We demonstrate the effect that the growth of different *Fusarium* fungi on wheat and barley leaves has on the SERS spectra of the samples. We obtained that the contamination of plants resulted in the presence of several spectral lines that are typical for each pathogen. These lines were observed in the SERS spectra even when there were no visible differences between the infected and healthy leaves.

In addition, we studied the dynamics of the fungi growth on the leaf surface during time. It showed the increase of the overall intensity of a spectral region 1100–1750 cm^{-1}, several spectral lines became more noticeable or gave a rise to a shoulder of the neighboring broad band. The example of such dynamics, obtained for barley plants infected with *Fusarium Graminearum* (*F. Gram.*), is presented in Fig. 1.

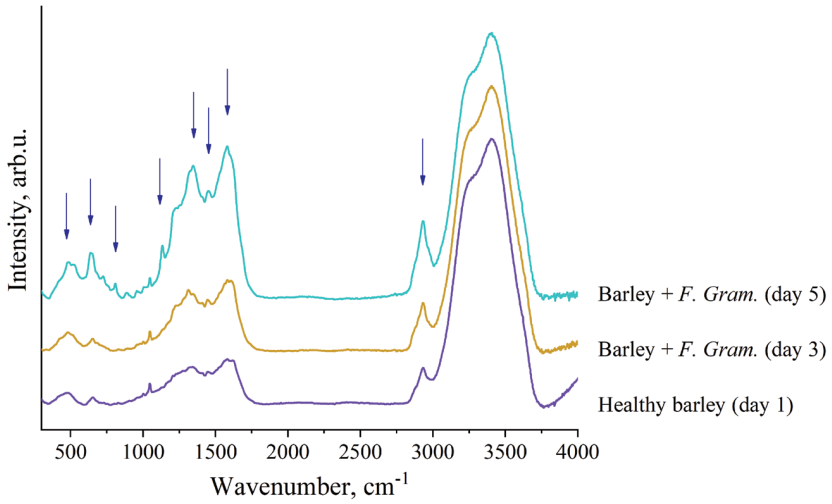

Fig. 1. SERS spectra of healthy barley leaves and leaves infected with *F. Gram*, recorded during several days after infection. Arrows point to the spectral lines that changed the most.

Thus, we developed a SERS spectroscopy technique of the identifying the growth of *Fusarium* fungi on agricultural plants. This technique is simple, fast and can be used with portable spectrometers.

This research was funded by a grant of the Ministry of Science and Higher Education of the Russian Federation for large scientific projects in priority areas of scientific and technological development (subsidy identifier 075-15-2024-540).

[1] S. Savary, L. Et al. The global burden of pathogens and pests on major food crops. // Nat. Ecol. Evol. – 2019. – V. 3. – P. 430–439. DOI: 10.1038/s41559-018-0793-y.

Nanostructured platforms for light-triggered thermal effects in biomedical applications

D. Nazarovskaia[1], P. Tyurin-Kuzmin[2,3], N. Yabbarov[4], B. Khamitov[1], J. Petrova[1], M. Vasilieva[1], M. Mollaeva[4], E. Nikolskaya[4], L. Osminkina[1,3]

1- Lomonosov Moscow State University, Faculty of Physics, Leninskie gory 1, Moscow, 119991 Russia
2- Lomonosov Moscow State University, Faculty of Medicine, Leninskie gory 1, Moscow, 119991 Russia
3- Institute of Biological Instrumentation, Russian Academy of Sciences, Institutskaya Street 7, Moscow oblast, Pushchino, 142290 Russia
4- N. M. Emanuel Institute of Biochemical Physics of Russian Academy of Sciences, Kosygina Street 4, Moscow, 119334 Russia

e-mail: nazarovskaia.da22@physics.msu.ru

Photothermal therapy (PTT) is minimally invasive cancer treatment wherein photothermal agents (PTAs) convert light into localized heat, selectively destroying tumor cells through hyperthermia. An ideal PTA require: a) strong absorption in the tissue-transparent near-infrared (NIR) windows (650–900 nm or 1000–1700 nm), b) efficient heat conversion (fast temperature raise up to 42–44 °C to induce cell apoptosis), and c) tumor-specific accumulation.

Among emerging efficient PTAs, porous silicon (PSi) nanomaterials fascinate the interest of researchers in recent years due to the combination of semiconductor properties and biocompatibility [1]. The intrinsic bandgap of bulk Si ~1.12 eV, or 1100 nm in wavelength equivalently, enables absorption across the bio-window (700–1100 nm) and can be extendable via quantum confinement in small Si nanocrystals. Moreover, PSi broad featureless absorption spectrum eliminates need for specialized light sources.

PSi consists of Si nanocrystals (nc-Si) and pores. The developed PSi surface is the result of its synthesis through electrochemical etching of crystalline Si (c-Si) and different porosity (20–95%), pore sizes (1.5–50 nm), and surface areas (100–1125 m^2/g) can be fabricated. In contrast to bulk c-Si, PSi exhibit photoluminescent (PL) properties due to quantum confinement effect in small nc-Si (2–7 nm). Photolumenescent PSi nanoparticles (NPs) and nanowires (NWs) have a broad excitation spectrum and can be recognized inside cells in vitro and in vivo by standard luminescent technics.

In PTT, hybrid porous silicon-gold (Au@pSi) nanostructures combine the advantages of both materials and can be used to create highly efficient heating systems when irradiated with light in the NIR range [2, 3]. Au@pSi nanoparticles can not only improve light absorption, but also provide precise targeted heating of cells, minimizing damage to surrounding healthy tissues. Importantly, such plasmonic systems have multifunctional potential and can be used for image-guided cancer therapy (for instance, with applications in PL microscopy, Surface-enhanced Raman scattering micro-spectroscopy), for targeted drug delivery as capacious nanocontainers.

In this work, the processes of heating of porous silicon-gold hybrid nanoparticles (Au@pSi) suspensions for application in PTT have been investigated. This study involves the synthesis of Au@pSi, analysis of their structural and optical properties, cytotoxicity studies, and measurements of their heating efficiency under infrared radiation in vitro.

The study was supported by the Russian Science Foundation grant No. 24-15-00137, https://rscf.ru/project/24-15-00137/.

[1] L.A. Osminkina, M.B. Gongalsky, Porous silicon for biomedical applications (Elsiever), Chapter 16, (2021).
[2] M. Cui, et. al, Fluorescent Silicon Nanorods-Based Nanotheranostic Agents for Multimodal Imaging-Guided Photothermal Therapy, Nano-Micro Letters, 11:73, (2019).
[3] E. Gerasimova, et. al, Single-step fabrication of resonant silicon–gold hybrid nanoparticles for efficient optical heating and nanothermometry in cells, ACS Applied Nano Materials, 6(20), 18848–18857, (2023).

Optical clearing improved transmission of low frequency and low power laser pulses in muscle

L. M. Oliveira[1], G. Rodrigues[1], M. R. Pinheiro[1], M. I. Carvalho[1], V. V. Tuchin[2]

1- Institute for Systems and Computer Engineering, Technology and Science (INESCTEC), Porto, Portugal
2- Saratov State University, Saratov, Russia

e-mail: lmanueloliveira@gmail.com

Tissue transmission of laser pulses is conditioned by various factors, such as the pulse frequency, pulse amplitude, and tissue absorption and scattering properties. Pulsed lasers have been used in various biomedical applications like imaging, fluorescence, therapy and surgery, but, in general, such applications require high laser power and high pulse repetition rates. In contrast, low-power, low-repetition-rate lasers demonstrate low efficiency, but for a number of biophotonic applications, such lasers are urgently needed both from the safety and cost points of view. One possible solution to this problem is tissue optical clearing to eliminate unnecessary losses of both probing and detectable photons that carry information about the object [1, 2].

In this work, using various 5 mW lasers, emitting between 405 and 850 nm, the intensity of the transmitted pulses was measured after crossing muscle samples with 0.5 mm thickness. The transmitted pulses showed increasing magnitude with increasing wavelength, which is according to the wavelength dependence of the absorption and scattering coefficients of the muscle. The study was repeated after treating the muscle samples with glycerol, sucrose, electronic cigarette liquid, or tartrazine solutions, showing improved transmittances for all the treated tissues. The tissues treated with sucrose solution presented the lowest improvement in pulse magnitude, while the ones treated with the tartrazine solution presented the highest improvement, but only for lasers with emission between 635 and 850 nm.

[1] L. Oliveira and V. V. Tuchin, The Optical Clearing Method: A New Tool for Clinical Practice and Biomedical Engineering, Basel: Springer Nature Switzerland AG, 2019.
[2] I. S. Martins, H. F. Silva, E. N. Lazareva, N. V. Chernomyrdin, K. I. Zaytsev, L. M. Oliveira, and V. V. Tuchin, Measurement of tissue optical properties in a wide spectral range: a review [Invited], Biomedical Optics Express, 14 (1), 249–298 (2023).

Hybrid porous silicon-gold nanoparticles: photonic properties and biomedical applications

L. Osminkina[1,2]

1- Lomonosov Moscow State University, Faculty of Physics, Leninskie gory 1, Moscow, 119991 Russia
2- Institute for Biological Instrumentation of Russian Academy of Sciences, Pushchino, Moscow Region, 142290 Russia

e-mail: osminkina@physics.msu.ru

Hybrid nanomaterials composed of porous silicon (pSi) and gold nanostructures represent a promising platform for multifunctional biomedical applications. These systems combine the advantages of silicon-based biodegradability and high internal surface area with the plasmonic and radiosensitizing properties of gold. In this study, we describe the synthesis, physicochemical characterization, and biomedical assessment of hybrid pSi-Au nanoparticles designed for simultaneous photothermal therapy, radiosensitization, and spectroscopic diagnostics.

Porous silicon nanoparticles were obtained through electrochemical anodization of crystalline silicon, followed by fragmentation and size selection in the sub-200 nm range. Gold nanostructures were introduced onto the surface or within the pores of the pSi matrix using in situ chemical reduction of gold salts (e.g., $HAuCl_4$) under controlled conditions. Scanning electron microscopy (SEM), transmission electron microscopy (TEM), and energy-dispersive X-ray spectroscopy (EDS) confirmed the hybrid composition and morphology of the resulting nanostructures.

Optical characterization via UV–Vis–NIR spectroscopy revealed a broad plasmonic absorption band in region of 500–700 nm, associated with the collective oscillation of electrons in gold nanostructures. This plasmonic behavior was further validated by laser-induced heating experiments, where exposure to red laser light (633 nm) resulted in rapid and localized temperature elevation. These results demonstrate the high photothermal conversion efficiency of the hybrid particles, making them suitable candidates for photothermal therapy (PTT) in oncological settings.

Raman spectroscopy of the hybrid nanoparticles exhibited significant signal enhancement, particularly for molecular species adsorbed onto the gold-modified surfaces. This surface-enhanced Raman scattering (SERS) effect was used to detect and distinguish biomolecules in complex environments, showing potential for label-free molecular diagnostics. Notably, the characteristic crystalline silicon (c-Si) peak at ~520 cm^{-1} remained visible, confirming the structural integrity of the pSi core.

In addition to their photonic properties, the hybrid nanoparticles exhibited radiosensitizing effects due to the high atomic number (Z) of gold, which increases local energy deposition upon X-ray irradiation. In vitro experiments using cancer cell lines demonstrated that the presence of pSi-Au nanoparticles significantly enhanced the cytotoxic effects of ionizing radiation compared to control groups. This radiosensitization is attributed to the generation of secondary electrons and reactive oxygen species (ROS) near the cellular nucleus, facilitated by nanoparticle internalization.

Moreover, the porous nature of the silicon matrix provides a favorable environment for drug loading and controlled release. By integrating multiple functionalities: light-activated heating, radiosensitization, and drug delivery, these nanoparticles represent a versatile theranostic platform. Their biodegradability and low systemic toxicity, confirmed in preliminary cytocompatibility assays, further support their potential for in vivo use.

Taken together, our findings highlight the unique combination of optical, thermal, and radiological properties in pSi-Au hybrid nanoparticles. These features can be tailored by controlling the porosity, gold distribution, and surface chemistry. Future directions include the addition of targeting ligands or aptamers to improve cellular uptake and selectivity toward tumor tissues, as well as evaluation in animal models of combined therapy.

This work contributes to the development of next-generation nanomedicine tools that synergize diagnostic and therapeutic capabilities, enabling precision interventions in cancer treatment.

The study was supported by the Russian Science Foundation grant No. 24-15-00137, https://rscf.ru/project/24-15-00137/.

Multi-wavelength laser speckle contrast imaging: from Monte Carlo simulations to phantom experiments

V. Perekatova, A. Kostyuk, D. Kurakina, Yu. Belozerov, K. Bylinskaya, E. Sergeeva, M. Kirillin

A. V. Gaponov-Grekhov Institute of Applied Physics of the Russian Academy of Sciences, Ul'yanov Street 46, Nizhny Novgorod, 603950 Russia

e-mail: valeriya1000@yandex.ru

Laser Speckle Contrast Imaging (LSCI) [1] is a non-invasive technique for characterizing microvascular blood flow by analyzing spatiotemporal fluctuations in dynamic speckle patterns generated by moving red blood cells, which provides real-time perfusion maps without contrast agents [2]. In this paper we report on development of a multi-wavelength LSCI system and a Monte Carlo-based model of LSCI image formation.

The Monte Carlo model is based on simulating light propagation in layered tissues and analyzing backscattered photons forming speckle patterns, tracking per-photon parameters: statistical weight, path length, exit coordinates, and scattering events on static/dynamic scatterers. Laser illumination of scattering media creates static speckle patterns through interference. Moving scatterers (e.g., red blood cells) induce dynamic speckle fluctuations, where flow velocity governs the fluctuation rate – a phenomenon called speckle decorrelation. A prototype LSCI imaging system was constructed featuring four laser sources operating at wavelengths from red and NIR bands (655 nm, 785 nm, 850 nm, 940 nm) and a synchronized camera for multi-wavelength speckle contrast acquisition, leveraging tissue-specific optical properties for depth-resolved imaging. System validation employed custom designed 3D-printed vasculature phantom (1 mm diameter vessels at 200 μm – 1.2 mm depth) with Lipoplus emulsion flow (0 – 6.3 mm/s, simulating microvascular hemodynamics), optically characterized via spectrophotometric measurements by Specord 250 Plus and OCT. The setup visualized vessels across all depths, demonstrating contrast-map broadening with depth. Spatial speckle contrast ($K = \sigma/\langle I \rangle$) inversely relates to flow velocity ($K \sim 1/V^{1/2}$), as faster flow accelerates speckle decorrelation, reducing K and enabling perfusion mapping in superficial tissue (~1–2 mm depth) without contrast agents (Fig. 1).

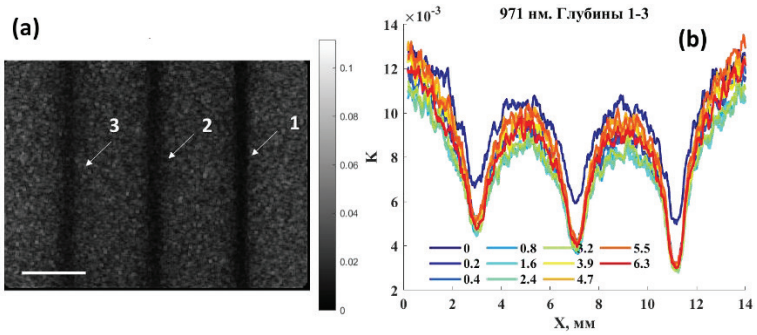

Fig. 1. (a) Spatial speckle contrast of a 3D-printed phantom containing cavities filled with moving Lipofundin at 971 nm for a flow velocity of 3.9 mm/s. Scale bar: 2.5 mm. (b) Spatial speckle contrast averaged along the vessel region vs. flow velocity in LSCI.

Vessel broadening on the contrast map with increasing depth was demonstrated. Analysis of spatial contrast demonstrated that the vessel diameter at 655 nm was overestimated by 50% (up to 200 μm), while at 908 nm and 971 nm the error did not exceed 20% (up to 600 μm). At the same time, temporal contrast maps at depths up to 800 μm showed vessel broadening at 908 nm and 971 nm not exceeding 10%, confirming the high potential of this approach. Spatial contrast decreases monotonically with flow velocity, enabling velocity assessment. However, at velocities above 2 mm/s, the system becomes insensitive to further changes thus limiting application to capillaries/arterioles where flow typically remains below this threshold.

The study is supported by the Russian Science Foundation (project No. 24-75-10068).

[1] D. Boas, and A. Dunn, Laser speckle contrast imaging in biomedical optics, Journal of biomedical optics, 15, 1, 011109–011109 (2010).
[2] W. Heeman, W. Steenbergen, G.M. van Dam, E. Boerma, Clinical applications of laser speckle contrast imaging: a review, Journal of biomedical optics, 24, 8, 080901-080901 (2019).

Evaluating tartrazine diffusion properties in the skeletal muscle

M. R. Pinheiro[1], G. Rodrigues[1], M. I. Carvalho[1], V. V. Tuchin[2], L. M. Oliveira[1]

1- Institute for Systems and Computer Engineering, Technology and Science (INESCTEC), Porto, Portugal
2- Saratov State University, Saratov, Russia

e-mail: maria.r.pinheiro@inesctec.pt

The evaluation of diffusion properties of novel optical clearing agents (OCAs) is critical for advancing biomedical diagnostic and therapeutic applications [1]. Tartrazine (TZ), a high absorbing food dye, has been recently demonstrated to have great potential to increase tissue transparency in tissues [2], but no studies have yet reported its characteristic diffusion properties. This study was conducted to evaluate the diffusion properties of TZ in skeletal muscle and characterize the tissue dehydration and the refractive index (RI) mechanisms that lead to the transparency created by this OCA. Kinetic collimated transmittance (T_c) and kinetic thickness measurements were performed on muscle samples under treatment with aqueous solutions of TZ with different osmolarities. The characteristic diffusion times that characterize the tissue dehydration and the RI matching mechanisms were calculated from kinetic T_c measurements at discrete wavelengths. The corresponding diffusion coefficients of TZ and water in the muscle were calculated from sample thickness data measured during treatments where the unique fluxes of TZ and water occur [3]. The obtained diffusion times for TZ and water were 323.4 s and 62.1 s, respectively. Using these values with the corresponding sample thicknesses during treatment, the corresponding diffusion coefficients (D) were calculated as 4.53×10^{-7} cm^2/s for TZ and 1.89×10^{-6} cm^2/s for water. These findings offer essential insights into the diffusion mechanisms of TZ in skeletal muscle and support its ongoing evaluation as a novel agent for optical clearing applications.

[1] L. Oliveira and V. Tuchin, The Optical Clearing Method – A New Tool for Clinical Practice and Biomedical Engineering (Springer), Chapter 1, (2019).
[2] Z. Ou et al., Achieving optical transparency in live animals with absorbing molecules, Science, 385, eadm6869, (2024).
[3] M. Pinheiro, V. Tuchin, and L. Oliveira, Invasive and minimally invasive evaluation of diffusion properties of sugar in muscle, IEEE J. Sel. Top. Quantum Electron., 29(4), (2023).

Study of extracellular matrix stiffness influence on the distribution and photophysical properties of photosensitizers using laser spectroscopy and FLIM microscopy

D. Pominova[1,2], A. Ryabova[1,2], I. Romanishkin[1], I. Markova[1,2]

1- Prokhorov General Physics Institute of the Russian Academy of Sciences, Vavilov 38, Moscow, 119991 Russia
2- National research nuclear university MEPHI, Moscow, Russia

e-mail: pominovadv@gmail.com

Tumor microenvironment stiffness, driven by dysregulated extracellular matrix (ECM) remodeling, critically compromises therapeutic efficacy in desmoplastic cancers (e.g., pancreatic, breast). Dense ECM creates biomechanical barriers that restrict drug penetration, induce hypoxia, and promote therapy resistance [1]. Photodynamic therapy (PDT) efficacy is particularly hindered by impaired photosensitizer diffusion and altered photophysics in rigid microenvironments. Quantifying ECM stiffness effects on photosensitizer behavior is essential for optimizing PDT protocols.

This study integrates laser spectroscopy and FLIM microscopy to decode how ECM stiffness modulates photosensitizer (PS) distribution, fluorescence, photobleaching dynamics, and metabolic responses in vitro. Changes in ECM parameters after PDT were also analyzed. Model systems included of varying stiffness, mimicking the dense stromal environment of tumors, as well as cell cultures (tumor cells and fibroblasts).

The photosensitizers (chlorin e6, aluminum phthalocyanine) distribution was quantified using fiber-optic reflectance and fluorescence spectroscopy. In rigid gels, photosensitizer penetration dropped compared to soft gels, correlating with a increase in scattering coefficients. Photobleaching rates under 660 nm irradiation (100 mW/cm^2, 5 min) slowed in dense gels due to oxygen diffusion limitations, confirmed by singlet oxygen sensor assays. FLIM microscopy (two-photon excitation at 740 nm) revealed shortened mean photosensitizer's fluorescence lifetimes in stiff matrices. In cellular models FLIM detected changes in NADH lifetime ratios, showing metabolic shifts and glycolytic adaptation. PDT efficacy in stiff gels declined sharply, with lower cell death and reduced singlet oxygen generation. A scattering coefficient change in the collagen gels after PDT was also observed, indicating a collagen damage. FLIM further captured photosensitizer lifetime changes post-PDT, providing dynamic readouts of treatment response.

These findings establish ECM stiffness as a regulator of PDT outcomes through: impaired photosensitizer diffusion, photophysical alterations, and hypoxia-mediated resistance. The synergy of laser spectroscopy and FLIM offers a transformative approach for adaptive PDT, enabling irradiation parametrs optimization via optical stiffness measurements.

The study was funded by a grant from the Russian Science Foundation (project №25-12-00436).

[1] Z. Yuan, Y. Li, S. Zhang et al, Extracellular matrix remodeling in tumor progression and immune escape: from mechanisms to treatments, Mol Cancer, vol. 22, Article number: 48, (2023).

Laser speckle contrast imaging: an application in experimental medicine

E. Potapova[1], N. Golubova[1,2], V. Dremin[1], I. Ryzhkov[2], K. Lapin[2], V. Prizemin[1], E. Seryogina[1], Y. Kalyuzhnaya[3], S. Demyanenko[3], A. Dunaev[1]

1- Research & Development Center of Biomedical Photonics, Orel State University, Orel, 302026 Russia
2- Federal Research and Clinical Center of Intensive Care Medicine and Rehabilitology, Moscow, 141534 Russia
3- Laboratory of Molecular Neuroscience, Academy of Biology and Biotechnology, Southern Federal University, Rostov-On-Don, 344090 Russia

e-mail: potapova_ev_ogu@mail.ru

Laser Speckle Contrast Imaging (LSCI) has emerged as a powerful, non-invasive optical technique for real-time visualization of blood flow dynamics in biological tissues. LSCI has rapidly gained traction across diverse domains of experimental medicine. The technique operates by analyzing the speckle pattern generated when coherent laser light scatters from moving red blood cells within microvasculature, enabling dynamic imaging of tissue perfusion with high spatial and temporal resolution. LSCI offers the advantages of being label-free, cost-effective, and suitable for continuous monitoring in both *in vivo* and *in vitro* settings. As such, it is increasingly applied in preclinical models of stroke, inflammation, wound healing, and tumor angiogenesis to elucidate microcirculatory behavior under physiological and pathological conditions.

This article explores the principles, advancements, and key applications of LSCI in experimental medicine, highlighting its potential to transform translational research and inform therapeutic strategies.

The LSCI system developed at the Research and Development Center of Biomedical Photonics (Orel State University, Orel) was used to capture images, including a 785 nm laser source (LDM785 laser source from Thorlabs, USA), a high-resolution CMOS camera (UI-3360CP-NIR-GL from IDS, Germany), NIR linear polarizer, and objective (MVL25TM23 from Thorlabs or MY5X-802-5X from Mitutoyo). Original software was used to analyze the data.

LSCI was used to map the cerebral vessels of a laboratory animal, as well as for spatial mapping of blood flow rhythms [1]. The proposed technology allowed not only measuring the relative cerebral blood flow, but also expanding diagnostic capabilities for a detailed analysis of the physiological mechanisms behind blood flow changes. LSCI was also used to monitor blood flow in the brain's arterioles and control reperfusion during the photothrombotic model of ischemic attack. It has been shown that exposure of the mouse cerebral cortex arterioles to a laser with a wavelength of 532 nm, after intravenous administration of 15 mg/kg of bengal rose, causes similar ischemic and reperfusion injuries that lead to the formation of microinfarctions [2]. To better understand the potential of the LSCI technique, studies on cerebral blood flow in rats were performed in an acute experiment involving thinning of the skull and acute blood loss [3]. These studies demonstrate that in order to obtain reliable LSCI data on cerebral perfusion, it is necessary to prepare the skull, and it was also found that moderate blood loss does not decrease cerebral blood flow to a level that compromises autoregulation. Additionally, studies have been conducted that show that microcirculatory disorders can be detected using the LSCI method through the optical channels of a standard laparoscope [4].

Laser Speckle Contrast Imaging represents a transformative tool in the field of experimental medicine, offering real-time, high-resolution insights into tissue perfusion and microvascular function.

This work was supported by the grant of the Russian Federation Government (075-15-2025-011).

[1] N. Golubova, E. Potapova, E. Seryogina, V. Dremin, Time–frequency analysis of laser speckle contrast for transcranial assessment of cerebral blood flow, Biomedical Signal Processing and Control, 85, 104969 (2023).
[2] Kalyuzhnaya Y.N., Logvinov A.K., Pashkevich S.G., Golubova N.V., Seryogina E.S., Potapova E.V., Dremin V.V., Dunaev A.V., Demyanenko S.V. An Alternative Photothrombotic Model of Transient Ischemic Attack, Translational Stroke Research, 15(4), (2024).
[3] N. Golubova, I. Ryzhkov, K. Lapin, E. Seryogina, A. Dunaev, V. Dremin, E. Potapova, Effect of thinned-skull cranial window on monitoring cerebral blood flow using laser speckle contrast imaging, IEEE Journal of Selected Topics in Quantum Electronics, 31(4), 7000108 (2025).
[4] E.V. Potapova, E.S. Seryogina, V.V. Dremin, D.D. Stavtsev, I.O. Kozlov, E.A. Zherebtsov, A.V. Mamoshin, Y.V. Ivanov, A.V. Dunaev, Laser speckle contrast imaging of blood microcirculation in pancreatic tissues during laparoscopic interventions, Quantum Elec. 50(1), 33–40 (2020)..

Possibilities and comparison of *in vivo* microscopy and *in vitro* laser aggregometry technique for assessment of erythrocyte aggregation in terminal capillaries and in blood samples

A. V. Priezzhev[1], Yu. I. Gurfinkel[2], L. I. Dyachuk[2], P. A. Moldon[1], A. E. Lugovtsov[1]

1- Physics Department and 2- Medical Research and Educational Institute, M. V. Lomonosov Moscow State University, Moscow, Russia

e-mail: avp@biomedphotonics.ru

The aim of this study was to develop means for *in vivo* quantitative assessment of the degree of erythrocyte aggregation in the microcirculation bed by optical capillaroscopy, which is particularly important for patients suffering from cardiovascular diseases, with the goal of *in vivo* identifying diagnostically significant markers [1]. Capacities and information content of *in vivo* measurements in human nail-bed capillaries was compared with those of *in vitro* measurements performed in whole blood samples by laser aggregometry technique. Hypothetically it was assumed that while being preferable for many patients, in vivo measurements yield sufficient information on the degree of erythrocyte aggregation for early diagnostics of microvascular dysfunction and monitoring the hemorheologic status of patients [2, 3].

As a results the study showed the presence of erythrocyte aggregates in nail-bed capillaries of patients suffering from such diseases as arterial hypertension, coronary artery disease, and atrial fibrillation compared to healthy people who do not have erythrocyte aggregates in their capillaries. The number of aggregates in nail bed capillaries correlated with increased erythrocyte aggregation characterized by the aggregation index measured *in vitro* in whole blood samples.

The calculated correlation matrices have shown that the alterations of the parameters measured *in vivo* and *in vitro* for patients with different stages of these diseases are interrelated. Good agreement between the results obtained with different techniques, and their applicability for the diagnostics of abnormalities of rheological properties of blood were demonstrated.

We conclude that these results open up new opportunities for early non-invasive *in vivo* assessment of erythrocyte aggregation capacity and microrheologic alterations, which are typical of patients suffering from many socially significant diseases.

This work was supported by the Russian Science Foundation (Grant № 25-15-00172).

[1] A. Lugovtsov, Y. Gurfinkel, P. Ermolinskiy, A. Maslyanitsina, L. Dyachuk, A. Priezzhev, Optical assessment of alterations of microrheologic and microcirculation parameters in cardiovascular diseases, Biomedical Optics Express vol. 10, 3974–3986 (2019).
[2] A. Maslianitsyna, P. Ermolinskiy, A. Lugovtsov, A. Pigurenko, M. Sasonko, Yu. Gurfinkel, A. Priezzhev, Multimodal diagnostics of microrheologic alterations in blood of coronary heart disease and diabetic patients. Diagnostics vol.11, 76 (2021). https://doi.org/10.3390/diagnostics11010076.
[3] A.V. Muravyov, A.V. Priezzhev, A.E. Lugovtsov, I.A. Tikhomirova, A.V. Zamyshlyaev, M.E. Shishikhin, A.V. Shishikhina, The relationship between hemodynamic parameters and microrheology of erythrocytes in individuals with arterial hypertension. Thrombosis, Hemostasis and Rheology No. 2, 17–22 (2023). DOI: 10.25555/THR.2023.2.1056 (in Russian).

Optical features of tumor extracellular matrix

A. Ryabova[1,2], D. Pominova[1,2], T. Savelieva[1,2], I. Romanishkin[1], I. Markova[1,2], K. Linkov[1], V. Makarov[1,2], A. Moskalev[1], D. Yakovlev[1,3]

1- Prokhorov General Physics Institute of the Russian Academy of Sciences, Vavilov 38, Moscow, 119991 Russia
2- National research nuclear university MEPHI, Moscow, Russia
3- Shemyakin-Ovchinnikov Institute of Bioorganic Chemistry, Russian Academy of Science, Moscow, Russia

e-mail: nastya,ryabova@nsc.gpi.ru

In recent years, increasing attention has been paid to the role of extracellular matrix (ECM) components in the processes of oncogenesis and metastasis. ECM density affects the metabolism of the tumor microenvironment, migration and malignancy, in addition, it is a significant barrier that limits the penetration of antitumor agents and reduces the effectiveness of therapy [1]. The development of new strategies for managing ECM density and increasing the permeability of tumor tissues is of great interest [2].

Optical coherence tomography, ultrasound, sonoelastography, and magnetic resonance imaging are used for noninvasive assessment of tissue mechanical properties at the macroscale [3]. Quantitative microelastography is a compression-based optical coherence tomography-elastography method that allows assessing tissue mechanical properties at the microscale and uses a compliant layer as an optical stress sensor placed between the imaging window and the tissue, which provides quantitative assessment of elasticity [4]. Noninvasive methods for measuring optical parameters of biological tissues and imaging are being intensively developed, such as thermography, laser speckle contrast imaging, spectral optical coherence tomography, and spatial frequency domain imaging [5].

The report will consider the possibility of using optical diagnostic methods for non-invasive assessment of ECM density and simultaneous study of processes at both tissue and cellular and molecular levels, including absorption and fluorescence spectroscopy, Raman spectroscopy, fluorescence microscopy for analysis of cell populations and distribution of collagen fibers in a tumor node, as well as time-resolved fluorescence microscopy for analysis of endogenous metabolic coenzymes and collagen matrix types. This approach will allow us to establish the relationship between macroparameters (ECM density and mechanical stress, hydrostatic pressure) and the composition of the ECM and the cellular microenvironment of the tumor.

The study was funded by a grant from the Russian Science Foundation (project №25-12-00436).

[1] T.R. Cox, The matrix in cancer, Nat Rev Cancer, vol. 21(4), pp. 217–238, (2021).
[2] C. Avendano, J.C. Menendez, Chapter 12 - Protein degradation-based cancer therapy, Medicinal Chemistry of Anticancer Drugs (Third Edition), Elsevier, pp. 637–679, (2023).
[3] M.R. Zanotelli, N.C. Chada, C.A. Johnson, C.A. Reinhart-King, The Physical Microenvironment of Tumors: Characterization and Clinical Impact, Biophys. Rev. Lett, vol. 15, pp. 51–82, (2020).
[4] K.L. Metzner, Q. Fang, R.W. Sanderson, Y.L. Yeow, C. Green, F. Abdul-Aziz, J. Hamzah, A. Mowla, B.F. Kennedy. A novel stress sensor enables accurate estimation of micro-scale tissue mechanics in quantitative micro-elastography, APL Bioeng, vol. 8(3), pp. 036115, (2024).
[5] D.M. McClatchy, E.J. Rizzo, W.A. Wells, C.C. Black, K.D. Paulsen, S.C. Kanick, B.W. Pogue, Light scattering measured with spatial frequency domain imaging can predict stromal versus epithelial proportions in surgically resected breast tissue, J Biomed Opt, vol. 24(7), pp. 1–11, (2018).

Development of specialized fiber-optic multichannel probes for biomedical applications of the frequency domain near infrared spectroscopy

L. Safonova[1], M. Belsheva[1], G. Danielyan[2], G. Nazarova[2], P. Saenko[3]

1- Bauman Moscow State Technical University, 2nd Baumanskaya st. 5, Moscow, 105005 Russia
2- «Optofiber» Limited Liability Company, Vavilova st. 38-5-1, Moscow, 119991 Russia
3- Moscow Engineering Physics Institute, Kashirskoe shosse 31, Moscow, 115409 Russia

e-mail: gldan@yandex.ru

Frequency domain near infrared spectroscopy (FD NIRS) is the method, which has been actively developed over the last thirty years [1], and is widely used for studies of biological tissues, organs and systems in functional diagnostics and in various fields of medicine. Recently, the capabilities of FD NIRS for intraoperative diagnostics have been demonstrated [2]. The main advantages of the method are its relative cheapness, the possibility of quantitative assessment of optical properties of biological tissues in monitor mode, quantitative estimation of structural and physiological features of a tissue volume from several tens of milliliters to several hundred milliliters, and in depth from several millimeters to several centimeters. The wide possibilities of the method are demonstrated by scientific research and development [3, 4]. However, the main limitation for its wide application in clinical practice is the extremely high complexity of the anatomical structure and significant variability of physiological parameters of different human organs and tissues. Each application requires taking into account the individual features of the biological object under study, the physical basis of the interaction of optical radiation with it and the development of an optical probe design suitable for the purposes of research and/or diagnostics.

In this area of biomedical photonics, fiber-optic multichannel probes [5] for local delivery and registration of backscattered light in tissues have proven themselves. Such optical probes allow to provide a small contact area with the investigated surface, a wide variety of mapping options over the region of interest, to vary the probing depth and spatial resolution, and to combine optical studies with other physical methods. The developed design solutions of specialized fiber-optic multichannel probes take into account the listed requirements to them and peculiarities of their application in biomedicine.

Special design solutions with a small contact area are required for mapping cerebral hemodynamics under the scalp [6]. To diagnose structural heterogeneities of small volumes of biological tissues intraoperatively, it is important to consider the size of the operating field, requirements for biocompatibility and sterilization of the probe, and physical limitations of the FD NIRS method (Fig. 1). For joint studies with MRI, EEG or electroimpedance probing, the materials used and design solutions with the possibility of personal customization of the multimodal probe are important.

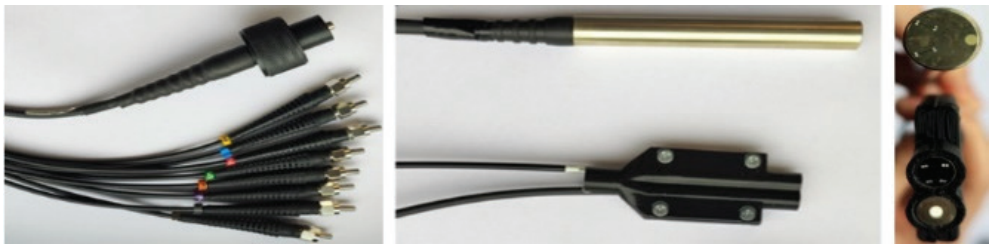

Fig. 1. Examles of the designed fiber-optic multichannel probes for structural and functional testing of a small tissue volume.

The purpose of this report is to demonstrate developed variants of specialized fiber-optic multichannel probes for biomedical applications of the FD NIRS method, design features of the probes and results of their application [7].

[1] J. Fishkin, P. So, A. Cerussi, S. Fantini, M. Franceschini, and E. Gratton, Frequency-domain method for measuring spectral properties in multiple-scattering media: methemoglobin absorption spectrum in a tissuelike phantom, Applied Optics, vol. 34, pp. 1143–1155, (1995).

[2] M. Belsheva, L. Safonova, A. Shkarubo, Sensitivity of frequency domain near infrared spectroscopy for neurovascular structure detection in biotissue volume: numerical modeling results, Journal of Biophotonics, e202400291, (2024).
[3] S. Fantini, A. Sassaroli, Frequency-domain techniques for cerebral and functional near-infrared spectroscopy, Frontiers in Neuroscience, vol. 14, article 300, (2020).
[4] X. Zhou, Y. Xia, J. Uchitel, L. Collins-Jones, S. Yang, R. Loureiro, R.Cooper, H. Zhao, Review of recent advances in frequency-domain near-infrared spectroscopy technologies [Invited], Biomedical Optics Express, vol. 14, pp. 3234–3258, (2023).
[5] U. Utzinger, R. Richards-Kortum, Fiber optic probes for biomedical optical spectroscopy, Journal of Biomedical Optics, vol. 8, pp. 121–147, (2003).
[6] A. Kassab and M. Sawan, Developments in near-infrared spectroscopy (IntechOpen), Chapter 1, (2017).
[7] I.S. Javelov, S.M.Kaplunov,G.L. Danielyan, Book: Fiber-optical measuring systems: Applied problems ,Moscow-Izhevsk, Chapter 2 (2011).

Laser microscopy with spectral signature for biophotonics

H. Schneckenburger

Aalen University, Institute of Applied Research, Beethovenstr. 1, Aalen, 73430 Germany

e-mail: herbert.schneckenburger@hs-aalen.de

Laser-assisted microscopy has become an inevitable tool in biophotonics, in particular since high resolution or super-resolution techniques as well as 3D methods have become available. In recent years, detection systems have become more and more sensitive, e.g. for fluorescence microscopy, so that many applications can be performed at low, non-phototoxic levels of illuminating light [1].

Often fluorescence microscopy needs spectral resolution, e.g., if tumor cells and less malignant cells are to be distinguished by the fluorescence of specific coenzymes [2]. Förster Resonance Energy Transfer (FRET) from an optically excited donor molecule to a fluorescent acceptor molecule has been used to measure cell metabolism upon apoptosis [3] or following the impact of a pharmacological agent [4]. More generally, spectrally resolved fluorescence microscopy is an appropriate tool to distinguish fluorescent components in complex biological systems, often in combination with statistical methods. An example is given for beech wood, whose main constituents cellulose and lignin can be distinguished semi-quantitatively in view of their technical application [5]. When using short pulse laser systems, spectrally resolved microscopy can be combined with Fluorescence Lifetime Imaging (FLIM) for a more detailed analysis of living cells or tissues.

[1] H. Schneckenburger and C. Cremer, Keeping cells alive in microscopy. Biophysica 5(1), 1 (2025).
[2] P. Weber, M. Wagner, P. Kioschis, W. Kessler and H. Schneckenburger, Tumor cell differentiation by label-free fluorescence microscopy, J. Biomed. Opt. 17(10), 101508 (2012),
[3] P. Weber, S. Schickinger, M. Wagner, B. Angres, T. Bruns and H. Schneckenburger, Monitoring of apoptosis in 3d cell cultures by FRET and light sheet fluorescence microscopy, Int. J. Mol. Sci. 16(3), 5375–5385 (2015).
[4] H. Schneckenburger, P. Weber, M. Wagner, S. Enderle, B. Kalthof, L. Schneider, C. Herzog, J. Weghuber and P. Lanzerstorfer, Combining TIR and FRET in molecular test systems, Int. J. Mol. Sci. 20, 648 (2019).
[5] H. Schneckenburger, K. Weber, K. Holderied, H. Janßen, S. Fischer, T. Wolfinger, W. Kantlehner: „Fluorescence analysis of wood chips and their constituents. Z. Naturforsch. 79b, 643–649 (2024).

Distribution of white blood cells and rigid red blood cells under flow in a rectangular microfluidic channel: a study by fluorescence confocal laser scanning microscopy

A. N. Semenov[1–3], Y. Rashidi[2], F. Mauer[2], A. E. Lugovtsov[3], V. V. Kovalyuk[1,4], A. V. Priezzhev[3], C. Wagner[2,5]

1- National University of Science and Technology MISIS, Moscow, Russia
2- Saarland University, Saarbrücken, Germany
3- M. V. Lomonosov Moscow State University, Moscow, Russia
4- National Research University Higher School of Economics, Moscow, Russia
5- University of Luxembourg, Luxembourg, Luxembourg

e-mail: a.semenov@misis.ru

Assessment of blood flow in microcirculation is critical for diagnosing cardiovascular diseases, guiding both surgical and conservative treatments. Understanding the mechanisms regulating microvascular flow is essential to maintain optimal blood transport function. A fundamental process in this context is margination – the migration of certain cells, such as white blood cells (WBC) and rigid red blood cells (RBC), toward the vessel walls during flow. While normal deformable RBC tend to concentrate in the vessel center, forming a central cell-rich core, WBC and rigid RBC – due to their lower deformability – are displaced toward the vessel wall, accumulating in the plasma-rich cell-free layer. This spatial segregation plays a crucial physiological role, i.e. WBC marginate to facilitate immune surveillance. Rigid RBC, which deformability is impaired due to aging or pathology such as cardiovascular diseases and diabetes mellitus, can adhere to the endothelium and promote vaso-occlusion.

In this study, we examined the flow-induced distribution of WBC and rigid RBCs in a rectangular PDMS microfluidic channel (30 μm height, 60 μm width, 3 cm length) using blood suspensions at 20% hematocrit. Three types of fluorescently labeled cells were studied: (1) WBC; (2) glutaraldehyde-fixed rigid RBCs, and (3) normal RBC. Cells were added to the suspensions and tracked using confocal microscopy at multiple channel positions and depths. Flow was driven by a constant pressure drop of 30 mbar using a high-precision controller.

The results revealed distinct margination profiles: rigid RBC exhibited wall-localized peaks, while deformable RBC formed a single central peak. WBC also marginate near the walls, although the effect was less pronounced, likely due to donor-dependent heterogeneity. Further experiments are underway to refine these observations.

Our findings underscore the potential of the "blood-on-a-chip" platform as a powerful tool to investigate microrheological phenomena and cellular margination in health and disease. Previously we demonstrated, how endothelialization of the rectangular microfluidic channel revealed novel peculiarities of the blood flow [3]. Here we show, how microfluidic offers new insights into studies of the blood cells margination patterns, which is particularly important in case of pathologies characterized by impaired cell deformability and abnormal microcirculatory behavior.

This work was supported by Russian Scientific Funding grant № 25-15-00172 (experimental study) and the Ministry of Science and Higher Education of the Russian Federation FSME-2025-0004 (fabrication).

[1] Lugovtsov A.E., Gurfinkel Y.I., Ermolinskiy P.B., Maslyanitsina A.I., Dyachuk L.I., Priezzhev A.V. Optical assessment of alterations of microrheologic and microcirculation parameters in cardiovascular diseases, vol. 10 (8), pp. 3974–3398 (2019).
[2] Umerenkov D.A., Ermolinskiy P.B., Lugovtsov A.E., Fabrichnova A.A., Gurfinkel Yu. I., Dyachuk L.I., Priezzhev A.V. Assessment of Microcirculation and Microrheological Parameters of Blood in Patients With Type 2 Diabetes Mellitus Using Biophotonics Techniques, Journal of Biophotonics, e202400485 (2024).
[3] Semenov A.N., Lugovtsov A. E., Ermolinskiy P.B., Priezzhev A.V. Laser Aggregometry Assessment of Blood Microrheology in a Slit Fluidic Channel Covered With Endothelial Cells, Journal of Biophotonics, e202400379 (2024).

Lymphatonics for revolutionary neurotechnologies

O. Semyachkina-Glushkovskaya

Laboratory "Smart Sleep", the Scientific Medical Center of the Saratov State University, Saratov, 410012 Russia

e-mail: glushkovskaya@mail.ru

Brain diseases account for 30% of all known pathologies in the world. This is due to the fact that many brain diseases are treated symptomatically due to the blood-brain barrier, which does not allow 98% of known drugs to enter the brain. Neurophotonics opens up innovative strategies in the development of non-pharmacological technologies for the treatment of brain diseases. However, despite progress in this direction and the emergence of commercial helmets for the treatment of brain injuries, Alzheimer's and Parkinson's diseases, depression, phototherapy remains an exclusively experimental method for treating brain pathology that has not been introduced into widespread medical practice. This is due to the limited knowledge of the mechanisms of the therapeutic effects of phototherapy. The generally accepted scientific concept is photo-activation of the mitochondrial enzyme cytochrome C oxides (COX) and an increase in the production of nitric oxide (NO) in the endothelium of blood vessels. Increasing the energy of neurons and microcirculation due to these mechanisms are important processes of neuroregeneration. However, they do not explain how phototherapy is able to influence complex cognitive processes of the brain, improve its immunity, memory and homeostasis. There is a gap between the understanding of systemic and molecular mechanisms of phototherapy for brain diseases. This is due to the lack of understanding of what is the systemic target for light, in addition to COX and NO.

The recent rediscovery of meningeal lymphatic vessels (MLVs) has changed the situation dramatically. Pioneering studies have proven that MLV perform an important function of cleansing brain tissue from toxins and metabolites, helping to maintain immunity and brain homeostasis. Dysfunction of MLVs underlies neurocognitive, oncological, metabolic, age-related and traumatic brain damage. Therefore, the creation of technologies for stimulation of the MLV functions is a priority and relevant area in modern medicine. However, the proposed methods of pharmacological stimulation of MLVs are limited by their invasiveness and side effects.

Since MLVs are located on brain surface, they are an ideal target for photobiomodulation (PBM). Indeed, recent findings have shown that PBM effectively stimulates brain drainage and lymphatic removal of beta-amyloid from its tissues, which is accompanied by a significant improvement in cognitive function of mice. PBM stimulates the MLV functions and promotes the removal of blood from the brain after the development of intracranial hemorrhages, which leads to rapid recovery of mice. PBM of the MLV functions leads to the development of resistance to the progression of glioma and brain damage caused by diabetes mellitus. PBM of brain drainage also contributes to the improvement of cognitive abilities in healthy animals. It has been proven that the preservation of MLVs is a necessary for the manifestation of the therapeutic effects of PBM. Damage to MLVs or age-related decline in their functions significantly reduce the therapeutic effects of PBM. The phenomenon of natural activation of MLV functions in deep sleep has been discovered. It has recently been discovered that sleep is a therapeutic window for PBM, in particular in the elderly. On this basis, a unique technology of PBM of the MLV functions in humans has been created, which is currently undergoing clinical trials in Russia on patients with the initial stage of Alzheimer's disease. Innovative technologies for photo-treatment of brain diseases during sleep have been proposed. A new direction in biophotonics has appeared – lymphatonics, based on the development of breakthrough photo-technologies of MLV stimulation for the neuromedicine of the future.

This research was supported by mega grant of the Russian Science Foundation (No. 23-75-30001).

Developing an algorithm for fast analysis of FLIM data

I. D. Shchechkin[1,2], S. A. Rodimova[1], N. V. Bobrov[1,3], A. M. Mozherov[4], V. I. Shcheslavsky[1], D. S. Kuznetsova[1,4]

1- Privolzhsky Research Medical University, Minin and Pozharsky Square 10/1, Nizhny Novgorod, Russia
2- Lobachevsky State University of Nizhni Novgorod, Gagarin Avenue 23, Nizhny Novgorod, Russia
3- Volga District Medical Center of the Federal Medical and Biological Agency, Marshal Voronov str. 20a, Nizhny Novgorod, Russia
4- I. M. Sechenov First Moscow State Medical University, Trubetskaya str. 8, Moscow, Russia

e-mail: iliahasa1992@gmail.com

Fluorescence-lifetime imaging microscopy (FLIM) allows the analysis of the fluorescence lifetimes of intracellular fluorophores. In particular, it is possible to analyze the fluorescence lifetimes of free (a1) and bound (a2) forms of NAD and NADPH (a3). These parameters are related to metabolic processes, including anaerobic glycolysis, oxidative phosphorylation, and biosynthetic processes, which makes it possible to assess the metabolic status of a cell. The aim of this work was to develop a method for rapid analysis of NAD(P)H fluorescence decay curves in cells.

To perform automatic analysis of FLIM images, a segmentation algorithm was developed based on the architecture of the UNet++ convolutional neural network using a multicomponent loss function, including: BCE, Focal and Dice loss functions and ELU activation function.

We analyzed 988 FLIM images of liver tissue during regeneration with pathology (steatosis and fibrosis). Using the segmentation algorithm, 20974 attenuation curves were accumulated for each individual segmented cell (11367 – steatosis, 9607 – fibrosis).

The decay curves were preprocessed, and an algorithm was developed for automatically determining the boundaries of the decay process. The axes were standardized and background noise was eliminated. The decay curves were analyzed using five methods: 1. Processing in SPCImage (manual processing); 2. Approximation based on an exponentially modified Gaussian function for two and three components; 3. Approximation based on an exponential function for two components; 4. Predictions using a perceptron (neural network); 5. Re-representation of curves using the principal component analysis (PCA) method.

As a result, we developed metrics to study the quality of decay curve analysis methods. We confirmed, that the distribution of the calculated decay parameters by all methods has similar patterns with manual processing using SPCImage. It was shown that the perceptron–based prediction method was the most comparable option for steatosis (F1 = 0.93), and the PCA method for fibrosis (F1 = 0.83). The distribution of parameter a2 has been evaluated to assess the stability of curve analysis by various methods. It has been shown that the most stable method for steatosis is the PCA (disp. Ind. = 0.558), for fibrosis, an approximation based on a modified Gaussian function for two components (disp. Ind. = 0.527) and the principal component method (disp. Ind. = 0.564). At the same time, the manual processing method showed values of dispersion index of 0.824 and 0.928 for the development of steatosis and fibrosis, respectively.

Thus, the most stable method of automatic processing of the NAD(P)H fluorescence decay curve is the PCA and modified Gaussian function for two components.

The work was supported by the Russian Science Foundation (grant No. 23-15-00421).

Unraveling biophysics of tumor cells: imaging of membrane microviscosity using FLIM with molecular rotors

L. Shimolina[1], A. Khlynova[1], N. Ignatova[1], I. Druzhkova[1], A. Gulin[2], V. Elagin[1], P. Sherin[3], M. Kuimova[3], M. Shirmanova[1]

1- Privolzhsky Research Medical University, Minin and Pozharsky sq. 10/1, Nizhny Novgorod, 603005 Russia
2- N. N. Semenov Federal Research Center for Chemical Physics RAS, Moscow, 119991 Russia
3- Department of Chemistry, Imperial College London, White City Campus, London, W12 0BZ United Kingdom

e-mail: shimolina.l.e@gmail.com

Cell membranes, despite their small size, are an integral component of any cell, and perform many functions to maintain its homeostasis and vital functions. The changes in biophisical parameters of membranes in a living cell can signal serious disorders, including tumor transformation. Recent studies show that the microviscosity of tumor cell membranes is involved not only in migration and metastasis processes, but also in the mechanisms of tumor cell response to treatment [1, 2].

The present work is aimed to study of plasma membrane's microviscosity in cancer cells using the fluorescent molecular rotor BODIPY 2 and fluorescence lifetime imaging microscopy FLIM.

The study was performed on cultured five colorectal cancer lines with different migratory ability: HT29, HCT116, Caco-2, SW480, SW837. The Hela Kyoto cell line (human cervical cancer) and Nude mice with subcutaneously grafted tumors were used. PDT was carried out with the chemical photosensitizer photoditazine (Veta-Grand, Russia) at a dose of 10 μM for in vitro, 5 mg/kg for in vivo. A laser scanning microscope LSM 880 (Carl Zeiss, Germany) equipped with a FLIM module SPC 150 TCSPC (Becker & Hickl GmbH, Germany) and a Mai Tai HP femtosecond laser, 80 MHz, 140 fs (Spectra Physics, USA) was used in the study. Fluorescence lifetime analysis was performed in the SPCImage software 8.3 (Becker&Hickl GmbH, Germany). Microviscosity was measured in individual cell plasma membranes using a BODIPY2 fluorescent molecular rotor (eg 850 nm, em 500–550 nm) [3].

It was found that in the range of cell lines we selected, HT29 cells have the most fluid membranes, 427±30 cP. Caco-2, HCT116, and SW837 cells have slightly more viscous membranes vs. HT29, with microviscosities 448±51 cP, 456±33 cP, and 457±27 cP, respectively [4]. The highest values of microviscosity were observed in SW480 cell membranes – 457±27 cP.

In context of therapy, during PDT, the microviscosity of the membranes increased from 339±40 cP to 415±22 cP in the first minutes after PDT. Analysis of changes in viscosity of tumor cells in vivo showed that in control samples without exposure, the microviscosity was 252±35 cP. However, after PDT in both cellular and vascular regimes, a statistically significant increase in viscosity was observed to approximately 400 cP. And 7 days after PDT, the viscosity value in tumor cells was recovering to control values [5].

The presented study is important for a deep understanding of the mechanisms of cancer cells response to therapy. Our results provide new data which will be useful for the development of new diagnostic approaches in oncology.

This work is supported by the Russian Science Foundation under grant No: 23-74-00045.

[1] Rebillard A. et al. Cisplatin-induced apoptosis involves membrane fluidification via inhibition of NHE1 in human colon cancer cells, Cancer Res. 67, 7865–7874, (2007).
[2] Zeisig R, Koklic T, et al. Arch Biochem Biophys. 459(1), 98–106, (2007).
[3] Shimolina LE et al, Scientific Reports. 7, 41097, (2017).
[4] Efremov YM, Shimolina LE et al. Cells. 12(21), 2583, (2023).
[5] Shimolina LE et al, JPPB, 259(12),113007, (2024).

Optical spectroscopy for surgery guidance: the choice of modalities and clinical translation

E. Shirshin

M. V. Lomonosov Moscow State University

e-mail: eshirshin@gmail.com

Biophotonics has emerged as a transformative tool in surgical oncology and minimally invasive procedures, offering high-resolution imaging, precise tissue differentiation, and real-time therapeutic feedback. This study explores the integration of laser-based biophotonic technologies – including fluorescence imaging, Raman spectroscopy, diffuse reflectance spectroscopy (DRS) – for intraoperative guidance in urological and endocrine surgeries. Key applications include: (1) Laser Lithotripsy Control: Real-time spectral feedback during laser lithotripsy to differentiate stone composition and optimize laser parameters, reducing collateral damage and improving stone fragmentation efficiency; (2) Tumor Margin Detection: fiber-based spectroscopy and imaging to delineate malignant versus healthy tissue in bladder, colorecta, and endocrine surgeries, enhancing oncological outcomes; (3) Endocrine Surgery Navigation: Near-infrared (NIR) fluorescence and DRS for parathyroid and thyroid gland identification, preserving critical structures during resection; (4) AI-Enhanced Biophotonics: Machine learning algorithms for rapid interpretation of optical data, enabling automated decision support in tumor margin assessment and lithotripsy monitoring. We present clinical case studies, ex vivo validations, and preclinical results demonstrating improved precision, reduced operative times, and lower complication rates. The convergence of laser technologies with biophotonics promises to redefine precision surgery in urology and endocrinology, paving the way for standardized, image-guided protocols.

Fungicidal action of laser and LED radiation sources in visible spectral region

A. L. Shmitko[1], A. I. Tretyakova[1], A. V. Mikulich[1], A. N. Sobchuk[1], R. K. Nahorny[1], T. S. Ananich[1], N. D. Prokopenko[1], S. V. Yakimchuk[1], I. A. Leusenka[1], L. G. Plavskaya[1], O. N. Dudinova[1], O. A. Emeliyanova[2], N. V. Dudchik[2], V. Y. Plavskii[1]

1- State Scientific Institution "B. I. Stepanov Institute of Physics of the National Academy of Sciences of Belarus", Minsk, Belarus
2- Research Institute of Hygiene, Toxicology, Epidemiology, Virology and Microbiology, Minsk, Belarus

e-mail: v.plavskii@ifanbel.bas-net.by

Interest in optical drug-free methods of suppressing the growth of fungal microorganisms is due to their increasing resistance to pharmaceuticals, as well as the presence of pronounced side effects of most antifungal drugs on the patient's body. In addition, the use of fungicidal agents in the food industry is practically unacceptable.

In this work it is shown that the effect of optical radiation of laser and LED sources in blue spectral region on fungal microorganisms (yeast-like *Candida albicans*, mold fungi of the *Penicillium candidum* species formed on hard cheeses) leads to inhibition of their growth, and at a higher energy dose – to their death. It has been established that photochemical processes sensitized by endogenous porphyrins and flavins contribute mainly to the photoinactivation of microorganisms. The presence of these photosensitizers in the cells of *C. albicans* and *P. candidum* is confirmed by spectral-fluorescence methods, as well as by kinetic spectrofluorometry methods. The data obtained indicate the presence of two compounds of porphyrin nature in the cells: coproporphyrin III and protoporphyrin IX. The conducted evaluation showed that the concentration of endogenous porphyrins in *C. albicans* is approximately 8 nM per 1 ml of intracellular content.

It was found that the rate of fungal photoinactivation increases with increasing the energy dose. It was concluded that each cell has several photosensitive vital targets, and a certain number of photodamages must be accumulated for cell inactivation (multi-impact process).

Using chemiluminescence assay, the mechanism of photodamage of microorganisms and the dependence of the damaging effect on the wavelength of the acting radiation were studied. The determining role of reactive oxygen species (and, primarily, singlet oxygen) in the mechanism of photodamage of fungal microorganisms was shown. No fundamental differences in the action of laser and LED sources were revealed. The maximum damaging effect is observed when exposed to radiation with a wavelength of 405 nm, corresponding to the maximum of the Soret absorption band of porphyrins and a local minimum in the absorption spectrum of flavins (riboflavin, flavin mononucleotide, flavin adenine dinucleotide), which indicates the important role of porphyrins in the implementation of self-sensitized death of fungal microorganisms.

Authors are grateful to the Belarusian Republican Foundation for Fundamental Research for supporting this study within the framework of the project F25UZB-132.

Trophectoderm biopsy of mammalian blastocysts using infrared femtosecond laser pulses

D. Sitnikov[1], V. Agentova[1], M. Filatov[2]

1- Joint Institute for High Temperatures of the Russian Academy of Sciences, JIHT RAS, Izhorskaya st. 13, Bd. 2, Moscow, 125412 Russia
2- Institute of Gene Biology Russian Academy of Sciences, IBG RAS, Vavilova str. 34/5, Moscow, 119334 Russia

e-mail: sitnik.ds@gmail.com

In modern assisted reproductive technology practice, millisecond laser systems are extensively utilized not only for assisted hatching but for trophectoderm (TE) biopsy at the blastocyst stage as well. The main goal is to perform preimplantation genetic testing in order to detect chromosomal anomalies that lead to severe syndromes: Down's, Patau's, Edwards's, Varkany's, Shereshevsky-Turner's and Klinefelter's, among others.

In our previous study, we evaluated the efficacy of using an infrared femtosecond laser (with a pulse duration of 280 fs and a wavelength of 1028 nm) in combination with standard microsurgical instrumentation, including holding pipettes for TE biopsy on mice blastocysts [1]. A combined "Femtosecond laser scalpel-optical tweezers system" developed in JIHT RAS was used [2].

Laser radiation was focused to a spot of 3 μm in diameter at $1/e$ level. The experimental results confirmed that laser pulses with intensities $I = 10–65$ TW/cm^2 effectively detached the biopsy specimen, regardless of the sample thickness. It has been shown that the higher the intensity, the smaller the number of pulses required to cut off a biopsy specimen of a given thickness. The disadvantage of maximum I values is that a strong shock wave is formed in the area where the laser beam is focused, which can negatively affect the surrounding cells of the embryo. So, special care should be taken.

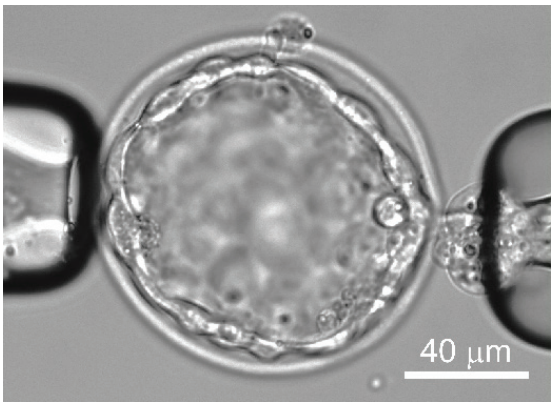

Fig. 1. Trophectoderm cells are being cut using a femtosecond laser pulse (I = 38 TW/cm^2, sample thickness H = 8 μm, mouse).

Our study is aimed at checking the efficacy of femtosecond laser pulses on a novel object – human blastocysts. The study was conducted on cryopreserved human embryos that remained after the completion of IVF programs and were donated by patients for research purposes to the FSBI "National Medical Research Center for Obstetrics, Gynecology, and Perinatology named after Academician V. I. Kulakov." The human blastocyst is 1.5 times larger in diameter, with larger cell sizes that greatly influenced the procedure. We found that $I < 40$ TW/cm^2 are too delicate to detach the TE sample. Data on the number of infrared femtosecond laser pulses required for TE biopsy, as a function of sample thickness, are obtained.

This work was supported by the Russian Science Foundation (Grant number 23-19-00424, https://rscf.ru/en/project/23-19-00424/).

[1] D. Sitnikov and M. Filatov, 'Biopsy of embryo trophectoderm cells using infrared femtosecond laser pulses,' Quantum Electronics, vol. 54, pp. 661–667, (2024).
[2] D. Sitnikov, D. Muhdina, M. Filatov, Y. Silaeva. Determination of the Optimal Impact Parameters for Microdissection of Zona Pellucida Using Femtosecond IR Laser Pulses. High Temp. vol. 62, pp. 121–130, (2024).

Reconstruction accuracy in diffuse optical spectroscopy with multiple source-detector distances

I. Turchin

A. V. Gaponov-Grekhov Institute of Applied Physics of the Russian Academy of Sciences, Ul'yanov Street 46, Nizhny Novgorod, 603950 Russia

e-mail: ilya@ipfran.ru

Diffuse optical spectroscopy (DOS) is a non-invasive method for studying tissues based on broadband illumination in the visible and/or near-infrared wavelength range and detection of diffusely scattered light. Numerical processing of the recorded spectrum enables the reconstruction of tissue chromophore concentrations (oxygenated and deoxygenated hemoglobin, water, lipids, melanin, collagen, etc.) using their known absorption spectra and a model of light propagation in tissues. DOS is used for various biomedical applications, including brain function studies, tumor boundary detection, differential diagnosis of neoplasms, monitoring of malignant tumor treatment, diagnostics of skin diseases, etc. The accuracy of chromophore concentration reconstruction depends on two key factors: (1) the precision of extinction spectrum measurements, accounting for instrumental characteristics of the DOS system (source spectral brightness, detector sensitivity, fiber transfer functions), and (2) the accuracy of the physical model describing light propagation in tissues.

To improve measurement accuracy, a self-calibration method can be employed, utilizing two sources and two detectors arranged symmetrically (with each source measured by both detectors). Although this approach increases measurement time, it offers superior accuracy compared to the traditional ratiometric method (which uses one source and two detection fibers) and reduces the influence of optical inhomogeneities at the probe-tissue interface [1].

Concerning the reconstruction accuracy, we present comparative analysis of different analytical models of diffuse reflectance (Green's function, conventional model applied in DOS [2], and a refined model published recently [3]) with the Monte Carlo-simulated reflectance in a wide range of optical parameters. The refined model demonstrates the best accuracy among all three analytical models for source-detector distances (SDDs) exceeding 2 mm. It was shown in [4] that a semi-analytical fit of massive Monte Carlo reflectance is proposed which possesses a discrepancy of less than 2% in the entire range of considered absorption and scattering and at SDDs below 2 mm. The accuracy of chromophore concentration recovery from MC simulated spectra of reflectance for a soft tissue is evaluated for all the discussed models.

Regarding reconstruction accuracy, we present a comparative analysis of different analytical models of diffuse reflectance (Green's function, the conventional DOS model [2], and a refined model proposed recently [3]) against Monte Carlo-simulated reflectance across a wide range of optical parameters [4]. The refined model demonstrates the highest accuracy among the three for source-detector distances exceeding 2 mm. A semi-analytical fit of Monte Carlo-simulated reflectance was proposed, achieving less than 2% discrepancy across all considered absorption and scattering values at source-detector distances below 2 mm.

A proposed broadband DOS device with a self-calibrating probe has been successfully applied in biomedical studies, including skin graft viability assessment [5] and monitoring tumor physiological parameter dynamics during chemotherapy [6].

[1] Perekatova, V., Kostyuk, A., Kirillin, M., Sergeeva, E., Kurakina, D., Shemagina, O., Orlova, A., Khilov, A., Turchin, I. VIS-NIR diffuse reflectance spectroscopy system with self-calibrating fiber-optic probe: Study of perturbation resistance. Diagnostics 2023, 13, 457.
[2] Farrell, T.J., Patterson, M.S., Wilson, B. A diffusion theory model of spatially resolved, steady-state diffuse reflectance for the noninvasive determination of tissue optical properties in vivo. Medical Physics 1992, 19, 879–888.
[3] Sergeeva, E., Kurakina, D., Turchin, I., Kirillin, M. A refined analytical model for reconstruction problems in diffuse reflectance spectroscopy. Journal of Innovative Optical Health Sciences 2024, 2342002.
[4] Perekatova, V., Sergeeva, E., Kirillin, M., Khilov, A., Kurakina, D., Turchin, I. Comparative analysis of accuracy of analytical models and Monte-Carlo-based empirical approximation for diffuse reflectance spectroscopy. Optics Communications 2025, 579, 131440.
[5] Turchin, I., Beschastnov, V., Peretyagin, P., Perekatova, V., Kostyuk, A., Orlova, A., Koloshein, N., Khilov, A., Sergeeva, E., Kirillin, M., Ryabkov, M. Multimodal optical monitoring of auto- and allografts of skin on a burn wound. Biomedicines 2023, 11, 351.
[6] Druzhkova, I., Bylinskaya, K., Plekhanov, A., Kostyuk, A., Kirillin, M., Perekatova, V., Turchin, I. Effects of FOLFOX chemotherapy on tumor oxygenation and perfused vasculature: An in vivo study by optical techniques. Journal of Biophotonics 2024, e202400339.

Deep learning in analysis of optical properties of biotissues

B. Yakimov[1,2], E. Shirshin[1,2]

1- Faculty of Physics, M. V. Lomonosov Moscow State University, Leninskie Gory 1-2, Moscow, 119234 Russia
2- Laboratory of Clinical Biophotonics, Biomedical Science and Technology Park, Sechenov First Moscow State Medical University, Trubetskaya 8, Moscow, 119048 Russia

e-mail: bp.jakimov@physics.msu.ru

Exploring the parameters related main optical responses of cellular and tissue molecules is essential for enhancing the development and application of optical diagnostic methods. A key aspect of this research involves identifying new endogenous target molecules – naturally occurring substances within the body – that display unique optical properties. In this study, we show that such molecules can be identified not only through experimental techniques but also by employing machine learning and quantitative structure-property relationship methods on existing open-access databases that contain information on metabolites, pharmaceuticals, and other biomolecules found in humans. We begin by assessing the accuracy of models developed to reconstruct main optical characteristics, and then we demonstrate how these models can aid in the discovery of new optical biomarkers within the cells and biotissues.

The work was supported by the Non-commercial Foundation for the Advancement of Science and Education INTELLECT.

Advances in the interaction of laser radiation with upconversion nanoparticles in tissues

I. Yu. Yanina[1,2]

1- Saratov State University (National Research University), Institute of Physics, Astrakhanskaya str. 83, Saratov, 410012 Russia
2- Tomsk State University (National Research University), Laboratory of laser molecular imaging and machine learning, Lenin's av. 36, Tomsk, 634050 Russia

e-mail: irina-yanina@list.ru

This paper reviews research findings on the toxicity of various types of upconversion nanoparticles [1–4]. Upconversion nanoparticles are promising for imaging biological tissues and organs under luminescent light, as well as for use in disease diagnostics and photoinduced therapy. The review examines nanoparticles with additional coatings or functionalized surfaces modified with targeting or photoactive molecules, allowing the creation of multimodal particles. Special attention is given to the phototoxicity of these particles. When using nanoparticles for therapeutic or diagnostic applications in living organisms, toxicity is a crucial consideration. The toxic effects of upconversion nanoparticles on an organism depend on their concentration upon administration and the total amount of nanoparticles relative to body weight. Based on histological and biochemical studies of concentration dependencies, it has been shown that these particles generally do not exhibit significant toxicity, and the maximum permissible concentration can be considered 2 mg/mL.

The study was supported by a grant Russian Science Foundation No. 25-22-00144, https://rscf.ru/project/25-22-00144/.

[1] I. Yu. Yanina, V. I. Kochubey, Toxicity of Upconversion Nanoparticles. Overview. Izvestiya of Saratov University. Physics, vol. 20, iss. 4, pp. 268–277 (2020).
[2] J. Li, X. Chang, X. Chen, Z. Gu, F. Zhao, Z. Chai, Y. Zhao, Toxicity of inorganic nanomaterials in biomedical imaging, Biotechnol Adv., vol. 32, no.4, pp. 727–743 (2014).
[3] M. Z. Ahmad, B. A. Abdel-Wahab, A. Alam, S. Zafar, J. Ahmad, F. J. Ahmad, P. Midoux, C. Pichon, S. Akhter, Toxicity of Inorganic Nanoparticles Used in Targeted Drug Delivery and Other Biomedical Application: An Updated Account on Concern of Biomedical Nanotoxicology, J nanosci nanotechno., vol. 16, no.8, pp. 7873–7897 (2016).
[4] A. Gnach, T. Lipinski, A. Bednarkiewicz, J. Rybka, J.A. Capobianco, Upconverting nanoparticles: assessing the toxicity, Chem Soc Rev., vol. 44, no.6, pp. 1561–1584 (2015).

Endoscopic laser speckle contrast imaging of blood flow

J. Yuan[2], Q. Han[1], J. Lu[2], P. Li[1,2]

1- MoE Key Laboratory for Biomedical Photonics, Advanced Biomedical Imaging Facility-Wuhan National Laboratory for Optoelectronics, Huazhong University of Science and Technology, Wuhan, Hubei, 430074 China
2- State Key Laboratory of Digital Medical Engineering, Key Laboratory of Biomedical Engineering of Hainan Province, School of Biomedical Engineering, Hainan University, Sanya 572025 China

e-mail: pengchengli@hainanu.edu.cn

Rigid endoscopy can observe and find abnormal lesions in the human body and has been widely used in minimally invasive surgery. Blood flow is essential for maintaining normal physiological functions of the human body. Combine the laser speckle contrast imaging (LSCI) of blood flow imaging with rigid endoscopy, can achieve rapid, high-resolution, label-free, and long-term blood flow perfusion monitoring in minimally invasive surgery. Endoscopic LSCI can help surgeons to provide visualization of blood flow in internal tissue, organs, and the endovascular inner wall during minimally invasive surgery [1–3]. However, conventional endoscopic LSCI uses low-coherency light illumination scheme where the laser passes through multimode glass fiber bundles and is coupled with the laparoscope's built-in illumination system (including light cones and built-in lighting glass fiber bundles) leading to restricted angles of illumination, compromised laser coherence, uneven laser intensity distribution, and low coupling efficiency, which degrade the performance of LSCI imaging in endoscopic applications. We proposed that conical fiber coupled high coherence laser can be used to achieve large angle, high coherence, high uniformity and high coupling efficiency laser illumination in the endoscopic environment. Through phantom and animal experiments, we reveal that conical fiber illumination significantly enhances LSCI performance. This technology expands the detectable flow range, broadens the imaging field of view. Moreover, it significantly improves signal to noise ratio, facilitates more sensitive detection of minute blood flow changes, and improve the signal background ratio of endoscopic LSCI imaging. Our findings suggest that conical fiber-based laser illumination stands as a highly promising advancement in endoscopic LSCI.

[1] J. H. Ronn, N. Nerup, R. B. Strandby, et al., Laser speckle contrast 646 imaging and quantitative fluorescence angiography for perfusion as-sessment," Langenbecks Arch. Surg. 505–515 (2019).
[2] W. Heeman, K. Dijkstra, C. Hoff, et al., "Application of laser speckle contrast imaging in laparoscopic surgery, Biomed. Opt. Express 10, 650 2010–2019 (2019).
[3] J. Yan, Q. Han, L. Meng, et al., High-quality Endoscopic Laser Speckle Contrast Imaging with Conical Fiber Illumination, Photonics Research, 3(3), 583–592 (2025)

Optical imaging for tissue engineering

E. Zagaynova[1,2], A. Kashina[2], A. Kashirina[2], P. Ermakova[2], N. Batenkin[3], S. Chesnokov[3], A. Bogomolova[1], A. Panova[1,4], V. Elagin[2]

1- Lopukhin Federal research and clinical center of physical-chemical medicine, Moscow, Russia
2- Institute of Biomedical Technologies, Privolzhskiy Medical Research University, Nizhny Novgorod, Russia
3- Federal State Budgetary Institution of Science G. A. Razuvaev Institute of Organometallic Chemistry, Russian Academy of Sciences, Nizhny Novgorod, Russia
4- Institute of Gene Biology, Russian Academy of Sciences, Moscow, Russia

e-mail: ezagaynova@gmail.com

Insulin-deficient conditions include: type 1 diabetes mellitus (T1DM) – an autoimmune disease with the destruction of β-cells, pancreatic diseases (necrosis, tumors, fibrosis) with the development of Langenhars islet deficiency [1]. Despite the success in islets transplantation for the treatment of insulin-deficient conditions, problems remain, such as a shortage of donor tissues of the required quality and immune rejection of the transplant.

The creation and implementation of the technology of transplantation of insulin-producing cells (islets) protected from the immune response will open up new prospects for the treatment of patients with insulin-deficient conditions.

Non-invasive technologies are needed to safely monitor the process of β-cells production, storage and transplantation. Multiphoton microscopy combined with fluorescence lifetime imaging (FLIM) is a high spatial resolution, label-free and non-invasive approach to study cells. It enables to investigate cells' and tissues' structure (multiphoton microscopy of endogenous fluorophores), a structure of a matrix (second-harmonic generation microscopy), and the metabolic status of single cells (FLIM).

Our team is developing several so-called tissue-engineered constructs for treatment of insulin-deficient conditions and for quality control uses optical technologies.

1. Isolation and autotransplantation of islets from the pathological pancreas. The task of optical imaging is to determine the quantity and quality of islets both in pancreatic tissue and after preservation before administration to the patient [2].

2. Isolation, accumulation, storage, encapsulation of islets in alginate capsules for allotransplantation. FLIM imaging evaluates the viability and activity of islets before and after encapsulation and before transplantation [3].

3. Creation of β-cells from induced pluripotent stem cells with reduced immunogenicity, encapsulation in improved alginate capsules and transplantation of tissue-engineered constructs to recipients. Optical imaging monitors the quality of capsules, β-cells activity inside the capsules (FLIM imaging). Distribution and preservation of labeled β-cells in the animal model in parallel with the activity of insulin production and maintenance of glucose levels (luciferin-luciferase genetically encoded construct and IVIS Spectrum Whole body imaging).

Research was supported by the Russian Science Foundation, project number 24-65-00044.

[1] Bellofatto K., Beat Moeckli B., Wassmer Ch.-H., et al. Bioengineered Islet Cell Transplantation // Current Transplantation Reports. V. 8. P. 57–66 (2021).
[2] Ermakova, P.; Kashirina, A.; Kornilova, I.; Bogomolova, A.; Myalik, D.; Naraliev, N.; Kuchin, D.; Lugovaya, L.; Zagaynova, E.; Zagainov, V.; Kashina, A. Contrast-Free FLIM Reveals Metabolic Changes in Pathological Islets of Langerhans. Int. J. Mol. Sci., 23, 13728 (2022).
[3] Ermakova P., Vasilchikova E., Baten'kin M., Bogomolova A., Konev A., Anisimova N., Egoshina A., Zakharina M., Tselousova J., Naraliev N., Kuchin D., Lugovaya L., Zagainov V., Chesnokov S., Kashina A., Zagaynova E. Probing of New Polymer-Based Microcapsules for Islet Cell Immunoisolation // Polymers. T. 16, №. 17, 2479 (2024).

Analysis of nonlinear elasticity of biotissues in optical coherence elastography using a new stress-strain equation inspired by nonlinearity of rocks

V. Y. Zaitsev, A. A. Sovetsky, L. A. Matveev, A. L. Matveyev

A. V. Gaponov-Grekhov Institute of Applied Physics RAS, Nizhny Novgorod, Russia

e-mail: vyuzai@ipfran.ru

The recently developed method of quasistatic Compression Optical Coherence Elastography (C-OCE) with reference silicone layers made it possible to obtain nonlinear stress-strain dependences relating the applied uniaxial compressive stress and the axial component of the resultant strain in the tissue. In many tissues we observed quite universal nonlinear-elastic behavior. Namely, at the initial stage of compression, tissues exhibit pronounced increase in the slope of the stress-strain dependence with subsequent trend to almost linear asymptotics, which strongly resembles elastic nonlinearity of compressed cracked rocks. By analogy with geomechanics we consider that such a nonlinear elastic response of tissues is mostly determined by the histologically confirmed presence of interstitial gaps/pores resembling cracks in rocks, in which highly compliant narrow cracks can easily be closed by applied compressing stress. Similarly, in biotissues, after closing most of compliant pores by the applied stress when performing C-OCE examination, the elastic response of the sample becomes nearly linear and is determined by the Young's modulus of the host tissue. For describing the distribution of the cracks/gaps over closing pressures, an analogy with geophysics is also used. In contrast to often used phenomenological approaches, the parameters introduced in the new model have clear physical meaning and characterize the total content of compliant pores, their characteristic closing stress and the Young modulus of the host tissue [1].

For diverse tissues examined using C-OCE (eye cornea, pericardium, various components of malignant tumors, lymph nodes, etc.), the model well describes the observed nonlinear stress-strain dependences and is useful for differentiating various types/states of tissues important for solving important biomedical problems [1–7].

The preparation of this report was supported by the RSF grant No 22-12-295.

[1] V. Y. Zaitsev et al., "Geophysics-Inspired Nonlinear Stress–Strain Law for Biological Tissues and Its Applications in Compression Optical Coherence Elastography," Materials (Basel)., v. 17(20), p. 5023, (2024) doi: 10.3390/MA17205023.
[2] A. A. Plekhanov et al., "Tissue Elasticity as a Diagnostic Marker of Molecular Mutations in Morphologically Heterogeneous Colorectal Cancer," Int. J. Mol. Sci., v. 25(10), p. 5337, (2024), doi: 10.3390/ijms25105337.
[3] E. B. Kiseleva et al., "Detecting emergence of ruptures in individual layers of the stretched intestinal wall using optical coherence elastography : A pilot study," J. Biophotonics, v. 17(8), e202400086, (2024), doi: 10.1002/jbio.202400086.
[4] V. Y. Zaitsev et al., "Application of compression optical coherence elastography for characterization of human pericardium: A pilot study," J. Biophotonics, 16(3), e202200253, (2023) doi: 10.1002/jbio.202200253.
[5] A. A. Plekhanov et al., "Compression OCT-elastography combined with speckle-contrast analysis as an approach to the morphological assessment of breast cancer tissue," Biomed. Opt. Express, v. 14(6), p. 3037, (2023) doi: 10.1364/BOE.489021
[6] E. V Gubarkova et al., "Quantification of linear and nonlinear elasticity by compression optical coherence elastography for determining lymph node status in breast cancer," Laser Phys. Lett., v. 20(6), p. 65601, (2023) doi: 10.1088/1612-202X/accdcf
[7] A. A. Plekhanov et al., "Towards targeted colorectal cancer biopsy based on tissue morphology assessment by compression optical coherence elastography," Front. Oncol., v. 13, 1121838, (2023), doi: 10.3389/fonc.2023.1121838

Multimodal assessment of microcirculatory parameters using optical diagnostics techniques

K. Bylinskaya, M. Kirillin, A. Kostyuk, E. Sergeeva, I. Turchin, V. Perekatova

A. V. Gaponov-Grekhov Institute of Applied Physics of the Russian Academy of Sciences, Ul'yanov Street 46, Nizhny Novgorod, 603950 Russia

e-mail: k.bylinskaya@ipfran.ru

Assessment of microcirculatory bed parameters using optical methods is a rapidly developing field of biomedical diagnostics that allows for the noninvasively or minimally invasively study of blood flow in small vessels (arterioles, capillaries, venules) responsible for the exchange of substances between blood and tissues, which is critical for understanding and diagnosing various diseases.

Diffuse optical spectroscopy (DOS) is a non-invasive diagnostic technique that allows for the assessment and monitoring of the biochemical state of tissues. DOS is commonly used to measure chromophore concentrations in tissues *in vivo* [1]. Optical coherence tomography (OCT) is an imaging technique which generates cross-sectional images of tissue with high resolution [2]. The combined use of OCT and DOS enables a comprehensive assessment of the microvasculature by integrating morphological imaging with functional probing, opening new avenues for research and diagnostics. In our study, we performed multimodal monitoring of microvascular parameters of human skin using OCT and DOS since their combined use yields information inaccessible when either is used alone.

The study involved 18 healthy volunteers (8 females, 10 males). Multimodal monitoring included acquiring 3D OCT and OCT-A images and DOS spectra from different skin areas: the wrist (proximal wrist crease), palm (thenar eminence), and web space between the thumb and index finger.

The setup for broadband self-calibration DOS measurements, previously developed in IAP RAS, was employed for the estimation of the parameters of microvascular bed [3]. The spectra of effective attenuation coefficient demonstrate differences for different age groups, especially in the range of 450–500 nm, characterizing the levels of melanin and blood (Fig. 1). The difference is mostly pronounced for the spectra obtained from the web space.

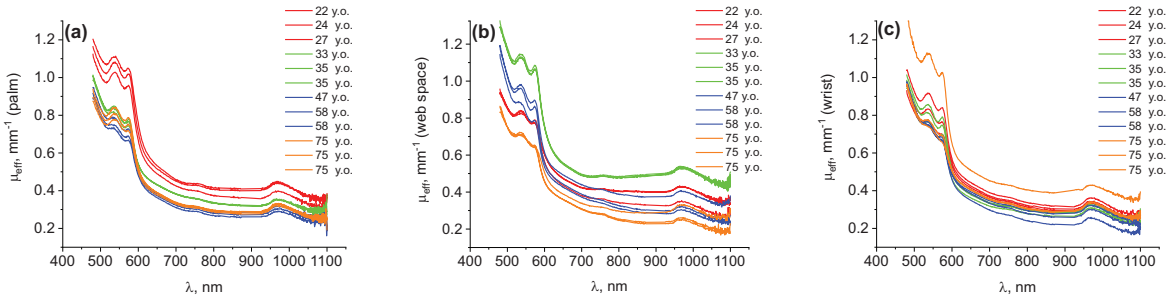

Fig. 1. Typical effective attenuation coefficient spectra of skin from the palm (a), web space (b), and wrist (c) in volunteers of different age groups, derived from detector channel data at source-detector distances of 2.4 mm and 3.6 mm.

Reconstruction of the biotissue parameters governing the absorption spectrum was performed using the refined analytical model for small acceptance angle [4].

Preliminary statistical analysis of the reconstructed chromophore concentrations showed statistically significant differences between phototypes 1 and 2 for blood, water and melanin content, and between phototypes 1 and 3 for water and melanin content.

The study is supported by the Russian Science Foundation (project No. 24-75-10068).

[1] O'Sullivan T.D., Dehghani H., Re R. Diffuse Optical Spectroscopy: Technology and Applications: introduction to the feature issue // Biomed. Opt. Express. 2024. Vol. 15, № 11. P. 6516–6520.
[2] Aumann S. et al. Optical Coherence Tomography (OCT): Principle and Technical Realization // High Resolution Imaging in Microscopy and Ophthalmology: New Frontiers in Biomedical Optics / ed. Bille J.F. Cham (CH): Springer, 2019.
[3] Perekatova V. et al. VIS-NIR Diffuse Reflectance Spectroscopy System with Self-Calibrating Fiber-Optic Probe: Study of Perturbation Resistance // Diagnostics. Multidisciplinary Digital Publishing Institute (MDPI), 2023. Vol. 13, № 3.
[4] Sergeeva E. et al. A refined analytical model for reconstruction problems in diffuse reflectance spectroscopy // J. Innov. Opt. Health Sci. 2024. Vol. 17.

Development and application of multichannel fiber-optic sensor for laser spectrometry, biomedicine and automatization's

G. L. Danielyan[1], N. A. Ivanov[1], O. V. Vikhrova[1], O. D. Morozova[1], G. V. Nazarova[2], I. N. Molokovich[3]

1- General physics institute RAS, Vavilova str. 38, Moscow, 119991 Russia
2- LLC Optofiber, Vavilova str. 38-5, Moscow, 119333 Russia
3- Central Institute of Aviation Motors, CIAM, Aviamotornaya str. 2, Moscow, 111116 Russia

e-mail: gldan@yandex.ru

Multichannel fiber-optic Bundles (MFOB) have become widely used not only as motion sensors, but also in various physical experiments, in biomedicine and in industrial installations using lasers and various spectroscopy methods [1, 2]. Moreover, their role in modern research and hardware improvement tasks is unique and allows make remote measurements in very harsh conditions [3–5]. However, the problem of designing and implementing fiber-optic sensors based on MFOB is constrained by several factors: 1. the complexity of choosing the optimal structure and its numerical modeling of the MFOB; 2. the choice of a construction and e distance between the sensitive end of the probe; 3. the ineffective use of new special fibers in the structure of the MFOB [5].

Methods: We presented an improved theoretical model of the MFOB containing a large number (up to 630) of fibers, dividing into groups of emitting and receiving channels (up to20), which maximizes the efficiency of lighting collection in MOFOB probes. Various numerical models have been developed for measuring the necessary data and optical reflections in tasks of physical research and tasks using laser fluorescence diagnostics. In general, MFOB numerical model are applicable as cheap fast simplified modeling. To demonstrate the theory, various MFOBs have been developed, ranging from sensors for monitoring turbine blades of gas aircraft engines to MFOBs in various physical experiments for fluorescence spectrometry in the field of Biomedical R&D [6].

Results: Our experimental results and designed devises show optimal dependence of the collection efficiency on the distance between the probe and the research sample. Designed probes are generally consistent with our MFOB numerical model. In the report presents the practical results of the development of a large number of optimal MFOB structures for motion sensors, spectral sensors for the UV-VIS-NIR1-3 ranges (from 200 to 2400 nm), sensors for plasma monitoring and for other laser systems.

Conclusions: We have studied the effectivity of MFOB numerical model for use in probes for physical and biomedical applications. It is determined that the decisive factor in MFOB is the optimal selection of the type of multimode fibers, their geometric dimensions and their relative location in the MFOBs structure. Determined that there is an optimal distance between the probes and the object under study. This optimal distance, depends not only on the diameter of the fiber and its numerical aperture, but also on the structure of the channels and their location in MFOB. To increase the signal-to-noise ratio, it is effective to use a metal coated opto-fibers in the channels for receiving and transmitting laser radiation. For a large class of tasks related to fluorescence spectroscopy, an optical fiber structure consisting of metal-emitting quartz-coated fibers and receiving glass fibers with a high numerical aperture is very effective.

[1] J. Javelov, I. Kaplunov, G. Danielyan, Fiber-optical measuring systems: Applied problems, Chapter 1, (2011).
[2] L. Wang et al. BioMed. Engineering OnLine, 2011, 10:95; http//biomedical-engineering-online/content/101/95.
[3] U. Utzinger et al, Fiber optic probes for biomedical spectroscopy. J. Biomed. Opt. 8:121–147, (2003).
[4] G. Danielyan, Multichannel Fiber Optic Bundles and Sensors for Biomedical Applications, Proc. SPIE v. 5566, pp. 198–203.
[5] G. Danielyan, W. Neuberger , USA patent 5453838-09, Sensing system with multi-channel fiber optic bundle sensitive probe ,USA patent Bulletin, 17, (1997).
[6] G. Danielyan, S. Ivanov, I. Molokovich et al., High temperature fiber optic sensor for monitoring gaps in aircraft engines, J. Fotonika, special pub. (2019), DOI 10.24411/2308-6920-2019-16171.

Classification of low-molecular-weight ligands of nicotinic acetylcholine receptors by Raman spectroscopy

A. A. Gilfanova[1,2], K. A. Prokhorov[2], Yu. N. Utkin[3], V. I. Tsetlin[3]

1- Institute for Physical Research and Technologies,
Peoples' Friendship University of Russia named after Patrice Lumumba, Moscow, Russia
2- Department of Coherent Radiation Interaction with Matter,
Prokhorov General Physics Institute of the Russian Academy of Sciences, Moscow, Russia
3- Institute of Bioorganic Chemistry named after academicians M. M. Shemyakin and Yu. A. Ovchinnikov of the Russian Academy of Sciences, Moscow, Russia

e-mail: gilfanova_0703@mail.ru

Raman spectroscopy is a highly informative method for investigating molecular structures based on their vibrational characteristics. In this study, the method was applied to analyze nine low-molecular-weight ligands of nicotinic acetylcholine receptors (nAChRs), including agonists, antagonists, and modulator. These organic substances are of great interest to biologists as signaling molecules of neuroreceptors that control important human systems. However, until now, most of these substances have not been studied using Raman spectroscopy methods.

We examined the ligands in their natural polycrystalline form. Microdoses of the samples were analyzed using a Raman spectrometer combined with an optical microscope. Laser excitation wavelength was 532 nm. The recorded spectra varied greatly from sample to sample. To identify patterns and recognize groupings within the all spectral data, principal component analysis (PCA) was applied. As shown in Fig. 1, this approach revealed stable ligand clusters that reflect both molecular structure and functional activity with respect to nAChRs. Notably, only tubocurarine deviated from the typical distribution of antagonists**.** This can be attributed to the effect of fluorescence and low intensity of the Raman signal that distort individual Raman lines. The deeper reasons may lie in the fact that many ligands change the mechanisms of their action depending, for example, on the cell type or the concentration of the ligand itself. Therefore, a more subtle and in-depth classification of ligand functionality is desirable.

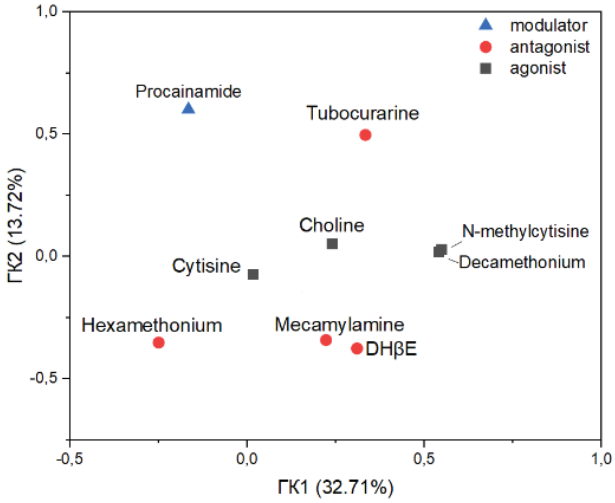

Fig. 1. PCA of all ligands based on Raman spectra.

Additionally, we used our spectral data for hierarchical cluster analysis, which allowed systematizing and visualizing objects by their similarity. The results were quite satisfactory, further identifying the spectral proximity between ligands of certain specificity.

The approach we used, which included cost-effective Raman spectroscopy followed by statistical data analysis, demonstrated good efficiency in the identification and classification of biologically active substances. It offers promising potential for analyzing new receptor-targeted ligands in pharmacological research.

Effect of Pt-Pd nanoparticles on auto- and photooxidation of tetrahydrobiopterin

D. A. Makarova[1], A. S. Nizamutdinov[1], T. A. Telegina[2], Yu. L. Vechtomova[2], A. A. Buglak[3]

1- Kazan (Volga Region) Federal University, Kremlevskaya str. 18, Kazan, 420008 Russia
2- A. N. Bach Institute of Biochemistry, Federal Research Center "Fundamentals of Biotechnology" of the Russian Academy of Sciences, Leninsky pr-t. 33, building 2, Moscow, 119071 Russia
3- Physics Department of St. Petersburg State University, Universitetskaya nab., 7–9, St. Petersburg, 199034 Russia

e-mail: makarovadaryaaa@mail.ru

Tetrahydrobiopterin (H4Bip) as a coenzyme of phenylalanine hydroxylase is involved in the oxidation of phenylalanine to tyrosine (a precursor of melanin). Studies have shown that the affected area of the skin contains an excess of tetrahydrobiopterin and its oxidation products [1]. There is a hypothesis that excess tetrahydrobiopterin leads to the accumulation of hydrogen peroxide [2]. Its excess either contributes to the induction of GTF cyclohydrolase or leads to oxidative stress. Thus, we have a "vicious circle" that maintains an excess of tetrahydrobiopterin [3].

One of the most relevant areas for preventing pathology is phototherapy, which prevents the oxidation of tetrahydrobiopterin by dimerizing dihydropterin [4]. Today, excimer laser radiation with a wavelength of 308 nm is actively used, but such therapy has only a temporary result. In addition to ultraviolet radiation, in recent decades, nanoparticles of noble metals (such as gold, platinum, palladium) have also been used as a therapy for vitiligo, acting as antioxidants due to their high catalytic activity [5]. In this context, the aim of the present studies is to study the effect of Pt-Pd nanoparticles on the auto- and photooxidation of tetrahydrobiopterin.

The oxidation products were studied by optical absorption spectroscopy. A Shimadzu spectrophotometer was used to record absorption spectra. The xenon lamp light of a Horiba FluoroMax-4 spectrofluorimeter was used as a UV radiation source. Irradiation was carried out at two wavelengths (325 and 308 nm) for 3 minutes. The purchased colloid of Pt-Pd nanoparticles diluted in a phosphate buffer (0.01 M; 7.2 pH) at concentrations of C_0 = 6 μl/ml, C_1 = 1.2 μl/ml and C_2 = 0.3 μl/ml were used as samples.

The percentage of dimer formation of dihydropterin was calculated relative to tetrahydrobiopterin, taking into account that the dimer is a double molecule. The gray bars indicate the periods of ultraviolet irradiation. The highest percentage of dimer formation was about 87.52 and was obtained when the solution was irradiated with ultraviolet light with a wavelength of 325 nm and a nanoparticle concentration of 1.2 μl/ml.

The highest quantum yield of dihydropterin dimers was also obtained under UV irradiation (325 ± 10 nm) with the addition of Pt-Pd nanoparticles at a concentration of C_1 = 1.2 μl/ml. The concentration of nanoparticles C_2 = 0.3 μl/ml also showed positive dynamics in the formation of dimers, but was less effective.

[1] Bergqvista Ch., Ezzedine Kh. Vitiligo: A Review, Dermatology, vol. 236., pp. 571–592, (2020).
[2] Schallreuter K.U., Moore J., Wood J.M., Beazley W.D., Gaze D.C., Tobin D.J., In vivo and in vitro evidence for hydrogen peroxide (H_2O_2) accumulation in the epidermis of patients with vitiligo and its successful removal by a UVB-activated pseudocatalase, J Investig Dermatol Symp Proc., vol. 4., pp. 91–96, (1999).
[3] Telegina T.A., Vechtomova Yu.L., Kritsky M.S., Nizamutdinov A.S., Madirov E.I., Makarova D.A., Buglak A.A Photooxidation of tetrahydrobiopterin as the basis of vitiligo phototherapy , Optics and Spectroscopy, vol. 5, № 5., pp. 602–607, (2022).
[4] Buglak A.A., Telegina T.A., Lyudnikova T.A., Vechtomova Yu.L., Kritsky M.S. Photooxidation of tetrahydrobiopterin under UV irradiation: possible pathways and mechanisms, Photochemistry and photobiology, vol. 90, Iss. 5., pp. 1017–1026, (2014).
[5] Bae J.M. Jung Min Bae, Han Mi Jung, Bo Young Hong, Phototherapy for Vitiligo: A Systematic Review and Meta-analysis, Original Investigation., vol. 153(7)., pp. 666–674, (2017).

Tumor node tracking using fluorescence monitoring during photodynamic therapy

A. Savelyev, M. Kirillin, I. Turchin

A. V. Gaponov-Grekhov Institute of Applied Physics of the Russian Academy of Sciences, Ul'yanov Street 46, Nizhny Novgorod, 603950 Russia

e-mail: a.savelyev@ipfran.ru

Fluorescence imaging is one of the most easy-to-use and effective noninvasive techniques for real-time assessment of therapeutic response during photodynamic therapy (PDT). This technique enables monitoring of photosensitizer (PS) accumulation and photobleaching in the tumor node and surrounding tissues. The degree of PS photobleaching defined as the relative decrease in fluorescence intensity as a result of the PDT procedure can serve as a criterion for PDT efficacy and a basis for intraprocedural therapeutic dose correction. Such implementation of the personal medicine principle is essential to minimize damage to healthy tissues and reduce the risk of recurrence [1].

Real-time assessment of PS photobleaching during clinical PDT procedure requires automatic tracking of the irradiated pathological area. However, this process is complicated by several factors, including shifts of the target region within the frame induced by patient movement and the presence of extraneous objects (e.g., medical instruments or adjacent PS localization areas) in the acquired images. These objects may obscure the region of interest or introduce artifacts due to glare and intrinsic fluorescence. Additionally, the gradual decrease in fluorescence intensity during therapy further complicates visual tracking. In this connection, selecting a robust algorithm capable of overcoming these challenges is crucial for accurate PDT fluorescence monitoring.

This study presents an experimental evaluation of the following tracking algorithms: Median Flow [2], TLD [3], MOSSE [4], and CSRT [5]. A comparative analysis was performed on image series obtained using a fluorescence imaging system previously developed by our team [6] during 8 PDT procedures in clinical environment. Each series contained conjugated images acquired upon excitation at 405, 660, and 780 nm, together with dark field images used to subtract background level. Fluorescence imaging at several wavelength provides additional information about fluorophore localization [7].

Additional experiments with a phantom object containing a chlorin-based PS were conducted to evaluate algorithm robustness against shifts, tilts, and occlusions of the target area.

The results demonstrate that the optimal method for tracking the pathological area is the CSRT algorithm, supplemented by MOSSE to maintain tracking in cases of fluorescence area overlapping.

The developed algorithm facilitates individualized laser dose adjustment and enhances PDT efficacy by providing reliable, automated assessment of PS photobleaching during treatment.

The study is supported by the Russian Science Foundation (project 24-15-00175).

[1] Gamayunov, S.V., et al., Fluorescence imaging for photodynamic therapy of non-melanoma skin malignancies – A retrospective clinical study. Photonics & Lasers in Medicine, 5 (2016).
[2] Kalal, Z., K. Mikolajczyk, and J. Matas. Forward-backward error: Automatic detection of tracking failures. in 2010 20th international conference on pattern recognition. IEEE (2010).
[3] Kalal, Z., K. Mikolajczyk, and J. Matas, Tracking-learning-detection. IEEE transactions on pattern analysis and machine intelligence, 34(7): pp. 1409–1422 (2011).
[4] Bolme, D.S., et al. Visual object tracking using adaptive correlation filters. in 2010 IEEE computer society conference on computer vision and pattern recognition. IEEE (2010).
[5] Lukežič, A., et al., Discriminative Correlation Filter with Channel and Spatial Reliability. International Journal of Computer Vision, 2018. 126.
[6] Kleshnin, M. S., et al. Compact and fully automated system for monitoring photodynamic therapy, based on two LEDs and a single CCD. Laser Physics Letters 12.11, 115602 (2015).
[7] M. Kirillin, et al. Dual-wavelength fluorescence monitoring of photodynamic therapy: from analytical models to clinical studies. Cancers, 13(22), 5807 (2021).

32nd INTERNATIONAL CONFERENCE
Advanced Laser Technologies
ALT'25

LASER SYSTEMS AND MATERIALS

Development of optically pumped rare gas laser (OPRGL)

Yu. A. Adamenkov, M. A. Gorbunov, A. A. Kalacheva, V. A. Shaidullina, A. V. Yuriev

FSUE «RFNC-VNIIEF» Mira prosp. 37, Sarov, Russia

e-mail: oefimova@otd13.vniief.ru

Optical pumped rare gas Laser (OPRGL) on metastable atoms of inert gases is new promising optical generator in which high quantum efficiency is combined with good optical quality of the output beam. The optical medium of the laser consists of a mixture of rare gases containing a buffer gas (usually helium) and a gas on the atoms of which generation occurs – Ne, Ar, Kr or Xe. The content of generating gas in the mixture ranges from 1 to 5%. Since receiving the first generation on inert gas atoms (Kr) in 2012 [1], studies of the active medium [2, 3] have been carried out aimed at optimizing laser parameters, such as increasing the generation output and the efficiency of using optical pumping.

This paper presents the results of experiments on the study of a laser on a mixture of inert gases with optical pumping (LONIG). Dependence of generation power on repetition frequency of discharge pulses and on gas mixture flow rate for medium 2% Ar + 98% He is presented. The second harmonic generation at wavelength 456 nm was achieved.

Pulse-periodic discharge was used to create active medium. During the experiments, the following parameters were varied: pressure and flow rate of the gas medium, transmission coefficient of the mirrors of the optical resonator, repetition rate of electric discharge pulses. The maximum generation power obtained in the experiments was 4.5 Watts. The achieved power of second harmonic generation was less than 1 mWt.

[1] J. Han, M.C. Heaven. Gain and lasing of optically pumped metastable rare gas atoms // Optics Letters. -2012. -Vol. 37, No. 11, pp. 2157–2159.
[2] Sun P., Zuo D., Mikheyev P.A., Han J., Heaven M.C. Time-dependent simulations of a CW pumped, pulsed DC discharge Ar metastable laser system // Opt. Express., 27, 22289 (2019).
[3] П.А. Михеев. Лазеры на метастабильных атомах инертных газов с оптической накачкой // Квантовая электроника, 2015, 45, № 2.

Using low-loss chalcogenide and tellurite fibers for quantum and nonlinear optical applications

A. V. Andrianov[1], E. A. Anashkina[1], N. I. Salnikov[1,2], S. E. Motorin[1,3], V. V. Dorofeev[1,3]

1- A. V. Gaponov-Grekhov Institute of Applied Physics of the Russian Academy of Sciences, Ulyanov Street 46, Nizhny Novgorod, 603950 Russia
2- Lobachevsky State University of Nizhny Novgorod, Gagarin Ave. 23, Nizhny Novgorod, 603022 Russia
3- G. G. Devyatykh Institute of Chemistry of High-Purity Substances of the Russian Academy of Sciences, Tropinin Street 49, Nizhny Novgorod, 603950 Russia

e-mail: andrian@ipfran.ru

The trend toward miniaturizing optical devices that operate at relatively low power requires using highly nonlinear materials. In this context, chalcogenide and tellurite glasses ("soft" glasses) are of great interest due to their significantly higher nonlinearity than commonly used materials. Tellurite glasses have a third-order nonlinearity that is 10–20 times higher than fused silica, and chalcogenide glasses have a nonlinearity that is 100–500 times higher, depending on their composition. Additionally, these glasses exhibit exceptional transparency in the mid-infrared (mid-IR) range: up to ~6 μm for tellurite and 8–12 μm for chalcogenide glass. Recent advances in glass preparation technologies and the fabrication of optical fibers and chip-scale waveguides have enabled significant reductions in propagation losses. This has made it possible to use these glasses for demanding applications. We consider two applications of soft glasses that rely on low losses and high nonlinearity: the generation of quantum squeezed light and nonlinear optical switching in multicore fibers (MCFs).

Squeezed light is a key resource in photonic quantum technology. One of the most prominent applications of squeezed light states is measurement beyond the standard quantum limit. Various nonlinear interactions can produce squeezing. Here, we focus on the optical Kerr effect because it can potentially be implemented in a wide variety of materials and arrangements. We have experimentally demonstrated the generation of a specific type of squeezed light, polarization-squeezed light, in a short (few cm) piece of solid-core chalcogenide (As_2S_3) fiber via the Kerr effect. We used a femtosecond laser at 1.56 μm as a source of pump light in a coherent state. Directly measured squeezing of –2.8 dB was obtained in a setup without active stabilization. Numerical simulations were in good agreement with the experimental results. Using a similar setup and a piece of suspended-core fiber made of tellurite glass (TeO_2-WO_3-La_2O_3 composition) we obtained polarisation-squeezed light with squeezing at the level of –1 dB. Comprehensive numerical simulation of quantum dynamics revealed that near-zero dispersion at the pump wavelength leads to a complex quantum-mode structure of the output pulse, which provides worse squeezing that would be expected from simplified models.

The high nonlinearity of soft glasses makes them promising candidates for nonlinear applications, such as all-optical switching. Here, we report on the fabrication of a tellurite MCF (TeO_2-WO_3-La_2O_3-Bi_2O_3 core and TeO_2-WO_3-La_2O_3 cladding) using specially developed technology based on assembling an MCF preform from single-core preforms with ground and polished edges. This technology enables the production of MCFs with a small, controlled distance between the cores (~16 μm), ensuring the necessary coupling. We experimentally observed the effect of nonlinear optical switching of 220-femtosecond ultrashort pulses in an 8-cm long piece of manufactured two-core fiber. As the input energy increased, the output energy was redistributed between the cores. It was possible to suppress the radiation in one of the cores at certain input pulse energy. The experimental results were supported by numerical simulation. This effect was observed at relatively low pulse energies of 2 nJ, which is of interest for developing saturable absorbers for mode-locked fiber lasers.

[1] A. Andrianov, A. Romanov et al., Polarization squeezing in chalcogenide fibers, Optics Letters, vol. 49, pp. 6661–6664 (2024).
[2] A. Andrianov, N. Salnikov et al., Nonlinear Optical Switching of Ultrashort Pulses in a Two-Core Tellurite Light Guide, Optoelectronics, Instrumentation and Data Processing, vol. 61, pp. 12–18 (2025).

Widely tunable narrow-linewidth mid-IR solid-sate coherent sources for long-distance environmental monitoring and wireless communication

O. Antipov[1,2], I. Eranov[1], A. Dobrynin[1,2], Yu. Getmanovskiy[1], V. Sharkov[1,2]

1- Institute of Applied Physics of RAS, Nizhny Novgorod, Russia
2- Nizhny Novgorod State University, Nizhny Novgorod, Russia

e-mail: antipov@ipfran.ru

Tunable mid-infrared (IR) sources (at wavelength range of 2–14 μm) have applications in environmental monitoring, wieless communication, remote sensing, surgery and diagnostics, materials processing, science [1]. Last years a tunable mid-IR coherent sources based on Cr^{2+}:ZnSe (Fe^{2+}:ZnSe) lasers or optical parametric oscillators (OPOs) operated using the pump wavelength tuning and selection of intracavity gratings and etalons have been reported [1–3]. This paper presents the narrow-linewidth light sources based on Cr^{2+}:ZnSe laser and OPO with high pulse energy and electronic wavelength tuneability within wavelength ranges of 2.3–2.7 μm and 3.4–5.5 μm.

An electronically-tunable high-average-power solid-state laser system based on a polycrystalline Cr^{2+}:ZnSe was studied [4]. The laser system architecture comprised a tunable Cr^{2+}:ZnSe master oscillator and Cr^{2+}:ZnSe power amplifier pumped with 10–40 kHz pulse repetition rate by a Ho^{3+}:YAG master oscillator and a Ho^{3+}:YAG power amplifier, respectively. An intracavity electronically-tuned acousto-optical filter provided 2.3…2.7 μm wavelength tunability of narrow-linewidth generation of the Cr^{2+}:ZnSe laser. An advanced procedure of Cr^{2+}:ZnSe-element surface improvement was applied for LID-threshold increasing, that resulted in an increase of the output power of the laser system. The wavelength-tunable narrow-linewidth operation in a high-quality beam with an average output power of up to 10 W was demonstrated [4].

The tunable optical parametric system included an OPO and an optical parametric amplifier (OPA) built on $ZnGeP_2$ (ZGP) nonlinear crystals was created [5]. The ZGP crystals of the OPO and OPA were pumped by 10-Hz repetitively pulsed Ho^{3+}:YAG laser at 2091 nm. A Si plate (with 30-μm thickness) was inserted into the OPO single-resonant ring cavity as an intracavity Fabri-Perrot filter. The OPO operational wavelength was tuned by adjusting the temperature on the Si plate, and the temperature and optical axis orientation of the ZGP crystal. The tuning range of the signal and idler waves were 3.4–4.1 μm and 4.3–5.5 μm, respectively. The frequency-comb OPO operation was also achieved. The ZGP OPA was used to increase the pulse energy. The combined energy of the signal and idler of the OPO-OPA source in a high-quality beam reached 4 or 20 mJ for the narrow-line or broadband repetitively-pulsed radiation, respectively.

The design and assembly of the Cr^{2+}:ZnSe laser system were carried out within the framework of the project "Technology-SG-3.2.1.2". The research regarding the optimization of the Cr^{2+}:ZnSe laser and the tunable OPO system was supported by the Russian Science Foundation (project No. 22-12-20035).

[1] Konstantin L. Vodopyanov, Laser-based Mid-infrared Sources and Applications, Wiley: , USA, 2020, 287 p.
[2] S. Mirov, I. Moskalev, S. Vasilyev, V. Smolski, V. Fedorov, D. Martyshkin, J. Peppers, M. Mirov, A. Dergachev , and V. Gapontsev, IEEE J. Sel. Top. Quantum Electron., v. 24 (iss. 5), pp. 1–29 (2018).
[3] S. Das, Optical parametric oscillator: status of tunable radiation in mid-IR to IR spectral range based on $ZnGeP_2$ crystal pumped by solid state lasers, Opt. and Quantum Electron, v. 51, 70 (2019).
[4] Oleg Antipov, Ilya Eranov, Stanislav Balabanov, Anton Dobryinin, Yuri Getmanovskiy, Valeriy Sharkov, Nikolay Yudin, Photonics v. 11, 555 (2024).
[5] I. Eranov, O. Antipov, A. Dobrynin, Yu. Getmanovskiy, V. Sharkov, J. of Optical Technology, v. 92, iss. 11, paper 483-2025 (2025).

Infrared luminescence and light amplification in mixed crystal $BaY_{1.8}Lu_{0.2}F_8:Er^{3+}$

A. V. Astrakhantseva[1], A. A. Shavelev[1], A. G. Nikolaev[2], K. N. Boldyrev[3], A. S. Nizamutdinov[1]

1- Institute of Physics, Kazan Federal (Volga Region) University, Kazan, Russia
2- Institute of Geology and Oil and Gas Technologies, Kazan Federal (Volga Region) University, Kazan, Russia
3- Institute of Spectroscopy of the Russian Academy of Science, Troitsk, Moscow, Russia

e-mail: av.astrakhantseva@mail.ru

Nowadays gas analyzers based on lasers emitting in the infrared (IR) range of the spectrum are used to detect and control the concentration of greenhouse gases in the atmosphere [1]. The Er^{3+} ion provides the infrared laser oscillation at wavelengths of about 1.5 and 2.7 μm, which correspond to the groups of lines of the absorption of water, carbon dioxide and methane [2].

IR laser oscillation at a wavelength of about 2.7 μm in matrices doped with Er^{3+} ions is realized between two excited states $^4I_{11/2}$ and $^4I_{13/2}$. This transition is self-limited for most solid-state laser media. The self-limitation effect means that the lifetime of the lower laser level is longer than the lifetime of the upper one. The phenomena of cross-relaxation and up-conversion at high concentrations of the active impurity help to populate the lower state of the Er^{3+} ion $^4I_{13/2}$ and provide the population of the upper laser level $^4I_{11/2}$ [3, 4].

In this work the spectral-kinetic characteristics in the IR region of the spectrum of the concentration series of $BaY_{1.8}Lu_{0.2}F_8:Er^{3+}$ crystals were investigated. The lifetime of the excited states $^4I_{11/2}$ and $^4I_{13/2}$ was determined and it was shown that at high concentrations of Er^{3+} ions (20 and 30 at.%) the lifetime of the upper laser level $^4I_{11/2}$ becomes longer than the lifetime of the lower laser level $^4I_{13/2}$. It was shown that for $BaY_{1.8}Lu_{0.2}F_8:Er^{3+}$ crystals the line of the intermultiplet transition at a wavelength of 2.7 μm is broadened compared to the $LiYF_4:Er^{3+}$ crystal.

Experiments on obtaining lasing for a concentration series of $BaY_{1.8}Lu_{0.2}F_8:Er^{3+}$ crystals (5, 15 and 30 at.%) at a wavelength of 2.7 μm are also discussed. Conclusions on the effect of removing the self-limitation condition of the $^4I_{11/2} \rightarrow {}^4I_{13/2}$ transition on obtaining lasing are discussed.

The work was carried out within the framework of a subsidy allocated to Kazan (Volga Region) Federal University for the implementation of a state assignment in the field of scientific activity, project No. FZSM-2024-0004.

[1] P. Siozos, et al, Autonomous Differential Absorption Laser Device for Remote Sensing of Atmospheric Greenhouse Gases, Remote Sensing, vol. 14, № 3, p. 460, (2022).
[2] K. N. Gorbachenya, A. S. Yasukevich et.al, Synthesis and Laser-Related Spectroscopy of Er:Y2O3 Optical Ceramics as a Gain Medium for In-Band-Pumped 1.6 μm Lasers, Crystals, vol. 12, № 4, p. 519, (2022).
[3] F. Auzel, Up-conversions in RE-doped Solids, Springer Series in Materials Science, vol. 83, pp. 266–319, (2005).
[4] A. M. Tkachuk et. al, Upconversion processes, luminescence kinetics, and cw diode-pumped 2.8-um laser action in Er-doped double-fluoride crystals, Laser Optics 2000: Solid State Lasers, vol. 4350, pp. 81–89, (2001).

Gas-discharge hollow core fiber lasers: first results and prospects

I. A. Bufetov, A. V. Gladyshev

Prokhorov General Physics Institute of the Russian Academy of Sciences, Dianov Fiber Optics Research Center, Vavilov st. 38, Moscow, Russia

e-mail: iabuf@fo.gpi.ru

As a result of the combination of two well-known technologies, hollow core fiber technology and gas-discharge laser technology, the fundamental feasibility of implementing gas-discharge fiber lasers (GDFLs) was demonstrated in 2023 [1]. At present, GDFLs based on mixtures of noble gases He:Ar:Xe, He:Xe, He:Ar, and He:Kr in the hollow core of revolver fibers (RFs) have been demonstrated. Operating wavelengths of these GDFLs are in the range from 2 to 2.5 μm. A maximum output peak power was ~2 mW in quasi-continuous mode [1–4]. In contrast to other types of fiber lasers, GDFLs do not use other lasers for pumping, and they are characterized by a deliberately narrow spectral bandwidth of generation. But, like bulk gas-discharge lasers, they have low efficiency.

To evaluate the possibilities for increasing the output power of GDFLs, it is necessary to determine such parameters of the gas-discharge plasma in the core of the hollow fiber, as the small signal gain (g_0) and the saturation power (P_{sat}) [5].

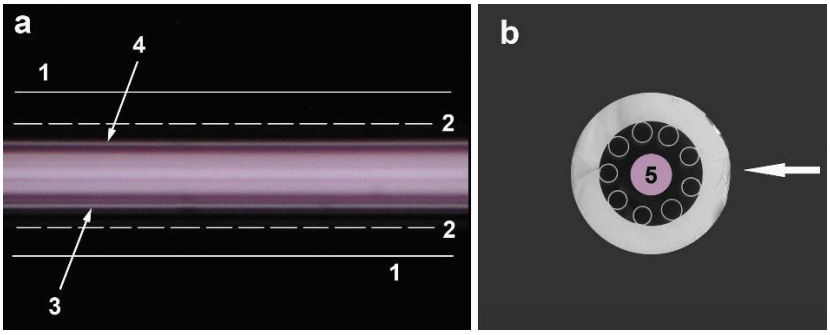

Fig.1. (a) Picture of the intrinsic luminescence of the microwave discharge plasma in the hollow core of the RF, taken with an optical microscope in a direction perpendicular to the RF axis. Lines 1 show the position of the outer boundaries of the RF, dotted lines 2 show the position of the inner diameter of the RF support tube; numbers 3 and 4 indicate the local intensity maxima corresponding to the boundaries of the RF core (reflection of plasma radiation from the walls of the capillaries forming the RF reflecting layer). (b) Electron microscope picture of the RF cross-section. The arrow indicates the direction of observation in (a); number 5 indicates a circle, the dimensions of which are equal to the diameter of the microwave plasma column (at the level of 1/2 of the luminescence intensity). Figures (a) and (b) have the same scale, the outer diameter of the RF is 335 μm, the inner diameter of the support tube is 218 μm, the diameter of the hollow core is 130 μm, the diameter of the plasma column is 85 μm.

For the mixture of He:Xe = 100:1 (at 120 torr) our measurements give the values of g_0 ~ 10 dB/m and P_{sat} ~ 10 mW [6]. Values g_0 and P_{sat} allow us to estimate the maximum power that can be obtained in quasi-continuous mode from the GDFL. Undoubtedly, an increase in the length of the active medium allows for an increase in the output power of the GDFL. And this is of particular interest, since fibers with a hollow core with extremely low optical losses at the level of α_R ~ 0.1 dB/km have been created recently [7]. With a fiber length of $1/\alpha_R$, the lasing power can reach $P_{MAX} \approx (g_0/\alpha_R) \cdot P_{sat}$ ~ 1 kW. Thus, GDFLs can be considered as potentially sources of high-power narrow wavelength band laser radiation in a wide range from UV to mid-IR.

This research was supported by Russian Science Foundation (grant No. 25-19-00559).

[1] A.V. Gladyshev, D.G. Komissarov, S.M. Nefedov, A. F. Kosolapov, V. V. Velmiskin, A. P. Mineev, I. A. Bufetov, Gas-Discharge Fiber Laser with Microwave Pumping. Bull. Lebedev Phys. Inst., vol. 50, pp. 403–408, (2023).
[2] A.V. Gladyshev, D.G. Komissarov, S.M. Nefedov, A. F. Kosolapov, V. V. Velmiskin, A. P. Mineev, I. A. Bufetov, Gas-Discharge He-Xe Fiber Laser, IEEE JSTQE, vol. 30, paper 0900107, (2024).
[3] A.V. Gladyshev, D.G. Komissarov, S.M. Nefedov, A. F. Kosolapov, V. V. Velmiskin, A. P. Mineev, I. A. Bufetov. Argon Gas-Discharge Fiber Laser. Bulletin of the Lebedev Physics Institute, Vol. 51, Suppl. 10, pp. S800–S808, (2024).
[4] Bufetov I., Komissarov D., Nefedov S., Kosolapov A., Velmiskin V., Mineev A., Gladyshev A. He-Kr Gas-Discharge Laser Based on Hollow-Core Fiber. Photonics, vol. 11, paper 1102, (2024).
[5] W. W. Rigrod. Saturation Effects in High Gain Lasers. J. Appl. Phys., vol. 36, pp. 2487–2490, (1965).
[6] I. A. Bufetov, A. V. Gladyshev, D. G. Komissarov et al. Laser parameters of plasma in He-Xe gas-discharge fiber lasers. Opt. Lett., (2025), (to be published).
[7] Y. Chen et al. Hollow core DNANF Optical Fiber with <0.11 dB/km Loss. Conference OFC 2024, paper Th4A.8, (2024).

Turn-on and heating dynamics of mid-IR quantum-cascade lasers

E. Cherotchenko, I. Vrubel, V. Dudelev, D. Mikhailov, D. Chistyakov, G. Sokolovskii

Ioffe Institute, St. Petersburg, 194021 Russia

e-mail: echerotchenko@gmail.com

Mid-infrared quantum cascade lasers (MIR QCLs), operating in the 8–14 μm wavelength range, are widely used in remote sensing, chemical and trace gas analysis, industrial process control, and biomedical applications [1–4]. These devices rely on intersubband transitions within an active region composed of a semiconductor superlattice. It is well known that QCLs generate significantly more heat than light, making thermal management a critical technological challenge. Effective thermal control directly impacts key laser parameters such as emission stability, wall-plug efficiency, and build-up time.

Using the measured temperature-dependent wavelength chirp and the build-up time in a pulsed pump regime in two different QCL-structures as examples, we provide the analytical description of the arising thermal effects [5–7]. We demonstrate the fundamental nature of refractive index variation with temperature in III-V semiconductors, and validate a method for measuring the internal temperature of the QCL active region by analyzing the Fabry–Pérot pattern drift. Our theoretical results are compared with numerical simulations and experiment, and show good agreement. The findings reveal fundamental technological limitations associated with overheating, providing valuable insights for the design and optimization of QCL-based devices.

The work is supported by Russian Science Foundation (Grant № 21-72-30020-П).

[1] Y. Yao, A. J. Hoffman, and C. F. Gmachl, "Mid-infrared quantum cascade lasers", Nat. Photonics 6(7), 432 (2012).
[2] R. F. Curl, F. Capasso, C. Gmachl, A. A. Kosterev, B. McManus, R. Lewicki, M. Pusharsky, G. Wysocki, and F. K. Tittel, "Quantum cascade lasers in chemical physics", Chem. Phys. Lett. 487(1–3), 1 (2010).
[3] A. Kosterev, G. Wysocki, Y. Bakhirkin, S. So, R. Lewicki, M. Fraser, F. Tittel, and R. F. Curl, "Application of quantum cascade lasers to trace gas analysis", Appl. Phys. B 90(2), 165 (2008).
[4] S. Rassel, C. Xu, S. Zhang, and D. Ban, "Noninvasive blood glucose detection using a quantum cascade laser", Analyst 145(7), 2441 (2020).
[5] Cherotchenko, E., et al. "Thermally stimulated chirp in a pulsed QCL: Microscopic origins behind Fabry-Perot pattern drift", International Journal of Thermal Sciences 210 (2025): 109618.
[6] Vrubel, I. I., Cherotchenko, E. D., Kusakina, K. V., Abdulrazak, S. H., Dudelev, V. V., Sokolovskii, G. S. An effect of a pump pulse rising edge on the QCL build-up time: the analytical approach. Applied Physics B, 131(4), 85. (2025)
[7] Cherotchenko, E. D., et al. "Observation of long turn-on delay in pulsed quantum cascade lasers", Journal of Lightwave Technology 40.7: 2104–2110.(2021).

Polarization properties of laser-diode-pumped 1-μm ceramic lasers

E. Dobretsova[1], D. Guriev[1], S. Kuznetsov[1], V. Tsvetkov[1], V. Zhmykhov[1], I. Chikulina[2], M. Nikova[2], V. Tarala[2], D. Vakalov[2]

1- Prokhorov General Physics Institute of the Russian Academy of Sciences, Moscow, Russia
2- North Caucasus Federal University, Stavropol, Russia

e-mail: tsvetkov@lsk.gpi.ru

Ceramic laser materials demonstrate good thermal, mechanical, and spectral characteristics and also can be manufactured in large sizes. Together with Yb:YAG ceramics Yb:YSAG (yttrium-scandium-aluminum garnet) could meet the laser operating requirements. The Yb:YSAG ceramics have garnered attention for their superior thermal stability and broader optical properties compared to traditional laser media like YAG.Moreover, when producing the YSAG ceramics it is easier to maintain stoichiometry than in the case of YAG ceramics.

Despite of the cubic crystal structure of the Yb:YSAG ceramics it's lasing polarization characteristics depends on several factors, including the intrinsic properties of the material and their operational conditions. Linearly polarized output of Yb:YSAG lasers have been observed and attributed primarily to the thermally induced mechanical stresses in the active medium.

The degree of polarization of the output radiation was studied using a Glan prism in the temperature range of 295–400 K. In all cases, it was determined that the lasing radiation was linearly polarized. The results of the polarization study of the $Y_{2.35}Yb_{0.25}Sc_{1.00}Al_{4.40}O_{12}$ and $Y_{2.52}Yb_{0.25}Sc_{0.38}Al_{4.85}O_{12}$ for different temperatures in the pulsed repetion mode lasing are presented.

Transparent glass-ceramics based on Ti^{3+}-doped spinel nanocrystals

O. Dymshits[1,2], S. Maltsev[3], I. Alekseeva[1], M. Tsenter[1], K. Bogdanov[4], S. Zapalova[1], A. Volokitina[1,2], A. Zhilin[5]

1- S. I. Vavilov State Optical Institute, Babushkina st. 36, St. Petersburg, 192171 Russia
2- Ioffe Institute, Russian Academy of Sciences, Politekhnicheskaya 26, St. Petersburg, 194021 Russia
3- Peter the Great St. Petersburg Polytechnic University, Polytechnicheskaya 29, St. Petersburg, 195251 Russia
4- ITMO University, Kronverkskiy pr. 49, St. Petersburg, 197101 Russia
5- D. V. Efremov Institute of Electrophysical Apparatus, Metallostroy, Doroga na Metallostroy, 3 Bld., St. Petersburg, 196641 Russia

e-mail: vodym1959@gmail.com

Titania, TiO_2 is an effective nucleating agent to obtain transparent glass-ceramics of aluminosilicate systems. Trivalent titanium (Ti^{3+}) ions in crystals and glasses are known for their broadband emission in the visible and near-IR spectral range, which could be used for tunable laser development. For instance, lasers based on Ti:sapphire (Ti^{3+}:Al_2O_3) crystals find different scientific and medical applications. The search for new materials with Ti^{3+} ions exhibiting broadband emission properties is a challenging task. Spinels comprise an important class of compounds with a combination of high melting point, high strength, hardness, chemical and thermal resistance and high isomorphic capacity. Spinel-based transparent glass-ceramics have advantages of high homogeneity and scalable production. When nucleated by titania and melted under reducing conditions, they can accommodate Ti^{3+} ions substituting for the Al^{3+} in octahedral (O_h) sites in nanocrystals with spinel structure. Development of transparent glass-ceramics containing Ti^{3+} ions in nanocrystals of gahnite ($ZnAl_2O_4$), and γ-Al_2O_3 with defect spinel structure is important for the elaboration of rare-earth-free Ti^{3+}-doped materials with the broadband emission.

The model lithium (LAS) and zinc aluminosilicate (ZAS) glasses nucleated by TiO_2 were melted in oxidizing (with addition of arsenic oxide) and different reducing conditions (without arsenic oxide, with an addition of carbon and with an addition of aluminum powder) at a temperature of 1580 °C and heat-treated from 680 to 1350 °C to obtain glass-ceramics based on nanocrystals of γ-Al_2O_3, lithium aluminosilicate solid solutions with β-quartz and β-spodumene structure (LAS) and gahnite (ZAS). They were studied by differential scanning calorimetry, X-ray diffraction analysis, Raman spectroscopy, transmission electron microscopy, absorption and luminescence spectroscopy.

Phase assemblage of glass-ceramics of both systems and sequence of phase transformations are independent of the redox conditions of glass melting, while the rate of these transformations is significantly higher in glasses melted in reducing conditions.

In LAS and ZAS glass-ceramics prepared from glasses melted under reducing conditions, broadband absorption is observed in the range of 400–1200 nm due to the $T_{2g} \rightarrow E_g$ transition of Ti^{3+} ions in O_h positions in nanocrystals with spinel structure, the Ti^{3+}–Ti^{4+} pairs and the appearance of Ti^{3+} self-doped rutile (ZAS) or Al_2TiO_5 and β-quartz solid solutions (LAS). The intensity of the band in the range of 400–1200 nm increases with an increase in the volume fractions of spinel crystals. In samples synthesized under oxidizing conditions, the absorption is due to the Ti^{4+}–O^{2-} charge transfer band.

Luminescent properties of glass-ceramics under excitation by a laser with a wavelength of 453 nm, are determined by impurity ions Cr^{3+} and Ti^{3+} in O_h positions in crystals with spinel structure. In the samples obtained under strongly reducing conditions, the luminescence of Ti^{3+} ions predominates.

Variation of the red-ox conditions of the glass melting makes it possible to control the content of titanium ions in various oxidation states in nanocrystals with spinel structure and their spectral properties.

Mode dynamics in multimode LD-pumped Raman fiber laser with fs-inscribed FBG or thin-film output mirror

M. D. Gervaziev, A. G. Kuznetsov, A. A. Revyakin, V. A. Simonov, A. V. Dostovalov, V. S. Terentyev, D. S. Kharenko, S. A. Babin

Institute of Automation and Electrometry SB RAS, Novosibirsk, 630090 Russia

e-mail: babin@iae.nsk.su

Development of laser devices is mainly focused on their integrability into optoelectronic circuits in case of low-power chip-scale lasers, and on the design of robust diode-pumped high-power laser schemes with all-solid-state or all-fiber performance where laser cavity optics and pump elements are integrated into single unit free of adjustable discrete parts. For both these extremes, hybrid schemes consisting of fiber and integrated optical elements produced with the use of various laser micro-fabrication technologies are being actively developed recently [1].

In addition to well-known LD-pumped Yb-doped fiber lasers (YDFLs) operating in 1–1.1 μm band, impressive results have been achieved in generating relatively high-power radiation at short-wavelength domain (0.95–0.98 μm) in all-fiber LD-pumped Raman fiber lasers (RFLs) based on passive multimode graded-index (GRIN) fibers [2]. The use in the laser cavity of output couplers based on a FBG inscribed by femtosecond (fs) pulses in the near-axis area of GRIN fiber core maximally overlapping with the fundamental mode, made it possible to maximize the effect of beam cleaning for the generated Stokes radiation. Such all-fiber cavity consisting of highly-reflective UV-inscribed FBG and fs-inscribed output FBG in a 1-km passive GRIN fiber of ~100 μm core diameter directly pumped by highly multimode LDs with beam quality parameter $M^2 \approx 34$ at 940 nm allows for generation of high-quality ($M^2 \approx 2$) Stokes beam at 976 nm with output power of ~50 W [3]. In spite of relatively large threshold pump power (~120 W), this experiment has demonstrated a record pump-to-Stokes brightness enhancement factor of about 73 in RFLs of this type.

As alternative opportunity of transverse mode selection, a dielectric thin-film mirror (R ~ 20%) has been micro-fabricated on the central area of the end face of the same GRIN fiber [4]. In the cavity with highly-reflective UV-FBG, Raman lasing of Stokes wave at 976 nm starts at lower threshold pump power (~80 W). Mode-selective properties of mirrors with various diameters were tested experimentally and compared with calculations in COMSOL with optimum diameter found to be around 12 μm. The measured Raman laser output beam at 976 nm has quality factor $M^2 \sim 2$ near the threshold that confirms rather good selection of the fundamental transverse mode. Around 35 W output power with about 60% slope efficiency and narrow spectrum has been demonstrated at the expense of slight worsening of beam quality to $M^2 \sim 3$ without any sign of thin-film mirror degradation.

Since two types of in-fiber output couplers exhibit different output beam properties, we study transverse mode distribution and mode dynamics as a function of output power with the use of holographic (based on SLM) mode decomposition technique [5] allowing for real-time measurements. In case of fs-inscribed FBG output coupler, the mode distribution is measured to have predominant content (~40%) of fundamental mode and exponentially decreasing amplitudes of high-order modes (as a function of their quantum number). This distribution is rather stable and weakly varying with increasing power (measured up to 20 W). In case of output thin-film mirror, the fundamental mode content is nearly the same, but the mode distribution is not exponential and significantly changes with increasing power, as well as fluctuations of mode amplitudes observed in ms time domain. The relative fluctuations decrease from 40% (near the Raman threshold), to ~10% (at 20 W).

The details of these studies will be presented at the conference.

This work is supported by Russian Science Foundation (№21-72-30024-П).

[1] S. Angstenberger, P. Ruchka, M. Hentschel, T. Steinle, H. Giessen, Hybrid fiber–solid-state laser with 3D-printed intracavity lenses, Optics Letters, vol. 48, pp. 6549-6552 (2023).
[2] S.A. Babin, E.A. Zlobina, S.I. Kablukov, Multimode Fiber Raman Lasers Directly Pumped by Laser Diodes, IEEE J. Sel. Top. Quantum Electron, vol. 24, pp. 1–10 (2018).
[3] A.G. Kuznetsov, S.I. Kablukov, E.V. Podivilov, S.A. Babin, Brightness enhancement and beam profiles in an LD-pumped graded-index fiber Raman laser, OSA Continuum, vol.4, p. 1034 (2021).
[4] A.G. Kuznetsov, V.S. Terentyev, V.A. Simonov, H.A. Rizk, I.N. Nemov, K.A. Bronnikov, A.V. Dostovalov, S. A. Babin, Raman lasing and transverse mode selection in a multimode graded-index fiber with a thin-film mirror on its end face, Micromachines, vol.15, p. 940 (2024).
[5] D.S.Kharenko. M.D. Gervaziev, A. G. Kuznetsov, E. V. Podivilov, S. Wabnitz, S. A. Babin, Mode-resolved analysis of pump and Stokes beams in LD-pumped GRIN fiber Raman lasers, Optics Letters, vol. 47, pp. 1222–1225 (2022).

Erbium-doped fiber laser with vibration-induced sweeping and sweeping rate control

E. K. Kashirina, I. A. Lobach, S. I. Kablukov

Institute of Automation and Electrometry, Siberian Branch of the Russian Academy of Sciences, Ac. Koptyug ave. 1, Novosibirsk, 630090 Russia

e-mail: kashirina@iae.nsk.su

Fiber self-sweeping lasers are of interest due to the simplicity of their design, since the self-induced tuning of the laser wavelength in time occurs due to internal processes associated with the formation of dynamic population gratings [1]. Recently, we reported an erbium-doped fiber laser with vibration-induced sweeping [2], in which, on the one hand, the optical frequency tuning is similar to self-sweeping lasers (it is not tied to an externally controlled and widely tunable selector), but, on the other hand, unlike them, moments of frequency tuning can be locked to a sertain phase of external vibrations. In our previous work [2], the vibrations were a parasitic effect, their frequency was fixed (77 Hz), and the vibrations of a laser cavity section were induced in a specially designed mechanical resonator. In the new laser scheme (Fig. 1a), the cavity length oscillations were induced within a piezoelectric fiber length modulator (PFLM) (highlighted by a cyan ellipse in Fig. 1a), which allows controlling not only the vibration amplitude but also their frequency using an arbitrary waveform generator (AWG) and a PZT amplifier. It should be noted that without length modulation, the laser operates in the single longitudinal mode generation regime.

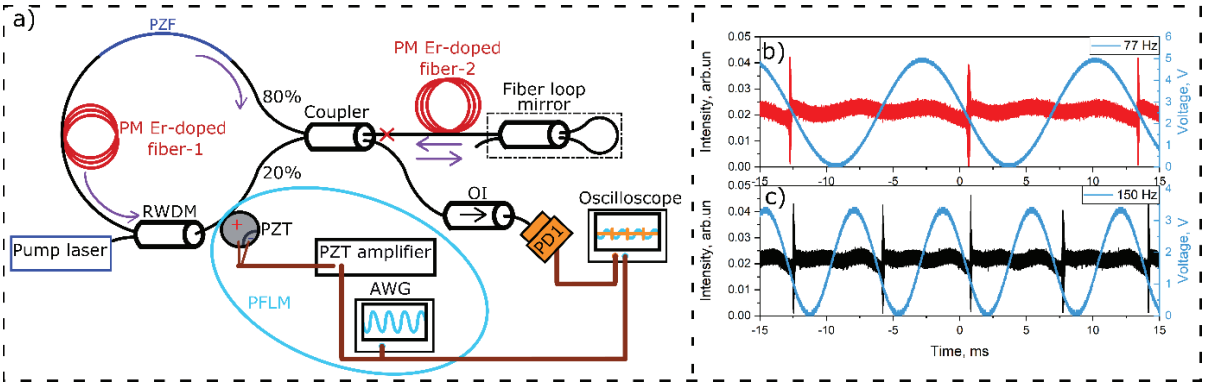

Fig. 1. Schema of the ring Erbium-doped fiber laser with vibration-induced sweeping (a) and its intensity dynamics with the corresponding control voltage at a frequency of 77 Hz (b) and 150 Hz (c).

We used a positive sine wave at the AWG to control the piezoelectric element. At a modulation frequency of 77 Hz, regular intensity bursts were observed in the laser output power, shown in Fig. 1b by the red curve for sinusoidal voltage modulation with an amplitude of 4.8 V and a repetition period of 13 ms (cyan curve in Fig. 2b). The moments of intensity bursts correspond to hops of the optical frequency by the value of the free spectral range (FSR) of the cavity of ~9.6 MHz. It is worth noting that the optical frequency hops always occur on a falling sine wave, and it was also independently confirmed using a wavelength meter that the mode-hops occur by single FSR in the same direction, and the sweeping range exceeds 1 nm. The repetition rate of the regular intensity bursts increases linearly with the frequency on the AWG (see blue curve in Fig. 1c measured at 150 Hz). Independent measurements using a wavelength meter showed that with an increase in frequency from 77 Hz to 150 Hz, the wavelength tuning speed also increases from 6.4 pm/s to 12.4 pm/s. More details about the study of the controlled vibro-sweeping fiber laser will be given in the report.

The study was supported by the grant of the Russian Science Foundation No. 25-12-00186, https://rscf.ru/project/25-12-00186/. In the presented work, the equipment of the Multiple-access center "High-resolution spectroscopy of gases and condensed matters" in IA&E SB RAS, was used.

[1] N. Poddubrovskii, R. Drobyshev, I. Lobach, S. Kablukov, Fiber lasers based on dynamic population gratings in rare-earth-doped optical fibers, Photonics, vol.9, No.9, p. 613, (2022).
[2] E. Kashirina, I. Lobach, S. Kablukov, Vibration-Induced Sweeping Operation in Fiber Lasers, Photonics, vol.11.No.8, p.731. MDPI, (2024).

Mid-IR and long wavelength IR InAsSb(P) based photodiodes

A. A. Klimov, R. E. Kunkov, A. A. Lavrov, T. C. Lukhmyrina, B. A. Matveev, M. A. Remennyi

Ioffe Institute, Polytechnicheskaya 26, St. Petersburg, 194021 Russia

e-mail: mremennyy@mail.ioffe.ru

The overview is devoted to InAsSb and InAsSbP based photodiodes (PDs) operating in mid-IR (3–6 mm) and longwave IR (6–15 mm) spectral bands developed at Ioffe Institute (St. Petersburg). It focuses on PDs operating parameters in the 200–500 K temperature range as well as on their practical applications in industry, medicine and scientific research. The PDs developed for the 3–4 mm wavelength region exhibit specific detectivity at peak wavelength as high as $1.5 \cdot 10^{10}$ and $2.5 \cdot 10^{11}$ cmHz$^{1/2}$W^{-1} for the bare chip and immersion lens (D = 3.5 mm) designs correspondingly (see Fig.1). The above values are at least 2 fold higher than those at the market.

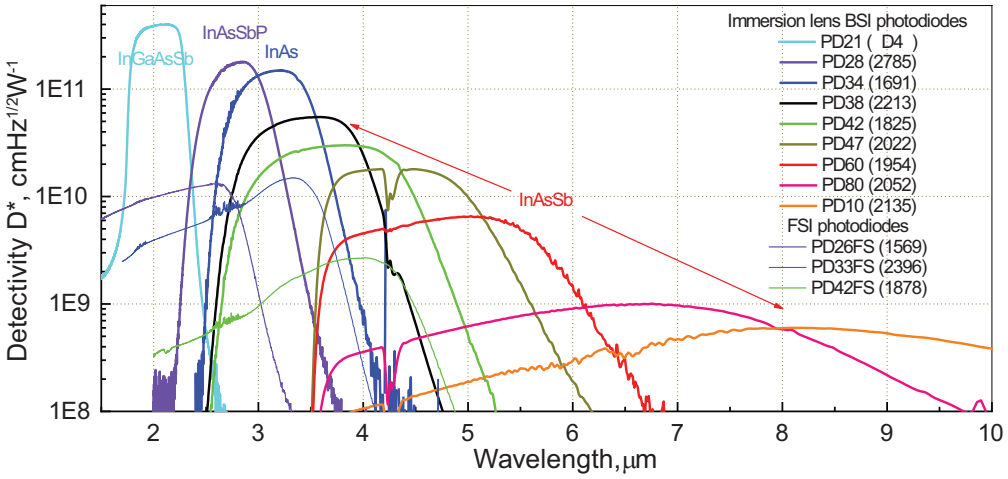

Fig. 1. Spectral detectivity for InAsSb(P) photodiodes with immersion lens (D = 3.5 mm) at room temperature

Modern trends in the implementation of Artificial Intelligence algorithms for distributed fiber sensors

A. Kokhanovskiy

School of Physics and Engineering, ITMO University, St. Petersburg, 197101 Russia

e-mail: alexey.kokhanovskiy@gmail.com

Recent advances in artificial intelligence (AI) have created new opportunities for improving the performance and functionality of distributed fiber-optic sensor (DFOS) systems. This presentation examines the integration of various AI techniques – including deep learning algorithms such as convolutional neural networks (CNNs), long short-term memory (LSTM) networks, and autoencoders, as well as machine learning methods like CatBoost and k-nearest neighbors (k-NN) – to address critical challenges in DFOS applications.

The first part of the presentation reviews recent progress made by other research groups, where AI algorithms have been applied to tasks such as anomaly detection, event classification, and the inverse design of fiber-optic sensors.

The second part focuses on our recent work involving distributed fiber Bragg grating (FBG) sensors for temperature and strain measurements. A CNN-based approach enabled a fivefold improvement in spatial resolution – achieving an interrogation resolution of 5 pm – while maintaining high temperature sensitivity [1]. A combination of CatBoost regression and k-nearest neighbors (k-NN) was applied in a tactile sensor prototype, resulting in high accuracy in predicting both impact force and contact position [2]. We also present experimental results on reconstructing a two-dimensional temperature field across a 250 × 250 mm sensor panel using a feedforward neural network to interpret signals from an optical backscatter reflectometer [3]. Finally, we propose a multicore fiber platform for distributed temperature sensing, enhanced by machine learning algorithms.

The study also emphasizes that the most resource-intensive stage of AI integration remains data acquisition and labeling. To address this, we propose solutions such as transfer learning and the development of open datasets. Overall, our results demonstrate the effectiveness of AI in overcoming classical limitations of DFOS systems, particularly in achieving high-resolution, multi-point temperature sensing in compact and scalable configurations.

[1] [2] Kokhanovskiy, Alexey, et al., Highly dense FBG temperature sensor assisted with deep learning algorithms. Sensors 21(18) 6188 (2021).
[2] Shabalov, N., et al., Soft 2D tactile sensor based on fiber Bragg gratings and machine learning algorithms. Sensors and Actuators A: Physical 369 115219. (2024).
[3] Wolf, Alexey, et al., 2D temperature field reconstruction using optical frequency domain reflectometry and machine-learning algorithms. Sensors 22(20) 7810 (2022).

Quantum-dot based microlasers with resonator of broken symmetry for on-chip data processing and transmission

N. Kryzhanovskaya, E. Moiseev, K. Ivanov, N. Fominykh, I. Fedosov, I. Makhov, A. Zhukov

International Laboratory of Quantum Optoelectronics, HSE University, Soyuza Pechatnikov str. 16, St. Petersburg, 190008 Russia

e-mail: nataliakryzh@gmail.com

Technological progress makes it possible to significantly reduce the size of semiconductor laser emitters to microscales commensurate with the emission wavelength. Extreme laser miniaturization can be achieved using disk or ring resonators supporting high-Q whispering gallery modes (WGM). WGM lasers are interesting not only due to small mode volume, but also for their long times of light-matter interaction, unique capabilities of sensing and so on. On the other hand, small losses for the output of emission in high-Q resonators, which typically lead to low optical power, can negate the practical benefits of the laser or even completely hide the peculiarities of the light physics inside the cavity. In this study, we attempted to summarize the data on the achieved optical output power in different III-V injection microlasers and analyzed the key characteristics that limit the maximum output power, especially influence of the active region self-heating at cw operation and impeded light extraction out of WGM cavities. We compared various III-V materials and fabrication methods developed for improving emission output. A promising approach to improve the emission output is to use the deformation of the cavity shape from the circle to break rotational symmetry. We focus on the progress that has been made so far in terms of improving far-field diagram and directional coupling of WGM to increase a wall-plug efficiency. Most promising results have been obtained for microlasers with limaçon [1, 2] and quadrupole deformations [3] of the resonator shape. In this work lasing in limaçon and quadrupole μ-lasers with InGaAs/GaAs quantum dots in the active region has been demonstrated at elevated temperatures (up to 90 °C). The quality factor of structures is estimated to be at least 10^5. One directional lobe dominates in the far field of limaçon-microlasers, while quadrupole microlasers are characterized by two lobes in opposite directions. The angular divergence of the lobe of the directional diagram of the limaçon-laser was about 50° in the lateral direction and about 8° in the vertical direction. Therefore, limaçon and quadrupole lasers combining directional emission, low current threshold and on-chip fabrication characters could be considered to be a useful device in optoelectronic integration applications in future.

Laser emission can be transferred to other optical components not only by open channel (via air) but also by vertical or lateral coupling with closely spaced waveguide. We report on InGaAs/GaAs quantum dot injection microdisk lasers laterally connected with a bus waveguide fabricated by planar technology from the same epi-structure. Various coupling schemes of microlaser with waveguide are studied including a microlaser attached to a waveguide (zero gap), a 100 nm gap for evanescence light outcoupling, and with a waveguide surrounding the resonator. The modes outcoupling and microlaser's loss (Q-factor) are analyzed by simulation of the lasers. We study the spectral and lasing parameters of the microdisk lasers, as well as characteristics of the outcoupled emission, and demonstrate efficient light outcoupling for 30 and 40 μm diameter continuous wave operating microdisk laser up to 96 °C. We demonstrate the reduce of absorption losses in a waveguide by applying a forward bias to it. When a current of about 60 mA was applied to the optical waveguide, a sharp increase of almost an order of magnitude in the output optical power of the microlaser was observed, which we associate with the achievement of transparency in the waveguide. An integrated optocoupler is presented in which the radiation source is a microdisk laser coupled to a waveguide, and the radiation receiver is a waveguide photodetector.

The research was supported by a grant of Russian Science Foundation № 25-72-20048, https://rscf.ru/project/25-72-20048.

[1] Q. Song, W. Fang, B. Liu, S.-T. Ho, G. S. Solomon, and H. Cao, «Chaotic microcavity laser with high quality factor and unidirectional output», Phys. Rev. A, 80, 041807 (2009).
[2] J.-W. Ryu, J. Cho, I. Kim, and M. Choi, «Optimization of conformal whispering gallery modes in limaçon-shaped transformation cavities» Sci. Rep., 9, 8506 (2019).
[3] H. G. L. Schwefel, N. B. Rex, H. E. Tureci, R. K. Chang, and A. D. Stone, in Summaries of Papers Presented at the Quantum Electronics and Laser Science Conference (Opt. Soc. America, 2002), 74, pp. 24–25.

Influence of annealing atmosphere during diffusion doping on spectral characteristics of Cr:ZnSe active elements lasing

S. V. Kurashkin[1,2], D. V. Savin[2], O. V. Martynova[1]

1- National Research Lobachevsky State University of Nizhny Novgorod, Gagarin ave. 23, Nizhny Novgorod, 603022 Russia
2- Devyatykh Institute of Chemistry of High-Purity Substances, Russian Academy of Sciences, Tropinin str. 49, Nizhny Novgorod, 603137 Russia

e-mail: svkurashkin@gmail.com

The work investigated the influence of the annealing atmosphere (Ar or Zn vapor) during diffusion doping on the luminescent and laser properties of the obtained Cr:ZnSe active elements. The conditions for high-temperature annealing of the samples were the same: temperature of about 1000 °C, holding time of 216 hours.

Laser generation was obtained in an L-shaped cavity with a diffraction grating. A silicon plate served as the output mirror. The Q-switch Tm:YAP pump laser radiation was fed to the AE through a dichroic ultra-wideband mirror (R > 98% in the wavelength range of 2.25–2.9 μm), and a 300 lines/mm diffraction grating with a gold coating was used instead of a high-reflection mirror.

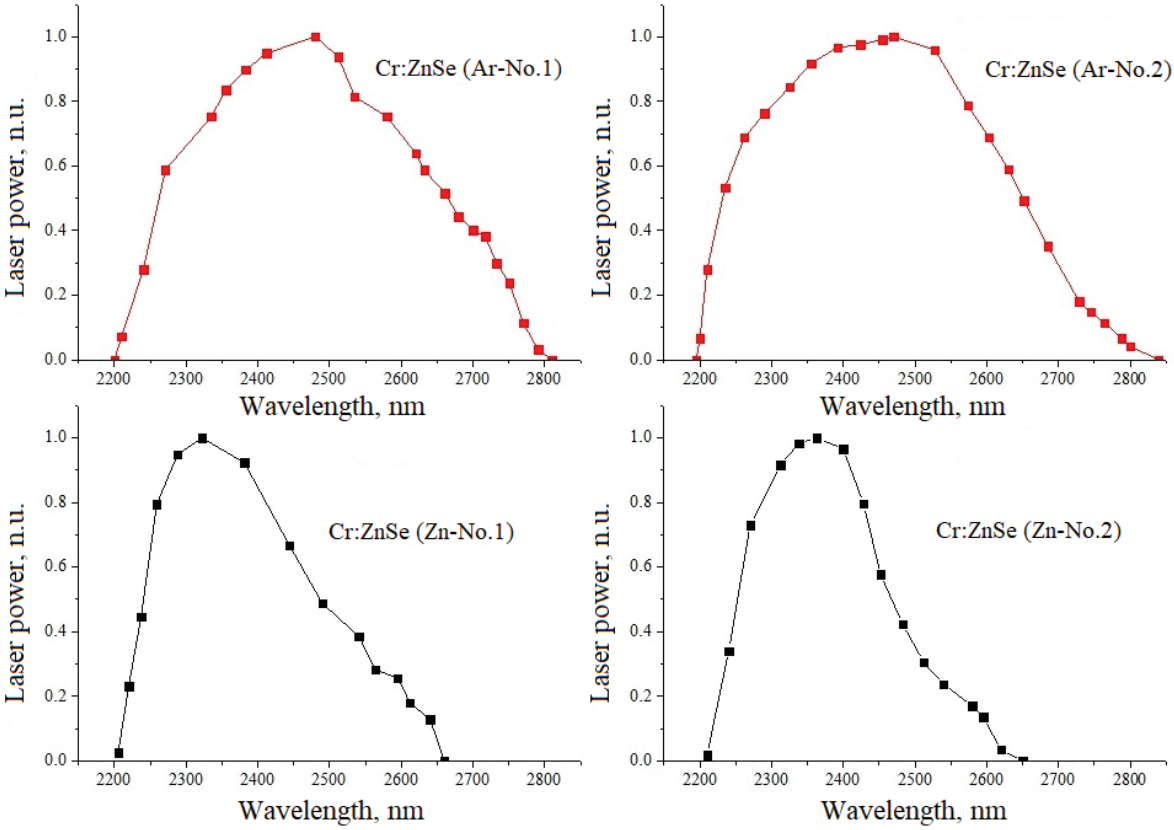

Fig. 1. Cr:ZnSe laser wavelength tuning spectra.

Fig. 1 shows the laser tuning curves for Cr:ZnSe active elements obtained by diffusion annealing in Zn and Ar atmospheres.

As can be seen from fig. 1, lasing at longer wavelengths can be obtained on Cr:ZnSe active elements annealed in argon. The results of the study show that polycrystalline active elements obtained by diffusion annealing in an argon atmosphere are better suited for creating long-wavelength Cr:ZnSe lasers.

The study of laser characteristics was supported by the "National Project Science and Universities" (FSWR-2024-0004), the production of active elements was supported by the Ministry of Science and Higher Education of the Russian Federation (FFSR-2025-0004).

Specificities of coherent beam combining in a multichannel Yb:YAG laser of high peak and average power

I. Kuznetsov, S. Chizhov, D. Trunov, N. Karpov, O. Palashov

A. V. Gaponov-Grekhov Institute of Applied Physics of the Russian Academy of Sciences (IAP RAS), Ul'yanov str. 46, Nizhny Novgorod, 603950 Russia

e-mail: kuznetsov@ipfran.ru

High peak power lasers are widely used for charged particles acceleration, generation of X-ray and THz radiation, and so on. However, practical implementation of these developments requires an increase in the average power of lasers, or the pulse repetition rate. Today, ytterbium solid-state lasers are the most successful technology on this way. A promising method for increasing the peak and average power is to use a multi-channel laser scheme with coherent beam combining. The method involves splitting a laser beam into several replicas, amplifying the replicas in different amplifiers, and then coherent combining them into a single beam, which is achieved by controlling the phase of each replica. The method can be very effective for Yb lasers, however, to date there are only a few pioneering results [1]. The key problem is the creation of identical channels, which is aggravated by the strong thermal effects.

In this paper, we propose a new architecture of a multichannel laser amplifier that allows us to significantly simplify the task of channel multiplication. The idea is to amplify several beams in one active element (AE), when the beams are located symmetrically relative to the AE axis and along its cooled side surface. In this case, the AE is effectively cooled through the side surface, since the heat sources are distributed in close proximity to it. Additionally, all beams are in symmetric conditions, which ensures the equivalence of the channels. Based on the presented geometry, a MOPA laser system with a 4-channel Yb:YAG amplifier and coherent beam combining is implemented, the scheme of which is shown in Fig. 1 [2].

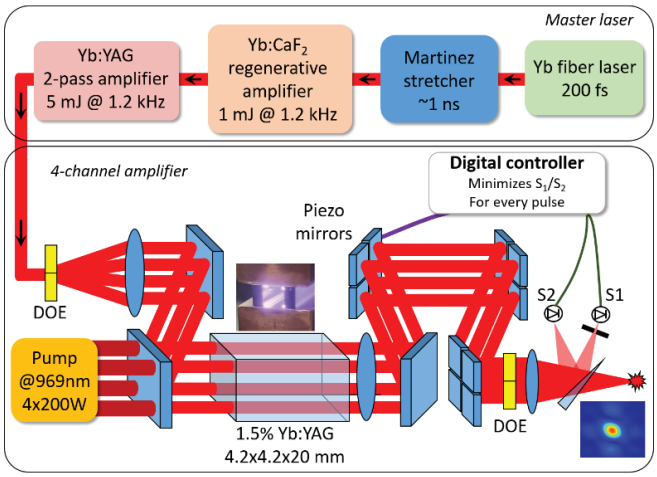

Fig. 1. Laser scheme. DOE – diffraction optical element.

To date, such a system has achieved pulse energy >17 mJ at an average power of ~20 W. Coherent channel combining according to the "tiled aperture" principle with 57% power in the central lobe of the beam has been implemented. Phase fluctuations in the channels, mainly concentrated in the band up to 10 Hz, are effectively suppressed by the digital controller. It maximizes the power in central beam lobe normalized to the full beam power. This normalization allows to eliminate the influence of pulse energy instability. The RSD of residual fluctuations of the target function was <1%.

This work was supported by Russian Science Foundation No. 23-12-00199, https://rscf.ru/en/project/23-12-00199/.

[1] M. Kienel, M. Müller, S. Demmler, J. Rothhardt, A. Klenke, T. Eidam, J. Limpert, A. Tünnermann, "Coherent beam combination of Yb:YAG single-crystal rod amplifiers", Opt. Lett. 39, 3278-3281 (2014).
[2] I. Kuznetsov, S. Chizhov, D. Trunov, P. Smolin, N. Karpov, O. Palashov, "MOPA laser system with a 4-channel Yb:YAG single-rod amplifier and coherent beam combining", Opt. Lett. 50, 3158-3161 (2025).

Luminescence of the Sb-clusters in yttrium-aluminoborate glasses

G. Malashkevich[1], V. Kouhar[1], A. Ramanenka[1], A. Sukhodola[2], N. Golubev[3], M. Ziyatdinova[3], E. Ignat'eva[3], V. Sigaev[3]

1- B. I. Stepanov Institute of Physics, National Academy of Sciences of Belarus, Minsk, Belarus
2- Belarusian National Technical University, Minsk, Belarus
3- Russian University of Chemical Technology, Moscow, Russia

e-mail: g.malashkevich@ifanbel.bas-net.by

Glasses of the $(Y_{1-x}Ln_x)_2O_3$–Al_2O_3–B_2O_3 system, particularly those with a composition close to the huntite-like stoichiometry, are known to exhibit a record-high minimum Ln–Ln distance for oxide matrices, amounting to ~0.67 nm [1]. Recent research has revealed that in similar glasses of the composition (mol %) $10Y_2O_3$–$30Al_2O_3$–$60B_2O_3$, when doped with antimony in excess of 100%, a significant deviation from the specified stoichiometry can be occurred and it leads to the formation of isolated Sb–O–Sb clusters [2]. These clusters exhibit broadband luminescence ($\Delta\lambda \approx 280$ nm), peaking at $\lambda_{max} \sim 700$ nm (see Fig.), excited within the band gap. This contrasts with the luminescence of isolated Sb^{3+} ions, which is excited via the interband transition. Recognizing the need for diverse active materials suitable for tunable near-IR lasers, this work presents an in-depth study of the spectral-luminescent properties of such clusters. It was shown that their luminescence is excited on the long-wavelength wing ($\lambda \geq 350$ nm) of a relatively broad band at $\lambda_{max} \approx 305$ nm, the position of which is practically independent of the recording wavelength (see Fig. 1). The luminescence decay kinetics of these clusters follow Förster behavior and occur within the microsecond range. A quantum yield reaching 40% is achieved at a Sb_2O_3 concentration of 15.0 mol % and a peak absorption coefficient of 5.5 cm^{-1} in the region of the main vibration of impurity OH^--groups ($\lambda \approx 2.83$ μm). Based on [3], this allows us to expect a noticeable increase in luminescence quantum yield upon complete dehydration, classifying these glasses with the considered clusters as promising active materials for tunable lasers with LED pumping.

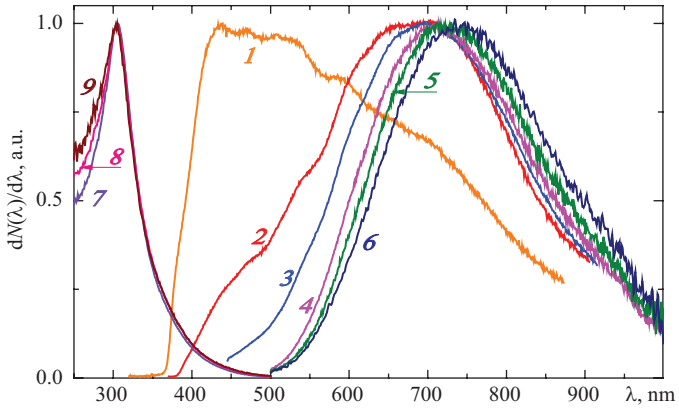

Fig. 1. Luminescence and excitation spectra of glass with the composition (mol %) $10Y_2O_3$–$30Al_2O_3$–$60B_2O_3$+$15.0Sb_2O_3$. λ_{exc}, nm: (*1*) 320, (*2*) 350, (*3*) 370, (*4*) 420, (*5*) 440, (*6*) 460; λ_{rec}, nm: (*7*) 700, (*8*) 750 (*9*) 800.

The work was partially supported by the State Program of Scientific Research "Photonics and Electronics for Innovations" (task 1.2) and the scientific and technical program of the Union State "Component-F" (event 3.1).

[1] G.E. Malashkevich, V.N. Sigaev, N.V. Golubev, E.Kh. Mamadzhanova, A.A. Sukhodola, A. Paleari, P.D. Sarkisov, A.N. Shimko, Spectroscopic properties of Sm-containing yttrium-aluminoborate glasses and analogous huntite-like polycrystals, Mater. Chem. Phys., 137, 48–54, (2012).
[2] G.E. Malashkevich, V.V. Kouhar, A.A. Romanenka, A.A. Sukhodola, I.V. Prusova, N.V. Golubev, M.Z. Ziyatdinova, E.S. Ignat'eva, V.N. Sigaev, Spectral-luminescent and optical properties of antimony-doped yttriumalumoborate glasses, Zh. Prikladnoy Spektroskopii, 92, 336–342, (2025).
[3] G.E. Malashkevich, V.V. Kouhar, E.V. Pestryakov, V.N. Sigaev, N.V. Golubev, M.Z. Ziyatdinova, A.A. Sukhodola. Spectral-luminescent and laser properties of the $(Y_{1-x}Yb_x)_2O_3$–Al_2O_3–B_2O_3 glasses, Optical Materials, 76, 253–259, (2018).

Nd-doped amplifiers efficiency related to lower level relaxation rate

V. B. Morozov, A. N. Olenin, D. V. Yakovlev

Physics Faculty of M. V. Lomonosov Moscow State University, Leninskiye Gory, Moscow, 119899 Russia

e-mail: morozov@phys.msu.ru

Crystalline and glass Nd-doped laser media are widely used to produce and amplify high-peak-power picosecond and short nanosecond pulses. Most often, laser action occurs between the Stark sublevels of the $^7F_{3/2} \rightarrow {}^4I_{11/2}$ transition, which is usually addressed as a classical 4-level scheme. However, when amplifying pulses with duration comparable to or shorter than the lifetime of the lower laser level, the aspiring to implement the most energetically favorable amplification regime closed to saturation, can meet so-called "bottleneck" effect [1]. Population accumulates at the lower laser level during the pulse amplification and tends to be equalized with the upper level population. As a result, the medium becomes more optically transparent and the gain drops. In turn, sufficiently rapid relaxation of the lower laser level population, contributes to the partial recovery of the population difference and, respectively, to the amplifying ability of the medium. Thus, the detailed description of short pulse amplification represents a substantially non-stationary task depending on specific parameters of the amplifying medium. Here we focus on the lower level relaxation.

Based on the available data on the lower laser level lifetimes in various Nd-doped crystalline and glass matrices, one can conclude that the values differ quite significantly. For example, in the cases of widely used popular media such as Nd:YAG, Nd:YLF, Nd:glass etc. the values range from near 100 ps to over 10 ns [1]. These important nuances should be taken into account when developing advanced energy-effective laser systems. Two-pass amplifying schemes are the mportant structural components of many linear laser amplifying systems providing operation near the saturation condition and representing optimal solution from the point of view of pump conversion efficiency. They offer near uniform complete exhaustion of population inversion along the entire length of the pumped laser medium [2]. This seemingly obvious statement may not be entirely correct if to neglect the terminal laser level population relaxation conditions. Thus, the value of the lifetime of the lower laser level should be adequately taken into account when creating efficient, especially two-pass, schemes for amplifying picosecond and short nanosecond pulses. However, reference information on this matter is often only approximate, and the data from the most systematic studies [1] upon closer examination appear to be the result of indirect measurements.

Previously, we proposed and implemented experimentally an approach for direct measurement the dynamics of partial gain recovery of a probe pulse following the saturating one with a variable delay in Nd:YAG amplifier [3, 4]. The performed analysis showed that the lifetime of the lower level is at least no more than 100 ps. Further refinement and obtaining a lower estimation value require more detailed measurements, saturating and probe pulses better time reference, as well as adequate modeling of the gain under the partial saturation and the accompanying lower level population relaxation. We develop these approaches in the present work. The experiments are performed with a picosecond laser delivering 40 ps pulses of several mJ energy, split into saturating and probe channels with orthogonal polarizations and with a relative time shift by means of an optical delay line. In the case of Nd:YAG, a significant complicating factor is the closeness of the values of the relaxation time being studied and the duration of the laser pulses employed in the scheme. Based on the experimental data and calculations, we came to a more accurate estimation 60±20 ps of the lower level relaxation time in Nd:YAG.

We modified a widely used model of laser pulse amplification [5] by introducing corrections that take into account the finite value of the relaxation rate of the lower laser level. This approach allowed possibility of accurate and adequate analysis of practical schemes for two-pass side- and end-pumped picosecond pulse amplifiers. Also, it looks attractive when applied to short nanosecond amplifier schemes on Nd:glass.

[1] C. Bibeau, S.A. Payne, H.T. Powell. J. Opt. Soc. Am. B 12(10) 1981–1992 (1995).
[2] V.B. Morozov, A.N. Olenin, D.V. Yakovlev. ALT 2024, Vladivostok, Book of Abstracts, 135 (2024).
[3] V.B. Morozov, A.N. Olenin, D.V. Yakovlev. ALT 2023, Samara, Book of Abstracts, LS-0-14 (2023).
[4] V.B. Morozov, A.N. Olenin, D.V. Yakovlev. ICLO 2024, IEEE Photonics Society, 17 (2024).
[5] L.M.Frantz, J.S.Nodvik. J. Appl. Phys. 34(8) 2346–2349 (1963).

Ultraviolet laser systems on Ce^{3+}-based active media and photodynamic processes

A. Nizamutdinov[1], D. Makarova[1], A. Shavelev[1], V. Semashko[1,2], Stella Korableva[1]

1- Kazan Federal University, Kremlevskaja str. 18, Kazan, 420008 Russia
2- FRC Kazan Scientific Center of RAS, Zavoisky Physical-Technical Institute, Sibirsky tract 10/7, Kazan, 420029 Russia

e-mail: anizamutdinov@mail.ru

Today technologies express demand on lasers oscillating in ultraviolet (UV) spectral range and having short pulse duration [1]. Main methods of obtaining UV laser radiation are nonlinear and parametric conversion of non-UV laser radiation. These methods can be technically difficult and it takes a lot of space. But on the other hand one can obtain UV lasing by use of fluoride crystals doped by Ce^{3+} ions as active media [2]. Among the trivalent lanthanide ions the ion of Ce^{3+} has minimal energy of 5d configuration with the value of about 50000 cm^{-1} [3]. And ultraviolet laser radiation in Ce-doped fluoride crystals is driven by stimulated emission resulting from interconfigurational 5d-4f transitions in Ce^{3+} ions excited by UV laser pump. Fluoride crystals doped by ions Ce^{3+} allow us to obtain short pulses with duration from several to tens of nanoseconds and even in subnanosecond time domain.

Here we discuss developments in design of practical laser systems based on $LiCaAlF_6$ and $Li(Lu,Y)F_4$ crystals doped with Ce^{3+} ions. These are solid state active media capable to generate laser light in the range of 280–340 nm [4, 5]. The discussed advantages are wide wavelength tuning for intracavity spectroscopy or selective tissue treatment, and also possibility to manage the output characteristics inside the cavity [6].

At the same time there are photodynamic processes in UV active medium resulting in formation of color centers [7]. Color centers in there turn absorb energy of laser radiation and cause losses in active medium [7, 8]. Level of losses due to color centers depends on amount of laser radiation inside the cavity and doesn't remain constant during experiment [7, 8]. This gives an opportunity to utilize the color center losses for arrangement the modulation of Q-factor of the cavity or even mode-locking. Here we discuss additional light and temperature approach for control of UV laser output chatacteristics. For example, Laser oscillation was obtained in active medium $Ce:LiLu_{0.7}Y_{0.3}F_4$ in a pulse mode at the wavelength λ = 311 nm as single pulse with duration t = (400±10) ps in the low Q-factor cavity. We expect that shortening of the pulse duration was achieved by passive Q-switch, which is caused by bleaching of color centers in the volume of the active medium absorbing the laser radiation. Thus measured contrast of losses level dependence on pump energy appeared to be 1.8 and methods of Q-switch control are change of pumping energy, output mirror reflection and additional illumination intensity.

[1] A. Saliminia, A. Proulx, R. Vallée, Optics Communications, 333, 133-138, (2014).
[2] M. Dubinskii, V. Semashko, A. Naumov, R. Abdulsabirov, S. Korableva, J. Mod. Opt., 40, 1–5, (1993).
[3] L. Brewer, JOSA, 61, 1666–1682, (1971).
[4] A. Shavelev, A. Nizamutdinov, A. Shakirov, S. Korableva, D. Zverev, A. Rodionov, E. Lukinova, V. Semashko, Bulletin of the Russian Academy of Sciences: Physics, 88, S600–S608, (2024).
[5] A. Nizamutdinov, L. Nurtdinova, V. Semashko, S. Korableva, Optics and Spectroscopy, 116, 732-738, (2014).
[6] D. Makarova, A. Nizamutdinov, A. Shavelev, T. Minnebaev, Bulletin of the Russian Academy of Sciences: Physics, 88, S651-S653, (2024).
[7] A. Shakirov, A. Nizamutdinov, A. Shavelev, S. Batygov, S. Kuznetsov, V. Semashko, Bulletin of the Russian Academy of Sciences: Physics, 88, S609-S614, (2024).
[8] V. Semashko, M. Dubinskii, R. Abdulsabirov, S. Korableva, A. Naumov, A. Nizamutdinov, M., Zhuchkv, M.S., Proceedings of SPIE, 4766, 119-126, (2002).

Narrow-band fiber lasers for microwave photonics and sensing

I. Panyaev[1], P. Itrin[1], V. Ribenek[1], D. Korobko[1], A. Fotiadi[1,2]

1- Ulyanovsk State University, Leo Tolstoy Street 42, Ulyanovsk, 432970 Russia
2- Ioffe Physical-Technical Institute of RAS, Politekhnicheskaya 26, St. Petersburg, 194021 Russia

e-mail: paniaevis@ulsu.ru

Injection locking is a powerful method for stabilizing laser output in photonic integrated circuits, especially for applications requiring a narrow spectral linewidth and low phase noise. Unlike conventional phase stabilization techniques that rely on complex and costly optoelectronic systems, lasers based on injection locking achieve passive stabilization by locking to a high-Q resonator mode. While high-Q resonator technology is still under development, fiber laser configurations have already achieved record Q-factors due to their long cavity lengths. The presentation will demonstrate experimental implementations of narrow-linewidth fiber lasers built from standard telecommunications components and discuss the features of injection locking mechanisms that are promising for future integration into photonic chips.

Here we report a simple narrow-band laser configuration based on a DFB laser coupled to an all-fiber ring cavity that operates in the self-injection-locking regime. We use a low-cost USB-DAQ and a simple phase shifter to stabilize the laser system and prevent mode-hopping. The self-injection-locking mechanism ensures continuous coupling between the DFB laser and the external fiber ring cavity, resulting in exceptionally low-noise narrow-band lasing. Unlike previous designs, our laser configuration is entirely composed of polarization-maintaining (PM) fiber components. Furthermore, similar to [1], we employed a fiber ring cavity constructed (and subsequently integrated into the configuration) using just one fiber coupler, instead of the two couplers utilized in many earlier configurations. Such a cavity design potentially reduces optical losses in the ring cavity (by a factor of two compared to [2]), offering an enhanced Q-factor. Thanks to the new laser design, the performance characteristics of the laser have been significantly improved. The laser's Lorentzian linewidth has been reduced to approximately 75 Hz. To the best of our knowledge, this is the narrowest laser linewidth reported for DFB lasers that are self-injection locked to an external fiber cavity. The laser output power of approximately 8 mW allows for potential scaling with external amplifiers. The laser operates at frequencies tightly locked to the ring cavity resonances, with frequency drift primarily influenced by environmental temperature changes. By applying thermal control to the entire laser configuration, we've reduced the laser frequency drift to roughly 0.5 MHz/min, ensuring absolute fluctuations of the laser frequency are less than 8 MHz. Utilizing the PM fiber configuration negates the need for polarization controllers, making the laser setup more robust and adjustment-free. Compared to non-PM configurations, the laser's noise performance improves by approximately 10 dBc/Hz and 50 dBc/Hz for measured relative intensity noise (RIN) and phase noise power spectral density (PSD), respectively.

Overall, our findings enhance the understanding of the self-injection-locking mechanism in semiconductor lasers, paving the way for new possibilities in manipulating and controlling their properties. The ability to generate a sub-100 Hz laser linewidth is particularly valuable for applications such as high-resolution spectroscopy, phase-coherent optical communications, microwave photonics, coherent optical spectrum analyzers, and distributed fiber optic sensing, especially in phase-OTDR acoustic sensing [3, 4].

The work was funded by the Ministry of Education and Science (FEUF-2023-0003) and Russian Science Foundation (23-79-30017).

[1] V. V. Spirin, et al, Dual-frequency laser comprising a single fiber ring cavity for self-injection locking of DFB laser diode and Brillouin lasing, Optics Express, vol. 28, pp. 37322–37333, 2020.
[2] V. V. Spirin, et al., Sub-kilohertz Brillouin fiber laser with stabilized self-injection locked DFB pump laser, Optics & Laser Technology, vol. 141, p. 107156, 2021.
[3] I. S. Panyaev, P. A. Itrin, D. A. Korobko, and A. A. Fotiadi, Sub-100-hz dfb laser injection-locked to pm fiber ring cavity, Journal of Lightwave Technology 42, 2928–2937, 2024.
[4] А. А. Фотиади, Д. А. Коробко и И. О. Золотовский, Бриллюэновские лазеры и сенсоры: Тенденции и перспективы, Автометрия 59, 74–86, 2023.

Prospects for all-fiber mid-IR spectroscopy: systems and components

E. A. Romanova[1], V. S. Shiryaev[2]

1- Saratov State University, Astrakhanskaya 83, Saratov, 410012 Russia
2- Devyatykh Institute of Chemistry of High-Purity Substances of RAS, Tropinin str. 49, Nizhny Novgorod, 603951 Russia

e-mail: romanovaelena@sgu.ru

I. ***Fiber-optic evanescent wave spectroscopy (FEWS) and diffuse reflectance spectroscopy (DRS)***

Remote chemical analysis of various substances in real time is a challenging problem. Different application areas include healthcare, industry, agriculture, ecology, defense and security. The middle-infrared (mid-IR) spectral range that is a "fingerprint" region of molecular bonds is most suitable for the chemical analysis. Development of compact and cheap fiber-optic sensors for *FEWS* mid-IR spectroscopy is possible because some part of radiation propagating in a fiber is penetrating through the fiber core side surface to an external medium. In *DRS*, a unique property of optical fibers to deliver light to a micron-size point and collect light from that point is utilized.

II. ***Laboratory experiments with fiber-optic sensing elements integrated into FTIR***

To date, most *FEWS* experiments have been carried out in labs with fiber-optic sensing elements shaped as bent probes [1, 2]. Broadband IR radiation emitted in a Fourier Transform IR (*FTIR*) spectrometer by a Globar was launched into a probe made of chalcogenide glass for interaction with an analyte. Transmittance spectra at the probe output were measured using *FTIR*. Action of the probes and their sensitivity was also studied in computer models on the base of the wave optics theory [3]. *DRS* sensors are usually made of polycrystalline fibers, which are less fragile than chalcogenide fibers [4].

III. ***Towards an all-fiber sensor: the need for a broadband fiber-optic light source***

To create compact and portable sensors for *FEWS* or *DRS*, fiber-optic sources of broadband radiation are to be developed. Spectral supercontinuum generation in mid-IR was obtained in chalcogenide fibers pumped by parametric oscillators [5] near zeros of group velocity dispersion at wavelengths in mid-IR. Cheaper light sources for pumping are currently being developed – mid-IR fiber lasers [6]. Broadband mid-IR emission in rare earth doped chalcogenide fibers is considered as another option for creating all-fiber spectroscopic sensors [7].

IV. ***What is currently used and what is in demand***

In medicine, both *FEWS* and *DRS* are in demand. Biosensors made of chalcogenide fibers have been used in *FEWS* for cancer diagnostics, to monitor bacterial films and live cell cultures [8]. *DRS* probes integrated into FTIR were developed by Art photonics (Berlin, Germany) for endoscopic diagnostics in oncology [4]. There is no urgent need for portable all-fiber devices for medical diagnostics in hospital laboratories. In other application areas, the lack of compact and cheap sources of broadband radiation slows down the actual implementation of such sensors.

[1] Boussard-Pl´edel, C.: Chalcogenide waveguides for infrared sensing. In: Chalcogenide Glasses. Preparation, Properties and Applications. 1st ed., J.-L. Adam, X. Zhang (Eds.), Woodhead Publishing, pp. 381–410 (2014).
[2] Velmuzhov, A.P., Shiryaev, V.S., Sukhanov, M.V., Kotereva, T.V., Stepanov, B.S., Snopatin, G.E.: Mid-IR fiber-optic sensors based on especially pure Ge20Se80 and Ga10Ge15Te73I2 glasses. J Non-Cryst Solids 579, 121374 (2022).
[3] Romanova, E., Korsakova, S.: Light waves interaction with an analyte in fiber-optic sensors for mid-IR spectroscopy. Opt and Quant Electron 53(11), 650 (2021).
[4] Artyushenko V., Bocharnikov A., Sakharova T., Usenov I. Mid-infrared Fiber Optics for 1–18 μm Range: IR-fibers and waveguides for laser power delivery and spectral sensing. Opt. Photon., 4, 35–39 (2014).
[5] C.R. Petersen, U. Møller, I. Kubat, B. Zhou, S. Dupont, J. Ramsay, T. Benson, S. Sujecki, N. Abdel-Moneim, Z. Tang, D. Furniss, A. Seddon and O. Bang, Mid-infrared supercontinuum covering the 1.4–13.3 μm molecular fingerprint region using ultra-high NA chalcogenide step-index fibre, Nature Photonics 8, 830–834 (2014).
[6] V.V. Koltashev, B.I. Denker, B.I. Galagan, G.E. Snopatin, M.V. Sukhanov, S.E. Sverchkov, A.P. Velmuzhov, V.G. Plotnichenko, 150 mW Tb^{3+} doped chalcogenide glass fiber laser emitting at $\lambda > 5$ μm, Opt. & Laser Technol., 161, 109233 (2023).
[7] V. Nazabal, J.-L. Adam, Infrared luminescence of chalcogenide glasses doped with rare earth ions and their potential applications, Opt. Mater.: X, 15, 100168 (2022).
[8] Lucas P., Coleman G.J., Jiang S., Luo T. , Yang Z., Chalcogenide glass fibers: Optical win-dow tailoring and suitability for bio-chemical sensing. Opt. Mat. 47, 530–536 (2015).

Bipolar Gunn effect in high-voltage GaAs diodes: towards impact-ionization lasers once again?

A. V. Rozkhov, V. Kh. Kaibyshev, A. A. Toropov, P. B. Rodin

Ioffe Institute, St. Petersburg, Russia

e-mail: rodin@mail.ioffe.ru

Bipolar Gunn effect is an electron-hole plasma instability caused by the negative differential mobility of electrons in GaAs. It is drastically different from the classical monopolar Gunn effect, traditionally associated with microwave electronics. Bipolar Gunn domains are multiple narrow moving domains of strong ionizing electric field. Spontaneous appearance of such field domains is a powerful mechanism of rapid non-equilibrium carrier generation through intense impact ionization within the domains. This mechanism manifests itself in various GaAs devices of pulse power electronics.

In this presentation bipolar Gunn effect and its consequences are investigated in high-voltage (~300–500 V) GaAs diodes that are switched from blocking to conducting state by a steep (~1 kV/ns) voltage ramp applied to reversely biased diode and in-series load [1–3]. Electric and optical experiments, as well as numerical simulations, have been performed. We argue that impact ionization in bipolar Gunn domains is responsible for both subnanosecond switching [1] and submirosecond maintaining of the conducting state after switching (so called *lock-on effect*) [2]. We demonstrate that the electron-hole plasma concentration achieved after the subnanosecond switching is sufficient for stimulated emission [3].

Narrow (~10 μm) high current density (10^5 A/cm^2) filaments are formed in the diode. Recombination emission kinetics have been measured using time correlated single photon counting (TCSPC) method. The recombination fall time varies between 200 and 700 ps for different filaments but is well below the nanosecond range for all filaments, indicating stimulated emission. A significant narrowing of the averaged emission spectra is observed. Narrow laser-like spectra are observed for singe pulses, despite the absence of specially designed mirrors in the power diodes under study. However, the spectra measured for electrical pulse trains, and spatial filamentary patterns in the device do not repeat themselves from pulse to pulse. Numerical simulations reveal complex chaotic dynamics of the ionizing bipolar Gunn domains.

Our results bear some similarities with research on impact-ionization lasers based on streamer discharge in bulk semiconductor samples [4, 5]. We have shown that stimulated emission can be achieved in reversely biased homo-junction GaAs diode driven to the impact ionization by a steep voltage ramp. However, the filaments in our diodes are not streamers in their physical nature, and the mechanism that leads to high carrier concentration is not just avalanching. In fact, this mechanism only involves avalanche breakdown at the initial stage, while ionizing bipolar Gunn domains play a leading rolde at the next and most important stage. Controlling the location of current filaments by means of appropriate structural design has the potential to achieve lasing in diodes pumped by ionizing bipolar Gunn domains.

[1] M.S. Ivanov, A.V. Rozhkov, P.B. Rodin, Subnanosecond switching of GaAs diode due to impact ionization in collapsing bipolar Gunn domains, Solid State Commun., vol.379, 115420 (2024).
[2] A.V. Rozhkov, M.S. Ivanov, P.B. Rodin, Self-Sustaining of the Conducting State and Bipolar Ionizing Gunn Domains in Pulse Avalanche Gallium Arsenide Diodes. Bull. Russ. Acad. Sci. Phys., vol.87, pp. 765–770 (2023).
[3] A.V. Rozhkov; V.Kh. Kaibyshev, A.A. Toropov, P.B. Rodin, Subnanosecond kinetics of recombination radiation of a high-voltage gallium arsenide diode in impact-ionization switching. Tech. Phys. Lett., v.50, 3, 2024, pp. 52–55 (2024).
[4] N.G. Basov, A.G. Molchanov, A.S. Nasibov, A.Z. Obidin, A.N. Pechenov, Yu.M. Popov, Solid state streamer lasers, Zh. Eksp. Teor. Fiz., vol.70, pp.1751–1761 (1976).
[5] G.A. Mesyats, A.S. Nasibov, V.G. Shpak, S.A. Shunailov, M.I. Yalandin, Lasing in zinc selenide single crystals pumped by high-voltage subnanosecond pulses, Quantum Electronics, vol.38, pp.213–214 (2008).

MOPA architectures for ultrafast crystalline Raman lasers with various wavelengths

S. N. Smetanin, D. P. Tereshchenko, Yu. A. Kochukov, A. G. Papashvili, K. A. Gubina, P. D. Kharitonova, B. D. Ovcharenko, V. V. Bulgakova, P. A. Chizhov, A. A. Ushakov, V. E. Shukshin, I. S. Voronina, L. I. Ivleva

Prokhorov General Physics Institute of the Russian Academy of Sciences, Vavilova 38, Moscow, 119991 Russia

e-mail: ssmetanin@bk.ru

Development of fundamentally new photonics devices of various spectral ranges can be based on the study of the interaction of various nonlinear phenomena in active media under the action of high-intensity ultrashort laser pulses. Namely, highly transient stimulated Raman scattering (SRS) with various frequency shifts, nonlinear phase modulation, supercontinuum generation, filamentation, parametric and laser amplification can be used.

When the laser pump pulse was shorter than a phase relaxation time of a Raman resonance, SRS in various scheelite-type crystals occurred in a highly transient regime with combined (short ~300 cm^{-1} and long ~900 cm^{-1}) Raman shifts not only on primary, but also secondary Raman modes having comparable integral cross-sections of Raman scattering [1]. Under pumping by a subpicosecond powerful Yb-fiber laser (λ_p = 1.03 μm), it resulted to efficient ultrafast SRS generations at wavelengths of λ_s = 1.06 and 1.14 μm without narrowing the Stokes spectral lines (the linewidth is ~10 nm like the pump laser) with the output Stokes pulse energies of a μJ level. Therefore, we have a wide range of options for laser and parametric amplification of crystalline Raman laser radiation at various wavelengths in architectures of master oscillator power amplifier (MOPA).

In this work, we optimized MOPA architectures for ultrafast crystalline Raman lasers with various wavelengths. First, it was done for laser amplification of ultrashort pulses of Raman radiation with both short and long Raman shifts in promising laser crystals with neodymium ions (~1.06 μm) and F_2^- color centers (~1.14 μm) in the near infrared range, for the amplified subpicosecond pulse energies of a 1-mJ level. We found optimum laser crystals having an enough gain linewidth and achieved multifold amplification of the 10-nm linewidth Stokes pulses in $CaMoO_4$:Nd^{3+} at 1.06 μm and in LiF:F_2^- at 1.14 μm. Second, we developed MOPA architectures for parametric amplification of the Raman laser radiation in promising quadratically nonlinear crystals with difference frequency generation at an idle wavelength of $\lambda_i = (\lambda_p^{-1} - \lambda_s^{-1})^{-1}$ for advancing into the mid-infrared range, including for spectral positioning at wavelengths of known infrared lasers with ferrum ions (4-6 μm) and with CO_2 (10.6 μm), for the amplified subpicosecond pulse energies in the mid-infrared range of a 1-μJ level. A subpicosecond version of the system is now being implemented, which previously provided generation of 50-microjoule 20-picosecond pulses in the mid-infrared range (4–11 μm) using $LiGaS_2$ and $LiGaSe_2$ nonlinear crystals with various crystalline Raman laser seedings [2].

This research was supported by Russian Science Foundation – Project No 24-12-00448 (https://rscf.ru/project/24-12-00448/).

[1] Yu. A. Kochukov, K. A. Gubina, D. P. Tereshchenko, S. N. Smetanin, A. G. Papashvili, P. A. Chizhov, A. A. Ushakov, V. E. Shukshin, E. E. Dunaeva, I. S. Voronina, L. I. Ivleva, Multiwavelength highly transient stimulated Raman scattering on dual Raman modes in $Sr(MoO_4)_{0.8}(WO_4)_{0.2}$ and $Sr(MoO_4)_{0.4}(WO_4)_{0.6}$, Opt. Lett. **49** (19), 5575–5578 (2024).

[2] S. N. Smetanin, M. Jelínek, V. Kubeček, A. F. Kurus, V. N. Vedenyapin, S. I. Lobanov, L. I. Isaenko, 50-μJ level, 20-picosecond, narrowband difference-frequency generation at 4.6, 5.4, 7.5, 9.2, and 10.8 μm in $LiGaS_2$ and $LiGaSe_2$ at Nd:YAG laser pumping and various crystalline Raman laser seedings, Optical Materials Express, **10** (8), 1881–1890 (2020).

Universal critical indices predicting erbium laser behavior

A. M. Smirnov[1–3], A. V. Dorofeenko[1,2,4,5], O. V. Butov[1]

1- Kotelnikov Institute of Radioengineering and Electronics of RAS, Mokhovaya 11-7, Moscow, 125009 Russia
2- Moscow Institute of Physics and Technology, Institutskiy pereulok 19, Dolgoprudny, 141700 Russia
3- Faculty of Physics of Lomonosov Moscow State University, Leninskie Gory 1-2, Moscow, 119991 Russia
4- Institute for Theoretical and Applied Electromagnetics RAS, Izhorskaya 13, Moscow, 125412 Russia
5- Dukhov Research Institute of Automatics, Suschevskaya 22, Moscow, 127055 Russia

e-mail: alsmir1988@mail.ru

Lasers and amplifiers based on fibers doped with erbium ions, the luminescence of which lies mainly at the telecommunications range of 1.55 microns, have become essential elements of advanced fiber communication lines with network densification, fiber sensor systems and the application of ultra-wideband erbium fiber lasers with ultrashort pulses. The creation of short fiber lasers requires an increase of the doping elements concentration in the core. In this case, there is a clusterization problem of rare-earth elements, which has a detrimental effect on the amplifying properties of the optical fiber. The erbium clusterization effect in the core material of the fiber laser leads to the pulsed operation regime.

We present the analysis of erbium heavily-doped fiber lasers operation, which demonstrate two thresholds, the first one associated with an onset of lasing in the pulsed regime, and the second with a transition to continuous-wave (CW) operation. Lasing features near these two thresholds have been investigated experimentally. For the first time, a power-law behavior of the system parameters – pulses frequency, duration and peak intensity – was revealed in a wide range of pump rates around both thresholds (Fig. 1). The power exponents were associated with critical indices of phase transition. Their values were convincingly determined different from integers and half-integers. Critical indices were shown weakly dependent on the Fabry-Perot and distributed feedback (DFB) laser cavity parameters, which made it possible to experimentally establish the universal dependence of the pulse frequency and duration on the lasing power [1].

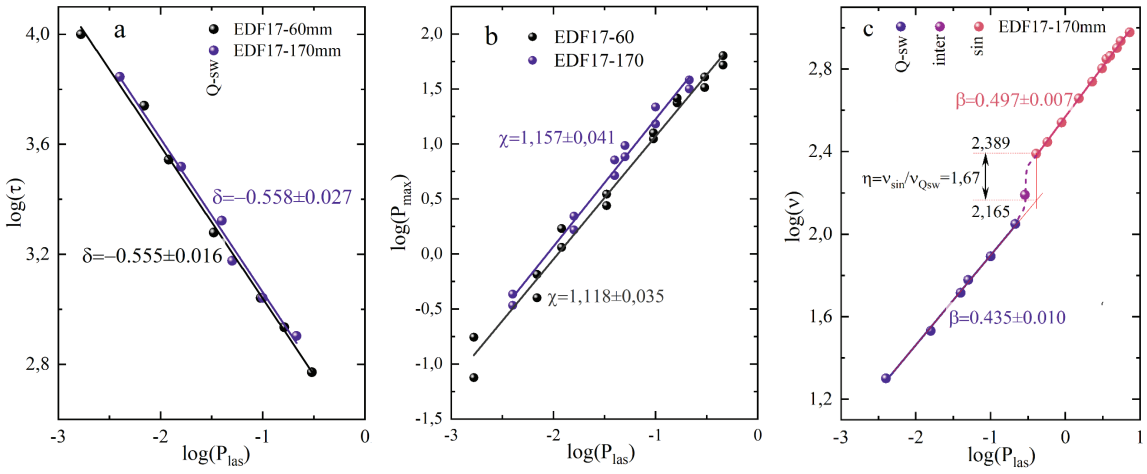

Fig. 1. Pulse duration (a), amplitude (b) and frequency (c) logarithm dependence on the operation power logarithm for heavily-doped erbium fiber lasers. Experimental data are approximated by the dependencies: $\log(\tau) = \delta\log(P_{las}) + \text{const}$ (a); $\log(P_{max}) = \chi\log(P_{las}) + \text{const}$ (b); $\log(\nu) = \beta\log(P_{las}) + \text{const}$ (c).

Thus, the linear log-log dependences represent a direct consequence of the system's critical behavior above the lasing threshold. In the theory of critical phenomena, universal dependences between indices are known. In our case, such relation originates from an apparent identity $P_{las} = P_{max\ v\tau}$. After logarithmising we retrieve a relation $\alpha = \chi + \beta + \delta$, where critical index $\alpha = 1$ is the slope efficiency of linear dependence $P_{las} = \alpha(P_{pump} - P_{th})^{\alpha}$. The results of the work are extremely useful for determining and predicting the parameters of the designed erbium lasers, due to universality of the critical indices.

[1] A.M. Smirnov, A.A. Rybaltovsky, I.A. Nechepurenko, A.V. Dorofeenko, O.V. Butov, Critical behavior of erbium fiber lasers in pulsed and relaxation oscillations regimes, Optics and Laser Technology, Volume 181, Part B, 111823 (2025).

Fiber-based source of bright ultrabroad photon pairs at pulse and cw regimes

M. A. Smirnov[1], I. V. Fedotov[2], A. F. Khairullin[1], O. A. Ermishev[1], A.M. Smirnova[1], A. B. Fedotov[2], S. A. Moiseev[1]

1- Kazan Quantum Center, Kazan National Research Technical University named after A. N. Tupolev, K. Marks st. 10, Kazan, 420111 Russia
2- Faculty of Physics, Moscow State University named after M. V. Lomonosov, ter. Leninskie Gory 1, Moscow, 119991 Russia

e-mail: maxim@kazanqc.org

The development of sources of quantum states of light is of great importance for modern quantum technologies. By now, sources of correlated photon pairs (biphotons), which represent a two-photon state of light, have been greatly developed [1]. Due to their non-classical properties, photon pair sources find application in various areas of quantum technologies [2], including the development of quantum repeaters, quantum computers, quantum visualization methods, quantum spectroscopy and microscopy.

One of the key goals for the practical use of the developed methods is the integration of such sources into an optical platform, ensuring their compactness and scalability. The use of optical fiber as a nonlinear medium for generating photon pairs has significant potential for implementing this approach.

The report presents the key results obtained over the past several years. The research was conducted at the Kazan National Research Technical University named after A. N. Tupolev – KAI (KNITU-KAI), in particular, at its division Kazan Quantum Center, together with colleagues from the Moscow State University named after M. V. Lomonosov (MSU). The operation of a bright ultra-wideband (≈180 THz) fiber source of biphotons with widely spectrally separated signal and idler photons was experimentally demonstrated [3]. Such a two-photon source is realized due to the joint use of broadband synchronism of interacting light waves and high optical nonlinearity of photonic crystal fiber with a quartz core. In addition, the degree of quantum entanglement was numerically estimated based on the Schmidt mode analysis for ultra-wideband biphoton states generated in a photonic crystal fiber. Also the generation of interband photon pairs with wavelengths near 0.5 and 1.6 μm in a photonic crystal fiber was also experimentally demonstrated using continuous (cw) low-power optical pumping by a diode laser with a central wavelength of 0.8 μm [4]. It was found that the generation rate of entangled photons with continuous pumping is comparable to the values obtained using pulsed pumping with a Ti:sapphire femtosecond laser if the average continuous pump power is an order of magnitude higher than the average pulsed pump power. The results highlight the potential of using such photon pair sources for quantum technologies, including quantum spectroscopy, imaging and communications, due to their compactness and scalability. Optical fibers as sources of photon pairs (biphotons) represent a promising and promising platform for the development of quantum optics and quantum technologies. The achievements presented in the report demonstrate the possibilities of generating photon pairs with high efficiency, forming specified spectral profiles and controlling quantum entanglement.

This research was supported by Ministry of Education and Science of the Russian Federation (Reg. number NIOKTR 125012300688-6).

[1] Klyshko D. N. The Einstein-Podolsky-Rosen paradox for energy-time variables, Soviet Physics Uspekhi, vol. 32 (6), p. 555, (1999).
[2] Erhard M., Krenn M., Zeilinger A. Advances in high-dimensional quantum entanglement, Nature Reviews Physics, vol. 2 (7), pp. 365–381, (2020).
[3] Smirnov M. A. et al. Bright ultra-broadband fiber-based biphoton source, Optics Letters, vol. 49 (14), pp. 3838–3841, (2024).
[4] Khairullin A. F. et al. Visible–Telecom Photon Pair Source Based on a Photonic-Crystal Fiber under Continuous-Wave Pumping, JETP Letters., vol. 119 (5), pp. 345–351, (2024).

High-speed photonics on the base of composite fluorinated polymer materials

V. I. Sokolov

NRC «Kurchatov Institute», Academician Kurchatov square 1, Moscow, Russia

e-mail: visokol@rambler.ru

The development of modern high-speed photonics and integrated optics requires the new optical mate-rials, possessing ultra-high transparency in telecom wavelength regions around 850, 1300 and 1550 nm, ultra-low material dispersion, environmental stability and high manufacturability. Moreover, synthesis of optically active and nonlinear optical materials, which permit fabrication of compact wave-guide am-plifiers and single-frequency distributed feedback lasers as well as high-speed (>100 GHz) optical waveguide modulators is of great importance.

We report the creation of new optical materials on the basis of amorphous fluorine-containing polymers with embedded nanocrystals (NCs) $NaYF_4$, $NaLuF_4$ etc. doped with rare-earth elements (Yb, Er, Tm, Ce), which possess intense down-conversion photoluminescence (PL) around 1530 nm, as well as pol-ymers with embedded fluorinated electro-optical chromophores. We present the review of high-pres-sure (15–16 MPa) technique for synthesis of new amorphous fully fluorinated (perfluorinated) poly-mers (Fig. 1), methods for synthesis of nanocrystals (Fig. 2) and chromophores as well as methods for embedding NCs and chromophores into polymer matrix. We also present advanced laser technologies for fabricating single-mode optical waveguides and waveguide elements using the composite polymer materials (Fig. 3). These elements include waveguide splitters, directional couplers, Mach-Zhender in-terferometers, narrowband waveguide filters with submicron Bragg gratings, and optical waveguide amplifiers for 1530–1565 nm telecom wavelength region as well as high-speed polymer optical bus on printed circuit board for microprocessor computing systems.

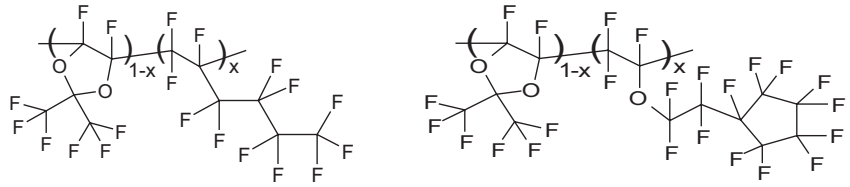

Fig. 1. New amorphous perfluorinared polymers synthesized using high-pressure (15–16 MPa) technique.

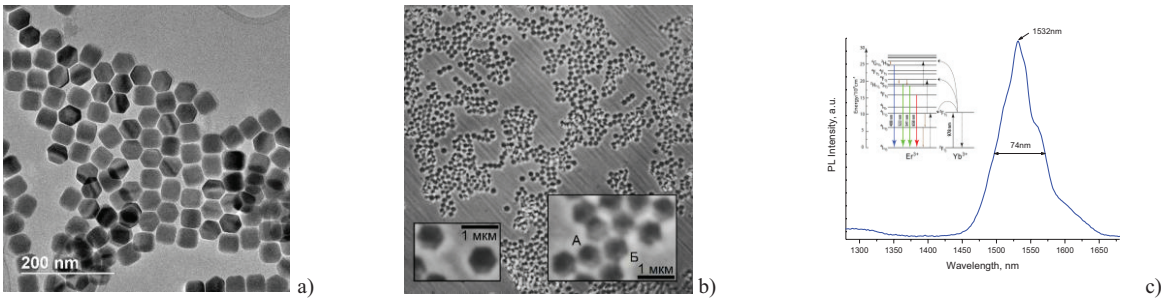

a) b) c)

Fig. 2. (a) TEM photo of β-$NaYF_4$:Yb^{3+},Er^{3+} nanocrystals. (b) Photo of NCs taken using deep UV optical microscopy (235 nm). (c) PL down-conversion spectrum of β-$NaYF_4$:Yb^{3+},Er^{3+} NCs pumped with 980 nm laser light.

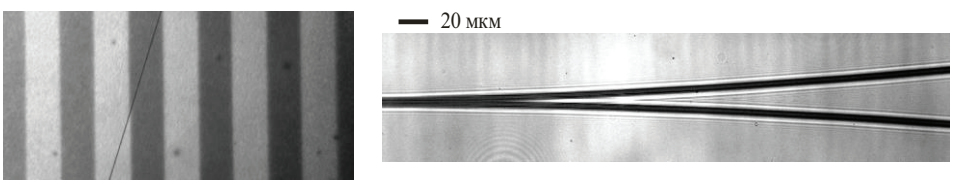

Fig. 3. Photographs of single-mode polymer waveguides with embedded fluorinated chromophores fabricated using direct laser writing technique.

The work was carried out within the state assignment of NRC "Kurchatov Institute".

Growth and investigations of the novel promising laser hosts, $Mg_{1-x}Zn_xWO_4$ mixed single crystals

K. Subbotin[1,2], Yu. Zimina[1,2], A. Titov[1], P. Popov[3], L. Iskhakova[1], D. Lis[1], S. Pavlov[1,2], E. Zharikov[1]

1- Prokhorov General Physics Institute of the Russian Academy of Sciences, Vavilova st. 38, Moscow, Russia
2- Mendeleev University of Chemical Technology of Russia, Miusskaya sq. 9, Moscow, Russia
3- Petrovsky Bryansk State University, Bezhitskaya st. 14, Bryansk, Russia

e-mail: soubbot@lsk.gpi.ru

In the last years, $MgWO_4$ and $ZnWO_4$ crystals with monoclinic wolframite-like structure doped by rare-earth ions (RE, R^{3+}) have attracted much attention as promising active laser media. They possess a complex of good properties: inhomogeneously broadened optical absorption and luminescence bands with high peak transitions cross-sections and large Stark splitting of ground states of RE-ions. Besides that, $MgWO_4$ crystal has good thermal conductivity, up to 10 W/m·K. However, this crystal cannot be grown from melt because of the polymorph phase transformation below the melting point. Moreover, the distribution coefficients of RE-ions between this crystal and a parent media are rather low. Therefore, introduction of the essential concentrations of RE-ions into this crystal is a quite difficult task. On the other hand, $ZnWO_4$ crystal can easily be grown by Czochralski. A proper choice of a charge compensator for heterovalent substitution of Zn^{2+} by R^{3+} can raise the distribution coefficient of RE-ions upto 0.4 or even 0.5. However, thermal conductivity of $ZnWO_4$ is worse, only about 5 W/m·K, depending on the particular crystallographic direction.

It is known that $MgWO_4$ and $ZnWO_4$ form the continuous series of $Mg_{1-x}Zn_xWO_4$ solid solutions in very wide concentration range. Moreover, some properties (e.g. the scintillation light yield) of these solid solutions are better than those of $MgWO_4$ and $ZnWO_4$ crystals. The use of such mixed crystals as the laser hosts should additionally broaden the absorption and luminescence bands of RE-dopants and smoothen the contours of these bands. Besides that, even rather low value of x appeared to open the possibility of growing the crystals by the Czochralski technique. However, the particular "threshold" value of x remained unknown, and it was unclear how doping the crystal by RE-ions affects for this value. Besides that, it was not clear, whether thermal conductivity and mechanical strength characteristics of the mixed crystals drastically worsen as compared to the individual crystals.

In the frame of our work we have performed the attempts to grow the concentration series of eight $Mg_{1-x}Zn_xWO_4$ single crystals by Czochralski with x = 0.1 to 1.0. Six attempts were successful: the crystals with the compositions starting from x = 0.2 have high optical quality. Besides that, the Tm:Li:$Mg_{0.8}Zn_{0.2}WO_4$ single crystal with 0.5 at.% of Tm^{3+} had also been successfully grown. The attempts of Czochralski growth of the $Mg_{1-x}Zn_xWO_4$ crystals with x = 0.1 and 0.15 were failure: they resulted in obtaining the polycrystalline samples, consisting of the mixtures of high-temperature and low-temperature $MgWO_4$ like phases. Thus, the "threshold" value of x was refined with the precision of ±0.005 f.u. to be 0.185. Moreover, the addition of 0.5 at.% of Tm^{3+} does not shift this "threshold" x towards larger values.

In order to measure the properties of the whole concentration series of the $Mg_{1-x}Zn_xWO_4$ crystals in the range of x from 0 to 1, $MgWO_4$ single crystal was additionally grown from flux. The unit cell parameters for all the samples were calculated from X-ray powder diffraction analysis with the Rietveld treatment of the obtained patterns. The actual crystals compositions along the boules were measured by energy-dispersive microprobe analysis with the approximation of the obtained results by Gulliver-Pfann equation. The hydrostatic densities of different parts of the grown crystals were measured, and compared with the theoretical X-ray densities. Besides that, thermal conductivities and mechanical strength characteristics (micro-hardness and crack-resistance) of the samples have been measured. Thermal conductivity of $Mg_{0.8}Zn_{0.2}WO_4$ crystal appeared to be, at least, not worse than for $ZnWO_4$, whereas the mechanical strength characteristics of the mixed crystals are better than those for $MgWO_4$ and $ZnWO_4$.

The study was supported by the Russian Science Foundation, grant no. 23-22-00416.

Period-doubling bifurcation of the temporal pulse bunch width of noise-like pulses in a passively mode-locked fiber laser

A. Sudin[1], I. Volkov[1], S. Ushakov[1,2], K. Nishchev[1]

1- National Research Mordovia State University, Bolshevistskaya Street 68, Saransk, Republic of Mordovia, 430005 Russia
2- Prokhorov General Physics Institute of the Russian Academy of Sciences (GPI), Vavilova Street 38, Moscow, 119991 Russia

e-mail: alexander.sudin1999@yandex.com

Noise-like pulses represent one of the generation regimes in passively mode-locked fiber lasers. Due to their broad optical spectrum and short coherence length, lasers generating noise-like pulses are attractive for applications in spectroscopy, metrology, and supercontinuum generation.

The schematic of the Er/Yb-doped fiber ring laser is shown in Fig. 1. The mode-locking mechanism is based on the nonlinear polarization rotation technique. The cavity length is 321 m, corresponding to a fundamental pulse repetition rate (f0) of 635.73 kHz. By adjusting the pump power of the laser diode and the rotation angles of the polarization controller plates, various noise-like pulse regimes with distinct temporal profiles were observed.

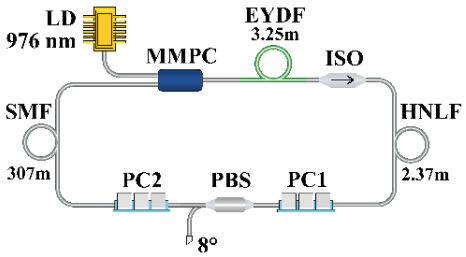

Fig. 1. Experimental setup:
EYDF – Er/Yb-doped fiber; HNLF – highly nonlinear fiber;
ISO – fiber isolator; LD – pump laser diode;
MMPC – multimode pump combiner;
PC – polarization controller; PBS – polarization beam splitter;
SMF – single mode fiber.

The output characteristics of the noise-like pulse with a square-shaped temporal profile are shown in Fig. 2. The optical spectrum was broadened to 1200 nm, with a full width at half maximum (FWHM) of 37 nm. The FWHM of the coherence spike was 90 fs (inset in Fig. 2a). Notably, two square-shaped pulses with different temporal widths were observed in the cavity. As shown in Fig. 2b, the temporal width of the first pulse was 7.4 ns (black curve), while that of the second was 10.3 ns (red curve). Analysis of the oscillogram over a 20 μs range revealed that these pulses exhibit a 2-roundtrip periodicity. This behavior can be characterized as a period-doubling bifurcation [1]. This observation is further corroborated by the radio frequency spectrum analysis (Fig. 2c), which exhibits a signal at half the fundamental pulse repetition rate.

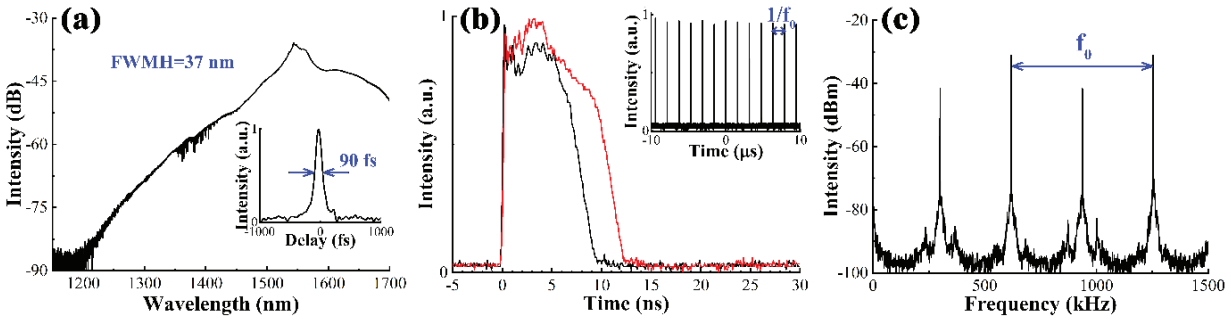

Fig. 2. (a) Optical spectrum (inset: autocorrelation trace of the coherent spike); (b) Oscilloscope trains in the range of 35 ns (inset: oscilloscope train in the range of 20 μs); (c) RF spectrum.

We have experimentally demonstrated the generation of noise-like pulses in a passively mode-locked Er/Yb-doped fiber ring laser, accompanied by a period-doubling bifurcation of the temporal pulse bunch width.

[1] Z. Wang, A. Coillet, S. Hamdi, Z. Zhang, and P. Grelu, Spectral Pulsations of Dissipative Solitons in Ultrafast Fiber Lasers: Period Doubling and Beyond, Laser & Photonics Reviews, 17, 2200298, (2023).

Enhanced 1.5-μm luminescence of Er^{3+} in ZBLAN glasses by additional doping with Tb^{3+} and Yb^{3+} ions

K. E. Sumachev, A. P. Savikin

Lobachevsky State University of Nizhny Novgorod, Gagarin Avenue, Nizhny 23, Novgorod, 603950 Russia

e-mail: sumachev09@gmail.com

The efficiency of 1.5 μm luminescence of erbium ions at the transition $^4I_{13/2} \rightarrow {}^4I_{15/2}$ directly depends on the optimal conditions of populating the $^4I_{13/2}$ state. The structure of energy levels of Tb^{3+} ions in the IR region 3500–5500 cm^{-1} is of interest due to the occurrence of interionic energy transfer processes with Er^{3+} ions, which can affect the populations of $^4I_{13/2}$ and $^4I_{11/2}$ states. Low phonon energy fluoride matrices doped with rare-earth ions demonstrate a higher efficiency (compared to oxide matrices) of interionic energy transfer processes with a lower probability of nonradiative intracenter relaxation [1, 2], which can be used for a more efficient populating of the $^4I_{13/2}$ state due to the cross-relaxation of Er^{3+} ion states with the participation of co-doped ions.

The luminescence properties of ZBLAN (ZrF_4-BaF_2-LaF_3-AlF_3-NaF):1%Er^{3+}+3%Yb^{3+}+x%Tb^{3+} (x = 0, 0.1, 0.2, 0.4, 0.6, 1 mol.%) glasses were investigated. The enhanced of 1.5 μm luminescence of Er^{3+} ions under excitation by 940 nm wavelength radiation in ZBLAN:1%Er^{3+}+3%Yb^{3+} composition with additional doping of Tb^{3+} ions was presented. The yield of 1.5 μm luminescence at the optimum Tb^{3+} ions concentration value of 0.4% was 6 times higher compared to the composition without Tb^{3+} ions.

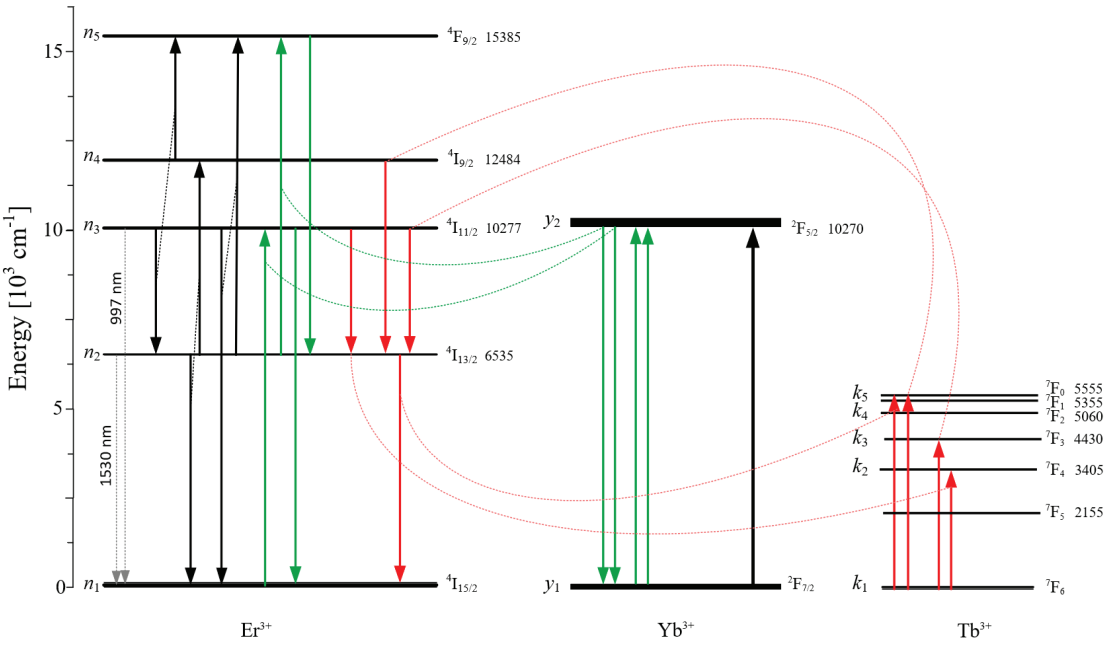

Fig. 1. The cross-relaxation and energy transfer processes of Er^{3+}, Yb^{3+} and Tb^{3+} ions in ZBLAN glass.

The presence of the concentration extremum for the $^4I_{13/2}$ state can be explained by analyzing the competitive processes of interionic energy transfer ($^4I_{11/2} \rightarrow {}^4I_{13/2}$) – ($^7F_6 \rightarrow {}^7F_4$) + ($^7F_6 \rightarrow {}^7F_3$) and ($^4I_{13/2} \rightarrow {}^4I_{15/2}$) – ($^7F_6 \rightarrow {}^7F_0$) with the participation of Tb^{3+} ions (Fig. 1). The compiled theoretical model based on a balance equations taking into account non-resonant transitions allowed to estimate the $^4I_{13/2}$ and $^4I_{11/2}$ states populations of Er^{3+} ions and explain the increasing the population of the $^4I_{13/2}$ state in three-component alloying.

The work was supported by the Ministry of Science and Higher Education of the Russian Federation (FSWR-2024-0003).

[1] F. Gun, Optical properties of fluoride glasses: a review, Journal of Non-Crystalline Solids. 184. 9–20, (1995).
[2] P. Zhang, J. Yin, B. Zhang, L. Zhang, J. Hong, J. He, Y. Hang, Intense 2.8 μm emission of Ho^{3+} doped PbF_2 single crystal, Optics Letters, 39, 3942–3945, (2014) https://doi.org/10.1364/OL.39.003942.

Long wavelength lasers on the basis of Rare-Earth doped chalcogenide glasses

S. E. Sverchkov[1], B. I. Denker[1], M. P. Frolov[2], B. I. Galagan[1], V. V. Koltashev[3], V. G. Plotnichenko[3], M. V. Sukhanov[4], A. P. Velmuzhov[4]

1- Prokhorov General Physics Institute of RAS, Moscow, Russia
2- Lebedev Physical Institute of RAS, Moscow, Russia
3- Prokhorov General Physics Institute of RAS, Dianov Fiber Optics Research Center, Moscow, Russia
4- Devyatykh Institute of Chemistry of High-Purity Substances of RAS, Nizhny Novgorod, Russia

e-mail: glasser@lst.gpi.ru

The prospects of chalcogenide glasses as materials for bulk and fiber lasers emitting at $\lambda > 4$ μm, i.e. at wavelengths inaccessible for fluoride glass lasers, have been recognized for several decades already. Dozens of works have been devoted to the synthesis and spectroscopy of rare earth doped sulfide and selenide glasses. Nevertheless, attempts to obtain mid-infrared laser action in them did not bring success for many years. It was a curious situation: lots of papers with the words "mid infrared laser" in the title have been published, but no laser action was demonstrated (with the exception of 1.08 μm lasing in Nd^{3+} doped sulfide glass). Now it is clear, that the absence of the laser effect in the mid-infrared was due to the absorption losses caused by hydrogen-containing impurities (S-H, Se-H, Ge-H groups) in the doped glasses.

The situation has begun to change in 2020 after the first demonstration of 5 μm lasing effect Tb^{3+} doped selenide glass [1]. Now a whole new class of mid-infrared bulk and fiber lasers have been developed on the basis of rare earth doped selenide glasses. For the first time laser action between the first excited and the ground levels of Ce^{3+}, Pr^{3+}, Nd^{3+} and Tb^{3+} ions was demonstrated. The spectral range of these transitions extends from 4.5 μm to 6.1 μm (see Fig. 1).

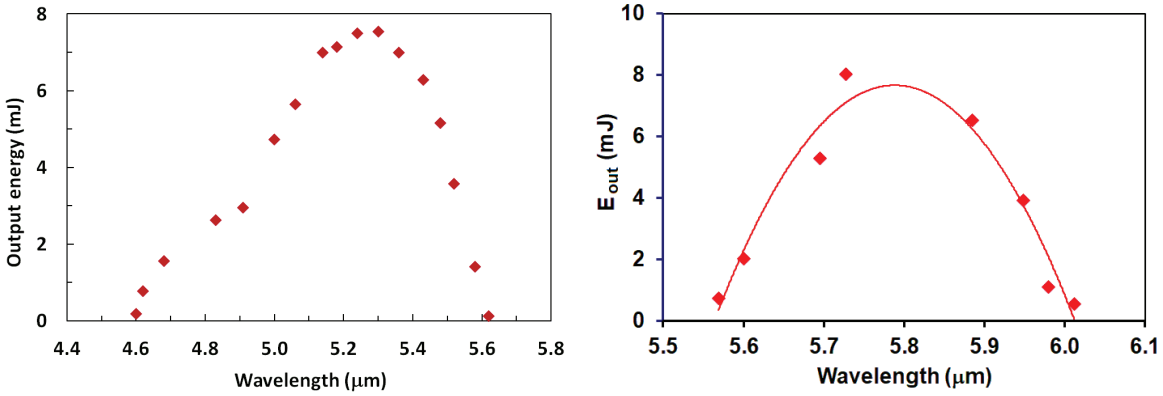

Fig.1. Tuning curves of bulk Ce^{3+} (left plot) and Nd^{3+} (right plot) doped selenide glass lasers.

The highest output parameters for bulk glass lasers (over 40 mJ of output energy) were obtained with Ce^{3+} doped glass at room temperature [2]. The longest lasing wavelengths for any glass laser and tunability within the 5.56–6.1 μm spectral band (complementing Ce^{3+} and Tb^{3+} tuning ranges) were shown with Nd^{3+} ions [3].

Multimaterial optical fibers with rare earth doped selenide glass core surrounded by undoped sulfide glass cladding were developed. Room-temperature CW laser action was obtained in Tb-doped and Ce-doped fibers. The highest output parameters for fiber lasers (150 mW at 5.1–5.3 μm under continuous pumping) were demonstrated with Tb^{3+} ions [4].

Thus, practically significant output parameters are already demonstrated by both bulk and fiber chalcogenide glass lasers emitting in the 4.5-6.1 μm spectral band.

The work was supported by RSF grant 25-13-00245.

[1] M.Churbanov et al, First demonstration of ~ 5 μm laser action in terbium doped selenide glass, Applied Physics B, 126, 117 (2020)
[2] M.Frolov et al, Current progress in Ce^{3+} -doped selenide glasses for mid-infrared lasers, Opt. Mater. Express 12, 4619-4629 (2022)
[3] M.Frolov et al, Cross-relaxation processes in Nd-doped selenide glass and 5.7 μm laser action in it, J. of Lumin. 280,121089 (2025)
[4] V.Koltashev et al, 150 mW Tb-doped chalcogenide glass fiber laser emitting at λ>5μm, Optics and Laser Technology, 161,109233 (2023)

Modeling of dual-wavelength pump schemes for optically pumped Ar-He laser

A. Torbin[1], R. Kuramshin[1,2], M. Zagidullin[1]

1- Lebedev Physical Institute, Samara Branch, Novo-Sadovaya str. 221, Samara, 443011 Russia
2- Samara National Research University, Moskovskoye shosse 34, Samara, 443086 Russia

e-mail: torbin.ap@yandex.ru

Presently, the most advanced laser systems capable of delivering both high power and diffraction-limited beam quality are hybrid gas lasers utilising diode optical pumping. Exemplary systems of this kind include diode-pumped alkali vapor lasers (DPAL) and optically pumped metastable rare gas lasers (OPRGL). In contradistinction to solid-state gain media, gaseous active media proffer the advantage of diminished thermal effects on beam quality and minimised optical distortions. Consequently, gas lasers facilitate the extraction of higher energy limits per unit volume of the active medium in comparison with their solid-state counterparts.

OPRGL is a direct analogue of DPAL, also capable of providing an output of 10^2 W per cubic centimetre, but without a number of its disadvantages, such as a chemically active laser medium and the need to heat the gas cell. OPRGL operates using a three-level scheme. Metastable Rg* atoms are generated in glow discharge plasma. Optical pumping is performed from the lower metastable state $1s_5$ to the $2p_9$ or $2p_8$ level. As a result of collisions between the excited Rg* atom and the He atom, the $2p_{10}$ level is populated. Inverse population occurs between the $2p_{10}$ and $1s_5$ levels. Amplification and lasing have been observed at optical pumping of metastable atoms of heavy inert gases Rg* = Ne*, Ar*, Kr* and Xe*. The maximum output powers of OPRGL achieved to date are 12.5 W (Ar*-He OPRGL) [1], 4.1 W (Ar*-He) [2] and 1.3 W (Xe*-He) [3]. The OPRGL system based on an Ar*-He mixture is assumed to be the most promising due to the lowest cost of gases used therein and the best knowledge of argon-helium plasma compared to similar inert gas mixtures.

One of the primary obstacles impeding the augmentation of the output power of OPRGL pertains to the depletion of the metastable lower laser level upon the initiation of optical pumping. This phenomenon transpires as a consequence of a sequence of collision and spontaneous emission transitions to the proximate $1s_4$ level, which does not partake in the laser cycle but is radiatively coupled to the ground state. Consequently, the loss of metastable atoms is increased, and the efficiency of converting pumping into laser radiation is decreased. The most promising approach to resolving this issue is to utilise additional optical pumping to facilitate the return of atoms from the $1s_4$ level to the laser cycle [4, 5].

The report will present the results of a kinetic modeling of a lasing medium for a dual-wavelength optically pumped rare gas laser. Analytical formulas were derived for the frequency of Ar* radiation losses, population of the energy levels involved in the laser cycle and specific powers for pump absorption and lasing in the limit of bleaching of pump and lasing transitions taking into account dual-wavelength optically pump.

The study was supported by the grant from the Russian Science Foundation No. 25-22-00392, https://rscf.ru/project/25-22-00392/.

[1] P. Lei, Z. Chen, Y. Shen, X. Wang and D. Zuo, Demonstration of a metastable argon laser of 10 W by transverse pumping, Optics Letters, 49(17), pp. 4918–4921. (2024).
[2] J. Han, C. R. Sanderson, B. Hokr, C. W. Ballmann, A. B. Clark and M. C. Heaven, Optically pumped rare gas lasers, Proc. SPIE, 11042, p. 1104202 (2019).
[3] C. R. Sanderson, C. W. Ballmann, J. Han, A. B. Clark, B. H. Hokr, K. G. Xu and M. C. Heaven, Opt. Express, 27, pp. 36011–36011 (2019).
[4] J. Gao, P. Sun, X. Wang and D. Zuo, Modeling of a dual-wavelength pumped metastable argon laser, Laser Physics Letters, 14(3), p. 035001, (2017).
[5] P. Sun, D. Zuo, X. Wang, J. Han and M. C. Heaven, Investigation of dual-wavelength pump schemes for optically pumped rare gas lasers, Optics Express, 28(10), pp. 14580–14589, (2020).

Spectroscopic and mechanical strength characteristics of the Tm,Li:$ZnWO_4$ promising laser crystal

Y. Zimina[1,2], K. Subbotin[1,2], A. Titov[1], A. Popov[1,3], P. Volkov[4], D. Lis[1], S. Pavlov[1,2], Y. Didenko[1,2], E. Chindyasova[1,2]

1- Prokhorov General Physics Institute of the Russian Academy of Sciences, 38 Vavilova st., Moscow, Russia
2- Mendeleev University of Chemical Technology of Russia, 9 Miusskaya sq., Moscow, Russia
3- Institute of Theoretical and Applied Electrodynamics of the Russian Academy of Sciences, 13 Izhorskaya st., Moscow, Russia
4- National Research Center «Kurchatov Institute» IREA, 1 Academician Kurchatov square, Moscow, Russia

e-mail: yulia_zimina@inbox.ru

In the last years, $ZnWO_4$ crystals with a monoclinic wolframite-like structure doped with rare-earth ions have attracted much attention as promising active laser media of the visible and near-IR ranges [1]. In this work we report on the investigation of the absorption spectra, luminescence decay kinetics and mechanical strength characteristics of the concentration series of Tm,Li:$ZnWO_4$ single crystals.

The series of Tm,Li:$ZnWO_4$ single crystals was grown by the Czochralski method in air using a Pt crucible. The actual concentrations of the dopants were measured by inductively coupled plasma atomic emission spectroscopy. It was shown that the use of Li^+ as charge compensators for the entry of Tm^{3+} ions into the Zn^{2+} site can increase the segregation coefficient of Tm^{3+} in the crystal from 0.2 to 0.4.

Optical absorption spectra of Tm,Li:$ZnWO_4$ crystals were systematically studied for the spectral transitions in the range of 700–2000 nm, Fig. 1. The difference in shapes of the absorption spectra for different orientations of the magnetic field strength vector of the probe beam relative to the optical indicatrix axes at the same orientation of the electric field strength vector of probe beam was revealed.

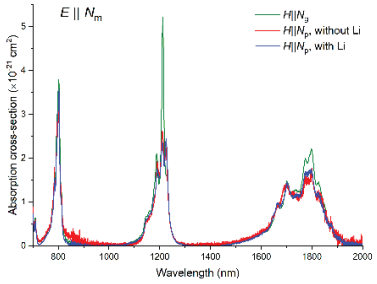

Fig. 1. Polarized optical absorption spectra of Tm,Li:$ZnWO_4$ crystals.

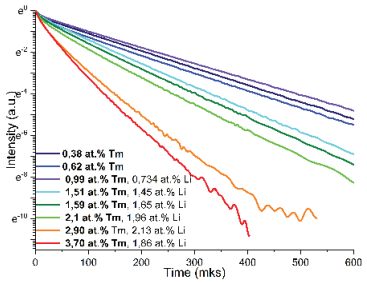

Fig. 2. Luminescence decay kinetics of Tm,Li:$ZnWO_4$ crystals, T = 300 K.

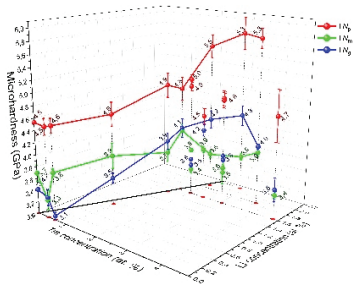

Fig. 3. Microhardness of Tm,Li:$ZnWO_4$ crystals.

The luminescence decay kinetics near 800 nm ($^3H_4 \rightarrow {}^3H_6$) was measured 300 K (Fig. 2).The cross-relaxation ($^3H_4 \rightarrow {}^3F_4$; $^3H_6 \rightarrow {}^3F_4$) efficiency was calculated according to the formula:

$$\beta^{I}_{\mathrm{Tm}\rightarrow\mathrm{Tm}} = \left(1-\left(\int (I(t)/I(0))\,\mathrm{d}t \Big/ \int (I'(t)/I'(0))\,\mathrm{d}t\right)\right)\cdot 100\% \ .$$

In our previous work, the 2 mm CW laser operation was demonstrated at the Tm,Li:$ZnWO_4$ sample with the actual concentration of Tm^{3+} 1.6 at. % with a maximum output power of 282 mW and a slope efficiency of only 14.7% [2]. It was found that the cross-relaxation efficiency in that crystal was only 56%, while the efficiency in the sample with the highest Tm^{3+} concentration (3.7±0.3 at.%) is much higher (71%). This suggests that a laser operation with better characteristics can be expected at the sample with a higher Tm^{3+} concentration.

Mechanical strength characteristics (Fig. 3) of the Tm,Li:$ZnWO_4$ crystals were measured by the indentation method for different directions. Dependences of the measured values on the actual dopant concentrations were revealed.

The study was supported by the Russian Science Foundation, grant no. 23-22-00416.

[1] A. Volokitina, S. P. David, P. Loiko et. al., Monoclinic zinc monotungstate Yb^{3+},Li^+:$ZnWO_4$: Part II. Polarized spectroscopy and laser operation, J. Lumin. 231, 117811 (2021).
[2] G. Z.Elabedine, K.Subbotin, P. Loiko et. al., Growth, spectroscopy and 2 μm laser operation of monoclinic Tm^{3+}:$ZnWO_4$ crystal, Optical Materials, 157, 116039 (2024).

Multi-wavelength MOPA laser system based on $Cr:LiCaAlF_6$ crystals for medical optoacoustic tomography

R. D. Aglyamov[1], A. K. Naumov[1,2], A. S. Nizamutdinov[2], A. A. Shavelev[2], O. A. Morozov[1,2], Yu. P. Brodnikovsky[3], V. V. Semashko[1,2]

1- Kazan E. K. Zavoisky Physical-Technical Institute (KPhTI), Sibirsky tract, 10/7, Kazan, 420029 Russia
2- Kazan Federal University, 18 Kremlyovskaya str., Kazan, 420008 Russia
3- Tomowave Laser LLC, Kazan, 420008 Russia

e-mail: aglyam92@mail.ru

The development of medical optoacoustic tomography using human blood as an endogenous contrast agent is hampered by the lack of reliable, easy-to-use and inexpensive sources of powerful pulsed laser radiation in the 750–900 nm spectral range [1–2]. Currently used titanium-sapphire, alexandrite lasers or parametric oscillators do not provide the required and stable output characteristics, besides they are technically complex and have their cost up to half of the cost of diagnostic optoacoustic system. Here the results of the development of a laser based on $Cr^{3+}:LiCaAlF_6$ (Cr:LiCAF) crystals are discussed, which avoids many of the above-mentioned drawbacks and provides powerful 50 ns-pulsed tunable laser radiation in the region of the absorption bands of oxy- (~840 nm) and -deoxyhemoglobin (~757 nm) in blood are presented and the prospects of it application in scientific & diagnostic tomography.

Cr:LiCAF crystals (c = 3 at.%) were synthesized in Kazan Federal University by the Bridgman technique in graphite crucibles in a fluorinating atmosphere under exceeded argon pressure (P = 1500 GPa). Increase of the concentration of Cr^{3+} ions up to 3 at.% slightly decreased the lifetime of the upper laser level (at about ~165 μs), but allowed to increase the efficiency of absorption of pump lamp radiation. The laser elements were cylinders 4 and 8 mm in diameter for laser oscillator and power amplifier, respectively, and 90 mm in length with the optical axis of the crystal oriented perpendicular to the cylinder's formant. Such geometry allows generating π-polarized laser radiation corresponding to the maximum gain. The working surfaces of the active elements were polished and parallel to each other with an error of less than 10". No any antireflection coating was applied.

A lamp-pumped laser system consisting of a Q-switched oscillator and a double-pass amplifier (MOPA) was realized. Two-lamp cavities with diffuse reflectors and with "high density packing" of active elements and pump lamps were used. A specially designed laser resonator consisting of dielectric mirrors with high reflection coefficient and 2 m radius of curvature, a flat output mirror, a polarizer, apertures and an electro-optic modulator allows alternately generating laser pulses with a duration of ~45–50 ns at wavelengths ~757 and ~840 nm. The programmable system from Tomovave Laser LLC (Russia) provided independent energy setting for each pumping act (up to 250 J @ 180 μs) in order to equalize the laser intensity at these wavelengths. The MOPA-laser operates at a pulse repetition rate of 10 Hz with an output pulse energy of up to 300 mJ.

Taking into account the limitations associated with physiological movements and other features of the patient's tissues, the duration of laser pulses and their energy allow molecular and functional high-contrast visualization to a depth of up to 5–7 cm with a spatial resolution not worse than 1 mm. The modularity and flexibility of the developed system allows the possibility of varying the wavelengths of laser generation within 750–890 nm spectral range, multiple scaling of output characteristics, as well as the use of amplifiers based on Cr:LiCAF crystals for improvement of existing optoacoustic medical diagnostic systems.

[1] S. Manohar, D. Razansky, Adv. Opt. Photon., 8, 586–617 (2016).
[2] A.A. Oraevsky, A.A. Karabutov, S.V. Solomatin, E.V. Savateeva, V.A. Andreev, Z. Gatalica, H. Singh, R. D. Fleming, SPIE Proc., 4256, (2001).
[3] A.A. Shavelev, A.A. Shakirov, E.V. Lukinova, R.D. Aglyamov, A.K. Naumov, V.V. Semashko, A.S. Nizamutdinov, P.A. Palianov, Y.N. Panchenko, S.M. Bobrovnikov, SPIE Proc., 11322, 113221L

Synthesis, structure and luminescent properties of glass-ceramics based on the $PbCl_2$-TeO_2 system doped with Dy^{3+}, Ho^{3+}, and Er^{3+} ions

A. Bakaeva[1], D. Butenkov[1,2], P. Strekalov[1], N. Simonenko[2], P. Loiko[3], O. Petrova[1]

1- D. Mendeleev University of Chemical Technology, Miusskaya sq. 9, Moscow, 125047 Russia
2- N. S. Kurnakov Institute of General and Inorganic Chemistry RAS, Leninsky Prospekt 31, Moscow, 119991 Russia
3- Centre de Recherche sur les Ions, les Matériaux et la Photonique (CIMAP), UMR 6252 CEA-CNRS-ENSICAEN, Université de Caen Normandie, 6 Boulevard Maréchal Juin, Caen Cedex 4, 14050 France

e-mail: bakaevanna@mail.ru

Crystalline lead chloride exhibits attractive spectral-luminescent properties, including a wide transparency spectral window (0.3–20 μm) and a low phonon energy value (up to 180 cm^{-1}) [1, 2]. However, it has several significant disadvantages, such as hygroscopicity and weak mechanical properties, which limit its application as a material for infrared (IR) technologies. These drawbacks can potentially be mitigated by developing glass-crystalline materials based on oxychloride lead glasses. In this context, the oxide glass phase containing $PbCl_2$ crystallites can protect the $PbCl_2$ phase from aggressive environmental influences. Glass-ceramics can combine the advantageous characteristics of crystalline $PbCl_2$ and the oxide glass phase. However, to date, there is no available information on the preparation of glass-ceramics that incorporate a crystalline lead chloride phase [3, 4].

This study presents glass-ceramic samples produced through the thermal treatment of glasses in the $x$$PbCl_2$-(100-$x$-$y$)$TeO_2$-y$REF_3$ system, where x varied from 10 to 50 mol% and y was set at 0 mol% or 1 mol% for Dy^{3+} and Ho^{3+}, and 2 mol% for Er^{3+}. The identification of the crystalline phases in these samples was conducted using X-ray phase analysis and Raman spectroscopy. First, the crystallization of undoped glass compositions under various heat treatment conditions was investigated. Under specific conditions, the desired $PbCl_2$ crystalline phase was successfully obtained in some of the samples. The lattice parameters of $PbCl_2$ calculated for the glass-ceramics show slight variations from the reference values. This discrepancy can be attributed to the influence of the residual glassy phase and the small size of the crystallites.

Further, glass-ceramic samples doped with Dy^{3+}, Ho^{3+}, and Er^{3+} were produced under identical heat treatment conditions. These glass-ceramic samples were also analyzed using X-ray diffraction (XRD) and Raman spectroscopy. The impact of crystallization on the luminescence of Dy^{3+}, Ho^{3+}, and Er^{3+} ions was examined through luminescence spectroscopy; concurrently, the excited state lifetimes of these rare-earth ions were measured.

Research was done using equipment of «Research Chemical and Analytical Center NRC «Kurchatov Institute» Shared Research Facilities.

[1] Brown E., Hömmerich U., Bluiett A.G., Trivedi S.B., Zavada J.M., Synthesis and spectroscopic properties of neodymium doped lead chloride, Journal of Applied Physics, vol. 101, p. 113103 (2007).
[2] T.T. Basiev, Y.K. Danileiko, L.N. Dmitruk, B.I. Galagan et al., The purification, crystal growth, and spectral-luminescent properties of PbCl2:RE, Optical Materials, vol. 25, pp. 295–299 (2004).
[3] J. Pisarska, R. Lisiecki, G. Dominiak-Dzik, W. Ryba-Romanowski et al., Influence of PbX_2 (X = F, Cl, Br) content and thermal treatment on structure and optical properties of lead borate glasses doped with rare earth ions, Optica Applicata, vol. 40, pp. 351–358 (2010).
[4] S.A. Avanesov, M.I. Vatlina, B.V. Ignatiev, V.A. Isaev, A.V. Lebedev et al., Luminescence of Er^{3+} ions in germanate based lead-fluoride-chlorine glasses and glass-ceramics, Ecological Bulletin of Research Centers of the BSEC, pp. 5–13 (2007).

Change in EPR of arsenic selenide as a result of irradiation

A. G. Berezovsky[2], S. M. Dubrovskikh[2], V. V Karzanov[3], A. N. Kachemtsev[1], A. A. Konovalov[2], I. V. Skripachev[1], M. F. Churbanov[1]

1- «G. G. Devyatykh Institute of Chemistry of High-Purity Substances of RAS», Tropinina str. 49, Nizhny Novgorod, 603951 Russia
2- «RFNC-VNIITF named after academician E. I. Zababakhin», Vasilyeva str. 13, Snezhinsk, Chelyabinsk region, 456770 Russia
3- «Lobachevsky National Research Nizhny Novgorod State University», Gagarina pr. 23, Nizhny Novgorod, 603022 Russia

e-mail: kachemcev@ihps-nnov.ru

Glassy arsenic selenide has a number of unique properties that make it possible to use this material in various fields, including fiber optics. Obtaining waveguides from arsenic selenide with extremely low losses is complicated by the polyvalence of chalcogens. One of the possible options for controlling the properties of non-crystalline semiconductor materials is irradiation by high-energy particles, for example, gamma rays. The electron paramagnetic resonance (EPR) spectroscopy method is widely used to determine the nature of defects or complexes of defects in a semiconductor. The EPR spectrum of arsenic sulfides and selenides has been studied in a number of papers, for example, [1]. The change in the EPR of arsenic sulfide and selenide as a result of irradiation is considered in [2]. The results obtained earlier mainly relate to samples in the form of films formed on substrates by various methods. The fiber is drown by the crucible method from bulk ingots of arsenic selenide. The aim of the work was to study possible ways to increase the transparency of arsenic selenide in the near and middle infrared range by changing the near and middle order in the glass structure [1].

To conduct the experiments, samples of especially pure arsenic selenide of various chemical compositions with a deviation from the stoichiometric formula As_2Se_3 in both directions were produced at the IHPS RAS. The glasses were obtained by quenching from a melt of arsenic selenide of a given weight ratio: 42% arsenic – 58% selenium; 40% arsenic – 60% selenium and 36% arsenic – 64% selenium. Precursors having a purity level of at least 5N were further purified by distillation methods. The required amount of substances was loaded into an ampoule made of high-purity quartz glass with a minimum content of OH^--groups. Glass synthesis was carried out at a temperature of 750 °C in a rocking furnace, followed by annealing at a temperature close to the glass transition temperature Tg. Three arsenic selenide samples in the form of rectangular parallelepipeds of identical sizes were made from the ingots obtained. The surface contamination of the samples was removed by etching in a weak hydrochloric acid solution.

The EPR spectra of arsenic selenide samples were taken at room temperature using an automated Bruker EMX+ spectrometer. To improve the signal-to-noise ratio, multiple magnetic field scans were used, followed by computer averaging of the measurement results. The EPR was calculated taking into account the Q-factor of the resonator, and the background signal was subtracted. The EPR spectra were measured in the range of magnetic field strength from 1.500 to 4.500 Gs.

The samples were irradiated under normal conditions at an isotope source of ^{60}Co for several months. During the experiment, the samples were placed in a glass ampoule filled with nitrogen. The absorbed dose level of gamma radiation was 0.91 MGr (91 Mrad).

After the end of the irradiation, the EPR spectrum was measured again under conditions similar to the previous measurement. The EPR spectra of three arsenic selenide samples of different chemical compositions were compared before and after radiation exposure. It is shown that deviations from the stoichiometric composition of arsenic selenide significantly affect the EPR of irradiated samples.

The study was supported by the Russian Science Foundation, RSF grant No. 22-13-00226-П.

[1] I.D. Likholit, V.M. Lyubin, V.F. Masterov, V.A. Fedorov, Study of photostructural transformations in As_2S_3 films by photoinduced paramagnetic resonance method, Physics of the Solid State, vol. 26, № 1, pp. 172–178 (1984).
[2] A.O. Matkovsky, K.K. Schwartz, F.V. Pirogov, O.I. Shpotyuk, I.V. Savitsky Radiation and photostimulated processes in glassy arsenic trisulfide and triselenide (Academy of Sciences of the Latvian SSR, Institute of Physics, Salaspils), LAFI – 142 Preprint, (1988).

Cadmium doping in $CsPbBr_3$ nanocrystals: a route to lower ASE thresholds

O. Burdulenko[1], D. Gets[1], L. Zelenkov[1,2]

1- School of Physics and Engineering, ITMO University, Saint Petersburg, Russia
2 - Faculty of Physics and Optoelectronic Engineering, Harbin Engineering University, Harbin, Heilongjiang, People's Republic of China

e-mail: dmitry.gets@metalab.ifmo.ru

Lead-halide perovskites have been recognized as promising materials for next-generation optoelectronic applications due to their high photoluminescence quantum yield, broad absorption spectrum, and direct bandgap [1–4].

Among various fabrication approaches, nanocrystal-based perovskite films are especially attractive due to their facile synthesis, high packing density, and capability to exhibit amplified spontaneous emission (ASE) under pulsed excitation – the first step toward a practical laser gain medium [5].

Yet it is the defect structure that ultimately governs both efficiency and long-term stability [6]. Theory and experiment reveal that even in so-called "defect-tolerant" perovskites a broad spectrum of point and extended defects – including halide and lead vacancies, Schottky pairs and grain-boundary dislocations – introduce trap that accelerate non-radiative recombination, intensify the Auger process that dominates under strong optical pumping and over time drive photo-induced degradation. The result is a significant rise in ASE thresholds and a shortened operational lifetime of laser and LED devices. Strategies such as chemical doping [7] which tunes the electronic structure and surface passivation with suitable ligands [8, 9] or additives can partly offset these limitations by lowering trap densities, slowing carrier recombination and improving mobility thereby restoring the material's attractive optoelectronic properties.

In this study, lecithin-coated $CsPbBr_3$ nanocrystals were synthesized using a hot-injection method and doped with cadmium ions at varying concentrations (0.05, 0.1, 0.15, 0.2, 0.25 molar fraction). Cadmium incorporation was found to alter the recombination dynamics and enhance carrier mobility by passivating surface and lattice defects. Optical characterization confirmed that Cd^{2+} doping leads to modified photoluminescence quantum yields, prolonged emission lifetimes, and notably reduced ASE thresholds.

[1] L. Protesescu, S. Yakunin, M. I. Bodnarchuk, F. Krieg, R. Caputo, C. H. Hendon, R. X. Yang, A. Walsh, and M. V. Kovalenko, Nanocrystals of cesium lead halide perovskites ($CsPbX_3$, X = Cl, Br, and I): novel optoelectronic materials showing bright emission with wide color gamut, Nano Letters, vol. 15, pp. 3692–3696, (2015).
[2] R. Chen, Z. Liang, W. Feng, X. Hu, and A. Hao, Solution-processed all-inorganic perovskite $CsPbBr_3$ thin films for optoelectronic application, Journal of Alloys and Compounds, vol. 864, p. 158125, (2021).
[3] B. R. Sutherland and E. H. Sargent, Perovskite photonic sources, Nature Photonics, vol. 10, pp. 295–302, (2016).
[4] L. Chouhan, S. Ghimire, C. Subrahmanyam, T. Miyasaka, and V. Biju, Synthesis, optoelectronic properties and applications of halide perovskites, Chemical Society Reviews, vol. 49, pp. 2869–2885, (2020).
[5] L. Lei, Q. Dong, K. Gundogdu, and F. So, Metal halide perovskites for laser applications, Advanced Functional Materials, vol. 31, p. 2010144, (2021).
[6] J. Ye, M. M. Byranvand, C. O. Martínez, R. L. Hoye, M. Saliba, and L. Polavarapu, Defect passivation in lead-halide perovskite nanocrystals and thin films: toward efficient LEDs and solar cells, Angewandte Chemie, vol. 133, pp. 21804–21828, (2021).
[7] Y. Zhang, D. Tu, L. Wang, C. Li, Y. Liu, and X. Chen, Transition metal ion-doped cesium lead halide perovskite nanocrystals: doping strategies and luminescence design, Materials Chemistry Frontiers, vol. 8, pp. 192–209, (2024).
[8] S. Milanese, M. L. De Giorgi, G. Morello, M. I. Bodnarchuk, and M. Anni, Role of the capping ligand in $CsPbBr_3$ nanocrystals amplified spontaneous emission properties, ACS Applied Nano Materials, vol. 8, pp. 3964–3973, (2025).
[9] F. Krieg, Q. K. Ong, M. Burian, G. Raino, D. Naumenko, H. Amenitsch, A. Süess, M. J. Grotevent, F. Krumeich, M. I. Bodnarchuk, I. Shorubalko, F. Stellacci, and M. V. Kovalenko, Stable ultraconcentrated and ultradilute colloids of $CsPbX_3$ (X = Cl, Br) nanocrystals using natural lecithin as a capping ligand, Journal of the American Chemical Society, vol. 141, pp. 19839–19849, (2019).

Optical spectroscopy of oxychloride lead tellurite glasses doped with Tm^{3+}, Er^{3+} and Ho^{3+} ions

D. Butenkov[1,2], A. Vasilenkova[2], A. Bakaeva[2], K. Runina[2], P. Strekalov[2], K. Veselský[3,4], P. Loiko[3], A. Braud[3], M. Brekhovskikh[1], O. Petrova[2]

1- N. S. Kurnakov Institute of General and Inorganic Chemistry RAS, Leninsky prospekt 31, Moscow, 119991 Russia
2- D. Mendeleev University of Chemical Technology, Miusskaya sq. 9, Moscow, 125047 Russia
3- Centre de Recherche sur les Ions, les Matériaux et la Photonique (CIMAP), UMR 6252 CEA-CNRS-ENSICAEN, Université de Caen Normandie, 6 Boulevard Maréchal Juin, Caen Cedex 4, 14050 France
4- Faculty of Nuclear Sciences and Physical Engineering, Czech Technical University in Prague, Břehová 7, Prague, 11519 Czech Republic

e-mail: dabutenkov@gmail.com

Tellurium dioxide-based glasses are attracting attention due to the wide variability in their compositions and properties. The advantages of these glasses include chemical resistance, thermal stability, relatively low phonon energies (about 800 cm^{-1}), and broad transmission ranges [1]. The introduction of heavy metal oxides and halides Me_xX_y (where Me = Zn, Cd, Sb, Pb, Bi, and X = F, Cl, Br and I) into the glass composition enhances transparency in both the UV and IR spectral ranges, as well as improves the luminescence efficiency of rare-earth activators [2]. While oxide and oxyfluoride systems have been extensively studied laser gain media, oxychloride systems remain relatively underexplored [3].

We report on the synthesis, thermal, vibrational, and spectral-luminescent properties of novel $PbCl_2$-TeO_2 oxychloride glasses doped with rare-earth ions (Tm^{3+}, Er^{3+}, and Ho^{3+}) up to 2 mol% with the goal of developing low-phonon-energy active materials for the short-wave infrared. These glasses are obtained by melt-quenching technique at a relatively low temperature of 800 °C. As host matrices, these glasses exhibit good thermal stability (ΔT = 63 °C), broadband transparency (0.35–6.20 μm), prominent Raman peaks at 90–180 cm^{-1} attributed to Pb-Cl vibrations (Fig. 1a). The broadband luminescence of the dopant ions is observed in the spectral range of 2 to 3 μm (Fig. 1b).

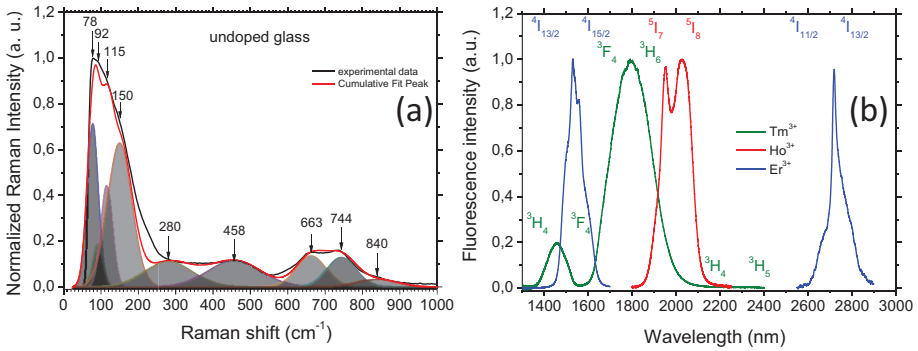

Fig. 1. Properties of $PbCl_2$-TeO_2 glasses: (a) Raman spectrum; (b) Fluorescence spectra of Tm^{3+}, Er^{3+}, and Ho^{3+} doped $PbCl_2$-TeO_2 oxychloride glasses in the short-wave infrared.

The luminescence lifetimes of the excited states responsible for these emissions are exceptionally long among TeO_2-based oxide and oxyhalide glasses, paving the way for potential applications of these glasses in fiber lasers and amplifiers.

This work was supported by the Ministry of Science and Higher Education of the Russian Federation as part of the State Assignment of Kurnakov Institute of General and Inorganic Chemistry of the Russian Academy of Sciences.

[1] F. Désévédavy, C. Strutynski, A. Lemière, P. Mathey, G. Gadret, J. Jules, B. Kibler, F. Smektala, Review of tellurite glasses purification issues for mid-IR optical fiber applications, J. Am. Ceram. Soc., Vol. 103, pp. 4017–4034 (2020).
[2] A. Sennaroglu, A. Kurt, G. Özen, Effect of cross relaxation on the 1470 and 1800 nm emissions in Tm^{3+}:TeO–$CdCl_2$ glass, J. Phys.: Condens. Matter, Vol. 16, pp. 2471–2478 (2004).
[3] P. Kostka, J. Zavadil, J. Pedlikova, M. Poulain, Preparation and optical characterization of $PbCl_2$–Sb_2O_3–TeO_2 glasses doped with rare earth elements, Physica Status Solidi (a), Vol. 208, pp. 1821–1826 (2011).

Van der Waals epitaxial growth of AlN nanowires on h-BN

A. M. Dautov[1,2], T. Shugabaev[2], K. P. Kotlyar[2], A. Kuznetsov [3], G. E. Cirlin[2], A. D. Bolshakov[3], V. O. Gridchin[1,2]

1- Faculty of Physics, St. Petersburg State University, Universitetskaya Embankment 13B, St. Petersburg, 199034 Russia
2- Laboratory of epitaxial nanotechnologies, Alferov University, Khlopina 8/3, St. Petersburg, 194021 Russia
3- Moscow Centre for Advanced Studies, Kulakova 20, building 1, Moscow, 123592 Russia

e-mail: amdautov24@gmail.com

Currently, one of the key research areas involves the epitaxial synthesis of semiconductors structures on two-dimensional (2D) materials – van der Waals (vdW) epitaxy. Notably, 2D materials can serve as platforms for integrating optoelectronic devices with silicon-based electronics. In addition, the absence of dangling bonds on 2D surfaces prevents the formation of mismatch dislocations in heterostructures grown on these 2D materials. Hexagonal boron nitride (h-BN) substrates are among the most promising substrates for growing III-N-based semiconductor structures. Despite its wide bandgap, h-BN's potential for effective p-type conductivity makes it a compelling material for applications in ultraviolet (UV) radiation sources, particularly in AlN/h-BN heterostructures [1]. It should be noted highly promising application of nanowires (NWs) structures based on III-N semiconductors, particularly AlN grown on h-BN. The near-perfect crystalline quality of NWs, combined with the absence of lattice-mismatch dislocations between h-BN and III-N materials, enables the fabrication of highly efficient semiconductor heterostructures. However, to the best of our knowledge, the growth of AlN nanowires on two-dimensional h-BN structures has not been reported previously. This work presents, for the first time, experimental results on the formation processes and properties of AlN NWs grown on two-dimensional h-BN flakes.

The NWs growth was performed using plasma-assisted molecular beam epitaxy (PA-MBE) in a Riber Compact 12 system (France) onto h-BN flakes. Monocrystalline h-BN flakes were mechanically exfoliated onto a silicon substrate coated with a 50 nm thick SiO_x layer. A series of growth experiments was conducted at different substrate temperatures. The structural properties of the samples were characterized using a Zeiss SUPRA 25 scanning electron microscope (SEM) and a Horiba Jobin-Yvon LabRAM HR 800 Raman spectrometer.

An array of NWs with an average height of ~260 nm and diameter ~60 nm was formed in all samples. The grown NWs exhibit a high surface density of approximately 1.2×10^{10} cm^{-2}. Plane-view (SEM) observations of the NWs reveal hexagonal morphology at the nanocrystalls top. It is noteworthy that partial NWs coalescence into continuous walls is also evident in certain regions. The resulting coalesced walls exhibit lengths ranging from 10 to 15 μm. Typically, such growth behavior is attributed to local variations in the III/V material ratio near step edges due to an increased group-III flux.

Raman spectroscopy analysis of the NWs revealed characteristic peaks at 656 cm^{-1} and 1.365 cm^{-1}, corresponding to AlN and h-BN, respectively [2]. The full width at half maximum of 5.1 cm^{-1} of AlN peak indicates exceptionally high crystalline quality in the examined AlN structure.

In this work, we have developed a growth technology for AlN/h-BN nanowires and characterized the structural quality of the resulting AlN NWs. The results of this work expand the possibilities for fabricating functional heterostructures based on AlN NWs, while also demonstrating significant potential for silicon-based optoelectronic applications. The experimental findings highlight the potential of h-BN as a substrate for vdW epitaxy of III-N semiconductors.

The work was carried out with the support of the St. Petersburg State University for a research project No. 129360164.

A. K. thanks the Ministry of Science and Higher Education of the Russian Federation (project FSMG-2025-0005) for support of nanostructures optical characterization.

[1] Laleyan D. Molecular Beam Epitaxy of Wide Bandgap Al (Ga) N and h-BN for Deep-Ultraviolet Optoelectronics : дис. -2020.
[2] Lughi V., Clarke D. R. Defect and stress characterization of AlN films by Raman spectroscopy //Applied physics letters. -2006. -Т. 89. -№.24.

Measurement of the optical absorption coefficient of lithium-sodium molybdate crystal at a wavelength of 1064 nm

D. Yu. Demushkin[1], D. A. Denisov[1], A. V. Konyashkin[2]

1- Moscow Institute of Physics and Technology, Institutsky lane, 9, Dolgoprudny, 141701 Russia
2- Fryazino branch of the Kotelnikov Institute of Radioengineering and Electronics of RAS, Vvedensky pass. 1, Fryazino, 141190 Russia

e-mail: demushkin.diu@phystech.edu

Lithium-sodium molybdate $LiNa_5Mo_9O_{30}$ (LNM) is a fairly new nonlinear-optical crystal. This material is transparent in 0.36–5.26 μm wavelength range, it has high laser damage threshold 2.64 GW/cm^2 (at 1064 nm wavelength, 10 ns pulses, 1 Hz repetition rate), high birefringence ($\Delta n = 0.1932$ at 1014 nm wavelength) and nonlinear optical coefficients $d_{31} = 1.4$ pm/V, $d_{32} = 4.3$ pm/V, $d_{33} = 1.1$ pm/V [1]. As follows, LNM crystals are good candidates for the fabrication of the polarization prisms with high radiation strength [2].

In this work, the value of the optical absorption coefficient α of the LNM crystal (3.0 × 3.3 × 9.0 mm^3) was measured by the piezoelectric resonance laser calorimetry (PRLC) method [3]. As a radiation source, CW linearly polarized fiber laser operating at 1064 nm wavelength with the beam quality parameter $M^2 = 1.05$ was used. The polarization was perpendicular to the crystallographic axis b, the beam waist diameter was 30 μm.

It is shown that in the power range of 15–60 W the coefficient α remains constant, and its average value is $(2.0 \pm 0.1) \times 10^{-3}$ cm^{-1} (see Fig. 1).

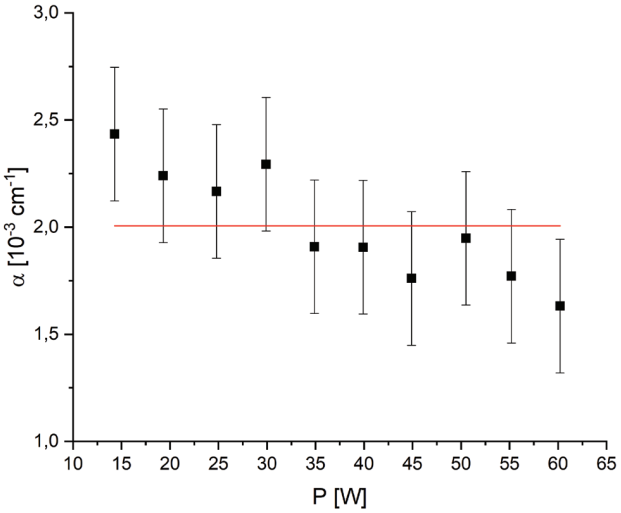

Fig. 1. Dependence of the optical absorption coefficient of the LNM crystal on the laser radiation power at 1064 nm wavelength.

The work was carried out within the framework of the state task of the Kotelnikov Institute of Radioengineering and Electronic of RAS.

[1] W. Zhang et al., LiNa5Mo9O30: Crystal growth, linear, and nonlinear optical properties, Chemistry of Materials, vol. 28(12), pp. 4483–4491, (2016).
[2] X. Du et al., High laser damage threshold LiNa5Mo9O30 prism: for visible to mid-infrared range, Chinese Optics Letters, vol. 20(5), p. 051602, (2022).
[3] O.A. Ryabushkin et al., Piezoelectric resonance calorimetry of nonlinear-optical crystals under laser irradiation, Photonic Fiber and Crystal Devices: Advances in Materials and Innovations in Device Applications VII, vol. 8847, pp. 141–149, (2013).

The growth and study of Yb^{3+} $MgMoO_4$ potential laser crystal

Y. S. Didenko[1,2], K. A. Subbotin[1,2], A. I. Titov[1], D. A. Lis[1], Y. I. Zimina[1,2], L. D. Iskhakova[1]

1- Prokhorov General Physics Institute of Russian Academy of Sciences, Vavilova st. 38, Moscow, 119991 Russia
2- Mendeleev University of Chemical Technology of Russia, Miusskaya sq. 9, Moscow, 125049 Russia

e-mail: ia.didenko@yandex.ru

Monoclinic magnesium monotungstate crystal $MgWO_4$ [1–4] has been identified as interesting laser host matrices for doping with rare-earth ions (RE^{3+}), in particular, for broadly tunable and femtosecond mode-locked solid-state lasers. This crystal has high thermal conductivity, strong birefringence, intense absorption and emission bands of RE^{3+} ions for polarized light, strong crystal fields resulting in large Stark splitting of RE^{3+} manifolds. $MgWO_4$ melts incongruently, and, consequently, it is grown from the flux [4] resulting in relatively small crystals and tolerated optical quality. There exists its monomolybdate counterpart, $MgMoO_4$ [5–6] which melts congruently and can be grown from the melt.

Yb^{3+}:$MgMoO_4$ crystal was grown by the Czochralski method. The Yb^{3+} concentration in the starting melt for Yb:$MgMoO_4$ growth was set to 7 at.% (considering the substitution of Mg^{2+} ions). The actual Yb^{3+} doping level in the crystal was determined to be 0.2 at.%. The structure was refined by the Rietveld method, and it was confirmed that the crystal belongs to the monoclinic class (sp. gr. *C*2/*m*, lattice constants: a = 10.276(9)Å, b = 9.289(6)Å, c = 7.027(6)Å and β = 106.903(8)°). The segregation coefficient Yb^{3+} in this crystal (K_{Yb}) is about 0.029, which requires solutions to improve the efficiency of using the material. Polarized Raman spectra were measured, and an intense mode at 969 cm^{-1} corresponding to symmetric vibrations of valence bonds in $[MoO_4]^{2-}$ tetrahedra was detected. Spectroscopic studies of the crystal were performed. The studies have shown a wide absorption band with the main peak at 978 nm and relatively wide luminescence bands with the main peak at 1031 nm, and peak stimulated emission cross-section $\sigma_{SE} = 0.76\times10^{-20}$ cm^2. The luminescence decay kinetics is single-exponential with the lifetime of 0.63 ms at 300 K. Compared to Yb:$MgWO_4$ [1], Yb:$MgMoO_4$ crystal has better prospects for the application for ultrafast lasers around 1 μm because of wider and smooth luminescence band.

Low-temperature (12 K) spectroscopic studies indicate the multi-site behavior of Yb^{3+} ions in $MgMoO_4$. At least 8 nonequivalent optical centers were found that correspond to different charge compensation mechanisms of heterovalent substitution of Mg^{2+} by Yb^{3+}: ytterbium ions can be localized both in the regular Mg1 and Mg2 magnesium positions with non-local charge compensation, and as associates with various charge compensators, such as cationic vacancies, oxygen interstitials, and random impurities of alkaline ions. This polycentricity causes a strong inhomogeneous broadening of the spectra, which is useful for laser applications.

The introduction of additional dopants, such as Li^+, can increase the ytterbium distribution coefficient in the crystal and reduce the number of optical centers or change their relative concentrations. This study expands the understanding of the mechanisms of rare-earth doping in monoclinic crystals with the formula $M^{2+}XO_4$ (where M = Mg, Zn and X = W, Mo). The data obtained will make it possible to take the gain band of Yb^{3+} ions for generating pulses with a duration of less than 100 femtoseconds. Additional broadening of the absorption and luminescence bands can be promoted by the creation of "mixed" Yb:Mg(W,Mo)O_4 crystals.

[1] P. Loiko et al., Opt. Lett. 45, 1770–1773, (2020).
[2] L. Zhang et al., Opt. Mater. Express, 12, 2028–2040, (2022).
[3] L. Zhang et al., J. Lumin. 213, 316–325, (2019).
[4] L. Zhang et al., Opt. Express 25, 3682–3693, (2017).
[5] L. Li et al., PLoS One. 7, e30327, (2012).
[6] K. Subbotin et al., Opt. Mater. 138, 113648, (2023).

Spectroscopic properties of lithium aluminosilicate glass-ceramics nucleated by (Tm^{3+},Yb^{3+}):$YNbO_4$ nanocrystals

O. S. Dymshits[1,2], E. V. Vilejshikova[3], I. Alekseeva[2], S. Zapalova[2], M. Ya. Tsenter[2], A. A. Volokitina[1,2], A. M. Malyarevich[3], K. V. Yumashev[3], A. A. Zhilin[4]

1- Ioffe Institute, Russian Academy of Sciences, Politekhnicheskaya 26, St. Petersburg, 194021 Russia
2- S. I. Vavilov State Optical Institute, Babushkina st. 36, St. Petersburg, 192171 Russia
3- Belarusian National Technical University, Nezavisimosti ave. 65/17, Minsk, 220013 Belarus
4- D. V. Efremov Institute of Electrophysical Apparatus, Metallostroy, Doroga na Metallostroy, bld. 3, Saint Petersburg, 196641 Russia

e-mail: vodym1959@gmail.com

Transparent glass-ceramics of the lithium aluminosilicate (LAS) system nucleated by rare-earth orthoniobates are multiphase materials that contain two functional crystalline phases. The nucleating agent, yttrium orthoniobate, is a promising host for various trivalent rare-earth ions, while the main crystalline phase, β-quartz solid solutions, ensures near zero expansion of resultant glass-ceramics.

Recently we demonstrated [1] that glass-ceramics obtained by isothermal heat-treatments of glasses at 700–900 °C contain $YNbO_4$ nanocrystals with the distorted tetragonal structure, T'. In samples heated at 1000 °C and above, the monoclinic features are observed. The monoclinic M (S.G. *I2/a*) phase is formed at cooling the glass-ceramics after such heat-treatments, when $YNbO_4$ nanocrystals with tetragonal (S.G. $I4_1/a$) T structure undergo the second-order ferroelastic transition at ~550 °C. Optical properties of these glass-ceramics are directly linked to the structure of rare-earth orthoniobates, which changes from the defect tetragonal to the tetragonal, and then, to the monoclinic form with the increase of the temperature of the secondary heat-treatment.

For this study, the model glass of the composition (mol%) 18 Li_2O, 27 Al_2O_3, 55 SiO_2, was doped with 0.5 Tm_2O_3, 0.5 Yb_2O_3, 2.2 Y_2O_3, and 3.2 Nb_2O_5 (mol%) added above 100% as nucleating agents. The glass was melted in air at 1580 °C for 4 h with stirring, bubbled with oxygen for 0.5 h to remove the OH^- groups from the melt, cast onto a metal plate and annealed at 720 °C. The transparent glass was heat-treated in isothermal conditions from 720 to 1350 °C for 6 h by the two-stage heat-treatments with the first hold at 720 °C for 6 h.

Differential scanning calorimetry, X-ray diffraction analysis, Raman spectroscopy and optical spectroscopy were used to study structural and spectroscopic parameters of the glass and glass-ceramics. (Tm^{3+},Yb^{3+}):$YNbO_4$ nanocrystals with sizes increasing from ~7 to 25 nm appear and grow in glass with increasing the heat-treatment temperature. Their absorption, luminescence, and up-conversion luminescence spectra significantly change following the T' to T to M phase transition of the niobate phase. The main crystalline phase, β-quartz solid solutions appear during heat-treatment at 800 °C and converts to ß-spodumene solid solutions at 1100 °C.

The transparent glass-ceramics look promising for laser operation in the spectral range of ~2 μm, up- and down-conversion phosphors.

The work was supported by the Russian Science Foundation (Grant № 25-23-20131).

[1] O. Dymshits, A. Bachina, et al. Phase transformations upon formation of transparent lithium alumosilicate glass-ceramics nucleated by yttrium niobates. Ceramics, vol. 6, pp. 1490–1507 (2023).

Functional dielectric crystals and the specifics of their testing

N. Kozlova, E. Zabelina, V. Kasimova, V. Umylin, A. Korchagin

National University of Science and Technology «MISIS», Leninsky pr. 4, b. 1, Moscow, 119049 Russia

e-mail: kozlova_nina@mail.ru

Dielectric ion crystals are the most important materials for electronic and microelectronic technologies. Many crystalline dielectric materials have been tested for use as media for generation, control of the optical characteristics of systems, and for the electronic and microelectronic industries. However, only a few of them have found practical application. Characteristic features of crystals are the anisotropy and symmetry of physical properties due to the crystallographic regularity of their internal structure [1]. Formation of crystal structure strictly obeys the laws of crystallography [1, 2]. Among the 32 symmetry classes of crystal structures, 21 classes belong to the polar and polar-neutral classes, the rest belong to the nonpolar classes. And this already leads to a difference in properties, i.e. to anisotropy of properties due to the crystal structure, which can be observed visually without using research equipment, and assume which class of symmetry the crystal belongs to and which properties can be observed.

However, in the process of crystal growth occurs the following: growth defects, point growth defects, dislocations, uncontrolled impurities entering the crystal from the charge, the growing atmosphere and other environmental factors. All this disrupts the shape of the grown crystals, but the main property – anisotropy – remains. Additional careful research is required to understand this statement. In addition to the anisotropy of the structure in dielectric (ionic) crystals, non-obvious properties are observed, such as optical activity or gyrotropy, dichroism, birefringence. And in experimental studies we do not obtain reproducibility of the results with multiple measurements.

External influences even on crystals of nonpolar classes, such as temperature, radiation fields, mechanical influences, or the introduction of the dopants, especially in case of elements with a different oxidation state, can lead to a change in the properties of the crystals. These effects affect the change and deformation of the crystal structure, leading to the formation of structural defects, and thereby the properties of crystals. And not only on the properties of crystals, but also on the technology of obtaining crystals [4].

In the case of studies of electro-optical crystals, i.e. when additional exposure to electric fields is needed, this requires the application of conductive coatings on the surface of the samples. This introduces additional testing difficulties to obtain reliable results, foremost, the choice of the electrode conductive coating material and the choice of measurement schemes. It is known that the application of conductive coatings to the polar surfaces of sample immediately leads to electrochemical processes on the surfaces, and during temperature tests in the volume of crystals, additional scattering centers can be observed, i.e. to increase the concentration of point defects.

Our long-term research experience has allowed us to present the model of ionic dielectric crystals as an external structure based on the strict laws of crystallography, weakly subject to external influences, and numerous structural point defects that control the properties of crystals and can be exposed to external influences, thereby it is possible to adjust the properties of already grown crystals. Thus, the approach «structure – point defects of structure – properties – application of defects to control properties – correction of crystal production technology» works to study the physical parameters of dielectric crystals.

Studies were carried out in the accredited laboratory «Single crystals and stock on their base» NUST MISIS with financial support from the Ministry of Education and Science of Russia within the framework of the state assignment to universities FSME-2023-0003.

[1] M.P. Shaskolskaya, Crystallography (Moscow: Higher School), 1984.
[2] I.S. Zheludev Physics of crystalline dielectrics (Moscow: Nauka), 1968.
[3] A.A. Blistanov, Features of structural defects in ionic crystals (dielectrics), News of Higher educational institutions. Electronic equipment materials, vol. 4, pp. 4–15, (2005).
[4] N.S. Kozlova, E.V. Zabelina, V.M. Kasimova, Features of Testing and Monitoring Optical Qualities of Dielectric Single Crystals, Measurement Standards. Reference Materials, vol. 21, pp. 72–85, (2025).

Tailoring optical properties of huntite-like solid solutions

A. Kuznetsov[1], M. Rakhmanova[2], A. Jamous[1,3], A. Kokh[1]

1- Sobolev Institute of Geology and Mineralogy SB RAS, Novosibirsk, 630090 Russia
2- Nikolaev Institute of Inorganic Chemistry SB RAS, Novosibirsk, 630090 Russia
3- Tomsk State University, Tomsk, 634050 Russia

e-mail: ku.artemy@igm.nsc.ru

$RM_3(BO_3)_4$ (where R = Y, La-Lu, M = Al, Ga, Cr, Fe), classified as orthoborates, are recognized as excellent candidates for optical applications. These materials, referred to as huntites, are isotypic with the mineral $CaMg_3(CO_3)_4$, crystallizing in the *R*32 space group [1]. Within this family, aluminum-containing huntites are particularly promising for nonlinear optical, phosphor, and laser applications [2]. In comparison to RBO_3, these materials exhibit reduced concentration quenching of luminescence. Furthermore, they demonstrate chemical stability, mechanical strength, and significant thermal conductivity. $RAl_3(BO_3)_4$ is one of the most extensively studied crystals in this category, noted for several advantageous properties.

However, in contrast to the traditional exploration of simple compositions of $RM_3(BO_3)_4$, recent research has increasingly focused on more complex compositional strategies within this class of compounds. A substantial body of work has been dedicated to investigating scenarios where the R position is occupied by two or three different rare earth elements simultaneously, and/or where multiple atomic species (e.g., combinations of Al, Ga, Cr, or Fe) are present in the M position. A key advantage of such an approach to elementary substitutions is its ability to maintain the desired structural framework of huntite. Concurrently, these complex multi-element substitutions open up extensive opportunities for precise control or even the creation of entirely new functional properties in the material.

In the present study, the optical properties of $RM_3(BO_3)_4$ crystals (R = Y, La-Lu, M = Al, Ga, Sc), synthesized via the (TSSG), were evaluated. The investigation revealed a deviation from stoichiometric composition in the obtained crystals, presumably linked to gradual changes in the melt composition during crystallization. Experiments conducted on solid-state synthesis confirmed the potential for forming non-stoichiometry in all $RM_3(BO_3)_4$ compounds (R = Y, La-Lu, M = Al, Ga, Sc) [3, 4]. Structural analyses of the obtained crystals were performed using single-crystal and powder X-ray diffraction methods. The optical properties, specifically luminescence and second harmonic generation (SHG), were assessed employing standard luminescent spectroscopy and the Kurtz-Perry technique, respectively. The results of these comprehensive studies revealed that even minor structural distortions in the crystal lattice are attributed to the observed non-stoichiometry. The identified non-stoichiometry correlates with a decrease in the quantum yield of luminescence and a reduction in the efficiency of SHG, underscoring the critical importance of composition control for optimizing the optical functionality of these huntite-like solid solutions.

This work was supported by the RSF project (№ 23-19-00617).

[1]A.D. Mills, Crystallographic Data for New Rare Earth Borate Compounds, $RX_3(BO_3)_4$, Inorg Chem vol.1, pp. 960–961, (1962).
[2]N.I. Leonyuk, V. V. Maltsev, E.A. Volkova, O. V. Pilipenko, E. V. Koporulina, V.E. Kisel, N.A. Tolstik, S. V. Kurilchik, N. V. Kuleshov, Crystal growth and laser properties of new $RAl_3(BO_3)_4$ (R = Yb, Er) crystals, Opt Mater (Amst) vol.30, pp.161–163, (2007).
[3] Kuznetsov, A. B., Jamous, A. Y., Rakhmanova, M. I., Simonova, E. A., Svetlichnyi, V. A., Kokh, A. E., Yudin, V. N., Solodovnikov, S. F., Shevchenko, V. S., Kokh, K. A.: Nonstoichiometry as a hidden aspect of $TbAl_3(BO_3)_4$ optical properties. Dalton Transactions, 53(46), 18653–18661, (2024).
[4] Kokh, K. A., Jamous, A. Y., Svetlichny, V. A., Kuznetsov, A. B., Yelisseyev, A. P., Bogdanov, N. E., Goreyavcheva, A. A., Kokh, A. E.: Redistribution of rare-earth dopants (Eu, Dy, Ho, Er, Tm, Yb) in $LaSc_3(BO_3)_4$ structure and influence on optical properties. Optical Materials, 159, 116655, (2025).

KRS-5 optics production by diamond turning and milling

M. S. Kuznetsov, K. S. Zaramenskikh, A. V. Osipov, M. V. Morozov, S. M. Pilyushko, A. R. Korneeva

JSC «State Research and Design Institute of Rare Metal Industry «Giredmet» named after N. P. Sazhin, Moscow, 115524 Russia

e-mail: msekuznetsov@rosatom.ru

Crystals of thallium halides have uniform transparency over a very wide wavelength range, covering the visible and mid-IR spectral ranges from 0.35 μm to 50 μm (depending on the composition), 0.54 μm – 50 μm for KRS-5 (TlBr–TlI). Transmission is up to 70% in the absence of absorption bands. The combination of unique optical characteristics, chemical resistance and mechanical strength makes it possible to improve the properties of equipment in comparison with existing analogues in the range up to 10 μm, as well as to create devices operating in the range from 10 to 50 microns that have no analogues when using KRS-5 crystals.

The main problem is the complicacy in optical processing of thallium halide crystals due to the material's softness and plasticity, high coefficient of thermal expansion, low thermal conductivity, and significant anisotropy. Traditional processing technologies lead to the formation of a deep damaged layer in the crystal structure during grinding and low yield during final finishing of the optical surface by manual polishing.

As an alternative method, diamond tool processing on ultra-precision machine tools has been proposed, which avoids the formation of significant damaged layers, embedding of abrasive particles on the processed surface, and high processing temperatures.

A methodology for processing KRS-5 (TlBr–TlI) crystals by diamond turning and milling has been developed and implemented, consisting of two stages: determining the optimal orientation of the workpiece during milling, at which no brittle fracture is observed; and processing the workpiece with proper orientation. The conducted studies have made it possible to understand the features of processing and the physics of the cutting process of KRS-5 crystals, revealing that shape accuracy is related to the anisotropy of KRS-5 crystals, variations in hardness in different directions, and unequal cutting conditions.

The processing technology has been optimized, and cutting parameters have been selected to achieve surface accuracy and quality parameters ($N = 0.6$ μm, $\Delta N = 0.5$ μm, $Ra = 0.01$ μm) sufficient for standard optical products, such as windows, beamsplitters, etc. The proposed method of processing KRS-5 crystals has increased the productivity of optical component manufacturing while ensuring the required accuracy and quality.

The authors express gratitude to the team of LLC "RPA Asferika" V. V. Lapshin and E. M. Zakharevich

Electronic properties of $CuInS_2$ compounds. Theory and experiment

I. A. Mamedova[1], I. Q. Qasimoglu[1], Z. A. Jahangirli[1,2], Kh. A. Hidiyev, S. S. Ragimov[1,2], T. G. Mammadov[1], N. A. Abdullayev[1,2]

1- Institute of Physics, Ministry of Science and Education of Azerbaijan, Baku, Azerbaijan
2- Baku State University, Baku, Azerbaijan

e-mail: irada_mamedova@yahoo.com

I–III–VI_2 compounds are ternary analogues of the well-known ZnS and CdS compounds. $CuInS_2$ crystallizes in a tetragonal chalcopyrite-type structure with a space group $I\bar{4}2d$. On the one hand, $CuInS_2$ crystals attract attention of researchers in view of their large birefringence; they are promising as non-linear optical materials [1]. At the same time, the band gap of $CuInS_2$ crystals makes it possible to use them as elements of efficient solar cells [2].

We have obtained and characterized by X-ray diffraction and Raman spectroscopy crystals of defective chalcopyrite $CuInS_2$. Ab initio calculations of electronic, including optical, properties were carried out on the basis of DFT using the method of full-potential linearized augmented plane waves (FP-LAPW) implemented in the Wien2k code. Spectral ellipsometry was used to experimentally study the optical characteristics of $CuInS_2$ semiconductor compounds [3]. The calculation results show that the dependences of the real part of the dielectric function on the energy Re ε(E) (Fig. 1a, curves 1 and 2) have a similar appearance with maxima at energies E ~ 0.9 eV and 2 eV. In this case, the values of the dielectric functions are almost identical. The dependences of the imaginary part of the dielectric function on the energy Im ε(E) (Fig. 1b, curves 1 and 2) also have a similar appearance with an inflection in the vicinity of ~ 1 eV and maxima at energies E ~ 2.2 eV and 2.8 eV, respectively.

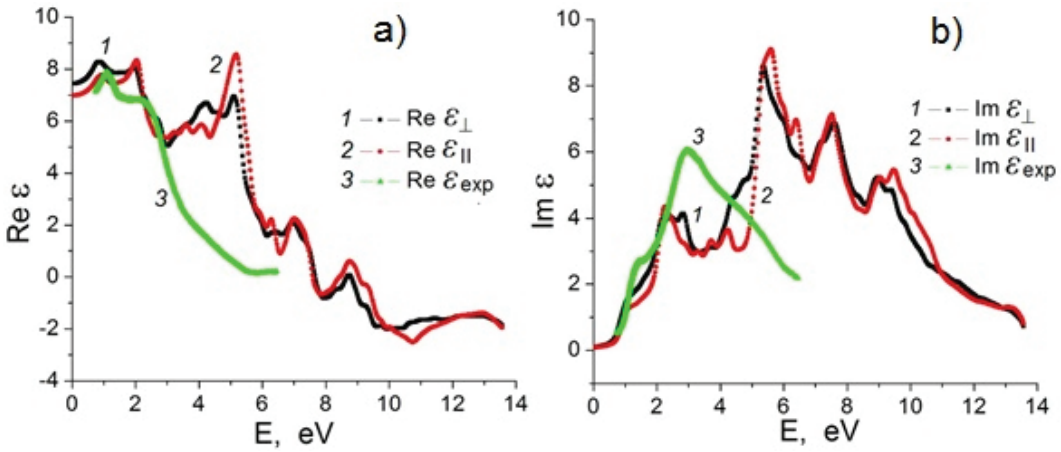

Fig. 1. Calculated and experimental real and imaginary parts of dielectric function of $CuInS_2$

The absorption coefficient α, refractive n and extinction k indices, band gap E_g were determined and calculated, the values of which are compared with the literature data.

The values of the nonlinear refractive index n_2, nonlinear susceptibilities of the first $\chi^{(1)}$ and third order $\chi^{(3)}$ were calculated and found to be equal to 3.1×10^{-10} esu, 0.61 esu, 2.4×10^{-11} esu, respectively.

[1] A. Reshak and S. Auluck, Electronic structure, linear, nonlinear optical susceptibilities and birefringence of $CuInX_2$ (X = S, Se, Te) chalcopyrite-structure compounds, *PMC Physics B* **1** No.12, (2008).
[2] M. Nakamura, K. Yamaguchi, Y. Kimoto, Y. Yasaki, T. Kato, and H. Sugimoto, Cd-Free Cu(In,Ga)$(Se,S)_2$ Thin-Film Solar Cell With Record Efficiency of 23.35%, *IEEE Journal of Photovoltaics* **9** (6), 1863–1867 (2019).
[3] Z. A. Jahangirli, I. Q. Qasimoglu, I. A. Mamedova, et al. Physics of Wave Phenomena, **33** (1), 36–45 (2025).

Study of As-Ge-Se and As-Ge-Te chalcogenide systems by the method of X-ray diffraction

S. I. Mekhtiyeva[1] , A. I. Isayev[1], H. I. Mammadova[1,2], R. I. Alekberov[1]

1- The Ministry of Science and Education of the Republic of Azerbaijan, Institute of Physics, G. Javid ave 131, Baku, AZ1073 Azerbaijan
2- Azerbaijan University of Architecture and Construction, Baku, Azerbaijan

e-mail: physics.humay@mail.ru

This work is devoted to the interpretation of the results obtained from the study of the local structure, topological and mechanical properties of the layers obtained on the basis of As-Ge-Se and As-Ge-Te chalcogenide systems by the method of X-ray diffraction. On the basis of X-ray diffraction experiments, the local structure parameters (quasiperiod and correlation length in the medium order region) of the As-Ge-Se glassy system were determined. Also, the dependence of physical parameters (density, packing coefficient, compactness, average value of atomic volume, number of unpaired electrons, cohesive energy) on average coordination number and parameter R, which determines the character of chemical bond between atoms, was determined. X-ray diffraction curves of As-Ge-Se and As-Ge-Te layers obtained by thermal evaporation in vacuum is shown in Fig. 1.

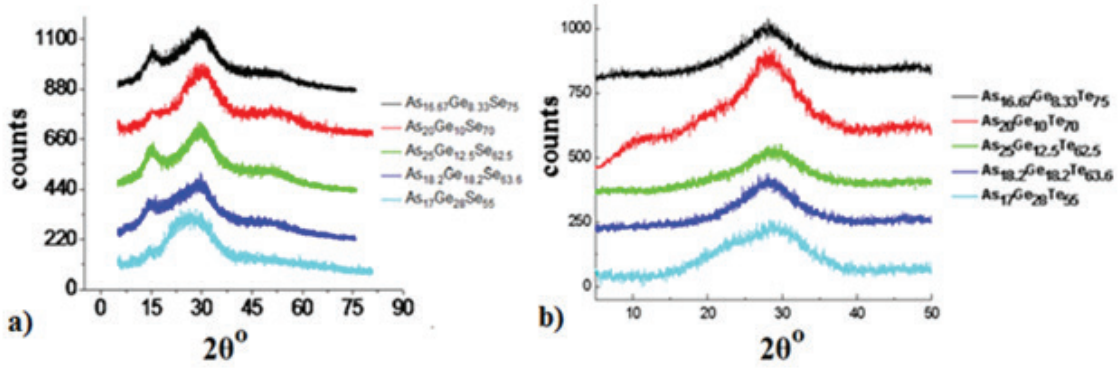

Fig 1. Intensity distribution in X-ray diffraction of As-Ge-Se (a) and As-Ge-Te (b) layers obtained by thermal evaporation in vacuum.

The wide maxima observed in the diffraction pattern prove the amorphous nature of the studied samples. In As-Ge-Se systems, the first sharp diffraction peak (FSDP), which differs from other diffraction peaks due to its anomalous dependence on temperature and pressure typical of most glassy substances, is observed in the X-ray diffraction scattering intensity distribution graph (Fig. 1a) [1, 2]. In the As-Ge-Te system, FSDP is observed only in layers with chemical composition $As_{20}Ge_{10}Te_{70}$ (Fig. 1b). Based on modern points of view about the local structure of non-crystalline substances, it can be concluded that the difference observed in the diffraction pattern of the studied objects is related to the difference in their local structure characteristics. In other words, the observation of FSDP in all studied chemical compositions of the As-Ge-Se system indicates the formation of an medium order range in them. In the As-Ge-Te system, the observation of FSDP in a layer with a chemical composition such as $As_{20}Ge_{10}Te_{70}$, which corresponds to the value of the average coordination number of 2.4, shows that the medium order range is formed only in that composition. Thus, this experimental fact indicates that the structure of the As-Ge-Te system has a higher degree of disorder. The observation of FSDP only in $As_{20}Ge_{10}Te_{70}$ can be explained by the formation of topological regularity (Z = 2,4) [3, 4].

[1] Elliott, S.R., Second sharp diffraction peak in the structure factor of binary covalent network glasses // Phys. Rev. B, 51(13), pp. 8599–8602 (1995).
[2] Lee, J.H., Simulation evidence for the origin of the first sharp diffraction peak / J.H. Lee, S.R. Elliott // Journal of Non-Crystalline Solids, 192-193, -pp. 133–136, (1995).
[3] Phillips, J.C., Topology of covalent non-crystalline solids I: Short-range order in chalcogenide alloys // Journal of Non-Crystalline Solids, 34, pp.153–181. (1979).
[4] Tich, L., / Covalent bond approach to the glass-transition temperature of chalcogenide glasses / L. Tich, H. Ticha // J. of Non-Crystalline Solids, 189(2), pp. 141–146, (1995).

The new view on the laser properties and abilities of the $LaF_3:Nd^{3+}$ crystals

A. K. Naumov[1,2], R. D. Aglyamov[1], S. L. Korableva[2], V. V. Semashko[1,2]

1- Kazan E. K. Zavoisky Physical -Technical Institute (KPhTI), Sibirsky tract 10/7, Kazan, 420029 Russia
2- Kazan Federal University, Kremlyovskaya str. 18, Kazan, 420008 Russia

e-mail: aglyam92@mail.ru

"Laser fever" associated with the search for new laser materials, which took place at the dawn of the development of quantum electronics, often led to publications obtained on insufficiently perfect crystalline samples with the presence of numerous structural defects and uncontrolled impurities. The situation was also aggravated by the fact that at that time for lamp-pumped laser tests it was necessary to synthesize crystals several centimeters long, which a-priori increased the probability of defect formation and affected their spectroscopic and laser properties. As a result, experimental data of different authors varied from each other and conclusions about the promising application of crystals of various chemical composition in quantum devices turned out to be erroneous. In particular, it appeared in the case of studies of crystals of trifluorides of rare-earth elements with tisonite structure (LaF_3, CeF_3, etc.) [1, 2], characterized by high crystallization temperatures and tendency to formation of microblock's structure. Modern opportunities of laser diode pumping allow us to revise the earlier conclusions by more careful studies of spectral-kinetic, polarization-dependent, and laser properties of these crystals.

The precise polarized absorption and luminescence spectra of the $LaF_3:Nd^{3+}$ with the doping level 0.5–10 at.% crystal were obtained in the wide spectral range (200–1100 nm) at room temperature and stark's structure of 4f-states of Nd^{3+} ions were clarified.

Unlike wide-band flash-lamp pumping the resonant diode pumping makes it possible to pump the $Nd:LaF_3$ crystals to the most favorable absorption bands at 788 and 796.6 nm by π-polarized beam or at 790.8 for σ-polarized one. It allows to avoid undesirable excitation of high-lying 4f-manifolfs of Nd^{3+} ions, decrease a heat release and leads to a lower lasing threshold and increased the total efficiency. The laser experiments in both π- and σ-orientations of the active elements relative to the resonator axis and the CW pumping beam were performed. The single wavelength laser action was observed at a wavelength of 1063.05 nm for the π-orientation and simultaneous multi-wavelength lasing at 1040, 1058.9, ~1062.5, 1064.5 and 1066.8 nm were realized for the σ-oriented active medium, respectively. It was also discovered that the multiwavelength lasing spectra were dependent on wavelength and polarization of the pumping. The CW output properties of the several $Nd:LaF_3$ active crystals with different orientations of the optical axis and the various diode-pumping conditions were studied and analyzed. The typical CW slope efficiency of the most of tested $Nd:LaF_3$ active crystals was above 12%. The impact of anisotropy, microdomain structure and Nd^{3+} ions content in the LaF_3 crystals to laser properties are discussed.

The obtained results prove the prospects of $Nd:LaF_3$ crystals application as active media and open the opportunity to design for the new compact multi-wavelength diode-pumped laser systems especially for THz radiation sources.

[1] E. Y. Wong, O. M. Stafsudd, D. R. Johnston, Optical absorption spectrum of Nd^{3+}-doped LaF_3 single crystal: The evidence of a hidden selection rule, Phys. Rev., v. 131, n. 3, pp. 990–993, (1963).
[2] C. K. Asawa, M. Robinson, Temperature-dependent concentration quenching of fluorescence by cross relaxation of Nd^{3+} in LaF_3, Phys. Rev., v. 141, n. 1 pp. 251–258, (1966).

Lead-gallate glasses doped with Tm^{3+}, Er^{3+} and Ho^{3+} ions for IR applications

O. B. Petrova[1], A. B. Terekhova[1], D. A. Butenkov[1,2], K. N. Boldyrev[3]

1- D. Mendeleev University of Chemical Technology, Miusskaya sq. 9, Moscow, 125047 Russia
2- N. S. Kurnakov Institute of General and Inorganic Chemistry RAS, Leninsky prospekt 31, Moscow, 119991 Russia
3- Institute of spectroscopy RAS, Fizicheskaya str. 5, Troitsk, Moscow, 108840 Russia

e-mail: petrova.o.b@muctr.ru

Oxide glasses containing heavy metals are characterized by high density, high refractive index, chemical resistance and good transmittance of radiation in the near and mid-infrared range. The listed characteristics are especially in demand in the creation of medical lasers, weapons homing systems, passive optics elements, as well as in many other areas of scientific research [1].

One of the promising objects of research is the PbO-Ga_2O_3 system. It is known that the system has a wide glass formation region with a high content of lead oxide, due to which the glasses are transparent up to 7 μm [2]. The purpose of the presented work was a systematic study of the spectral properties of glasses in the PbO-Ga_2O_3 system and the selection of the best matrix for doping with REs.

Synthesis of glasses was carried out according to the classical method of melt quenching. The melt was kept at 1100 ºC for 1 h and cast into steel molds. Synthesis was carried out in corundum crucibles with a covers, the weight of the batch was 50 g. PbO (99.99 wt.%, Chemkraft) and Ga_2O_3 (99.95 wt.%, Reachim) were used as starting reagents. The 50PbO-50Ga_2O_3 sample was completely crystallized, the crystalline phases of the initial oxides of orthorhombic PbO (*Pbma*) and monoclinic Ga_2O_3 (*C*2/*m*) were identified. The 60PbO-40Ga_2O_3 sample, despite its amorphous nature, turned out to be opaque, which is presumably the result of liquation. The sample containing 90 mol% lead oxide was obtained partially crystallized. The structure of the glasses was established by vibrational spectroscopy methods. The most optically successful compositions are 70PbO-30Ga_2O_3 and 80PbO-20Ga_2O_3: the transparency range was from 450–470 nm to 7470–7340 nm (Fig. 1a), refractive index n_d (λ = 588.6 nm) 2.197-2.245, Abbe number 14–13.5, density 7.286–7.504 g/cm^3, Vickers hardness 3.6–3.2 GPa, the glass transition temperature T_g was 421–383 °C, respectively.

70PbO-30Ga_2O_3 glass, which was chosen as the matrix for doping with Ho^{3+} (1 mol%), Tm^{3+} (2 mol%), and Er^{3+} (2 mol%). The glasses have a luminescence distribution within 2–3 μm (Fig. 1b).

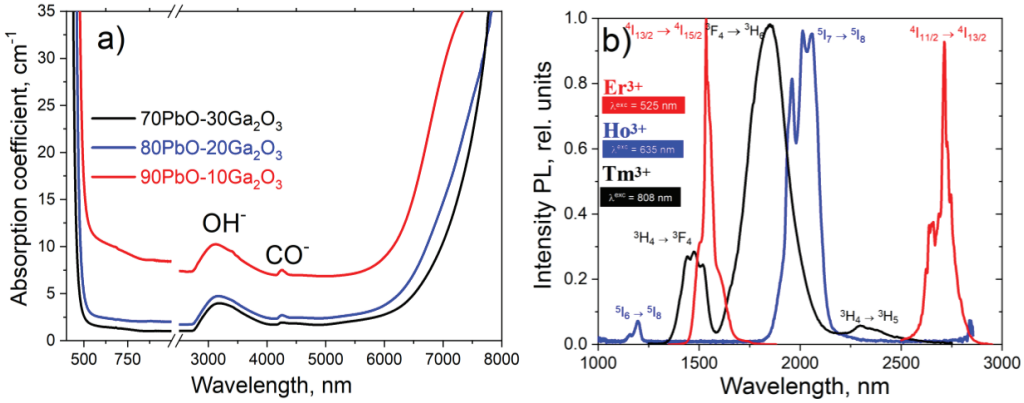

Fig. 1. Absorption spectra of undoped glasses (a); Fluorescence spectra of Er^{3+}, Tm^{3+} and Ho^{3+} doped PbO-Ga_2O_3 glasses in the infrared (b).

The values of the refractive indices and the running optical dispersion allow taking into account the glasses for superheavy flints, which in combination with the reduced phonon energy, the wide transmission range of the system makes it promising for applications as matrix materials for doping with rare earth ions, as well as in passive optics.

[1] Dumbaugh W.H., Lapp J.C., Heavy-Metal Oxide Glasses, J. of the Amer. Cer. Soc., v. 75, № 9, pp. 2315–2326 (1992).
[2] Shelby J.E., Lead Galliate Glasses, Am. Cer. Soc., v.71, №. 5, pp. 254–256 (1988).

Silver halide-based light guides for the IR range: preparation and investigation

S. Pilyushko, M. Kuznetsov, K. Zaramenskikh, A. Korneeva, G. Polyakova, L. Butvina

JSC «State Research and Design Institute of Rare Metal Industry «Giredmet», Moscow

e-mail: vorpat2402@bk.ru

The demand for power and wave optics in the mid- and far-infrared range continues to grow due to the constant development of such fields as space research, environmental monitoring, medical diagnostics and treatment of diseases (including dental), synthesis of organic and pharmaceutical substances [1].

Among crystalline materials, silver halides and their compounds are promising. They are transparent in the 10-micron region, poorly soluble, have a disinfecting effect, are safe for humans, have not only a wide spectral range of transmittance (from 2 to 20 microns), but also satisfactory strength properties and chemical stability [2]. The most important quality of silver halides that determines their application as a material for fiber optics is plasticity, which allows to produce light guides by extrusion of single crystal blanks [3].

In this work, 1.5 m and 2 m step-index optical fiber samples were manufactured by extrusion from a single-crystal composite blank. The blank was machined on an ultra-precision lathe using diamond quasi-plastic turning to obtain contact surfaces of maximum quality.

To study some parameters of the obtained optical fiber, a laboratory stand was prepared, consisting of a fiber spectrophotometer and a system for inputting laser radiation with a wavelength of 10.6 μm. The main parameters of the manufactured light guides were obtained, such as: spectral transmission, spectral dependence of attenuation by the break method, as well as the value of attenuation when inputting laser radiation. According to the spectral dependence, it can be said that in the range from 3.5 μm to 15.5 μm, the attenuation is less than 0.5 dB/m. When inputting laser radiation into an optical fiber using a lens system, the attenuation coefficient was 0.64 dB/m with an error of 0.05 dB/m.

[1] K.S. Zaramenskikh, M.S. Kuznetsov, L.N. Butvina, et al., Obtaining of shell fiber infrared light guides from silver and thallium halides, Photon Express, No. 6 (174), pp. 315–316, (2021).
[2] L. Butvina, "Polycrystalline Fibers" in the book "Infrared Fiber Optics" (A.S. Sanghera, I.D. Aggarwal, CRC Press, Boca Raton), pp. 209–249, (1998).
[3] S.M. Pilyushko, V.O. Umnov, M.S. Kuznetsov, et al., Measurement of the attenuation coefficient of a silver halide optical fiber, Lasers in science, technology, medicine: Collection of scientific papers of the XXXIII International Conference, Vol. 33, pp. 102–106, (2022).

Chalcogenide fiber based luminescence source for mid-IR spectroscopy

E. A. Romanova[1], M. V. Sukhanov[2], V. V. Koltashev[3]

1- Saratov State University, Astrakhanskaya 83, Saratov, 410012 Russia
2- Devyatykh Institute of Chemistry of High-Purity Substances of Russian Academy of Sciences, Nizhny Novgorod, Russia
3- Prokhorov General Physics Institute of the Russian Academy of Sciences, Dianov Fiber Optics Research Center, Moscow, Russia

e-mail: romanovaelena@sgu.ru

A fiber-optic source of broadband radiation is a part of an all-fiber sensor for mid-IR spectroscopy. Chalcogenide fibers doped with rear earth (RE) ions as luminescence sources allow us to move further into the mid-IR in the 4–6 μm range [1, 2].

In this work, computer modeling of the output luminescent radiation characteristics was carried out in comparison with experimental data obtained for chalcogenide fiber with a 20 μm core made of Ga-Ge-Sb-Se glass doped with terbium (Tb^{3+}) ions.

The numerical model used a three level system for Tb^{3+} ion and assumed that the levels from $^7F_0$ to $^7F_4$ were thermally coupled (inset in Fig. 1a). The base model parameters included pumping at 1.98 μm (2.0 μm), $^7F_6 \rightarrow {}^7F_1$ transition, and 4–6 μm range luminescence from the first excited level to the ground level, $^7F_5 \rightarrow {}^7F_6$ transition.

Pump and emission powers variation along the fiber was investigated in a numerical model comprising kinetic equations for populations of Tb^{3+} ion levels and differential equations for the pump and emission powers. Parameters for the fiber and coefficients for the equations solution were the same as in [3]. However to fit experimental data, optical loss at λ_p was taken 20 times greater than that measured for the fiber without a RE dopant and used in [3]. Such great losses make a significant contribution at 100–400 cm fiber lengths. An explanation can be given by the effect of radiation leakage from the fiber due to a change in the pump field profile in the fiber transverse cross-section under conditions of constant absorption and power exchange between different modes of the fiber [3].

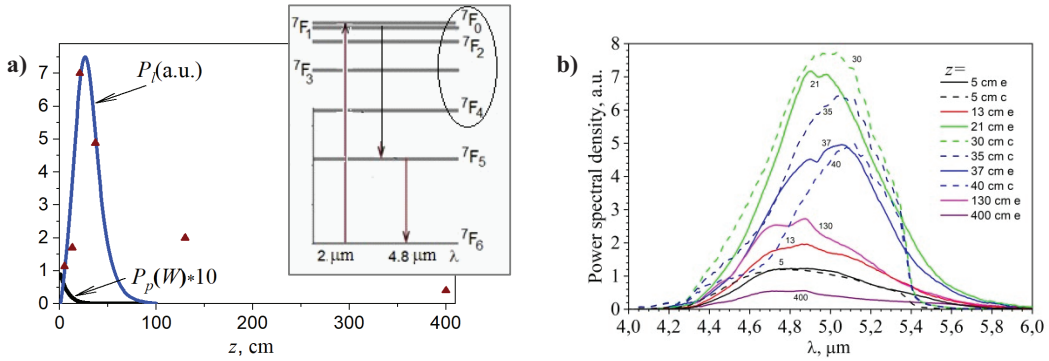

Fig. 1. a) Pump power and emission power calculated (solid curves) and measured (symbols) at λ = 5 μm, inset: energy levels of Tb^{3+}; b) measured (solid lines) and calculated (dashed lines) emission spectra at different distance z along the fiber. $P_p(0)$ = 90 mW (with account of reflections and radiation field loss at the input facet).

As shown in Fig. 1, numerical data fit experiment in the range of the emission power P_l increase to the maximum and then at some distance of the power decrease. At $z \sim 100$ cm, calculated emission power tends to zero, but in experiment, emission was registered at longer distances (symbols in Fig. 1a) where the pump power P_p is assumed zero. Upconversion luminescence is the effect, which can be responsible for such long decay of the emission radiation along the fiber.

[1] V. Nazabal, J-L. Adam, Infrared luminescence of chalcogenide glasses doped with rare earth ions and their potential applications, Opt. Mater.: X, 15, 100168 (2022).
[2] V.V. Koltashev, B.I. Denker, B.I. Galagan, G.E. Snopatin, M.V. Sukhanov, S.E. Sverchkov, A.P. Velmuzhov, V.G. Plotnichenko, 150 mW Tb^{3+} doped chalcogenide glass fiber laser emitting at λ > 5 μm, Opt. & Laser Technol., 161, 109233 (2023).
[3] E.A. Romanova, N.D. Parshina, V.S. Shiryaev, The influence of the mode intensity profile on the population kinetics of terbium ion levels and the excitation of luminescence in a few-mode chalcogenide fiber, Bull. of the Lebedev Phys. Inst., 50, S1225–S1239 (2023).

Tailoring molybdenum disulfide for optoelectronic applications through functionalization

A. R. Rymzhina[1], I. N. Kozlova[1], F. V. Gneushev[1], V. A. Reichert[1], A. D. Razorvin[1], V. S. Pavelyev[1], P. Sharma[1,2], V. I. Platonov[1], N. Tripathi[1]

1- Samara National Research University, Moskovskoye Shosse 34, Samara, 443086 Russia
2- School of Electronics Engineering (SENSE), Vellore Institute of Technology (VIT), Vellore, 632014 India

e-mail: nishant.tripathi.11@gmail.com

Advancing sensor technologies requires superior materials with enhanced performance. Two-dimensional materials stand out due to their exceptional sensitivity, chemical stability, and substrate compatibility, making them ideal for next-generation sensing systems [1].

Near-IR sensors find key applications in different fields such as healthcare (non-invasive glucose/oxygen monitoring [2–3]), industry (hazardous substance detection [4]), agriculture (quality control [5]). Their compact design enables integration into fiber-optic and machine vision systems [6].

Within this work, a heterostructure based on MoS_2 decorated with gold nanoparticles on a Si substrate with previously deposited Cr contacts was examined. MoS_2, by virtue of its 2D properties, including a 1.8 eV direct bandgap, demonstrates effective interaction with photons in the near-IR range.

Gold nanoparticles induce the localized surface plasmon resonance effect (LSPR), which can be interpreted as the presence of numerous p–n junctions at the Au/MoS_2 interface [7]. This phenomenon leads to a significant enhancement of the local electromagnetic field near these interfaces, thereby substantially increasing the light absorption efficiency in the heterostructure.

In this work, the photodetector was fabricated as follows: symmetrical Cr contacts were formed on a Si substrate using standard photolithography process, after which MoS_2 was deposited between them using dielectrophoresis method followed by drop cast of Au nanoparticles. It was established experimentally that Au nanoparticles deposition leads to the resulting sensor detectable spectral range extension. The authors attribute this to the LSPR emergence. This effect not only broadens the device spectral response but also significantly enhances its sensitivity by amplifying the local electromagnetic field and improving the photoinduced charge carriers separation. The photodetector current measurements were carried out in a light-absorbing chamber with a chopper that blocked the LED radiation every 4 seconds.

Under illumination with a wavelength of 940 nm at a power density of 1000 μW/cm², a photocurrent of 0.675 μA was recorded in the absence of external bias. According to the calculations, the fabricated photodetector exhibited a response time of 30 ms and a recovery time of 40 ms.

The obtained characteristics demonstrate the future outlook of the proposed approach for creating near-IR photodetectors based on two-dimensional materials. Of particular note is the plasmon-induced photoresponse enhancement, associated with the increased local electromagnetic field near Au nanoparticles and improved photo-carrier separation efficiency.

The study was supported by the grant of the Russian Science Foundation No. 25-23-00494, https://rscf.ru/project/25-23-00494/.

[1] Rymzhina A. Recent trends in the fabrication of photodetectors: A detailed analysis on the photodetection properties of new 2D-TMCs / A. Rymzhina, P. Sharma, V. Pavelyev, P. Mishra, N. Tripathi // Journal of Nanomaterials and Optoelectronics. -2025. -Vol. 38, -No. 5. -P. 112–127.
[2] Zhao Y. Review of non-invasive continuous glucose monitoring technologies based on optical methods / Y. Zhao, W. Zhang, J. Lu, Y. Zhao, S. Wang, Y. Guo // Sensors. -2022. -Vol. 22, -No. 13. -P. 4855.
[3] Hina A. Noninvasive Blood Glucose Monitoring Systems Using Near-Infrared Technology—A Review / A. Hina, W. Saadeh // Department of Electrical Engineering, Lahore University of Management and Sciences. -2025. -P. 1–15.
[4] Kosterev A. A. Application of quantum cascade lasers to trace gas analysis / A. A. Kosterev, G. Wysocki, Y. Bakhirkin, S. So, R. Lewicki, M. Fraser, F. Tittel, R. F. Curl // Rice Quantum Institute, Rice University, 6100 Main St., Houston, TX 77005, USA. -2003. -P. 1–15.
[5] Ren W. Research progress in near-infrared spectroscopy for detecting the quality of potato crops / W. Ren, Q. Jiang, W. Qi // Journal of Agricultural Science and Technology. -2024. -Vol. 30, -No. 5. -P. 123–136.
[6] Di J. Using Fiber Optic Bundles to Miniaturize Vision-Based Tactile Sensors / J. Di, Z. Dugonjic, W. Fu, T. Wu, R. Mercado, K. Sawyer, V. R. Most, G. Kammerer, S. Speidel, R. E. Fan, G. Sonn, M. R. Cutkosky, M. Lambeta, R. Calandra // Journal of Robotics and Vision Engineering. -2024. -Vol. 35, -No. 4. -P. 215–229.
[7] Li K.-H. Design strategies toward plasmon-enhanced 2-dimensional material photodetectors / K.-H. Li, X. Chen, D. Su, Y. Sun, H. Zhou, Z.-G. Liu, P. Xia, X. Zhang // Advanced Devices & Instrumentation, -2023, -Vol. 2, Article -No. 0017, -P. 1–20.

NV^- diamond laser illumination system for direct registration of fast-moving objects

A. Savvin, E. Zaloznaya, A. Dormidonov

Dukhov Automatics Research Institute, Federal State Unitary Enterprise,
Suschevskaya str. 22, Moscow, 127055 Russia

e-mail: ed.zaloznaya@physics.msu.ru

The report presents the results of experimental and numerical studies on the use of NV^- diamond laser as an illumination system for shadow photographic recording of fast-moving dust phase objects.

The shadow photographic recording is one of the widely used methods for investigation of the dynamics of multiphase medium in gas dynamic experiments, which consists in transferring the image of an object formed by scattered rays of illumination light to a photosensitive area. To implement this method, it is necessary to highlight the objects under study using a pulsed bright light source of short duration – shorter than 1 ns. When using a laser source with high temporal coherence for this purpose, distortions associated with interference noise appear on the recorded images, the elimination of which will avoid the appearance of speckle patterns in images and increase the resolution (approximately twice) of the shadow photographic recording method. Therefore, an additional requirement for an illumination system is a low temporal coherence of light.

According to [1, 2], all the specified requirements for the illumination system for shadow photographic recording can be satisfied using an NV^- diamond laser pumped with a picosecond 532-nm Nd:YAG laser. The 200-ps pulse at the carrier wavelength of 715 nm generated by the NV^- diamond laser has a spectral band with a width of 12 nm, which, according to the Wiener-Khinchin theorem, ensures low temporal coherence of a pulse and, consequently, high resolution of a shadow method.

Fig. 1a shows a shadow image of the explosion of a copper wire bridge when illuminated with the picosecond pulse of an NV^- diamond laser with low temporal coherence. For comparison, Fig. 1b shows a similar shadow image obtained when illuminated with a picosecond pulse of a Nd:YAG laser with a high temporal coherence. In both cases, the delay of the illumination pulse was 20 μs. As one can see, in the shadow image in Fig. 1a there are practically no noise interference speckles, which makes it possible to distinguish individual particles of the order of 5 μm in size, while due to the noise components in Fig. 1b, small-scale fragments of wire cannot be distinguished.

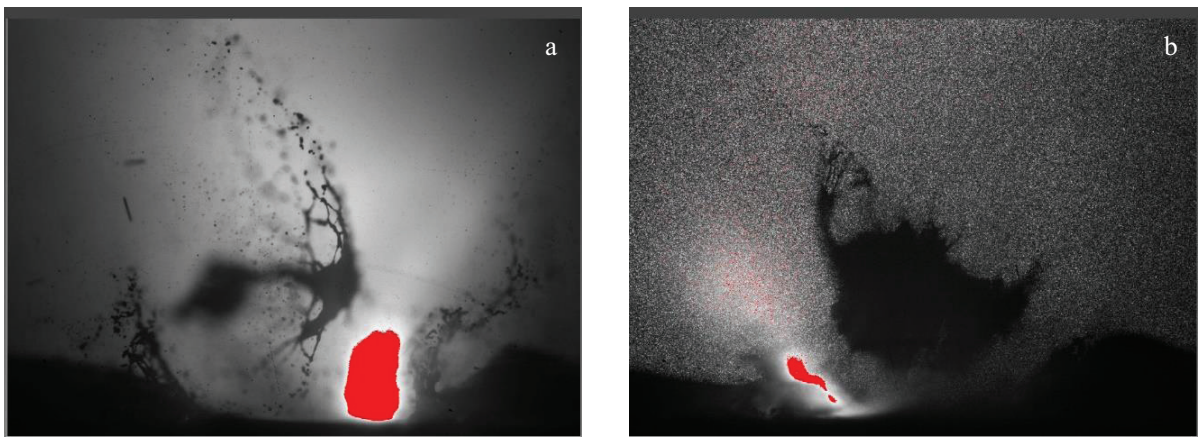

Fig.1. Shadow image of the copper wire explosion with a 20-μs delay of the illumination pulse (a) with low temporal coherence, (b) with high temporal coherence.

[1] A. Savvin, A. Dormidonov, E. Smetanina et al., NV^- diamond laser, Nature Communications 12, 7118 (2021).
[2] D. Genin, E. Lipatov, M. Shulepov et al., Microjoule-Range Diamond NV-Laser with Optical Pumping, Phys. Status Solidi RRL 1, 2300062 (2023).

Tailoring ultrabroadband NIR emission in Bi_2O_3-GeO_2-Tm_2O_3 glasses by Er^{3+}/Ho^{3+}/Yb^{3+} co-doping

K. Serkina[1], O. Knyazkova[1], A. Eliseeva[1], A. Korol[1], I. Stepanova[1], E. Sektarov[2,3]

1- D. Mendeleev University of Chemical Technology of Russia, Moscow, Russia
2- Institute of Spectroscopy RAS (ISAN), Troitsk, Moscow, Russia
3- National Research University "Higher School of Economics", Moscow, Russia

e-mail: serkina.k.s@muctr.ru

Bismuth-doped germanate glasses have long been known as a promising material for optical fibers operating in the near-IR range. Bismuth ions in the germanate matrix can form bismuth active centers (BACs), which have a characteristic wide luminescence band in the range of 1000–1700 nm [2]. These glasses can be used as frequency-tunable laser media [1]. To expand the working spectral range of luminescence of bismuth-containing glasses, it is proposed to dope them together with rare-earth ions that exhibit luminescence in the near-IR range. Tm^{3+} ions and Er^{3+} ions are characterized by luminescence in the ranges of 1700–2100 nm and 1450–1550 nm, respectively, due to which doping with them can expand the spectral range of luminescence of bismuth-germanate glasses in the long-wave region. Ho^{3+} ions have luminescence in the region of 1000–2200 nm, which makes it possible to further expand the luminescence range. Yb^{3+} ions are sensitizers for both BACs and thulium ions. Based on this [2], it was assumed that joint of bismuth-germanate glasses doped with thulium and erbium oxides or thulium and holmium oxides will make it possible to significantly broaden the luminescence band.

Bi_2O_3-GeO_2 glasses were synthesized by classic melt-quenching technique. The compositions can be described by the general formula $10Bi_2O_3$–$90GeO_2$–$0.025Tm_2O_3$ co-doped with 0.05 mol.% Ho_2O_3, or Er_2O_3, or Yb_2O_3. High purity Bi_2O_3, GeO_2, Tm_2O_3, Er_2O_3, Ho_2O_3, Yb_2O_3 were melted at 1100 °C during 30 min, then hardened on a metal substrate. The emission spectra of polished glass samples were recorded on a Bruker IFS 125HR IR Fourier spectrometer with an original luminescent module. Excitation sources was 808 nm laser diode with 600 mW power.

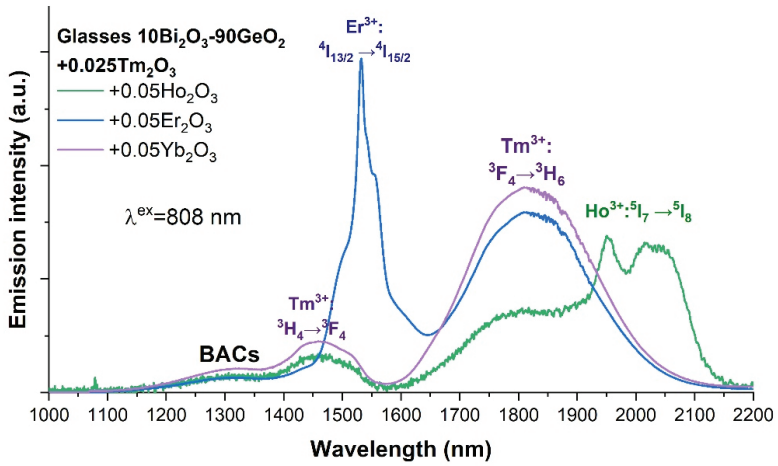

Fig. 1. Emission spectra of synthesized glass.

The luminescence spectra of glasses are a superposition of the BACs and the RE ions emission bands. The greatest broadening of luminescence in the long-wave region was obtained by doping with holmium oxide. The erbium emission band lies in the interval between the BACs and thulium bands, which makes it continuous. The introduction of ytterbium made it possible to enhance the luminescence of thulium and BACs in the NIR region.

[1] E. M. Dianov, Nature of Bi-related near IR active centers in glasses: state of the art and first reliable results, Laser Phys. Lett., vol. 12, pp. 51–56, (2015).
[2] G. Lakshminarayana, R. Vidya Sagar, S. Buddhudu NIR luminescence from Er^{3+}/Yb^{3+}, Tm^{3+}/Yb^{3+}, Er^{3+}/Tm^{3+} and Nd^{3+} ions-doped zinc-borotellurite glasses for optical amplification, J. of Luminescence, vol. 125, pp. 690–695, (2008).

Upconversion emission in Er^{3+}/Tm^{3+} co-doped sodium-germanate glasses

K. Serkina[1], O. Knyazkova[1], I. Stepanova[1], E. Sektarov[2,3]

1- D. Mendeleev University of Chemical Technology of Russia, Moscow, Russia
2- Institute of Spectroscopy RAS (ISAN), Troitsk, Moscow, Russia
3- National Research University "Higher School of Economics", Moscow, Russia

e-mail: serkina.k.s@muctr.ru

In this work, Er^{3+}/Tm^{3+} co-doped sodium-germanate glasses were obtained by melt-quenching method. Synthesized glasses were made in the form of cubes with dimensions of 2×2×2 mm. The opposite faces were polished plane-parallel and had optical quality. Upconversion characteristics of polished glass samples were recorded on a on an OpticInsight USB2000+ fiber optic spectrometer with 10 nm resolution at room temperature. Excitation sources were 808 nm (1.6 W optical power, 204 W/cm^2 power density at the focus) and 980 nm (0.8 W power, 26 W/cm^2 power density at the focus) laser diodes.

Upconversion luminescence spectra consists of Er^{3+} and Tm^{3+} characteristic emission bands in visible range. The intense green (525 and 550 nm), red (650 nm) and dark-red (790 and 800 nm) emissions are simultaneously observed. The dark-red emission was originated from the $^1F_2 \rightarrow {}^3H_6$ and $^3H_4 \rightarrow {}^3H_6$ transitions of Tm^{3+}; the green (525 and 550 nm), and red (650 nm) upconversion luminescence were identified from the $^2H_{11/2} \rightarrow {}^4I_{15/2}$, $^4S_{3/2} \rightarrow {}^4I_{15/2}$ and $^4F_{9/2} \rightarrow {}^4I_{15/2}$, transitions of Er^{3+} respectively [1].

Efficient energy transfer from Er^{3+} to Tm^{3+} were demonstrated for obtained glasses. The significant enhancement in upconversion emissions of Er^{3+} have been observed due to the Tm^{3+}-associated energy transfer pathways [2].

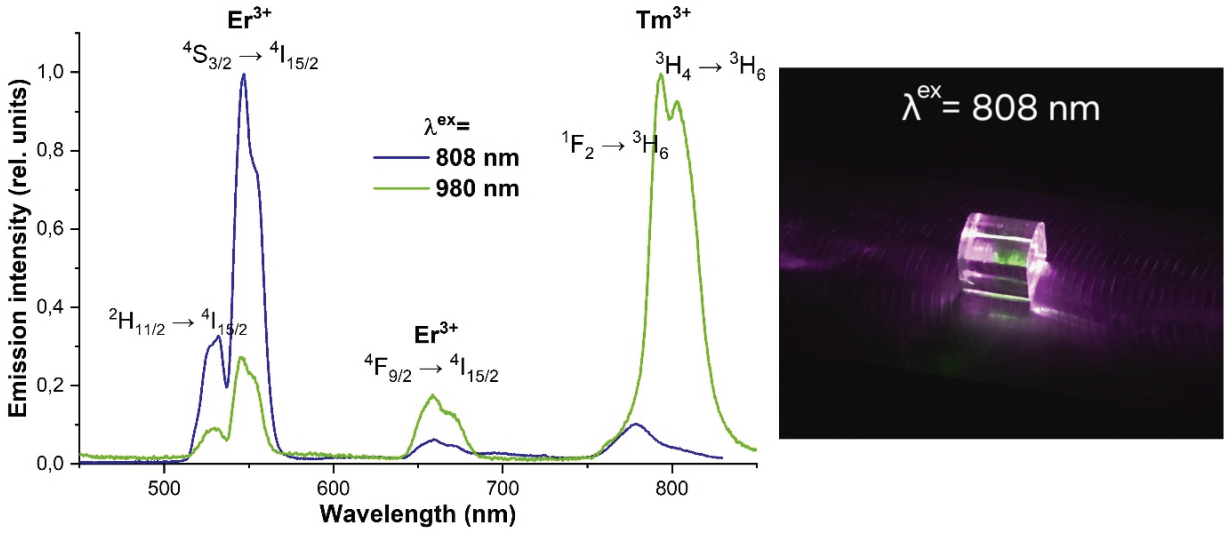

Fig. 1. Emission spectra of synthesized glass and appearance of the sample under 808 nm laser excitation.

The intensity ratio of Er^{3+} and Tm^{3+} observed with a change in excitation, turning blue-green to yellow-green light were achieved. In addition, the Er^{3+}/Tm^{3+}-doped sodium-germanate glasses could be applied as an infrared imaging device based on coupled levels of Er^{3+}, exhibiting high sensitivities. These results will pave an avenue to novel RE-doped glasses for color-tunable NIR visualization.

[1] W. Lozano, C. Araújo, Y. Messaddeq Enhanced frequency upconversion in Er^{3+} doped fluoroindate glass due to energy transfer from Tm^{3+}, J. of Non-cryst. Sol., vol. 311, pp. 318–322, (2015).
[2] T. Grzyb, I. R. Martín, R. Popescu The use of energy looping between Tm^{3+} and Er^{3+} ions to obtain an intense upconversion under the 1208 nm radiation and its use in temperature sensing, J. Nanoscale, vol. 16, pp. 1692–1702, (2024).

Investigation of the optical properties of bulk β-BaB_2O_4 crystals grown from the BaO-B_2O_3-Na_2O-MoO_3 system

E. Simonova[1], A. Kuznetsov[1], A. Goreyavcheva[1], E. Khan[1], A. Kokh[1], D. Ezhov[2], V. Svetlichnyi[2]

1- Sobolev Institute of Geology and Mineralogy SB RAS, Novosibirsk, 630090 Russia
2- Tomsk State University, Tomsk, 634050 Russia

e-mail: simonovaea@igm.nsc.ru

Barium metaborate β-BaB_2O_4 (BBO) crystals occupy a special place among such crystals [1–3]. It should be noted that two polymorphic modifications are known for BBO: a low-temperature non-centrosymmetric β-form and a high-temperature centrosymmetric α-form, between which a phase transition occurs at a temperature of 925 °C. The main method of growing BBO crystals is crystallization from a melt solution using the seed crystal growth technique in the near-surface layer (top-seeded solution growth) [4].

The optical properties of β-BaB_2O_4 (BBO) crystals grown in the BaB_2O_4-$NaBaBO_3$-$BaMoO_4$ system are investigated. The study is aimed at evaluating the prospects of using the compositions of this system as solvents to improve the quality and increase the size of crystals, which is an urgent task in nonlinear optics. Using the methods of X-ray phase analysis and differential scanning calorimetry, the BaB_2O_4-$NaBaBO_3$-$BaMoO_4$ system was studied. Experiments on the growth of bulk β-BBO crystals have been carried out, and their linear and nonlinear optical properties have been studied. The results obtained demonstrate the potential of the BaB_2O_4-$NaBaBO_3$-$BaMoO_4$ system as an effective solvent for the growth of high-quality β-BBO crystals.

For optical measurements, optical elements with dimensions of 10×10×10 mm and plane-parallel plates measuring 10×10×2 mm were fabricated from the selected β-BaB_2O_4 crystal. These elements were oriented along and perpendicular to the *z*-axis. Additionally, a sample cut at angles of $\theta = 47.7°$ and $\varphi = 90°$, with a thickness of 10 mm, was prepared to evaluate the efficiency of second harmonic generation (SHG) in the UV range (266 nm) under excitation by radiation at a wavelength of 532 nm.

The resulting crystals have demonstrated excellent optical properties. In particular, low absorption coefficients were recorded, which indicates a high purity and uniformity of the material. In addition, the high efficiency of second harmonic generation in the ultraviolet range confirms the suitability of such crystals for use in devices requiring high optical power and frequency conversion efficiency of laser radiation. As a result of the study, it was revealed that the BaB_2O_4-$NaBaBO_3$-$BaMoO_4$ system has significant potential for growing large β-BaB_2O_4 crystals characterized by high optical quality.

This work was supported by the RSF project (№ 25-23-20004).

[1] Chen C.T., Wu Y.C., Jiang A.D., Wu B.C., You G., Li R.K., Lin S.J. New nonlinear optical crystal LiB_3O_5 // J. Opt.Soc. Am. B. 1989. V.6, №4. P. 616–621.
[2] Nikogosyan, D. N., [Nonlinear Optical Crystals: A Complete Survey], Springer-Verlag, New York (2005).
[3] Chen, C., Sasaki, T., Li, R., Wu, Z., Lin, Z., Mori, Y., Hu, Z., Wang, J., Uda, S., Yoshimura, M. and Kaneda, Y., [Nonlinear Optical Borate Crystals: Principals and Applications], Weinheim Wiley-VCH (2012).
[4] Feigelson R.S., Raymakers R.J., Route R.K. Solution growth of barium metaborate crystals by top seeding // Crystal Growth. 1986. V.97. P. 352.

Comparative study of $LiGaSe_2$ and $LiGaS_2$ crystals with antireflection microstructures for mid-IR parametric down-conversion via intracavity-pumped OPO

S. N. Smetanin[1], P. D. Kharitonova[1,2], A. G. Papashvili[1], L. I. Isaenko[2,3], A. F. Kurus[2,3], A. P. Yelisseyev[2,3], A. A. Goloshumova[2,3], A. A. Bushunov[2,4], A. A. Teslenko[2,4], V. A. Lazarev[4], M. K. Tarabrin[2,4]

1- Prokhorov General Physics Institute of the Russian Academy of Sciences, Moscow, 119991 Russia
2- Novosibirsk State University, Novosibirsk, 630090 Russia
3- V. S. Sobolev Institute of Geology and Mineralogy SB RAS, Novosibirsk, 630090 Russia
4- Bauman Moscow State Technical University, Moscow, 105005 Russia

e-mail: polincharik@ya.ru

This work demonstrates parametric down-conversion of 1047-nm Nd:YLF laser radiation into the mid-infrared range (4874 nm) using $LiGaSe_2$ (LGSe) and $LiGaS_2$ (LGS) crystals with antireflection microstructures (ARM). The experimental setup featured an intracavity-pumped Nd:YLF laser (1047 nm, 25 ns pulses, 5 Hz repetition rate) coupled to a high-Q cavity (Fig. 1a). A dual-cascade intracavity optical parametric oscillator (OPO) design was employed: a $KTiOAsO_4$ (KTA) crystal (8.3×8.4×20.8 mm^3, Θ = 58°, φ = 0°) generated type II-b (o-oe) phase-matched two-micron radiation at 1724 nm and 2668 nm, achieving up to 2 mJ combined pulse energy, followed by difference-frequency mixing in ARM-coated LGSe or LGS crystals produced mid-IR output at 4874 nm via type II-a (eo-e) phase matching. The ARM technology [1], applied to polished surfaces of LGSe (5×5×9 mm^3, Θ = 90°, φ = 39°) and LGS (5×5×10 mm^3, Θ = 90°, φ = 42°) crystals, enhanced transmission from ~70% to ~80% across 1.5–9 μm, minimizing Fresnel losses without compromising laser damage thresholds.

Despite LGSe's higher nonlinear coefficient, LGS-ARM outperformed LGSe-ARM, yielding 100 nJ at 4874 nm (vs. 2 nJ for LGSe-ARM), attributed to superior optical quality. Output at 4874 nm exhibited a 21-nm spectrum width (Fig. 1b) and was tunable by ±15 nm via crystal rotation. The intracavity pumping scheme proved to be critical in reducing the lasing thresholds and increasing the output pulse energy in the mid-IR range by two times compared to previous extracavity designs [2]. Results confirm ARM-coated LGS as a promising material for high-power mid-IR generation, with future improvements possible via KTA crystal pairing or thermal tuning for broader spectral coverage in spectroscopy applications.

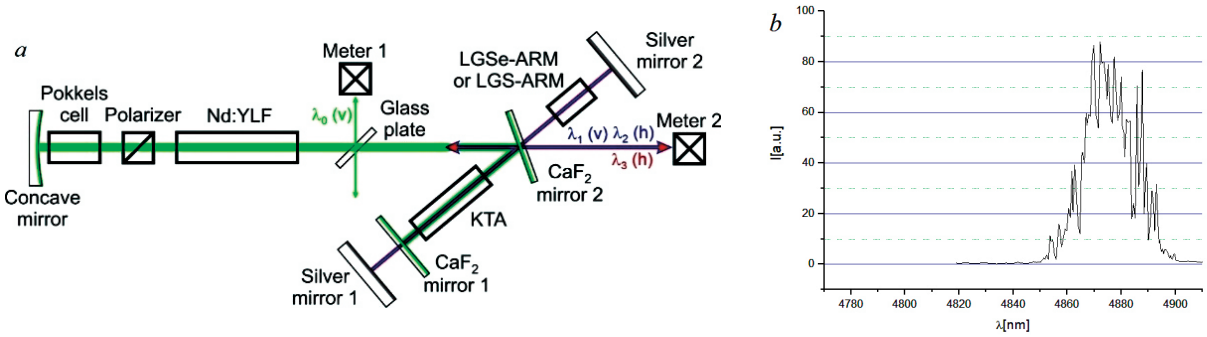

Fig. 1. a) Optical diagram of the setup: λ_0 (v) and λ_1 (v) are vertically polarized radiation components with wavelengths λ_0 = 1047 and λ_1 = 1724 nm; λ_2 (h) and λ_3 (h) are horizontally polarized radiation components with wavelengths λ_2 = 2668 nm and λ_3 = 4874 nm. b) Registered radiation spectrum at wavelength λ_3 = 4874 nm.

The study was supported by the Russian Science Foundation, grant no.20-72-10027-P (https://rscf.ru/project/23-72-50012/) and partly done on state assignment of IGM SB RAS No.122041400031-2 (analysis of the charge composition for the crystal synthesis).

[1] A.A. Teslenko, A.A. Bushunov, L.I. Isaenko, A.A. Shklyaev, A.A. Goloshumova, S.I. Lobanov, V.A. Lazarev, M.K. Tarabrin. Antireflection microstructures fabricated on the surface of a $LiGaSe_2$ nonlinear crystal. Opt. Lett. 48 (5), 1196–1199 (2023).
[2] P.D. Kharitonova, S.N. Smetanin, L.I. Isaenko, I.V. Smirnov, A.A. Sirotkin, P.G. Zverev, A.G. Papashvili, S.I. Lobanov, A.P. Yelisseyev, A.A. Goloshumova, A.A. Bushunov, A.A. Teslenko, V.A. Lazarev, M.K. Tarabrin. Study of operability of a nonlinear converter based on a $LiGaSe_2$ crystal with surface antireflection microstructures under nanosecond laser excitation. Optika i Spektroskopiya (in Russian) 133 (3), 267–273 (2025).

Luminescence properties of rare-earth (Ho^{3+}, Er^{3+}, Tm^{3+}) doped novel lead germanate oxychloride glasses

A. Terekhova[1], D. Butenkov[1,2], E. Sektarov[3,4], O. Petrova[1]

1- D. Mendeleev University of Chemical Technology, Miusskaya sq. 9, Moscow, 125047 Russia
2- N. S. Kurnakov Institute of General and Inorganic Chemistry RAS, Leninsky prospect 31, Moscow, 119991 Russia
3- Institute of Spectroscopy of the Russian Academy of Sciences, Troitsk, Fizicheskaya st. 5, Moscow, 108840 Russia
4- Higher School of Economics, Myasnitskaya st. 20, Moscow, 101000 Russia

e-mail: nastt2001@mail.ru

Among heavy-metal-based glasses investigated for mid-infrared applications, lead-germanate glasses demonstrate relatively low phonon energy and infrared transparence comparable to tellurite glasses, while exhibiting superior mechanical strength and thermal stability [1]. Incorporation of metal halides into lead-germanate oxide glasses reduces both phonon energy and OH^- absorption coefficients, while simultaneously enhancing luminescent properties [1, 2].

Glasses in the xPbCl$_2$-(50-0.5x)PbO-(50-0.5x)GeO$_2$ system (x = 0–50 mol%, with 10 mol% increments) were synthesized. The 30PbCl$_2$-35PbO-35GeO$_2$ composition as optimal for rare-earth ion (Ho^{3+}, Er^{3+}, Tm^{3+}) doping by comprehensive physicochemical characterization identified. The glass matrix exhibited: crystallization stability (ΔT) – 82 °C, transparency range 350–6450 nm, refractive index (n_d) – 2.0888, Abbe number – 16.7, density – 6.210 g/cm^3, Vickers microhardness – 159 kg/mm^2. Vibrational spectroscopy revealed a maximum matrix phonon energy of 795 cm^{-1}.

The luminescence spectra of rare-earth-ion-doped oxychloride lead germanate glasses in the 1.3–3 μm range are presented in Figure 1.

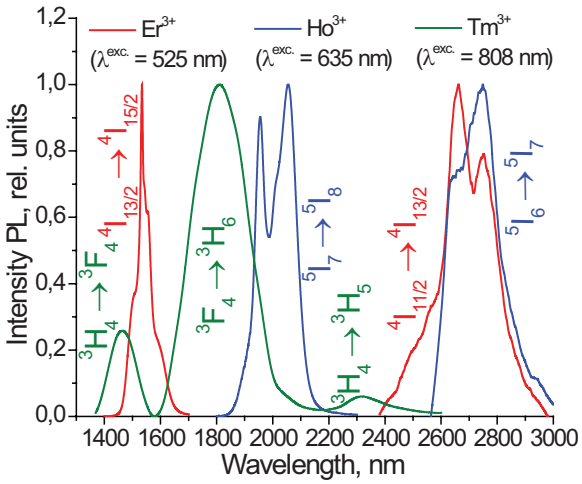

Fig. 1. Luminescence spectra of 29.975PbCl$_2$-34.975PbO-35GeO$_2$-0.15ReF$_3$ (Re = Ho^{3+}, Er^{3+}, Tm^{3+}) glasses.

The presented spectra show characteristic mid-IR luminescence bands typical for the studied rare-earth ions.

This work reports the first synthesis and characterization of oxychloride lead-germanate glasses. The results demonstrate that rare-earth ion doping renders these glasses promising luminescent and laser materials for the 1–3 μm spectral range.

[1] Wang, P., Bei, J., Ahmed, N., Ng, A. K. L., & Ebendorff-Heidepriem, H. Development of low-loss lead-germanate glass for mid-infrared fiber optics: I. Glass preparation optimization. Journal of the American Ceramic Society, 104(2), 860-876, (2021).
[2] Brown, E., Hömmerich, U., Bluiett, A. G., Trivedi, S. B., & Zavada, J. M. Synthesis and spectroscopic properties of neodymium doped lead chloride. Journal of applied physics, 101(11), (2007).

Features of the near-electrode processes in polar dielectric crystals

V. Umylin, N. Kozlova, E. Zabelina, A. Korchagin, A. Temirov

University of Science and Technology MISIS; Leninsky avenue 4, Moscow, 119049 Russia

e-mail: v.umylin@mail.ru

At this time the piezo-devices are highly demand. The working elements of these devices are fabricated on polar cuts of single crystal piezoelectric materials with applied conductive coatings on their sides. Such devices are compact and highly reliable. However, their service life is limited due to degradation and aging processes of crystal element surfaces which contact with conductive coatings. Such processes may result in breakdown of dielectric element. Degradation is usually associated with external effects. They lead to significant changes in operating properties. This results in unreliability of the readings that the devices transmit. And can affect the shortening of their working life.

Consideration of the contribution of conductive coatings to fatigue effects and aging is usually limited to such processes as delamination of conductive coatings, changes in their microstructure or geometric parameters. However, the conductive coating can affect the electrophysical and dielectric properties. And even the phase stability of the material. This leads to degradation and aging of the surfaces of crystal elements and performance degradation of the functional characteristics of devices and instruments. In polar cut samples without stimulating external influences (temperature, electrical and radiation) the short-circuit currents (SCC) arise, when conductive coatings (which applied to the surface) are short-circuited. The processes of their occurrence are poorly studied.

The aim of this work was to study the features of occurrence of the SCC and near-electrode processes in α-$LiIO_3$ crystals with different materials of conductive coatings and according to different measurement schemes.

The polar cut samples of model crystal α-$LiIO_3$ of hexagonal modification with different materials of conductive coatings (In, Al, Ar, Cr) were used for investigations. The samples with symmetrical (identical) and asymmetrical (different) conductive coatings relative to the polarity of the sample side were studied. The polarity of the samples was determined using a piezotester. The SCC and their temperature dependences were measured from the room temperature to 210 °C without applying an external electric field. The SCC on the samples were recorded using the hardware complex with the special software developed in our laboratory (certificate of state registration of the computer software No. 2025615960).

Temperature dependences of the SCC were obtained. The magnitudes and direction of current flow depend on the material of conductive coatings and the polarity of the side of their application on the sample. Temperature dependences of cooling do not match with heating. This may indicate the irreproducibility of processes and the formation of new phases.

Studies of the electrophysical parameters in polar crystals were carried out in the accredited laboratory of semiconductor materials and dielectrics «Single crystals and stock on their base» NUST MISIS with financial support from the Ministry of Education and Science of Russia within the framework of the state assignment to universities FSME-2023-0003.

Spectral luminescence and structural properties of silica glasses with CeO_2: Ni and Ce_2O_3: Ni nanoparticles

N. Varapai, V. Kouhar, A. Ramanenka, G. Malashkevich

B. Stepanov Institute of Physic, NAS of Belarus, Minsk, Belarus

e-mail: n.varapay@ifanbel.bas-net.by

It is known that Ln^{3+} ions incorporated into CeO_2 and Ce_2O_3 nanocrystals are characterized by cubic symmetry of optical centers, weak cross-relaxation quenching of luminescence, and its effective sensitization by labile photoreduced $(Ce^{3+})^+$ and stable Ce^{3+} ions [1]. This allows us to propose optical materials with such nanocrystals for solving a number of specific tasks. Given the increased interest in recent decades in glass ceramics with nanocrystals activated by nickel ions, it was decided to investigate the "spectroscopic behavior" of the latter in nanocrystals of cerium oxides in a silica matrix.

The experimental samples were synthesized from a solution using the sol-gel method, which included hydrolysis of $(C_2H_5O)_4Si$ in an aqueous-alcoholic solution in the presence of HCl as a catalyst until a sol is obtained, the introduction of aerosil and activator salts into it, neutralization of the resulting colloidal system with a solution of ammonia, gel formation, drying, and sintering to a transparent glass state.

Fig. 1 shows the diffractograms of the synthesized samples. As can be seen, the initial sample is characterized by the presence of weak Bragg reflections at angles (indicated by red arrows), corresponding to the cubic lattice of the CeO_2 lattice with the space group Fm3m. Further annealing of this sample in air leads to an increase in the intensity of these reflections, and annealing in hydrogen leads to a weakening of these reflections and the appearance of new ones, indicating a restructuring of the formed nanocrystals. The inset in Fig. 1 shows the optical density spectra, indicating the presence of intense absorption at $\lambda \leq 400$ nm and a number of weak bands in the visible and near-IR regions of the spectrum.

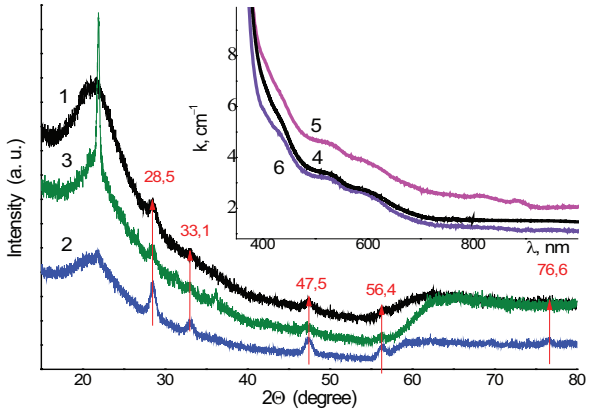

Fig. 1. Diffraction patterns and absorption spectra of samples before (1, 4) and after (2, 5) annealing in air and hydrogen (3, 6).

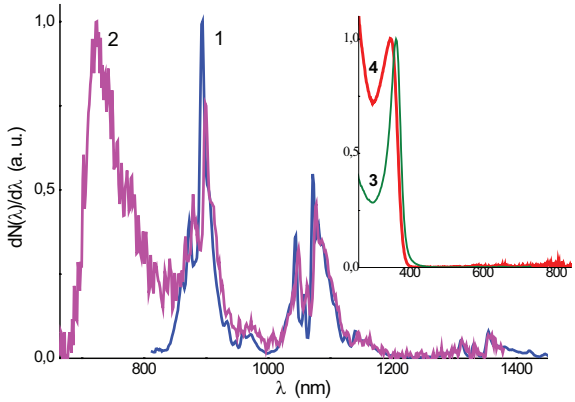

Fig. 2. Luminescence and its excitation spectra of samples after annealing in air (1, 3, 4) and hydrogen (2). λ_{exc} = 320 nm, λ_{rec}, nm: 896 (3), 1085 (4).

Fig. 2 shows the IR luminescence spectra of the annealed samples. It can be seen that the sample annealed in air shows an intense structural band at $\lambda_{max} \approx 900$ nm, a less intense band at $\lambda_{max} \approx 1100$ nm, and a weak band at $\lambda \approx 1380$ nm, which can be attributed to Ni^{4+} electronic transitions. For the hydrogen-annealed sample, an additional weakly structured band appears at $\lambda_{max} \approx 720$ nm, which may be associated with the luminescence of F^+ centers [2] or the luminescence of Ni^{3+}. The inset in Fig. 2 shows the luminescence excitation spectrum of these samples, indicating the most effective excitation in the UV region.

Thus, the synthesized glass-ceramic possesses sufficiently high transparency and may be of interest as UV sensors, and special phosphors, and in the fiber-optic version, which allows pumping into long-wave absorption bands of nickel ions, as an active material for IR lasers.

[1] G.E. Malashkevich, V.N. Sigaev, G.I. Semkova, B. Champagnon, Nanocrystalline Nature of High-Symmetry Ce^{4+}-Eu^{3+} Centers in Silica Gel Glasses, Physics of the Solis State, vol. 46, pp. 552–556, (2004).
[2] S. Tiwari, G. Rathore, N. Patra, A.K. Yadav, D. Bhattacharya, S.N. Jha, C.M. Tseng, S.W. Liu, S. Biring, S. Sen, Oxygen and Cerium defects mediated changes in structural, optical and photoluminescence properties of Ni substituted CeO_2, J. Alloys Compd., vol. 782, pp. 689–698, (2019).

Effect of post-growth isothermal annealing on the optical properties of langasite family crystals

E. Zabelina[1], N. Kozlova[1], V. Kasimova[1], O. Buzanov[2]

1- National University of Science and Technology «MISIS», Leninsky pr. 4, b. 1, Moscow, 119049 Russia
2 - FOMOS-Materials, Buzheninova st. 16, Moscow, 107023 Russia

e-mail: zabelina.ev@misis.ru

The crystals of the langasite family are langasite (LGS, $La_3Ga_5SiO_{14}$), langatate (LGT, $La_3Ga_{5.5}Ta_{0.5}O_{14}$) and catangasite (CTGS, $Ca_3TaGa_3Si_2O_{14}$). These are crystals with the structural type of calcium-gallium germanate, point group of symmetry 32 [1], therefore, they are optically anisotropic, exhibit birefringence, dichroism and gyrotropy. CTGS is referred to ordered crystals, while LGS and LGT are referred to disordered crystals.

The symmetry of crystals determines the possibilities of manifestation of properties in them [2, 3]. At the same time, the physical properties of real crystals are determined by their defect structure [4, 5]. Defects can arise during the crystal growth with impurities and dopants, especially in case of elements with a different oxidation state, in dependence on growth atmosphere, as a result of technological features of growth processes and other environmental factors. External post-growth influences on crystals such as temperature, radiation fields, mechanical influences can lead to a change in the defect structure of the crystals and significantly affect all their properties. Optical properties are extremely sensitive to crystal defect structure.

The purpose of this work was a comprehensive study of the post-growth annealings in air and vacuum on the optical properties of LGS, LGT and CTGS.

The crystals were grown in the company «FOMOS-Materials» by the Czochralski method in Ir crucibles in an atmosphere of argon and argon with the addition of oxygen.

The optical properties of the crystals were studied in the accredited laboratory «Single crystals and stock on their base». The spectral dependences of the transmission of ordinary (To) and extraordinary (Te) waves were measured on a Cary-5000 spectrophotometer with a universal measuring accessory UMA in polarized light. The specific rotation of the plane of polarization ρ was measured when light propagated along the axis of the 3rd order (optical axis) by the direct method at a wavelength of $\lambda = 630$ nm and by spectrophotometric methods presented in [6, 7], using spectral transmission dependences in the analyzer-crystal-polarizer system with different angles between the analyzer and the polarizer.

Studies were carried out in the accredited laboratory «Single crystals and stock on their base» NUST MISIS with financial support from the Ministry of Education and Science of Russia within the framework of the state assignment to Universities FSME-2023-0003.

[1] B.V. Mill, A.V. Butashin, Modified rare-earth gallates with the $Ca_3Ga_2Ge_4O_{14}$ structure, Reports of the USSR Academy of Sciences, vol. 264, pp. 1385–1389, (1982).
[2] M.P. Shaskolskaya, Crystallography (Moscow: Higher School), 1984.
[3] I.S. Zheludev Physics of crystalline dielectrics (Moscow: Nauka), 1968.
[4] A.A. Blistanov, Features of structural defects in ionic crystals (dielectrics), News of Higher educational institutions. Electronic equipment materials, vol. 4, pp. 4–15, (2005).
[5] N.S. Kozlova, E.V. Zabelina, V.M. Kasimova, Features of Testing and Monitoring Optical Qualities of Dielectric Single Crystals, Measurement Standards. Reference Materials, vol. 21, pp. 72–85, (2025).
[6] E.V. Zabelina, R. Shahin, N.S. Kozlova, V.M. Kasimova Determination of the polarization plane specific rotation in gyrotropic crystals of the middle category by the spectrophotometric method. News of Higher educational institutions. Electronic equipment materials, vol. 26, pp. 181–189, (2023).
[7] T.G. Golovina, A.F. Konstantinova, V.M. Kasimova, E.V. Zabelina, N.S. Kozlova, G.Yu. Deev, O.A. Buzanov, Effect of Annealing of $Ca_3TaGa_3Si_2O_{14}$ Catangasite Crystals on Their Optical Activity, Crystallography Reports, vol. 69, pp. 704–710, (2024).

KRS-5 single crystal growth process optimization by calculation of temperature gradient using finite element method

K. S. Zaramenskikh, M. S. Kuznetsov, S. V. Erohin, S. M. Pilyushko, A. R. Korneeva

JSC «State Research and Design Institute of Rare Metal Industry «Giredmet» named after N. P. Sazhin, Moscow, 115524 Russia

e-mail: kszaramenskikh@rosatom.ru

Thallium halides, in particular KRS-5 (TlBr–TlI), represent one of the most promising classes of optical crystals for applications in the mid- and far-infrared ranges. Nevertheless, the high quality standards applied to materials used for such applications present considerable challenges in the manufacture of single thallium halide crystals. In particular, when failing to adhere to exacting growth conditions, the samples exhibit polycrystalline characteristics, rendering them unsuitable for utilization.

Given the high cost of experiments carried out to ascertain the optimal conditions for growth, computer modeling may present a viable alternative. When taking such an approach to satisfy the specific requirements, it becomes possible to analyze key effects as standalone entities, thus avoiding unnecessary complications resulting from the introduction of a high number of simultaneous unknown variables. Thus, the aim of the present work is to ascertain the causes of polycrystallinity in the samples and identify the optimal parameters for the growth conditions of KRS-5 single crystal.

In order to solve the problem, the finite element method was used for the calculation of temperature distribution, shape and position of the crystallization front. All calculations were performed in the MATLAB package using the Partial Differential Equation Toolbox (PDEs) module. The issue of temperature distribution was addressed by means of an axisymmetric approximation. The height of the ampoule model was 0.35 m, the radius was 0.04 m, and the angle at the tip of the cone was 45°. The ampoule model was divided into a grid with triangular elements no larger than 0.005 m in size with a quadratic division of the grid nodes and a mesh growth rate of 1.5. Based on the calculations, samples of the KRS-5 crystal were grown in EDG11-D4 Sunfire furnace (MELLEN) in JSC Giredmet.

A computer simulation was employed to calculate the temperature distribution within the material during the growth process. This was used to determine the position and shape of the crystallization front. It is established that polycrystalline samples develop as a consequence of the crystallization front assuming a flat configuration. The optimum temperature in the furnace was determined. The work demonstrated the successful growth of a KRS-5 single crystal under the calculated conditions.

32nd INTERNATIONAL CONFERENCE
Advanced Laser Technologies
ALT'25

LASER DIAGNOSTICS AND SPECTROSCOPY

Scanning probe lithography for all-dielectric nanophotonics

P. A. Alekseev, M. E. Popov, K. A. Gasnikova, B. R. Borodin

Ioffe Institute, Polytechnicheskaya 26, Saint Petersburg, 194021 Russia

e-mail: prokhor@mail.ioffe.ru

In recent years, advancements in research and synthesis have given rise to a variety of novel materials, each exhibiting distinctive properties. Van-der-Waals (vdW) materials and halide perovskites are of particular interest in this study. The optical properties of vdW materials are unique due to the essential anisotropy of the crystal lattice in the in-plane and out-of-plane directions. This results in giant birefringence and a record high refractive index in the spectral range with near-zero absorption [1]. Furthermore, vdW materials can be obtained in the form of a monomolecular layer. Transition metal dichalcogenides (TMDCs), exhibit strong excitonic photoluminescence at room temperatures. Halide perovskites also have large exciton binding energy, which makes them favorable for study of the exciton-related physics at room temperatures [2].

In order to employ the perspective optical properties of the aforementioned materials in the domains of photonics and optoelectronics, it is necessary to create elemental photonics circuit units. Specifically, stripe waveguides and light-emitting cavities. However, conventional mask lithography methods are not well developed for vdW materials and halide perovskites. In this study, we propose an universal maskless scanning probe lithography (SPL) for the prototyping of the dielectric nanophotonics units (stripe waveguides and microdisk resonators). The approach is based on the mechanical scanning probe lithography, in which a sharp diamond probe carves the desired structures with a lateral resolution of less than 20 nm. The roughness of the carved structures is determined by several factors, including the mechanical properties of the material, the shape of the probe, the moving direction, the probe pressure force, and the moving velocity. These parameters are the subject of extensive study, aimed at revealing the key features of the carving process that are necessary to obtain the desired structures.

The employment of revealed features has enabled the fabrication of a variety of structures from the advances nanophotonic materials. A 20-μm-long stripe waveguide was carved from a 70-nm-thick $InGaS_3$ (vdW material) flake, conducting visible light within the 500–1100 nm spectral range. The creation of a waveguide was achieved through the optimization of the cutting direction, a factor that was governed by the in-plane crystal lattice and the probe shape. The creation of a photonic crystal that supports room-temperature exciton-polariton formation was realized for the quasi 2D halide perovskite layer. The alteration of a particular period within the photonic crystal enables the modulation of Rabi splitting [2]. From the 200-nm-thick GaP layers grown on sapphire, various stripe waveguides and microdisks with an optical quality exceeding 1000 were created.

The use of TMDC materials with a record high refractive index facilitates the fabrication of microdisk resonators of reduced size, thereby enabling effective control of photoluminescence (PL) spectra. For instance, a microdisk with a thickness of 70 nm and a diameter of 2.5 μm has been shown to enhance the in-direct excitonic PL by a factor of 100, a consequence of the Purcell effect [3]. In order to further exploit the high intensity PL of the TMDC monolayer and the high refractive index of the bulk TMDC, a double heterostructure was fabricated in which a monolayer $MoSe_2$ was embedded in a 50-nm-thick WS_2 layer. A heterostructure disk with a diameter of 2.35 μm exhibited a $MoSe_2$ excitonic PL modulated by narrow whispering gallery modes. These modes possessed a Q-factor of 700, which exceeded the theoretically predicted value, indicating the emergence of amplified spontaneous emission [4]. Thus, m-SPL is an effective universal tool for the creation of high-quality nanophotonic structures.

The work is supported by Russian Science Foundation, 24-12-00209.

[1] A.S. Slavich, G.A. Ermolaev, M.K. Tatmyshevskiy, et al, "Exploring van der Waals materials with high anisotropy: geometrical and optical approaches," Light: Science & Applications 13(1), 68 (2024).
[2] N. Glebov, M. Masharin, B. Borodin, P. Alekseev, F. Benimetskiy, S. Makarov, and A. Samusev, "Mechanical scanning probe lithography of perovskites for fabrication of high-Q planar polaritonic cavities," Applied Physics Letters 122(14), 141103 (2023).
[3] B.R. Borodin, F.A. Benimetskiy, V.Y. Davydov, et al, "Indirect bandgap $MoSe_2$ resonators for light-emitting nanophotonics," Nanoscale Horizons 8(3), 396–403 (2023).
[4] P.A. Alekseev, I.A. Milekhin, K.A. Gasnikova, et al, "Engineering whispering gallery modes in $MoSe_2/WS_2$ double heterostructure nanocavities: Towards developing all-TMDC light sources," Materials Today Nano 30, 100633 (2025).

Terahertz pulse shaping controlled by photoinduced metallization in GaAs

T. V. Dolgova, M. A. Kiryanov, I. A. Novikov, V. I. Stadnichuk, A. A. Fedyanin

Faculty of Physics, Lomonosov Moscow State University, Moscow, 119991 Russia

e-mail: dolgovatv@my.msu.ru

One of the key challenges in terahertz (THz) photonics is the development of compact and dynamically reconfigurable elements for real-time control over the spatial and temporal structure of THz radiation. This includes controlling THz wavefronts, spectral properties, and polarization states. Significant progress has been made in passive THz optics, including the development of filters, polarizers, lenses, and beam splitters. These elements are typically fabricated from materials with low refractive indices and must be physically thick to accumulate the required phase shift. Besides, the static nature of such components restricts their real-time functionality.

Consequently, there is a growing demand for active and quasi-planar THz devices whose functionality can be reconfigured in real time. A promising solution to this problem is the optical generation of transient THz metasurfaces that are functional patterns formed by spatially modulated femtosecond laser excitation on the surface of a semiconductor. These photoinduced structures locally alter the dielectric function by generating electron-hole plasma, giving rise to diffraction, reflection, and resonance effects in the THz range. Compared to fabricated metamaterials, this approach offers full reconfigurability and high switching speeds.

In this work, we demonstrate an experimental approach to the ultrafast terahertz pulse shaping in gallium arsenide (GaAs) via femtosecond-laser-induced metallization. The relatively long wavelength of THz radiation (hundreds of microns) enables practical geometries in which the wavefronts of the THz probe and the optical pump can be matched with interferometric accuracy. For example, in a configuration where the sample surface normal bisects the angle between the THz and optical wave vectors, ensuring efficient spatial overlap between the excitation profile and the THz field. By projecting optical pulses onto the GaAs surface, we generate transient carrier distributions that reach and exceed the metallization threshold, forming reflective and plasmonically active regions. A modified time-domain spectroscopy technique is used to directly resolve the temporal evolution of the transmitted and reflected THz fields, capturing both the main pulse and time-delayed satellites arising from photoexcited areas. We report experimentally resolved THz pulse shaping effects in both the non-metallic and metallic photoexcitation regimes. By varying the pump fluence, we observe a pronounced modulation of the satellite THz pulse, including changes in amplitude and temporal profile. Using one-dimensional photoexcitation patterns, we induce resonant excitation of surface plasmon polaritons on GaAs, enabling plasmon-assisted reshaping of THz fields. This approach paves the way toward complex, on-demand THz waveform generation and all-optical spatiotemporal control of THz radiation.

This work was supported by Russian Science Foundation (24-12-00210).

Comparative analysis of optical supercontinuum generation in high-pressure He, N_2, Ar, and CO_2 gases

Yu. E. Geints[1], V. O. Kompanets[1,2], S. V. Chekalin[1,2]

1- V. E. Zuev Institute of Atmospheric Optics SB RAS, Acad. Zuev Square 1, Tomsk, 634055 Russia
2- Institute of spectroscopy RAS, Fizicheskaya str. 5, Troitsk, Moscow, 108840 Russia

e-mail: ygeints@iao.ru

The generation of coherent optical radiation with an anomalously broadened spectral composition (supercontinuum) during the nonlinear propagation (self-focusing, filamentation) of high-power femtosecond laser pulses in transparent media, including high-pressure gases, holds considerable practical interest for the obtaining of extremally ultrashort optical pulses. This is crucial for advancing modern attosecond spectroscopy and the study of matter under extreme conditions. We report on the results of systematic experiments on the generation of broadband supercontinuum in an optical cell filled with various atomic and molecular gases, including He, Ar, N_2, and CO_2, at pressures ranging from 1 to 50 bar achieved through the focused nonlinear propagation of 40 fs pulses from a multi-terawatt Ti:sapphire-laser.

Our measurements (Fig. 1) demonstrate that, with the exception of He, all supercontinuum (SC) spectra exhibit similar pressure-dependent behavior, when an initial strong spectral broadening is followed by saturation of the spectral bandwidth and, in the case of CO_2, even a noticeable reduction relative to its maximum achievable value. To elucidate these findings, we carry out theoretical simulations based on the unidirectional propagation equation for an ultrashort optical wave packet. Our analysis reveals that the most likely explanation for the observed effects is the enhanced role of free-electron kinetics, such as absorption and refraction of the laser pulse, in the self-generated plasma as the gas pressure increases. These findings provide valuable insights into the mechanisms governing supercontinuum generation in high-pressure gaseous media.

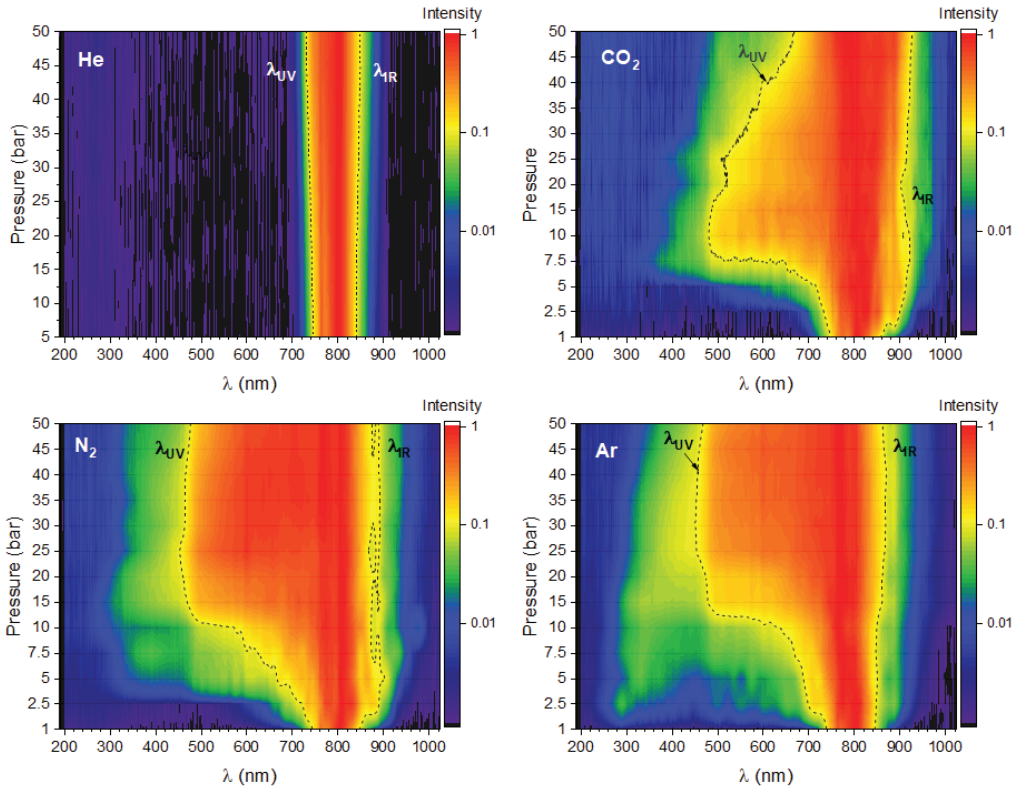

Fig. 1. SC spectrum of laser pulse after filamentation in different pressurized gases. The dashed contours mark the cutoff wavelengths of the spectrum in the UV (λ_{UV}) and IR (λ_{IR}) bands.

Silver/Gold modified silicon nanowires for optical diagnostics of hazardous substances

K. A. Gonchar[1,2], A. D. Kartashova[1], L. A. Osminkina[1,2]

1- Lomonosov Moscow State University, Physics Department, Leninskie Gory 1, Moscow, 119991 Russia
2- Institute of Biological Instrumentation of the Russian Academy of Sciences, Pushchino, Moscow Region, 142290 Russia

e-mail: k.a.gonchar@gmail.com

Modern public safety challenges require the development of compact and highly sensitive sensors for the rapid detection of trace amounts of hazardous substances. In this study, we present sensor substrates based on arrays of silicon nanowires modified with gold and silver nanoparticles (AuAg@SiNWs), designed for the detection of 5-hydroxytryptamine (5-HT) and 2,4-dinitrotoluene (2,4-DNT) as a model substances via surface-enhanced Raman scattering (SERS) spectroscopy.

The substrates were fabricated using metal-assisted chemical etching of crystalline silicon followed by deposition of noble metals. We demonstrate the possibility of recording the spectra of the target substances directly from human fingerprints (Fig. 1).

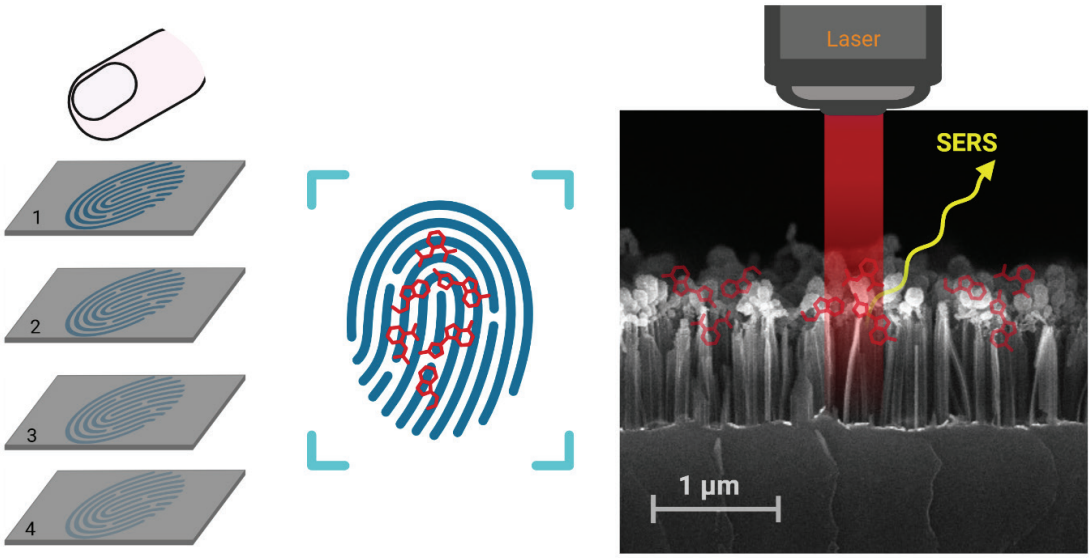

Fig. 1. Schematic representation of the procedure for applying sequential fingerprints on sensor substrates and recording the SERS signal from traces of molecules on the surface of AuAg@SiNWs.

It was found that the spectral signals remain detectable for up to four sequential fingerprints in the case of 2,4-DNT and up to two for 5-HT, without significant loss of intensity. These results confirm the potential of the developed AuAg@SiNWs substrates as compact, low-cost, and sensitive sensors for rapid on-site (in situ) analysis, including security screening at transportation hubs and in public facilities.

The study was supported by the Russian Science Foundation, grant No. 24-15-00137, https://rscf.ru/project/24-15-00137).

Time-resolved broadband two-dimensional spectroscopy with ultrashort pulses in the visible and mid-infrared range

G. D. Ivanov[1], A. S. Shvedov[1], E. A. Stepanov[1,2], A. A. Lanin[1,3], A. B. Fedotov[1–3]

1- Lomonosov Moscow State University, Physics Department, Moscow, 119991 Russia
2- Russian Quantum Center, Skolkovo, Moscow Region, 143025 Russia
3- LIFT Center LLC, Skolkovo Innovation Center, Moscow, 121205 Russia

e-mail: a.b.fedotov@physics.msu.ru

Nonlinear optics methods offer unique opportunities for studying fast processes in complex physical, chemical, and biological systems. Multidimensional nonlinear spectroscopy is one of the most promising and dynamically developing area [1–2]. Unlike conventional one-dimensional spectroscopy, multidimensional spectroscopy allows one to identify physically and chemically significant classical [3–6] and quantum [7] correlations in nonlinear response spectra, as well as to study the dynamics of fast processes in complex atomic and molecular systems [2, 6]. In recent years, a noticeable number of variations of 2D-FTIR spectroscopy have been developed.

Our study by two-dimensional infrared spectroscopy is carried out using three ultrashort laser pulses, with precisely controlled time characteristics. Our experimental studies are based on a multifunctional Ti:Sapphire femtosecond laser complex consisting of master oscillator, regenerative amplifier, optical parametric amplifier and difference frequency generation scheme. We have developed set-up for measuring two-dimensional infrared Fourier spectra in the mid-IR range and investigated the molecule of dicobalt octacarbonyl. The method allows one to correctly reconstruct the two-dimensional spectrum of dicobalt octacarbonyl and observe the change in absorption of the sample on a picosecond time scale, which is associated with the transformation of the molecule from one isomeric state to another [8, 9].

A cross-range version of two-dimensional Fourier spectroscopy with a spectral resolution of 0.6 cm^{-1} along both axes of detection frequencies has been implemented in our work. The experimental scheme has been successfully tested by recording the relaxation of vibrational levels of a DCM organic dye solution in the frequency range of 1430–1820 cm^{-1} (5.5–7 μm) upon electronic excitation of the sample by visible broadband radiation. It has been shown that in a polar solvent, the relaxation of electronic excitation of the DCM dye is accompanied by the activation of Franck-Condon vibrational modes, which appear in the two-dimensional Fourier spectrum at frequencies of 1547 and 1576 cm^{-1}. It has been demonstrated that the technique allows one to reconstruct the phase of nonlinear absorption and resolve the effects of spontaneous emission and absorption from an excited state.

The work was supported by Russian Science Foundation grant # 25-12-00211.

[1] S. Mukamel.Principles of Nonlinear Optical Spectroscopy. Oxford University Press, New. York, (1995).
[2] P. Hamm, M. Lim, R.M. Hochstrasser. Structure of the amide band of peptides measured by femtosecond nonlinear-infrared spectroscopy Journal of Physical Chemistry B, 102, 6123 (1998).
[3] S. Mukamel, Y. Tanimura, P. Hamm. Coherent Multidimensional Optical Spectroscopy, Accounts of Chemical Research, 42, 1207 (2009).
[4] P. Hamm, M. Zanni. Concepts and Methods of 2D Infrared Spectroscopy. Cambridge University Press (2011).
[5] S.T. Cundiff, S. Mukamel. Optical multidimensional coherent spectroscopy. Phys. Today, 66, 44 (2013).
[6] X. Dai, A.D. Bristow, D. Karaiskaj, S.T. Cundiff. Two-dimensional Fourier-transform spectroscopy of potassium vapor. Physical Review A 82, 052503 (2010).
[7] K.E. Dorfman, F. Schlawin, S. Mukamel. Nonlinear optical signals and spectroscopy with quantum light. Rev. Mod. Phys., 88, 045008 (2016).
[8] Е.А. Степанов, А.Н. Жданов, И.В. Савицкий, П.Б. Глек, А.А. Ланин, А.Б. Федотов, А. М. Желтиков. Широкополосная двумерная спектрохронография с использованием сверхкоротких импульсов среднего инфракрасного диапазона. Квантовая электроника, 52, 227 (2022).
[9] Е.А. Степанов, Г.Д. Иванов, А.Н. Жданов, А.А. Воронин, А.С. Шведов, И.В. Савицкий, А.А. Ланин, А.Б. Федотов. Широкополосная двумерная инфракрасная спектроскопия с регистрацией сигнала в видимой области спектра в процессе нелинейно-оптического преобразования частоты. Оптика и спектроскопия, 131, 1001 (2023).

Optical properties and applications of InAs(P,N,Bi)-based nanowires

A. Kaveev[1,2], I. Mukhin[2,3], V. Fedorov[2,3], A. Pavlov[2,3], D. Miniv[2], D. Kirilenko[1,3], A. Nadtochiy[4], A. Goltaev[2], R. Ustimenko[3], D. Karaulov[3], E. Moiseev[2,4], M. Vinnichenko[3]

1- Ioffe Institute, St. Petersburg, 194021 Russia
2- St. Petersburg Academic University, St. Petersburg, 194021 Russia
3- Peter the Great St. Petersburg Polytechnic University, St. Petersburg, 195251 Russia
4- HSE University Saint Petersburg, International Laboratory of Quantum Optoelectronics, St. Petersburg, 194100 Russia

e-mail: kaveevandrei@yandex.ru

InAs(P,N,Bi)-based nanoheterostructures are in great demand in mid-infrared photonics for telecom and sensing applications. While the vapor–liquid–solid grown nanowires have demonstrated the potential to control the crystal phase and vary the InAs(P,N,Bi) alloy composition in a wide range, the use of a foreign gold catalyst adversely affects their optoelectronic properties. Here we address the limitations of a catalyst-free approach, revealing that self-induced InAs(P,N,Bi) nanowires with a high P-content of 49%, greater than that previously reported, can be grown on silicon wafers via solid-source plasma-assisted molecular beam epitaxy on a SiOx / Si (111) substrate. The interplay between arsenic, phosphorus and nitrogen incorporation was studied, revealing that an increased phosphorus flux suppresses the nanowire axial growth rate, decreasing the length to diameter aspect ratio. It was shown that Bi can be incorporated into nanowires during their growth providing InAsBi alloy and can be considered as a catalyst providing the axial growth.

The relationship between the InAs(P,N) nanowire composition and crystal structure was studied using transmission electron microscopy and X-ray diffraction reciprocal space mapping. It was found that, for all compositions achieved, nanowires grow in a random hexagonal wurtzite phase. In the case of InAsBi nanowires monocrystalline sphalerite structure can be obtained.

Low-temperature photoluminescence studies and *ab initio* density functional theory calculations were performed to evaluate the dependence of the bandgap on the structure and composition of the InAs(P,N,Bi) alloys. Room temperature photoluminescent response at wavelengths as short as 1480 nm was demonstrated, revealing the suitability of grown nanowires for applications in photobiology and remote sensing. Additional passivation of the nanowire surface with InP leads to a decrease in the intensity of nonradiative recombination and an improvement in the photoluminescent response of the nanowires, which makes it possible to detect photoluminescence emission at room temperature.

The obtained experimental results indicate that by introducing nitrogen, phosporous or bismuth and changing their concentration, as well as by forming a core / shell structure based on InAs nanowires, it is possible to significantly control the efficiency and sensitivity limit of photosensitive devices developed on their basis.

The NW synthesis and study are financially supported by the project of the Ministry of Education and Science of the Russian Federation (state assignment No. FSEG-2023-0016)

Nonlocal photonics of spatially confined media

S. Kharintsev, E. Battalova, A. Minibaev

Department of Optics and Nanophotonics, the Leader of Quantum Photonics and Metamaterials Lab, Institute of Physics, Kazan Federal University, Kremlevskaya str. 16a, Kazan, 420008 Russia.

e-mail: skharint@gmail.com

Nonlocal photonics is an emerging field in optics that studies the interaction of light and matter with strong spatial dispersion. Spatial dispersion (or spatial nonlocality) can drastically change the principles of light-matter interaction. In nonlocal media, electron-photon momentum matching can be achieved, leading to indirect optical transitions. These phenomena are governed by structural inhomogeneities that provide spatial localization of photons.

Examples of nonlocal media are perovskites, spinels, liquid crystals, colloidal systems, high-entropy crystals, ceramics, amorphous and porous materials, polymers, water, micelles, proteins, etc. [1]

In this talk, we consider such semiconductors as silicon [2, 3] and metal-halide perovskites [4], in which electron scattering of light is observed [1, 2, 4]. Similar effects are demonstrated in free and spatially confined water. It will be shown that broadband inelastic radiation causes an anomalous increase in the refractive index of heterogeneous media, an increase in electrical conductivity and leads to their optical heating [5]. This talk will consider some applications in the field of optoelectronics, biomedicine and renewable energy.

[1] S. S. Kharintsev, E. I. Battalova, V. Mkhitaryan, V. M. Shalaev. How near-field photon momentum drives unusual optical phenomena: opinion // Optical Materials Express, – V. 14. – P. 2017–2022, (2024).
[2] S. S. Kharintsev, E. I. Battalova, A. I. Noskov, J. Merham, E. O. Potma, D. A. Fishman. Photon-Momentum-Enabled Electronic Raman Scattering in Silicon Glass // ACS Nano, – V. 18. – P. 9557–9565, (2024).
[3] S. S. Kharintsev, A. I. Noskov, E. I. Battalova, L. Katrivas, A. B. Kotlyar, J. G. Merham, E. O. Potma, V. A. Apkarian, D. A. Fishman. Photon Momentum Enabled Light Absorption in Silicon // ACS Nano, – V. 18. – P. 26532–26540, (2024).
[4] S. S. Kharintsev, E. I. Battalova, I. A. Matchenya, A. G. Nasibulin, A. A. Marunchenko, A. P. Pushkarev. Extreme Electron-Photon Interaction in Disordered Perovskites // Adv. Sci., – V. 11. – P. 2405709, (2025).
[5] S. S. Kharintsev, E. I. Battalova, I. Heat Generation in Spatially Confined Solids Through Electronic Light Scattering // Nanophotonics, 2025 (accepted).

Raman bands about 850 cm^{-1} as universal marker of *gauche*-conformers in molecular backbones of ethylene glycol, 1,3-propylene glycol and polyethylene glycols

L. Yu. Kozlova[1], V. V. Kuzmin[1], M. O. Bosyukh[2], L. Yu. Ustynyuk[2], G. Yu. Nikolaeva[1], V. S. Novikov[1]

1- Prokhorov General Physics Institute of the Russian Academy of Sciences, Vavilov str. 38, Moscow, 119991 Russia
2- Chemistry Department, M. V. Lomonosov Moscow State University, Moscow, 119991 Russia

e-mail: vs.novikov@kapella.gpi.ru

Simplest glycols, such as ethylene glycol (EG) and 1,3-propylene glycol (1,3-PG), and higher-molecular-weight glycols, such as polyethylene glycols (PEGs), are widely used in numerous areas, including pharmaceutical, cosmetic, food, and chemical industries. Aqueous solutions of low-molecular-weight glycols are used as heat transfer agents, antifreezes, de-icing fluids, cryoprotectants.

Solid PEGs have semicrystalline structure with predominant molecular conformation of helix 7_2 and monoclinic crystalline lattice. Molecules of liquid glycols can adopt multiple conformations with relative contents depended on environmental conditions. Evaluation of the molecules conformational composition is very important because of strong dependence of the structure and properties of glycol-containing systems on this characteristic.

Raman spectroscopy is powerful technique to evaluate the conformational composition of molecules. However, determination of the relative contents of molecules in numerous conformations is quite complex task. For rapid, but representative analysis, it is convenient to choose a parameter, which gives some average quantitative characteristic of the conformational composition.

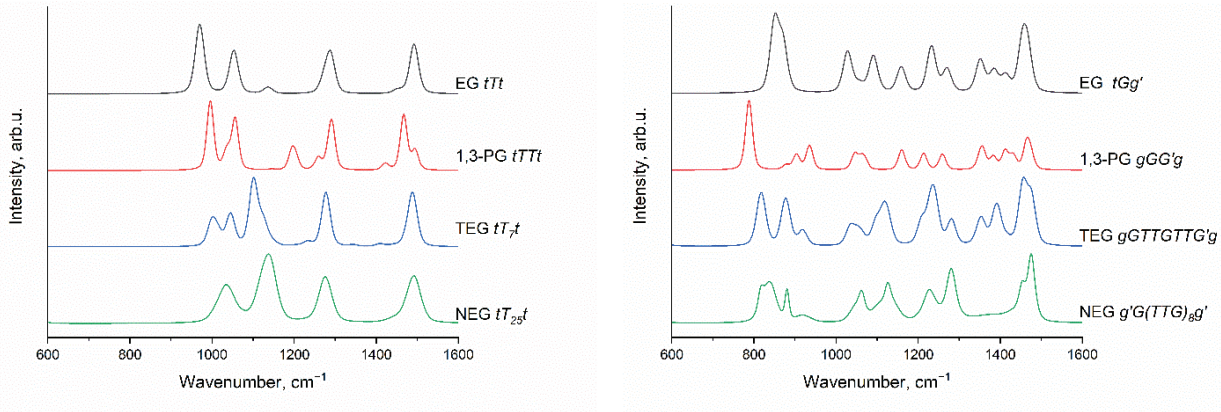

Fig. 1. Calculated (OLYP/4z, gas phase approximation) Raman spectra of molecules of EG, 1,3-PG, triethylene glycol (TEG) and nonaethylene glycol (NEG) in the *all-trans* conformation (left) and the conformation with the minimal energy (right).

Based on quantum-chemical modeling we revealed that the Raman spectra of the molecules of EG, 1,3-PG and oligomers of EG in the *all-trans* conformation do not contain any bands in the region about 850 cm^{-1} (Fig. 1). On the examples of EG and 1,3-PG, we showed that the spectra of the molecules in all the conformation with *gauche*-conformers in the molecular backbones contain noticeable bands in the region about 850 cm^{-1}. The bands at about 1450 cm^{-1} are the deformation vibrations of CH_2 groups, they depend less significantly on the conformational composition and can be used as the reference bands. Thus, we propose to use the ratio of intensities of the bands at about 850 and 1450 cm^{-1} as a measure of the content of *gauche*-conformers in molecular backbones of EG, 1,3-PG and PEGs. Taking into account that the wavenumbers and intensities of the bands about 850 cm^{-1} depend on the type of conformation, more detailed analysis of the conformational composition can be carried out.

This study was supported by the Russian Science Foundation under the grant №25-22-20065, https://rscf.ru/project/25-22-20065/.

Anharmonic phonon decay and electron-phonon coupling in topological insulators revealed by Raman spectroscopy

N. Kumar[1,2], A. S. Krylov[3], S. N. Krylova[3], D. V. Ishchenko[1], I. A. Milekhin[1,4], A. V. Korsakov[5], A. G. Milekhin[1,4], O. E. Tereshchenko[1,4]

1- Rzhanov Institute of Semiconductor Physics, SB RAS, Novosibirsk, 630090 Russia
2- Tomsk State University, Lenin ave. 36, Tomsk, 634050 Russia
3- Kirensky Institute of Physics, Federal Research Center KSC SB RAS, Krasnoyarsk, Russia
4- Novosibirsk State University, Novosibirsk, 630090 Russia
5- V. S. Sobolev Institute of Geology and Mineralogy, SB RAS, Novosibirsk, 630090 Russia

e-mail: kumar@isp.nsc.ru

This work employed resonantly excited, temperature-dependent and polarization-resolved Raman scattering spectroscopy to investigate the surface and bulk vibrational modes of Bi_2Te_3 and $Bi_{2-x}Sb_xTe_{3-y}Se_y$ (BSTS) topological insulator thin films, revealing critical insights into their electronic and phononic interactions. Near-resonant excitation at 1.57 eV above the Fermi energy confirmed the existence of unoccupied surface states in Bi_2Te_3, which enhanced electron-phonon coupling and induced a resonant enhancement of the A^1_{1g} (LO) mode, while in BSTS, a stronger resonance of this mode at 2.54 eV was attributed to bulk interband electronic transitions. The low-energy A^1_{1g} (LO) phonon mode exhibited minimal temperature sensitivity, whereas the high-energy A^2_{1g} (LO) mode demonstrated significant intensity reduction and linewidth broadening, reflecting an increased phase space for multiphonon decay processes (3-phonon and 4-phonon scattering) at elevated temperatures due to enhanced anharmonic interactions. The E^2_g mode in topological insulators showed weak temperature dependence in Raman spectra because its in-plane vibrations couple weakly with thermal phonons, while lower energy A^1_{1g} mode restricts phase space for anharmonic decay by limiting available phonon combinations that conserve both energy and momentum, thereby reducing thermal broadening and intensity variations. Temperature-dependent Raman studies further uncovered three distinct phonon scattering regimes: a quadratic increase in optical phonon linewidth at $k_BT \ll \Theta_D$ (electron-phonon scattering), linear behavior near $k_BT \sim \Theta_D$ (3-phonon scattering), and a nearly inverse quadratic trend at $k_BT \gg \Theta_D$ (4-phonon scattering), demonstrating the dynamic evolution of phonon interactions across thermal regimes. The stronger electron-phonon coupling in BSTS ($\lambda = 0.28$) compared to Bi_2Te_3 ($\lambda = 0.23$) led to enhanced momentum scattering of Dirac fermions, reducing conductivity ($\sigma \propto 1/\lambda$) while suggesting to potentially improving thermoelectric efficiency, an effect likely originating from larger electron-phonon matrix elements influenced by topological surface states or defects, particularly near Dirac points where scattering effects are most pronounced. These findings collectively provide a comprehensive understanding of the interplay between electronic transitions, phonon dynamics, and scattering mechanisms in topological insulators, offering critical insights for optimizing their performance in quantum devices and thermoelectric applications.

In-situ chemical sensing by laser induced breakdown spectroscopy

V. N. Lednev, P. A. Sdvizhenskii, A. V. Rogachevskaya

Prokhorov General Physics Institute, Russian Academy of Science, Moscow, Russia

e-mail: lednev@kapella.gpi.ru

The in-situ sensing is essential for control systems development due to advancing new complicated technologies such as microelectronics technologies and the additive manufacturing, wherein component failure cannot be tolerated (such as the aerospace industry). These technologies are based on complicated and multiparametric processes making feedback a mandatory requirement to ensure stable processing and high-quality products. Multiple instrumental techniques (e.g., machine vision, pyrometry, acoustic sensing) have been suggested for on line monitoring but chemical composition quantification remains challenging in modern industry applications [1]. According to the in-situ sensing requirements, the quantitative elemental analysis should be carried out within a few seconds so any sample preparation is not possible thus the majority of analytical techniques cannot be utilized. Laser induced breakdown spectroscopy (LIBS) is a good candidate to win this challenge due to the absence of sample preparation and remote sensing capability. A brief review of in-situ LIBS was presented with focusing on recent achievements in industrial applications. Some examples of spotlights are provided: additive manufacturing and welding processes diagnostics by LIBS to reveal chemical composition in a key spot (melt pool) [2]. Large datasets study of LIBS signals revealed that signals distribution functions are biased from a Gaussian profile so the careful data processing by statistical methods is required to achieve reliable results [3].

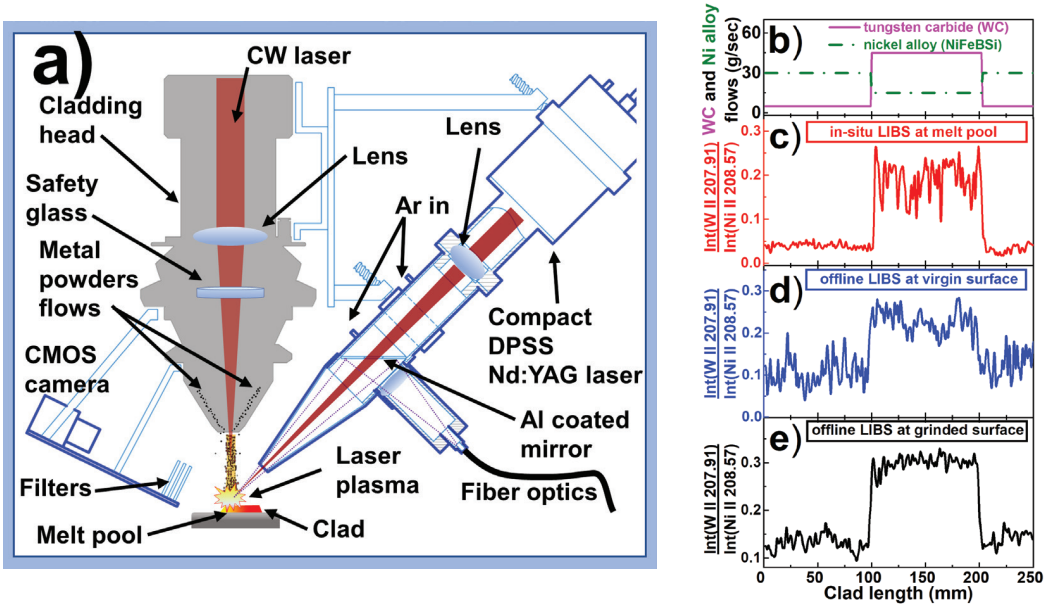

Fig. 1. Scheme of the in-situ chemical analysis by laser induced breakdown spectroscopy (LIBS) in additive manufacturing (a). LIBS measurements for clad synthesized with varying concentrations of NiFeBSi and WC: (b) – flows of tungsten carbide (WC) and NiFeBSi powders; (c) – in-situ LIBS inside melt pool; (d) – offline LIBS of solid clad; (e) – offline LIBS after surface grinding.

The authors gratefully acknowledge financial support from the Russian Science Foundation (RSF) (agreement № 25-29-00835), https://rscf.ru/en/project/25-29-00835/.

[1] S.K. Everton, et al., Review of in-situ process monitoring and in-situ metrology for metal additive manufacturing, Materials & Design, vol. 95, pp. 431–445 (2016).
[2] V.N. Lednev, et al., In situ multi-elemental analysis by laser induced breakdown spectroscopy in additive manufacturing, Addit. Manuf., vol. 25, pp. 64–70 (2019).
[3] V.N. Lednev, et al., LIBS signals statistics for gated and time-integrated acquisition, Spectroch Act. B, vol. 228, p.107181 (2025).

Optically pumped magnetometers: physical principles, applications and prospects

A. O. Makarov[1,2], K. S. Kozlova[1,2], D. V. Brazhnikov[1], A. N. Goncharov[1–3]

1- Institute of Laser Physics SB RAS, Lavrentyev Avenue 15B, Novosibirsk, 630090 Russia
2- Novosibirsk State University, Pirogov Street 1, Novosibirsk, 630090 Russia
3- Novosibirsk State Technical University, Karl Marks Avenue 20, Novosibirsk, 630073 Russia

e-mail: werklore@mail.ru

High-sensitivity atomic magnetometers (AMs) have found many applications in fundamental physics (e.g., search for the dark matter or the permanent electric dipole moment of the neutron) as well as in applied sciences: medicine, biology, geophysics, space missions, etc. These quantum devices are based on laser spectroscopy of alkali-metal vapors and demonstrate sub-picotesla sensitivity. State-of-the-art high-sensitivity miniature AMs employ rubidium or cesium atoms, operating in the suppressed spin-exchange relaxation (SERF) regime. This regime requires a relatively high vapor cell temperature (150–200 °C), limiting the scope of applications.

In this paper, two novel methods for monitoring magneto-optical resonances in miniature (~0.1 cm^3) alkali-metal vapor cells at temperatures less than 90 °C are proposed. The first one concerns the Bell-Bloom method [1, 2] of scalar magnetic field measurements. This method commonly uses a modulated light beam with circular polarization. We propose to use an elliptically polarized beam and a polarimeter to monitor a change in the beam's ellipticity which is caused by circular dichroism in the medium (Fig. 1a). In our experiments, we use a buffer-gas-filled 5 mm long ^{87}Rb vapor cell. The second method (Fig. 1b) is a modification of the Hanle technique (zero-field level crossing resonances) [3, 4]. In both methods, an elliptically polarized resonant light beam is used, and the resonances are detected in the change of the ellipticity parameter of the beam.

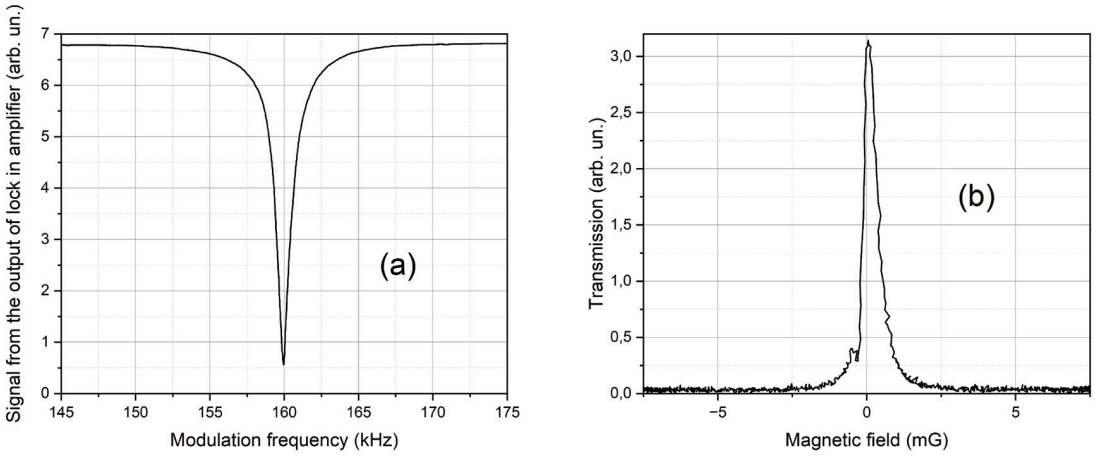

Fig. 1. Magneto-optical resonances, observed in the change in ellipticity of a light wave: (a) Bell-Bloom resonance, (b) Hanle resonance

The achieved reduction in the operating temperature of the sensor is extremely important for some applications, especially for medical diagnostics. The shot-noise limited sensitivity of magnetic-field measurements in the proposed schemes is of the order of 10 fT/√Hz, which compete with the best commercial AMs operating in the SERF regime.

The work was supported by Russian Science Foundation (Grant no. 23-12-00195).

[1] A. Makarov, K. Kozlova, D. Brazhnikov, V. Vishnyakov, A. Goncharov, Optics Communications, vol. 577, p. 131369, (2025).
[2] W. E. Bell and A. L. Bloom, Phys. Review Letters, vol. 6, p. 280, (1961).
[3] A.O. Makarov, D.V. Brazhnikov, A.N. Goncharov, JETP Letters, vol. 117, p. 509 (2023).
[4] E. B. Aleksandrov, A. M. Bonch-Bruevich, V. A. Khodovoi, Optics and Spectroscopy, vol. 23, p. 151 (1967).

Application of multi-excitation ultraviolet fluorescence spectroscopy for brain cells studying

N. Maslov[1], N. Gubanova[2]

1- Khristianovich Institute of Theoretical and Applied Mechanics SB RAS, Novosibirsk, Russia
2- Institute of Cytology and Genetics SB RAS, Novosibirsk, Russia

e-mail: nmaslov@itam.nsc.ru

Multi-excitation fluorescence spectroscopy allows for the characterization of the distribution of fluorophores in samples of various origins and is a powerful tool for chemical, biological, and medical diagnostics. The use of ultraviolet radiation leads to the simultaneous excitation of multiple fluorophores. Using a laser with a tunable wavelength allows manipulation of fluorophores' contributions by measuring laser-induced fluorescence (LIF) excitation-emission matrices (EEM), and gathering additional diagnostic information. One of the promising tasks for ultraviolet LIF spectroscopy is the identification of brain tumor tissues, in particular gliomas, for which accurate intraoperative determination of the border is a critical factor. It is known that tryptophan plays an important role in tumor cell metabolism, and at the same time, it is the main intrinsic fluorophore present in biological tissues. Its fluorescence behavior depends on its molecular surroundings and can be registered by spectroscopic methods. At the same time, bulk tissue diagnostics is complicated by several factors. The multilayer structure of biological tissues, fluorescence of surrounding cell media, possible presence of unidentified fluorophores, significant overlap of fluorophores' emission spectra, and their possible instability make qualitative and especially quantitative estimation of tissue properties problematic. To simplify the analysis, model studies were carried out using glioblastoma cell line U87MG and primary cell culture of human brain.

The EEMs of the samples under study were measured using a tunable OPO laser system and spectrometer. The excitation wavelength was scanned in the 210–290 nm region with 10 nm steps. Fluorescence was registered in the 295–800 nm spectral region. Using the MTT assay and LIF spectroscopy, it was shown that there is a dose-dependent toxic effect of laser radiation affecting the viability of cells in culture and their spectral properties. Nevertheless, at radiation doses below 10 mJ/cm^2, no toxic effects were detected, and the LIF spectra did not change. Such energy levels are more than enough to measure multiple fluorescence spectra, making them suitable for diagnostics. All spectra had one dominant peak, which can be attributed to tryptophan, but its shape was wavelength-dependent, and its maximum may shift in the 222–230 nm region. These features indicate that several fluorophores are present in the samples, and they are initially unknown. Several statistical methods are appropriate for EEM spectral decomposition, but they either give ambiguous solutions or are applicable only for optically thin samples. In real practice, various inner filtering effects do not allow the use of these methods directly and require appropriate prior correction specific for each sample. Assuming that fluorescence reabsorption is negligible, we iteratively found appropriate correction coefficients for excitation variations using the least squares method for their calculation and principal component analysis. Due to the correlated nature of EEM, this allowed us to decompose them without any assumptions about light illumination and collection geometry. Model experiments with simulated spectral data and real fluorophores showed good agreement between the calculated spectra and real fluorescence spectra of the pure substances. Experiments with various optical depth cell suspensions also showed that this approach allows for spectral decomposition for thick samples. Two spectral components were found, and their relative contributions depended on cell type and viability. The developed approaches and measured characteristic spectra can be used as a basis for the LIF analysis of more complex tissues.

The research was funded by Russian Science Foundation (project No. 24-22-20078) with financial support from the Government of the Novosibirsk Region.

Nanoscopy of semiconductor nanostructures

A. G. Milekhin[1], I. A. Milekhin[1,2], N. N. Kurus[1], L. S. Basalaeva[1], A. V. Taranenko[1], R. B. Vasiliev[3], L. N. Dvoretckaia[4], I. S. Mukhin[4], A. V. Latyshev[1,2], E. O. Chiglintsev[5,6], A. I. Chernov[5,6], D. R. T. Zahn[7]

1- A. V. Rzhanov Institute of Semiconductor Physics, Lavrentjev av. 13, Novosibirsk, 630090 Russia
2- Novosibirsk State University, Pirogov str. 1, Novosibirsk, 630090 Russia
3- Department of Material Science, Moscow State University, Moscow, Russia
4- Alferov University, Khlopina st. 8, St. Petersburg, 194021 Russia
5- Russian Quantum Center, Skolkovo Innovation City, 194021 Moscow, 121205 Russia
6- Center for Photonics and 2D Materials, Moscow Institute of Physics and Technology, Dolgoprudny, 141700 Russia
7- Semiconductor Physics, Chemnitz University of Technology, Chemnitz, D-09107 Germany

e-mail: milekhin@isp.nsc.ru

Nanoscopy including Tip-enhanced Raman scattering and Photoluminescence (TERS and TEPL, respectively) takes advantages of structural methods such as Atomic Force or Scanning Tunneling Microscopies (AFM or STM) and optical techniques (conventional Raman scattering and Photoluminescence) and allows studying the phonon and electron spectra of semiconductor nanostructures with the nanometer spatial resolution.

Here, the results of TERS and TEPL studies of 0D, 1D, and 2D semiconductor nanostructures are presented. Comparison of TERS and TEPL spectra and hyperspectral images with AFM maps of the nanostructures provides information of their local properties such as built-in mechanical strain or structural defects, and emission properties.

AFM maps, TERS, TEPL spectra and images were obtained using an AFM AIST-NT coupled with a Raman spectrometer (Xplora, Horiba). All PL and Raman spectra were recorded using an objective (100×, 0.7 NA) at normal light incidence under laser excitation with a wavelength of 532, 638, and 785 nm at room temperature. Self-made TERS probes metallized with Au or Ag/Au were used in the experiments.

CdSe nanocrystals with a size of 6 nm deposited of Au nanodisks were used to establish the mechanism of TERS enhancement and distribution of local electric field in the vicinity of Au nanodisks [1]. Structure peculiarities in single GaAs nanocrystal (NC) of different size were studied with a spatial resolution of about 10 nm in TERS and TEPL experiments. TERS by vibrational modes from arsenic nanoclusters allows their spatial distribution over the GaAs NC surface was established.

TEPL and TERS images of single GaAs, AlN, and GaP nanocolumns with a spatial resolution of about 10 nm were obtained. The role of localized surface plasmon originated at metallized TERS tip as well as the tip coatings for visualization of semiconductor nanostructures is discussed. The importance of the laser radiation polarization for analysis of TERS images of AlN nanocolumns is emphasized.

Resonant gap-mode TERS and TEPL of atomically thin MoS_2, graphene and multigraphene flakes [2] on the plasmonic (Au) nanodisks with strong enhancement factors were realized. The energies of phonon and exciton modes derived from TERS and TEPL spectra of the 2D nanostructures, provide detailed information on their structural defects and built-in mechanical strain with a spatial resolution down to 2 nm.

This work was supported by the Russian Science Foundation (project 22-12-00302).

[1] I.A. Milekhin, M. Rahaman, A.V. Tsarev, K.V. Anikin, E.E. Rodyakina, T.A. Duda, B.M. Saidzhonov, R.B. Vasiliev, A.G. Milekhin, A.V. Latyshev, D.R.T. Zahn, Applied Surface Science, vol. 686, p.162144, (2025).
[2] N.N. Kurus, V. Kalinin, N.A. Nebogatikova, I.A. Milekhin, I.V. Antonova, E.E. Rodyakina, A.G. Milekhin, A.V. Latyshev, D.R.T. Zahn, RCS Advances, 14, pp. 3667–3674 (2024).

Nonlinear-optical diagnostics of structures with inhomogeneous magnetization

T. V. Murzina, V. B. Novikov, I. A. Kolmychek

Department of Physics, M. V. Lomonosov Moscow State University, Leninskie Gory, Moscow, 119991 Russia

e-mail: murzina@mail.ru

The inhomogeneity of material properties of various types of optical structures is commonly perceived as a small correction, which has a little effect on their functional properties and is neglected in most of the studies. At the same time, inhomogeneity is inevitable for nanostructured media and can provide exciting new properties, such as hyperbolic dispersion for the case of anisotropic metal-dielectric nanocomposites [1] or giant magnetoresistance in various types of magnetic ones [2]. A special place belongs to magnetic composite structures, which provide an excellent platform for the development of functional materials with improved properties. On the other hand, in view of extra possibilities provided by modern fabrication technologies, nowadays one can study new physical phenomena specific for magnetic composite structures of special design. Nonlinear optics plays a significant role in these studies due to its high sensitivity to all types of symmetry breaking of a medium or structure, including magnetic ones [3]. The second important property of nonlinear optical processes, such as optical second harmonic generation (SHG), consists in high relative values of the magnetization-induced modulation of the nonlinear response as compared to the linear magneto-optical case, which allows to study tiny magnetic effects inaccessible to linear optics.

In this work we review our recent studies of a number of effects that appear in the linear and nonlinear optical responses of structures with inhomogeneous magnetization. Different types of structures are considered, including (i) domain structure in pristine epitaxial garnet films and of that modified by regular 1D or 2D surface arrays of planar structures made of ferromagnetic metals, (ii) surface arrays of cobalt triangular-shape submicron particles with vortex magnetization on quartz substrate, (iii) a few nanometer thick Co/Pt bilayer film. The experiments are performed using the nonlinear optical microscopy technique providing a submicron spatial resolution, or in a common scheme of transmitted or reflected SHG when a surface area of about 30 mm in diameter is illuminated; as the pump source the radiation of a femtosecond Ti-sapphire laser was used. For all the structures linear optical and magnetooptical effects were compared to nonlinear optical ones.

We demonstrate that, due to a complicated spatial distribution of magnetization in domains and domain walls of rare-earth garnet films, the SHG response attained for different combinations of linearly polarized fundamental and SHG waves allows to visualize not only bulk stripe domains, but also the surface closure ones. Moreover, in-depth thickness of the latter was estimated through the SHG microscopy studies. We observe the pinning effect of the bulk stripe domains of garnet in the presence of a surface lattice of ferromagnetic particles or stripes. This effect appears as a variation of the domains width close to the periods of the external ferromagnetic lattice; the relative variation of this parameter being up to several percent. Another evidence of pinning is the azimuthal tilt of the domains' orientation relative to the external magnetic field due to their arrangement along the Co/Au stripes. In arrays of cobalt triangular-shaped particles on a nonmagnetic substrate the contribution of the macroscopic toroidal moment of magnetization to the SHG response was found. Its value reaches 20% of the non-magnetic component of the SHG intensity and can be observed clearly with circularly polarized laser radiation. Finally, in the case of a bilayer film consisting of a ferromagnetic (cobalt) and heavy (platinum) metals we suggested and experimentally observed a new mechanism of the second-order nonlinear response associated with magnetization dynamics induced by the magnetic field of an intense femtosecond laser pulse. It can provide the SHG contribution comparable with the common magnetization-induced effect.

This work was supported by RSF Grant No. 19-72-20103-P.

[1] A. Poddubny, I. Iorsh, P. Belov, Y. Kivshar, Hyperbolic metamaterials, Nature Photonics, vol. 7, pp. 958–967 (2013).
[2] G. Binasch, P. Grünberg, F. Saurenbach, W. Zinn, Enhanced magnetoresistance in layered magnetic structures with antiferromagnetic interlayer exchange, Phys. Rev. B, vol. 39, pp. 4828–4830 (1989).
[3] R.-P. Pan, H. D. Wei, Y. R. Shen, Optical second-harmonic generation from magnetized surfaces, Phys. Rev. B, vol. 39, p. 1229 (1989).

Use of neural network generated spectra to improve solution of spectroscopy inverse problem

A. Mushchina[1,2], I. Isaev[1], S. Burikov[1,2], T. Dolenko[1,2], S. Dolenko[1]

1- D. V. Skobeltsyn Institute of Nuclear Physics, M. V. Lomonosov Moscow State University
2- Physical Department, M. V. Lomonosov Moscow State University

e-mail: dolenko@srd.sinp.msu.ru

From the point of view of data processing, the main problem in spectroscopy is solving inverse problems (IP) that consist of restoring the target parameters of the studied object by its spectra. Problems of such kind often possess well-know negative properties hampering solving them – they are often ill-posed or even incorrect, due to low stability and non-uniqueness of their solution.

Besides that, additional properties inherent to most spectroscopic inverse problems are their high input dimension (a large number of channels in the spectrum) and non-linearity, making solving them with conventional IP solution methods too complex, computationally expensive or even impossible with adequately low error. For this reason, an alternative class of methods effective in solving IP are machine learning (ML) methods, which can often cope well with the listed difficulties.

However, ML methods suffer from their own difficulties, the main of which is need of a large enough amount of data required to train ML models. Meanwhile, obtaining experimental spectroscopic data is often expensive, requiring high-cost equipment, reagents and high qualification of the personnel.

Leaving aside use of special methods to reduce input dimensionality of spectra, in this study we concentrate on an alternative approach: expanding the experimental set of spectra with model spectra, calculated or generated. The main criterion of success here is reduction of IP solution error on a separate independent set of experimental data when ML models are trained on the expanded training dataset.

Unfortunately, in this situation most of the commonly used methods of obtaining extra data usually fail. Interpolation among the experimental spectra may easily produce non-physical spectra that cannot be obtained in experiment. Applying noise to experimental spectra may increase noise resilience of ML models [1], but it cannot reduce the IP solution error. Finally, direct expanding of the dataset with spectra obtained in other experiments is impossible without applying special domain adaptation procedures due to differences in experimental conditions among various experiments, resulting in extra variations in the data that do not allow improving the IP solution quality.

In this study, we investigate use of generation of additional spectra by a special architecture of artificial neural networks – variational autoencoders (VAE) [2]. This type of neural networks first encodes an experimental spectrum into a space of lower dimension (latent space) and then decodes it back to the space of the initial spectra. A special training procedure provides similarity of the decoded spectra to the spectra of the initial set, and also makes the distribution of the spectra in the latent space close to normal distribution. This allows using the decoder part of the VAE to generate model spectra from data points sampled from the latent space, and the distribution of such model spectra turns out to be close to the distribution of experimental spectra also in the initial spectra space. This gives hope that expanding the training set of experimental spectra with such model spectra could improve the result of IP solution.

In this study, we compare use of conventional VAE and the so-called conditioned VAE [3, 4], and we generate model spectra from normal and from uniform distribution in the latent space. The spectroscopic task is to simultaneously determine the concentrations of 8 ions (Cu^{2+}, Ni^{2+}, Fe^{3+}, Zn^{2+}, Li^{+}, NH_4^{+}, SO_4^{2-}, NO_3^{-}) in multi-component aqueous solutions by their optical absorption spectra.

It is demonstrated that expanding the training set of data with model spectra generated by VAE from uniform distribution in the latent space provides reduction of IP solution error, statistically significant for Zn^{2+} and Li^{+} ions. Therefore, the studied approach is promising, and it needs further study.

This study has been performed at the expense of Russian Science Foundation grant no. 24-11-00266, https://rscf.ru/en/project/24-11-00266/.

[1] I. Isaev et al, Lectures Notes in Computer Science, vol.11139, pp. 435–444, (2018). DOI 10.1007/978-3-030-01418-6_43
[2] D.P. Kingma and M. Welling, Foundations and Trends in Machine Learning, vol.12(4), pp. 307–392, (2019). DOI 10.1561/2200000056
[3] K. Sohn, X. Yan, H. Lee, Learning structured output representation…, Advances in Neural Information Processing Systems, vol.28, (2015).
[4] A. Efitorov et al, Studies in Computational Intelligence, vol.1064, pp. 557–565, (2023). DOI 10.1007/978-3-031-19032-2_56

Raman spectral study of near-surface ice-like layer formation in water at room temperature

S. M. Pershin[1], P. S. Smerchansky[2], M. Ya. Grishin[1]

1- Prokhorov General Physics Institute of the Russian Academy of Sciences, Vavilova street 38, Moscow, 119991 Russia
2- National Research University "Higher School of Economics", Myasnitskaya street 20, Moscow, 101000 Russia

e-mail: mikhail.grishin@kapella.gpi.ru

It has been noticed by a number of researchers that liquid water tends to form spontaneously a near-surface layer with properties different from that of bulk water. For example, the authors of [1] have observed the formation of a "clear zone" near the water surface in a water suspension of polystyrene microspheres. Optical studies on stimulated Raman scattering of nanosecond [2] and picosecond [3] laser pulses have revealed that in the presence of an optical breakdown caused by focusing the laser beam at the water surface, a characteristic spectral band of ice appears in the Raman spectrum of liquid water at room temperature.

In this work we present the results of our recent experiments on Raman spectroscopy of near-surface water layer. Spontaneous Raman scattering measurements have been carried out using low energy laser pulses (Nd^{3+}:YLF, 527 nm, 10 ns, 100 μJ/pulse, 12 Hz) that do not produce optical breakdown and thus do not disturb the sample (unlike the above-mentioned studies [2, 3]). We have observed the Raman OH band shift by ~10 cm^{-1} towards the characteristic ~3200 cm^{-1} ice band in liquid water when focusing the laser beam near the surface compared to the case of focusing in bulk water. It should be noted that the detected OH band shift formed during ~2 hours after filling the sample cuvette (see Fig. 1).

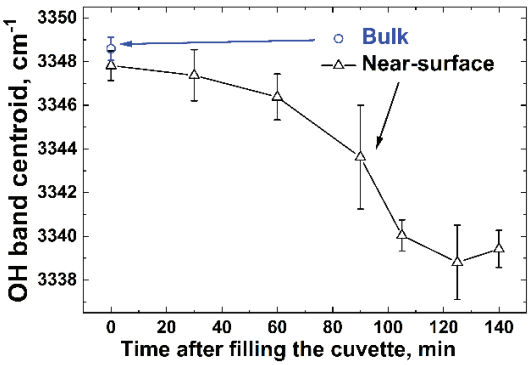

Fig. 1. Time dependence of the water Raman OH band centroid in the near-surface layer.

The presented results are in consistence with our previous findings: the formation of ice-like hydrate shells of SiO_2 nanoparticles in water suspension [4].

The authors acknowledge the financial support of the Russian Science Foundation (grant no. 23-42-10019).

[1] K. Ovchinnikova and G.H. Pollack, Cylindrical phase separation in colloidal suspensions, Physical Review E, vol. 79, 036117 (2009).
[2] Z. Men, W. Fang, Z. Li et al., Hydrated-electron resonance enhancement O-H stretching vibration of water hexamer at air-water interface, Optics Letters, vol. 40, pp. 1434–1437 (2015).
[3] H. Yui, H. Fujiwara, T. Sawada, Spectroscopic analysis of total-internal-reflection stimulated Raman scattering from the air/water interface under the strong focusing condition, Chemical Physics Letters, vol. 360, pp. 53–58 (2002).
[4] S.M. Pershin, A.F. Bunkin, M.A. Davydov et al., Ice-like structure of the hydrate shell of quartz nanoparticles in an aqueous suspension, JETP Letters, Vol. 121, pp. 84–88 (2025).

Chemiluminescence enhancement inside an open nanocavity for oxidation stress sensing

N. S. Petrov, D. R. Dadadzanov, T. A. Vartanyan

ITMO University, Kronverksky Pr. 49, bldg. A, St. Petersburg, 197101 Russia

e-mail: tavartanyan@itmo.ru

Chemiluminescence is a curious phenomenon widespread in nature, in particular, in the form of bioluminescence, and an important analytical technique that has found applications in forensic science, medical diagnostics and environmental monitoring. Of special interest is its ability to detect highly reactive free radicals, in particular, reactive oxygen species, that cannot be observed by other methods because of their very short life time. To further expand the use of chemiluminescence, it is necessary to increase its intensity. As the quantum yield of the most popular chemiluminescent probe – luminol – is rather low, about 0.01 [1], it is tempting to interfere with the final step of photon irradiation by alternating the dielectric environment of the reactive species. This approach, already termed as metal-enhanced chemiluminescence [2], employs nanostructured materials that strongly modify the density of photonic states in the close proximity of the radiating molecule. Accelerated in this way radiation transitions win the competition against nonradiative relaxation, thus ensuring the quantum yield growth.

Metal nanostructures in the form of thin films and periodic arrays of metal nanocylinder possessing localized surface plasmons resonance were considered as promising means of radiation transitions speed up [3, 4]. Unfortunately, the Purcell factor, which numerically characterizes the degree of acceleration of the radiative transition, strongly depends on the distance to the nanoparticles. Because of this, the proportion of reactants affected by the enhancement of the quantum yield is small. On the other hand, it is known that the field enhancement factor inside a spherical nanoshell made of plasmonic metal is homogeneous. The same is true for the local density of photonic states. Thus, the Purcell factor is homogeneous inside the shell as well. Of course, in order for reagents to enter and light to exit, the cavity must be open. In the hope that the density of photon states does not change too much when the cavity is open and nonspherical, we explored the spatial distribution of the radiation transition acceleration factor inside the reservoirs formed in the thin periodically perforated metal film.

The radiation intensity of a dipole located in different parts of cylindrical holes with diameters in the range from 10 to 60 nm in a thin aluminum film with a thickness of 5 to 40 nm was calculated using COMSOL Multiphysics® and compared with the radiation intensity of the same dipole in a homogeneous space with a refractive index of 1.33, corresponding to the refractive index of the aqueous medium in which the luminescent molecules are located. The boundary conditions were chosen to simulate a square lattice of holes with a period of 220 to 250 nm. The refractive index of the substrate on which the aluminum film was located was taken to be 1.46, which corresponds to the refractive index of fused quartz. The dispersion of the refractive index of quartz was not taken into account due to its smallness in the relevant wavelength range around 425 nm – the the maximum of luminol chemiluminescence. By varying the film thickness, the diameters of the holes and the grating period, we were able to tune the perforated aluminum film into resonance with the chemiluminescence spectrum of luminol and achieve a tenfold increase in the radiation intensity of the dipole inside the cylindrical hole compared to the radiation intensity in a homogeneous medium, and this increase changed slightly throughout the entire volume of the hole.

This study was supported by a grant from the Russian Science Foundation (Project 23-72-00045 https://rscf.ru/project/23-72-00045/).

[1] H.R. Schroeder and F.M Yeager, Chemiluminescence yields and detection limits of some isoluminol derivatives in various oxidation systems, Anal. Chem., vol. 50, pp. 1114–1120, (1978).
[2] K. Aslan and C.D. Geddes, Metal-enhanced chemiluminescence: advanced chemiluminescence concepts for the 21st century, Chemical Society Reviews, vol. 38, pp. 2556–2564, (2009).
[3] D.R Dadadzhanov, A.V. Palekhova, T.A. Vartanyan, Metasurface of aluminum nanocylinders to enhance the chemiluminescence of luminol, Optics and Spectroscopy vol.131, pp. 1646–1650, (2023).
[4] D.R Dadadzhanov, I. A. Gladskikh, M.A. Baranov, A. Karabchevsky, T.A. Vartanyan, Self-organized plasmonic metasurfaces: The role of the Purcell effect in metal-enhanced chemiluminescence (MEC), Sensors and Actuators B: Chemical. vol. 333, p. 129453 (2021).

Features of resonant Raman in ultrahard amorphous sp^3 carbon synthesized in the pressure range of 20–160 GPa and temperatures of 300–2300 K

M. Popov[1], F. Khorobrykh[2], S. Klimin[3], D. Ovsyannikov[4], A. Kvashnin[5]

1- Prokhorov General Physics Institute of the Russian Academy of Sciences, Vavilov str. 38, Moscow, 119991 Russia
2- Scientific and Technological Center of Unique Instrumentation, Russian Academy of Sciences, Butlerova str. 15, Moscow, 117342 Russia
3- Institute of Spectroscopy, Russian Academy of Sciences, Troitsk, Moscow, 108840 Russia
4- Federal State Budgetary Institution «Technological Institute for Superhard and Novel Carbon Materials of National Research Centre «Kurchatov Institute», Centralnaya str 7a, Troitsk, Moscow, 108840 Russia
5- Skolkovo Institute of Science and Technology, Bolshoy Boulevard 30, bld. 1, Moscow, 121025 Russia

e-mail: mikhail.yu.popov@mail.ru

The resonance phenomena of Raman scattering in carbon nanoclusters formed by sp^3 bonds have been studied. It is known that the Raman cross section for carbon materials formed by sp^2 bonds is 50 times higher than for sp^3 bonds when excited in the visible wavelength range, and the cross sections are equal when excited at ~257 nm (~5 eV). Another type of resonance phenomenon is observed in ultrahard amorphous carbon materials consisting of clusters of carbon atoms with 3 and 4 covalent sp^3 bonds [1, 2]. In this case, sp^3 bonding means the absence of π electrons despite the presence of carbon atoms bonded to only three neighbors. Such clusters are characterized by the appearance of high frequency (above 1332 cm^{-1} in diamond, up to 1640 cm^{-1}) Raman modes corresponding to fragments of the structure with three sp^3 bonds and caused by higher force constants than in diamond. Accordingly, such clusters are characterized by a higher bulk modulus (~600 GPa) than diamond (443 GPa) [1, 2].

Nanoclusters were synthesized in three regions of the recently updated carbon phase diagram at temperatures reaching 2300 K and pressures of 20–25 GPa (within the diamond stability region), 70 GPa (within the diamond instability region), and 160 GPa (also within the diamond stability region) [3].When fullerite is heated under a pressure of 20–25 GPa, partial diamond formation is observed. An increase in pressure up to 160 GPa and heating to 2300 K does not result in the formation of diamond from fullerite, although at pressures above 115 GPa graphite is transformed into diamond. Therefore, the issue of the stability of the carbon phase at pressures exceeding 115 GPa remains a topic for further investigation.

Two types of Raman resonances are observed in carbon clusters formed by sp^3 bonds. The first type is associated with the well-known resonant enhancement of the Raman spectrum intensity near the absorption edge and is observed in this work at excitations of ~1 eV (1064 nm) and ~2.3 eV (532 nm), depending on the synthesis conditions. In this case, all the high frequency modes of the cluster from 1380 to 1640 cm^{-1} appear in the Raman spectrum. The second type of resonance manifests itself in the activation of one of the modes in the range 1380–1640 cm^{-1}, depending on the wavelength of the excitation radiation (except for the wavelength at which the first type of resonance is observed). The frequency of the active mode depends linearly on the wavelength of the excitation radiation. The Raman line at 1640 cm^{-1} is observed when excited at 257 nm. Piezospectroscopy at pressures up to 90 GPa has shown that clusters with high bulk modulus participate in Raman processes when excited at shorter wavelengths.

[1] F. Khorobrykh, S. Klimin, S. Kulnitskiy, F.N. Jalolov, A. Kvashnin, A. Eliseev, A. Kirichenko, V. Prenas, V. Denisov, N. Mel'nik, P. Sorokin, M. Popov, Cluster structure of ultrahard fullerite revealed by Raman spectroscopy. Carbon 214, 118314, (2023).
[2] M. Popov, F. Khorobrykh, S. Klimin, V. Churkin, D. Ovsyannikov, A. Kvashnin, Surface Tamm States of 2–5 nm Nanodiamond via Raman Spectroscopy. Nanomaterials, 13696 (2023).
[3] D. Ovsyannikov, F. Khorobrykh, K. Bulatov, B. Kulnitskiy, V. Zhukov, P. Sorokin, S. Klimin, M. Popov, Transformations of C60 fullerite in the regions of stability and instability of diamond on the carbon phase diagram in the pressure range of 20–160 GPa and temperatures of 300–2300 K. Carbon, 238, 120165 (2025).

Laser induced breakdown spectroscopy for molten cast iron elemental analysis

P. A. Sdvizhenskii[1,2], V. N. Lednev[1], A. V. Rogachevskaya[1], E. A. Volkov[3]

1- Prokhorov General Physics Institute, Russian Academy of Science, Moscow, Russia
2- National University of Science and Technology MISIS, Moscow, Russia
3- JSC Severstal, Mira Street 30, Vologda region, city of Cherepovets, 162608 Russia

e-mail: pausdw@gmail.com

Laser-induced breakdown spectroscopy (LIBS) [1] is an optical emission technique for elemental analysis, requiring minimal sample preparation and enabling real-time measurements. It is versatile for solids, liquids, and gases, particularly effective for light elements, and suitable for harsh environments like molten metals that why LIBS has been widely applied in metallurgy, including real-time molten metal analysis.

The impact of overheated molten cast iron (1450–1550 °C) on LIBS performance have been studied in details, focusing on Si quantification. Additionally, the accuracy of LIBS melt analysis was compared for gated and non-gated spectrometers.

A laboratory setup was based on an induction furnace (MC 100 V, Indutherm) and a custom LIBS probe (Fig. 1). A diode pumped Nd:YAG pulsed laser (1064 nm, 65 mJ/pulse) was focused onto molten cast iron in an argon-shielded crucible. Plasma emission was collected directed via a pierced mirror, lens and fiber to a gated spectrograph coupled with iCCD camera (iStar) or non-gated spectrograph Avantes AvaSpec-2048.

Results showed that higher melt temperatures (1550 °C) resulted in better calibration curve linearity and accuracy, likely due to enhanced mixing in the crucible. However, the difference was negligible and surface oxide layers had a greater influence on analysis than temperature. It was shown that the alternating magnetic field from induction furnace did not affect the properties of the LIBS plasma or the results of the quantitative analysis [2].

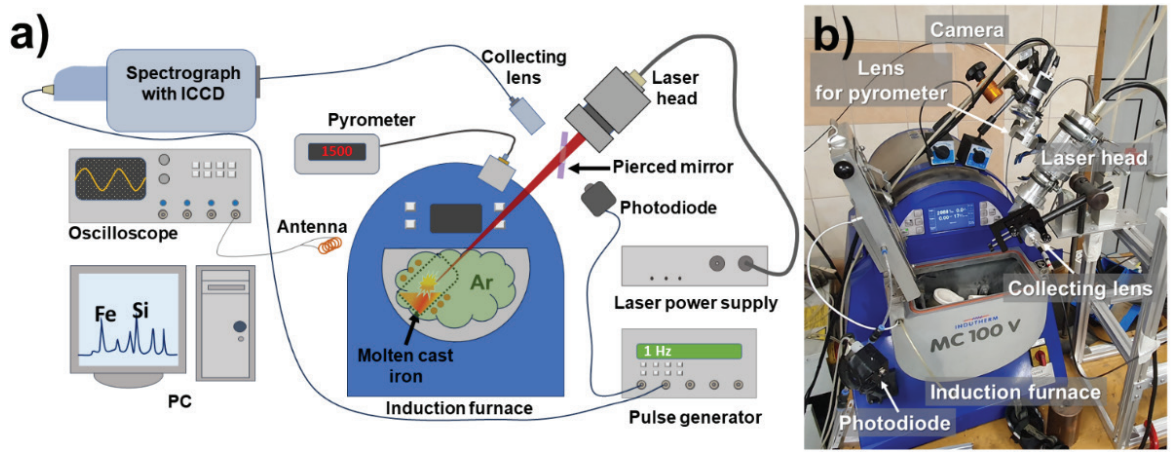

Fig. 1. Scheme (a) and photo (b) of laser induced breakdown spectroscopy (LIBS) setup for cast iron molten samples analysis at different temperatures. Cast iron samples were heated by an induction furnace in an argon atmosphere.

The authors gratefully acknowledge financial support from the Russian Science Foundation (RSF) (agreement № 25-29-00835), https://rscf.ru/en/project/25-29-00835/

[1] D.A. Cremers, L.J. Radziemski, Handbook of Laser-Induced Breakdown Spectroscopy, John Wiley & Sons, (2013).
[2] Sdvizhenskii P. A., Karpenkov D. Y., Rogachevskaya A. V., Volokhov S. V., Galeru K. E., Kuznetsov, D. V., & Lednev V. N. Superheated pig iron elemental analysis by LIBS. Optics & Laser Technology, 183, 112378, (2025).

Anisotropic femtosecond laser-induced structuring of thin chalcogenide films for infrared polarization optics applications

D. Shuleiko[1], P. Pakholchuk[1,2], D. Pomazkin[1,2], A. Musorin[1], D. Archibasov[1], V. Gushchina[1,3], S. Kozyukhin[3], P. Kashkarov[1,4]

1- Lomonosov Moscow State University, Leninskie Gory 1/2, Moscow, 119991 Russia
2- Lebedev Physical Institute of the RAS, Leninsky Avenue 53, Moscow, 119991 Russia
3- Kurnakov Institute of General and Inorganic Chemistry of the RAS, Leninsky Avenue 31, Moscow, 119991 Russia
4- National Research Center «Kurchatov Institute», Akademika Kurchatova sq. 1, Moscow, 123182 Russia

e-mail: shuleyko.dmitriy@physics.msu.ru

Chalcogenide vitreous semiconductors (ChVS) possess significant interest for telecommunications, optical data storage with polarization-dependent coding, as well as infrared (IR) polarization optics, due to their high refractive index, transparency in the near-IR range [1], and possibility to form laser-induced periodic surface structures (LIPSS) on them under the action of ultrashort laser pulses [2]. Combining high refractive index with deep surface laser-induced submicro- and nanorelief allows achieving substantial optical anisotropy in ChVS [3]. Additionally, photostructural transformations, including reversible phase transitions [4], occur in such materials under laser irradiation. The effects of photostructural transformations in ChVS, such as photodarkening and photobleaching [5], are associated with the formation/rupture of «wrong» homopolar bonds, and may manifest in the photoluminescence (PL) spectra of these materials.

Therefore the aim of this work was to create an optically anisotropic LIPSS on thin ChVS films via laser irradiation, and analyze possibilities to increase their polarizing contrast. The latter includes numerical simulation for the obtained polarization contrast and spectral dependences of the transmittance and reflection coefficients for laser-nanostructured ChVS films. We also aimed to identify the effect of laser-induced structural changes in the ChVS films on their PL.

To produce periodic submicro- and nanorelief on the surface of 1-μm-thick ChVS (As_2S_3, As_2Se_3 and $As_{50}Se_{50}$) films, femtosecond laser pulses (515 nm, 300 fs, fluence 8–270 mJ/cm^2, frequency up to 2 kHz) were used. The obtained LIPSS represented one-dimensional gratings with a period from ~170 to ~500 nm and a depth from 30 to 100 nm, or hierarchical structures containing two mutually orthogonal gratings with different periods. The possibility to control the optical anisotropy of LIPSS formed on the ChVS by changing the number and fluence of the laser pulses is demonstrated: the optical retardance value in the LIPSS varies from 0 to 30 nm for one layer of ChVS film. The possibility of increasing the optical retardance using layer-by-layer deposition of ChVS with subsequent LIPSS formation on each layer is presented.

We also demonstrated correlation between the photoluminescence intensity of laser-modified As_2S_3 films and the concentration of defects in them. Twofold increase in the PL intensity observed for the modified As_2S_3 films, can be attributed to laser-induced creation of defect states in the form of homopolar bonds in the Urbach edge. These defects act as radiative recombination centers for the carriers, while paramagnetic defects in the form of dangling sulfur bonds, detected in the samples by electron paramagnetic resonance measurements, are shown to not contribute to the luminescence.

The obtained results are promising for future development of polarizing near-IR optics based on laser-nanostructured thin ChV films.

The work was supported by the Russian Science Foundation (project 22-19-00035-П), https://rscf.ru/en/project/22-19-00035/.

[1] J.S. Sanghera, L.B. Shaw, L.E. Busse, et al. Fiber and Integrated Optics 19(3) 251 (2000).
[2] D. Shuleiko, S. Zabotnov, O. Sokolovskaya et al. Materials, 16(13), 4524 (2023).
[3] E. Kuzmin, S. Zabotnov, D. Shuleiko, et al. Bulletin of the Russian Academy of Sciences: Physics, 88(Suppl.3), S370–S374 (2024).
[4] A.V. Kolchin, S.V. Zabotnov, D.V. Shuleiko et al. Opt. Spectrosc. 131(2), 137 (2023).
[5] .P. De Neufville, S.C. Moss, S.R. Ovshinsky, J. Non-Cryst. Solids, 13(2), 191–223 (1974).

Optical diagnostics of nanoparticles in aqueous solutions: real possibilities and applications

G. O. Silaev[1,2], A. T. Shaydulin[1,3], Yu. V. Orlovskii[3], Yu. G. Vainer[1,2],

1- Institute of spectroscopy RAS, Physicheskaya st. 5, Troitsk, Moscow, 108840 Russia
2- Higher School of Economics National Research University, Myasnitskaya st. 20, Moscow, 101000 Russia
3- Prokhorov General physics Institute of RAS,, Vavilova st. 38 Moscow, 119991 Russia

e-mail: vainer@isan.troitsk.ru

The most widely used methods of nanoparticles (NPs) visualizing are electron and probe microscopy, which are characterized by high spatial resolution. However, they require expensive equipment, are characterized by a long and complex procedure for sample preparation and measurements, and have a strong effect on the sample. A fundamental disadvantage of electron microscopy is that this method is practically unsuitable for research in aqueous media, which greatly limits the real possibilities of their applications.

Optical microscopy methods are characterized by high efficiency and are much more accessible. They allow you to obtain a wide variety of information about nanoobjects of various natures, including biological ones, as well as observe and study not only single NPs, down to a few nanometers in size, but also single atoms and molecules. An important advantage of optical methods is their negligible impact on the object under study. The report is devoted to the presentation of the real capabilities of the laser ultramicroscope "light sheet" developed by us, based on the registration of elastic light scattering signals and intended for visualization and study of single NPs in aqueous solutions. The results of using the created microscope in solving a number of problems relevant to nanophysics, nanotechnology, biology and medicine are considered.

The developed microscope allows studying NPs with sizes of up to 5 nm and less and determining individual values of their hydrodynamic radius based on the analysis of their Brownian motion trajectories. Using the developed microscope, it is possible to obtain information on the spatial structure of the NPs under study, for example, to answer the question: "Do the observed particles have a continuous internal structure or is it an aggregate formed from several NPs?", as well as to obtain other information on the objects under study.

The report presents the results of comparing the data on the sizes of the NPs under study obtained using the developed microscope with the values obtained using other methods, in particular, the dynamic scattering method, atomic force microscope and transmission electron microscope. Examples of studying the properties of aqueous solutions of nanoparticles promising for use in medical purposes, in particular for phototherapy of solid cancer tumors, are considered.

Photoluminescent and nonlinear-optical diagnostics of redistribution of CdSe/ZnS quantum dots in liquid-crystal matrix under UV irradiation

O. I. Sokolovskaya[1], N. D. Presnov[1], A. A. Ezhov[1,2], Ya. I. Derikov[1,2], G. A. Shandryuk[1,2], O. N. Karpov[1,2], A. S. Merekalov[2], L. A. Golovan[1]

1- Lomonosov Moscow State University, Department of Physics, Moscow, Russia
2- A. V. Topchiev Institute of Petrochemical Synthesis RAS, Moscow, Russia

e-mail: golovan@physics.msu.ru

Embedding semiconductor quantum dots (QDs) into liquid-crystal (LC) matrix allows their spatial distribution to be controlled, which is of great importance for fabrication of novel light-emitting devices with designed QD distribution. Employing LC with embedded chromophores opens possibility to control LC phase state by means of their photoisomerization activated by ultraviolet (UV) light at temperature below the LC temperature of isotropization. In the LC phase of the matrix QDs tend to leave it and form aggregates, whereas in isotropic phase all QD are homogeneously dissolved in the matrix [1].

In this study, azochromophores of extended (EA) or branched (BA) structure (10 wt.%) were used as isotropization agents for nematic LC. CdSe/ZnS QDs (1 wt.%) were embedded into LC matrix. The migration of QDs in phase-changing LC matrix was studied with the help of transmission measurement, fluorescent optical microscopy with cw excitation at wavelength of 532 nm and UV photoinduced (365 nm) phase transition in LC matrix. UV illuminated region demonstrates isotropization accompanied by QDs homogeneous distribution was observed, whereas in LC areas QDs are in an aggregated state.

Second – and third harmonic (SH, TH) and upconversion luminescence (UC) signals (Cr:forsterite laser, 1250 nm, 80 fs, 80 MHz, 150 mW) along with transmission signal in crossed polarizers (diode laser, 780 nm) were measered in nematic LC with the aforementioned azochromophores and QDs. The transmission signal demonstrates drastic fall at the temperature of isotropization of LC (62 °C), whereas all nonlinear-optical signals decreases with the temperature increase and reach mininmun at lower temperature (about 55 °C), which possibly indicates additional structural variation inside the LC.

Thus, LC phase transition accompanied by QD migration has been demonstrated and optical harmonic and up-conversion signals are markers for these structural changes.

This research was funded by the Russian Science Foundation, grant number № 23-19-00246, https://rscf.ru/project/23-19-00246/.

[1] M.A. Osipov, M.V. Gorkunov, Nematic liquid crystals doped with nanoparticles: phase behavior and dielectric properties. In: Liquid Crystals with Nano and Microparticles. (2016).
[2] O.I. Sokolovskaya, V.Yu. Nesterov, et al. Diagnostics of ultraviolet-induced isotropic phase transitions in nematic liquid crystal with azochromophore, Liq. Cryst. and their Appl., vol. 25, pp. 90–98 (2025).

Bound states in the continuum and other resonance phenomena in the luminescence response of two-dimensional photonic crystals

M. Stepikhova[1], A. Peretokin[1], S. Dyakov[2], E. Smolina[3], D. Yurasov[1], M. Shaleev[1], D. Shengurov[1], E. Rodyakina[4], A. Novikov[1]

1- Institute for Physics of Microstructures RAS, Nizhny Novgorod, 603950 Russia
2- Skolkovo Institute of Science and Technology, Moscow, 143025 Russia
3- Federal Research Center A. V. Gaponov-Grekhov Institute of Applied Physics RAS, Nizhny Novgorod, 603950 Russia
4- Rzhanov Institute of Semiconductor Physics, Siberian Branch of Russian Academy of Sciences, Novosibirsk, 630090 Russia

e-mail: mst@ipmras.ru

Low-dimensional photonic structures currently being developed (with sizes comparable to and even smaller than the wavelength of radiation) open up new possibilities for controlling emission properties of the active medium, as well as observing new phenomena, such as, for example, bound states in a continuum (BIC). Bound states in the continuum are resonant states localized in the continuous spectrum of radiation, with a long (in theory tending to infinity) lifetime. It turns out that such states can be observed in photonic crystals [1], low-dimensional Mie resonators [2], metastructures [3], etc. In this paper, the possibilities of observing bound states in the continuum of different nature in two-dimensional photonic crystals (PhCs) will be discussed. Bound states in the continuum observed at the Γ point of the Brillouin zone, the cause of which is a mismatch between the symmetry of the field of the resonant mode and the modes of the radiation continuum (the so-called symmetry protected BIC), as well as Friedrich-Wintgen bound states in the continuum observed beyong the Γ point of the Brillouin zone, will be considered. The reason for the emergence of the latter is destructive interference of modes, accompanied by the phenomenon of "avoided crossing". We will show that the Friedrich-Wintgen BICs can be observed only for modes of the same symmetry and polarization, whereas the interaction of modes of different symmetry and polarization leads to the so-called phenomenon of mode "crossing", which manifests itself in the photoluminescence spectra as bright spots of high intensity. Another topic that will also be discussed concerns topological defects in photonic crystals, a feature of which is their robustness to structural imperfections [4]. We will demonstrate a new type of topological defects in photonic crystals, namely the so-called "loop defects", and describe their properties.

A special feature of this work is the observation of bound states in the continuum and other resonant phenomena in the luminescent response of two-dimensional photonic crystals. Photonic crystals were formed on silicon structures with Ge(Si) nanoislands, which are of interest for integrated photonics. To observe the phenomena discussed above, an original method of luminescence measurements with angular resolution was used. This method allows to analyze not only the band structure of the studied photonic crystals, but also the features of the modes polarization in the far field. In particular, we will show that the bound states in the continuum that we observe are characterized by the presence of vortex polarization and a certain topological charge, the value of which depends on the symmetry of the electromagnetic field of the mode. The specificity of the emissivity of topological defects in the far field will also be considered.

The work was funded by the Russian Science Foundation (grant # 25-22-00386).

[1] C.W. Hsu, B. Zhen, A.D. Stone, et al., Bound states in the continuum, Nature Reviews Materials, vol. 1, p. 16048 (2016).
[2] M.V. Rybin, K.L. Koshelev, Z.F. Sadrieva, et al. High-Q supercavity modes in subwavelength dielectric resonators. Physical Review Letters, vol. 119, p. 243901 (2017).
[3] К.Л. Кошелев, З.Ф. Садриева, А.А. Щербаков и др., Связанные состояния непрерывного спектра в фотонных структурах, Успехи Физических Наук, т. 193, № 5, с. 528–553 (2023).
[4] X. Zhang, F. Zangeneh-Nejad, Z.-G. Chen, et al., A second wave of topological phenomena in photonics and acoustics, Nature, vol. 618, pp. 687–697 (2023).

Structural and optical properties of heterostructures based on group IV materials (Ge, Si, Sn)

V. Timofeev[1], I. Skvortsov[1], V. Mashanov[1], I. Loshkarev[1], D. Kolyada[2], D. Firsov[2], O. Komkov[2]

1- Institute of Semiconductor Physics, Siberian Branch of the Russian Academy of Sciences, Lavrentyev Avenue 13, Novosibirsk, 630090 Russia
2- Saint Petersburg Electrotechnical University 'LETI', Prof. Popov 5, Saint Petersburg, 197376 Russia

e-mail: vyacheslav.t@isp.nsc.ru

An urgent task in the development of electron-photonic integrated circuits is to obtain new materials compatible with silicon technology, allowing to expand the operational spectral range of devices, while also advancing miniaturization, increasing speed, and enhancing energy efficiency. The class of Ge-Si-Sn materials is one of the most promising for addressing these challenges [1]. Incorporating Sn to the GeSi matrix allows to control the band structure of the original material, reducing the bandgap. This makes it possible to regulate of the operating wavelength for nanophotonic devices based on GeSiSn materials within the near and mid-infrared (IR) range from 1.55 to 8 μm [2, 3]. In contrast, devices utilizing Ge and Si are limited to the near IR range.

As a result of performed studies, a growth technology of multilayer structures, including GeSiSn/Si(Ge) quantum wells and quantum dots with the Ge content of up to 84% and the Sn content of up to 18%, was developed using the molecular beam epitaxy method. A kinetic diagram of the growth of GeSiSn layers with high Sn content in the temperature range of 100–300 °C was established. Based on these kinetic diagrams, the thickness range corresponding to the pseudomorphic state was identified. The advantage of such films over thicker layers in the absence of dislocations. By comparing the measurements of the parameters of GeSiSn/Si heterostructures using the Doppler broadening of the annihilation line and IR photoluminescence (PL) methods, it was shown that the emission band consisting of a series of individual peaks within the energy range of 0.3–0.55 eV is related to the emission of vacancy complexes. The density of these defects significantly decreases upon annealing the structure due to the vacancy complexes formation, which in turn leads to a decrease in the PL intensity of defects and promotes an increase in PL intensity from GeSiSn/Si multiple quantum wells (MQWs). It was found that annealing the GeSiSn/Si MQW structures in the temperature range of 500–700 °C causes a transition in the PL mechanisms from luminescence involving radiative vacancy complexes to interband luminescence. Interband PL was obtained for MQW structures with the GeSiSn quantum well width ranging from 0.5 to 3 nm, as well as with different Ge and Sn contents. The PL peak position for the annealed GeSiSn/Si MQW samples shifts toward the long-wavelength region, up to 2 μm.

The application of the IR Fourier spectroscopy of photoreflectance to study the band structure of GeSiSn solid solutions enabled the experimental observation of direct interband transitions in GeSn and GeSiSn epitaxial layers of different compositions. For the studied samples, the transition energies were obtained, their temperature dependences were determined, and the impact of annealing on the optical properties of the samples was demonstrated. In the photoreflectance spectra of GeSn/Ge heterostructures, a splitting of the main peak was observed, indicating the splitting of the GeSn valence band into heavy and light hole subbands due to mechanical strains in the structure. This finding illustrates the possibility for a contactless assessment of the degree of mechanical strain in the GeSn layer by measuring the magnitude of signal splitting in the IR photoreflectance spectra.

The work was carried out within the state assignment of the Ministry of Education and Science of the Russian Federation, No. FWGW-2024-0001.

[1] D. Grützmacher, O. Concepción, Q. Zhao, D. Buca, Si–Ge–Sn alloys grown by chemical vapour deposition: a versatile material for photonics, electronics, and thermoelectrics, Applied Physics A, vol. 129, p. 235, (2023).
[2] M. Atalla, S. Assali, A. Attiaoui, C. Lemieux-Leduc, A. Kumar, S. Abdi, O. Moutanabbir, All-Group IV Transferable Membrane Mid-Infrared Photodetectors, Adv. Funct. Mater., vol. 31, p. 2006329, (2020).
[3] V. Reboud, O. Concepcion, W. Du, M. El Kurdi, J.M. Hartmann, Z. Ikonic, S. Assali, N. Pauc, V. Calvo, C. Cardoux, E. Kroemer, N. Coudurier, P. Rodriguez, S. Yu, D. Buca, A. Chelnokov, Advances in GeSn alloys for MIR applications, Phot. Nano. Fund. Appl., vol. 58, p. 101233, (2024).

Precision control of 2D excitons in chiral atomically thin $A^{II}B^{VI}$ semiconductors: from dielectric screening to self-assembly into superstructures

R. B. Vasiliev, D. A. Kurtina, M. Yu. Skrypnik, A. I. Lebedev

Lomonosov Moscow State University, Leninskie Gory, Moscow, 119991 Russia

e-mail: romvas@inorg.chem.msu.ru

Two-dimensional (2D) semiconductors exhibit strong excitonic effects due to reduced dielectric screening and enhanced Coulomb interactions, making them potential candidates for new optoelectronic applications [1]. In present work, we discusses a new representative of the class of 2D semiconductors based on $A^{II}B^{VI}$ compounds: organic-inorganic nanostructures of the composition [M(n+1)E(n)L(2)], where M = Cd or Zn, E = S, Se or Te, L is an X-type organic or inorganic ligand in anionic form, and n is the number of monolayers. The organic (or inorganic) ligands included in the composition terminate the basal planes of the nanostructure and compensate for the charge of the positively charged core of the nanostructure. The hybrid organic-inorganic composition of such nanostructures opens up new possibilities for inducing desired properties due to organic ligands covalently hybridized with the inorganic core, which is unachievable for both classical quantum wells obtained by the MBE method and exfoliated 2D nanostructures. We consider the possibilities of controlling the exciton properties of such two-dimensional semiconductors due to organic molecules on the surface, changing the permittivity of the medium, and self-assembly of structures into superstructures.

We used a colloidal method for the growth of atomically thin nanostructures (nanosheets) of cadmium and zinc chalcogenides with a thickness of less than 1 nanometer (only 2 or 3 monolayers in thickness) and lateral sizes up to 1 micron (anisotropy factor up to 1000). A system of cadmium (zinc) acetate/octadecene/oleic acid/oleylamine was used for the nanostructure growth in the temperature range of 110–250 °C [2–4] and we achieved the formation of nanostructures with a precise (with an accuracy of 1 monolayer) thickness in the range of 0.6–0.9 nm. Ligand exchange protocols were developed for the exchange of native oleic acid ligand for different organic and inorganic molecules. A detailed study using TEM, HAADF-STEM, SAED and XRD methods showed the composition of nanostructures followed the ratio $[M_{n+1}E_nL_2]$ (M – zinc or cadmium, E – chalcogen, L – organic ligand, n – number of atomic planes) with n = 2 and 3.

The optical properties of nanostructures were studied by optical absorption, luminescence and luminescence excitation spectroscopy. For chiral enantiomeric ligand we used CD spectroscopy, magnetic CD spectroscopy, and polarimetry. Optical spectra of nanostructures showed distinct, narrow bands related to 2D excitons at room temperature. Well-resolved LH, HH, and SO exciton transitions was found and a pronounced exciton luminescence band were observed. The exchange of ligands led to a spectral shift of excitonic bands due to hybridisation of ligand and inorganic core. We discuss the effect of organic molecules on the surface, changing the permittivity of the medium, and self-assembly of structures into superstructures on the excitonic properties. For example, variation of dielectric constants of solvents led to a change in the contributions of HH and LH excitons to the absorption spectra and variation in the spectral position of excitons, which can be explained by the effect of dielectric screening of 2D excitons. The results of the work are of interest for the development of new approaches to controlling the exciton properties of 2D semiconductors.

This work was supported by the Russian Science Foundation (grant № 25-13-00416).

[1] Mueller, T., Malic, E. Exciton physics and device application of two-dimensional transition metal dichalcogenide semiconductors. npj 2D Mater Appl 2, 29 (2018).
[2] Kurtina D.A. et.al., Atomically Thin Population of Colloidal CdSe Nanoplatelets: Growth of Rolled-up Nanosheets and Strong Circular Dichroism Induced by Ligand Exchange, Chem. Mater., 31, 9652–9663, (2019).
[3] Kurtina, D.A. et al. Induction of Chirality in Atomically Thin ZnSe and CdSe Nanoplatelets: Strengthening of Circular Dichroism via Different Coordination of Cysteine-Based Ligands on an Ultimate Thin Semiconductor Core. Materials, 16, 1073 (2023).
[4] Kurtina, D.A. et al. Chirality in Atomically Thin CdSe Nanoplatelets Capped with Thiol-Free Amino Acid Ligands: Circular Dichroism vs. Carboxylate Group Coordination. Materials 17, 237 (2024),

Combining classical and multivariate analyses of Raman spectra as an efficient tool for the quality evaluation of dietary omega-3 supplements

D. D. Vasimov[1,2], S. M. Kuznetsov[1], V. S. Novikov[1], E. A. Sagitova[1]

1- Prokhorov General Physics Institute of the Russian Academy of Sciences, Vavilov Str. 38, Moscow, 119991 Russia
2- Moscow Institute of Physics and Technology, Institutskiy Per. 9, Dolgoprudny, Moscow Region, 141700 Russia

e-mail: sagitova@kapella.gpi.ru

Currently, multivariate analysis of spectra is becoming more and more popular in vibrational spectroscopy. In this study, we applied a classical approach and two multivariate methods – principal component analysis (PCA) and partial least-squares (PLS) regression – in order to analyze the Raman spectra of dietary omega-3 supplements, which are widely used to address deficiencies of omega-3 polyunsaturated fatty acids (ω-3 PUFA) and promote health. We revealed that the classical approach allows detecting two characteristics of the dietary omega-3 supplements. Namely, monitoring the intensity of the Raman band at 1658 cm^{-1}, relating to the stretching vibration of C=C bonds (ν(C=C)), enables the determination of the total ω-3 PUFA content. Monitoring the wavenumbers of the Raman bands, assigned to the stretching vibration of C=O bonds (ν(C=O)) and deformation CH_2 vibration (δ(CH_2)), allows for distinguishing between the forms (ethyl esters (EE) or triglycerides (TG)) in which ω-3 PUFAs are present in the supplements. Figure 1 shows the Raman spectra of omega-3 supplements that differ in the forms and content of ω-3 PUFAs.

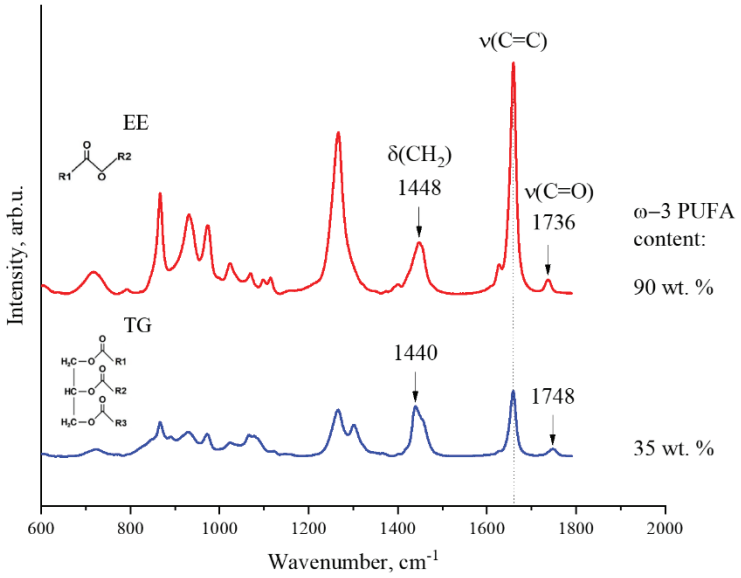

Fig. 1. Raman spectra of omega-3 supplements with different forms (EE and TG) and contents of ω-3 PUFAs.

We found out that multivariate analysis could be used to extract information about the ratio of EPA and DHA contents in omega-3 supplements from the Raman spectra. We demonstrated that this information can be obtained using both PCA and PLS regression applied to the spectral region of 540–1200 cm^{-1}. However, the form of ω-3 PUFAs should be identified before such analysis. Thus, we concluded that the development of Raman spectroscopy methods for rapid quality assessment of omega-3 supplements should be based on a combination of both classical and multivariate data analysis approaches.

This work was supported by the RSF grant № 24-22-20100, https://rscf.ru/project/24-22-20100/.

Laser diagnostics in terahertz and infrared ranges using free-electron lasers and synchrotron radiation sources

S. L. Veber[1,2], A. R. Melnikov[1,2], N. A. Tashkeev[1,2], I. A. Milekhin[2,3], Ya. V. Getmanov[4], O. A. Shevchenko[4], A. G. Milekhin[3], K. V. Zolotarev[2], N. A. Vinokurov[4], Y. V. Zubavichus[2]

1- International Tomography Center SB RAS, Novosibirsk, Russia
2- Center for Collective Use "SKIF", Boreskov Institute of Catalysis SB RAS, Koltsovo, Russia
3- Rzhanov Institute of Semiconductor Physics SB RAS, Novosibirsk, Russia
4- Budker Institute of Nuclear Physics SB RAS, Novosibirsk, Russia

e-mail: sergey.veber@tomo.nsc.ru

Large-scale research infrastructures, often referred to as "megascience" facilities, define the frontier of experimental capabilities in modern science. In the infrared (IR) and terahertz (THz) spectral ranges, such radiation can be produced by state-of-the-art sources like synchrotrons and free-electron lasers (FELs). In the Russian Federation, two major facilities are dedicated to this purpose: the Novosibirsk Free Electron Laser (NovoFEL), which delivers record-breaking power in the THz domain, and the emerging Siberian Circular Photon Source (SKIF), scheduled for commissioning in the near future.

The NovoFEL is a user-oriented facility that provides narrowband, tunable THz-IR radiation for advanced fundamental and applied studies [1]. Thanks to its recuperation-based design, NovoFEL operates in both quasi-continuous and flexible pulsed modes, with the possibility to tailor pulse duration and repetition rate [2]. It hosts more than ten experimental stations covering applications from biology to plasma physics. Its intense radiation – with pulse peak power up to 1 MW, focused intensity above 1 GW/cm^2 – has enabled studies of nonlinear THz phenomena such as ablation and THz-induced gas discharges.

One of the prominent research directions at NovoFEL involves magneto-optical studies of molecular magnetic materials, particularly single-molecule magnets (SMMs). For instance, investigations on Co(II)-based SMMs using tunable high-power THz radiation have demonstrated the capability of FEL-driven pump-probe experiments to access otherwise inaccessible spin dynamics. These studies are complemented by EPR spectroscopy experiments at THz frequencies, performed at the BESSY II synchrotron [3].

SKIF represents the next-generation 4+ synchrotron light source designed to support a wide range of cutting-edge experiments [4]. Among its second-stage beamlines under development is the IR Diagnostics Station, covering an exceptionally soft photon energy range for a synchrotron – from the THz to ultraviolet domain (approximately 5 meV to 5 eV). The beamline will enable a suite of techniques such as IR microscopy and nano-IR, and also magneto-dipole spectroscopy. Its design includes a custom optical layout and a dedicated high-vacuum photon collection chamber. The beamline is designed to provide advanced tools for cutting-edge studies of light–matter interactions with applications to solid-state physics, molecular systems, and advanced materials.

This research was supported by the Ministry of Science and Innovation Policy of the Novosibirsk Region, Agreement No. 30-2025-000858, project No. 25-13-20039.

[1] G.N. Kulipanov et.al., Novosibirsk Free Electron Laser—Facility Description and Recent Experiments, IEEE Trans. Terahertz Sci. Technol. 5, 798–809, (2015).
[2] O.A. Shevchenko et.al., Electronic Modulation of THz Radiation at NovoFEL: Technical Aspects and Possible Applications, Materials 12, 3063, (2019).
[3] O.V. Minakova et.al., Intermolecular Exchange Interaction in Bis-(Phenoxy Schiff Base) Co(II) Complexes: an In-depth Insight into the Magneto-Structural Nature of Single-Molecule Magnets, submitted, (2025).
[4] A.V. Bukhtiyarov et al., Synchrotron Radiation Facility "Siberian Circular Photon Source" (SRF SKIF), Crystallogr. Rep. 67, 690–711 (2022).

Plurality of luminophores in synthesis of carbon dots from citric acid and ethylenediamine

A. Vervald[1], K. Laptinskiy[1,2], T. Dolenko[1]

1- Faculty of Physics, Lomonosov Moscow State University, Building 1, Leninskie Gory 2, Moscow 119991 Russia
2- Skobeltsyn Institute of Nuclear Physics, Lomonosov Moscow State University, Building 1, Leninskie Gory 2, Moscow, 119991 Russia

e-mail: alexey.vervald@physics.msu.ru

Hydrothermal treatment of an aqueous solution of citric acid (CA) and ethylenediamine (EDA) leads to their polymerization, dehydration, carbonization, and possible graphitization [1, 2]. Sufficiently large structures synthesized in this way are called carbon dots (CDs). Under certain conditions, such CDs – classified as polymer nanostructures – are known to produce ultra-bright luminescence in the violet-blue region with a quantum yield up to ~100%. Our study [2] of 392 CA and EDA samples subjected to hydrothermal synthesis with varying EDA:CA ratio in the range of 0–20:1, temperature in 80–200 °C, and reaction time in 0.5–6 h, showed that the formation of samples' main luminophores starts with the polymerization of precursors, accelerates with the initial carbonization of the samples, while the stage of graphitizing carbonization – formation of CDs' cores – brings their partially destruction. Most publications suggest that this main – and only – luminophore is IPCA (5-oxo-1,2,3, 5-tetrahydroimidazo[1,2-a]pyridine-7-carboxylic acid or 5-oxo-1,2,3,5-tetrahydroimidazo[1,2-a]pyridine-7-carboxylic acid) [3]. The present study points to a much more complex picture.

The analysis of luminescence maps of 392 samples of CA and EDA reaction (examples in Fig. 1) allowed to identify 8+ different fluorescence signatures and track the stages of their appearance and extinction at different stages of CD synthesis. Some of these signatures merge or become absorbed by photoluminescence in the main maximum in the $\lambda_{ex}/\lambda_{em}$ 350/440 nm/nm region. To check whether different fluorescence signatures belong to separate molecular systems, choice samples were subjected to gel electrophoresis. The separation indicates the existence of up to 7 different fractions in the samples, differing in charge, luminescence, its quantum yield, and composition of functional groups.

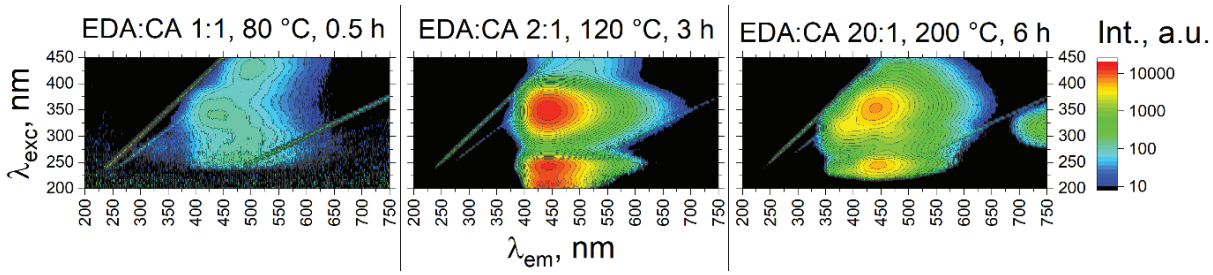

Fig. 1. Excitation-emission maps of EDA-CA samples' luminescence.

The study was supported by the grant from the Russian Science Foundation No. 22-12-00138, https://rscf.ru/en/project/22-12-00138/.

[1] N. Papaioannou, M.-M. Titirici, A. Sapelkin, Investigating the effect of reaction time on carbon dot formation, structure, and optical properties, ACS Omega, 4, pp. 21658–21665, (2019).
[2] A. M. Vervald, K. A. Laptinskiy, M. Yu. Khmeleva, T. A. Dolenko, Toward carbon dots from citric acid and ethylenediamine, part 1: Structure, optical properties, main luminophore at different stages of synthesis, Carbon Trends, 19, 100452, (2025).
[3] P. Duan, B. Zhi, L. Coburn, C. L. Haynes, K. Schmidt-Rohr, A Molecular fluorophore in citric acid/ethylenediamine carbon dots identified and quantified by multinuclear solid-state nuclear magnetic resonance, Magn. Reson. Chem., 58, pp. 1130–1138, (2020).

Spectroscopy of donor–acceptor properties of carbon nanoparticles in solutions

A. Vervald[1], K. Laptinskiy[1,2], A. Korepanova[1], S. Burikov[1], T. Dolenko[1]

1- Department of Physics, Lomonosov Moscow State University, Leninskiye Gory 1/2, Moscow, 119991 Russia
2- Skobeltsyn Institute of Nuclear Physics, Lomonosov Moscow State University, Leninsky Gory 1/2, Moscow, 119991 Russia

e-mail: tdolenko@mail.ru

Effective use of carbon dots (CD) in various fields of science and technology requires a more detailed understanding of the mechanisms of formation and change of their photoluminescence as a result of their interaction with the environment. In this study, CD synthesized via a hydrothermal method from citric acid (CA) and ethylenediamine (EDA) in their different ratios are studied in solvents by FTIR spectroscopy, optical absorption spectroscopy and photoluminescence spectroscopy including time-resolved one. Particular attention is paid to the properties of CD with various nitrogen content (Fig. 1) in solvents with different values of acidity SA and basicity SB.

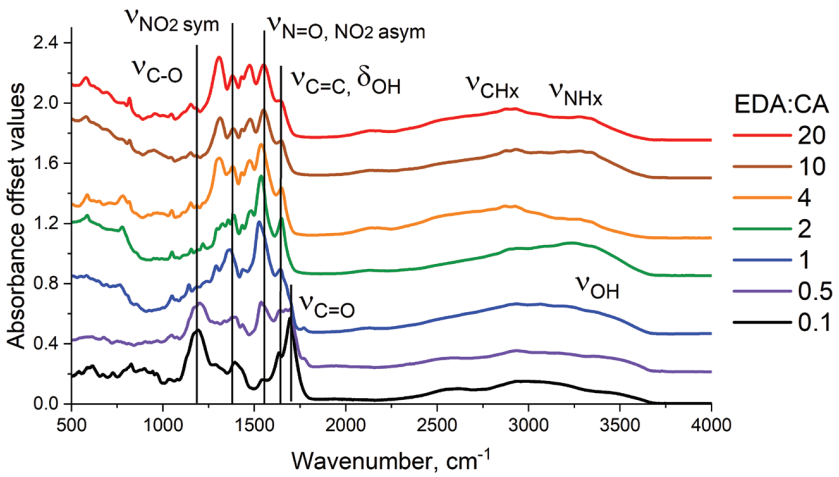

Fig. 1. FTIR absorption spectra of PCD powders with varying nitrogen content evaporated from water.

The analysis of the obtained experimental results demonstrated a significant dependence of the spectral characteristics of PCD photoluminescence on the acidity and basicity of the solvent. It was determined that the reason for this dependence is the formation of hydrogen bonds of varying strength between PCD functional groups and solvent molecules.

In this case, in solutions with different acidity and basicity, nitrogen-deficient CD act as basicity centers, i.e. hydrogen bond acceptors. Nitrogen-rich CD in the studied solvents act as acidity centers, i.e. hydrogen bond donors.

The obtained results are of extreme importance for the targeted development of CD-based nanosensors and medical agents in various environments. Knowledge of the mechanisms of medium parameters influence on the photoluminescence of carbon nanomaterials allows one to solve many fundamental problems in nanotechnology and material science.

The research was carried out at the expense of the grant from the Russian Science Foundation № 22-12-00138-P, https://rscf.ru/en/project/22-12-00138/.

Ratiometric thermometry via anti-Stokes excitation of NV-centers in microdiamonds

G. Voskanyan[1], N. Kurochkin[2,3], A. Gritsienko[2,3]

1- Bauman Moscow State Technical University, 2-nd Baumanskaya Str. 5, Moscow, 105005 Russia
2- Moscow Institute of Physics and Technology (National Research University), Institutskiy per. 9, Dolgoprudny, Moscow Region, 141700 Russia
3- P. N. Lebedev Physical Institute of the Russian Academy of Sciences, Leninskiy Ave. 53, Moscow, 119991 Russia

e-mail: g.voscaniantz@gmail.com

Precise and accurate temperature measurement at the cellular scale is critical for a range of applications, most notably in hyperthermia-based cancer therapies [1]. Luminescence thermometry provides the highest spatial resolution among existing techniques. In biological systems, luminescent probes must be excitable and detectable within the 600–900 nm near-infrared (NIR) biological transparency window to minimize absorption and scattering. Previously reported rapid ratiometric methods involving nitrogen-vacancy (NV) color centers rely on Stokes excitation outside this window, which is suboptimal for biological environments [2]. NV centers also permit anti-Stokes excitation [3], which we exploit in this study to develop a ratiometric thermometry technique that enables fast temperature readout fully within the biological transparency window.

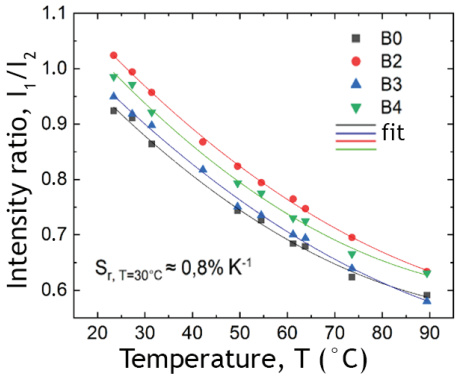

Fig. 1. Temperature dependence of the luminescence intensity ratio (I_1/I_2) for a selection of microdiamonds under anti-Stokes excitation.

In this research, we investigated the temperature-dependent luminescence response of NV centers in HPHT microdiamonds (average size ~30 μm) under anti-Stokes laser excitation at 685 nm. In our setup, we split the reflected luminescence signal from the sample into two paths and spectrally filtered them, with Channel 1 transmitting 580–620 nm and Channel 2 transmitting 626–646 nm. We then measured the ratio of the intensities of luminescence signals in the two channels (I_1/I_2) across a temperature range of 23–90 °C. Figure 1 shows the I_1/I_2 ratio as a function of temperature for several microdiamonds. As the temperature rises, this ratio decreases non-linearly, which we fit with an exponential function. Note, that the temperature-dependent luminescence response ratio exhibits consistent behaviour for all microdiamonds. The method yields a relative temperature sensitivity of $S_r = 0.8\%\ K^{-1}$ at 23 °C and a noise floor of 1 $K \cdot Hz^{-1/2}$.

To conclude, we demonstrated a ratiometric thermometry method based on anti-Stokes excitation of NV-centers in microdiamonds with non-linear temperature dependence. Its high relative sensitivity coupled with diamond biocompatibility make this method a compelling candidate for biological thermometry applications.

[1] Piñol, R., Brites C. D. S, Silva et al., Nanoscale Thermometry for Hyperthermia Applications., Micro and Nano Technologies, pp. 139-172, (2019).
[2] T. Plakhotnik, H. Aman, H.-C. Chang, All-Optical Single-Nanoparticle Ratiometric Thermometry With A Noise Floor of 0.3 K $Hz^{-1/2}$. Nanotech., vol. 26, 245501, (2015).
[3] M. H., Alkahtani, F. Alghannam, L. Jiang, Fluorescent Nanodiamonds for Luminescent Thermometry in the Biological Transparency Window, Opt. Lett. vol. 43(14), pp. 3317–3320, (2018).

Microjoule eye-safe LiDAR without "dead zone" for docking

V. A. Zavozin

Prokhorov General Physics Institute of the Russian Academy of Sciences

e-mail: vzavozin@kapella.gpi.ru

The new microjoule and eye-safe LiDAR without "dead zone" based on diode laser with picosecond step at the front of the pulse and strobe Single Photon Avalanche Diode (SPAD) was developed and testing. In our laboratory we develop diode laser for eye-safe LiDAR in time-correlating single photon counting (TCSPC) mode. We used injection commercial laser (SPL PL90_3, OSRAM) with three AlGaAs diodes in stack. We applied current generator with field-effect transistor (FET) as switcher for feed circuit. This laser generates pulses with specific form. This is a new lasing mode of nanosecond laser with a 200-ps-long step at the leading edge of a 4-ns-long pulse. It improves the accuracy of range in LiDAR with quick-response strobe single photon avalanche diode receiver [1].

We sensing flat target in distance about 35 m by LiDAR in TCSPC mode with different backscattering energy that achieve receiver. The energy is varied by changing the receiving diaphragm. In one session was 10^5 laser pulses. The histograms are presented in Fig. 1.

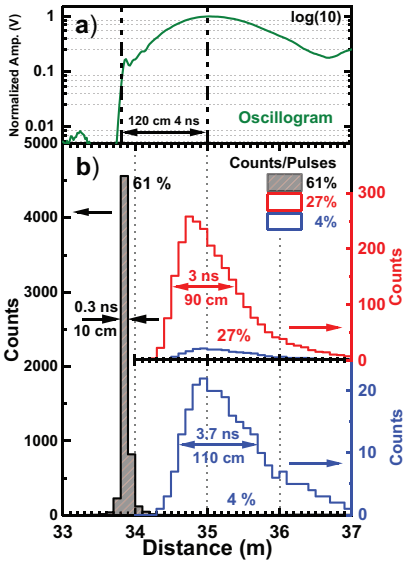

Fig. 1. Laser pulse oscillogram in logarithmic scale (a). Histograms with different ratio counts/pulses measured by TCSPC LiDAR (b)

Histogram profile has changed by increase of backscattering energy that achieve SPAD. Main position of maximum in graphs shifts closer to LiDAR. This happens because strobed SPAD detect only one backscattering photon from single laser pulse. The receiver detects photons from front of laser pulse more often when diaphragm is open. Thus, accuracy of range depends on the duration of pulse front when other things being equal. In this case it depends on duration of 200-ps-long step.

This LiDAR with this diode laser can be used in different modes. First mode when receiver detect about 1% of laser pulses. There histogram present backscattering photons from different particles such as aerosols or vapors. The second mode when receiver detects more then 50% of laser pulses. There histogram presents distance to the target with improves accuracy of range. This mode actually same as time of light technic.

Thus, LiDAR in this dual mode excellent fit for approach and docking. In far zone we locate target then in near zone we measure distance with improves accuracy of range up to touch.

This work was supported by the Russian Science Foundation (project No. RSF-23-42-10019).

[1] Pershin, S. M., and others, 'New Lasing Mode of a Diode Laser: A 200-Picosecond Leading Edge of a Nanosecond Pulse', Bulletin of the Lebedev Physics Institute, 50.3, pp. S383–88 (2023), doi:10.3103/S1068335623150125

Linear and nonlinear spectroscopy of Mie-resonant high refractive index nanoparticles

D. M. Zhigunov[1], D. A. Shilkin[2], V. O. Bessonov[2,3], D. A. Chermoshentsev[1], S. A. Dyakov[1], A. G. Nasibulin[1], A. A. Fedyanin[2]

1- Skolkovo Institute of Science and Technology, Bolshoy Boulevard 30, bld. 1, Moscow, 121205 Russia
2- Faculty of Physics, M. V. Lomonosov Moscow State University, Leninskie Gory 1, Moscow, 119991 Russia
3- Frumkin Institute of Physical Chemistry and Electrochemistry, Russian Academy of Sciences, Moscow, 119071 Russia

e-mail: d.zhigunov@skoltech.ru

Optical resonant nanostructures made of semiconductor materials with a high refractive index, such as Si, Ge and GaAs, are currently the focus of attention of researchers developing approaches to control light at the nanoscale. This is facilitated by relatively low absorption losses at optical frequencies and pronounced Mi-type resonances, which make it possible to enhance the local electromagnetic field inside individual nanoparticles by exciting characteristic magnetic and electric modes in the visible and near-infrared regions of the spectrum.

In this work, the optical properties of Si, Ge, and SiGe nanoparticles obtained by femtosecond laser printing from the corresponding thin films were studied [1–3]. The ordered arrays of crystalline single Ge and $Si_{1-x}Ge_x$ nanoparticles with sizes from 100 to 300 nm were obtained by laser printing and their scattering spectra in the visible region of the spectrum were measured [1]. It is shown that the best ordering and control of the size of nanoparticles can be achieved by selecting the wavelength and energy of a femtosecond laser pulse in combination with the required thickness of the donor film, which leads to an optimal volume of the molten part of the film.

Due to the absorption and scattering of light and its finite thickness, the substrate can reduce the Q-factor of the optical resonances of nanoparticles located on it. In order to minimize the influence of the environment on the properties of resonant nanoparticles, it was proposed to use single-walled carbon nanotube (SWCNT) membranes as a receiving substrate in the laser printing process. For the first time, laser transfer of Si nanoparticles about 200 nm in size was first performed on a 20 nm thick SWCNT membrane [2]. It was demonstrated that the electric and magnetic quadrupole Mi-type resonances, which are poorly distinguishable in the scattering spectra of Si nanoparticles located on a cover glass substrate, become noticeably more pronounced upon transition to the SWCNT membrane. Moreover, the optical contrast of the bright field microscopy images of the Si NPs on the surface of the pristine SWCNT membrane has been shown to increase by an order of magnitude in comparison with the contrast obtained in the case of a glass substrate.

The nonlinear optical response from Si nanoparticles about 300 nm in size was studied by excitation spectroscopy near the magnetic quadrupole (mq) resonance in the scattering spectrum [3]. It has been shown that resonance enhances both the efficiency of second harmonic generation and the photoluminescence signal caused by multiphoton absorption of light when pumped by femtosecond laser pulses with a variable wavelength. Additional irradiation of Si nanoparticles with femtosecond pulses led to a significant modification of the particle shape due to their melting and subsequent solidification, which was accompanied by suppression or complete disappearance of resonances in the scattering spectra. At the same time, the intensity of the total nonlinear response from the irradiated nanoparticle significantly decreased, which confirms the key role of Mi resonances in enhancing the effectiveness of nonlinear optical phenomena for Si nanoparticles.

[1] D.M. Zhigunov, A.B. Evlyukhin, A.S. Shalin, U. Zywietz, B.N. Chichkov, Femtosecond laser printing of single Ge and SiGe nanoparticles with electric and magnetic optical resonances, ACS Photonics, 5, 977–983 (2018).
[2] D.M. Zhigunov, D.A. Shilkin, N.G. Kokareva, V.O. Bessonov, S.A Dyakov, D.A. Chermoshentsev, A.A. Mkrtchyan, Yu.G. Gladush, A.A. Fedyanin, and A.G. Nasibulin, Single-walled carbon nanotube membranes as non-reflective substrates for nanophotonic applications, Nanotechnology, 32, 095206 (2021).
[3] D.M. Zhigunov, D.A. Shilkin, V.O. Bessonov, I.M. Antropov, D.A. Chermoshentsev, S.V. Semin, A.V. Kimel, A.A. Fedyanin, Linear and nonlinear optical response of Mie-resonant Si nanoparticles and its modification induced by femtosecond irradiation post-treatment, Opt. Mater. 154, 115616 (2024).

The complex "duality lemma" and scattering of radiation in absorbing media

L. A. Apresyan, V. I. Krasovsky

Federal State Budgetary Institution of Science A. M. Prokhorov Institute of General Physics, Russian Academy of Sciences, Moscow, Russia

e-mail: leon_apresyan@mail.ru

The classical theory of scattering is based on the assumption that scattering objects (which can be both macroscopic particles and quantum scatterers – atoms and molecules) are located in a non-absorbing medium, usually in free space [1, 2]. Meanwhile, every real medium is to some extent absorbing. Taking this into account leads to a noticeable complication of the theory, since, unlike the free propagation, the energy characteristics of radiation in the absorbing medium change during the propagation between scattering acts. This complicates even the description of the simplest model of scattering on a homogeneous spherical particle in an absorbing medium [3, 4]. In the article [5], when considering coherent scattering on a system of macroscopic particles in lossless medium, a simple relation was obtained, called the "duality lemma", the use of which simplifies the description of the energy balance, allowing us to consider the energy exchange between arbitrarily selected volumes of the medium with scatterers. In this paper, we consider the general complex form of this lemma for dielectric and magnetic scatterers in a lossy medium. Taking the real part of it gives the time average power flows. Taking the imaginary part corresponds to the description of reactive powers, the fluxes of which are not preserved even for the free propagation of radiation. The latter generally do not have a direct energetic meaning, but are widely used in applications as an auxiliary tool. As an example of the application of the lemma, we consider the conditions of the energy balance between an external source and a scatterer in an absorbing medium.

[1] H. C. Van de Hulst: Light Scattering by Small Particles. Wiley, New York (1957); Dover (1981).
[2] J. R. Taylor: Scattering Theory. The Quantum Theory of Nonrelativistic Collisions. Wiley, New York (1972).
[3] M. I. Mishchenko and J. M. Dlugach: .Scattering and extinction by spherical particles immersed in an absorbing host medium. J. Quant. Spectrosc. Radiat. Transfer/ 211, 179–187 (2018).
[4] M. I. Mishchenko, G. Videen, P. Yang: Extinction by a homogeneous spherical particle in an absorbing medium. Opt. Lett. 42(23), 4873–4876 (2017) DOI: 10.1364/OL.42.004873
[5] L. A.Apresyan, V. I. Krasovsky, S. I. Rasmagin: Energy balance for coherent scattering of radiation by a system of many particles (Tech. Phys., 2025, in print)

Spectral phase retrieval using a hybrid Gerchberg-Saxton algorithm

E. Bogatova[1], A. Burkov[1], N. Tereshchenko[2], E. Tulnikov[1]

1- Moscow Institute of Physics and Technology, Institutskiy pereulok 9, Dolgoprudny, Russia
2- VPG Laserone, Vvedenskogo sq. 1, Fryazino, Moscow Region, Russia

e-mail: burkov.as@phystech.edu

Accurate spectral phase retrieval is critical for applications like ultrafast optics, coherent control, and fiber Bragg grating characterization [1]. While the Gerchberg-Saxton (GS) algorithm is an established tool for phase reconstruction, its performance degrades for complex nonlinear systems [2] (e.g., chirped gratings with dispersion and self-phase modulation) due to stagnation in local minima [3]. Recent advances propose hybrid approaches combining GS with stochastic optimization to overcome these limitations.

We demonstrate robust spectral phase retrieval of ultrashort pulses using a modified Gerchberg-Saxton (GS) algorithm combined with genetic optimization techniques. The method iteratively reconstructs the spectral phase from intensity measurements in two domains: the laser output spectrum and output of fiber, spliced at the end of the laser. Initially validated on analytical data with known phase profiles (e.g., quadratic chirp, SPM-distorted phases), the algorithm achieved >80% accuracy in phase reconstruction, as shown below (Fig. 1). For experimental data, we introduced a hybrid approach integrating GS with crossover and mutation operators from genetic algorithms (GA) to escape local minima and improve convergence. Key innovations include such features as genetic hybridization: crossover of phase solutions and random mutations diversify the search space, reducing stagnation.

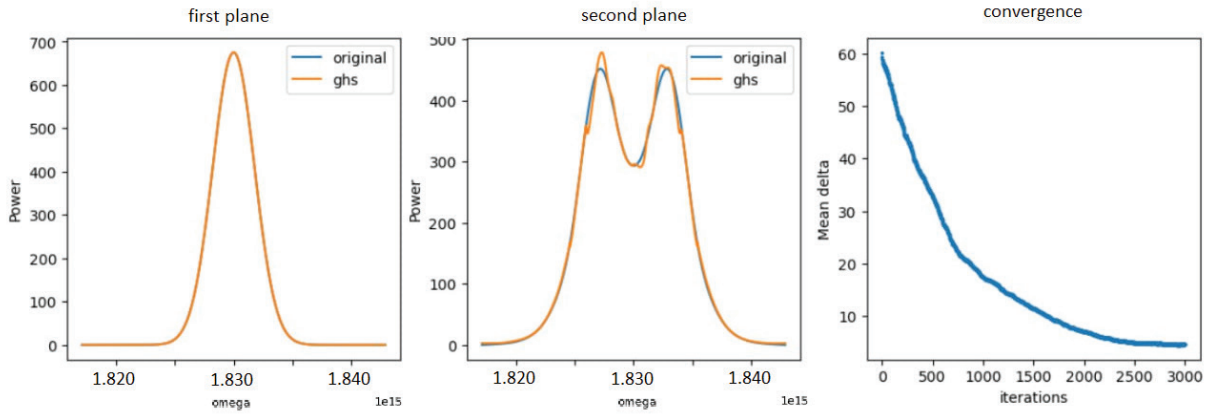

Fig. 1.

Experimental validation demonstrated that the hybrid GS-GA algorithm significantly outperformed classical GS, which exhibited instability even when initialized with the correct phase in analytical test cases. This approach enables precise phase control in nonlinear pulse shaping and coherent phonon generation applications.

[1] J. A Conway, G. A Sefler, J. T. Chou, G. C. Valley, Phase ripple correction: theory and application, Optics letters, 33(10), 1108-1110, (2008).
[2] A. Rundquist, A. Efimov, D. H. Reitze, Pulse shaping with the Gerchberg–Saxton algorithm, Journal of the Optical Society of America, B 19.10, 2468-2478, (2002).
[3] A. K. Hansen, Coherent laser phase retrieval in the presence of measurement imperfections and incoherent light, Applied Optics 56.26, 7341–7345, (2017).

Development of ion nanosensors using various machine learning methods

G. Chugreeva[1], A. Guskov[1], G. Kupriyanov[1], K. Laptinskiy[1,2], I. Isaev[2], S. Dolenko[1,2], T. Dolenko[1]

1- Faculty of Physics, M. V. Lomonosov Moscow State University, Moscow, Russia
2- D. V. Skobeltsyn Institute of Nuclear Physics, M. V. Lomonosov Moscow State University, Moscow, Russia

e-mail: chugreeva.gn17@physics.msu.ru

Carbon dots (CD) are nanoparticles whose optical properties, in particular stable intense photoluminescence (PL), are extremely sensitive to changes in environmental parameters [1]. The selectivity of optical properties with respect to changes in a particular parameter opens up broad prospects for the use of CD as optical nanosensors of liquid media [2, 3]. In all known publications the authors present the results on creation of CD nanosensors, capable to determine only 1-2 environmental parameters, while in most applications it is necessary to monitor the changes in several parameters at once.

This study shows that using various machine learning methods (ML), it is possible to solve the inverse multiparametric problem of optical spectroscopy for determining the type and concentration of ions in water from PL CD spectra. To find the best solution of determining ion concentration with maximum accuracy, several ML methods were used: multilayer perceptrons, convolutional neural networks, Kolmogorov-Arnold networks, and learning transfer. Research conducted to find the optimal neural network architecture has shown that two-dimensional convolutional neural networks achieve the best results. Such a neural network model is able to determine the concentration of Cu^{2+}, Ni^{2+}, Co^{2+}, Pb^{2+}, Al^{3+}, Cr^{3+}, NO_3^- ions in aqueous solutions with an mean absolute error of 0.68 mM, 0.95 mM, 0.3 mM, 1.38 mM, 1.06 mM, 0.2 mM, 2.42 mM, accordingly. The accuracy of solving the inverse nanosensory problem meets the needs of monitoring the composition of industrial waters.

The study was supported by the grant from the Russian Science Foundation No. 22-12-00138-P, https://rscf.ru/en/project/22-12-00138/.

[1] A.M. Vervald, K.A. Laptinskiy, G.N. Chugreeva, S.A. Burikov, T.A. Dolenko. Quenching of Photoluminescence of Carbon Dots by Metal Cations in Water: Estimation of Contributions of Different Mechanisms // J. Phys. Chem. C, vol. 127, pp. 21617–21628, (2023).
[2] Panigrahi, A., Behera, R. K., Mishra, L., Kumar, S., Dubey, P., Dutta, S., & Sarangi, M. K. Exploring optoelectronic properties of undoped and amine-doped carbon dots: Impact of surface functionalization and pH. Carbon, vol. 206, pp. 114–123, (2023).
[3] Laptinskiy, K. A., Burikov, S. A., Chugreeva, G. N., Sarmanova, O. E., Tomskaya, A. E., & Dolenko, T. A. The influence of the type of ions hydration on photoluminescence of carbon dots in aqueous suspensions. Fullerenes, Nanotubes and Carbon Nanostructures, vol. 29, Issue 1, pp. 67–73, (2020).

Luminescent proline-stabilized copper nanoclusters: synthesis and examination in bioanalysis by fluorometry and capillary electrophoresis

A. Demenshin, E. Kolobova, E. Solovyeva

Institute of Chemistry, Saint Petersburg State University, Universitetskaya nab. 7/9, Saint Petersburg, 199034 Russia

e-mail: svenszivaldemar@gmail.com

Metal nanoclusters are widely used in various fields of chemistry and biology. Their most prominent applications include sensing, bioimaging and catalysis. In analytical chemistry, numerous methods have been proposed for the spectral determination of important metabolites, such as glucose, utilizing metal nanoclusters [1]. However, the preparation of stable and highly luminescent nanoclusters remains challenging. Additionally, the development of new applications for metal nanoclusters is in high demand.

Copper nanoclusters are inexpensive, easy to synthesizable, highly stable and have numerous applications [2]. In this work, the protocol for the synthesis of copper nanoclusters stabilized with L-proline was optimized, resulting in Cu nanoclusters with intense emission near 450 nm (Fig. 1A). Various copper to L-proline (Cu^{2+}:L-Pro) molar ratios were tested, and the optimal ratio was found to be 1:250. Obtained nanoclusters were analyzed by reverse phase high-performance liquid chromatography (Fig. 1B) and capillary electrophoresis.

A major part of the work was dedicated to the evaluation of synthesized clusters in capillary electrophoresis as additives in background electrolytes. Different model mixtures of bioactive compounds were investigated to determine whether L-proline-Cu nanoclusters can improve the performance of capillary electrophoresis. It was confirmed that L-proline-Cu nanoclusters enhance the efficiency and separation selectivity of some analytes due to specific interactions, which were validated by spectroscopic methods.

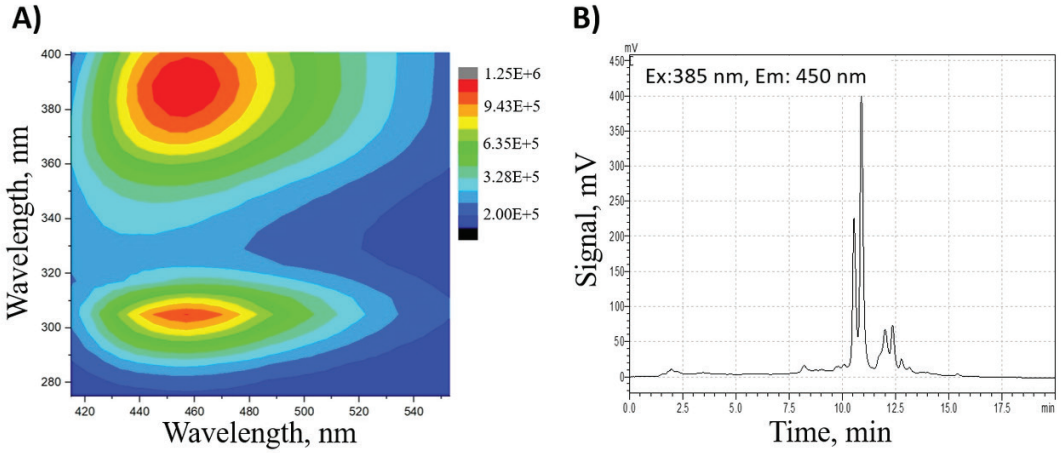

Fig. 1. A) 3D fluorescence spectra and B) chromatogram of synthesized L-proline-Cu nanoclusters.

The work was supported by Saint Petersburg State University, project № 122040800256-8. The authors thank the resource centers of SPBU Research Park: "Chemical Analysis and Material Research", "Optical and Laser Materials Research".

[1] L. Zhihe, W. Zhennan, Y. Qiaofeng, C, Yitao, Chai, C. Osburg Jin Huang, X. Jianping, Correlations between the fundamentals and applications of ultrasmall metal nanoclusters: Recent advances in catalysis and biomedical applications, Nano Today, 36, 101053, (2021).
[2] A. Baghdasaryan, T. Bürgi, Copper nanoclusters: Designed synthesis, structural diversity, and multiplatform applications, Nanoscale, 13(13), pp. 6283–6340, (2021).

Magnetic inhomogeneities in Fe_3Al epitaxial thin films probed by FMR and time-resolved magnetooptics

A. Kh. Kadikova[1], A. V. Petrov[1], Kh. Sh. A. Taqi[1], B. F. Gabbasov[1], A. I. Gumarov[1], I. V. Yanilkin[1], L. R. Tagirov[1,2], R. V. Yusupov[1]

1- Institute of Physics, Kazan Federal University, Kremlevskaya st. 16A, Kazan, 420008 Russia
2- Zavoisky Physical-Technical Institute, FRC Kazan Scientific Center of RAS, Sibirskiy Trakt 10/7, Kazan, 420029 Russia

e-mail: anelyakadikova11@gmail.com

Systems based on the Fe_3Al intermetallic compound remain relevant due to the diversity of properties achievable through alloying this system. When vanadium (V) and tungsten (W) are added, the system exhibits high thermoelectric properties [1], while the addition of cobalt (Co) results in high spintronic characteristics [2]. Additionally, the magnetism of various structural phases formed near the stoichiometric ratio Fe:Al = 3:1 is of particular interest. For example, the saturation magnetization of the A2 phase – a disordered solid solution of Al in α-Fe – is higher than that of the B2 phase (an ordered solid solution). This fact is an exception to the general rule for magnetic alloys undergoing ordering. Regarding spintronic materials, a critical parameter of ferromagnets is their magnetic homogeneity. In [3], the influence of A2-B2 antiphase boundaries in Fe-Al thin-film systems on their magnetic properties is examined in detail. However, the authors use transmission electron microscopy (TEM), electron holography, and Lorentz microscopy for their analysis.

This work presents the results of magnetic inhomogeneity studies in thin epitaxial Fe_3Al films on MgO (001) substrates using ferromagnetic resonance (FMR) and time-resolved magnetooptical spectroscopy, demonstrating the complementary character of these techniques. It is shown that the magnetic homogeneity of the films depends on their composition and synthesis conditions, which is reflected in the frequency spectrum and magnetization precession damping. We found that Fe_3Al thin-film systems tend to exhibit island-like morphology, regardless of synthesis conditions. Additionally, aluminum segregation to the surface has been observed.

The Gilbert damping constant was estimated to be $\alpha = (2.84 \pm 0.17)\times10^{-2}$ for a magnetically homogeneous $Fe_{70}Al_{30}$ thin film with a thickness of 20 nm. This value corresponds to the constant typical of Fe_3Al in the disordered A2 phase. Nearly all synthesized thin-film systems exhibit two FMR lines in their spectra, consistent with time-resolved magneto-optical measurements. For example, $Fe_{75}Al_{25}$ and $Fe_{70}Al_{30}$ thin films deposited at room temperature and annealed in vacuum at 450 °C are magnetically inhomogeneous, as evidenced by at least two or even three frequency components in the magnetization precession and its rapid damping. $Fe_{75}Al_{25}$ films synthesized at a substrate temperature of 400 °C exhibit both low-frequency (3–6 GHz) and high-frequency (18–19 GHz) precession components in a 0.3 T field applied along the normal direction. The latter is associated with either of the precession of magnetization in multiple magnetic phases within the Fe_3Al films, the coupled precession of magnetic domains, or both of them simultaneously.

[1] van der Rest C., Dupont V., Erauw J. P., Jacques P. J., On the reactive sintering of Heusler Fe_2VAl-based thermoelectric compounds, Intermetallics, 125, 106890, (2020).
[2] Ahmad A., Mitra S., Srivastava S.K., Das A.K., Structural, magnetic, and magnetocaloric properties of Fe_2CoAl Heusler nanoalloy, Journal of Magnetism and Magnetic Materials, 540, 168449, (2021).
[3] Murakami Y., Niitsu K., Tanigaki T., Kainuma R., Park H. S., Shindo D., Magnetization amplified by structural disorder within nanometre-scale interface region, Nature communications, 5, 1, 4133, (2014).

Raman analysis of PLLA-PEG-PLLA hydrogels

L. Yu. Kozlova[1], S. O. Liubimovskii[1], Yu. S. Fomina[2], Yu. D. Zagoskin[2], N. G. Sedush[2,3], V. S. Novikov[1]

1- Prokhorov General Physics Institute of the Russian Academy of Sciences, Vavilov str. 38, Moscow, 119991 Russia
2- National Research Centre "Kurchatov Institute", Akademika Kurchatova pl. 1, Moscow, 123182 Russia
3- Enikolopov Institute of Synthetic Polymeric Materials of the Russian Academy of Sciences, Profsoyuznaya str. 70, Moscow, 117393 Russia

e-mail: lus.kozlowa2011@kapella.gpi.ru

Hydrogels on the base of biocompatible polymers, such as copolymers of poly(L-lactide) (PLLA) and poly(ethylene glycol) (PEG), are increasingly used in medicine for fabrication of tissue-engineering constructions [1]. In this regard, the development of new methods for studying hydrogels is an urgent task. Raman spectroscopy is a highly informative and non-destructive method of research, it makes possible to obtain information about the structure of both crystalline and non-crystalline areas of polymers, conformational composition of molecules, relative contents of polymers and water. However, there are only limited number works in which PLLA-PEG-PLLA hydrogels was studied by Raman spectroscopy [2].

In this work, Raman spectra of hydrogels based on PLLA-PEG-PLLA triblock copolymers (Fig. 1) were analyzed. The molecular weight of PEG was 4600 and 12000 Da. The ratio of monomer units LA/EG was in the range from 0.5:1 to 1.5:1.

A number of spectral differences were observed in the hydrogels depending on the PEG segment length. First, the degree of crystallinity of the PLA blocks was higher when shorter PEG chain was used as macroinitiator. It's indicated by the intensity and profiles of the bands around 401 and 411 cm^{-1}. Second, comparison of the hydrogel spectra with those of liquid and semi-crystalline PEG revealed a predominance of disordered PEG conformations. Third, Raman spectra of partially dried hydrogels were recorded, showing that water content does not exert a significant influence on the structure. Finally, the analysis of the Raman spectra enabled estimation of the relative content of PLLA, PEG, and water within the hydrogels.

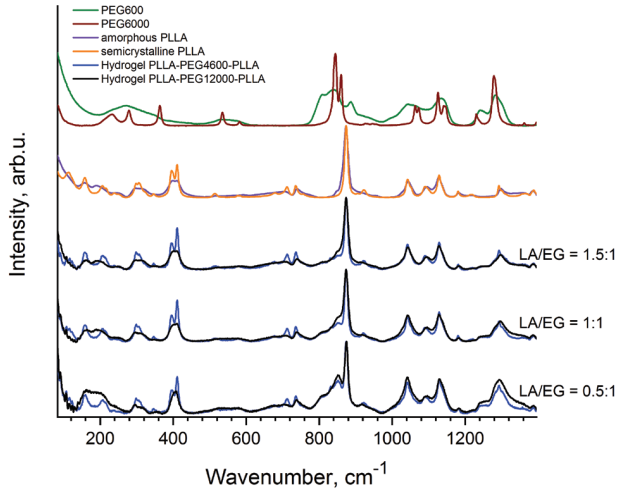

Fig. 1. Raman spectra of hydrogels with different length of PEG and PLLA blocks.

[1] Z. Yazdanpanah, J. D. Johnston, D. M. L. Cooper, and X. Chen, "3D Bioprinted Scaffolds for Bone Tissue Engineering: State-Of-The-Art and Emerging Technologies," Front. Bioeng. Biotechnol., vol. 10, no. April, (2022). doi: 10.3389/fbioe.2022.824156.
[2] S. Li and M. Vert, "Synthesis, Characterization, and Stereocomplex-Induced Gelation of Block Copolymers Prepared by Ring-Opening Polymerization of L(D)-Lactide in the Presence of Poly(ethylene glycol)," Macromolecules, vol. 36, no. 21, pp. 8008–8014, (2003). doi: 10.1021/ma034734i.

Raman structural analysis of linear oligomers of L-lactide and D,L-lactide

L. Yu. Kozlova[1], S. O. Liubimovskii[1], A. M. Semin[1,2], S. M. Kuznetsov[1], K. T. Kalinin[3], A. V. Bakirov[3,4], N. G. Sedush[3,4], V. S. Novikov[1]

1- Prokhorov General Physics Institute of the Russian Academy of Sciences, Vavilov str. 38, Moscow, 119991 Russia
2- D. I. Mendeleev Russian University of Chemical Technology, Miusskaya Ploshchad 9, building 1, Moscow, 125047 Russia
3- National Research Centre "Kurchatov Institute", Akademika Kurchatova pl. 1, Moscow, 123182 Russia
4- Enikolopov Institute of Synthetic Polymeric Materials of the Russian Academy of Sciences, Profsoyuznaya str. 70, Moscow, 117393 Russia

e-mail: lus.kozlowa2011@kapella.gpi.ru

Oligomers of lactide (LA) have a great potential in development of biocompatible and biodegradable systems for medical purposes, they also can serve as models for studying LA copolymers and branched LA oligomers. Varying the degree of polymerization (DP), the enantiomeric composition and post-treatment conditions, one can effectively change the structure and properties of the oligomers. Therefore, it is important to have an informative and convenient method for evaluation of key parameters of LA oligomers. The aim of this work is to determine the dependence of Raman spectra of linear oligomers of L-lactide (L-LA) and D,L-lactide (D,L-LA) on the DP and crystallinity degree (CD).

We showed that the ratio of intensities of the band of 1,12-dodecanediol (co-initiator of the synthesis) at 2850 cm^{-1} and the band of LA oligomers at 2947 cm^{-1} can be used to estimate the DP of the oligomers with length less than 50 monomeric units.

We revealed that the ratio of the intensities of the polylactide (PLA) bands at 411 and 874 cm^{-1} (Fig. 1) is a measure of the CD of the oligomers. This approach to the CD evaluation was proven early for neat PLA [1] and PLA blocks in copolymers of L-LA and CL in the whole range of compositions. We obtained that the CD of the oligomers of L-LA increases with growth of PD.

Thus, we showed that Raman spectroscopy is a powerful method for evaluation of the PD and CD of LA oligomers.

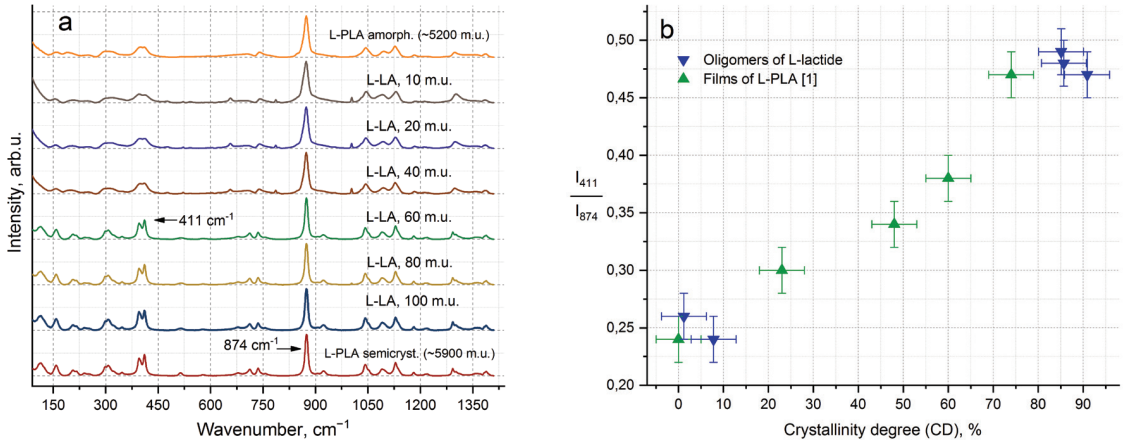

Fig. 1. a – Raman spectra of the oligomers of L-LA with various PD, semicrystalline (CD = 86%) and amorphous (CD = 0%) L-PLA in the spectral range of 80–1410 cm^{-1}; b – the ratio of the peak intensities of the PLA bands at 411 and 874 cm^{-1} as a function of the CD, obtained by X-ray diffraction analysis.

[1] S.O. Liubimovskii et al., Raman Evaluation of the Crystallinity Degree of Poly(L-Lactide)-Based Materials, Phys. Wave Phenom., vol. 32, no. 2, pp. 140–149, Apr. 2024, doi: 10.3103/S1541308X24700080.

Rapid evaluation of carotenoid content in vegetable oils and dietary supplements by Raman spectra

S. M. Kuznetsov[1], A. A. Ashikhmin[2,3], V. S. Novikov[1], E. A. Sagitova[1]

1-Prokhorov General Physics Institute of the Russian Academy of Sciences, Vavilov str. 38, Moscow, 119991 Russia
2- Pushchino Science Center for Biological Research, Russian Academy of Sciences, Pushchino, Moscow oblast, Russia
3- Bach Institute of Biochemistry, Research Center of Biotechnology Russian Academy of Sciences, Leninsky pr-t 33, bld. 2, Moscow, 119071 Russia

e-mail: kuznetsovsm@kapella.gpi.ru

Vegetable oils have numerous beneficial properties due to the presence of fatty acids in their content. Besides that, a number of oils contain different carotenoids that play an important role in nature and human health. Carotenoids are pigments that perform antioxidant and photoprotective functions in living organisms (mammals, plants and bacteria). Individual carotenoids can possess provitamin, antimutagenic, anticarcinogenic and immunostimulatory actions [1]. Vegetable oils can increase stability and bioavailability of carotenoids, and this property of oils is used in the creation of dietary supplements.

In this work, we developed a quantitative Raman technique of determining the carotenoid content in vegetable oils and dietary supplements. In order to do this, we prepared model solutions of sunflower oil (that originally did not contain carotenoids) with different content of carotenoids (β-carotene, lycopene, astaxanthin), and recorded their Raman spectra at the laser excitations with the wavelengths (λ) of 532 and 785 nm.

We observed three main Raman bands at about 1006, 1150, 1520 cm^{-1}, which are associated with the vibrations of carotenoid molecules. We obtained dependences of their peak intensities on the carotenoid content. Fig. 1 reveals such dependence obtained for the Raman band (λ = 532 nm) at about 1520 cm^{-1}, which relates to the stretching vibrations of C=C bonds of β-carotene molecules in the β-carotene enriched sunflower oil. A minimal content of β-carotene, which was reliably detected in this oil, is $2.5 \cdot 10^{-3}$ mass.%.

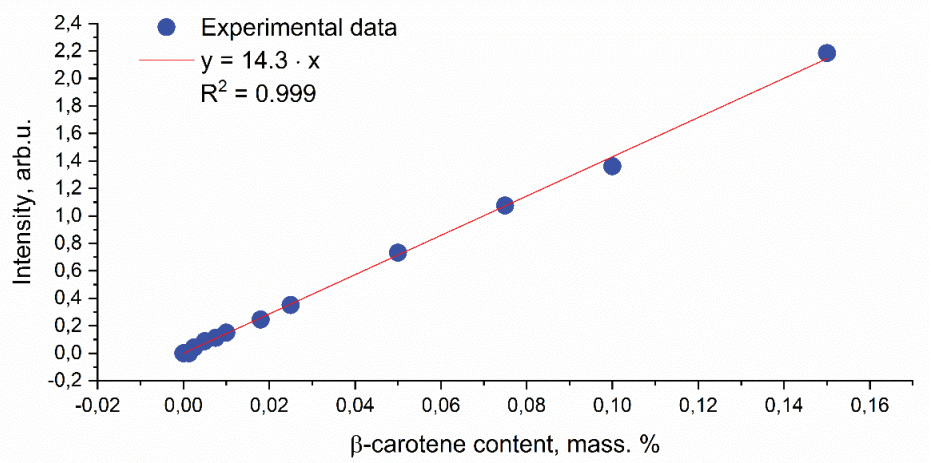

Fig. 1. Peak intensities of the C=C band in Raman spectra of β-carotene enriched sunflower oil *vs* β-carotene content; λ = 532 nm.

Thus, this contribution shows that the developed Raman technique can be applied to the detection of various carotenoid content in vegetable oils and commercial dietary supplements based on them. In addition, minimal levels of detection were studied for each used carotenoid.

This work was supported by the RSF grant № 24-22-20100, https://rscf.ru/project/24-22-20100/.

[1] Stahl W., Sies H. Bioactivity and protective effects of natural carotenoids. // Biochim. Biophys. Acta - Mol. Basis Dis. – 2005. – V. 1740, N. 2. – P. 101–107. DOI: 10.1016/j.bbadis.2004.12.006.

Bubble dynamics study for in situ chemical analysis of bulk oils by double pulse laser induced breakdown spectroscopy

V. N. Lednev[1], P. A. Sdvizhenskii[2], A. V. Rogachevskaya[1], A. A. Khaziev[2]

1- Prokhorov General Physics Institute, Russian Academy of Science, Moscow, Russia
2- Federal State Budgetary Educational Institution of Higher Education "Moscow Automobile and Road Construction State Technical University (MADI)", Moscow, Russia

e-mail: lednev@kapella.gpi.ru

The in situ chemical analysis of process fluids inside the units (internal combustion engines, drive-train, aircraft hydraulic systems, etc.) during its operation is highly demanded in aviation, automotive and energy industries. The online monitoring of metal impurities in the engine oil inside the operating unit will provide valuable information for understanding engine deterioration. Laser-induced breakdown spectroscopy (LIBS) is a good candidate for in situ chemical analysis of any sample type including liquids. However, laser induced plasma emission is quenched inside liquid so double pulse LIBS should be used to get plasma spectra suitable for quantitative chemical analysis: first nanosecond laser pulse to create a bubble inside the liquid, and the second laser pulse to induce plasma inside this bubble at the liquid-vapor interface. To optimize LIBS analytical performance and choose the best delay for second pulse ablation a detailed study of bubble dynamics in liquid has been studied by fast shadowgraph photography. The impact of oil temperature and laser pulse energy on bubble dimensions in different periods of its evolution have been quantified. The different delays between first and second laser pulses were varied to induce plasma by the second nanosecond laser pulse and find out an optimal delay for getting plasma spectra with the highest signal-to-noise ratio.

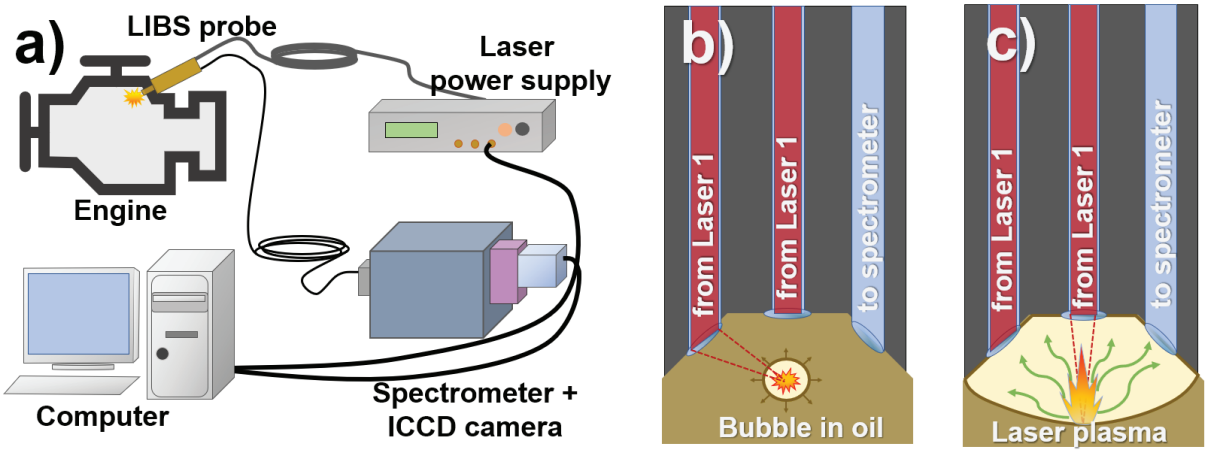

Fig. 1. The concept sketch of laser induced breakdown spectroscopy (LIBS) system for in situ chemical analysis of oil during engine exploitation (a) and key idea of double pulse method with bubble generation (b) and laser plasma induction (c).

The authors gratefully acknowledge financial support from the Russian Science Foundation (RSF) (agreement № 25-29-00835), https://rscf.ru/en/project/25-29-00835/.

An impact of inhomogeneous pump on ultrafast photoinduced magnetization precession in permalloy-based thin film structures

D. A. Makarov[1], A. Kh. Kadikova[1], A. I. Gumarov[1], I. V. Yanilkin[1], B. F. Gabbasov[1], A. V. Petrov[1], L. R. Tagirov[1,2], R. V. Yusupov[1]

1- Institute of Physics, Kazan Federal University, Kremlyovskaya str. 16a, Kazan, Russia
2- Zavoisky Physical-Technical Institute, Sibirsky tract 10/7, Kazan, Russia

e-mail: damakarov@yandex.ru

The magneto-optical Kerr effect (MOKE) is a powerful tool for studying magnetization dynamics in thin-film structures. It enables precise detection of magnetization variations, with sensitivity to optical polarization changes as small as 10^{-7}–10^{-8} radians [1] and ability to resolve fast magnetization dynamics.

In this work, photoinduced magnetization precession in thin permalloy (Py) films and permalloy/platinum (Py/Pt) bilayers were studied with time-resolved MOKE (TR-MOKE), and the Gilbert damping constants were determined. To minimize the influence of inhomogeneity of the probed region, measurements were performed with varying probe spot sizes while keeping the pump spot size fixed.

Our results reveal a strong dependence of the precession damping on the probe spot size for both Py and Py/Pt samples (Fig. 1). Notably, even when the probe spot is more than ten times smaller than the pump spot, a non-negligible dependence on the probe size persists. This observation contrasts with conventionally conducted measurements, where the probed region is often assumed to be sufficiently homogeneous at pump-to-probe spot size ratios of 3:1 [2–4].

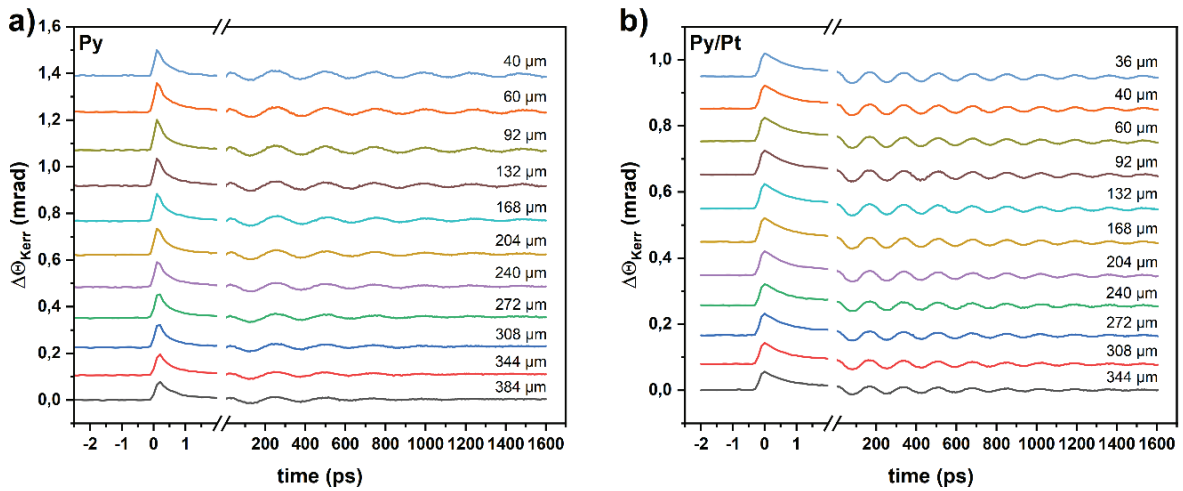

Fig. 1. Magnetization precession in a) Py and b) Py/Pt films, measured with different probe spot sizes at fixed pump spot size (600 μm).

The acquired data indicate that the homogeneity of the probed region plays a crucial role in the accurate determination of the Gilbert damping constant. The most reliable evaluation was achieved using the smallest probe spot size and further validated by comparison with ferromagnetic resonance (FMR) measurements, which showed good agreement (0.0082 for Py and 0.0108 for Py/Pt from TR-MOKE vs 0.007 for Py and 0.0102 for Py/Pt from FMR).

These findings highlight the importance of careful adjustment of the pump-to-probe spot size ratio in MOKE experiments to ensure precise determination of the Gilbert damping constant.

[1] J. M. D. Coey and S. S. P. Parkin, Handbook of Magnetism and Magnetic Materials (Springer), Magneto-optics and Laser-Induced Dynamics of Metallic Thin Films, (2021).
[2] H. J. Mohamad, L. R. Shelford, M. Aziz, U. A. S. Al-Jarah, R. Al-Saigh, R. A. J. Valkass, S. Marmion, B. J. Hickey, and R. J. Hicken, Thermally induced magnetization dynamics of optically excited YIG/Cu/Ni81Fe19 trilayers, Physical Review B., vol. 96, pp. 134431-1–134431-12, (2017).
[3] F. Busse, M. Mansurova, B. Lenk, M. von der Ehe, M. Münzenberg, A scenario for magnonic spin-wave traps, Scientific reports, vol. 5, pp. 12824-1–12824-6, (2015).
[4] C. S. Gonçalves, A. S. Silva, D. Navas, M. Miranda, F. Silva, H. Crespo, D. S. Schmool, A dual-colour architecture for pump-probe spectroscopy of ultrafast magnetization dynamics in the sub-10-femtosecond range, Scientific reports, vol. 6, pp. 22872-1–22872-11, (2016).

Phenomena of catalyzed oxidation of β-blockers on gold nanoparticle

K. Makarova, E. Kolobova, E. Solovyeva

Saint Petersburg State University, Institute of Chemistry, Saint Petersburg, Russia

e-mail: st107419@student.spbu.ru

Gold nanoparticles (GNPs) have unique properties that make them promising for analytical chemistry, pharmacology and medicine. Localized surface plasmon resonance (LSPR) underlies the physico-chemical properties of GNPs and causes a number of phenomena at the metal-solution interface that do not occur on the non-plasmonic surfaces. Interface phenomena involving chiral molecules are of particular interest from the point of view of bioanalytical applications of gold nanoparticles and surface-enhanced Raman spectroscopy (SERS), so their study is extremely important. The propranolol drug from the β-blockers family is one of the molecules for which a chiral recognition by SERS using chiral selector-modified noble metal nanoparticles has been reported in the literature [1].

This work presents the comprehensive study of β-blockers adsorption on GNPs under various conditions. The experiment included the exposure of β-blockers (propranolol, amlodipine, carvedilol, sotalol et al.) to a dispersion of GNPs, centrifugal separation of GNPs and solution with subsequent analysis of the solid phase by the SERS method, and the liquid phase by capillary electrophoresis. After adsorption of propranolol and sotalol drugs on GNPs, unknown peaks were observed in the electropherograms of the supernatants in addition to the peaks of R and S enantiomers. HPLC-MS analysis showed that these peaks arise from the products of molecules N-dealkylation and OH-group oxidation. Thus, it was revealed the conversion of some β-blockers into corresponding metabolites on the surface of GNPs. The assessment of influence of pH, oxygen content and presence of radical trap (sodium azide) on the degree of β-blockers conversion allowed us to propose the mechanism of single-electron transfer for the discovered reactions (Fig. 1).

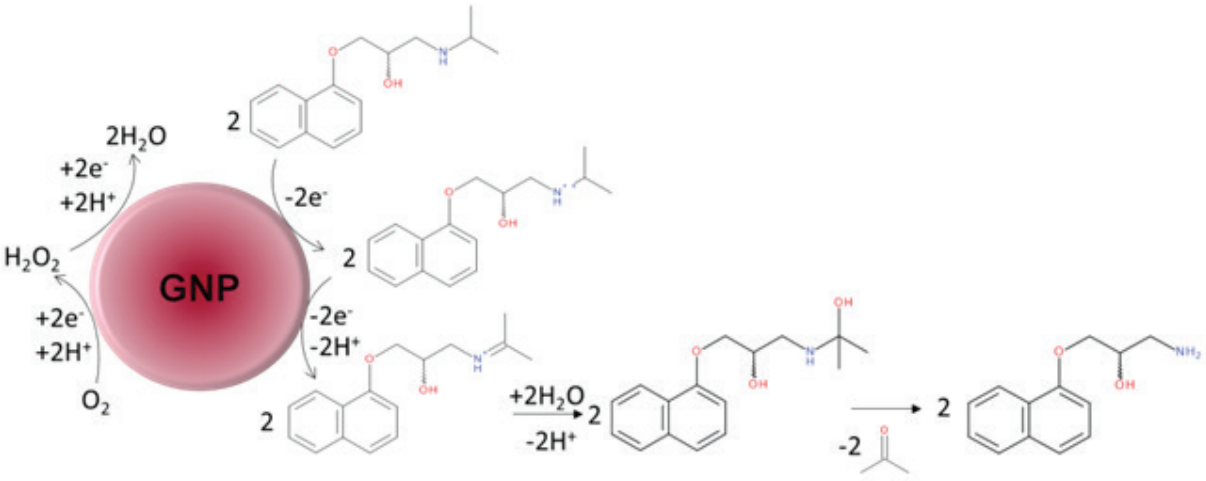

Fig. 1. Proposed mechanism of N-dealkylation of propranolol on gold nanoparticles.

This work was supported by Russian Science Foundation, grant № 22-73-10052. The authors thank the resource centers of SPBU Research Park: "Chemical Analysis and Material Research", "Optical and Laser Materials Research".

[1] E. Bodoki, M. Oltean, A. Bodoki, Rares Stiufiuc Chiral recognition and quantification of propranolol enantiomers by surface enhanced Raman scattering through supramolecular interaction with b-cyclodextrin, Talanta, vol. 101, pp. 53–58 (2012).

Eye-safe laser remote sensing of water flows underneath the ice of Lake Baikal

S. M. Pershin[1], M. Ya. Grishin[1], V. A. Zavozin[1], V. N. Lednev[1], V. S. Makarov[2], M. M. Makarov[3], K. M. Kucher[3]

1- Prokhorov General Physics Institute of the Russian Academy of Sciences, 38 Vavilova street 38, Moscow, 119991 Russia
2- Space Research Institute of the Russian Academy of Sciences, Profsoyuznaya street 84/32, Moscow, 117133 Russia
3- Limnological Institute Siberian Branch of the Russian Academy of Sciences, Ulan-Batorskaya street 3, Irkutsk, 664033 Russia

e-mail: mikhail.grishin@kapella.gpi.ru

Detection of water flows and layers underneath the ice is of growing demand in scientific and technological applications. The interest to such research has been increasing in the last decades due to oil and gas production in Arctic region and global climate changes monitoring. In laboratory measurements, different techniques can be used depending on the research goals while monitoring of vast natural areas can be carried out only by means of remote sensing. Laser remote sensing (LIDAR) is a promising way to reveal physical properties of both ice and open water, but only eye-safe systems are allowed.

For the first time, stratification layers in bulk water under ice have been detected by an eye-safe compact LIDAR developed in Prokhorov General Physics Institute to reveal any small fluctuation in water properties. The LIDAR was based on a Nd:YAG laser (532 nm, 3 ns, 2 μJ/pulse, 4 kHz) and a single-photon avalanche photodiode (SPAD) detector for underwater sensing (Fig.1a). The LIDAR was installed on the ice surface about 3 km from the coastline of Bolshoye Goloustnoye village (52.009420°N, 105.368420°E) at Lake Baikal (Fig.1b). The LIDAR measurements were compared with the space resolved temperature measurements by a STD probe (Fig.1c). It can be seen that at depths of 5 and 7 m scattering layers are present in water formed by a suspension of microparticles of different sizes that are stratified without convection in the subglacial volume on the shelf. Stratification layers can be explained by combined impact of two factors: a) the sub-ice water flow from a small creek located nearby; b) the displacement of water layers due to cyclonic circulation [1]. Based on the experimental measurements and signal-to-noise ratio, the LIDAR is capable to detect water flows at depths down to 50 m. Due to small footprint, low mass and energy efficiency, the developed LIDAR can be installed on lightweight boats [2] or unmanned quadcopters [3], so the automatic monitoring of freshwater reservoirs can be performed continuously, for example, by underwater drones.

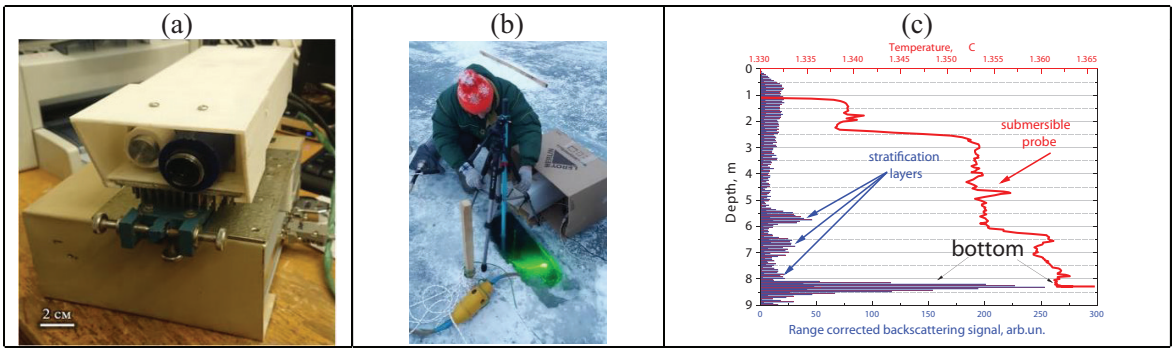

Fig. 1. (a) – A photograph of the compact eye-safe LIDAR. (b) – photograph of LIDAR measurements on the ice of Lake Baikal. (c) – LIDAR backscattering signal profile (blue color) and water temperature profile measured by the submersible probe (red color).

The authors are grateful to the Russian Science Foundation for the financial support of the study (grant no. 23-42-10019).

[1] E. Troitskaya, V. Blinov, V. Ivanov et al., Cyclonic circulation and upwelling in Lake Baikal, Aquatic Sciences, vol. 77, pp. 171–182 (2015).
[2] S.M. Pershin, B.G. Katsnelson, M.Ya. Grishin et al., Laser Remote Sensing of Lake Kinneret by Compact Fluorescence LiDAR, Sensors, vol. 22, 7307 (2022).
[3] M.Ya. Grishin, V.N. Lednev, S.M. Pershin and P.O. Kapralov, Ultracompact Fluorescence Lidar Based on a Diode Laser (405 nm, 150 mW) for Remote Sensing of Waterbodies and the Underlying Surface from Unmanned Aerial Vehicles, Doklady Physics, vol. 66, pp. 153–155 (2021).

Selenium quantification in soil by laser induced breakdown spectrometry

A. V. Rogachevskaya, V. N. Lednev, P. A. Sdvizhenskii

Prokhorov General Physics Institute of the Russian Academy of Sciences, Vavilova Street 38, Moscow, Russia

e-mail: rogachevskaya.alexa@gmail.com

Development of new techniques for soil elemental analysis without any sampling is of high demand in modern agriculture. Online control of the elemental composition allows both to produce healthy foods by preventing its poisoning and to improve an agricultural holding financial efficiency.

The conventional soil elemental analysis is complex and time consuming due to the soil dissolution in acids. In contrast, laser induced breakdown spectrometry (LIBS) has proven itself as an express element quantification technique that may not require sample preparation. However, matrix effects, humidity and other soil properties reduce the LIBS sensitivity and complicate the analysis. That is why several time-consuming sample preparation techniques, such as milling, sieving and pelleting, are used for soil in order to achieve good accuracy of measurements. The quantification of soil microelement, such as selenium, presents an additional challenge, as microelement concentration in soil is low and therefore requires more method sensitivity. Nevertheless, analysis by LIBS is a promising solution for online determination of soil elements under field conditions.

In the research LIBS is used for selenium quantification in soil. Se I 196.09 nm emission line was chosen as the analytical line due to its most insignificant spectral interference with the other soil components lines. The impact of simple soil samples preparation techniques on LIBS analytical performance have been compared (Fig. 1). The best limit of detection (LOD) was 15 mg/kg for 3 averaged spectra of tableted samples, which take more time to prepare. Though mounted on tape and loose soil powder showed the same LOD result if more signal accumulated. The study results show the potential of using the automated LIBS technique for online selenium control in the field.

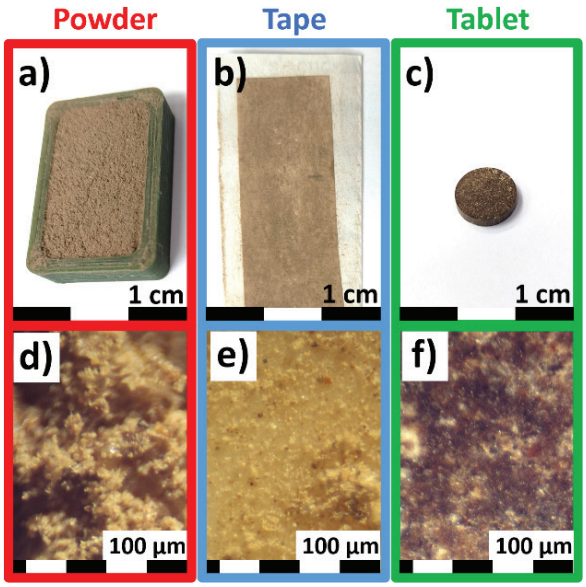

Fig. 1. Soil samples photographs: loose soil powder in a container (a), tape adhesive-mounted soil powder (b) and pressed into tablet soil powder (c). Close-up view of sample surfaces: loose (d), tape adhesive-mounted (e) and tableted soil powder (f).

This research was funded by a grant from the Ministry of Science and Higher Education of the Russian Federation for large scientific projects in priority areas of scientific and technological development (subsidy identifier 075-15-2024-540).

Chaos-order phase transition in water at room temperature: competition of hydrogen bonds and Brownian motion

P. Smerchanskiy[1,2], M. Grishin[2], S. Pershin[2]

1- Prokhorov General Physics Institute of the Russian Academy of Sciences, Vavilov str. 38, Moscow, 119991 Russia
2- National Research University Higher School of Economics, Myasnitskaya st. 20, Moscow, 101000 Russia

e-mail: pershin@kapella.gpi.ru, pavelsmerchanskiy@gmail.com

It is known that optical breakdown in a layer near the water surface in the field of nanosecond [1] and picosecond (532 nm) pulses [2] reduces the threshold of forced raman scattering (WRC) in water due to free electrons (according to the authors' interpretation). The breakdown modifies the structure of hydrogen-bonded complexes to an ice structure with a characteristic band of ~3200 cm^{-1} in the OH band envelope. Using spontaneous raman (532 nm 100 μJ, 7 ns), for the first time without optical breakdown, as far as we know, we detected a shift of the center of the OH band of RAMAN in the layer near the surface towards the ice component ~3200 cm^{-1}. This result correlates with the formation of ice-like structures of hydrate layers of nanoparticles in water, which we have recently discovered [3]. Significantly, the dynamics of the phase transition of the formation of ice structures in a layer up to 1 mm thick during 150 minutes after filling the cuvette with water has been revealed.

[1] Zh. Man, Opt. Lett. (2015).
[2] H. Yui, Chem. Phys. Lett. (2002).
[3] S. Pershin, A. Bunkin et al., Letters to the JETF (2025).

32nd INTERNATIONAL CONFERENCE
Advanced Laser Technologies
ALT'25

NONLINEAR AND TERAHERTZ PHOTONICS

THz generation and electron acceleration in gas-cluster jet under sub-TW laser excitation

A. V. Balakin[1], N. A. Kuzechkin[2], P. M. Solyankin[2], A. P. Shkurinov[1]

1- Faculty of Physics, Lomonosov Moscow State University, Moscow, Russia
2- National Research Centre "Kurchatov Institute", Moscow, Russia

e-mail: a.v.balakin@physics.msu.ru

Study of laser-plasma interaction and yielding from phenomena is intensively evolving field of knowledge which gives a great background for next implementation in a plenty of applications. Fast developing of generation techniques of ultra-intense laser pulses such as chirped pulse amplification technique allowed to achieve relativistic intensities (>10^{18} W/cm^2) and even up to as huge as 10^{25} W/cm^2 [1]. These special laser complexes of "mega-science" level that generate TW- and PW-power pulsed radiation are used in most experiments to form plasma in gaseous and condensed media in order to produce bunches of high-energy charged particles, secondary electromagnetic radiation in UV and X-ray range [2–4].

In turn, the use of less powerful, but more accessible and compact sub-TW level laser systems for laser-driven generation of energetic charge particles is not so popular. Here we substantiate that the small-footprint sub-TW laser can be used effectively for laser-plasma generation of accelerated electron bunches and accompanied THz radiation in gas-cluster jet. Ti:Sapphire regenerative amplifier system generated 35 fs pulses with energy of up to 7 mJ at 1 kHz repetition rate and provided sub-relativistic intensities up to 10^{17} W/cm^2 was used in our experiments for excitation of gas-cluster jet produced under adiabatic expansion of gas into vacuum through a special supersonic nozzle. This target inherits such unique features as high local and relatively low average density of the matter, and effectively interacts with high-intensity femtosecond laser pulses.

Here we present and discuss our recent results on study of generation of electron bunches and accompanied THz radiation under various conditions of the gas-cluster target excitation depending on: laser pulses energy, duration and polarization, localization of laser focus position in the jet, stagnation pressure of the working gas.

This work was funded partly within the state assignment of Lomonosov Moscow State University (A.V.B., A.P.Sh.) and partly within the state assignment of NRC "Kurchatov Institute" (N.A.K., P.M.S.).

[1] Mourou G. Nobel Lecture: Extreme light physics and application // Reviews of Modern Physics. -2019. -Vol. 91. -No. 3. -P. 030501.
[2] Esarey E., Schroeder C. B., Leemans W. P. Physics of laser-driven plasma-based electron accelerators // Reviews of modern physics. -2009. -Vol. 81. -No. 3. -P. 1229–1285.
[3] Hudson L. T., Seely J. F. Laser-produced X-ray sources //Radiation Physics and Chemistry. -2010. -Vol. 79. -No. 2. -P. 132–138.
[4] Nasr A.M. Hafz. Stable generation of GeV-class electron beams from self-guided laser–plasma channels // Nature Photonics -2008. -Vol. 2 -P. 571.

Powerful THz gyrotrons with improved selection of operating mode

I. V. Bandurkin, D. V. Lazarev, Yu. K. Kalynov, I. V. Osharin, A. V. Savilov

Federal Research Center A. V. Gaponov-Grekhov Institute of Applied Physics, Russian Academy of Sciences, Nizhny Novgorod, 603950 Russia

e-mail: savilov@ipfran.ru

Gyrotrins are sources of coherent radiation based on cyclotron excitation of high-Q near-cutoff modes of open cavities by a beam of electrons rotating in strong magnetic fields. Since the frequency of a traditional fundamental-cyclotron-harmonic gyrotron is close to the electron cyclotron frequency, the advancement of such devices to the terahertz frequencies is limited by the attainable magnetic fields. A natural solution of this problem is the operation at the cyclotron harmonics. However, an increase in the operating cyclotron harmonic number leads to a dramatic decrease in the intensity of the electron–wave coupling and, as a result, to a strong competition from the parasitic waves excited at lower harmonics (especially at the fundamental one). Thus, a key problem is ensuring the selectivity of excitation of a higher cyclotron harmonic. This problem is especially severe in the sub-THz frequency range, where the use of highly oversized cavities is inevitable and the mode spectrum is dense, and its solution required the use of both electronic and electrodynamic methods of the mode selection.

We describe our theoretical and experimental activity in realization of THz-frequency-range Large-Orbit Gyrotrons (LOGs). This gyrotron configuration uses a powerful electronic method to improving the selectivity of excitation of high harmonics, namely, the use of an axial electron beam, which can interact with a transverse mode of a cavity with an azimuthal index m only at the cyclotron harmonic $s = m$. In our experiments, various electrodynamic methods are aresed to improve the high-harmonic operation. Two experimental LOG installations (namely, the "universal" CW 30 kV/0.7 A LOG and the pulsed 80–100 kV/0.7–1.0 A LOG) are currently functioning at the Institute of Applied Physics [1]. In fist experiments under the CW LOG, stable CW operation at the second and third cyclotron harmonics (0.26 and 0.39 THz, respectively) with power levels of 10^2 W was observed [2]. Now, works under achieving a frequency of 0.52 THz on the basis of the use of a special sectioned cavity are in progress. In addition, we plan to carry out a testing experiment demonstrating possibility of a broadband ($\Delta f/f \sim 10\%$) frequency tuning in a gyrotron with external reflection of the output wave signal.

In the recent experiment under the pulsed LOG [3], it was demonstrated that the use of a cavity with one short selective irregularity expands the range of parameters, in which selective single-wave excitation of the operating third-harmonic wave is provided. This allowd us to acieve a quite high (1.3 kW) level of the output power. This experiment was performed in the regime of 10 μs pulses of the output wave. Recently, in a new series of experiments the duration of the output wave pulse has been increased up to ~30 μs at practically the same level of the output power. In addition, in the long-pulse experiment we observed a regime of competitions of two axial mode, where the lowest axial mode was exited at the edges of the electron beam pulse, whereas in the center of the pulse the second axial mode (having lower ohmic losses and, therefore, higher power) was generated. Our futire plans are to achieve a power level of several kW when operating at the third cyclotron harmonic (1 THz), as well as to achieve selective excitation of the fourth cyclotron harmonic at a frequency close to 1.2 THz.

[1] I. V. Bandurkin, V. L. Bratman, Y. K. Kalynov, I. V. Osharin, A. V. Savilov, Terahertz large-orbit high-harmonic gyrotrons at IAP RAS: Recent experiments and new designs, IEEE Trans. Electron Dev., vol. 65, pp. 2287–2293 (2018).
[2] Y. K. Kalynov, V. N. Manuilov, A. S. Fiks, N. A. Zavolskiy, Powerful continuous-wave sub-terahertz electron maser operating at the 3rd cyclotron harmonic, Appl. Phys. Lett., vol. 114, p. 213502 (2019).
[3] Y.K. Kalynov, I. V. Bandurkin, I. V. Osharin, A. V. Savilov, Third-Harmonic 1 THz Large-Orbit Gyrotron With an Improved Quasi-Regular Cavity, IEEE Electron Device Lett., vol. 44, p. 1740 (2023).

Nonlinearities of graphene in microwave and terahertz ranges

S. Bodrov, A. Korytin, A. Korzhimanov, I. Oladyshkin, Y. Sergeev, A. Stepanov

Institute of Applied Physics, Russian Academy of Sciences, Nizhny Novgorod, 603950 Russia

e-mail: step1an@ipfran.ru

Since the synthesis of graphene in 2004, its investigations have been attracting tremendous interest due to its unique physical properties and numerous potential applications. Among them, we note the possibility of using graphene as elements of high-frequency electronics. In our presentation, the results of a study of nonlinear properties of graphene in the microwave and terahertz frequency ranges are presented.

In particular, the passage of a short THz pulse through graphene located on a transparent dielectric substrate was investigated. THz radiation generated by the tilted-pulse-front technique in a $LiNbO_3$ crystal provided a field value of up to 250 kV/cm when focused in the sample area. The dependence of the THz radiation transmission through a sample with graphene on the terahertz field value is shown in Fig. 1. The nonlinear bleaching of graphene observed in the experiment is associated with the interplay of two processes acting in opposite directions: interband ionization of graphene and heating of electrons by a strong THz field.

Next, we investigated the effect of a strong THz field on the transmission of optical radiation through a single-layer graphene sample on a dielectric substrate using the pump-probe method. As it turned out, a terahertz pulse causes an increase in the transmission of optical radiation through graphene. Moreover, the effect turns out to be anisotropic: the increase in the transmission of optics through graphene turns out to be greater with orthogonal orientation of the THz and optics polarizations.

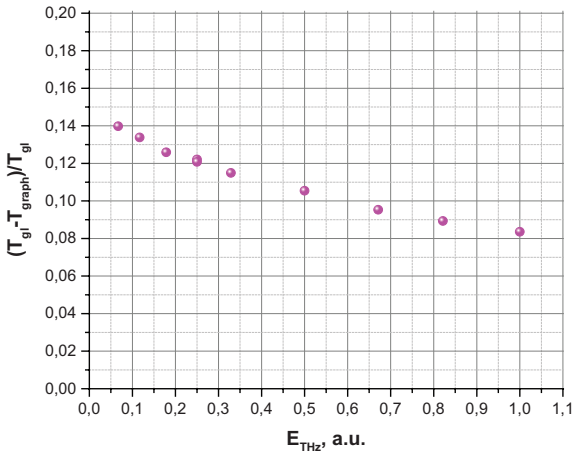

Fig. 1. Relative change in the transmission of a terahertz pulse through graphene from the magnitude of the THz field.

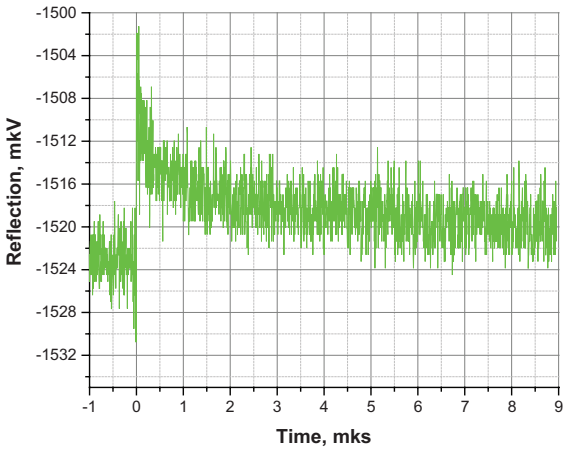

Fig. 2. Reflection of microwave radiation (173.5 GHz) from a graphene sample after exposure to a 70 fs laser pulse with an energy of 2 mJ.

Finally, a study was performed of the "slow" (on microsecond time scales) change in the reflectivity of graphene samples after exposure to nanosecond or femtosecond laser pulses in the microwave wavelength range of 100–200 GHz (Fig. 2). As it turned out, in addition to the rapid changes (which were characteristic of the first two experiments noted above), the time dependence of the reflection coefficient has a long time component determined by the thermal heating of the graphene and the substrate by the laser pulse.

The work was supported by the Russian Science Foundation the project No. 24-62-00032.

Gyrotrons: with great power comes great responsibility

G. G. Denisov[1], E. M. Tai[1,2], A. P. Fokin[1,2], A. N. Kuftin[1], Y. K. Kalynov[1], M. D. Proyavin[1], S. V. Samsonov[1], A. V. Savilov[1], E. A. Soluyanova[1,2], I. V. Zotova[1], M. Yu. Glyavin[1]

1- Institute of Applied Physics RAS, Ul'yanov str. 46, Nizhny Novgorod, Russia
2- GYCOM Ltd., Ul'yanov str. 46, Nizhny Novgorod, Russia

e-mail: glyavin@ipfran.ru

Gyrotrons [1, 2] are well known as sources of powerful coherent electromagnetic radiation in millimeter and sub-millimeter wavelength band. The key principles of efficient gyrotron operation are rotation phase bunching due relativistic cyclotron frequency dependence; radiation of electrons into the wave with "near-zero" longitudinal wave number which minimized effect of electron velocity spread, effective methods of mode selection for stable single mode operation; electrodynamic system with open cavities with large transverse size and effective conversion of high-order mode into paraxial microwave beam.

It should be noted that in recent years the importance of the above applications has increased significantly. Experiments have been conducted at nuclear fusion installations that confirm the fundamental need to use gyrotrons in its heating and current drive systems. At the beginning of the work on electron-cyclotron heating, it was believed that this approach was difficult, expensive and did not play the most important role. Today, the situation has changed dramatically, and the gyrotron complex of electron-cyclotron heating is considered absolutely necessary for tokamaks, playing a key role. In addition to the possibility of direct plasma heating, it should be noted that the gyrotron radiation flux can be focused into a spot with a characteristic size of several wavelengths, which allows locally increasing the plasma temperature in a given area and thus suppressing instabilities in the plasma or creating currents of the desired configuration in it. The international ITER project is in the stage of intensive construction and in 2024 a decision was made to increase the capacity of gyrotron complexes from 24 MW to 56 MW and, in the future, 80 MW. In the conceptual review of the DEMO project following ITER, increased requirements for gyrotrons were formulated: an increase in power by 1.5–2 times, an increase in frequency by 1.3–1.4 times, and an increase in efficiency to 60%. Such requirements undoubtedly require the solution of a number of scientific and engineering problems. Despite their rather rich history and significant results, gyrotrons continue to be the subject of intensive research.

The brightest achievements of present gyrotrons are: generations of MW power at frequencies up to 0.17 THz in CW mode with plans go to frequencies about 0.23–0.25 THz at the same power level; different tubes with operation frequency from 0.01 THz up to 1.3 THz; ability to capture frequency/phase (phased array); frequency stability better than $3 \cdot 10^{-12}$; wide instantaneous gain band (10%); continues frequency tuning – more than octave.

The report provides a brief overview of the key results obtained by IAP RAS/GYCOM teams, present some new ideas of formation electron beams with parameters good enough for effective electron beam-microwave energy exchange, methods of mode selection and examples of most attractive gyrotron applications.

Development of gyro devices was supported, in particular, by the IAP RAS projects FFUF-2022-0007 and FFUF-2024-0027.

[1] G.S.Nusinovich, M.K.A.Thumm, M.I.Petelin. "The Gyrotron at 50: Historical Overview". J. Infrared Milli Terahz Waves, 35, 325–381 (2014). doi :10.1007/s10762-014-0050-7
[2] A.G.Litvak, G.G.Denisov, M.Y.Glyavin. "Russian Gyrotrons: Achievements and Trends". IEEE Journal of Microwaves, 1, 1, 260–268, (2021). doi: 10.1109/JMW.2020.3030917

Spatiotemporal and spectral characteristics of mid-infrared single-cycle light bullets

A. Dormidonov[1], V. Kompanets[2], E. Zaloznaya[1], S. Chekalin[2]

1- Dukhov Automatics Research Institute, Federal State Unitary Enterprise, Suschevskaya str. 22, Moscow, 127055 Russia
2- Institute of Spectroscopy, Russian Academy of Sciences, Fizicheskaya str. 5, Troitsk, Moscow, 108840 Russia

e-mail: dormidonov@gmail.com

Filamentation of femtosecond laser pulse under conditions of anomalous group velocity dispersion leads to formation of a light bullet – wave packets extremely compressed in space and time with a high localization of the light field. The report briefly presents the current state of research on the phenomenon of mid-infrared single-cycle light bullets formed in transparent dielectrics [1].

Light bullets result from coupled processes of wave packet self-focusing in space and self-compression in time, which occur at an anomalous group velocity dispersion in the bulk of a third-order nonlinear medium under laser plasma generation conditions [2–4]. A light bullet is characterized by strong spatiotemporal optical field localization: the spatial and temporal scales of the localization region are a few wavelengths and one or two periods of optical oscillation.

Carrier-envelope phase shift during propagation of a near single-cycle light bullet causes synchronous oscillations of its spatial, temporal and energy parameters [5]. It causes periodical modulation of trace induced by light bullet in the medium (plasma channel or color centers structure). Such a dashed trace can be used to estimate the duration of a near single-cycle pulses [6].

Filamentation of mid-infrared light is accompanied by the generation of broadband supercontinuum, whose spectrum extends to the visible range and includes spectral components of the third, fifth, and subsequent odd harmonics of the fundamental frequency in the case of third-order nonlinearity and a continuous spectrum due to self-phase modulation. In the visible region of light bullet supercontinuum, an isolated anti-Stokes wing, separated by a broad minimum from the carrier wavelength band, is formed due to constructive interference of broadband light field [7]. The spectral maximum of the anti-Stokes band of the light bullet supercontinuum depends on linear parameters of the medium and can be determined by a simple dispersion equation [8].

[1] V.P. Kandidov, E.D. Zaloznaya, A.E. Dormidonov et al., Quantum Electron., 52, 233-246 (2022).
[2] Y. Silberberg, Optics Letters, 15, 1282 (1990).
[3] L. Bergé and S. Skupin, Physical Review Letters, 100, 113902 (2008).
[4] E.O. Smetanina, V.O. Kompanets, A.E. Dormidonov et al., Laser Phys. Lett., 10, 105401 (2013).
[5] E.D. Zaloznaya, V.O. Kompanets, A.D. Savvin et al., Laser Phys. Lett., 19, 075402 (2022).
[6] A.E. Dormidonov, E.D. Zaloznaya, V.O. Kompanets et al., JETP Letters, 116, 436 (2022).
[7] N. Garejev, G. Tamošauskas, A. Dubietis, Journal of the Optical Society of America B, 34, 88 (2017).
[8] A.E. Dormidonov, V.O. Kompanets, S.V. Chekalin, V.P. Kandidov, JETP Letters, 104, 175 (2016).

Mid-infrared optical parametric oscillator based on $BaGa_2GeS_6$ crystal

E. Erushin[1,2], S. Sere[2], M. Vostrikova[1,2], A. Boyko[1,2], G. Shevyrdyaeva[3], D. Badikov[3], N. Kostyukova[1,2]

1- Novosibirsk State University, Pirogova str. 1, Novosibirsk, 630090 Russia
2- Institute of Laser Physics of the SB of the RAS, Ac. Lavrentiev prosp. 15B, Novosibirsk, 630090 Russia
3- Kuban State University, Stavropolskaya str. 149, Krasnodar, 350040 Russia

e-mail: n.duhovnikova@gmail.com

The challenge of enhancing the spectral range and optimizing the conversion efficiency of mid-infrared radiation sources continues to be of significant importance. Research into barium chalcogenides is yielding important results, as these crystals exhibit a wide transparency range, significant nonlinearity, and high laser-induced damage threshold [1]. Among the barium chalcogenide crystals, the $BaGa_2GeS_6$ (BGGS) crystal is currently of particular interest. In recent years, successful implementations of sum-frequency generation for the broadband CO laser as well as a femtosecond optical parametric amplifier (OPA) pumped by a Cr:Forsterite laser using this crystal have been reported [2, 3]. In this context, we present what appears to be the first demonstration of a nanosecond optical parametric oscillator (OPO) based on a BGGS crystal pumped at 1.064 μm.

A 13.29 mm - long BGGS crystal with cut angles $\varphi = 17.3°$ and $\theta = 33.9°$ was used as a nonlinear element of the OPO. Both sides of the crystal were anti-reflection (AR) coated optimized for a central wavelength of 1.2 μm. The OPO was pumped by a diode-pumped, Q-switched Nd:YAG laser, which emitted pulses with an energy of up to 160 mJ within a 15 ns duration, operating at a repetition rate of 10 Hz. A single-pass pumping configuration was employed, where both cavity mirrors had a high transmission coefficient for pump wave. The output mirror was highly transparent for the idler wave, exceeding 70% over the entire tuning range, and highly reflective for the signal wave, ~90%. Concurrently, the front mirror of the cavity had a reflection coefficient for the signal wave of 99.9%. Fig. 1. demonstrate the wavelength tuning of the BGGS OPO radiation relative to the internal phase-matching angle: symbols depict the experimental data, while the curves are calculated utilizing Sellmeier equations from [4]. This figure also shows idler wave energy at 6.45 μm as a function of pump energy. The maximum idler energy (6.45 μm) of 2.064 mJ was obtained at a 92.6 mJ pump energy, and the idler wavelength tuning was 3.4–12.6 μm.

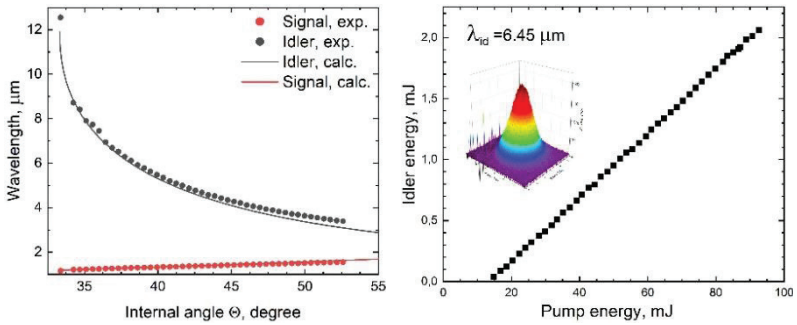

Fig. 1. Wavelength tuning of the BGGS OPO vs. an internal phase-matching angle: symbols (experimental data) and curves (calculated with Sellmeier expressions from [4] and idler energy at 6.45 μm vs. pump energy.

From the results obtained, it is evident that the BGGS crystal holds significant promise as a nonlinear medium for frequency-down conversion. This work was supported by the Russian Science Foundation and the Government of the Novosibirsk Region (Project no. 24-22-20049, https://rscf.ru/project/24-22-20049).

[1] N. Kostyukova, et al., Barium Chalcogenide Crystals: A Review, Photonics, vol. 11, p. 281 (2024).
[2] M. Ionin, et al., A Study of Effective Nonlinearity of $BaGa_2GeS_6$ Crystal by CO Laser Sum-Frequency Generation with Type-I and Type-II Phase Matching, Bull. Lebedev Phys. Inst., vol. 51 (Suppl 10), pp. S862–S869 (2024).
[3] E. Migal, et al., Unlocking superior performance of broadband powerful mid-IR optical parametric amplifiers with a $BaGa_2GeS_6$ crystal pumped at 1.24 μm, Opt. Lett., Vol. 49, pp. 4537–4540 (2024).
[4] K. Kato, et al., Temperature-dependent phase-matching properties of $BaGa_2GeS_6$ in the 0.767–10.5910 μm spectral range, Appl. Opt., vol. 61, pp. 10774–10777 (2022).

Broadband spectroscopy of astrophysical ice analogues: optical properties and scattering as a consequence of structural features.

A. A. Gavdush[1], B. M. Giuliano[2], V. E. Ulitko[3], K. I. Zaytsev[1], A. V. Ivlev[2], P. Caselli[2]

1- Prokhorov General Physics Institute of the Russian Academy of Sciences, Moscow, 119991 Russia
2- Max-Planck-Institut für Extraterrestrische Physik, Gießenbachstraße 1, Garching, 85748 Germany
3- Department of Engineering Physics, Polytechnique Montréal, Montreal, Quebec, H3C 3A7, Canada

e-mail: arsenii.a.gavdush@gmail.com

Understanding the physical and chemical properties of interstellar and circumstellar ices and their structure is crucial for a list of modern astrophysical problems [1]. Among other things, quantification of the terahertz (THz)–infrared (IR) optical properties of astrophysical ice analogues, having different molecular composition, phases, and structural properties, is required to model both the continuum emission by the dust grains covered with thick icy mantles and the radiative transfer in the dense cold regions of the interstellar medium [2–4]. Most of the ongoing laboratory research is concentrated on studying astrophysical ice analogues of different composition, while substantially less efforts have been put into obtaining information on structural features, such as porosity. These features depend on the experimental methodology of growing ice films, including different approaches and conditions (i.e., temperature, pressure, growth rate, etc.) of depositing ice on a cold substrate from the gas phase [5–7].

In our research we have focused on measurements and analysis of broadband optical properties of laboratory ices. The outcome of the first papers is the method for broadband (THz-IR) characterization of ices, which was then applied to study the dielectric response of CO, CO_2 [8, 9] and N_2 ices. The most recent efforts were made to develop a model that derive the relationship between the THz-IR optical properties, including scattering in ices, ice porosity and some structural features. A combined use of the Bruggeman EMT, Lorentz-Mie and Rayleigh scattering theories, as well as of the radiative transfer theory enables characterization of both the reduced effective optical properties of porous ices (occurring at all frequencies) and the additional wave extinction due to scattering on pores (increasing with frequency). This model shows that scattering in the studied ice samples occurs mainly in the Rayleigh regime. Also it can be concluded that scatterers of different shapes and dimensions can be approximated by spheres of effective radius. The scattering properties and porosity are retrieved by comparing the measured broadband response of our CO and CO_2 laboratory ices with the literature data on reportedly compact ices. Such an approach is relevant for modern laboratory astrophysics since it allows raw estimations on the morphological features of the deposited astrophysical ice analogues.

This work was supported by the Russian Science Foundation (RSF).

[1] A.C.A. Boogert, P.A. Gerakines, D.C.B. Whittet, Observations of the Icy Universe, Annual Review of Astronomy and Astrophysics, vol. 53(1), pp. 541–581 (2015).
[2] S.L. Widicus Weaver, Millimeterwave and Submillimeterwave Laboratory Spectroscopy in Support of Observational Astronomy, Annual Review of Astronomy and Astrophysics, vol. 57(1), pp. 79–112 (2019).
[3] D.V. Mifsud et al., The Role of Terahertz and Far-IR Spectroscopy in Understanding the Formation and Evolution of Interstellar Prebiotic Molecules, Frontiers in Astronomy and Space Sciences, vol. 8 (2021).
[4] D.V. Mifsud et al., Sulfur Ice Astrochemistry: A Review of Laboratory Studies, Space Science Reviews, vol. 217(1), p. 14 (2021).
[5] J.H.E. Cartwright, B. Escribano, C.I. Sainz-Diaz, The Mesoscale Morphologies of Ice Films: Porous and Biomorphic Forms of Ice under Astrophysical Conditions, The Astrophysical Journal, vol. 687(2), pp. 1406–414 (2008)
[6] M.J. Loeffler, M.H. Moore, P.A. Gerakines, The effects of experimental conditions on the refractive index and density of low-temperature ices: solid carbon dioxide, The Astrophysical Journal, vol. 827(2), p. 98 (2016)
[7] C. Millán, C. Santonja, M. Domingo, R. Luna, M. Á. Satorre, An experimental test for effective medium approximations (EMAs): Porosity determination for ices of astrophysical interest, Astronomy & Astrophysics, vol. 628, p. A63 (2019)
[8] B.M. Giuliano et al., Broadband spectroscopy of astrophysical ice analogues: I. Direct measurement of the complex refractive index of CO ice using terahertz time-domain spectroscopy, Astronomy & Astrophysics, vol. 629, p. A112 (2019).
[9] A.A. Gavdush et al., Broadband spectroscopy of astrophysical ice analogues: II. Optical constants of CO and CO_2 ices in the terahertz and infrared ranges, Astronomy & Astrophysics, vol. 667, p. A49 (2022).

Terahertz surface plasmon refractometry of metal, carbon and dielectric materials

V. V. Gerasimov[1,2], V. S. Vanda[1,2], V. D. Kukotenko[1], A. G. Lemzyakov[1,3], A. I. Ivanov[4], D. I. Krasnikov[5], N. I. Raginov[5], D. V. Fromichev[6], V. A. Stepanov[6], A. K. Nikitin[7]

1- Budker Institute of Nuclear Physics of SB RAS, Lavrentiev prospect 11, Novosibirsk, 630090 Russia
2- Department of Physics, Novosibirsk State University, Novosibirsk, 630090 Russia
3- Synchrotron Radiation Facility SKIF, Nikolsky pr. 1, Kol'tsovo, 630559 Russia
4- Rzhanov Institute of Semiconductor Physics SB RAS, Lavrentiev aven. 13, Novosibirsk, 630090 Russia
5- Skolkovo Institute of Science and Technology, Nobelya str. 3, Moscow, 121205 Russia
6- Joint Stock Company "Novosibirsk factory of semiconductor devise EAST", Krasny Ave. 18b, Novosibirsk, 630007 Russia
7- Scientific and Technological Centre of Unique Instrum. of RAS, Butlerova str. 15, Moscow, 117342 Russia

e-mail: v.v.gerasimov@inp.nsk.su

Currently, elements of terahertz (THz) optics and photonics are being actively developed. For sixth-generation (6G) communication systems, some of the key ones are plasmonic planar components based on solid and structured conducting nanomaterials [1]. Such materials can be metal, dielectric or semiconductor films, as well as carbon-containing materials and their composites. This paper presents the results of studies with the THz plasmon refractometry method of the optical characteristics of conducting gold films [2], composite layers of graphene nanoparticles with a small additive of the conducting polymer PEDOT:PSS [3], single-walled carbon nanotubes deposited on flat polished glass substrates [4]. The film thicknesses ranged from tens to several hundred nanometers. The Novosibirsk free-electron laser with a tunable wavelength in the range of 50–360 μm was used as a radiation source [5]. Due to their high conductivity, these materials have demonstrated the possibility of generating and controlling of characteristics of THz surface plasmon polaritons [6]. The possibility of measuring the optical constants of tetraaminodiphenyl films (with a thickness of an order of micron) used in pyroelectric detectors has also been demonstrated.

The study was partially supported by the grant of the Russian Science Foundation No. 25-22-20008 and with the financial support of the Government of the Novosibirsk Region (https://rscf.ru/project/25-22-20008/). The work was done at the shared research facility Siberian Center for Synchrotron and Terahertz Radiation on the basis of the Novosibirsk Free Electron Laser at Budker Institute of Nuclear Physics SB RAS. The authors thank the core facilities VTAN (Novosibirsk State University) for the access to the experimental equipment.

[1] V. J. Sorger, R. F. Oulton, R.-M. Ma, and X. Zhang, "Toward integrated plasmonic circuits," MRS Bull., vol. 37, no. 8, pp. 728–738 (2012).
[2] Gerasimov V V, Nikitin A.K., Vanda V.S., Lemzyakov A.G., and Azarov I.A. "Dispersion of attenuation of surface plasmon polaritons on metal in the terahertz range," J. Infrared Millim. Terahz. Waves, vol. 46, p. 32 (2025).
[3] Gerasimov V.V., Khasanov I.Sh., Kukotenko V.D., Lemzyakov A.G., Ivanov A.I., Antonova I.V., Cherevko A.G. "Terahertz Surface Plasmon Refractometry of Composite Graphene Nanoparticle Films," in IEEE Transactions on Terahertz Science and Technology, vol. 15, no. 1, pp. 61–68, (2025).
[4] E. S. Zhukova, A. K. Grebenko, A. V. Bubis, A. S. Prokhorov, M. A. Belyanchikov, A. P. Tsapenko, E. P. Gilshteyn, D. S. Kopylova,.Yu. G. Gladush, A. S. Anisimov, V. B. Anzin, A. G. Nasibulin, B. P. Gorshunov, "Terahertz-infrared electrodynamics of single-wall carbon nanotube films," Nanotechnology, vol. 28, p. 445204 (2017).
[5] Shevchenko, O.A., Vinokurov, N.A., Arbuzov, V.S., Chernov, K.N., Davidyuk, I.V., Deichuly, O.I., Dementyev, E.N., Dovzhenko, B.A., Getmanov, Ya.V., Gorbachev, Ya.I., Knyazev, B.A., Kolobanov, E.I., Kondakov, A.A., Kozak, V.R., Kozyrev, E.V., Krutikhin, S.A., Kubarev, V.V., Kulipanov, G.N., Kuper, E.A., Kuptsov, I.V., Kurkin, G.Ya., Medvedev, L.E., Motygin, S.V., Ovchar, V.K., Osipov, V.N., Petrov, V.M., Pilan, A.M., Popik, V.M., Repkov, V.V., Salikova, T.V., Scheglov, M.A., Sedlyarov, I.K., Serednyakov, S.S., Skrinsky, A.N., Tararyshkin, S.V., Tribendis, A.G., Tcheskidov, V.G., Vobly, P.D., Volkov, V.N.:"The Novosibirsk Free-Electron Laser Facility," Bull. Russ. Acad. Sci. Phys., vol. 83, p. 228–231 (2019).
[6] S. A. Maier, Plasmonics: Fundamentals and Applications. New York, NY: Springer US (2007).

Electric and spin currents induced by structured light

A. A. Gunyaga, M. V. Durnev, S. A. Tarasenko

Ioffe Institute, Saint Petersburg, 194021 Russia

e-mail: gunyaga@coherent.ioffe.ru

Microscopic and macroscopic inhomogeneities in semiconducting systems, e.g., crystal lattice without inversion center or edges of a sample, enable generation of dc electric and spin currents, which are non-linear in the incident field amplitude. On the other hand, electromagnetic field with spatially inhomogeneous parameters can also induce photocurrents even in homogeneous and isotropic media. In addition to the well-studied photothermoelectric currents that originate from the spatially varying intensity of incident radiation, photocurrents can also be driven by spatial variations in the radiation's polarization and phase [1, 2]. Prominent examples of such a structured radiation are vector beams with inhomogeneous polarization and beams of twisted photons carrying orbital angular momentum [3, 4].

Recently, the theory of photocurrents and second-harmonic generation induced by structured radiation has been developed for two-dimensional (2D) systems subject to radiation of classical frequency range with a photon energy being far less than the energy gap [2, 5]. This condition corresponds to microwave and terahertz spectral ranges in case of semiconductors. At the same time, the optical spectral range is also of great interest since the corresponding photon energy is of the same order as the typical energy gap in solids.

In this work, we study theoretically dc electric and spin currents emerging in 2D Dirac materials, e.g. graphene or transition metal dichalcogenides monolayers, under interband absorption of light with spatially inhomogeneous intensity, polarization or phase. It is shown that photocurrents originate from the optical orientation of electron spins by circularly polarized light, see Fig. 1. Additionally, the electric and spin currents get coupled due to the spin Hall and the inverse spin Hall effects. For the incident radiation with spatially varying phase, the photocurrent is generated due to momentum transition from photons to electrons, as in the photon drag effect.

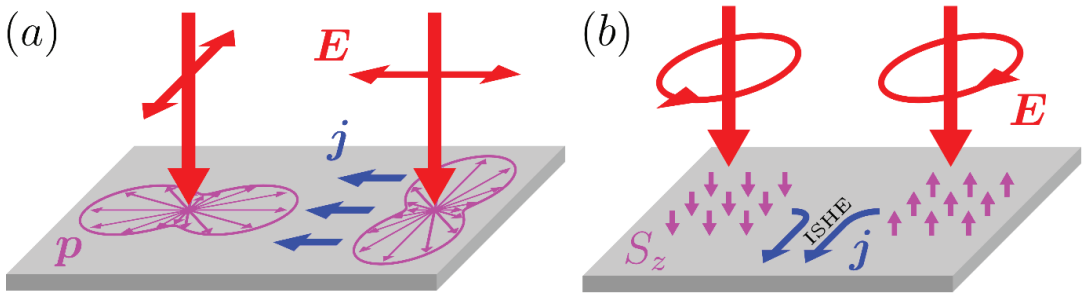

Fig. 1. Photocurrents induced by incident radiation with spatially inhomogeneous polarization.
(a) Rotating linear polartization causes non-uniform optical alignment of carriers' momenta, which leads to dc electric current.
(b) Spatially varying circular polarization creates non-uniform distribution of spin momentum, which transforms to electric currents due to the inverse spin Hall effect.

The developed theory is applied to investigate the currents induced by the vector and vortex optical beams. The generated currents have both radial and azimuthal components controlled by the beam polarization and the orbital angular momentum of photons.

Support by RSF (grant 22-12-00211-П) is acknowledged.

[1] Z. Ji, W. Liu, S. Krylyuk, X. Fan, Z. Zhang, A. Pan, L. Feng, A. Davydov, and R. Agarwal, Photocurrent detection of the orbital angular momentum of light, Science 368, 763 (2020).
[2] A. A. Gunyaga, M. V. Durnev, S. A. Tarasenko, Photocurrents induced by structured light, Phys. Rev. B, 108, 115402, (2023).
[3] A. Forbes, M. de Oliveira, and M. R. Dennis, Structured light, Nature Photonics 15, 253 (2021).
[4] B. A. Knyazev and V. G. Serbo, Beams of photons with nonzero projections of orbital angular momenta: new results, Physics-Uspekhi, 188(5), 508, (2018).
[5] A. A. Gunyaga, M. V. Durnev, S. A. Tarasenko, Second Harmonic Generation due to the Spatial Structure of a Radiation Beam, Phys. Rev. Lett., 134, 156901, (2025).

Novel optical materials for THz frequency range based on the artificial nano and microporous media

G. M. Katyba[1,2], A. S. Kucheryavenko[1], A.-E. P. Protopopova[1], A. N. Golikov[1], K. I. Zaytsev[2], V. N. Kurlov[1]

1- Institute of Solid State Physics of RAS, Academician Osipyan str. 2, Chernogolovka, 142432 Russia
2- Prokhorov General Physics Institute of RAS, Vaviliva str. 38, Moscow, 119991 Russia

e-mail: katyba_gm@issp.ac.ru

In recent decades, terahertz (THz) radiation has found increasing application in various fields of science and technology, including 6G communication and biomedical diagnostics. However, the rapid development of THz technologies is limited due to low efficiency or, even inaccessibility of THz optical materials, which can serve as the basis for various optoelectronic devices operating this frequency range. The development of new materials, including nanomaterials, artificial nanocomposite structures, and materials with tunable dielectric response (as well as devices based on them) is therefore a pressing task. In this work, several types of micro- and nanostructured media of different nature will be considered as novel materials for the GHz-THz frequency range.

Crystalline materials such as crystalline quartz, sapphire, and high-resistivity float-zone silicon (HRFZ-Si) exhibit a high refractive index and relatively low losses in the THz frequency range (for sapphire, n_0 ≅ 3.07 at a frequency of 1 THz). An original method for the growth of profiled crystals based on the edge-defined film-fed growth (EFG) technique [1] makes it possible to produce sapphire single crystals of complex geometries, which can serve as the basis for THz optical elements and artificial microstructured media, such as THz endoscopes [2] and bundles of fibers of various configurations [3].

Another promising artificial THz optical material is the nanoporous media based on submicron globules of amorphous silicon dioxide (SiO_2), forming an opal matrix [5, 6]. In this paper the problem of utilizing this material as the basis for optical elements with the capability to control the effective refractive index is discussed.

[1] P.I. Antonov and V.N. Kurlov, A review of developments in shaped crystal growth of sapphire by the Stepanov and related techniques, Progress in Crystal Growth and Characterization of Materials, 44(2), 63–122 (2002).
[2] G.M. Katyba, S.P. Lebedev, A.S. Kucheryavenko, I.N. Dolganova, N.V. Chernomyrdin, M.G. Burdanova, I.E. Spektor, M. Skorobogatiy, V.N. Kurlov, K.I. Zaytsev, Terahertz refractometry of hard-to-access objects using the sapphire endoscope suitable for harsh environments, Applied Physics Letters, 124(24), p. 243703, (2024).
[3] G.M. Katyba, M. Skorobogatiy, D.G. Melikyants, N.V. Chernomyrdin, A.N. Perov, E.V. Yakovlev, I.N. Dolganova, I.E. Spektor, V.V. Tuchin, V.N. Kurlov, K.I. Zaytsev, Superresolution Imaging Using a Tapered Bundle of High-Refractive-Index Optical Fibers, Physical Review Applied, 18(3), 34069 (2022).
[4] V.E. Ulitko, G.M. Katyba, V.A. Zhelnov, I.M. Shmytko, G.A. Emelchenko, I.E. Spector, V.M. Masalov, V.N. Kurlov, K.I. Zaytsev, M. Skorobogatiy, Opal-based terahertz optical elements fabricated by self-assembly of porous SiO_2 nanoparticles, Optics Express, 29(9), 13764–13777 (2021).
[5] V.E. Ulitko, G.R. Musina, V.M. Masalov, A.A. Gavdush, G.A. Emelchenko, V.V. Bukin, V.N. Kurlov, M. Skorobogatiy, G.M. Katyba, K.I. Zaytsev, Moisture adsorption by porous terahertz optical materials: a case study of artificial SiO_2 opals, Optical Materials Express, 13(4), 1163–1176 (2023).

THz modulators with dynamic tunable metasurfaces

M. Konnikova[1,2], A. Tretyakov[3], A. Shevchenko[4], A. Mumlyakov[4], M. Krasil'nikov[4], A. Anikanov[4], Yu. Kistenev[3], I. Ozheredov[1,2], A. Shkurinov[1]

1- Faculty of Physics, Lomonosov Moscow State University, Moscow, 119991 Russia
2- National Research Centre «Kurchatov Institute» (NRC «Kurchatov Institute»)
3- Laboratory of Laser Molecular Imaging and Machine Learning, Tomsk State University, Tomsk, Russia
4- Institute of Nanotechnology of Microelectronics of the Russian Academy of Sciences, Moscow, Russia

e-mail: konnikovamaria@gmail.com

For several decades now, research on metasurfaces has been rapidly advancing, and the range of new capabilities and operating frequency ranges is expanding significantly, especially in the terahertz range. The combination of metasurfaces and "active" layers, such as graphene, semiconductors, phase change materials (PCMs), e.t.c. has facilitated both new opportunities for the development of dynamic THz functional devices and significant achievements in THz modulators.

We propose a new approach to the study of thin films, such as semiconductors, metals and PCM's (GeTe), including simultaneous THz reflectance and transmittance measurements, which will minimize the uncertainty of the measured optical constants [1]. The obtained values of complex dielectric permittivity and conductivity of the films were used to design tunable THz planar devices [1]. The dynamic modulation methods of amplitude, phase, frequency, and polarization characteristics of the THz field have been experimentally demonstrated.

In general, the modulation rate and depth are critical metrics for modulators, so we focus our study on the improvement of these characteristics. According to the tuning time, we differentiate: 1) passive tuning by changing the angle of incidence and polarization of THz radiation, 2) active temperature tuning (a few minutes duration), and 3) active optical tuning (ns duration). It was determined that the fastest tunability is obtained for PCM-based metamaterials, which undergo a non-volatile phase transition from an amorphous (insulating) to a crystalline (conducting) state, changing their electrical and optical properties upon thermal or optical stimulation (see Fig.1a). The optical-induced amplitude modulation of the absorption spectrum of the GeTe-based metasurface is presented in Fig. 1b.

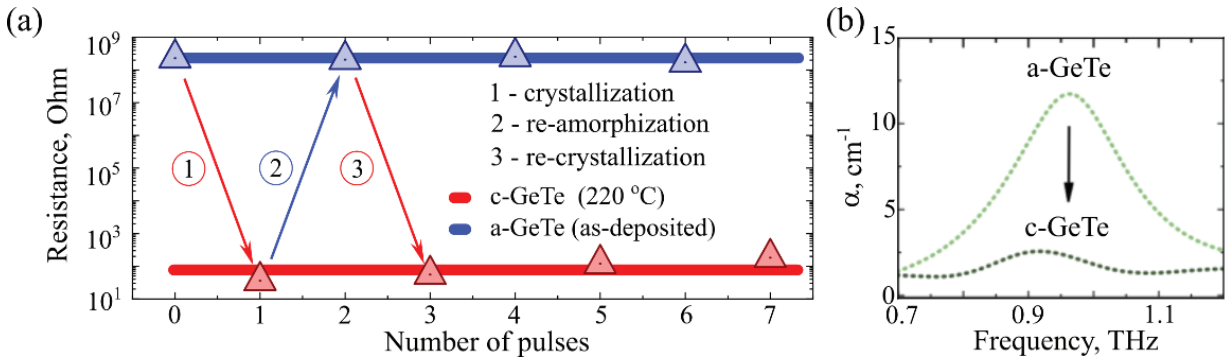

Fig.1. Resistivity-dependent crystallization of GeTe film under the influence of 30 ns KrF laser pulse (a). Tuning of the Fano resonance amplitude by optical crystallization of GeTe film (b).

Based on thin film studies, THz-active planar metasurfaces that ultrafastly modulate the frequency, amplitude, and polarization of the THz field have been designed and investigated.

The study was conducted partly under the state assignment of Lomonosov Moscow State University and NRC "Kurchatov Institute".

[1] M. Konnikova, A. Tretyakov, et al., "Novel method for extracting electromagnetic parameters of thin films based on dual-mode terahertz time-domain spectroscopy measurements ", Journal of Infrared, Millimeter, and Terahertz Waves, vol. 46(3), p. 18, (2025).
[2] M. Konnikova, M. Khomenko, et al., "$GeTe_2$ Phase Change Material for Terahertz Devices with Reconfigurable Functionalities Using Optical Activation" ACS Appl. Mater. Interfaces, vol. 15(7), (2023).

Optimum chirped pulse duration for terahertz yield in the dual-color femtosecond filament in air

O. Kosareva[1,2], I. Nikolaeva[1,2], J. Xie[3], D. Shipilo[1,2], N. Panov[1,2], A. Savel'ev[1,2], H. Zhao[3], W. Liu[3]

1- Faculty of Physics, Lomonosov Moscow State University, Leninskie Gory 1-62, Moscow, 119991 Russia
2- Lebedev Physical Institute of the Russian Academy of Sciences, Leninskiy pr. 53, Moscow, 119991 Russia
3- Institute of Modern Optics, Nankai University, Tongyan Road 38, Tianjin, 300350 China

e-mail: kosareva@physics.msu.ru

Among the terahertz (THz) sources, a two-color femtosecond filament in gases provides the coherent THz emission with the most broadband spectrum, which spans up to several tens of THz. Optical to terahertz conversion efficiency in the gas-based plasma reaches ~0.01% for the near infrared (800+400 nm) or up to 1% for the mid-infrared pump [1]. By positively chirping the initial pulse, one can increase the optical to THz conversion efficiency by an order of magnitude [2]. The THz yield depends strongly on the relative phase between the fundamental and the second harmonic radiation. Recently it was found that the relationship between THz pulse energy and chirp changes with variations in the specific phase difference between the first and second harmonics, and that the maximum THz energy might be attained not only for positively, but also for the negatively chirped pulse [3].

In this work we find both experimentally and numerically that the initial duration of the chirped pulse in the two-color (800+400 nm) filament in air is the major factor that determines the THz energy yield. By scanning through the relative (ω–2ω) phase shift in the range (0–180°) for each chirped pulse duration between –200 and 200 fs, we found that the optimum pulse duration, responsible for the maximum THz energy, does not change essentially with the chirp sign.

In the experiment the fundamental 800 nm, 4.5 mJ, 37 fs FWHM pulse with 9 mm beam diameter was focused with $f = 30$ cm lens followed by the beta-BBO crystal into air, where it created a filament. The THz radiation was collected by the two parabolic mirrors with $f = 15.4$ cm followed by the Golay cell. In the simulations we used 3D+t axially symmetric carrier-resolved code based on unidirectional pulse propagation equation. For each chirped pulse duration propagation and filamentation code run was performed for three phase shifts separated by 60° to find the maximum THz yield. We observed that for different initial relative (ω–2ω) phase φ the maximum THz energy can be obtained for either positively (red curves in Fig. 1) or negatively (green curves in Fig. 1) chirped pulse of the close duration. The largest for each particular chirped pulse duration THz energy is shown by stars in Fig. 1a. That is, while the geometry and the pump pulse energy remain unchanged, for each duration the initial phase shift φ is gradually adjusted in such a way that the THz yield takes its maximum.

The research was supported by Russian Science Foundation (project No. 25-49-00154) and National Natural Science Foundation of China (project No. W2412044).

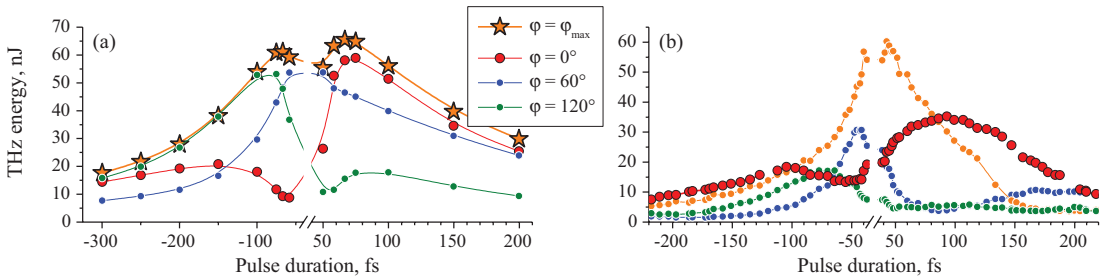

Fig. 1. THz yield from a 800+400 nm filament in the simulations (a) and experiment (b) for the chirped pulse durations ranged between –200 (negatively chirped) and 200 fs. Each curve except stars in panel (a) is obtained for the specific ω–2ω initial phase shift. Each THz energy value marked by a star on panel (a) corresponds to the optimized phase shift $\varphi = \varphi_{max}$, which varies with the chirped pulse duration.

[1] A. D. Koulouklidis, C. Gollner, V. Shumakova, V. Yu. Fedorov, A. Pugžlys, A. Baltuška, S. Tzortzakis, "Observation of extremely efficient terahertz generation from mid-infrared two-color laser filaments" Nat. Commun. 11, 292 (2020).
[2] T.-J. Wang, Y. Chen, C. Marceau, F. Théberge, M. Châteauneuf, J. Dubois, S. L. Chin "High energy terahertz emission from two-color laser-induced filamentation in air with pump pulse duration control" Appl. Phys. Lett. 95, 131108 (2009).
[3] A. Martinez, J. Houard, A. Hideur, D. Paparo, A. Vella "Controlling the time shape of terahertz pulses from two-color plasma by combining wavelength dispersion and laser chirp" Appl. Phys. Lett. 124, 021105 (2024).

Molecular gas spectroscopy with classical, gyrotron and synchrotron THz radiation sources for fundamental and applied goals

M. Koshelev

A. V. Gaponov-Grekhov Institute of Applied Physics RAS, Ulyanov Street 46, Nizhny Novgorod, Russia

e-mail: koma@ipfran.ru

Accurate laboratory studies of molecular spectra play an important role in fundamental science for understanding the molecular structure, physical processes of intramolecular dynamics and intermolecular interactions and also for various applications in medicine, gas analysis, atmospheric remote sensing, astrophysics, etc. The variety of studied objects and physical effects, as well as the accuracy and amount of information obtained in the study, are determined by the capabilities of the spectroscopic methods used. To acquire the most complete and reliable information on molecular spectra and physical processes, it is necessary to employ fundamentally different spectrometers covering the widest possible range of thermodynamic conditions.

Despite the fact that the THz range (also called as "THz gap") is quite narrow and has been challenging for the long time for spectral studies due to limited technical capabilities in both radiation sources and receivers, it offers a set of advantages that make it attractive to researchers. Advances in the development of THz radiation sources have spurred the progress of spectroscopic techniques and enabled the acquisition of new data on molecular spectra.

This report presents experimental studies of molecular spectra performed using several spectrometers equipped with both classical THz radiation sources (such as backward-wave oscillators) and more exotic sources, such as subTHz gyrotron combined with a radio-acoustic spectrometer or synchrotron radiation in combination with a Fourier-transform spectrometer. The particular results concern the contribution of various collisional effects to the shape of collisional-broadened resonant lines and the underlying physical mechanisms of the non-resonant (continuum) absorption in gases, including water vapor, which is of particular interest to atmospheric physics.

Enhanced terahertz emission from plasmonic antennas based on piezoelectric {InGaAs/InAlAs} heterostructures

P. M. Kovaleva[1], K. A. Kuznetsov[1], E. A. Klimov[2,3], S. S. Pushkarev[2], A. N. Klochkov[4]

1- Lomonosov Moscow State University, Physical Department, Moscow, Russia
2- National Research Centre "Kurchatov Institute", Moscow, Russia
3- Orion Scientific Product Association, Moscow, Russia
4- National Research Nuclear University MEPhI (Moscow Engineering Physics Institute), Moscow, Russia

e-mail: kovaleva.pm19@physics.msu.ru

Terahertz emission from semiconductor thin films and photoconductive antennas (PCAs) arises from ultrafast photocurrents driven by femtosecond optical excitation in the presence of a bias field.

In (111)A-oriented {InGaAs/InAlAs} heterostructures with elastically stressed layers due to mismatch in molar concentration of the Indium in each one strain-induced polarization provides an intrinsic vertical electric field, obviating the need for external electrodes. We demonstrate that this built-in field significantly enhances THz emission compared to unstrained reference structures. Through analysis of polarization and angular dependencies, we identify several THz generation mechanisms: optical rectification (OR), electric field induced optical rectification (EFIOR) [1], and presence of the dipole oscillating at an angle to the surface [2]. Moreover, we have successfully integrated plasmonic gratings with these piezoelectric heterostructures, achieving enhanced optical absorption and near-field confinement. These results establish strain-engineered, bias-free semiconductor emitters as a promising platform for compact and efficient THz sources.

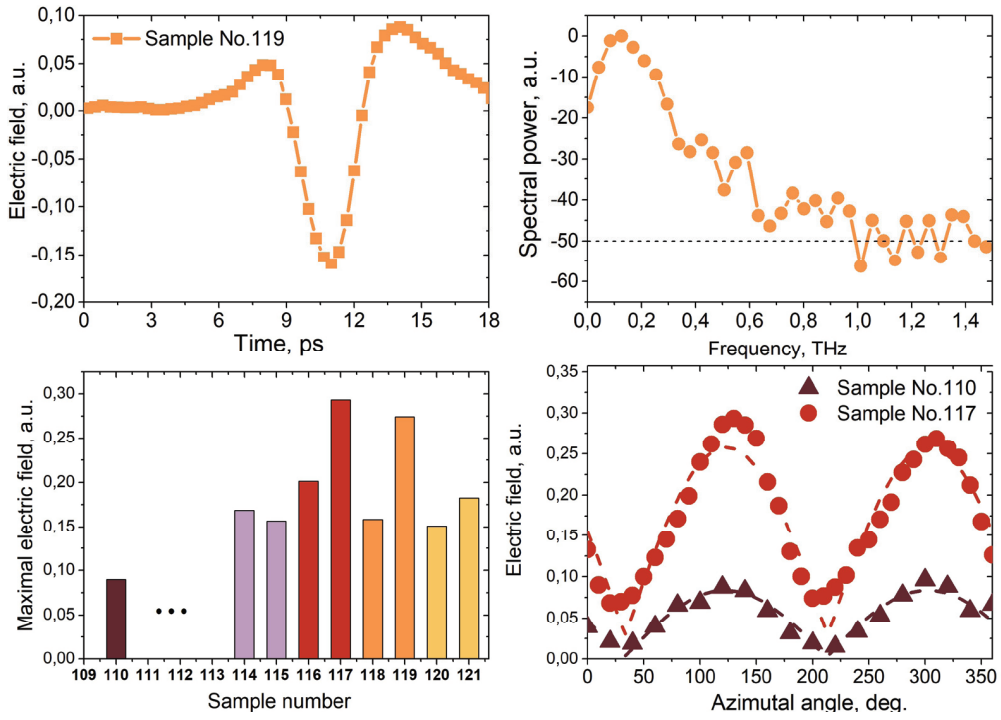

Fig. 1. (a) Typical THz radiation time-dependence from piezoelectric semiconductor heterostructure and its spectra (b), (c) Maximal amplitude of the THz signal from the different heterostructures, (d) Azimuthal angular dependence of the radiated THz signal from the heterostructure.

This work was supported by a grant from the Russian Science Foundation (project No. 22-19-00656) and by a grant from Theoretical Physics and Mathematics Advancement Foundation "BASIS" (grant No. 24-2-1-8-1)

[1] M. Reid, I. V. Cravetchi, and R. Fedosejevs, Phys. Rev. B, vol. 72, no. 3, p. 035201, Jul. (2005)
[2] I. Beleckaitė et al. , Electron. Lett., vol. 52, no. 23, pp. 1954–1956, Nov. (2016)
[3] E.A. Klimov et al. Opt. and. Spectr. Vol. 133, no. 3, Apr. (2025)

Optically controlled THz modulator based on transition metal dichalcogenide/silicon structure

E. Lebedeva, E. Bulavintseva, A. Alfer'ev, K. Kuznetsov, K. Brekhov, S. Lavrov, E. Mishina

MIREA – Russian Technological University, Vernadsky ave. 78, Moscow, 119454 Russia

e-mail: mishina_elena57@mail.ru

Two-dimensional (2D) materials, especially semiconductors, have good prospects for their application in THz devices, including optical and electro-optical modulators [1]. The unique characteristics of these materials, such as atomic thickness and high lateral mobility of charge carriers, allow for efficient control of their electronic and optical properties. Among the most promising 2D materials for creating THz modulators are transition metal dichalcogenides (TMDs), such as MoS_2, $MoTe_2$, WSe_2, and $MoSe_2$. When these materials are exposed to optical radiation, charge carriers are generated and excitons are excited. It was demonstrated that combined irradiation with photon energies of 2.33 eV (continuous) and 1.82 eV (pulsed) increases the charge carrier density to $4 \cdot 10^{14}$ cm^{-2} [2]. This increase caused a phase transition from interlayer excitons to layer-separated electron-hole plasma when the excitation density exceeded the Mott threshold. The phenomena of photogeneration of charge carriers are used for efficient modulation of terahertz radiation. Modulation of terahertz waves directly depends on the changes in the absorption coefficient caused by optical radiation. The development of optical modulators for terahertz radiation requires the identification of optimal two-dimensional materials and their combinations adapted to specific applications. Particular attention should be paid to expanding the frequency range and increasing the applicability of energy-saving technologies that include low-intensity modulating radiation. In addition, a comprehensive understanding of the interaction between photogenerated charge carriers and the resulting changes in the optical properties of materials in the terahertz spectrum is needed.

Here we present the results of experimental studies of the modulation characteristics of a THz modulator based on transition metal dichalcogenides (WS_2, WSe_2, $MoSe_2$) deposited on a silicon substrate. The TMD flakes were obtained by liquid exfoliation and had different sizes and thicknesses down to a monolayer. High-resistivity silicon with native oxide was used as a substrate. The deposited area was about 5 mm. All samples were characterized by scanning electron microscope (SEM, see Fig. 1a) and photoluminescence. THz pulses with a temporal width of 1.5 ps were centered at 1.5 THz with a spectral width of about 1 THz and were incident on the sample with a repetition rate of 3 kHz. Photoexcitation was achieved by continuous radiation at 532 nm (2.33 eV). The sizes of all optical spots on the sample were about 2 mm. Energy of the THz pulse was 50 nJ, the fluence of excitation radiation was up to 1 W/cm^2. The maximal modulation depth of 6% was achieved for WS_2 sample at 450 mW of excitation power.

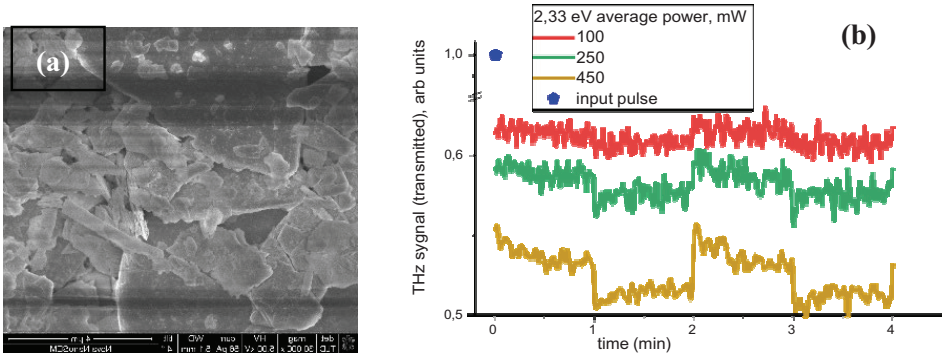

Fig. 1. (a) SEM image of the WS_2 sample; (b) modulated THz signal at different excitation power (532 nm).

The work is supported by Russian Science Foundation (Grant # 25-19-00575).

[1] A. Leitenstorfer, A.Moskalenko, T. Kampfrath, et al, The 2023 terahertz science and technology roadmap, J. Phys. D: Appl. Phys. 56, 223001 (2023).
[2] J. Wang J. Ardelean, Yusong Bai, et al., Optical generation of high carrier densities in 2D semiconductor heterobilayers, Science Advances 5, eaax0145 (2019).

Chiral metamembranes for far infrared and THz bands

R. O. Malikov[1], N. V. Valenko[1,2], S. G. Tikhodeev[1,2]

1- Moscow State University, Moscow, 119991 Russia
2- Prokhorov General Physics Institute, Russian Academy of Sciences, Moscow, 119991 Russia

e-mail: tikh@gpi.rus

Recently, much research attention has been given to the creation of artificial chiral metamaterials and metasurfaces, which have a wide range of applications, including optical and quantum informatics and sensing, such as biosensing. In particular, a chiral metasurface with selective reflection and transmission properties for circularly polarized radiation in the optical range of $\lambda = 870$ nm was proposed and realized experimentally based on a silicon nitride film [1]. These structures, called maximum chirality metasurfaces [2, 3], demonstrate selective properties for circularly polarized electromagnetic radiation. For example, they can reflect a circularly polarized wave of one handedness and absorb or transmit the other. These structures are promising for creating single-handed chiral cavities that efficiently interact with chiral emitters of matching handedness and for sensors based on them [4].

This talk will discuss maximum chirality metasurfaces in the far infrared and terahertz bands. We will analyze the physical origin of the maximum chiral response and address the peculiarities of electromagnetic field distributions in the near- and far-field zones. Recently, a photonic structure based on a nanocrystalline diamond metamembrane for $\lambda = 10$–15 μm was proposed in [5]. Additionally, we will present several designs of a metamembrane with maximum chirality based on silicon, optimized for the THz range ($\lambda = 600$ μm).

[1] B. Semnani, J. Flannery, R. Al Maruf, M. Bajcsy, Spin-preserving chiral photonic crystal mirror, Light-Sci. Appl., vol. 9, pp. 1–12 (2020).
[2] I. Fernandez-Corbaton, M. Fruhnert, C. Rockstuhl, Objects of maximum electromagnetic chirality, Phys. Rev. X, vol. 6, 031013 (2016).
[3] M.V. Gorkunov and A.A. Antonov, in All-Dielectric Nanophotonics, ed. A.S. Shalin, A.C.Valero and A.Miroshnichenko (Elsevier), Chapter 9 – Rational design of maximum chiral dielectric metasurfaces, pp. 243–286 (2024).
[4] K. Voronin, A.S. Taradin, M.V. Gorkunov, D.G. Baranov, Single-Handedness Chiral Optical Cavities, ACS Photonics, vol. 9, pp. 2652−2659 (2022).
[5] N.V. Valenko, O.A. Dmitrieva, S.G. Tikhodeev, Effect of losses on optical properties of chiral metamembranes, Computer Optics, vol. 48, pp. 816–822 (2024).

Plasmonic metamaterials for the systems of terahertz electronics

V. M. Muravev, M. S. Sokolova, K. R. Dzhikirba, P. A. Gusikhin, A. S. Astrakhantseva, I. V. Kukushkin

Osipyan Institute of Solid State Physics, Russian Academy of Sciences, Chernogolovka, 142432 Russia

e-mail: muravev@issp.ac.ru

Periodic metallic structures have the ability to simulate various homogeneous materials whose specific properties eventually do not exist for natural materials. We have realized a simple technology to assemble a 3D metamaterial consisting of stacked planar silicon chips with a metallic mesh lithographically fabricated on the chip surface. We use Fabry-Pérot resonance spectroscopy to accurately measure the metamaterial dispersion in the terahertz frequency range. It turned out that the electrodynamic response of the metamaterial can be described in terms of the effective dielectric permittivity. When the mesh period is small, the metamaterial demonstrates extremely large dispersion $\partial\varepsilon/\partial f$. Based on this metamaterial, we have made Fabry-Pérot resonators.

The Fabry-Pérot resonators have been constructed from high-resistivity (>30 kΩ×cm) silicon chips with dimensions of 1×1 cm², thickness d = 280 μm, and ε = 11.7. A metallic grid with periods a = 30–400 μm and a ribbon width w = 10–50 μm is lithographically fabricated on both sides of the semiconductor chip. The metallic layer, consisting of Cr (25 nm) and Au (700 nm), is thermally evaporated in a vacuum chamber. In experiments where field enhancement was measured, the Fabry-Pérot resonator was assembled from two silicon chips, each with a thickness of 150 μm. One chip features a PDB diode detector fabricated on one side of the substrate, while a grid or a homogeneous metallic layer is fabricated on the other side. The second silicon chip has only a metallic grid on the outer side of the substrate. The chips are aligned and pressed to form the Fabry-Pérot resonator.

A set of backward wave oscillators (BWOs) covering 50–500 GHz generates continuous terahertz radiation, which is directed normally at the sample. The transmitted power is detected synchronously using a pyroelectric detector [1].

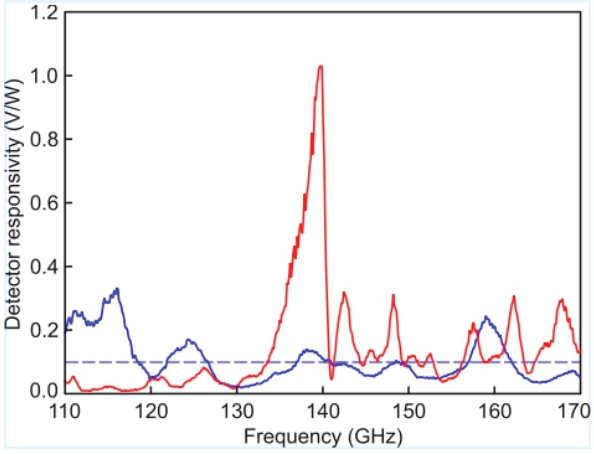

Fig. 1. The detector photo-voltage responsivity as a function of the frequency of incident electromsagnetic radiation. The red curve shows the detector responsivity placed into the plasmonic Fabry-Pérot resonator. The blue curve corresponds to the detector responsivity in the structure without a metallic grid on both chips. For this case, the dashed line indicates the average responsivity in the spectral range 110−170 GHz..

It is found that the resonator effectively accumulates and enhances the electric field of the incident electromagnetic wave. We have managed to directly measure the field enhancement by placing a diode detector inside the resonator. A remarkable forty-fivefold increase in the detector responsivity is achieved in the subterahertz frequency range (Fig. 1).

[1] G. Kozlov and A. Volkov, Topics in Applied Physics, vol. 74, Millimeter and submillimeter Wave Spectroscopy of Solids. Ed.: G. Gruner. Springer-Verlag Berlin-Heidelberg (1998).

Frequency resolved THz beam shaped by femtosecond plasma gradients in air

I. A. Nikolaeva[1,2], D. E. Shipilo[1,2], G. E. Rizaev[1,2], A. V. Koribut[2], T. A. Dick[2], D. V. Pushkarev[1], M. V. Levus[1,2], Ya. V. Grudtsyn[2], N. R. Vrublevskaya[1,2], N. A. Panov[1,2], L. V. Seleznev[1,2], A. A. Ionin[1,2], O. G. Kosareva[1,2]

1- Faculty of Physics, Lomonosov Moscow State University, Moscow, Russia
2- P. N. Lebedev Physical Institute of the RAS, Moscow, Russia

e-mail: nikolaevaia@lebedev.ru

Single-color femtosecond filament in air is a source of secondary emission such as supercontinuum and odd-harmonics [1] as well as terahertz (THz) emission [2] and second-harmonic [3]. The first two appear due to the third-order response of bound electrons and the transient photocurrent of free electrons and are well elaborated experimentally and in self-consistent simulations [4]. The last two are presumed to origin from the free electrons motion driven both by ponderomotive force that pushes the electrons out of the filament core thereby providing a quadruple source and by the light pressure force that pushes plasma electrons along the beam axis thereby producing a longitudinal dipole source [2].

Both models of the local plasma response were successfully used in combination with interference integral to reproduce the one-dimensional far-field distribution of THz radiation [2]. In its turn, measured second harmonic beam with the two lobes oriented along the laser polarization was explained qualitatively based on quadruple local source [3]. The particle in cell simulations demonstrated simultaneous THz and second-harmonic generation in tight focusing conditions [5].

In this work, we study in the experiment and numerical simulations the second harmonic and THz radiation from single-color filament formed in air by loosely focused 940-nm, 90-fs laser pulses with the energy of 0.5–3.5 mJ. The filament was formed by focusing 9-mm laser beam by the lenses with the focal lengths of 8, 40 and 100 cm. We measured the spectrum and spatial distribution of second harmonic and 2D spatial distribution [6] of THz radiation. The simulations are based on the vectorial diffraction integral with the source term given by the second-order nonlinear current [5] obtained on each step of the solution of laser pulse propagation equation. The 1–3 THz and second harmonic distributions exhibit two maxima located on the line perpendicular and parallel to the laser polarization direction, respectively (Fig. 1). Such deep azimuthal modulation in radially polarized THz beam appears due to destructive interference of THz waves driven by light pressure and ponderomotive force [6]. In contrast, the second harmonic is generated due to ponderomotive force solely. The second harmonic energy grows linearly with the pulse energy W due to the linear $(N_e L_{\text{fil}})^2$ scaling, where the plasma density $N_e \approx$ const taken from the ω–2ω phase-matched part of the filament before the pulse splitting. At the same time, the filament length L_{fil} is a square root of W.

The research was supported by Russian Science Foundation, project No. 24-19-00461 (https://rscf.ru/project/24-19-00461/).

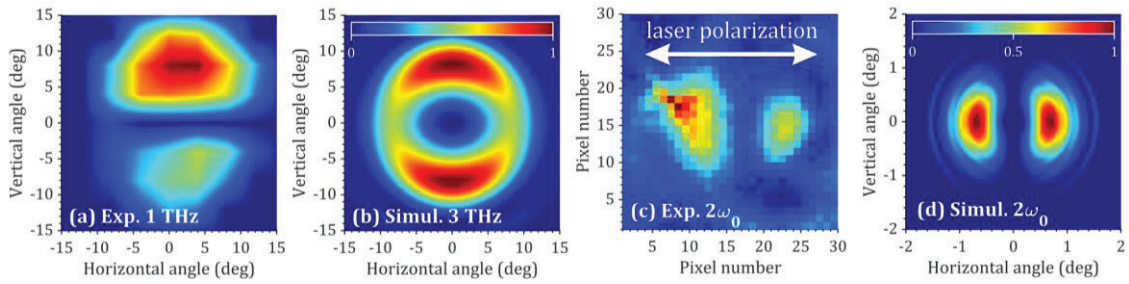

Fig. 1. Normalized spatial distributions of (a) 1 THz radiation measured in the experiment, (b) 3 THz radiation obtained in the simulations and the second harmonic obtained in (c) experiment and (d) simulations.

[1] A. V. Mitrofanov et al., Sci. Rep., 5, 8368 (2015).
[2] A. P. Shkurinov et al., Phys. Rev. E 95, 043209 (2017).
[3] G. Li et al., Opt. Lett., 39, 961 (2014).
[4] A. Couairon et al., Eur. Phys. J. Spec. Top., 199, 5 (2011).
[5] I. Thiele et al., Phys. Rev. E 94, 063202 (2016).
[6] I. A. Nikolaeva et al., Opt. Express 31, 41406 (2023).

Statistical features of the photo response of a superconducting hot-electron bolometer to week THz pulses generated by spontaneous parametric down-conversion

T. Novikova, A. Osipenkov, P. Prudkovskii, G. Kitaeva

Lomonosov Moscow State University, Leninskie Gory 1-2, Moscow, 119991 Russia

e-mail: gkitaeva@physics.msu.ru

The use of terahertz wave (THz) radiation generated under spontaneous parametric downconversion (SPDC) of short laser pulses in a nonlinear crystal located together with a cooled THz detector in the same cryostat makes it possible to exclude the influence of other sources and to study the statistics of the detector response to weak THz pulses containing few photons.

We studied statistical distributions of the photocurrent readings of a superconducting HEB detector [1] exposed to weak pulses of 1.5 THz frequency generated by SPDC in strongly non-degenerate mode [2] in Mg:$LiNbO_3$ crystal cooled down to 4.5 K. The number of THz photons incident on the HEB was varied by changing the average power of 25 ns SPDC pump pulses at 523 nm wavelength. Asymmetric histograms of readings obtained at low signal-to-noise ratios were then analyzed numerically to identify the parameters of some elementary current pulses that might form them.

A similar procedure of deconvolution to a Poisson sum of elementary contributions with Gaussian statistics was successfully applied earlier for photoelectric detectors and made it possible to determine the number and average values of elementary contributions usually associated with the absorption of single photons [3–6]. However, for a superconducting HEB detector such deconvolution gave fundamentally different results. It was found that not only the number of elementary contributions to HEB readings, but also their average value and dispersion change with a change in the power of the incident radiation. The average value of the contributions and their standard deviation monotonically increase with power, while the number of contributions has a clear tendency to reach saturation.

The nature of such elementary fluctuations of the HEB response, and their connection with the "hot spots" that arise in the superconducting film upon absorption of terahertz photons are discussed.

The work was done under financial support of the Russian Science Foundation (Grant No. 22-12-00055-П).

[1] S. Seliverstov, S. Maslennikov, S. Ryabchun, M. Finkel, T. M. Klapwijk, N. Kaurova, Yu. Vachtomin, K. Smirnov, B. Voronov, and G. Goltsman, Fast and sensitive terahertz direct detector based on superconducting antenna-coupled hot electron bolometer, IEEE Trans. Appl. Supercond., vol. 25, No. 2300304 (2015).
[2] G.Kh. Kitaeva, A.A. Leontyev, P.A.Prudkovskii, Quantum correlation between optical and terahertz photons generated under multimode spontaneous parametric down-conversion, Phys. Rev. A, vol. 101, p. 053810 (2020).
[3] R. Dossi, A. Ianni, G. Ranucci, O.Ju. Smirnov, Methods for precise photoelectron counting with photomultipliers, Nucl. Instrum. Methods Phys. Res. A, vol. 451, pp. 623–637 (2000).
[4] I. Chirikov-Zorin, I. Fedorko, A. Menzione, M. Pikna, I. Sýkora, S. Tokár, Method for precise analysis of the metal package photomultiplier single photoelectron spectra, Nucl. Instrum. Methods Phys. Res. A, vol. 456, pp. 310–324 (2001).
[5] D.Coquelin, T.Jobin, W.Kemmerer, P.Maxwell, S.Merten, E.Moller, W.Morris, G.Niculescu, I.Niculescu, W.Shaver, Practical considerations in modeling the low light response of photomultiplier tubes in large batch testing, Nucl. Instrum. Methods Phys. Res. A, vol. 928, pp. 43–50 (2019).
[6] D.A. Safronenkov, P.A. Prudkovskii, A.V. Osipenkov, G.Kh. Kitaeva, Elementary responses of analog photodetectors and absolute calibration of their efficiency, J. Appl. Phys., vol. 137, p. 184402 (2025).

Ultraviolet femtosecond filamentation: effects of nonlinearity delayed on sub-femtosecond timescale

N. A. Panov[1,2], N. R. Vrublevskaya[1,2], D. E. Shipilo[1,2], I. A. Nikolaeva[1,2], D. V. Pushkarev[1,2], G. E. Rizaev[1,2], M. V. Levus[1,2], A. A. Ionin[2], L. V. Seleznev[1,2], O. G. Kosareva[1,2]

1- Faculty of Physics, M. V. Lomonosov Moscow State University, Moscow, Russia
2- P. N. Lebedev Physical Institute of the RAS, Moscow, Russia

e-mail: napanov@ilc.msu.ru

The delay of 'the escape of an electron from an atom' during the tunnel ionization was estimated as $\tau \approx 100$–200 as in the time-of-flight experiments [1, 2]. Physically, this sub-femtosecond delay corresponds to the characteristic time of the electron cloud motion in strong laser field. In the filamentation regime, when one focuses the infrared femtosecond pulse into the bulk gas, the delay τ manifests in the fine effects of the rotation of the polarization of harmonics generated in the filament [3]. However, during ultraviolet (UV) filamentation one can expect to observe much coarser effects caused by the inertial electronic nonlinearity since the period of UV wave $T \leq 1$ fs becomes comparable with the time τ. The long-wavelength asymmetrical shift of 248-nm filament spectrum reported in [4] for different experimental conditions was not reproduced in simulations [4, 5], performed without the account for the inertial electronic response. In this work, we show experimentally and theoretically that the long-wavelength shift of the pulse spectrum in ~250-nm filament is caused by the delayed by ~200 as cubic nonlinearity of bound electrons.

In the experiment we focused ~100-fs, 0.2-mJ pulses centered at the wavelength $\lambda_0 \approx 250$ nm ($T \approx 800$ as) into the cuvette filled with air or argon at variable pressure and measured their spectra after the filamentation. The recorded spectra experience almost the same long-wavelength shift both in diatomic air and monatomic argon, if the pressure is the same (Fig. 1a). So, the spectral shift is the result of the interaction between the UV pulse and the electronic subsystem, but not with the rovibrational one. Using time-dependent Schrödinger equation, in the wide range of UV pulse intensities and durations we calculated the nonlinear polarization (Fig. 1d) induced by the field $E(t)$ of this pulse in the gas under the study. For the moderate intensities of 10–20 TW/cm^2, corresponding to the ones in ~250-nm filament [5], the spectrum of nonlinear polarization is shifted to the longer wavelengths (Fig. 1b) in qualitative agreement with the experiment. At the leading edge of the pulse, where the ionization is negligible, the delayed by ~200 as cubic response of the gas (Fig. 1c, d) is the main contribution into the nonlinear polarization. This nonlinearity delayed on sub-femtosecond timescale provides the observed long-wavelength shift of pulse spectrum during UV filamentation.

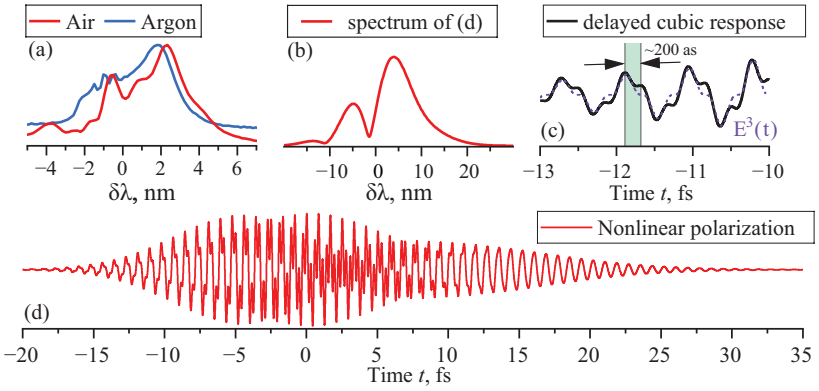

Fig. 1.
(a) Measutred spectra $S(\delta\lambda = \lambda - \lambda_0)$ after the filamentation in 1-atm air and argon (here λ is a wavelength).
(b) Simulated spectrum $S_p(\delta\lambda)$ of air polarization induced by 20-fs, 28-TW/cm^2 pulse.
(d) Nonlinear polarization of air.
(c) The leading edge of nonlinear polarization shows the cubic response delayed by ~200 as.

The research was supported by Russian Science Foundation, project No. 24-19-00461 (https://rscf.ru/project/24-19-00461/).

[1] M. Schultze et al., Science 328, 1658 (2010).
[2] U.S. Sainadh et al., Nature 568, 75 (2019).
[3] I. Babushkin et al., Nature Physics, https://doi.org/10.1038/s41567-022-01505-2 (2022).
[4] S. Tzortzakis et al., Opt. Commun. 197, 131 (2001).
[5] A. Couairon and L. Bergé, Phys. Rev. Lett. 88, 135003 (2002).

Terahertz-induced nonlinear response of solids: fundamental and practical aspects

F. Potemkin

Prokhorov General Physics Institute

e-mail: potemkin@physics.msu.ru

Modern photonics is aimed at developing new information technology devices that have a higher speed of information processing and reduce energy consumption. One of these areas is magnetic electronics and straintronics, which is based on a heterostructure consisting of a piezoelectric and magnetic material. The limiting factor of magnetic straintronics is the mechanical contact between the piezoelectric and the magnetic material. The contact limits the transmission speed at the GHz level, which corresponds to the capabilities of modern electronics. To overcome this barrier, it is possible to abandon the piezoelectric for domain repolarization control and use intense terahertz (THz) radiation. Studies of processes in a strong (quasi)static field have so far been mainly limited to theoretical studies, and consideration of nonlinear effects in the field of terahertz radiation has been limited to relatively weak fields, at a level of several tens of kV/cm [1].

Here we report on the first to our knowledge experimental observation of nonlinear effects by introducing a bichromatic approach for high order harmonic generation (HHG) in a semiconductor that combines an intense, ultra-short duration near- or mid-infrared excitation field with a strong terahertz radiation field. A wide-range (from VUV to THz) ultra-short duration coherent radiation source developed in the laboratory [2] provides a completely new quality when implementing multispectral exposure to matter, providing microjoule energy level pulses throughout the entire spectral range. This makes it possible to study nonlinear optical effects under bichromatic action on a sample under conditions of laser pulses in the IR and THz ranges that are close in intensity and the generated harmonics are in the transparency range of the semiconductor [3]. This fundamentally distinguishes the conducted research from previously published ones [4], since it makes it possible to generate harmonics from the volume, and not from the thinnest near-surface layer, and thereby increasing the efficiency of conversion to optical harmonics to extreme, record values. It is worth noting that registered THz-driven even harmonics demonstrate linear dependence on THz field that prove the four-wave mixing nature of the generation. All experimental studies were supported by the developed theoretical model based on Kohn-Sham equations.

This work was supported by Russian Science Foundation (Project № 25-22-00084).

[1] Li, S., Tang, Y., Ortmann, L. et al. High-order harmonic generation from a thin film crystal perturbed by a quasi-static terahertz field. Nat Commun 14, 2603 (2023).
[2] Pushkin, A.; Migal, E.; Suleimanova, D.; Mareev, E.; Potemkin, F. High-Power Solid-State Near- and Mid-IR Ultrafast Laser Sources for Strong-Field Science. Photonics 9, 90 (2022).
[3] E. A. Migal, A. V. Pushkin, and F. V. Potemkin, Even harmonic generation in semiconductors below and above the band gap assisted by an intense terahertz field Phys. Rev. B 110, 245201 (2024)
[4] Ovchinnikov, A.V., Chefonov, O.V., Mishina, E.D. et al. Second harmonic generation in the bulk of silicon induced by an electric field of a high power terahertz pulse. Sci Rep 9, 9753 (2019).

Optimal laser pulse parameters for terahertz emission from single-color filament

G. Rizaev[1,2], L. Seleznev[1,2]

1- P. N. Lebedev Physical Institute of RAS, Leninskiy pr. 53, Moscow, 119991 Russia
2- M. V. Lomonosov Moscow State University, Leninskie gory 1, Moscow, 119991 Russia

e-mail: rizaev@lebedev.ru

The plasma of a single-color laser filament serves as a broadband source of terahertz (THz) radiation [1, 2], now widely accessible in numerous laboratories. The plasma characteristics can significantly influence the properties of the THz emission [3, 4], which is crucial for applications.

In this study, we investigate the impact of experimental parameters on THz generation, including the laser pulse wavelength, energy, duration, and focusing conditions. The filament plasma was produced using laser pulses with a central wavelength of 750 nm, a minimum pulse duration of 90 fs, and energies up to 5 mJ. Detection of the THz emission was carried out using a cryogenic bolometer operating over the 0.1–12 THz range, with a set of narrowband filters with a relative bandwidth of $\Delta\nu/\nu = 0.1$.

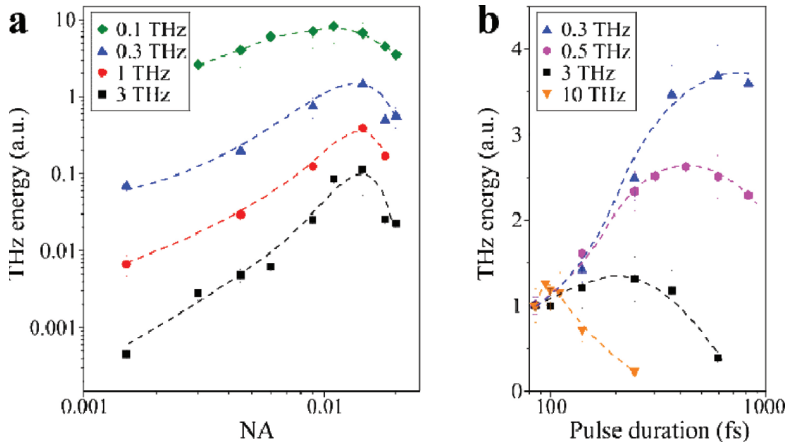

Fig. 1. Dependence of the THz radiation n energy on the beam numerical aperture at the minimum pulse dura ation (a) and on the pulse duration at NA = 0.18 (b).

Figure 1a presents the dependence of THz pulse energy at different frequencies on the laser beam numerical aperture (NA). At all frequencies, maximum generation efficiency is observed near NA = 0.015. Further analysis revealed that this aperture corresponds to a transitional regime between domination of geometric focusing and nonlinear Kerr self-focusing. Figure 1b shows how the THz energy at various frequencies depends on the laser pulse duration, which was adjusted via positive chirping. The experiments demonstrate that each THz frequency exhibits an optimal pulse duration, which rises as the frequency decreases. Therefore, for any given THz frequency, one can determine optimal laser pulse parameters that maximize the efficiency of THz generation.

The research is performed under the financial support of the Russian Science Foundation, grant number 24-19-00461, https://rscff.ru/en/project/24-19-00461.

[1] A. Couairon and A. Mysyrowicz, Femtosecond filamentation in transparent media, Physics reports, vol. 141((2-4), pp. 47–189, (2007).
[2] W. Sun, X. Wang, Y. Zhang, Terahertz generation from laser-induced plasma, Opto-Electronic Science, vol. 11(8), p. 220003, (2022).
[3] G. Rizaev, D. Pushkarev, L. Seleznev, Spectrum of terahertz emission from single-color filament plasma a under different laser beam focusing, Photonics, vol. 10(10), p. 1161 (2023).
[4] G. Rizaev, L. Seleznev, D. Mokrousova, D. Pushkarev, A. Ionin, Terahertz emission pattern from a single-color filament plasma, Optics Letters, vol. 47(22), pp. 5917–5920 (2022).

Formation of spatio-temporal vectorial optical vortices in elliptically polarized light pulse propagating in isotropic phase of a nematic liquid crystal with nonlocal nonlinear response

G. M. Shishkov, K. S. Grigoriev, V. A. Makarov

Lomonosov Moscow State University, Leninskie Gory 1 b.52, Moscow, Russia

e-mail: ksgrigoriev@ilc.msu.ru

The concept of spatio-temporal optical vortices (STOV) was first introduced by A. P. Sukhorukov and V. V. Yangirova in 2005 [1]. In cylindrically symmetric linearly polarized light pulses STOVs are special points in space and time, in which the complex amplitude of the electric field reaches zero, creating an analogy of widely known phase singularities in paraxial light beams. The study demonstrated that STOVs maintain their presence within a pulse during its propagation in free space. A linear-optical setup for generating such a pulse was proposed, and a forward-looking idea was briefly introduced regarding the possible existence of an optical soliton with an STOV in a Kerr nonlinear medium. Later on, STOVs were rediscovered at least twice by Bliokh [2] and, notably, Milchberg [3], who investigated the space-time phase profile of a high-power laser pulse during its filamentation in air with unparalleled precision. Despite the undeniable growing interest in this field, it is worth noting that, with very few exceptions, the aforementioned studies described STOVs in uniformly polarized pulses — an assumption that significantly simplifies the problem from both singular and nonlinear optics perspectives.

Polarization effects in nonlinear self-action of light are most pronounced in liquids with orientational nonlinearity, in which the impact of the cross-phase modulation of right and left circularly polarized components of a light pulse is 7 times greater than the impact of the self-phase modulation of these components. It was previously shown that multiple phase singularities of both components (vectorial optical vortices) arise during the paraxial beam propagation in such media. However, the behaviour of the beam is extremely sensible to its input power and the nonlinear collapse of the beam exceeding the critical power becomes a problem. These effects are mitigated in liquid crystals, especially near the phase transition temperature, when the medium has strong spatial nonlocality of optical response [4, 5].

In the present research we developed a new mathematical model of short elliptically polarized light pulse propagating in isotropic phase of a nematic liquid crystal, taking into account not only the nonlocality of its nonlinear orientational response, but the inertia of this response as well. In a wide series of numerical experiment we have detected the formation of spatio-temporal optical vortices in both circularly polarized components of the pulse. Two main scenarios of generation of STOVs were found: pairwise nucleation of vortices with opposite direction of energy flow and solitary vortex emergence from the axis of the light pulse. The peculiarities of the liquid crystal response are shown to provide stability of formed STOVs.

[1] A. P. Sukhorukov, V. V. Yangirova, Nonlinear Guided Waves and Their Applications, OSA Technical Digest (CD), paper WD15 (2005).
[2] K.Y. Bliokh, F. Nori, Phys. Rev. A, 86, 033824 (2012).
[3] H.M. Milchberg et al., Phys. Rev. X, 6, 031037 (2016).
[4] Makarov V.A., Grigoriev K.S., Shishkov G.M., Molecular Crystals and Liquid Crystals, 650, 1 (2017).
[5] Shishkov G.M., Grigoriev K.S., Makarov V.A., Las. Phys. Lett., 21, 2 (2024).

Simulation of THz field propagation in bioresorbable TPMS scaffolds: phase mapping and resorption monitoring

I. Shishkovsky

Lebedev Physical Institute of the RAS, Samara, 443011 Russia

e-mail: shiv@fian.smr.ru

Triply periodic minimal surface (TPMS) lattices fabricated from bioresorbable materials such as polylactic acid (PLA) are emerging as promising scaffolds for tissue engineering. However, monitoring scaffold resorption non-invasively remains a significant challenge. In this study, we investigate the use of terahertz (THz) wave propagation to monitor internal structural changes of 3D-printed TPMS scaffolds. We simulate electromagnetic wave propagation through gyroid-type TPMS made of PLA using the finite element method (FEM) implemented in MATLAB. The model incorporates realistic dielectric properties of PLA and soft tissue and allows time-resolved visualization of electric field amplitude and phase. Scaffold degradation is emulated by progressively reducing the solid phase in the PLA mask ($\phi = 0.7 \rightarrow 0.15$), and the field response is analyzed.

Amplitude maps $|E(x,y)|$ and phase plots $\arg E(x,y)$ show distinct spatial patterns depending on degradation level. Profiles of field magnitude along the central cross-section reveal increased transparency with lower PLA content. Shadow zone analysis highlights regions with attenuated field ($|E| < 0.001\ E0$), allowing identification of occluded regions. Spectral simulations in the 0.1–3 THz range demonstrate transmission dependence on frequency and structure type.

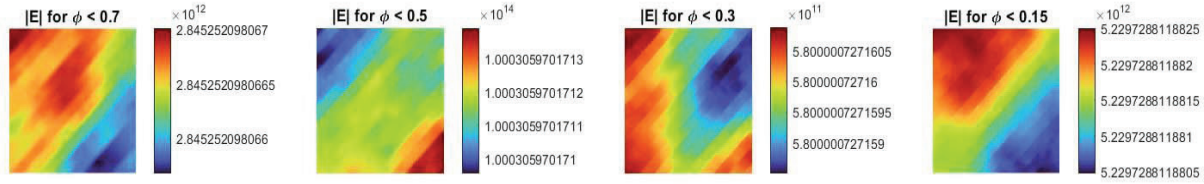

Fig. 1. 2D map of $|E(x, y)|$ at $\phi = 0.7 \rightarrow 0.15$.

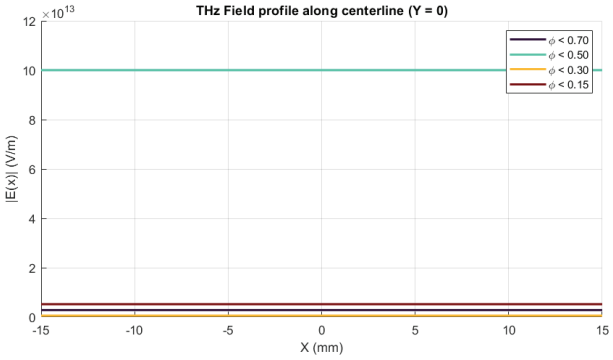

Fig. 2. Centerline field profiles for multiple ϕ.

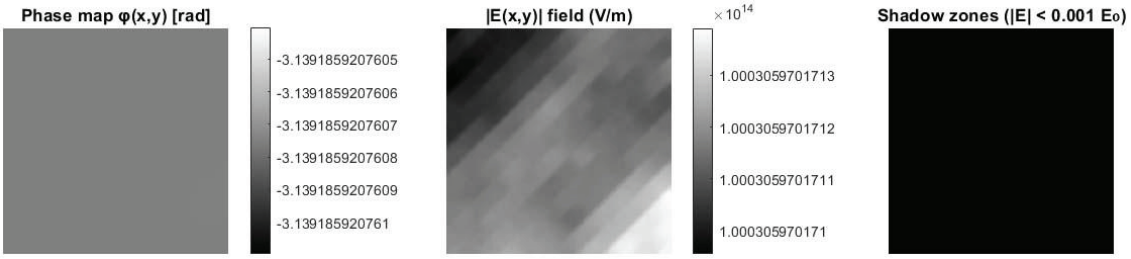

Fig. 3. Shadow zones.

These results demonstrate the potential of THz electromagnetic waves to characterize scaffold resorption with high spatial specificity. The combination of amplitude and phase diagnostics offers a robust framework for monitoring biodegradation, guiding scaffold design, and informing future THz imaging systems for biomedical applications.

Dynamic shielding of terahertz radiation using electrically controllable thin films of MXenes

V. V. Starchenko[1], Sh. Sun[2], M. I. Paukov[1], I. S. Kazantsev[3], A. V. Radivon[1], M. S. Mironov[3], A. A. Mkrtchyan[4], G. I. Tselikov[3], D. I. Yakubovsky[1], A. V. Shupletzov[1], A. I. Chernov[1], M. V. Shashkov[5], A. V. Xuy[1], G. A. Komandin[6], K. I. Zaitsev[6], Yu. G. Gladush[4], A. G. Nasibulin[4], A. V. Arsenin[1], V. Volkov[3], D. V. Krasnikov[4], Ya. Zhang[2], M. G. Burdanova[1,6,7]

1- Moscow Institute of Physics and Technology, Dolgoprudny, Russia
2- Beijing Key Laboratory of Metamaterials and Devices, Key Laboratory of Terahertz Optoelectronics, Ministry of Education of China, Beijing, China
3- XPANCEO, Dubai, United Arab Emirates
4- Skolkovo Institute of Science and Technology, Moscow, Russia
5- G. K. Boreskov Institute of Catalysis, Siberian Branch of the Russian Academy of Sciences, Novosibirsk, 630090 Russia
6- A. M. Prokhorov General Physics Institute of the Russian Academy of Sciences, Moscow, Russia
7- Institute of Solid State Physics of the Russian Academy of Sciences, Chernogolovka, Russia

e-mail: burdanova.mg@gmail.com

In recent years, there has been significant interest in the development of new materials and methods for shielding terahertz (THz) radiation, associated with their increasing applications in wireless communication systems, medical diagnostics, security, and spectroscopy [1].

Unlike many other two-dimensional materials, MXene films of $Ti_3C_2T_x$ demonstrate high stability of properties even with an increase in thickness. This stability results in a shielding efficiency exceeding 50 dB for films with a thickness of 2.5 μm, surpassing the performance of graphene, graphite, and metallic foil [2].

It is important to note that the previously unconsidered possibility of actively controlling THz radiation through electrical and optical modulation represents a significant advantage that enhances electromagnetic shielding efficiency. In this work, a transparent electrochemical cell was tested for the electrical control of THz radiation transmission through MXenes. The cell, consisting of a $Ti_3C_2T_x$ electrode, gold, and an ionic liquid, is sealed on the top and bottom with two quartz plates.

When a potential difference is applied between the sample and counter electrode, positive and negative ions accumulate at the surface of $Ti_3C_2T_x$ particles depending on the polarity of the voltage, forming a double electrical layer. As a result, it was shown that the significant shielding efficiency of electromagnetic radiation – 2.5×10^4 dB·g^{-1}·cm^2 – increases further due to electrochemical doping, reaching a level of 4×10^4 dB·g^{-1}·cm^2 when a voltage of +2 V is applied. Additionally, the initial shielding efficiency can be further enhanced by increasing the thickness of the material by up to 27 dB.

The ability to manipulate the properties of MXene films, as well as their compatibility with various substrates, makes these materials promising for applications in terahertz technologies and shielding systems.

MIP, AVR, and MGB acknowledge the Russian Science Foundation grant (project No 24-79-00143).

[1] A. Shafie, N. Yang, C. Han, J.M. Jornet, M. Juntti, T. Kürner, Terahertz communications for 6G and beyond wireless networks: Challenges, key advancements, and opportunities, IEEE Network, 37(3), 162–169, (2022).
[2] Feng W., Luo H., Wang Y., Zeng S., Deng L., Zhou X., Zhang H., Peng S., RSC Advances, V. 8(5), 2398–2403, (2018).

High-precision MMW and SMMW spectroscopy as a probe of intermolecular interactions

L. Surin, I. V. Tarabukin

Institute of Spectroscopy RAS, Fizicheskaya str. 5, Troitsk, Moscow, 108840 Russia

e-mail: surin@isan.troitsk.ru

Determination of intermolecular interaction parameters with high accuracy is necessary for interpretation of high-resolution spectroscopic and scattering data, including spectral data from studies of the interstellar medium, the Earth's atmosphere and planets. An important role here is played by experimentally obtained spectra of molecular complexes, the energy levels of which are very sensitive to the intermolecular interaction potential. This talk considers methods of precision spectroscopy of molecules and molecular complexes in the millimeter and submillimeter wavelength ranges. A new spectrometer with a molecular jet that propagates along the direction of radiation beam is presented [1]. A spectral resolution of 30–40 kHz and an accuracy of measurements of absolute frequencies of molecular transitions of about 3-5 kHz in the range of 50–260 GHz have been achieved. Observations of hyperfine structure of the rotational transitions of the astrophysically relevant molecules and weakly bound molecular complexes (CO isotopologues, NH_3–H_2, NH_3–CO, NH_3–Ne) are demonstrated.

The obtained hyperfine structure parameters (nuclear quadrupole, spin-rotational and spin-spin interaction constants) provide important information on both the structure and dynamics of molecular complexes and the interaction potential between monomers. In addition, the high specificity of the hyperfine structure pattern of rotational transitions helps to distinguish spectral features arising from different nuclear spin isomers of complexes containing molecules with equivalent nuclei [2].

This work was supported by the Russian Science Foundation through Grant No. 25-22-00506.

[1] I.V. Tarabukin, V.A. Panfilov, D.G. Poydashev, L.A. Surin, Millimeter-Wave Spectrometer for High-Precision Studies of Jet-Cooled Molecules and Weakly Bound Molecular Complexes, J. Infrared Millim. Terahertz Waves, 45, 645–656 (2024).
[2] L. Surin, I. Tarabukin, C. Pérez, M. Schnell, Microwave Spectra and Nuclear Quadrupole Structure of the NH_3–N_2 van der Waals complex and its Deuterated Isotopologues, J. Chem. Phys. 149, 224305:1–6 (2018).

Compact THz resonators based on superconducting MoRe film reflectors

A. Terentiev[1], A. Melentev[1], A. G. Shishkin[1], M. S. Sidelnikov[1,2], Z. V. Gagkaeva[1], V. S. Stolyarov[1], B. P. Gorshunov[1], E. S. Zhukova[1]

1- Moscow Institute of Physics and Technology, Dolgoprudny, 141700 Russia
2- Institute of Solid State Physics RAS, Chernogolovka, 142432 Russia

e-mail: terentev.a@phystech.edu

We demonstrate compact, high-performance terahertz (THz) Fabry-Pérot resonators utilizing superconducting $Mo_{0.6}Re_{0.4}$ films as reflectors. The resonators are constructed by depositing thin superconducting films (10, 20, and 30 nm thick) with critical temperatures T_c = 7–8 K on both sides of plane-parallel high-resistivity silicon substrates (0.5 mm thick, 8×8 mm^2 area). This monolithic design inherently maintains perfect alignment of the resonator reflectors without requiring mechanical adjustment systems. Using terahertz time-domain spectroscopy and high-resolution coherent-source backward-wave oscillator spectroscopy, we characterized resonator performance across frequencies ν = 3–50 cm^{-1} and temperatures T = 2.5–300 K. Record-breaking performance is achieved at T = 2.5 K: quality factor Q = 830 (resonance at ≈6 cm^{-1}) and finesse F = 580 (resonance at ≈3 cm^{-1}).

Additionally, we demonstrate polarization-sensitive operation of the resonator by patterning superconducting films into one-dimensional grids (50 μm wide stripes, 100 μm period). As shown in Fig. 1, strongly anisotropic performance is observed: for electric field of the THz radiation perpendicular to stripes (E⊥), the resonator becomes highly transparent approaching bare substrate transmission, while for parallel polarization (E∥) it exhibits sharp high-quality resonances with enhanced reflective properties.

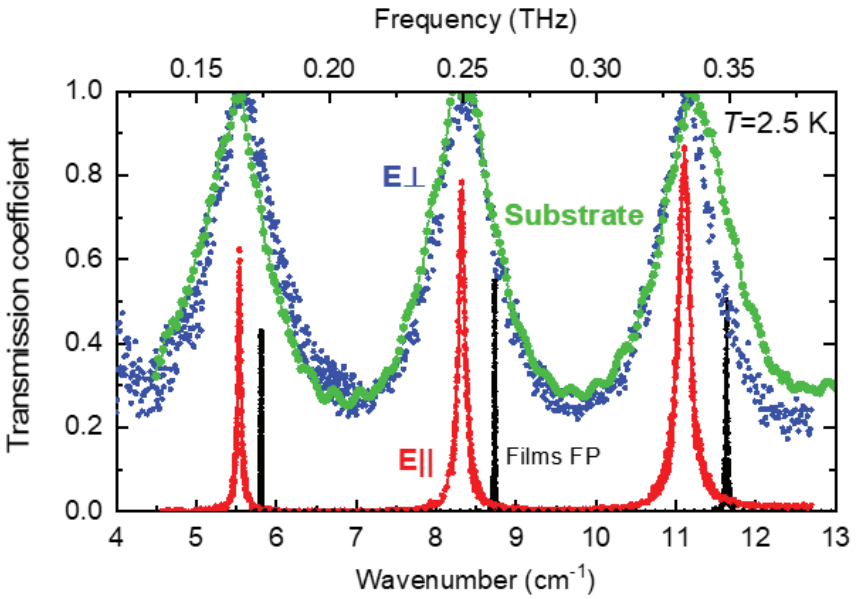

Fig. 1. Polarization-dependent transmission spectra of patterned Fabry-Perot resonator showing strong anisotropy between parallel (E∥, red) and perpendicular (E⊥, blue) polarizations of the E-vector of THz radiation relative to the stripes (inset). Green color shows the spectrum of bare substrate.

The $Mo_{0.6}Re_{0.4}$ films characteristics (temperature-dependent spectra of complex THz permittivity and conductivity) are obtained on a quantitative level and are well described within BCS theory. The proposed resonators are characterized by extreme compactness and simple monolithic construction, which makes them promising for terahertz applications.

The study supported by Ministry of Science and Higher Education of Russian Federation: projects FSMG-2025-0005 (THz experiments) and 075-15-2025-010 (data analysis).

Study of ENT organ neoplasms by high-resolution THz spectroscopy

V. L. Vaks[1,2], A. A. Ayzenshtadt[1,3], E. G. Domracheva[1,2], M. B. Chernyaeva[1,2], V. A. Anfertev[1], K. A. Glushkova[1,3], A. S. Cherniaeva[1]

1- Institute for Physics of Microstructures RAS, GSP-105, Nizhny Novgorod, 603950 Russia
2- Lobachevsky University, Gagarina av. 23, Nizhny Novgorod, 603022 Russia
3- Children Clinical Hospital No.1, Gagarina av. 76, Nizhny Novgorod, 603081 Russia

e-mail: elena@ipm.sci-nnov.ru

Currently, metabolic approaches for the diagnosis of various diseases and pathologies are actively developing in the world. Chromatographic methods, often combined with mass spectrometry, as well as spectroscopic methods, are most often used to identify pathology markers-metabolites in biological samples. However, the examination of biological tissues is carried out only using histological or chemical analysis. Currently, such large biological molecules as proteins (a specific protein of a tumor cell, an intracellular protein that inhibits cyclin-dependent kinases, a protein that regulates the cell cycle, and others) are distinguished among the biomarkers characteristic of sinonasal tumor tissues [1]. Terahertz spectroscopy based on nonstationary effects, which has high resolution and sensitivity simultaneously, makes it possible to identify the composition of the thermal decomposition products for tissues of ear-nose-throat (ENT) organs neoplasms and can provide important information about the differences in the chemical composition of the thermal decomposition products of healthy and pathologically altered tissues. This work is devoted to the study of the chemical composition of secondary metabolites formed at thermal decomposition of the tissues of ENT organ tumors using high-resolution THz spectroscopy for samples of relatively healthy mucous membranes and neoplasms (papillomas of the tonsils and larynx and cholesteatomas of the middle ear).

Spectroscopic measurements were carried out using a high-resolution THz spectrometer developed by the authors with phase switching of gas acting radiation with an operating range of 118–175 GHz, as well as a THz quantum cascade laser based spectrometer [2]. The studied tissue samples were heated, and a mixture of vapors and gaseous products of thermal decomposition was injected into a pre-evacuated measuring cell. According to the identified spectral lines, using on-line catalogs of spectroscopic data, substances whose composition differs for healthy tissues and pathologically altered tissues were identified. Absorption lines of methanol, propanediol, acetaldehyde, pyrrole, and ethylene sulfide are identified in the spectra of samples of relatively healthy mucous membranes and in the spectra of tumor tissues. However, their relative concentration in the thermolysis products of neoplastic tissue samples is higher than for relatively healthy tissues. A number of organic acids, aldehydes, nitriles, and other organic compounds have been identified, the absorption lines of which are absent in the spectra of relatively healthy tissues.

Identification of the initial substances in tumor tissues and revealing the differences between tumors of different types and healthy tissues can be the first step towards determining the metabolic profile of tissues during the tumor process. Thus, the potential possibility of using high-resolution THz spectroscopy to analyze the metabolic composition of neoplastic tissues is shown.

This research was funded by the Russian Science Foundation, grant No. 24-19-00623, https://rscf.ru/en/project/24-19-00623/.

[1] Lucidi D., Cantaffa C., Miglio M., Spina F., Alicandri Ciufelli M., Marchioni A., Marchioni D. Tumors of the Nose and Paranasal Sinuses: Promoting Factors and Molecular Mechanisms—A Systematic Review. // Int. J. Mol. Sci., vol. 24, p. 2670, (2023).
[2] Vaks V.L., Anfertev V.A., Balakirev V.Yu., Basov S.A., Domracheva E.G., Illyuk A.V., Kupriyanov P.V., Pripolzin S.I., Chernyaeva M.B. High resolution terahertz spectroscopy for analytical applications // Phys. Usp., vol. 63, pp.708–720 (2020).

Works in the field of terahertz waves in Russia in the pre-war period

O. Valkova

S. I. Vavilov Institute for the History of Science and Technology Russian Academy of Science, Baltiiskaia ul. 14, Moscow, 125315 Russia

e-mail: o-val2@yandex.ru

In the first decades of the 20th century, physicists around the world were focused on finding the shortest possible electromagnetic waves. They were trying to fill in the existing gaps in the electromagnetic spectrum, and there was a sense of urgency and competition among scientists to be the first to achieve this goal.

In 1914, V. K. Arkadiev (1884–1953), a physicist from the P. N. Lebedev scientific school, started work on this project in Moscow. However, his plans were interrupted by the outbreak of the First World War. Despite this setback, Arkadiev remained committed to this research. In 1921, he suggested that his wife A. A. Glagoleva-Arkadieva (1884–1945) also a professional physicist took his place. She turned out to be a talented and extraordinary experimenter. She abandoned attempts to reduce the Hertz vibrator, which was followed by her contemporaries, and designed a device she called a "mass radiator". It used a mixture of tiny metal filings immersed in a liquid dielectric. In 1922, she received waves with a length between 7 and 10 millimeters for the first time.

Already in 1922, she reported on her invention at the 3rd Congress of the Association of Russian Physicists in Nizhny Novgorod. She presented the report "A Method for Obtaining the Shortest Electromagnetic Waves" [1]. In 1924, the results of her experiments were published in the journal Nature [2]. The waves emitted by the mass emitter were superimposed on the one hand on short electromagnetic waves obtained by Niels and Tire, and on the other hand on Rubens' heat waves and, consequently, filled the existing gap on the scale of electromagnetic waves.

A. A. Glagoleva-Arkadieva was not the only researcher in our country who studied the shortest electromagnetic waves in the 1920s. You can mention M. A. Levitskaya's name, whose first work published in 1909 was devoted to studying a rectilinear resonator in the field of short electromagnetic waves. She has presented her work on "shortest Hertz waves" at several congresses of the Association of Russian Physicists in 1920th. However, the priority of Glagoleva-Arkadieva in this field turned out to undeniable. In the 1920s and 1930s, she continued to improve her instrument and study the waves obtained using it [3].

In the early 1930s, she founded a laboratory at the II Moscow State Medical Institute, with a small team that continued her research under her direct supervision. Based on extensive experimental data, they were able to explain the operation of a mass short-wave generator theoretically and describe its effects. They also studied the spectrum of the mass radiator, among other things. Although the results of these studies were published during or after the Great Patriotic War. The modest laboratory of Glagoleva-Arkadieva at the Medical Institute played a significant role in this research. The Maxwell Laboratory, which became part of the Moscow State University Physics Institute in 1933 and on which Glagoleva-Arkadieva worked, was a center for the study of the shortest electromagnetic waves in our country during the 1920s and 1930s. However, the war broke out, followed by the death of Glagoleva-Arkadieva in 1945, interrupting these studies [3].

[1] A. Glagolewa-Arkadiewa, Short electromagnetic waves of Wavelength up to 82 microns, Nature, vol. 113 (2844), p. 640, (1924).
[2] A. Glagoleva-Arkadieva, Metod polucheniya naibolee korotkih eletkromagnitnyh voln [Method of obtaining the shortest electromagnetic waves], Trudy III S'ezda Rossijskoj associacii fizikov 17–21 sentyabrya 1922 g. [Proceedings of the III Congress of the Russian Association of Physicists on September 17–21, 1922], Nizhny Novgorod, pp. 39–40 (1923).
[3] S. Vavilov, A. Ioffe A. Prof. A.A. Glagoleva-Arkadieva, Nature, vol. 159, pp. 296–297, (1947).

Terahertz biophotonics: progress and opportunities

K. I. Zaytsev

Prokhorov General Physics Institute of the Russian Academy of Sciences, Moscow, Russia

e-mail: kirzay@gmail.com

Terahertz (THz) technology was vigorously explored during the past decades [1, 2]. Nowadays, it offers a variety of application in medical diagnosis and therapy of socially important diseases, such as diabetes mellites [3] or malignant and benign neoplasms with different nosologies and localizations [4–7]. In this talk, recent progress in medical applications of THz technologies is considered [8–12]. Challenging problems, those hamper translation of THz technologies into a clinical practice, along with their possible solutions are also stressed. Among them: overcoming the Abbe diffraction limit in the THz range to bring the spatial resolution of THz medical spectroscopy and imaging to relevant values [12–19]; developing of hardware and methods for the quantitative THz endoscopy of hard-to-access tissues and internal organs [20–22]; improving the performance and information content of THz spectroscopy and imaging systems [23–25].

[1] H. Guerboukha et al., Advances in Optics & Photonics, vol. 10, pp. 843–938 (2018).
[2] O.A. Smolyanskaya et al., Progress in Quantum Electronics, vol. 62, pp. 1–77 (2018).
[3] G.G. Hernandez-Cardoso et al., Scientific Reports, vol. 12, p. 3110 (2022).
[4] K.I. Zaytsev et al., Journal of Optics, vol. 22, p. 013001 (2020).
[5] H. Lindley-Hatcher et al., Applied Physics Letters, vol. 118, p. 230501 (2021).
[6] O.P. Cherkasova et al., Journal of Biomedical Optics, vol. 26, p. 090902 (2021).
[7] N.V. Chernomyrdin et al., Opto-Electronics Advances, vol. 6, p. 220071 (2023).
[8] K.I. Zaytsev et al., Applied Physics Letters, vol. 106, p. 053702 (2015).
[9] A.A. Gavdush et al., Journal of Biomedical Optics, vol. 24, p. 027001 (2019).
[10] A.A. Gavdush et al., Biomedical Optics Express, vol. 12, pp. 69–83 (2021).
[11] A.S. Kucheryavenko et al., Physical Review Applied, vol. 20, p. 054050 (2023).
[12] N.V. Chernomyrdin et al., Scientific Reports, vol. 13, p. 16596 (2023).
[13] N.V. Chernomyrdin et al., Applied Physics Letters, vol. 113, p. 111102 (2018).
[14] N.V. Chernomyrdin et al., Optica, vol. 8, pp. 1471–1480 (2021).
[15] A.S. Kucheryavenko et al., Biomedical Optics Express, vol. 12, pp. 5272–5289 (2021).
[16] G.R. Musina et al., Biomedical Optics Express, vol. 12, pp. 5368–5386 (2021).
[17] N.V. Chernomyrdin et al., Applied Physics Letters, vol. 120, p. 110501 (2022).
[18] V.A. Zhelnov et al., Advanced Optical Materials, vol. 12, p. 2300927 (2024).
[19] V.A. Zhelnov et al., "Superresolution THz pulsed solid immersion microscopy," Applied Physics Letters, under review (2025).
[20] A.S. Kucheryavenko et al., Optics Express, vol. 31, pp. 13366–13373 (2023).
[21] G.M. Katyba et al., Appliied Physics Letters, vol. 124, p. 243703 (2024).
[22] G.M. Katyba et al., "Terahertz endoscopy of hard-to-access objects in the context of neoplasms diagnosis – A review," Light: Advanced Manufacturing, in press (2025).
[23] D.S. Ponomarev et al., Optics Letters, vol. 48, pp. 1220–1223 (2023)
[24] N.V. Zenchenko et al., Applied Physics Letters, vol. 124, p. 121107 (2024).
[25] D.S. Ponomarev et al., Physics-Uspekhi, vol. 67, pp. 3–21 (2024).

Microwave solitons of cyclotron-resonant self-induced transparency: theory and experiments

I. Zotova, N. Ginzburg, S. Samsonov, A. Sergeev, L. Yurovsky, V. Zaslavsky, A. Rostuntsova, N. Ryskin

A. V. Gaponov-Grekhov Institute of Applied Physics of the Russian Academy of Sciences, Russia

e-mail: zotova@ipfran.ru

In optics, a well-known effect is the self-induced transparency (SIT) of short light pulses during their resonant interaction with passive (non-inverted) media. As a result, the incident pulse is transformed into a SIT soliton, which propagates through the absorbing media without losses and changes in its shape. The SIT effect is realized when the duration of the input light pulse is less than the phase relaxation time, which is characteristic only for fairly exotic laser media.

In classical electronics, similar conditions arise during cyclotron-resonant interaction with a rectilinear magnetized electron beam, which acts as an analogue of a resonant non-inverted medium. Accordingly, in this case, one should expect the occurrence of the cyclotron-resonant SIT effect, which was theoretically predicted in [1]. At the same time, specific features of electron media are their motion, as well as large phase relaxation times. The latter factor is determined by the electron-electron or electron-ion collisions, which are typically neglected under normal operating conditions of electron-vacuum devices. The specified features lead to the emergence of new modes that have no analogues in optics. In particular, during resonant interaction with a counter-propagating wave, its modulation instability (MI) occurs [2, 3], as a result of which stationary radiation is transformed into a periodic or chaotic sequence of ultrashort pulses, which are the microwave SIT solitons. This effect is of interest for microwave modulation, which has been successfully demonstrated in recent Ka-band experiments.

The report presents the theory of the cyclotron-resonance SIT and the results of performed experiments.

This work was supported by the RSF project № 23-12-00291.

[1] N.S. Ginzburg, I.V. Zotova, A.S. Sergeev, Self-induced transparency and electromagnetic pulse compression in a plasma or an electron beam under cyclotron resonance conditions, Phys. Rev. Lett., vol.105, no.26, art.no.265001 (2010).
[2] I.V. Zotova, N.S. Ginzburg, A.S. Sergeev, E.R. Kocharovskaya, V.Yu. Zaslavsky, Conversion of an electromagnetic wave into a periodic train of solitons under cyclotron resonance interaction with a backward beam of unexcited electron-oscillators, Phys. Rev. Lett., vol.113, no.14, art.no.143901 (2014).
[3] A.A. Rostuntsova, N.M. Ryskin, I.V. Zotova, N.S. Ginzburg, Modulation instability of an electromagnetic wave interacting with a counter-propagating electron beam under condition of cyclotron resonance absorption, Phys. Rev. E, vol.106, no.1, art.no.014214 (2022).

Strain-induced magnetic anisotropy in Co/Pt THz spintronic emitter

A. L. Alferyev[1], P. Yu. Avdeev[1], M. V. Sapozhnikov[2], N. S. Gusev[2], A. M. Buryakov[1]

1- MIREA – Russian Technological University, Moscow, 119454 Russia
2- Institute for Physics of Microstructures RAS, Nizhny Novgorod, 603950 Russia

e-mail: seekingfornano@gmail.com

The terahertz (THz) range extends from approximately 100 GHz to 30 THz and is placed between the microwave and far-infrared regions of the electromagnetic spectrum [1]. This renders it particularly suitable for applications where compactness and controllability are essential, such as in the search for compact and controllable sources in the 'frequency gap' where traditional electronic and optical devices are inefficient. Spintronic emitters are regarded as being amongst the most promising sources in this field. They generate signals of up to approximately 20 THz and, due to an external magnetic field, allow precise polarisation [2]. The key conclusion to be drawn here is that spintronic structures combine high frequency 'performance' with the possibility of flexible tuning, since the amplitude, phase, and polarisation of THz pulses can be adjusted almost independently.

The primary mechanism for generating a terahertz signal in spintronic emitters involves the excitation of spin current by a femtosecond laser pulse in a ferromagnetic layer, and its subsequent conversion into a charge current due to the inverse spin Hall effect (ISHE). The resulting charge current functions as an 'antenna', emitting terahertz waves that form their time and polarisation structure [2].

Whilst it is already known that an external magnetic field enables the control of polarisation, recent studies have indicated that the range of available tuning methods can be significantly expanded. For instance, at the Co/Pt interface, the Dzyaloshinskii–Moriya interaction (DMI) has been demonstrated, whose magnitude can be tuned by strain with high precision [3]. This development presents a novel means to control the properties of the 'classical' Co/Pt spintronic emitter.

This work's primary objective is to study and analyse the influence of DMI on the characteristics of the Co/Pt spintronic emitter, in relation to the elastic strain that are induced in it. The structures of Co (2 nm)/Pt (2 nm), grown on SiO_2 by magnetron sputtering, were investigated. The experimental studies were conducted employing an amplified Ti:Sapphire-based femtosecond laser system (wavelength 800 nm, pulse repetition rate 3 kHz, pulse duration 35 fs) via terahertz time-domain spectroscopy (THz-TDS) in transmission mode.

The strain was applied by subjecting the sample to bending in crystallographic directions determined by the easy and hard axes of magnetic anisotropy of the ferromagnetic layer. The results demonstrated the potential for controlling the configuration of the terahertz hysteresis loop by regulating the amplitude of the applied strain. In the process of mechanical deformation along the easy axis of magnetisation, a transition from a hard hysteresis loop to an easy one was observed. Similarly, under deformation along the hard axis, the opposite phenomenon was observed: a transformation of the easy hysteresis loop into a hard one.

The work was supported by the Russian Science Foundation under Grant No 25-79-30019.

[1] Alfred Leitenstorfer et al, The 2023 terahertz science and technology roadmap, J. Phys. D: Appl. Phys. 56 (22), 223001 (2023).
[2] T.S. Seifert et al, Spintronic sources of ultrashort terahertz electromagnetic pulses, Appl. Phys. Lett., 120 (18), 180401, (2022).
[3] N. S. Gusev, A. V. Sadovnikov, Manipulation of the Dzyaloshinskii–Moriya Interaction in Co/Pt Multilayers with Strain, Phys. Rev. Lett. 124(15), 157202, (2020).

Frequency doubling of infrared laser radiation in type I phase matched lithium-sodium molybdate

D. A. Demushkin, D. A. Denisov, A. V. Konyashkin

Moscow Institute of Physics and Technology, Institutskii per. 9, Dolgoprudny, Moscow obl., 141701 Russia

e-mail: denisov.da@phystech.edu

Lithium-sodium molybdate ($LiNa_5Mo_9O_{30}$, LNM) is a rather new biaxial crystal of molybdate group. The crystal has a high laser damage threshold 2.64 GW/cm^2 (@ 1064 nm, 10 ns, 1 Hz) and large birefringence in range from 0.14 (@ 5 μm) to 0.26 (@ 0.435 μm), which makes it promising material for the fabrication of polarization affecting optical devices [1]. Theoretical research revealed LNM potential as a nonlinear optical crystal for laser frequency conversion, specifically second harmonic generation (SHG) and parametric conversion [2]. Experimental studies of frequency doubling of infrared (IR) radiation in lithium-sodium molybdate crystals has shown that the efficiency of the process in type II phase matched samples is extremely low (<4%) due to a considerable spatial walk-off caused by large birefringence [3]. Efficiency can be improved by compensating of the walk-off or using crystals with another phase matching type. In this work, the frequency doubling of IR radiation in type I phase matched LNM is realized.

LNM samples 2×5×10 mm^3 in size were cut in the direction of type I phase matching ($\theta = 90°$, $\varphi = 28°$) from single crystal boules grown by the Czochralskii method. Pulsed laser radiation (1030 nm, 2.4 ns, 100 kHz) with beam diameter of 0.3 mm was used as a pump radiation and was directed into the sample. Second harmonic (SH) and pump radiation was further separated by a dichroic mirror. Dependencies of the SH radiation power and the conversion efficiency on the pump power are shown at Fig. 1. The highest conversion efficiency was 13% at corresponding pump power of 8 W.

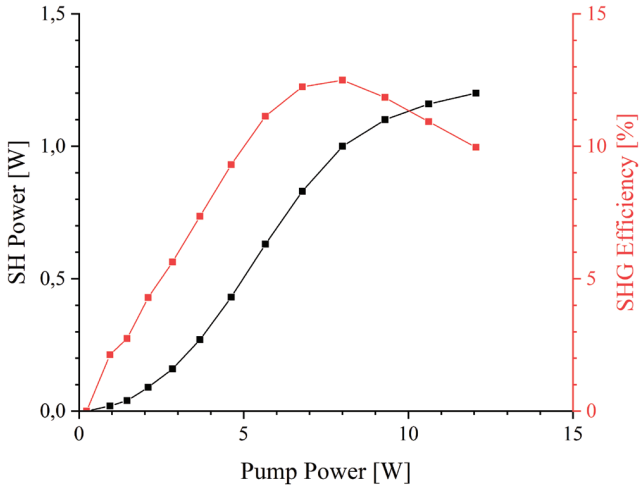

Fig. 1. Dependences of SH power and SHG efficiency on pump power

The study reveals that frequency doubling of IR radiation using the type I phase matched LNM crystals gives a more efficient result than using the type II phase matched ones.

[1] X. Du et. al., High laser damage threshold LiNa5Mo9O30 prism: for visible to mid-infrared range, Chinese Optics Letters, 20, 051602, (2022).
[2] S.G. Grechin et. al., $LiNa_5Mo_9O_{30}$ (LNM) crystal for nonlinear optical frequency conversion, Optical Materials, 135, 113226, (2023).
[3] D.A. Denisov et. al., Second-harmonic generation in $LiNa_5Mo_9O_{30}$ crystalline sample, ICLO 2024 Proceedings, (2024).

Low-thermal-gradient Czochralski growth of nonlinear $(Li,Na)_6Mo_9O_{30}$ crystals

V. D. Grigorieva[1], D. M. Ezhov[2]

1- Nikolaev Institute of Inorganic Chemistry SB RAS, Acad. Lavrentyev ave. 3, Novosibirsk, 630090 Russia
2- Tomsk State University, Lenin ave. 36, Tomsk, 634050 Russia

e-mail: grigoryeva@niic.nsc.ru

$(Li,Na)_6Mo_9O_{30}$ is a solid-solution variation of sodium molybdate $Na_6Mo_9O_{30}$ with an isovalent Na/Li substitution. In literature data orthorhombic crystal $LiNa_5Mo_9O_{30}$ is described, with its photonic properties making it a promising material for nonlinear optical applications [1]. $LiNa_5Mo_9O_{30}$ demonstrates a broad transparency range from 357 to 5260 nm. Compared to the well-known nonlinear crystal LBO, which belongs to the same mm2 point symmetry group, it demonstrates on average four times higher values of effective nonlinear susceptibility coefficients.

The compounds with solid-solution areas present higher requirements on thermal control during crystal growth in order to obtain bulk uniform crystals. Low-thermal gradient Czochralski technique (LTG Cz) characteristic feature is three independent heating zones in the growth chamber, with accurate weight control and crystal weight/temperature feedback loop [2]. This way, temperature gradients are reduced to 1 °/cm, which is two orders of magnitude lower compared to conventional Czochralski technique.

In this work, $LiNa_5Mo_9O_{30}$ and $LiNa_5Mo_9O_{30}$:Li crystals were obtained by LTG Cz technique. The crystals demonstated strong tendency to twinning along the c axis. During continuous crystal growth experiments stratification of the melt on lithium and sodium phases was observed. Quantative atomic emission spectroscopy analysis showed close compliance of loaded Li/Na ratio and the one in the grown crystals, with slight displacement toward the sodium fraction.

The optical and nonlinear optical properties of the crystal samples were investigated. The bandgap energies of the studied materials were determined using the Tauc plot method and derivative absorption spectrum fitting (DASF). The powder second-harmonic generation (SHG) test based on the Kurtz–Perry method was employed to evaluate the effective nonlinear susceptibility of the crystals. Fractionated samples of LBO and KTP nonlinear crystals were used as reference materials in the powder test.

The studied nonlinear crystals demonstrate an unusually strong dependence of the intensity of second-harmonic generation (SHG) of Nd:YAG laser radiation on the particle size compared to the reference samples. For large particle sizes, the SHG intensity of the $LiNa_5Mo_9O_{30}$ crystal grown from a melt with excess lithium concentration was found to be 6 times higher, whereas for the sample obtained from a stoichometric melt composition –4 times higher than that of the LBO crystal.

The study was supported by Russian Science Foundation grant No. 25-73-00328

[1] G. Grechin, N.A. Khohlov, D.G. Kochiev, V.A. Sukharev, A.P. Sadovsky, I. Ch Avetissov, $LiNa_5Mo_9O_{30}$ (LNM) crystal for nonlinear optical frequency conversion, Optical Materials, 135, 113226, (2023).
[2] V.N. Shlegel, Yu.A Borovlev, D.N. Grigoriev, V.D. Grigorieva, F.A. Danevich, N.V. Ivannikova, A.G. Postupaeva, Ya.V. Vasiliev, Recent progress in oxide scintillation crystals development by low-thermal gradient Czochralski technique for particle physics experiments, Journal of Instrumentation, V. 12, C08011, (2017).

Femtosecond laser printing of anti-reflective nanostructures on nonlinear crystals

A. Kurus[2,5], L. Lobanov[2,5], V. Fedyaj[1,2], S. Syubaev[3], A. Eliseev[2,5], A. Dostovalov[1,2], A. Kuchmizhak[3,4], L. Isaenko[2,5]

1- Institute of Automation and Electrometry of the SB RAS, Acad. Koptyug Ave. 1, Novosibirsk, 630090 Russia
2- Novosibirsk State University, Novosibirsk, 630090 Russia
3- Institute of Automation and Control Processes of the FEB RAS, Radio st. 5, Vladivostok, 690041 Russia
4- Far Eastern Federal University, Vladivostok, 690041 Russia
5- Sobolev Institute of Geology and Mineralogy SB RAS, Kopyug ave. 3, Novosibirsk, 630090 Russia

e-mail: kurusaf@igm.nsc.ru

Nonlinear crystals are key components in many infrared (IR) optical devices, including laser spectrometers operating in the near- and mid-infrared range. However, their high refractive index leads to significant Fresnel reflection losses, reducing overall efficiency. Antireflection microstructures (ARMs) represent a viable alternative to dielectric thin-film multilayer coatings, offering broadband performance, enhanced durability, damage resistance, and eliminate adhesion-related issues.

Compared to costly and complex techniques such as lithography, etching, or direct printing, femtosecond laser ablation provides a simpler, more versatile and effective method for ARM fabrication. Various approaches were demonstrated for ARMs fabrication: direct ablation to produce ARMs with increased depth and high aspect ratios [1, 2], laser ablation assisted with wet chemical etching to further increase depth [3], surface pattering based on laser-induced periodic surface structures (LIPSS), whose periods dependent on the laser wavelength resulting in broadband spectral range of ARM produced with UV laser radiation [4, 5].

In this study, we present the results of ARMs formation on nonlinear optical elements were fabricated from crystals grown by the low-gradient Bridgman method: GaSe, $BaGa_4Se_7$ (BGSe), $LiInS_2$ (LIS), using visible and IR femtosecond laser pulses. In this study, we present the results of ARM formation on nonlinear crystals: GaSe, $BaGa_2Se_4$ (BGSe), $LiInS_2$ (LIS) using visible and IR femtosecond laser pulses.. In particular, our results demonstrate that direct ablation with IR femtosecond pulses (1026 nm) on GaSe and LiS enhances transmission in the mid-IR range for single-side treatment by over 15% and 9%, respectively. Additionally, LIPSS formation on single side with visible laser radiation (513 nm) on BGSe crystals improves transmission from 65% to 73% in the near-IR range (1.3–2 μm). These results show the capabilities of femtosecond laser processing to improve the optical performance of nonlinear crystals in IR applications.

This work was supported by Russian Science Foundation (grant. № 25-79-20014).

[1] A. Yelisseyev, V. Fedyaj, V. Simonov, L. Isaenko, S. Lobanov, A. Shklyaev, A. Simanchuk, S. Babin, A. Dostovalov, Femtosecond laser direct writing of antireflection microstructures on the front and back sides of a GaSe crystal, Photonics, vol. 9, p.774, (2022).
[2] S. Syubaev, E. Modin, S. Gurbatov, A. Cherepakhin, A. Dostovalov, A. Tarasova, P. Krinitsin, A. Yelisseyev, L. Isaenko, A. Kuchmizhak SWIR anti-reflective nanostructures on nonlinear crystals by direct UV femtosecond laser printing, Applied Physics Letters, vol. 123, p. 061108, (2023).
[3] Teslenko, A., Konstantinova, T., Bushunov, A. et al. Antireflection microstructures on ZnSe for mid- and far-IR fabricated by femtosecond laser ablation assisted with wet chemical etching. Sci Rep 14, 10743 (2024).
[4] S. Syubaev, A. Dostovalov, A. Tarasova, A. Shevlyagin, L. Isaenko, A. Kuchmizhak, Femtosecond Laser-Induced Periodic Surface Nanostructuring of BaGa4Se7 Crystal for Near-Infrared Anti-Reflection Enhancement, Bulletin of the Russian Academy of Sciences: Physics, vol. 88, pp. 439–442, (2024).
[5] S. Gurbatov, Yu. Borodaenko, E. Mitsai, E. Modin, A. Zhizhchenko, A. Cherepakhin, A. Shevlyagin, S. Syubaev, A. Porfirev, S. Khonina, A. Yelisseyev, S. Lobanov, L. Isaenko, E. Gurevich, A. Kuchmizhak, Laser-Induced Periodic Surface Structures on Layered GaSe Crystals: Structural Coloring and Infrared Antireflection, The Journal of Physical Chemistry Letters, vol. 14, pp. 9357–9364, (2023).

Influence of the saturable absorber position on the output parameters and self-starting of a holmium UFL

A. Lobanov[1], V. Kamynin[1], S. Filatova[1], A. Ismail[1,2], N. Arutyunyan[1,2], E. A. Obraztsova[1,2], N. Komatsu[3], J. Kono[3], E. D. Obraztsova[1,2], V. Tsvetkov[1]

1- Prokhorov General Physics Institute of the Russian Academy of Sciences, Moscow, 119991 Russia
2- Moscow Institute of Physics and Technology (National Research University), Moscow, 141701 Russia
3- William Marsh Rice University, Houston, Texas 77251-1892, United States of America

e-mail: l0banov.a.i@yandex.ru

To create ultrafast lasers (UFLs), a mode-locking is used, often with saturable absorbers (SAs). In addition to characterization of SAs, it is necessary to know how a particular SA parameter affects laser generation. As shown in many works [1–3], the spectrum, pulse duration, its energy parameters, and the start time of continuous mode-locking are sensitive to changes in the SA parameters. At the same time, there are many problems for experimental confirmation of these dependencies. In this work, we present a method to study the effect of the modulation depth of the saturable absorber on mode-locking and CW mode-locking self-starting time.

For the experiment, we used a holmium fiber cavity based on polarization-maintaining fibers (Fig. 1a). A fiber coupler with a coupling ratio of 10/90 was used as an output of the laser and provided 10% output of laser power. Pumping was provided by a continuous-wave ytterbium fiber laser with a wavelength of 1130 nm via a PM WDM 1125/2100. A similar WDM was used to extract the unabsorbed pump. The gain medium was a 1-meter-long holmium-doped PM fiber, manufactured by IXBlue. An isolator with fast axis blocking was also used. An air optical section was integrated into the cavity, consisting of collimators aligned with each other and a confocal system of two lenses. The saturable absorber sample was placed at the center of the optical waist. By moving the sample along the optical axis, its modulation depth changed depending on the variation in the power density incident on the sample.

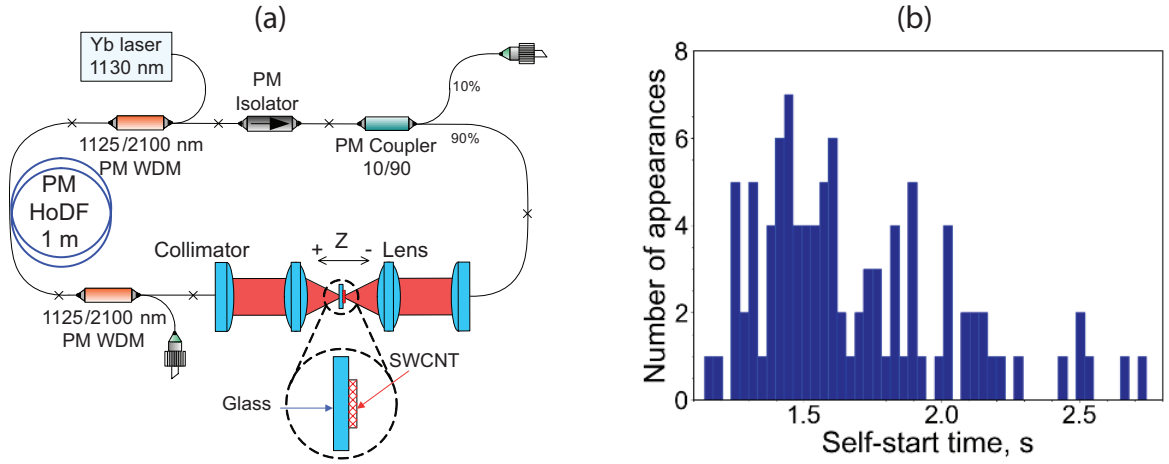

Fig. 1. (a) Schematic of the holmium resonator with an integrated optical path. HoDF – holmium-doped fiber, SWCNT – single-walled carbon nanotubes; (b) Histogram of self-start time at the center of the optical path waist.

For each sample position, the optical emission spectrum, average power, and self-start time of the system were recorded. The self-start time was recorded multiple times to collect statistical data. An example is shown in Fig. 1b.

Funding Russian Science Foundation (24-72-10120)

[1] C. Hönninger, R. Paschotta, F. Morier-Genoud, M. Moser, U. Keller, Q-switching stability limits of continuous-wave passive mode locking, 16 (2014) TuA6. https://doi.org/10.1364/assl.1999.tua6.
[2] C. Lecaplain, M. Baumgartl, T. Schreiber, A. Hideur, On the mode-locking mechanism of a dissipative- soliton fiber oscillator, Opt. Express 19 (2011) 26742. https://doi.org/10.1364/oe.19.026742.
[3] S.K. Turitsyn, B.G. Bale, M.P. Fedoruk, Dispersion-managed solitons in fibre systems and lasers, Phys. Rep. 521 (2012) 135–203. https://doi.org/10.1016/j.physrep.2012.09.004.

Second harmonic generation at 535 nm in LBO crystal pumped by an all-fiber passively Q-switched and Gain-switched Yb-doped laser

E. Maslova[1,2], P. Puyu[2]

1- National Research Nuclear University MEPhI, Kashirskoe shosse 31, Moscow, 115409 Russia
2- VPG Laserone, Vvedenskogo sq. 1, Fryazino, Moscow Region, 141190 Russia

e-mail: emaslova@vpglaserone.ru

Nonlinear frequency conversion processes are extensively used to enhance existing laser systems by generating coherent light in spectral ranges where direct sources are unavailable. Among these, second harmonic generation (SHG) serves as the primary method for producing 532 nm wavelength radiation [1].

In this abstract, we demonstrate second harmonic generation at 535 nm using an all-fiber passively Q-switched and Gain-switched laser as the pump source [2]. Employing a dual-cavity architecture that integrates both amplifier and saturable absorber, this laser system has performance parameters: 7 mJ pulse energy, 1200 W average output power, and 40 kW peak output power. Conversion efficiencies of 14%, 9.5%, and 8.3% were achieved for a 50-mm LBO crystal, a 20-mm LBO crystal, and two 20-mm LBO crystals (with one crystal rotated by 90°), respectively. The corresponding average output powers at the 535 nm second harmonic were 87 W, 57 W, and 100 W for these configurations.

In this work, we present experimental-numerical comparisons for single 50 mm and 20 mm LBO crystals, with the corresponding graphs shown below (Fig. 1). The configuration involving two sequential 20 mm crystals introduces additional complexity and is not included in this analysis.

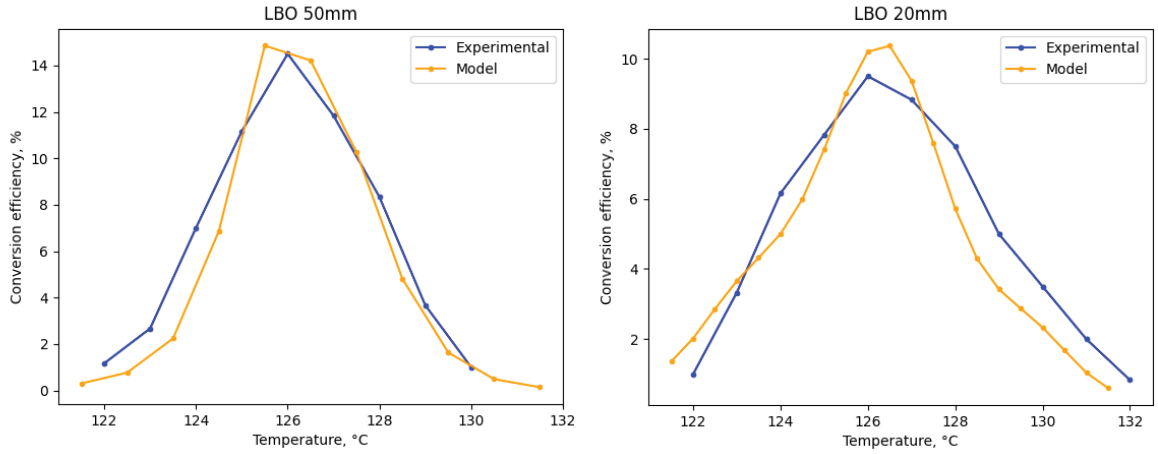

Fig. 1. Comparison of experimental and theoretical conversion efficiency as a function of crystal temperature for LBO crystal configurations: (left) 50 mm single crystal, (right) 20 mm single crystal.

Theoretical modeling, performed using a split-step beam propagation method with fast Fourier transform implementation (FFT-BPM) [3, 4], shows good agreement with experimental results**.** The model comprehensively accounts for diffraction effects due to finite beam aperture, anisotropic dispersion, and temperature/spectral/angular refractive index dependencies, providing a comprehensive framework for SHG optimization.

In the present study, the efficiency of second-harmonic generation is potentially limited by the pump source's random polarization, spectral width, and suboptimal pulse shape and duration, which could serve as optimization parameters in further research.

[1] A. J. W. Brown, M. S. Bowers, K. W. Kangas, and C. H. Fisher, "High-energy, high-efficiency second-harmonic generation of 1064nm radiation in KTP," Opt. Lett. 17, 109–111 (1992).
[2] A. A. Fotiadi, A. S. Kurkov, and I. M. Razdobreev, "All-fiber passively Q-switched Ytterbium laser," in IEEE, Proceedings of CLEO-Europe, 515, Munich, Germany, 12–17 June (2005).
[3] G. L. Pedrola, Beam Propagation Method for Design of Optical Waveguide Devices (John Wiley & Sons, Inc., New York, 2015).
[4] G. P. Agrawal, Nonlinear Fiber Optics (Elsevier/Academic Press, 2013).

Origin of the nonlinear vibrational response in complex-structured molecules within the THz frequency range

A. O. Nabilkova, M. S. Guselnikov, A. O. Ismagilov, M. V. Melnik, S. A. Kozlov, A. N. Tcypkin

Research and Educational Center of Photonics and Optical IT, ITMO University, Kadetskaya liniya 3/2, Saint Petersburg, Russia

e-mail: aonabilkova@itmo.ru

This study introduces a theoretical framework to predict the nonlinear refractive index coefficient n_2 in terahertz (THz) range of complex molecules by decomposing their vibrational nonlinear response into contributions from individual chemical bonds. Using reference materials with bonds analogous to those in isopropanol molecule – water (O-H bonds) [1], α-pinene (C-H bonds), and liquid CO_2 (C-O bonds) – we calculate bond-specific contributions and sum them to estimate n_2 for isopropanol. The theoretical prediction yields $n_2 = 4.7\times10^{-9}$ cm^2/W. Experimental validation via z-scan measurements with pulsed THz radiation (0.75 THz central frequency, 1 ps pulse duration) confirms a value of $n_2 = 2.5\pm0.5\times10^{-9}$ cm^2/W, demonstrating strong agreement.

We propose that the contribution of a specific oscillator (associated with a particular chemical bond in a complex molecule) can be derived from the n_2 of reference material with simpler structure dominated by the same bond. The nonlinear parameters *a* and *b*, which describe anharmonic oscillator behavior [2], depend solely on the properties of the individual oscillator. For systems with weak inter-bond interactions, the polarization response to the electric field from the same type of oscillator in different materials can be considered as equal. Building on this assumption and the theory of vibrational nonlinearity in the THz range [2], contribution $n_2^{\text{O–H}}$ to isopropanol's n_2 can be estimated through a nonlinear response n_2^{H2O} of water [1] adjusted by the concentration of O-H bond in the respective materials:

$$n_2^{\text{O-H}} = \frac{n_2^{\text{H2O}} n_0^{\text{H2O}} N_{\text{O-H}}^{2\,prop}}{n_0^{2\,prop} N_{\text{O-H}}^{\text{H2O}}}.$$

Here, n_2^{H2O} is the measured nonlinear refractive index coefficient for water, $N_{\text{O-H}}^{2\,prop}$ is concentration of O-H bonds in isopropanol, n_0^{H2O} linear refractive index of water, $N_{\text{O-H}}^{\text{H2O}}$ is concentration of O-H bonds in water and n_0^{2prop} is linear refractive index of isopropanol. The estimation of $n_2^{\text{C–O}}$ contribution using the same methodology is challenging due to the absence of experimental data for liquids composed purely of C–O bonds, for instance – carbon dioxide CO_2 in liquid form. So expression for n_2 from abovementioned theory [2] was used. Key parameters include bond concentration, linear refractive indices of vibrational and electronic nature (in THz and visible ranges), and main vibrational resonance frequencies [3, 4].

This work bridges molecular-level vibrational dynamics and macroscopic optical properties, offering a predictive tool for designing THz nonlinear materials. The large n_2 of isopropanol enables low-intensity THz nonlinear effects (e.g., self-focusing, Kerr effect), advancing applications in ultrafast optical switches, sensors, and frequency converters. The approach reduces reliance on direct experimental measurements, streamlining material optimization for THz technologies.

All authors acknowledge support from the Russian Science Foundation (Grant No. 24-22-00084).

[1] Tcypkin, A., Zhukova, M., Melnik, M., Vorontsova, I., Kulya, M., Putilin, S., Kozlov, S., Choudhary, S. and Boyd, R.W., Giant third-order nonlinear response of liquids at terahertz frequencies. Physical Review Applied, 15(5), p. 054009, (2021).
[2] Dolgaleva, K., Materikina, D. V., Boyd, R. W., & Kozlov, S. A., Prediction of an extremely large nonlinear refractive index for crystals at terahertz frequencies. Physical Review A, 92(2), 023809, (2015).
[3] Marin, T.W. and Janik, I., Ultraviolet spectroscopy of pressurized and supercritical carbon dioxide. Communications Chemistry, 4(1), p. 77, (2021).
[4] Khonakdar, D.R. and Raveshi, M.R., Mixed convection on a vertical plate in supercritical fluids by selecting the best equation of state. The Journal of Supercritical Fluids, 107, pp. 549–559, (2016).

Optical pump – terahertz probe of ultra-thin smooth gold films revealing their optoelectronic properties

M. I. Paukov[1], D. I. Yakubovsky[1], Sh. San[2], S. Kolar[1,3], K. A. Brekhov[1,3,4], G. A. Komandin[5] A. I. Chernov[1,3], K. I. Zaytsev[5] A. V. Arsenin[1], Y. Zhang[2], M. G. Burdanova[1,5,6]

1- Center for Photonics and 2D Materials, Moscow Institute of Physics and Technology (MIPT), Dolgoprudny, Russia
2- Capital Normal University, Beijing, China
3- Russian Quantum Center, Skolkovo, Russia
4- Moscow Institute of Radio Engineering, Electronics and Automation (MIREA – RTU MIREA), Moscow, Russia
5- A. M. Prokhorov General Physics Institute, Russian Academy of Sciences, Moscow, Russia
6- Y. A. Osipyan Institute of Solid State Physics, Russian Academy of Sciences, Chernogolovka, Russia

e-mail: paukov.mi@phystech.edu

We present an optical pump – terahertz probe (OPTP) spectroscopy study of ultra-thin smooth gold films (2–8 nm thickness) to elucidate their optoelectronic properties and carrier dynamics. The films, fabricated via a seed-free chemical synthesis method, exhibit exceptional homogeneity and reduced surface roughness, enabling precise probing of intrinsic electronic responses. Using OPTP – similar to methodologies in prior works – we measured transient terahertz conductivity dynamics following ultrafast photoexcitation. Results reveal a dependent on thickness terahertz photoconductivity. Relaxation dynamics, occurring on sub-picosecond timescales, further indicate efficient carrier thermalization mediated by electron-phonon coupling. Our findings demonstrate that ultra-thin smooth gold films offer tunable optoelectronic properties for advanced plasmonic and photonic devices, with direct implications for terahertz modulators and ultrafast sensors.

Dynamic terahertz focusing via electrically gated SWCNT structures

A. V. Radivon[1], G. M. Katyba[2,3], N. I. Raginov[4], A. A. Mkrtchyan[4], A. V. Chernykh[5], I. I. Rakov[4], M. I. Paukov[1], M. S. Mironov[1], M. A. Shashkov[1], G. A. Komandin[2], K. I. Zaytsev[2], Y. G. Gladush[4], N. V. Petrov[5,6], A. G. Nasibulin[4], A. V. Arsenin[1], D. V. Krasnikov[4], M. G. Burdanova[1,2,3]

1- Center for Photonics and 2D Materials, Moscow Institute of Physics and Technology, Dolgoprudny, Russia
2- Prokhorov General Physics Institute of the Russian Academy of Sciences, Moscow, Russia
3- Institute of Solid State Physics of the Russian Academy of Sciences, Chernogolovka, Russia
4- Skolkovo Institute of Science and Technology, Moscow, Russia
5- ITMO University, St. Petersburg, Russia
6- Qingdao Innovation and Development Center, Harbin Engineering University, Qingdao, China

e-mail: radivon.av@phystech.edu

The terahertz (THz) frequency range (0.1–10 THz) is the basis for modern technologies, including security systems, medical diagnostics and high-speed communications [1]. However, the lack of compact and tunable optical components remains the main limitation for their widespread use. In this paper, an electrochemically controlled Fresnel zone plate based on single-wall carbon nanotube (SWCNT) films is proposed, combining the functions of focusing and dynamic modulation of THz radiation.

SWCNT films synthesized by the CVD method [2] were deposited in the form of concentric rings necessary to form a Fresnel zone plate with a focal length of 2 cm at a frequency of 327 GHz. The final device consisted of SWCNT rings and gold counter contacts connected by an ionic liquid and encapsulated in a sandwich structure of two quartz plates. This configuration allows for the implementation of electrochemical doping according to a two-contact scheme. The field visualization behind the optical element was performed using a setup that included a backward-wave oscillator as a THz radiation source and a three-coordinate scanner with a fixed detector in the form of a Golay cell.

In the absence of voltage, the Fresnel zone plate operates as a lens with a focal length of 2 cm at 327 GHz, which confirms the possibility of using CNTs for such diffraction elements. Application of a potential difference from –2 to +2 V leads to a change in the field amplitude, with a modulation depth, i.e. a relative change in the signal, from –20% to +15%. In this case, the focus position remained virtually unchanged at the same potential difference values.

The obtained results demonstrate the promise of using electrochemical doping of SWCNTs to create adaptive THz devices. The main limitation is the relatively slow switching time (about 3 minutes) associated with diffusion processes in the ionic liquid, the selection of which is a further direction of research.

This work is supported by the RSF grant # 24-79-00143.

[1] A. Shafie, N. Yang, C. Han, J.M. Jornet, M. Juntti, T. Kürner, Terahertz communications for 6G and beyond wireless networks: Challenges, key advancements, and opportunities, IEEE Network, 37(3), 162–169, (2022).
[2] E.M. Khabushev, D.V. Krasnikov, O.T. Zaremba, A.P. Tsapenko, A.E. Goldt, A.G. Nasibulin, Machine learning for tailoring optoelectronic properties of single-walled carbon nanotube films, The journal of physical chemistry letters, 10(21), 6962–6966, (2019).

THz-IR spectroscopy of lead-free ferroelectrics with perovskite structure

M. V. Talanov[1], V. I. Kozlov[2,3], K. V. Zhivetev[1]

1- Moscow Institute of Physics and Technology (National Research University), Dolgoprudnyi, Russia
2- Research Institute of Solid-State Electronics Materials, MIREA − Russian Technological University (RTU MIREA), Moscow, Russia
3- Kapitza Institute for Physical Problems RAS, Moscow, Russia

e-mail: zhivetev.kv@phystech.edu

Ferroelectrics with the perovskite structure ABX_3 are widely used in the creation of piezoelectric devices such as piezoelectric sensors, actuators, and non-volatile data storage devices [1]. Currently, the most commonly used piezoelectric materials in technology are ferroelectric materials based on solid solutions of the $PbZr_{0.5}Ti_{0.5}O_3$ (PZT) system, which contain a significant amount of toxic lead, which contradicts modern environmental standards [2]. This has led to an increased focus on the search and development of new materials based on lead-free systems. The most extensively studied and promising system is $K_{0.5}Na_{0.5}NbO_3$ (KNN), which exhibits mediocre properties but serves as a basis for creating new materials with characteristics approaching those of PZT. The aim of this study was to determine the role of crystal lattice dynamics in the formation of the dielectric response of KNN ceramics, as the mechanisms primarily responsible for it remain unclear.

The objects of study were solid solutions of the systems (1-x)$K_{0.5}Na_{0.5}NbO_3$-x$Bi_{0.5}Na_{0.5}TiO_3$ (BNT) and (1-y)$K_{0.5}Na_{0.5}NbO_3$-y$Bi_{0.5}Na_{0.5}HfO_3$ (BNH) with x = 0, 0.025, 0.04, 0.06, and y = 0.02, 0.04, 0.06, 0.08, and 0.10, prepared using convenient ceramic technology. Dielectric properties in the radio-frequency range, infrared reflection spectra and terahertz complex transmission coefficient (amplitude and phase) were measured at temperatures from 300 to 5 K using a E7-20 immittance meter, Bruker Vertex 80v Fourier spectrometer and Menlo Tera K15 time-domain spectrometer, respectively. From THz data the reflection spectra were recalculated and combined with the infrared data. The resulting broadband reflection spectrum, along with the terahertz permittivity and transmission spectra, were fitted using a set of Lorentz oscillators (phonon modes): $\varepsilon(\nu) = \varepsilon_0 + \sum_j \frac{\Delta\varepsilon_j \cdot \nu_{0j}^2}{\nu_{0j}^2 - \nu^2 - i\nu\gamma_j}$.

Based on the fit parameters obtained in the studied temperature range, the temperature dependencies of the phonon mode contributions to the dielectric permittivity $\sum_j \Delta\varepsilon_j$ were calculated. It was found that compared to KNN ceramics, the magnitude of the phonon contribution to the dielectric permittivity at room temperature in the solid solutions increased more than threefold at x = 0.04 for (1-x)KNN-xBNT and y = 0.06 for (1-y)KNN-yBNH. Radio-frequency and terahertz dielectric permittivity were compared with its intrinsic contribution, showing similar behavior. This sharp increase in the dielectric permittivity of the studied solid solutions is attributed to the peculiarities of their structural evolution near the morphotropic phase boundaries.

The work was supported by a grant from the Ministry of Science and Higher Education of the Russian Federation, No. 075-15-2025-010.

[1] K. Uchino, Advanced piezoelectric materials: Science and technology, Woodhead Publishing, (2017).
[2] Directive 2011/65/EU, Official Journal of the European Union, 174(54), pp. 88–110 (2011).
[3] J.-L. Coutaz, F. Garet, V. Wallace, Principles of Terahertz Time-Domain Spectroscopy. – Jenny Stanford Publishing, (2018).

Non-saturated performance scaling of graphene bilayer sub-terahertz detectors at large induced bandgap

E. I. Titova, M. A. Kashchenko, A. V. Miakonkikh, A. D. Morozov, A. V. Shabanov, I. K. Domaratskiy, S. S. Zhukov, D. A. Mylnikov, V. V. Rumyantsev, S. V. Morozov, K. S. Novoselov, D. A. Bandurin, D. A. Svintsov

Moscow Institute of Physics and Technology, Moscow, Russia

e-mail: shabanov.av@phystech.edu

Electrically induced p-n junctions in graphene bilayer have shown superior performance for detection of sub-terahertz radiation at cryogenic temperatures, especially upon electrical induction of the bandgap E_G. Still, the upper limits of responsivity and noise equivalent power (NEP) at very large E_G remained unknown. Here, the cryogenic performance of graphene bilayer detectors at $f = 0.13$ THz is studied by inducing gaps up to $E_G \sim 90$ meV, a value close to the limits observed in recent transport experiments (Fig. 1). High value of the gap is achieved by using high-bottom hafnium dioxide gate dielectric. The voltage responsivity, current responsivity, and NEP optimized with respect to doping do not demonstrate saturation with gap induction up to its maximum values. The NEP demonstrates an order-of-magnitude drop from ~$400fWH^{-1/2}$ in the gapless state to ~$20fWH^{-1/2}$ at the largest gap. At largest induced bandgaps, plasmonic oscillations of responsivity become visible and important for optimization of sub-THz response.

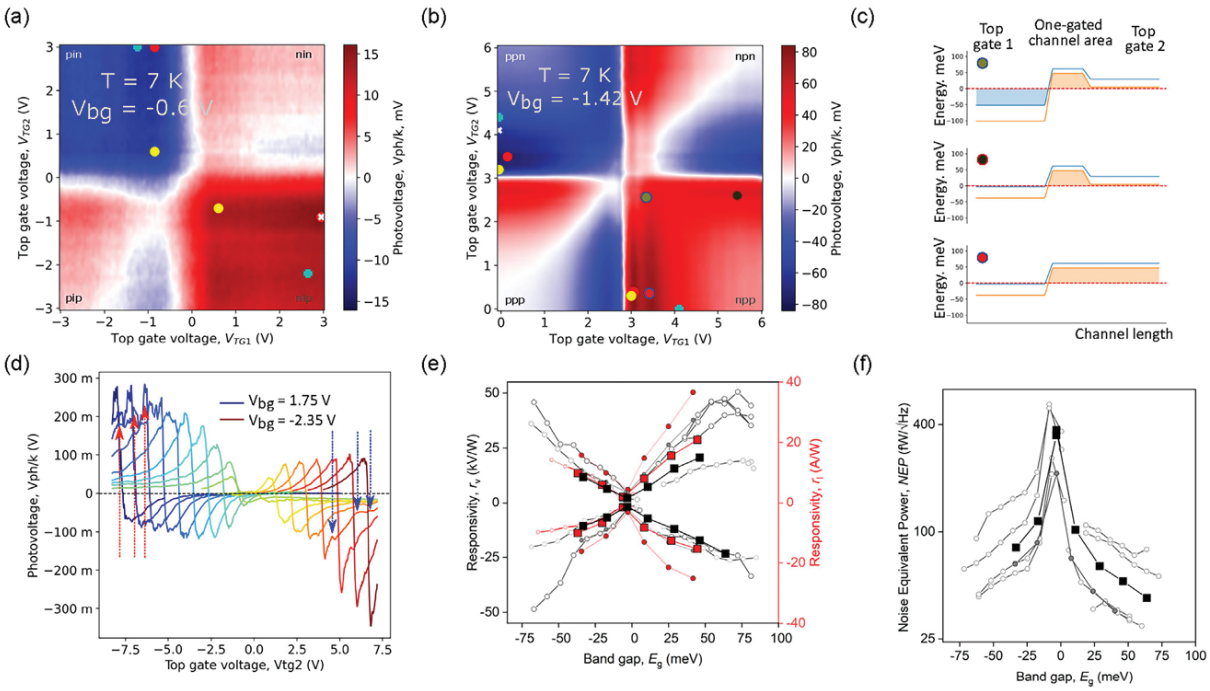

Fig. 1. Terahertz photoresponse of BLG detector with induced p-n junctions. (a), (b) Color map of BLG Sub-THz photovoltage as a function top gate voltages V_{tg1} and V_{tg2} controlling the density at two sides of the channel. k is the attenuation coefficient of the THz power. Panel (a) corresponds to the nominally gapless state, panel (b) – to the state with large induced band gap. Red dots on the color maps represent the optima of photovoltage V_{ph}^{max}, cyan dots – the optima of photocurrent I_{ph}^{max}, yellow – the optima of photovoltage per THz power dissipated in the channel $V_{ph} \times V_{ch}^{max}$, white – the minima of NEP. (c) Band diagrams along the BLG channel corresponding to high voltage responsivity. The respective doping voltages are indicated by color dots in panel (b). Red and black dots correspond to the largest responsivity. (d) Voltage responsivity obtained by scanning of the second gate voltage V_{tg2} while keeping the first gate voltage fixed, at different values of the back gate voltage marked by color. Red and blue arrows indicate the photovoltage oscillations arising from the excitation of graphene plasmons. (e) Extracted maximum voltage responsivity (gray) and current responsivity (red) as a function of induced bandgap. Filled and hollow symbols correspond to slightly different focusing conditions at different days of the measurement (f) Extracted noise equivalent power of the detector versus the induced bandgap.

Second-harmonic generation anisotropy in molybdenum disulfide nanostructures

M. D. Volkova[1], A. A. Popkova[1], S. M. Novikov[2], V. O. Bessonov[1], A. A. Fedyanin[1]

1- Faculty of Physics, Lomonosov Moscow State University, Moscow, 119991 Russia
2- Center for Photonics and 2D Materials, Moscow Institute of Physics and Technology, Dolgoprudny, 141700 Russia

e-mail: volkovamd@my.msu.ru

Efficient modulation of the optical response of nanostructures requires the ability to manipulate light–matter interactions at the nanoscale. One approach to achieving such tunability is the use of materials with optical anisotropy. Transition metal dichalcogenides (TMDs) exhibit strong in-plane covalent bonding and weak out-of-plane van der Waals interaction, which leads to significant optical anisotropy [1, 2]. Moreover, the high refractive index of TMDs, such as molybdenum disulfide (MoS_2), enables the fabrication of dielectric nanoresonators which support Mie-type resonances in the visible and near-infrared spectral ranges. Electromagnetic field localization within such nanoparticles amplifies nonlinear optical response of the material. Moreover, combining Mie-type resonances at the fundamental wavelength with material resonances at the second-harmonic wavelength leads to a significant increase in second-harmonic generation (SHG) [3].

In this work, cylindrical and cubic MoS_2 nanoparticles fabricated via electron-beam lithography followed by reactive ion etching were investigated. To determine the influence of nanostructure geometrical symmetry and material crystal symmetry on the efficiency of second-harmonic generation, we measured the SHG response dependence on the azimuthal angle of the sample rotation at pump wavelengths corresponding to various Mie resonances. Our results demonstrate that the SHG anisotropy is defined by the excited mode symmetry within the nanostructure and the crystalline symmetry of molybdenum disulfide.

This work is supported by the Russian Science Foundation, Project No. 24-19-00478.

[1] Gupta A., Sakthivel T., Seal S., Recent development in 2D materials beyond graphene, Progress in Materials Science, vol. 73, pp. 44–126 (2015).
[2] Ermolaev G.A., Grudinin D.V., Stebunov Y.V. et al., Giant optical anisotropy in transition metal dichalcogenides for next-generation photonics, Nature communications, vol. 12, p. 854 (2021).
[3] Popkova A. A., Antropov, I. M., Tselikov, G. I., et al., Nonlinear exciton–Mie coupling in transition metal dichalcogenide nanoresonators, Laser & Photonics Reviews, vol. 16, p. 2100604 (2022).

32nd INTERNATIONAL CONFERENCE
Advanced Laser Technologies
ALT'25

PHOTONICS IN QUANTUM TECHNOLOGIES

Theories of light scattering: features and limitations of the classical models

Yu. A. Akimov

Lebedev Physical Institute of the RAS, Troitsk branch, Troitsk, Moscow, 108840 Russia

e-mail: y.akimov@troitsk.lebedev.ru

Scattering theories are the classical tools for modelling of light-matter interaction. Despite the long history of success, scattering theories keep many fundamental questions unanswered. For instance, why scattering and absorption of light in those theories behave differently with change of scatterer size? How do they become resonant? If their resonances appear on eigen oscillations of electromagnetic fields, then why don't they grow infinitely with increased lifetime of the eigen oscillations? How anapole scattering appears in those theories for subwavelength metal particles, if it is forbidden by classical electrodynamics?

In this report, we review different scattering models and reveal their common features. We show the two common groups of current-sourced and current-free scattered fields, which appear in classical models [1] and exhibit independent dynamics. We demonstrate how by interfering each other these fields make the resultant scattered fields resonant and, thus, give rise to all the spectral features observed in the classical solutions for scattering and absorption of light.

Being a model feature, the current-free scattered fields naturally limit applicability of the theories bringing numerous conflicts with classical electrodynamics [1, 2]. We review those conflicts and clarify the common limitations of the classical models. To improve the scattering theories, we demonstrate the ways for further refinement of the models used. In particular, we show how by modifying the spatial distribution of the polarization currents one can get a physically consistent solution for excited electromagnetic fields [3]. Based on the physically consistent solution, we propose improved models of light scattering that enable sophisticated description of energy and momentum of electromagnetic fields.

[1] Yu.A. Akimov, "Interaction of light with subwavelength particles: Revealing the physics of the electric dipole moment in the classical scattering problem", J. Opt. Soc. Am. B, vol. 41, pp. 2114–2121 (2024).
[2] Yu. A. Akimov, "Mie scattering theory: A review of physical features and limitations", arXiv:2401.04146 [physics.optics].
[3] Yu. A. Akimov, "Paradox of radiant power and the issue of localized currents", Phys. Wave Phenom., vol. 33, pp. 214–220 (2025).

A toolkit for teaching and research on quantum key distribution

A. V. Borisova[1], V. L. Eliseev[1,2], A. E. Zhilyaev[1], A. S. Timoshenko[1,3]

1- JSC "InfoTeCS", Otradnaya 2B, build. 1, Moscow, Russia
2- National Research University "MPEI", Krasnokazarmennaya 14, build. 1, Moscow, Russia
3- MTUCI, Aviamotornaya 8A, Moscow, Russia

e-mail: vlad-eliseev@mail.ru

Quantum key distribution is one of the few commercially successful outcomes of the second quantum revolution, which has made quantum physics an area of interest for information technology specialists. This has led to an increasingneed for the development quantum informatics as an engineering discipline that requires simpler and more technologically advanced educational and research equipment than what is usually used in physics laboratories. On one hand, such equipment should have a low entry threshold for teaching students of information technology and information security departments. Such systems are already being produced [1, 2]. On the other hand, it is advisable to expand the functionality of educational equipment, enabling its use for more serious research and development.

In our work, we propose the architecture of a fiber-optic quantum key distribution system adapted for teaching and research purposes.The system allows two application: one for studying the principles of constructing quantum key distribution systems with a fixed quantum protocol, but with an open interface for configuring Alice and Bob parameters, and another for conducting research with single-photon pulses in the infrared telecommunication range. In the second application, the system is considered as a set of software-controlled devices that provide emission and detection of single-photon signals and allow its use in physical experiments of various directions. While specialized equipment exists that implements the necessary functions (for example, [3, 4]), transforming it into a research system of quantum key distribution is not trivial. Thus, the architecture we propose can be implemented as an instrumental system that provides a wide range of applications for teaching and research of quantum key distribution.

[1] ViPNet QKDSim | JCS InfoTeCS. https://infotecs.ru/products/vipnet-qkdsim/ (accessed June 19, 2025).
[2] Clavis XGR QKD System | ID Quantique SA. https://www.idquantique.com/quantum-safe-security/products/clavis-xgr-qkd-system/ (accessed June 19, 2025).
[3] The Power of Single Photons| Quandela. https://www.quandela.com/technology/the-power-of-single-photon-sources/ (accessed June 19, 2025).
[4] ID Qube Series NIR Gated | ID Quantique SA. https://www.idquantique.com/quantum-detection-systems/products/id230/ (accessed June 19, 2025).

Photon correlation methods for probing single emitter photophysics

I. Eremchev

Institute of Spectroscopy RAS, Troitsk, Russia

e-mail: eremchev@isan.troitsk.ru

Photon statistics analysis is a powerful tool for studying photophysical processes in single quantum emitters of various nature: molecules, color centers in diamonds, quantum dots, and nanoscale semiconductors. Photon statistics investigations commonly employ Hanbury Brown and Twiss intensity interferometry to quantify effects of anti-bunching and bunching of photons. The first effect reflects the inability of a single quantum emitter to produce two photons simultaneously. The second arises when emission is intermittently suppressed, leading to temporal clustering of photons. In single quantum systems, photon bunching could occur as a result of activation/deactivation of nonradiative recombination channels (in semiconductor nanocrystals) or transitions between singlet and triplet states (in chromophore molecules). In this regard, photon bunching analysis provides valuable insights into the transition rates between different metastable states of a single emitter. Photon statistics analysis can be used for studying biexciton luminescence in nanoscale semiconductors, estimation of the number of independent emitters in luminescent complexes, and determination of the luminescence lifetime.

This report presents an investigation of emitter photophysics using correlated photon-counting techniques, with emphasis on color centers in diamond – including the recently reported LX centers [1] – and on single perovskite nano- and microcrystals. A study of photon bunching in single LX centers has revealed that the observed hidden luminescence intermittency dynamics cannot be explained within the framework of a standard three-level model with a single metastable state. Analysis of perovskite photon statistics reveals surprisingly the effect of anti-bunching in the delayed photoluminescence $MAPbI_3$ microcrystals [2] and the photodegradation-induced transition from classical to sub-Poisson photon statistics in perovskite nanocrystals [3].

The work was funded by the Russian Science Foundation, Grant No. 25-22-00512, https://rscf.ru/project/25-22-00512.

[1] Neliubov et al, Phys. Rev. B 111 (15), 155420 (2025).
[2] Eremchev et al, Nano Lett. 23 (6), 2087–2093 92023),
[3] Baitova et al, JETP Lett. 118 (8), 560–567 (2023).

A quantitative model of single quantum dot blinking

P. A. Frantsuzov

Voevodsky Institute of Chemical Kinetics and Combustion, Siberian Branch of RAS, Institutskaya 3, Novosbrsk, 6300090 Russia

e-mail: frantsuzov@kinetcs.nsc.ru

The 2023 Nobel Prize in Chemistry was awarded for the discovery and synthesis of colloidal quantum dots, which have interesting structural and optical properties. One of the most interesting phenomena in this field is blinking: the fluctuation of the photoluminescence intensity of single quantum dots over time under continuous irradiation from an external light source. Interestingly, this fluctuation does not have a characteristic time scale. That is, one can observe this fluctuation at times of the order of milliseconds, seconds, thousands of seconds, even hours.

In spite of decades of comprehensive studies, the phenomenon of photoluminescence blinking in single semiconductor colloidal quantum dots still requires theoretical retreatment. The cause for this phenomenon is the nonradiative process of the QD photoexcited state recombination, the rate of which fluctuates with time. The are three basic microscopic mechanisms of the fluctuating nonradiative recombination proposed in the literature:

1. the Auger mechanism (AM) proposed by Efros and Rosen [1] describes a fast Auger recombination process that occurs in a charged QD;

2. the trapping mechanism (TM) proposed by Frantsuzov and Marcus [2] related to the relaxation of an excited QD through the trapping of a hole into a state in the band gap with subsequent non-radiative recombination with the remaining electrons;

3. the hot carrier trapping mechanism (HCTM) proposed by Galland et al. [3] which is a modified TM mechanism where a hot carrier (instead of a relaxed carrier) is trapped in a metastable trap.

There are three TM based models of blinking presented in the literature, namely, the Frantsuzov and Marcus model [1] and the multiple recombination center (MRC) model [4].

Here we present a recently proposed TM-based model [5], which suggests that the blinkng phenomenon is caused by fluctuations in the nonradiative relaxation rate due to temporal changes in the electron-phonon interaction. The model quantitatively reproduces the results of single CdSeS/ZnS core/shell quantum dots spectroscopy experiments.

[1] A. L. Efros and M. Rosen, Random Telegraph Signal in the Photoluminescence Intensity of a Single Quantum Dot, Phys. Rev. Lett., 78, 1110–1113 (1997).
[2] P.A. Frantsuzov and R.A. Marcus, Explanation of quantum dot blinking without the long-lived trap hypothesis, Phys. Rev. B, 72, 15532 (2005).
[3] C. Galland, Y. Ghosh, A. Steinbruck, M. Sykora, J. A. Hollingsworth, V. I. Klimov, and H. Htoon, Two types of luminescence blinking revealed by spectroelectrochemistry of single quantum dots, Nature, 479, 203–208 (2011).
[4] P. A. Frantsuzov, S. Volkan-Kacso, and B. Janko, Model of Fluorescence Intermittency of Single Colloidal Semiconductor Quantum Dots Using Multiple Recombination Centers, Phys. Rev. Lett., 103, 207402 (2009).
[5] E. A. Podshivaylov, M. A. Kniazeva, A. O. Tarasevich, I. Yu. Eremchev, V. Naumov, and P. A. Frantsuzov, Quantitative model of multi-scale single quantum dot blinking, Journal of Materials Chemistry C, 11, 8570–857 (2023).

Bright single-photon emission from an InAs/GaAs quantum dot in an elliptical micropillar with built-in Coulomb blockade

A. Galimov, M. Rakhlin, Yu. Serov, G. Klimko, M. Kulagina, Yu. Zadiranov, A. Toropov

Ioffe Institute, Polytekhnicheskaya str. 26, St. Petersburg, 194021 Russia

e-mail: galimov@mail.ioffe.ru

The development of efficient sources of indistinguishable single photons is an increasingly important topic for quantum technologies. Significant progress in this area has been achieved by realizing resonant excitation of epitaxially grown semiconductor quantum dots (QDs) inserted in optical microresonators. Elliptical micropillars currently achieve the highest end-to-end efficiency of 28% for monolithic quantum light sources [1]. To further improve efficiency, full charge-state stabilization of the emitting QD must be achieved. Until recently, the most effective approach was to use the Coulomb blockade effect in a microcavity p-n heterostructure with QDs [2]; however, implementing this method is exceptionally challenging, as it requires fabricating a high-Q microresonator containing a heavily doped active region with significant free-carrier absorption at the QD emission wavelength. In this paper, we present a simpler alternative method for implementing the Coulomb blockade in QDs, which allowed us to increase the efficiency of single-photon emission in elliptical micropillars up to 35%.

The single-photon source is an elliptical micropillar containing self-organized InAs/GaAs QDs sandwiched between 30 (bottom) and 18 (top) pairs of quarter-wave layers forming distributed Bragg reflectors [3]. The reactive ion etching method was optimized to obtain strictly vertical sidewalls of the micropillar with minimal roughness. The polarization degree of single-photon emission induced by the resonator asymmetry reached 86%, which made it possible to significantly reduce the losses from cross-polarization filtering during resonant excitation. Charge stabilization was achieved using the Coulomb blockade effect, realized directly during the epitaxial growth of the microcavity heterostructure by introducing a thin n-doped layer at a precisely controlled distance from the QD layer [4]. An analytical model was developed that allowed the implementation of doping profiles that provide precise adjustment of the Fermi level position and obtaining the required charge states of the QDs identified by measuring the spin dynamics and single-photon emission statistics. The use of weak auxiliary optical illumination allowed additional dynamic control of the charge-states of the QDs. Measurements of photon correlation statistics over extended time intervals demonstrated 97% stabilization fidelity for specific charge states. Thus, the presented approach allowed the implementation of a highly stable source of polarized single photons with record-high efficiency.

The work was supported by Rosatom in the framework of the Roadmap for Quantum computing (Contract No. 868-1.3-15/15-2021 dated 5 October 2021 and Contract No. R2152 dated 11 November 2021).

[1] H. Wang, Y.-M. He, T.-H. Chung et al. Towards optimal single-photon sources from polarized microcavities. Nat. Photonics 13, 770–775. (2019).
[2] R. Warburton, B. Miller, C. Dürr et al, Coulomb interactions in small charge-tunable quantum dots: A simple model, Phys. Rev. B 58, 16221 (1998).
[3] A. Galimov, M. Bobrov, M. Rakhlin et al., Towards Bright Single-Photon Emission in Elliptical Micropillars, Nanomaterials, 13, 9 (2023).
[4] A. Galimov, Yu. Serov, M. Rakhkin et al., Charge States of Single Quantum Dots in a Microcavity p–n–p Heterostructure with the Built-in Coulomb Blockade, Jetp Lett., 121, 5 (2025).

Numerical simulation of quantum optical state evolution via tensor networks

N. Kapridov[1,2], E. Tiunov[3], D. Chermoshentsev[1]

1- Russian Quantum Center, Bolshoy Boulevard 30, building 1, Skolkovo Innovation Center territory, Moscow, 121205 Russia
2- Moscow Institute of Physics and Technology, Institutskiy per. 9, Dolgoprudny, Moscow Region, 141700 Russia
3- Quantum Research Center, Quantum Algorithms, TII, Abu Dhabi, United Arab Emirates

e-mail: kapridov.na@phystech.edu

In recent years, significant attention has been devoted toward advancing technologies based on quantum optical effects [1]. A key aspect of this progress is the ability to accurately predict the evolution of quantum optical states in various processes. However, numerical simulations of quantum system dynamics face considerable challenges due to the high dimensionality of the Hilbert space.

To simulate quantum state evolution, one must solve the time-dependent Schrödinger equation. A common approach involves finding solutions in the Fock-state representation, where the Hilbert space size scales with the number of photons in the system. This becomes problematic for systems with large photon numbers. An alternative method uses continuous variables (CV) [2], such as position or momentum bases, where variables are discretized sufficiently to capture the wavefunction's details.

It turns out that with the help of tensor networks [3], it is possible to describe wave functions with exponentially high accuracy. The product matrix state (MPS) is the simplest one-dimensional tensor network that provides scalability and numerical tractability [4]. In this work, we utilize MPS to efficiently encode both wave functions and quantum operators. The MPS representation achieves exponential compression for both the wave function and the Hamiltonian. Time evolution is computed by directly solving the Schrödinger equation in the MPS format.

To validate our approach, we simulate the time evolution of degenerate spontaneous parametric down-conversion (SPDC). We analyze the joint dynamics of the "signal plus pump" wave function, initializing the pump mode in a coherent state $|\alpha\rangle = |20\rangle$ and the signal mode in a vacuum state. This configuration enables direct Fock-basis calculations, serving as a benchmark. A comparison of photon dynamics in the pump and signal modes – computed via both Fock-basis and tensor network methods – shows excellent agreement, confirming the accuracy of our approach.

Our results demonstrate that tensor networks can successfully simulate the quantum evolution of the signal and pump modes in SPDC. The close agreement with Fock-basis computations validates the method's precision. Future work will extend this framework to systems with multiple optical modes.

[1] J Wang, F Sciarrino, A Laing, MG Thompson, Integrated photonic quantum technologies, Nature Photonics, vol. 14, pp. 273–284, (2020).
[2] E Fedotova, N Kuznetsov, E Tiunov, AE Ulanov, AI Lvovsky, Continuous-variable quantum tomography of high-amplitude states, Physical Review A, vol. 108, p. 042430, (2023).
[3] S. R. White, Density matrix formulation for quantum renormalization groups, Physical Review Letters, vol. 69, pp. 2863–2866, (1992).
[4] I. V. Oseledets, Tensor-train decomposition, SIAM Journal on Scientific Computing, vol. 33, pp. 2295–2317, (2011).

Photoluminescence properties control using $Ge_2Sb_2Te_5$

O. Kushchenko[1], D. Litvinov[1], G. Verkhogliadov[1,2], E. Bodiago[1], D. Gets[1], P. Lazarenko[3], M. Rybin[1,4], A. Pushkarev[1,2], V. Shahnazaryan[1], A. Sinelnik[1]

1- Department of Physics, ITMO University, Saint Petersburg, Russia
2- Hybrid Photonics Laboratory, Skolkovo Institute of Science and Technology, Moscow, Russia
3- Herzen State Pedagogical University of Russua, St. Petersburg, Russia
4- Ioffe Institute, Saint Petersburg, Russia

e-mail: olga.kushchenko@metalab.ifmo.ru

Controlling light emission dynamically is essential for the progress of integrated photonic technologies [1–3], but traditional systems struggle with issues related to size reduction, efficiency, and tunability. In this work, we present a hybrid platform combining $Ge_2Sb_2Te_5$ (GST) [4] and perovskites [5] that enables versatile control of light emission within a compact structure. We showcase four distinct functionalities: reversible switching of intensity and wavelength, activation of perovskite photoluminescence via third harmonic generation in GST, and wavefront manipulation through beam focusing. By exploiting the fast phase-change properties and high refractive index contrast of GST, our approach allows for dynamic, non-volatile tuning without the need for lithography, using selective phase patterning or maskless etching instead. This integration of GST's tunability with the light-emitting capabilities of perovskites addresses the limitations of conventional static metasurfaces and offers a scalable path toward ultracompact, reconfigurable light sources for applications in quantum optics, holography, and on-chip sensing.

This research was supported by Priority 2030 Federal Academic Leadership Program.

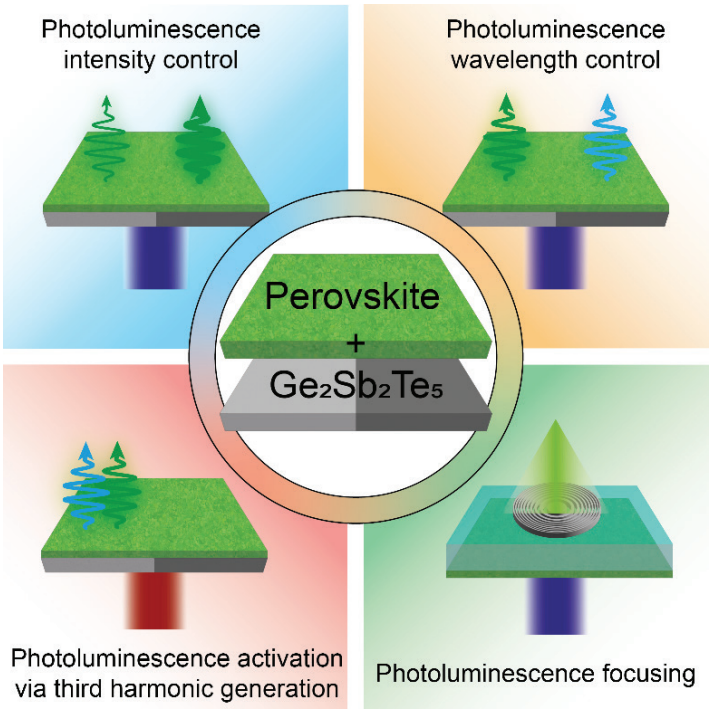

Fig. 1. Schematic diagram of photoluminescence properties control using $Ge_2Sb_2Te_5$.

[1] H. Kim et al., Optical Metasurfaces for Biomedical Imaging and Sensing, ACS Nano, 19, 3085–3114, (2025).
[2] H. Altug et al., Advances and applications of nanophotonic biosensors, Nature Nanotechnology, 17, 5–16, (2022).
[3] Q. Li et al. Metasurface-enhanced biomedical spectroscopy, Nanophotonics 14, 1045–1068, (2025).
[4] S. Raoux and M. Wuttig, Phase Change Materials: Science and Applications (Springer), 1–18, (2009).
[5] Protesescu L. et al., Nanocrystals of cesium lead halide perovskites ($CsPbX_3$, X = Cl, Br, and I): novel optoelectronic materials showing bright emission with wide color gamut, Nano Letters, 15, 3692–3696, (2015).

Nuclear optical clock

M. V. Okhapkin, O. N. Prudnikov, A. V. Taichenachev, V. I. Yudin

Institute of Laser Physics SB RAS, Novosibirsk, 630090 Russia

e-mail: taichenachev@mail.ru

In this talk we give a brief overview of recent advances in the field of optical clocks based on the transition between ground and isomeric states in the Th-229 nuclear. A short prehistory of the search for optical nuclear transition, starting from the paper [1], as well as pioneering proposals to use this transition for nuclear optical clocks [2, 3] will be present. Recent experimental observations of direct laser excitation of this transition [4–6] will be discussed in details. We also outline the main problems that should be solved on the way to creation of nuclear optical clock with relative uncertainty of the order of 10^{-19}–10^{-20}. Especial attention will be focused on our proposal on the two-photon optical nuclear clock [7].

[1] R. G. Helmer and C. W. Reich, Phys. Rev. C 49, 1845 (1994).
[2] E. V. Tkalya, JETP Lett. 55, 211 (1992).
[3] E. Peik, C. Tamm, Europhys. Lett. 61, 181 (2003).
[4] J. Tiedau, M. V. Okhapkin, K. Zhang, et al., Phys. Rev. Lett. 132, 182501 (2024).
[5] R. Elwell, Chr. Schneider, J. Jeet, et al., Phys. Rev. Lett. 133, 013201 (2024).
[6] C. Zhang, T. Ooi, J. S. Higgins et al., Nature 633, 63 (2024).
[7] V. I. Yudin, A. V. Taichenachev, O. N. Prudnikov et al., JETP Lett. 121, 365-374 (2025).

Measurement of the magneto-optical sensitivity of the spun optical fibers

Y. V. Przhiyalkovskiy[1,2], N. I. Starostin[1], S. K. Morshnev[1], A. I. Sazonov[1]

1- Kotelnikov Institute of Radio Engineering and Electronics (Fryazino Branch) of the Russian Academy of Sciences, Vvedensky Sq. 1, Fryazino, Moscow region, 141190 Russia
2- ERSO Transformer Solutions LLC, Elektrozavodskaya Street 21, Moscow, 107023 Russia

e-mail: yankus.p@gmail.com

Fiber-optic current sensors (FOCS) have become increasingly popular for measuring electric current in the power industry. The most common implementation of the FOCS is as an interferometer that detects the phase shift induced by the Faraday effect between two orthogonal elliptically polarized light waves propagating through a sensitive fiber [1]. A spun fiber, produced by drawing from a rotating highly birefringent preform, is the most effective sensing fiber [2].

The range of measured currents is determined by the spun fiber sensitivity, making it an important parameter. The latter is affected by two factors: the Verdet constant of the fiber's material and the average ellipticity of light polarization [3]. In practice, the polarization modes of spun fibers are close to the circular, which has the highest efficiency for accumulating the Faraday effect. Therefore, measuring the Verdet constant of spun fibers is an important task.

Direct measurement of the net value of the Verdet constant poses certain difficulties. In particular, measuring the rotation of linear polarization in a fiber requires coherent radiation sources. However, the polarization evolution of light in a spun fiber is greatly complicated. Detecting the $\pi/2$ phase shift using the FOCS also cannot provide the required accuracy because the interferometer would have low sensitivity in that case.

In this work, we propose using the differential method [4, 5] to measure the Verdet constant of a spun fiber which is integrated into a sensor. This method involves winding two equal parts of a single spun fiber around a current conductor in opposite directions. Such a configuration ensures a zero phase shift between light waves regardless of the current, resulting in a zero sensor output. However, it was shown in [5] that if modes coupling occurs in the region between the sensing parts (e.g., due to fiber bending), secondary waves appear, and their interference is determined by the Faraday phase shift only in the first half of the sensing fiber. But when a π phase shift occurs, secondary waves interfere with each other to produce a net result of zero, so for any mode coupling strength the signal will be zero. The intersection of the output current plots at different strengths of mode coupling indicates the point at which a π phase shift occurs. Due to the nature of interferometric detection, this point can be precisely determined. The experiment was carried out using a spun fiber with a beatlength of 10 mm at a wavelength of 1.55 μm and a pitch pitch of 3 mm. The value of the Verdet constant for this fiber was $7.3 \cdot 10^{-7}$ A/m.

The work was carried out within the framework of the state task No. 075-00395-25-00 of the Kotelnikov Institute of Radio Engineering and Electronics of the Russian Academy of Sciences.

[1] Bohnert, K., Gabus, P., Kostovic, J., & Brändle, H. Optical fiber sensors for the electric power industry. Optics and Lasers in Engineering, 43(3-5), 511–526, (2005).
[2] Laming, R. I., & Payne, D. N. Electric current sensors employing spun highly birefringent optical fibers. Journal of Lightwave Technology, 7(12), 2084–2094, (1989).
[3] Przhiyalkovskiy, Y. V., Starostin, N. I., Morshnev, S. K., & Sazonov, A. I. Polarization dynamics of light propagating in bent spun birefringent fiber. Journal of Lightwave Technology, 38(24), 6879–6885, (2020).
[4] Patent RF RU2792207C1 (PCT WO2023158334A1). "Volokonno-opticheskij chuvstvutelnij element datchika elektricheskogo toka i magnitnogo polja [Fiber optic sensing element of electric current and magnetic field sensor]", S.K. Morshnev, Y.V. Przhiyalkovsky, N.I. Starostin, M.Y. Yanin, Declared 15.02.2022. Published 20.03.2023. (In Russian).
[5] Przhiyalkovskiy, Y. V., Starostin, N. I., Morshnev, S. K., & Sazonov, A. I. Fiber-optic sensor for MA current measuring. Journal of Lightwave Technology, 42(9), 3423–3429, (2024).

Ultrafast all-optical logic and switching in organic polariton microcavities

A. D. Putintsev[1], D. A. Sannikov[1], M. Misko[1], A. V. Baranikov[1], A. V. Zasedatelev[1], U. Scherf[2], P. G. Lagoudakis[1]

1- Hybrid Photonics Laboratory, Skolkovo Institute of Science and Technology, Territory of Innovation Center Skolkovo, Bolshoy Boulevard 30, building 1, Moscow, 121205 Russia
2- Macromolecular Chemistry Group and Institute for Polymer Technology, Bergische Universität Wuppertal, Gauss-Strasse 20, Wuppertal, 42119 Germany

e-mail: anton.putintsev@skoltech.ru

The rising demand for high-speed, energy-efficient information processing has driven increasing interest in photonic logic systems that operate beyond the bandwidth limits of traditional electronics. Organic polaritonics – leveraging hybrid light-matter quasiparticles in organic semiconductor microcavities offers a promising route toward room-temperature all-optical logic and switching with sub-picosecond performance.

We report the realization of a universal, cascadable all-optical logic gate architecture based on non-ground-state polariton amplification in organic microcavities [1]. By exploiting vibron-mediated stimulated scattering under non-resonant optical excitation, we achieve functional NOT and NOR gates, enabling full Boolean logic with ultrafast switching times (~1 ps). The NOR gate, demonstrated as a multi-input logic element, suppresses spontaneous ground-state condensation in favor of higher-energy condensate formation when any input is present, establishing a robust pathway for complex logic circuit integration.

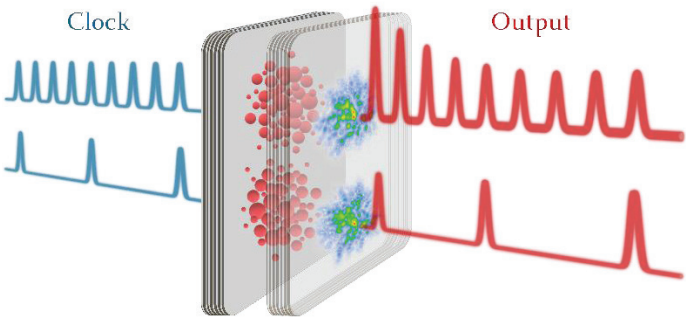

Fig. 1. Schematic of semiconductor microcavity as an I/O logic gate [2].

To complement the experimental realization, we develop a microscopic theoretical model capturing key relaxation and loss mechanisms – including thermalization, vibron relaxation, and bimolecular quenching – that govern the dynamics of polariton condensate formation. Using a pump-pump optical excitation scheme, we validate the theoretical predictions and identify kinetic losses as the principal factor limiting the achievable temporal separation between consecutive condensates. Our findings define an upper switching bandwidth approaching 240 GHz, pushing the boundaries of optical logic speed at ambient conditions [2].

Together, these results represent a critical advance in the field of organic polaritonics, demonstrating both the device-level feasibility and fundamental physical constraints of ultra-fast, room-temperature all-optical computing. This work paves the way for the development of next-generation photonic processors and integrated optoelectronic systems.

The work was carried out with the financial support of the RNF grant No. 23-72-00059.

[1] D. A. Sannikov, A. V. Baranikov, A. D. Putintsev, M. Misko, A. V. Zasedatelev, U. Scherf, and P. G. Lagoudakis, "Room temperature, cascadable, all-optical polariton universal gates", Nat. Commun. 15, 5362 (2024).
[2] M. Misko, A. D. Putintsev, D. Sannikov, A. Zasedatelev, U. Scherf, and P. G. Lagoudakis, "Temporal bandwidth of consecutive polariton condensation", Phys. Rev. B 111, L161403, (2025).

Three-photon laser excitation and three-body interactions of Rydberg atoms for quantum information

I. I. Ryabtsev[1,2], I. I. Beterov[1,2], E. A. Yakshina[1,2], D. B. Tretyakov[1], V. M. Entin[1], G. Suliman[1,2], N. N. Bezuglov[1,3], A. Cinins[4], K. Miculis[4,5], I. N. Ashkarin[6], P. Cheinet[6]

1- Rzhanov Institute of Semiconductor Physics SB RAS, Novosibirsk, 630090 Russia
2- Novosibirsk State University, Novosibirsk, 630090 Russia
3- Saint Petersburg State University, Saint Petersburg, 199034 Russia
4- Institute of Atomic Physics and Spectroscopy, University of Latvia, Riga, LV-1004 Latvia
5- National Research Nuclear University MEPhI, Moscow, 115409 Russia
6- Laboratoire Aime Cotton, CNRS, Univ. Paris-Sud, ENS Paris-Saclay, Orsay, 91405 France

e-mail: ryabtsev@isp.nsc.ru

Ultracold neutral atoms became recently one of the most promising platforms to implement quantum computation [1]. Such a computation is based on coherent laser excitation of atoms to strongly-interacting Rydberg states. In this talk, we will review our recent experimental and theoretical results on coherent three-photon laser excitation and coherent three-body interactions of Rb Rydberg atoms, which can be used in quantum information processing.

In our recent experiment on three-photon laser excitation $5S_{1/2} \rightarrow 5P_{3/2} \rightarrow 6S_{1/2} \rightarrow 37P$ of a single ^{87}Rb Rydberg atom in an optical dipole trap, we have observed for the first time three-photon Rabi oscillations between the ground and the Rydberg states [2]. A specific feature of the experiment was the usage of intense laser radiation at the wavelength of 1367 nm on the second excitation step, which provided the single-photon Rabi frequency up to 2 GHz to control the effective detunings of the intermediate levels of the three-photon transition due to ac Stark effect. We have detected Rabi oscillations with frequency from 1 to 5 MHz depending on the intensities of the laser pulses on the first and the second excitation steps.

Following the above experiment [2], we have built an extended theoretical model of three-photon excitation [3]. For a particular example of three-photon excitation scheme $5S_{1/2} \rightarrow 5P_{3/2} \rightarrow 6S_{1/2} \rightarrow nP$ in ^{87}Rb atoms, we have found that upon strong laser excitation on the second step with Rabi frequency Ω_2 and moderate excitation on the first and the third steps with Rabi frequencies Ω_1 and Ω_3, the three-photon Rabi frequency is given by $\Omega = \Omega_1\Omega_3/\Omega_2$. If we arrange the three exciting laser beams in such a way that spatial distributions of $(\Omega_1\Omega_3)$ and Ω_2 are identical, then Ω becomes independent of the atom position within laser beams, even for very tightly focused laser beams. This can provide a much better individual addressing of Rydberg excitation for adjacent atoms in trap arrays compared to commonly used two-photon excitation schemes.

Three-body interactions of Rydberg atoms at Förster resonances controlled by a dc electric field are of interest for the implementation of three-qubit quantum gates. In ref. [4], we proposed and analyzed a new kind of three-body Förster resonance $3 \times nP_{3/2} \rightarrow nS_{1/2} + (n+1)S_{1/2} + nP_{1/2}$ that can be realized with Rb Rydberg atoms for an arbitrary principal quantum number n. In subsequent theoretical work, we proposed schemes for implementing the three-qubit Toffoli quantum gates based on three-body Förster resonances of a new type [5, 6]. In our last work [7], an extended theoretical study of the above three-body Förster resonance was performed for various spatial configurations of three interacting Rb Rydberg atoms, and conditions for their experimental implementation were determined. It was found that one of the resonances has a weak dependence of the resonant electric field on the distance between atoms and it is therefore most suitable for performing experiments to observe coherent oscillations of populations and implement three-qubit quantum gates based on them.

This work was supported by the Russian Science Foundation Grant No 23-12-00067.

[1] D. Bluvstein et al., Nature 626, 58 (2024).
[2] I.I. Beterov et al., Zh. Eksper. Teor. Fiz. 166, 535 (2024), English translation: arXiv: 2410.01703.
[3] N. N. Bezuglov et al., arXiv: 2411.06607 (2024).
[4] P. Cheinet et al., Quant. Electr. 50(3), 213 (2020).
[5] I. N. Ashkarin et al., Phys. Rev. A 106, 032601 (2022).
[6] I. N. Ashkarin et al., Phys. Rev. Research 7, 013034 (2025).
[7] I. I. Ryabtsev et al., Zh. Eksper. Teor. Fiz. 168, 14 (2025).

Conversion of a phase-modulated CW laser field to pulses by phase control of its spectral components

R. Shakhmuratov

Zavoisky Physicsl-Technical Institute, FRC Kazan Scientific Center of RAS, Sibirsky Trakt 10/7, Kazan, 420029 Russia

e-mail: shakhmuratov@mail.ru

High repetition rate optical pulses are of interest in many applications related to optical communications, metrology, and signal processing [1]. Pulse generation by mode-locked lasers is one of the widespread technics. However, the repetition rate of these lasers is limited. New microresonators offer sources of short pulses with much higher repetition rate, which varies from 10 GHz to 1 THz depending on the resonator size [2]. However, their repetition rate is not tunable, as it depends on the mode spacing for a given device. In addition, such sources require thermal stabilization, and their parameters critically depend on the pump power, which requires special control. Meanwhile, tunable generation of high-repetition-rate optical pulses with arbitrary shape can be synthesized by phase-intensity spectral shaping of frequency combs [3]. Moreover, such combs with narrow and stable components can be implemented by a periodic phase modulation of a CW laser. Examples of phase-intensity spectral shaping of these frequency combs are discussed in [4, 5].

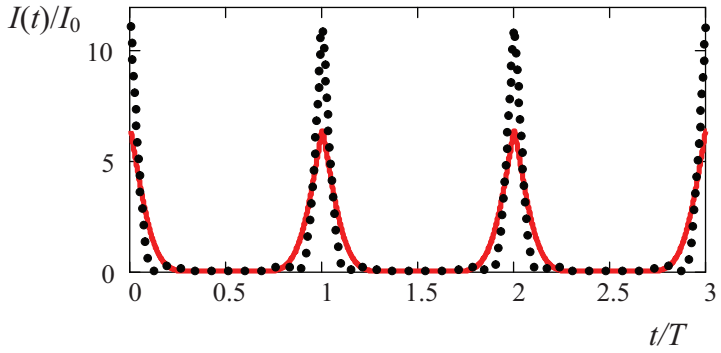

Fig. 1. Time evolution of the field intensity $I(t)$ of the phase modulated field after phasing of its spectral components. Modulation index of the fundamental frequency is 1.3 rad for red solid line and 2.6 rad for black dotted line. $T = 100$ ps is the period of fundamental frequency of the phase modulation (10 GHz) and intensity is normalazed to the intensity of the input SW field I_0.

In this report it is proposed to generate periodic train of pulses in a controllable way using three-tone phase modulation of the CW laser field in combination with liquid crystal phase modulators, which make all spectral components of the produced frequency comb in phase. This allows electronic readjustment of the shape, duration, and repetition rate of the pulses. Multiplication of the pulse repetition rate is also possible by this method. Three-tone phase modulation makes it possible to create frequency combs with unusual properties of their spectral components. Examples of the obtained picosecond pulses are shown in Fig. 1. Thus, electro-optical phase modulation and subsequent phase tailoring of the generated spectral components of the field by liquid-crystal phase modulators make it possible to carry out fully controlled generation of pulses. This proposal may have many interesting applications in optical communications.

[1] F. Quinlan, S. Ozharar, S. Gee, P. Delfyett, Harmonically mode-locked semiconductor-based lasers as high repetition rate ultralow noise pulse train and optical frequency comb sources, J. Opt. A: Pure Appl. Opt., vol. 11, p. 103001. (2009).
[2] T. J. Kippenberg, A. L. Gaeta, M. Lipson, M. L. Gorodetsky, Dissipative Kerr solitons in optical microresonators, Science, vol. 361, p. 6402, (2018).
[3] S. T. Cundiff and A.M.Weiner, Optical arbitrary waveform generation, Nature Photon., vol. 4, pp. 760–6, (2010).
[4] Z. Jiang, D. E. Leaired, and A.M.Weiner, Optical processing based on spectral line-by-line pulse shaping on a phase-modulated CW laser, IEEE Journal of Quantum Electronics, vol. 42, pp. 657–666, (2006).
[5] U. Andral, J. Fatome, B. Kibler, and C. Finot, Triangular spectral phase tailoring for the generation of high-quality picosecond pulse trains, Opt. Lett., vol. 44, pp. 4913–4916, (2019).

Lasing with superconducting quantum systems

P. Yu. Shlykov[1,2], Sh. V. Sandulianu[2], A. N. Bolgar[1], A. N. Vaseni[1,2], O. V. Astafiev[1,2]

1- Skolkovo Institute of Science and Technology, Bolshoy Boulevard 30-1, Skolkovo, Moscow, 121205 Russia
2- Moscow Institute of Physics and Technologies, Institutskii per. 9, Dolgoprudny, Moscow region 141700 Russia

e-mail: o.astafiev@skoltech.ru

Superconducting quantum systems are the key elements for a new field of physics – quantum optics with artificial atoms in the microwave range. The superconducting artificial atoms have a set of energy levels and, therefore, behave like natural ones, allowing to demonstrate phenomena of cavity quantum electrodynamics, quantum state control, single photon emission and many others. Such an "atom" has a number of properties that make it possible to realize the fundamental effects of quantum optics on a chip and observe previously unattainable phenomena. For example, it is easy to obtain a physically strong coupling with other circuit elements such as resonators, open transmission lines, other "atoms". This, in particular, allows one to realize the fundamental effects with just a single quantum system ("atom"). We will present a series of works on the implementation of the lasing effect on a single artificial atom. This is a current-pumped system – the first experimental realisation of lasing on the artificial atom [1]; a lasing effect with pumping using the Landau-Zener tunneling [2]; a lasing effect on an atom with a specially designed electromagnetic environment [3]; as well as a lasing effect in an acoustic system, where photons are substituted by phonons. The latest experiment (Fig. 1) is a breakthrough example of the capabilities of superconducting quantum technologies and one of the few effects of a new direction so far – quantum acoustics [4].

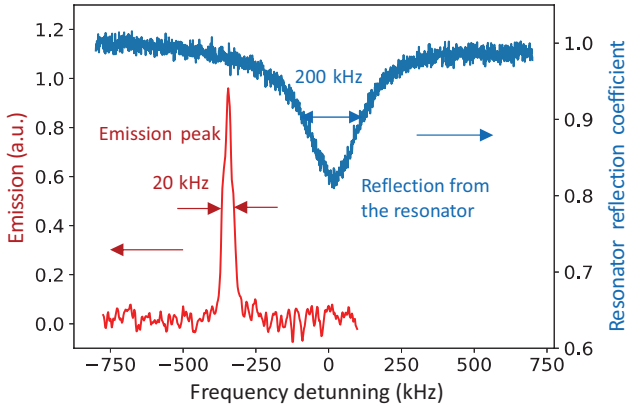

Fig. 1. Blue curve: reflection from the resonator, which demonstrates that the resonator linewidth is about 200 kHz. Red curve: an emission from the acoustic laser with typical width 20 kHz.

In the experiment, the artificial atom is coupled to a surface acoustic wave (SAW) resonator with the resonant frequency f_r = 3.15 GHz. The SAW resonator is formed by Bragg mirrors with metallic stripes and the electric filed is converted to acoustics one by inter-digitated transducers (IDT) – a set of metallic stripes with submicron step on a surface of quartz. Note that the base temperature in our refrigerator is T = 10 mK, so that $hf_r \gg k_BT$. By implementing a mechanism of population inversion in the "three-level atom" with the microwave excitation to the third energy level and relaxation to the first excited one. When the atom is in nearly resonant conditions, an emission of radiation is observed. Importantly that the emission linewidth exhibits strong line narrowing by one order of magnitude (Fig. 1). The number of phonons, estimated in the resonator is about 100.

[1] O. Astafiev, K. Inomata, A. O. Niskannen, T. Yamamoto, Yu. A. Pashkin, Y. Nakamura, and J. S. Tsai. Nature 449, 588–590 (2007).
[2] P. Neilinger, S. N. Shevchenko, J. Bogár, M. Rehák, G. Oelsner, D. S. Karpov, U. Hübner, O. Astafiev, M. Grajcar, and E. Il'ichev. Phys. Rev. B 94, 094519 (2016).
[3] A. A. Sokolova, G. P. Fedorov, E. V. Il'ichev, and O. V. Astafiev. Phys. Rev. A 103, 013718 (2021).
[4] Aleksey N. Bolgar, Julia I. Zotova, Daniil D. Kirichenko, Ilia S. Besedin, Aleksander V. Semenov, Rais S. Shaikhaidarov, and Oleg V. Astafiev. Phys. Rev. Lett. 120, 223603 (2018).

Stimulated downconversion of single-photon emission in a quantum dot-microcavity system

T. V. Shubina, I. V. Krainov, M. R. Rakhlin, A. A. Toropov

Ioffe Institute, St. Petersburg, 194021 Russia

e-mail: shubina@beam.ioffe.ru

Currently, two trends dominate in the implementation of single photon sources for quantum technologies, using: i) transitions in a semiconductor quantum dot (QD) placed in a microcavity, and ii) nonlinear effects – spontaneous parametric frequency downconversion and four-wave mixing. Each of them has its own peculiarities. InAs/GaAs QDs in microcavity are characterized by compactness, high generation efficiency of single photons, as well as their indistinguishability and purity close to unity. However, these QDs can emit efficiently only in the range of 900–950 nm, while the desired telecom C range (1550 nm) still remains a challenge. Another problem is the significant spread of QD emission energy that makes difficult to match it with a stable mode in the microcavity. In contrast, nonlinear single photon sources can have a fairly constant energy. The flexibility in tuning the photon energy by adjusting the pump laser wavelength makes these sources compatible with loss-limited fiber networks. At the same time, the spontaneous nonlinear processes are characterized by very low efficiency.

In this paper, we consider an alternative method that combines the advantages of these two approaches. We propose to implement nonlinear stimulated frequency downconversion directly in the QD inside a microresonator that is designed not for the exciton frequency in the QD, as usual, but for the target single-photon frequency, which is set by the difference between the energies of the exciton and the stimulating laser, as shown in Fig. 1.

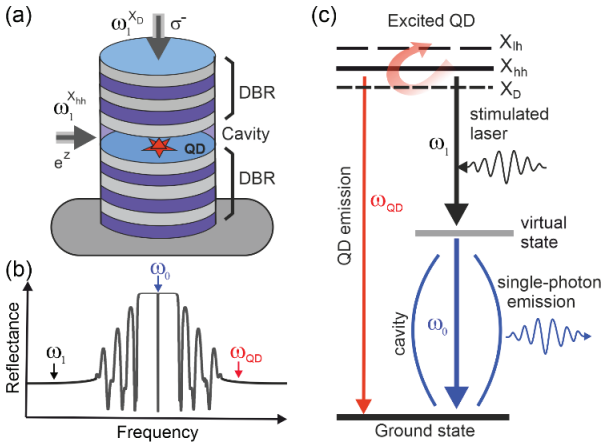

Fig. 1. (a) Single-photon source with a QD inside a target-frequency microcavity, the reflection spectrum of which is shown schematically in (b). The arrows indicate the excitation type for bright X_{hh} and dark X_D excitons in (a) and the frequency of the stimulating laser ω_1, cavity mode ω_0 and exciton radiation ω_{QD} in (b). (c) Scheme of single-photon generation during down-conversion in the QD-microcavity system.

Our theoretical modeling shows that a second-order nonlinear process can arise in this system due to the interaction of a heavy-hole exciton (or dark exciton) and a light-hole exciton in the stimulating laser field. For a telecom-band single photon source, we show that the downconversion efficiency can be comparable to direct emission from a 920 nm InAs/GaAs QD, and that the photon emission rate can approach ~1.3 MHz, which is significantly higher than that of typical nonlinear single-photon sources. The proposed nonlinear downconversion mechanism may be promising for on-demand single photon generation in telecom and other bands using well-established 920 nm InAs/GaAs QD technology such as molecular beam epitaxy.

This work was supported by Rosatom in the framework of the Roadmap for Quantum computing (Contracts No. 868-1.3-15/15-2021 dated 5 October 2021 and No. R2152 dated 11 November 2021).

[1] I.V. Krainov, M.V. Rakhlin, A.I. Veretennikov, and T.V. Shubina, Stimulated downconversion of single-photon emission in a quantum dot placed in a target-frequency microcavity, Optics Letters, vol. 50, pp. 2602-2605, (2025).

Structure and properties of proton-exchange layers of lithium niobate-tantalate solid solutions for photonic applications

A. Sosunov, I. Petukhov, E. Myasnikova, A. Kornilicyn

Perm state university, Bukirev str. 15, Perm, 614990 Russia

e-mail: avsosunov@psu.ru

The mixed lithium niobate-tantalate (LNT) crystals is a new system of solid solutions that promises new possibilities in lab-on-chip, integrated and nonlinear photonics. Proton exchange is one of the most widely used methods for creating optical waveguides, dielectric layers and activate surface. This work is dedicated to the study of structure and properties of *X*- and *Z*-cut LNT as a result of proton exchange followed by step-by-step annealing.

The structure and properties of the proton exchange layers in *X*- and *Z*-cut samples were systematically studied using various structural and integrated optical methods.

Direct proton exchange leads to the formation of a waveguide layer with a step-like refractive index profile. The waveguide substrate boundary is clear (not blurred). At this boundary, the parameters of the crystal lattice change abruptly. Proton exchange leads to with the formation of deformation twins and surface damage of the LNT crystal structure. The results of phase analysis of the samples indicate the presence of β-phases with high degrees of deformation of the crystal lattice. The calculated kinetic parameters of proton diffusion in LNT are significantly lower than for lithium niobate crystals, which is due to both the tantalum impurity and the greater disorder of the crystal lattice, and this leads to a decrease in the increment of the refractive index. The results provide a physical basis of diffuse process in mixed LNT solid solutions [1].

It was found that for both LNT cuts, the sequence of phase transitions $\beta \rightarrow \kappa \rightarrow \alpha$ is realized during annealing. The both proton content and refractive index increment ranges of the intermediate phases have been determined. For the *X*-cut LNT, the transformation process from the κ_2- to the κ_1-phase occurs with the formation of an unusual ordered pattern at surface. In this case, the protons do not move deeper the LNT crystal and refractive index does not change, respectively. For the *Z*-cut, such features are not observed due to smaller deformations of the LNT crystal lattice during annealing. The intermediate phases are characterized by higher vibration frequencies of OH-groups than these of proton-exchanged lithium niobate layers during the annealing. This is due to shorter "in plane" OH-bonds due to the slightly different composition and structure of LNT. The results will contribute to the predictability of the optical and structural characteristics proton-exchanged layers in LNT solid solutions for different applications [2].

The new method was developed for fast and non-destructive analysis of the parameters of channel gradient proton-exchange waveguides in integrated photonics devices. Gradient profiles of proton-exchange waveguides were reconstructed using the measuring of the OH-group line in the Raman spectrum in crystals of lithium niobate and LNT solid solution of *X*- and *Z*-cut. The profiles are in good agreement with the profiles obtained by the prism coupling method and theory. This allows to determine the depth of the waveguide layer with high accuracy. The refractive index increment can be determined from the calibration plot calculated in the work. The calibration plot give relationship between the intensity of Raman line of OH-groups and the refractive index increment. The relative error of calculating of refractive index increment is no more than 5% for *Z*-cut. This simple method allows to estimate all the main parameters of channel proton-exchange waveguides at any point for *Z*-cut samples. This is not available for other technics.

This work was funded by the RSF and the Perm region (project No. 24-22-20097).

[1] A. Sosunov, I. Petukhov, A. Kornilicyn, A. Mololkin, et. al., Structure and properties of proton exchange layers in lithium niobate-tantalate solid solutions, Solid State Ionics, vol. 417, p. 116692 (2024).
[2] A. Sosunov, I. Petukhov, E. Myasnikova, A. Kornilicyn, et. al., Structural-phase transformations during annealing of proton exchange layers in mixed lithium niobate-tantalate solid solutions, Materials Today Communications, vol. 43, pp. 111840-6, (2025)

Spectroscopy of metalloporphyrins

A. Starukhin

Stepanov Institute of Physics NAS RB, Minsk, Belarus

Dyakonov surface waveguide modes in ring resonators with chiral inclusions

I. I. Stepanov[1,2], O. V. Borovkova[1], S. A. Dyakov[3], N. A. Gippius[3], D. A. Chermoshentsev[1–3]

1- Russian Quantum Center, Bolshoy Boulevard 30, building 1, Skolkovo Innovation Center territory, Moscow, 121205 Russia
2- Moscow Institute of Physics and Technology, Institutskiy pereulok 9, Moscow Region, 141701 Russia
3- Skolkovo Institute of Science and Technology, Moscow Region, 143025 Russia

e-mail: stepanov.ii@phystech.edu

Among the many surface waves that exist under different conditions, Dyakonov surface waves can be distinguished separately. These waves propagate along the interface of two media, at least one of which is anisotropic. This type of surface waves was theoretically predicted at the interface of a semi-infinite isotropic and anisotropic medium in 1988 by Mikhail Dyakonov [1]. Later, the existence of Dyakonov surface waves were demonstrated in the finite-size structures composed of two straight waveguides made of the same anisotropic crystal with optical axes crossed at 90 degrees [2].

However, until now, the existence of this type of surface waves was not presented in ring microresonators, which are an important element of modern photonics. To confirm the existence of Dyakonov modes (DMs) in ring microresonators, we study the structure shown in Fig. 1. The system consists of two anisotropic uniaxial crystal resonators AM_1 and AM_2, whose optical axes (OA_1 and OA_2) rotate in the interface plane and form an angle of 90 degrees at any point of the ring.

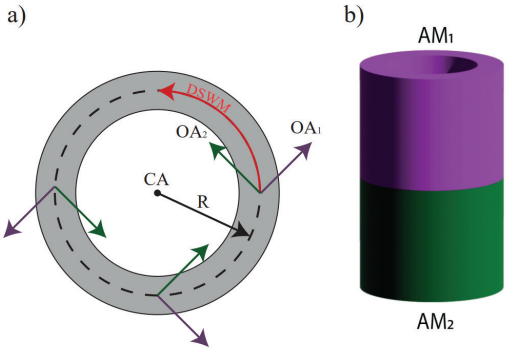

Fig. 1. (a) Top view of the ring resonator interface section, where CA indicates the cylinder axis and R – ring radius. OA_1 and OA_2 denote the optical axes of the anisotropic crystals. (b) General view of the simulated ring resonator geometry. AM_1 and AM_2 represent the corresponding anisotropic crystals.

We compare the results of numerical modeling of this system using the finite element method in COMSOL Multiphysics with the existing theory of DMs in a system of straight waveguides [3], supplemented by a condition on the wave vector specified by the ring. This can be done since in any radial section the orientation of the optical axes of the ring structure is identical to the case of straight waveguides. The polarization state and chirality density of the obtained DMs are considered. It was shown that the local chirality density of DMs is not zero and reaches local maxima at specific distances from the interface. Also, we demonstrate that an introduction of a gap between two anisotropic ring resonators significantly changes the chirality density and polarization state. The effect depends on the refractive index of the material in the gap, gap thickness, and the level of losses in the gap material.

Finally, the response of the system to placing a chiral material in the gap is measured, and assumptions are made on how to enhance this parameter.

The results obtained can be extremely useful in the implementation of an optical sensor for chiral structures, as well as other potential applications in sensing and communication systems.

[1] M. I. Dyakonov, "New Type of Electromagnetic Wave Propagating at an Interface," Sov. Phys. JETP, 67, 714–716, (1988).
[2] D. A. Chermoshentsev, E. V. Anikin, S. A. Dyakov, and N. A. Gippius, "Dimensional confinement and waveguide effect of dyakonov surface waves in twisted confined media," Nanophotonics, 9, 4785–4797, (2020).
[3] E. V. Anikin, D. A. Chermoshentsev, S. A. Dyakov, and N. A. Gippius, "Dyakonov-like waveguide modes in an interfacial strip waveguide," Phys. Rev. B, 102, 161113 (2020).

Dispersion engineering for optical parametric oscillators optimization in microresonators

N. Tatarinova[1,2], A. Shitikov[1], I. Bilenko[1,3], D. Chermoshentsev[1,2], V. Lobanov[1]

1- Russian Quantum Center, Moscow, Russia
2- Moscow Institute of Physics and Technology, Dolgoprudny, Russia
3- Moscow State University, Moscow, Russia

e-mail: n.tatarinova@rqc.ru

On-chip degenerate optical parametric oscillators (DOPOs) are key components in nonlinear and quantum optics, serving applications such as squeezed light generation [1] and coherent optical computing [2] across various pumping regimes. The threshold parameters, which are critical in defining the operational regime, are primarily determined by the integrated dispersion profile of the microresonator. Among the most effective strategies for reducing threshold power is dispersion engineering, which can be implemented in photonic crystal microresonators through periodic gratings and allow the deliberate introduction of forward-backward wave coupling, resulting in the splitting of selected cavity modes [3].

In this work, we numerically optimize DOPO threshold parameters and investigate approaches to reduce the total pump power, aiming toward the design of energy-efficient quantum photonic devices. Our theoretical framework is based on coupled-mode equations describing a symmetrically bichromatically pumped microresonator, providing control of individual resonant modes [4].

We begin by considering a model that excludes the backward-propagating wave. The analysis reveals that the threshold power depends only on the product $d_2 n^2$, where d_2 is the second-order dispersion coefficient and n denotes the number of free spectral ranges between each pump and the signal mode [5]. The effect of forward-backward coupling is introduced as an equivalent frequency shift of the modes. Specifically, a symmetric blue-shift $\Delta_{\pm 3n}$ applied to the modes with indices $\pm 3n$ – corresponding to the first generated sidebands in the non-degenerate four-wave mixing process – can reduce the threshold pump power by up to 40%. To refine the model, we incorporate the backward-propagating wave with forward-backward coupling coefficients β_μ, which are non-negligible only at the targeted modes $\beta_{\pm 3n}$. Although the nonlinear interaction between forward- and backward-propagating waves remains weak near the DOPO threshold, the presence of the backward wave introduces an additional energy conversion channel. This results in a slight increase in threshold power, yet the overall functional dependence remains similar to the simplified scenario (Fig. 1).

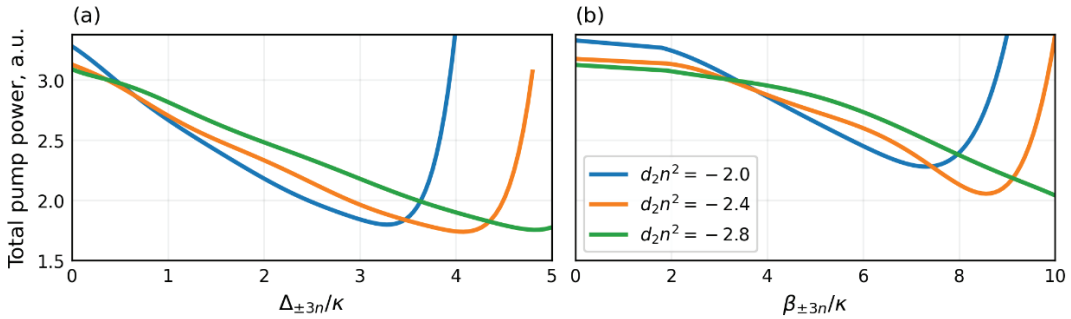

Fig. 1. Total pump power in the model without backward wave vs. shift $\Delta_{\pm 3n}$ (a) and total pump power in the model with backward wave vs. coupling rate $\beta_{\pm 3n}$ (b). All values are normalized on the cold cavity decay rate κ.

Our results show that careful tuning of the dispersion coefficients can lead to a significant reduction in the threshold power, improving the efficiency of these devices. These results lay the groundwork for the development of compact, low-power, and scalable quantum photonic systems.

The work was supported by the Russian Science Foundation (Grant No. 23-42-00111).

[1] Y. Zhao et al. "Near-degenerate quadrature-squeezed vacuum generation on a silicon-nitride chip", Physical Review Letters, 124.19, 193601, (2020).
[2] Y. Okawachi et al. "Demonstration of chip-based coupled degenerate optical parametric oscillators for realizing a nanophotonic spin-glass," Nature communications, 11.1, 4119, (2020).
[3] E. Lucas et al. "Tailoring microcombs with inverse-designed, meta-dispersion microresonators," Nature Photonics, 17.11, 943–950, (2023).
[4] N. Kondratiev and V. Lobanov. "Modulational instability and frequency combs in whispering-gallery-mode microresonators with backscattering," Physical Review A 101.1, 013816, (2020).
[5] N. Tatarinova et al. "Optimization of the degenerate optical parametric oscillations threshold in bichromatically pumped microresonator," arXiv preprint arXiv:2504.09224 (2025).

Domain-engineered PMN-PT crystals for electro-optic deflectors and modulators

A. D. Ushakov[1], W. Huang[2], M. Chuvakova[1], I. Kipenko[1], X. Liu[2], H. Zheng[2], X. Wei[2], V. Shur[1]

1- School of Natural Sciences and Mathematics, Ural Federal University, Ekaterinburg, 620000 Russia
2- Electronic Materials Research Laboratory, Key Laboratory of the Ministry of Education and International Center for Dielectric Research, Xi'an Jiaotong University, Xi'an, 710049 China

e-mail: bddah@ya.ru

In this study, we present the fabrication and characterization of electro-optic devices based on domain-engineered ferroelectric single crystals: deflector in PMN-PT and modulator in PIN-PMN-PT.

First, we demonstrate the electro-optic deflector with an engineered cascaded domain structure in multiaxial ferroelectric $Pb(Mg_{1/3}Nb_{2/3})O_3$–$PbTiO_3$. The working principle relies on electric field-induced birefringence $\Delta n(E)$, enabling beam deflection controlled solely by applied voltage. Recently, electro-optic deflector with cascaded domain structures created in lithium niobate have enabled fast beam steering, up to 3 MHz frequency and deflection efficiency of $5 \cdot 10^{-4}$ deg/V/mm [1]. The high electro-optic coefficient of crystals of PMN-PT family about 100 pm/V [2, 3] stimulated us to develop the prototype of the electro-optic deflector using [001]-cut PMN-PT crystals possessing tetragonal symmetry. After creation of the single-domain state, we fabricated a stable cascaded domain structure using a surface fixation technique. The second-harmonic generation microscopy allowed to approve the quality of the domain structure in the crystal bulk. The reached deflection efficiency $2.5 \cdot 10^{-4}$ deg/V/mm is comparable to prior results obtained in CLN [1].

Second, we show the ability to use a room-temperature poling technique to employ the [110]-oriented rhombohedral PIN-PMN-PT crystals for electro-optic modulators. Earlier, it was shown that conventional field-cooling techniques could be utilized for achieving high optical transmittance via formation of the laminar domain structure and removal of the light-scattering domain walls [4]. However, this procedure is time-consuming and does not prohibit the re-appearance of these domain walls. Here, we demonstrate the laminar domain structure formation using *in situ* domain imaging and offer a cost-effective alternative field treatment method which allow to use these crystals in modulators while preserving high electro-optic performance and optical transmittance.

Our results highlight the potential of domain-engineered ferroelectric PMN-PT-based crystals for high-performance electro-optic devices.

The authors are grateful for financial support of the Ministry of Science and Higher Education of the Russian Federation (state task FEUZ-2023-0017). The work was performed using the equipment of the Ural Center for Shared Use "Modern Nanotechnologies" UrFU (reg. No. 2968).

[1] J. Li et al., Cascaded domain engineering optical phased array for beam steering, Appl. Phys. Rev. 10, p. 031413 (2023).
[2] X. Wan et al., Refractive indices and linear electro-optic properties of $(1-x)Pb(Mg_{1/3}Nb_{2/3})O_3$–$xPbTiO_3$ single crystals, Appl. Phys. Lett. 85, pp. 5233–5235, (2004).
[3] Q. Hu et al., Achieve single domain state in (111)-oriented rhombohedral phase PMN-PT relaxor ferroelectric single crystals for electro-optical application, Appl. Phys. Lett. 115, p. 222901 (2019).
[4] X. Liu et al., Ferroelectric crystals with giant electro-optic property enabling ultracompact Q-switches, Science, 376, pp. 371–377 (2022).

Lanthanide-based OLEDs for electroluminescent thermometry

V. V. Utochnikova

M. V. Lomonosov Moscow State University, Leninskie gory 1/3, Moscow, Russia

e-mail: valentina@utochnikova.ru

Color-tunable organic light-emitting diodes (CTOLEDs) enable spectral modulation in response to external stimuli, with promising applications in adaptive lighting, displays, and smart sensors. We present a new class of CTOLEDs incorporating heterolanthanide coordination compounds $[Eu_xYb_{1-x}(dbm)_3(TDZP)]$ as dual-emitters, offering simultaneous electroluminescence and real-time temperature readout *via* the luminescence intensity ratio (LIR) between Eu^{3+} (red) and Yb^{3+} (NIR) emission bands.

These devices utilize internal Joule heating as a dynamic trigger for color modulation, enabling thermal feedback without additional temperature sensors or complex architectures. Upon electrical bias, Eu^{3+} emission undergoes progressive thermal quenching, while Yb^{3+} remains relatively stable, resulting in a strongly temperature-dependent LIR. The maximum relative thermal sensitivity in the photoluminescent mode reaches 8% K^{-1}, among the highest reported for molecular thermometers.

Electroluminescent studies under both cryogenic and ambient conditions reveal that the LIR – temperature behavior is reproducible under self-heating and external heating, allowing for accurate intrinsic temperature mapping within the active OLED layer. Importantly, voltage- and current-dependent spectral tuning is achieved without compromising device simplicity or operational stability.

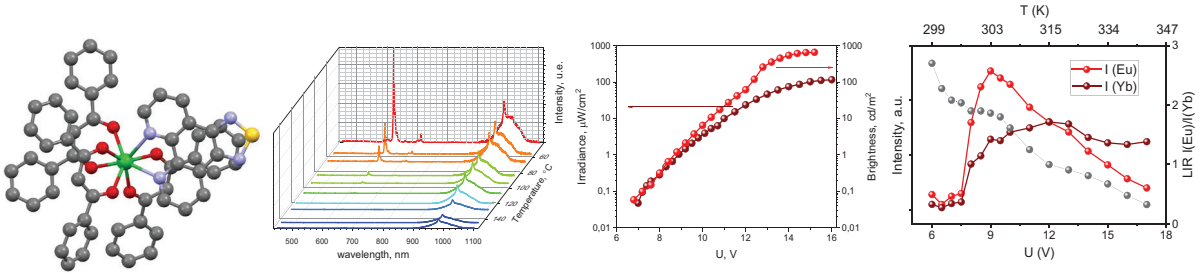

Fig. 1. From left to right: Crystal structure of $[Eu_{0.1}Yb_{0.9}(dbm)_3(TDZP)]$. Photoluminescence temperature dependence. Dual-emissive OLED operation. LIR as a function of voltage and operating temperature under self-heating conditions.

This multifunctional approach offers a compact, energy-efficient pathway for bias-modulated CTOLEDs with built-in thermal sensing. Such devices are highly promising for applications in photonic diagnostics, wearable electronics, and thermally adaptive light sources.

Photon superbunching in J-aggregates coupled to photonic bound-state metasurface

A. Vetlugin

Nanyang Technological University, Singapore, Republic of Singapore

e-mail: a.vetlugin@ntu.edu.sg

We experimentally demonstrate photon superbunching from J-aggregates coupled to high-Q silicon metasurface supporting bound states in the continuum. By leveraging the large oscillator strength of TDBC molecules in aggregated phase and the delocalized optical mode of the metasurface, we overcome the effects of dephasing and disorder at room temperature. This enables us to demonstrate superradiant emission accompanied by second-order correlation values $g^2(0)$ as high as 13 without the need for cryogenic cooling. We further investigate how the Rabi splitting influences emission intensity, lifetime, and photon statistics of both J-exciton and lower polariton states.

Radiation emission of a two-level atom driven by quantum electromagnetic field

R. Zakharov[1], A. Vasil'ev[1], O. Tikhonova[1,2]

1- Lomonosov Moscow State University, Leninskie Gory 1, Moscow, 119991 Russia
2- Russian Quantum Center, Bolshoy Boulevard 30, building 1, Skolkovo Innovation Center territory, Moscow, 121205 Russia

e-mail: ovtikhonova@mail.ru

The interaction of non-classical electromagnetic fields with matter is a very important and relevant problem of modern quantum optics and quantum information science. Such investigations provide a basis for the coherent control and managing the dynamics of quantum systems, methods of the storage and transfer of quantum information and developing fully quantum photon-matter interface which is extremely important for quantum information technologies. Now a wide variety of non-classical states of light are reproduced successfully in experiments. They include few-photons and coherent states with small mean photon number, biphoton pairs, multiphoton squeezed states etc. The interaction of these states with matter leads to new physical effects.

One of the very important but little explored problems concerns the peculiarities of the radiation emission of an atom driven by quantum light. The case of atomic emission under the pumping by resonance classical light is referred to the so-called resonance fluorescence [1]. This phenomenon is known to be accompanied by producing of the Mollow triplet in the atomic emission spectrum which is numerously investigated but still remains a very relevant problem. The specific features of the emitted radiation are well studied in the case of the classical pumping. Nevertheless the theoretical analysis of the atomic emission induced by quantum light is a rather difficult problem. In several papers [2] the theoretical approaches based on the solution of the Heisenberg-Langevin equations were developed with specific types of field correlators being taken into account. Another possibility consists in the solution of the density matrix equation with the relaxation term taken for example in the Lindblad representation [1]. However mutual influence between the atom and quantum field during the interaction can be very important especially in the case of few-photon or fragile squeezed field states. Moreover strong non-stationary character of the process plays an important role and leads to new features in the case of coupling with quantum light. These effects as well as the entanglement of emitted photons in the case of quantum pumping are still not investigated in details.

In this paper we develop a fully quantum theoretical approach to analyze from the fundamental principles a radiation emission of a two-level atom driven by the quantum electromagnetic field. To describe the emitted radiation a set of dissipative field modes which interact with the atom and can consequently influence each other are considered. In addition to the obtained numerical solution, we find an analytical solution to this problem in the limit of an infinite number of dissipative modes. Both solutions are in complete agreement with each other. We obtain the spectrum of atomic emission and analyze its formation during the time. We demonstrate the peculiarities of considered resonance fluorescence arising due to the non-classical character of the driving quantum field. The correlations between emitted photons are examined and their time evolution is analyzed. The correspondence of the obtained results to the classical limit of the Mollow triplet formation is discussed. The interaction of the emitted radiation with the second probe two-level atom is investigated and the resulting physical effects are analyzed. The obtained results are not only of fundamental importance, but also seem to be very promising for developing quantum technologies, since they describe the physical mechanisms of resonance fluorescence in quantum case and related wave mixing processes directly measured in experiments [3, 4].

[1] M. O. Scully and M. S. Zubairy Quantum Optics (Cambridge: Cambridge University Press), Chapter 10, (1997).
[2] C. W. Gardiner and A. S. Parkins, Driving atoms with light of arbitrary statistics, Phys. Rev. A, vol. 50, pp. 1792–1806, (1994).
[3] O. Astafiev et al. Resonance Fluorescence of a Single Artificial Atom, Science. vol. 327, pp. 840–843, (2010).
[4] A.Yu. Dmitriev et al. Direct experimental observation of sub-Poissonian photon statistics by means of multiphoton scattering on a two-level system, Phys. Rev. A, vol. 111, pp. 043715(11), (2025).

Optical resonator based on photonic crystal structures for diamond NV⁻ laser

V. V. Chashchin[1,2], D. E. Genin[1,2], E. I. Lipatov[1,2]

1- National Research Tomsk State University, Tomsk, Russia
2- Institute of High Current Electronics SB RAS, Tomsk, Russia

e-mail: lloodia@yandex.ru

It is known that, at the moment, laser generation has been achieved in NV⁻ color centers in diamonds, with a generation wavelength of λ ≈ 720 nm [1]. The generated pulse energy is approximately 50 μJ, with an optical pumping pulse energy of about 5.5 mJ, which corresponds to an efficiency of about 1% for the system [2].

However, the feedback provided by Fresnel reflection from the facets of the diamond is insufficient, which is why it is necessary to use an optical resonator in order to achieve the optimal feedback value. Using classical resonators based on external mirrors is not feasible due to the small geometric dimensions of the active diamond element (measured in millimeters) and the complexity of adjusting such a system.

This problem can be solved by creating a mirror with the desired reflection coefficient in a specific wavelength range directly on the surface of a diamond active element. A multilayer mirror, also known as a one-dimensional photonic crystal, can be "tuned" to the required reflection coefficient and wavelength range by adjusting the optimal parameters during its creation process.

This paper presents the results of increasing the energy of the laser pulse and the efficiency of a diamond laser by creating a reflective surface on one of the facets of a diamond laser element for the wavelength range λ = 710–730 nm. Figure 1 shows the dependence of the energy of the generation pulse on the energy of the pumping pulse for a diamond laser element with a blind mirror at the one of the facets.

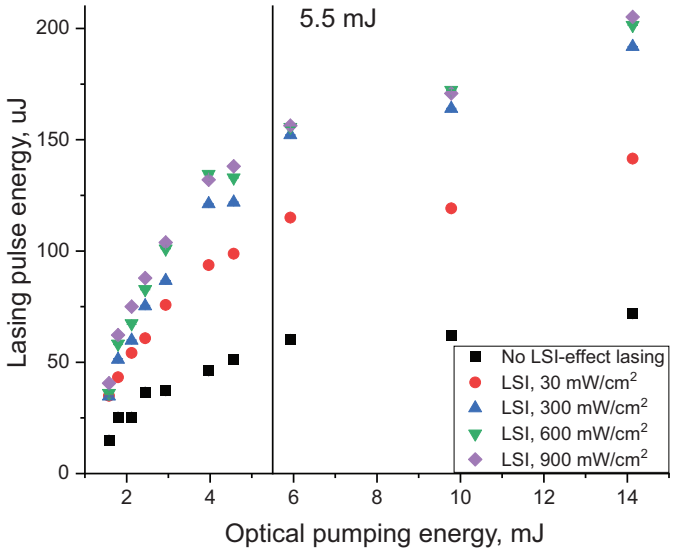

Fig. 1. Dependence of the generation energy on the optical pumping energy.

Figure 1 shows the relationship between the energy generated by a diamond laser and the optical pumping power, with a blind mirror at one end, under the influence of low-intensity, short-wavelength light [3].

[1] Savvin A. et al. NV-diamond laser // Nature communications. T. 12, № 1, c. 7118, (2021).
[2] Genin D. et al. Microjoule-Range Diamond NV-Laser with Optical Pumping // physica status solidi (RRL) – Rapid Research Letters. T. 18, №. 2, c. 2300062. (2024).
[3] Invention patent № 2813650 «A method for increasing the generation energy of a diamond NV⁻ laser», authors: Burachenko A.G., Vince V.G., Genin D.E., Eliseev A.P., Lipatov E.I., Ripenko V.S., Savvin A.D., Shulepov M.A., date of application 19.12.2022.

Modeling the creation of entangled states by non-gaussian beams

A. P. Gordeev[1], M. Yu. Goloshchapov[2], G. I. Struchalin[1], I. B. Bobrov[1], S. S. Straupe[1,2]

1- Quantum Technology Centre and Faculty of Physics, M. V. Lomonosov Moscow State University
2- Russian Quantum Center

e-mail: ar1emg0rdeev@gmail.com

This work is devoted to modeling the excitation of multi-qubit entangled states of neutral atoms using the Rydberg blockade effect and studying influence of different sources of noise [1]. We develop a numerical model that includes key noise sources related to hardware imperfections, such as fluctuations in the excitation laser and limitations in the cooling system. The latter affects the system by introducing atomic motion-related errors and setting a lower limit on the temperature that rubidium atoms can reach in the vacuum chamber [2]. Due to residual thermal motion, being irradiated, atoms experience varying amplitude and phase of electro-magnetic field, which disturbs controlled quantum operations.

One of the ways to reduce effect of thermal motion is to use beams with plain distribution of intensity near the atom (flat-top) instead of Gaussian beams [3]. They have sharper decline of intensity between neighboring atoms in array, so that influence of oscillations and crosstalk effects are reduced. We present method to construct such beams representing them as superposition of Laguerre-Gaussian or Hermite-Gaussian modes allowing to model propagation of electro-magnetic field phase and amplitude. Experimentally these beams achieved using spatial light modulators with phase masks calculated by special algorithm [4].

After reconstruction of the electro-magnetic field in space experienced by array of rubidium atoms in optical traps, we sample their coordinates and velocities from Boltzmann distribution and model evolution of the system by solving Gorini–Kossakowski–Sudarshan–Lindblad equation also taking into account multi-level structure of atoms, spontaneous decay and Doppler effect occurring from thermal motion. With this computational template field of arbitrary structure can be used to simulate evolution of energy levels population, so in combination with algorithms providing phase masks for spatial light modulators it can be used for optimization of experimental parameters.

Using this numerical model, we compare fidelity of multi-qubit entangled states in array of atoms in optical traps, obtained via beams with plain distribution of intensity of different shape and size, for various excitation protocols: with single laser pulse and several consequent pulses addressing neighboring atoms.

[1] A. Browaeys et al, Analysis of imperfections in the coherent optical excitation of single atoms to Rydberg states, Phys. Rev. A, vol. 97, p. 053803 (2018).
[2] J. Dalibard and C. Cohen-Tannoudji, Laser cooling below the Doppler limit by polarization gradients: simple theoretical models, JOSA B Vol.6, pp. 2023–2045 (1989).
[3] K. Gillen-Christandl et al, Comparison of Gaussian and super Gaussian laser beams for addressing atomic qubits, Appl. Phys. B, vol. 122, pp.131–151 (2016).
[4] E. Bolduc et al, Exact solution to simultaneous intensity and phase encryption with a single phase-only hologram, Opt. Lett., vol. 38, pp. 3546–3549 (2013).

RIN effect on phase noise spectra of lasers in heterodyne measurements

A. Kozlov, K. Zagorulko, N. Khatyrev

Russian Metrological Institute of Technical Physics and Radio Engineering, Mendeleevo, Russia

e-mail: alexkozlowv@yandex.ru

When measuring the phase noise (PN) PSD of single-frequency lasers, a minimum constant level can be observed at large frequency offsets (or increase of frequency noise in Hz2/Hz units). It was mentioned that the limitation may be due to relative intensity noise (RIN). In this paper, we performed an experimental study of possible origin of the minimum measurable level (MML) of PN.

For the experiment, we used common optical heterodyne setup. Beat notes (BN) of two fiber lasers (NKT Koheras BASIK) was obtained. In contrast to previous setup, output polarization-dependent isolator was excluded and polarization controllers were used to adjust the level of the BN regardless of the power (15+15 mW) incident on the photodetector (PD). BN frequency of the two lasers was tuned out of PD bandwidth and PSD level of the broadband noise of the DC signal (LBBN) was measured with a spectrum analyzer (at offset frequencies > GHz). The level was 77 dBm/Hz at RBW10 MHz that correspond to –147 dBm/Hz. Then the BN frequency was tuned to ≈4 GHz and amplitude noise (AN) and PN of BN were measured at various BN levels (adjusted by polarization controllers). The measurement results are shown in Fig. 1 (a, b). It can be seen that when the signal level decreases, the MML of PN increases. It can also be seen that the levels of AN and PN are the same at large frequency offsets. That suggests that the MML is determined not by the intrinsic noise of the measuring device and not by AN of BS. LBBN was subtracted from every measured AN and PN spectra (in linear format) taking into account the signal level. For example, the calculated noise floor level is –136.73 dBc for signal level –10.27 dBm (green curves). We subtract it in liner format from green AM and PN curves. The results are shown in Fig. 1 (c, d).

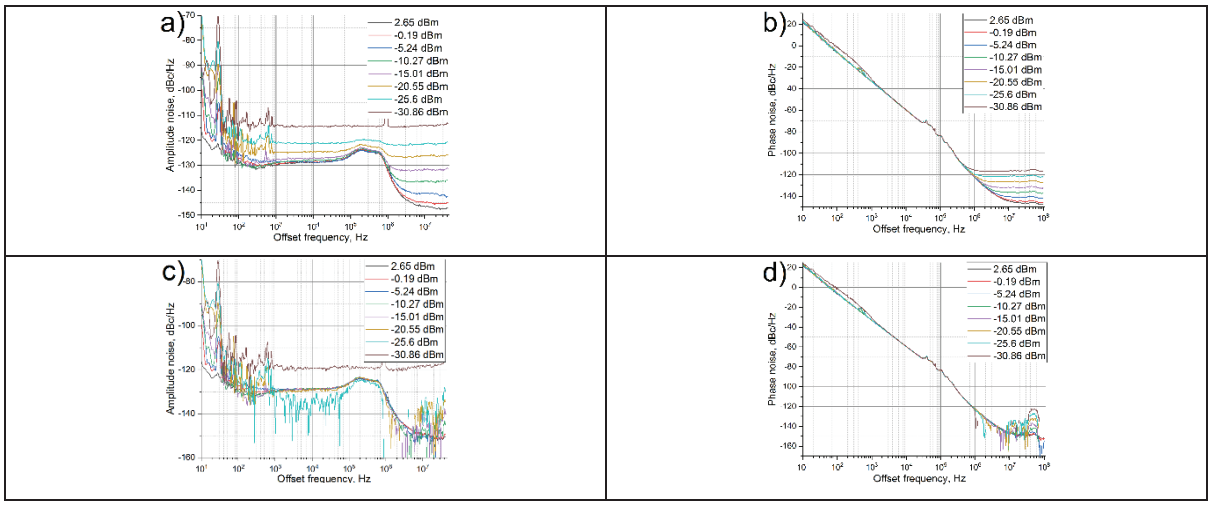

Fig. 1. AN (a) and PN (b) of beat note signal of various levels. The result of subtracting the LBBN from the AN (c) and PN (d).

Thus, it is shown that LBBN incident on PD are the origin of limiting MML of laser PN. The mentioned shot noise is a special case of the described restriction for very small DC signals. By subtracting the LBBN in the described way, it is possible to increase the range of measured values of PN. It is important to note that this factor affects all signals in systems where a DC signal is detected by a PD.

[1] R. Slavik et al. "Full characterization and comparison of phase properties of narrow linewidth lasers operating in the C-band", 21st International Conference on Optical Fiber Sensors. – SPIE, vol. 7753, p. 496–499 (2011).
[2] Pavlov, V.I., Balakireva, I.V., Brazhnikov, M.K., Khatyrev, N.P., "Frequency stabilization of diode lasers using lithium tantalate microresonators for laser cooling systems of a rubidium fountain", Almanac of modern metrology, Vol. 4, No. 32, 18–26 (2022).

Photophysics of single LX centers in diamond

M. Pavlenko[1,2,4], A. Neliubov[1,3,4], I. Eremchev[1,4], A. Naumov[1,4], E. Ekimov[5]

1- Institute for Spectroscopy of Russian Academy of Sciences, Troitsk, Fizicheskaya str. 5, Moscow 108840, Russia
2- National Research University Higher School of Economics, Staraya Basmannaya str. 21/4, Moscow, 109028 Russia
3- Skolkovo Institute Science and Technology, Nobel str. 1, Moscow, 121205 Russia
4- Institute of Spectroscopy RAS, Troitsk, Fizicheskaya str. 5, Moscow, 108840 Russia
5- Institute for High Pressure Physics, Russian Academy of Sciences, Moscow, Troitsk, 108840 Russia

e-mail: ritapavlenko00@gmail.com

Recent studies have unveiled a new class of defect centers in high-pressure-high-temperature (HPHT) microdiamonds, termed LX centers, which exhibit exceptional spectral properties [1]. These centers are characterized by bright, stable, and narrowband fluorescence with a full width at half maximum (FWHM) down to 0,5 nm at room temperature, that is an order of magnitude less than the corresponding parameter of well-known defects such as nitrogen-vacancy (NV) or group-IV vacancy centers (SiV, GeV, SnV). LX centers demonstrate negligible phonon sidebands and linearly polarized emission, that pave the way for applications in quantum optics as highly efficient single-photon sources, as well as bioimaging, and nanoscale thermometry.

Antibunching in second-order cross-correlation function $g^2(\tau)$ confirms single-photon emission, with a fluorescence lifetime of 1.5–2.5 ns. Despite the absence of observable blinking in emission of single LX centers, the luminescence is intermittent, which is confirmed by the presence of photon bunching in the $g^2(\tau)$-function together with antibunching. The observed intensity-dependent parameters of luminescence bunching could not be described in traditional model of three-level system. We consider a four-level energy model to explain the experimental data and provide additional numerical simulations to validate the model [2].

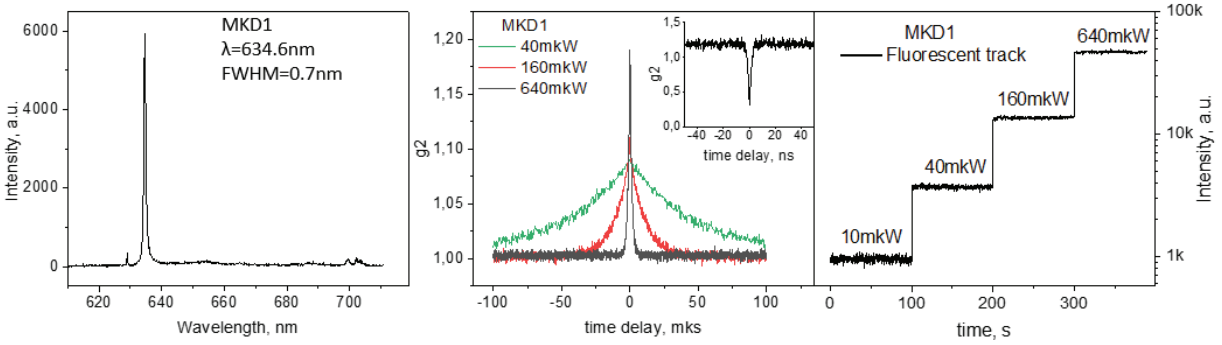

Fig. 1. Fluorescence properties of the MKD1 object. (a) Fluorescence spectrum of the LX center in diamond at room temperature. (b) Cross-correlation function of the investigated color center in microsecond scale obtained at different excitation power values. The inset shows the $g^2(\tau)$-function for the measurement at 640μW power. (c) Fluorescence track of the investigated staining center for several values of excitation power.

The research was carried out within the state assignment of The Ministry of Education of The Russian Federation (theme No. 124031100005-5).

[1] Neliubov A.Yu., Eremchev I.Yu., Drachev V.P., Kosolobov S.S., Ekimov E.A., Arzhanov A.I., Tarasevich A.O., Naumov A.V., Enigmatic color centers in microdiamonds with bright, stable, and narrow-band fluorescence. Phys. Rev. B 107, L081406 (2023).
[2] Neliubov A.Yu., Tarasevich A.O., Pavlenko M.I., Ekimov E.A., Naumov A.V., Eremchev I.Yu. Photophysics of single LX centers in high pressure--high temperature microdiamonds. Phys. Rev. B 111, 155420 (2025).

Hydrodynamic modeling of 3D-printing for chalcogenide glass IR photonics components design

B. Stepanov, L.Shabarova, I. Evdokimov, A. Stepanov

Institute of Chemistry of High-Purity Substances of the Russian Academy of Sciences (ICHPS RAS), Tropinina Str. 49, Nizhny Novgorod, Russia

e-mail: boris1885@gmail.com

Additive technologies are a relatively new and rapidly developing direction in the manufacture of functional photonics elements operating in the near and medium IR wavelength ranges. However, the choice of materials that can be used as filaments for 3D printing and have the required optical characteristics is limited. Chalcogenide glasses are one of the most promising IR materials for the manufacture of metalenses, sensor elements for evanescent spectroscopy, photonic crystals etc. with the possibility of using additive technologies for these purposes [1–3].

Extrusion processing is a key element of 3D printing technology [4]. A deep understanding of the technological aspects of the extrusion process will allow creating the theoretical foundations for the equipment design and manufacturing techniques for chalcogenide glass photonics components shaped by 3D-printing. The main goal of our research is to develop the physico-chemical fundamentals of technology for obtaining chalcogenide glass IR photonics components (sensor elements, splitters, couplers etc.) using 3D printing. We utilized hydrodynamic modeling as a powerful tool to obtain the deeper understanding the processes taking place during the extrusion. There are several features of extrusion process were discovered. The glass velocity and temperature fields during extrusion are depicted on Fig. 1. There is noticeable difference of the glass flow velocities in center of the extrusion die comparing with velocities at its wall leading to local heating of the glass in the central region of the die.

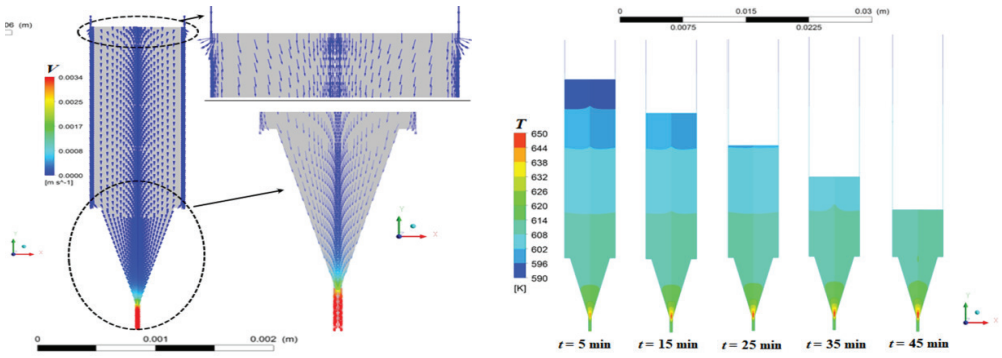

Fig. 1. The velocity field of the glass (left part) and temperature field (right part) in the extrusion die.

The obtained effect has a significant impact on the thermal and kinetic conditions of As-S glass flow during extrusion. Thereby the features of the glass flow include: 1) temperature inhomogeneities in the glass in the funnel of the die; 2) cooling parameters of the fiber at the exit of the die channel; 3) glass-air interface formation and the temperature field along the length and radius of the fiber as the glass flows out of the extrusion die and into the atmosphere.

Taking into account the results of hydrodynamic modeling of the extrusion process, as well as the physico-chemical properties of the glasses of the As-S system the requirements for the temperature and time modes of glass extrusion processing were formulated.

[1] Gu ZF, Gao YX, Zhou KS, et al. Surface-patterned chalcogenide glasses with high-aspect-ratio microstructures for long-wave infrared metalenses. Opto-Electron Sci 3, 240017 (2024).
[2] J.-L. Adam, X. Zhang (eds.) "Chalcogenide glasses: preparation, properties and applications" Woodhead Publishing Series in Electronic and Optical Materials: Number 44. 2014. Oxford Cambridge Philadelphia New Delhi. 607 p.
[3] E. Baudet, Y. Ledemi, P. Larochelle, S. Morency, and Y. Messaddeq 3D-printing of arsenic sulfide chalcogenide glasses Optical Materials Express V. 9, No. 5 PP.2307–2315 (2019).
[4] Keonkuk Kim et.al. Heat-Dissipation Design and 3D Printing of Ternary Silver Chalcogenide-Based Thermoelectric Legs for Enhancing Power Generation Performance Adv. Sci. 11, 2402934 (2024).
[5] Joël Charrier, Marie-Laure Brandily, Hervé Lhermite, Karine Michel, Bruno Bureau, Fréderic Verger, Virginie Nazabal Sensors and Actuators B: Chemical V. 173, , pp. 468–476 (2012).

Multitone high-fidelity Greenberger–Horne–Zeilinger gate simulation

F. Ushakov[1,3], E. Anikin[1,2], O. Lakhmanskaya[1], K. Lakhmanskiy[1–3]

1- Russian Quantum Center, Moscow, Russia
2- Moscow Institute of Physics and Technology, MIPT, Dolgoprudny, Russia
3- National Research Nuclear University MEPhI, Moscow, Russia

e-mail: fedoreverse@mail.ru

The production of multipartite entangled states presents a challenge for current quantum computers. In trapped-ion quantum computers, GHZ states can be generated by applying a bichromatic beam close to resonance with the center-of-mass (COM) motional mode, which creates spin-dependent forces on the ions [1]. However, for long ion chains, the fidelity of the GHZ state decreases due to an increase in the contribution of motional modes in the chain, leading to unwanted contributions to the spin-spin entangling phase [2].

We propose a method to reduce this error by using a polychromatic driving field, adding additional bichromatic tones to the beam that implements the spin-dependent force. This method works with an appropriate choice of additional tones, as we demonstrate. We model the ion chain illuminated by a polychromatic beam using a spin-dependent force Hamiltonian in the Lamb-Dicke approximation:

$$\hat{H} = \sum_{im\beta} \eta_{im}\Omega_{\beta}(t)\cos(\mu_{\beta}t + \psi)(a_m e^{-i\omega_m t} + a_m^{\dagger} e^{i\omega_m t})\sigma_x^{(i)}, \quad (1)$$

where η_{im} is the Lamb-Dicke parameter of specific ion and axial mode, Ω_{β} is the single spin Rabi frequency which is proportional to the illumination intensity, μ_{β} is the frequency detuning between carrier transition and one of the spectral components of the driving field, ω_m is the mode frequency, σ_x is the Pauli operator. Using this Hamiltonian, we find an approximate evolution operator:

$$U(t_0, t) = \exp\left(-\frac{i}{2}\sum_{i,j}\chi_{i,j}(t, t_0)\,\sigma_x^i\sigma_x^j\right), \quad (2)$$

where $\chi_{i,j}$ is the spin-spin coupling matrix, which we calculate for various polychromatic pulses Ω_{β}. From χ, the GHZ state fidelity is calculated using the formula:

$$F = 1 - \sum_{i<j}\left(\chi_{i,j} - \frac{\pi}{4}\right)^2, \quad (3)$$

Employing the model outlined above, we have computed the coupling matrix elements for each ion pair in the chain at the terminal moment of the gate operation, considering both the scenarios of preparing the GHZ state using a single tone and with the addition of a lower-intensity tone. In order to determine the intensity of the radiation of the additional tone, an empirical dependence of the gate infidelity and the ratio of the intensities of the main and additional tones was obtained. To present the results, we selected a finite matrix corresponding to the optimal value of infidelity. The resulting scaled χ matrices are presented in Fig. 1.

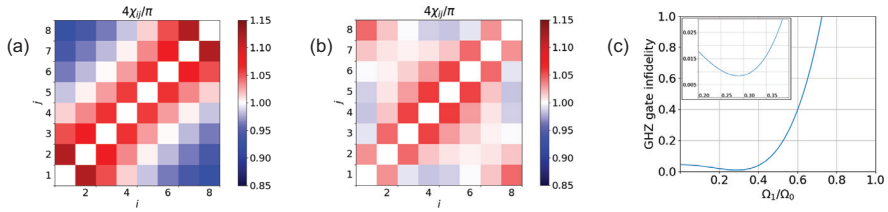

Fig. 1. Numerical calculation results of the interaction of a smoothed rectangle driving pulse with duration – 100 μs with 8-ion chain with radial mode frequency – 1.6 MHz and axial mode frequency – 150 kHz. (a) Finite coupling matrix in single-tone case: Ω_0 = 395 kHz, μ_0 = 873 kHz. (b) Finite coupling matrix in optimal double-tone case: Ω_1 = 115 kHz, μ_1 = 1.7 MHz, Ω_0, μ_0 are the same as in case (a). (c) Graph of the gate infidelity dependence on the ratio of tone intensities with a minimum at Ω_1/Ω_0 = 0.29.

By incrementing the number of tones by one, we achieved an improvement in the fidelity of the Greenberger–Horne–Zeilinger state, raising it from 95.7% to 99.2%. Subsequent computations were conducted with an greater number of tones, enabling us to perform GHZ state with even higher fidelity.

This work was supported by Rosatom in the framework of the Roadmap for Quantum computing (Contract No. 868-1.3-15/15-2021 dated October 5).

[1] Yotam Shapira et al. Physical Review A 101.3, p. 032330, (2020).
[2] Brandon P Ruzic et al. Physical Review Applied 22.1, p. 014007, (2024).

Effect of phonon-induced decoherence on the indistinguishability of single telecom C-band photons emitted by a coherently pumped InAs/InGaAs quantum dot

A. I. Veretennikov, Yu. M. Serov, A. I. Galimov, M. V. Rakhlin, S. V. Sorokin, G. V. Klimko, I. V. Sedova, N. A. Maleev, M. A. Bobrov, M. M. Kulagina, Yu. M. Zadiranov, Yu. A. Saliy, D. S. Berezina, A. A. Toropov

Ioffe Institute, St. Petersburg, 194021 Russia

e-mail: veretennikov.a01@mail.ru

The realization of deterministic single-photon sources (SPSs) represents a fundamental challenge in the development of scalable photonic quantum information processing. Epitaxially grown quantum dots (QDs) have emerged as one of the most promising platforms for SPSs, offering short radiative lifetimes and high internal quantum efficiency [1]. Among the various spectral regions, the telecom C-band is of particular interest due to its minimal transmission losses in silica optical fibers. A promising route to achieve C-band emission involves the growth of InAs QDs on $In_xGa_{1-x}As$/GaAs metamorphic buffer layers (MBLs) with graded composition profiles [2].

A key requirement for SPSs in linear optical quantum computing is the high indistinguishability of emitted photon wave packets, essential for enabling two-photon interference effects [3]. In QD-based systems, photon indistinguishability is predominantly limited by dephasing processes of charge carriers arising from their interaction with the surrounding environment [4]. Yet, the underlying decoherence mechanisms in MBL-based structures remain insufficiently explored.

In this work, we present a systematic study of two-photon interference visibility in a telecom C-band SPS based on InAs/InGaAs QDs embedded in a monolithic cylindrical microcavity above an $In_xGa_{1-x}As$/GaAs MBL. The source exhibits a low multi-photon probability with $g^{(2)}(0) = 0.019$ and a high single-photon count rate of 4.2 MHz. The degree of photon indistinguishability, measured via the Hong-Ou-Mandel interference experiment, reaches 35% at a temperature of 8.3 K.

Temperature-dependent coincidence measurements near zero delay reveal a reduction in the transverse dephasing time T_2^* from 790 ps at 8.3 K to 245 ps at 18 K, indicating a strong phonon-induced contribution. Notably, no significant dependence of T_2^* on the time delay between interfering photons was observed. Under resonant excitation, two primary sources of decoherence were identified: electron–phonon interactions and spectral diffusion. Fitting the experimental data allowed for the extraction of quantitative coupling parameters characterizing the underlying dephasing mechanisms. The experimentally observed Rabi oscillations were well reproduced by the fitted model, yielding a preparation fidelity of the QD excited state of approximately 88%.

These results provide essential insights into phonon-mediated decoherence in InAs/InGaAs QD systems and offer practical guidance for optimizing SPS performance for applications in the telecom C-band.

The work was supported by Rosatom in the framework of the Roadmap for Quantum computing (Contract No. 868-1.3-15/15-2021 dated 5 October 2021 and Contract No. R2152 dated 11 November 2021).

[1] T. Heindel, J.-H. Kim, N. Gregersen et al. Quantum dots for photonic quantum information technology, Advances in Optics and Photonics. 15(3) pp. 613–738, (2023).
[2] S.V. Sorokin, G.V. Klimko, I.V. Sedova et al. Metamorphic InAs/InGaAs Quantum Dot Heterostructures for Single-Photon Generation in the C-Band Spectral Range, JETP Letters, 120, p. 694, (2024).
[3] C. Couteau, S. Barz, T. Durt et al. Applications of single photons to quantum communication and computing, Nat. Rev. Phys. 5, pp. 326–338, (2023).
[4] H. Vural, S. L. Portalupi, P. Michler, Perspective of self-assembled InGaAs quantum-dots for multi-source quantum implementations. Appl. Phys. Lett. 117, 030501, (2020).

Towards 2D ion trap with integrated SSPD and waveguides for quantum computing

S. Zarutskiy[1], A. Podlesnyy[1], K. Sedykh[2,3], Y. Suleimen[1,4], V. Baturo[1], V. Kovalyuk[2,3], G. Goltsman[1,2], K. Lakhmanskiy[1]

1- Russian Quantum Center, Bolshoy Bulvar 30, bld. 1, Skolkovo, Moscow, 121205 Russia
2- National Research University,"Higher School of Economics", Moscow, 109028 Russia
3- National University of Science and Technology MISiS, Moscow, 119049 Russia
4- Moscow Pedagogical State University, Moscow, 119991 Russia

e-mail: zarutskiysy@my.msu.ru

In terms of tackling Noisy Intermediate-Scale Quantum Computing (QC) problems trapped-ion platform is one of the most promising [1]. However, the standard optical systems needed for quantum operation on trapped ions involve bulky setups to focus ion fluorescence on camera and individually address ions with lasers.

Integrated photonics is a promising solution to this problem: on-chip waveguides [2] and Superconductive Single-Photon Detectors (SSPD) [3] enable opportunities for scaling of ion addressing and state readout. However, field of the trap's RF electrode affects the performance of integrated SSPDs. The degrading impact of the nearby RF-electrode on the SSPD performance was observed to increase with both V_{RF} and Ω_{RF} in [4].

To support future SSPD integration, we design a surface ion trap optimized for low-voltage RF operation (see Fig. 1). While typical traps use hundreds of volts, in our design we limited V_{RF} to 60 V. In the design the ion-electrode separation is maintained at approximately 60 μm with the stability parameter $q \approx 0.6$. The trap depth is 40 meV, with an ion height of 58 μm at $\Omega_{RF} = 2\pi\times22$ MHz. Secular frequencies are well-separated and approximately equal (1.7, 3.7, 4.9) MHz.

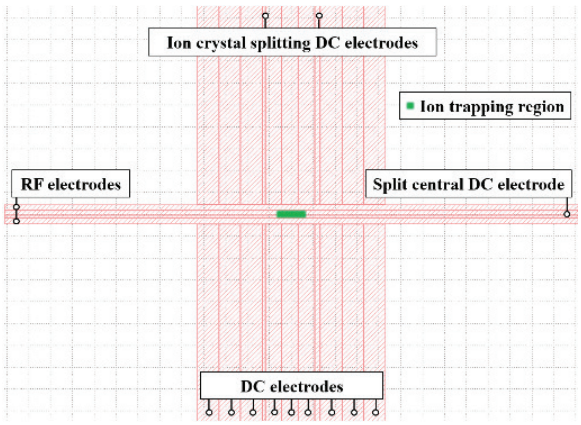

Fig. 1. The surface ion trap geometry. Ion trapping region is highlighted in green. Central trapping zone and additional vertical DC electrodes are separated by DC electrodes for ion crystal splitting. Central DC electrode is segmented to enable control over the orientation of radial modes.

The trap includes multiple vertical DC electrodes, including two pairs for ion transport and crystal splitting. An asymmetric central DC electrode allows control of radial mode orientation – essential for efficient cooling. This low-V_{RF}, low-Ω_{RF} ion trap is well suited for future SSPD integration. Our next step is to manufacture a trap on-chip SSPD and experimentally study the influence of RF fields under realistic trapping conditions, including cryostat vibration, cryogenic temperatures, and optical noise.

This work was supported by Rosatom in the framework of the Roadmap for Quantum computing (Contract No. 868-1.3-15/15-2021 dated October 5).

[1] C. D. Bruzewicz et al., Appl. Phys. Rev. 6, 021314 (2019).
[2] S. Todaro et al., Phys. Rev. Lett. 126, 010502 (2021).
[3] K. K. Mehta et al., Nature 586, 533 (2020).
[4] K. O. Sedykh et al., Tech. Phys. 68, 908 (2023).

Fabrication and characterization of integrated optical fiber diverging microlenses

L. O. Zhukov, R. S. Ponomarev

Perm State University, Integrated photonics laboratory, Perm, Russia

e-mail: leonidgp@bk.ru

This paper presents the fabrication and investigation of a diverging lens at the end of an optical fiber using the anisotropic etching method. Such a lens is a microscopic conical recess with a rounded top. Doping the fiber core with Ge reduces the activation energy of the etching process: Ge–O bonds have lower energy compared to Si–O bonds (343 kJ/mol [1] vs. 464 kJ/mol [2]). Optical imaging methods, including dark-field and bright-field microscopy, as well as measurements of the outgoing radiation profiles using an IR camera, were used to control the geometry of the resulting structure.

Experimental studies were conducted at two wavelengths: 980 nm and 1550 nm, characteristic of telecommunications and laser applications. It was found that the output radiation has a ring shape with a divergence angle of 42±3° at a wavelength of 980 nm and 40±2° at a wavelength of 1550 nm. These data were obtained by analyzing the three-dimensional distribution of intensity at the lens output.

For a deeper understanding of the physical processes occurring in the created microstructure, numerical modeling of the propagation of electromagnetic radiation in the medium was performed in Comsol Multiphysics 6.2. The modeling was based on solving Maxwell's equations in the frequency domain using the finite element method. During the numerical experiment, various parameters of the cone geometry were investigated, including the apex angle, cavity depth, and apex radius. A comparison of the simulation results with experimental data showed good agreement for parameters such as the divergence angle and the shape of the output spot. For example, the model divergence angle was 40° at a wavelength of 980 nm and 41° at a wavelength of 1550 nm, which is within the measurement error.

The results obtained demonstrate the high potential of such microstructured diverging lenses in various fields of integrated photonics. They can be used for light distribution systems, as well as components of fiber optic sensors and light field control devices.

The study was funded by the Russian Science Foundation grant No. 24- 91-21001.

[1] A. O. Borisova, Chemical Bonding in Coordination Compounds Based on Precision X-ray Diffraction Studies . Ph.D. dissertation, A. N. Nesmeyanov Institute of Organoelement Compounds, Russian Academy of Sciences, (2012).
[2] T. N. Kleimyonova and O. V. Raetskaya, "Use of silicon compounds," J. Electrotechnics , p. 74, (2019).

Calculation of interaction parameters of Pu^{3+} ions with spins of fluorine nuclei in CaF_2

R. R. Ziatdinov, M. V. Eremin

Institute of Physics of Kazan (Volga Region) Federal University, Kazan, Russia

e-mail: razik.ziat@gmail.com

Experimental data obtained by ENDOR method [1] revealed that the interaction of Pu^{3+} 5f-electrons with fluorine nuclei in CaF_2 crystal differs significantly from the classical dipole-dipole interaction. There is a large isotropic electron-nucleus interaction with the A_s parameter, which was found to be negative. The reason for this anomalous phenomenon has not yet been explained.

In this work, we consider the effect of mixing the 5f-electron wave functions of the Pu^{3+} ion with the 2s- and 2p-wave functions of fluorine on the values of the electron-nuclear double resonance (ENDOR) parameters A_s and A_p. Using the technique of irreducible tensor operators, we derive expressions for the spin Hamiltonian parameters of A_s and A_p via the hybridization parameters $\lambda_{f\sigma} = s_{f\sigma} + \gamma_{f\sigma}$, $\lambda_{f\pi} = s_{f\pi} + \gamma_{f\pi}$ and $\lambda_{fs} = s_{fs} + \gamma_{fs}$. In addition to this generally accepted covalent approach, the virtual transfer processes of 2s- and 2p-electrons of fluorine into the empty 6d-shell of plutonium have been taken into account. All overlap integrals were calculated on the Hartree-Fock wave functions of plutonium taken from [2], which were previously approximated by Gaussian-type orbital expansions. In the numerical evaluations of A_s and A_p, the covalency parameters $\gamma_{5f\sigma}$, $\gamma_{5f\pi}$, $\gamma_{6d\sigma}$, $\gamma_{6d\pi}$ were assumed to be proportional to the overlap integrals $s_{f\sigma}$, $s_{f\pi}$, s_{fs}, interaction with the A_s parameter, which was found to be negative. As it could be expected on the basis of transferred hyperfine interaction analysis, for rare-earth compounds (see, for example, [3]), the magnitude and sign of A_s for the Pu^{3+} ion in CaF_2 can be explained by virtual processes of transfer of 2s- and 2p-electrons of fluorine to the empty 6d-shell of plutonium. Moreover, using the experimental data of [1] we obtained the covalence parameters of 5f- and 6d-electrons of Pu^{3+} in CaF_2.

[1] W. Kolbe, N. Edelstain. Electron-Nuclear Double Resonance of Pu^{3+} in CaF_2 // Phys. Rev. B. Vol. 4, No. 9, pp. 2869–2875, (1971).
[2] G. Schreckenbach, P. J. Hay, R. L. Martin. Density Functional Calculations on Actinide Compounds: Survey of Recent Progress and Application to $[UO_2]^{2+}$ // J. Comput. Chem. Vol. 20, pp. 70–90, (1999).
[3] M. L. Falin, M. V. Eremin, H. Bill, D. Lovy. ENDOR and transferred hyperfine interaction of impurity rare-earth ions with nearest diamagnetic ions in crystals // Appl. Magn. Reson. Vol. 9, pp. 329–354., (1995).

32nd INTERNATIONAL CONFERENCE
Advanced Laser Technologies
ALT'25

NANOPHOTONICS

Novel mirrors, cavities, and analytical results for chiral nanophotonics

D. G. Baranov

Center for Photonics and 2D Materials, Moscow Institute of Physics and Technology, Dolgoprudny 141700 Russia

e-mail: baranov.mipt@gmail.com

Chirality is a universal geometric property of an object to be not compatible with its reflection by a series of rotations and translations in 3D. Chirality is common among various biological molecules and qualitatively changes the optical response of media containing chiral elements. When acting on a biological receptor, opposite enantiomers of the same molecule can cause different responses. This circumstance is even more critical for pharmaceuticals, where the opposite enantiomer of a medicinal molecule can be toxic. Thus, the development of technologies related to the separation of chiral enantiomers is critically important for modern biotechnology, pharmacology, and medicine.

Interaction of chiral matter with circularly polarized electromagnetic fields leads to the effect of circular dichroism, which underlies numerous methods for distinguishing molecular enantiomers. Enhancement of circular dichroism effects is usually achieved by interaction of chiral molecules with optical resonators. In this context, the problem of development of optical resonators that could selectively interact only with a given molecular enantiomer, and the search for novel fundamental effects in this family of physical systems presents a challenging and highly relevant problem.

In this talk, I will overview the fundamentals of chirality of light and matter, present optical designs required for realization of chiral polaritonic states, discuss recently developed theoretical models, and speculate on the exciting phenomena that can be enabled by strong coupling between chiral light and matter. I will present various strategies to the design of handedness preserving mirrors, in particular ones based on low-symmetry resonant dielectric metasurfaces, as well as the ones based on helical van der Waals homostructures with chiral properties that do not call for sophisticated nanofabrication techniques. Finally, I will highlight recent theoretical efforts indicating that chiral polaritonic systems may feature non-trivial optical phenomena, where the interplay of light and matter chirality plays the key role in determining not only its elastic its response to external electromagnetic fields, but also the asymmetry of the ground (vacuum) state of a chiral system with respect to the molecular handedness.

The work was supported by the Russian Science Foundation (grant No. 23-72-10005).

Study of chiral polariton spectra in asymmetric optical resonators

O. I. Blokhin, D. G. Baranov

Moscow Institute of Physics and Technology, Dolgoprudny, 141700 Russia

e-mail: blokhin.oi@phystech.edu

Light–matter coupling is at the heart of many optical phenomena. Polaritons are eigenstates with mixed photonic–material character, merging the properties of photonic and electronic excitations. Owing to this hybrid nature, polaritons open new avenues for controlling electronic transport and even chemical kinetics [1].

The study of chiral polaritons focuses on the interaction of chiral matter with electromagnetic modes of a defined handedness formed in purpose-designed resonators [2]. Unlike conventional cavities, which are symmetric with respect to a change in light polarization, the asymmetric cavity of [2] enhances coupling with a selected enantiomer. This cavity supports only a right-handed circularly polarized mode; placing a Pasteur medium (containing a single molecular enantiomer) inside it yields a chiral polariton state through coupling between the cavity mode and the medium.

In contrast to the quantum description that treats the collective interaction of many quantum emitters with a cavity [3], we adopt a classical approach that considers the macroscopic medium and classical fields, allowing a more transparent analysis of polaritonic-mode formation. Spectral analysis reveals a mode anti-crossing manifested by a change in dispersion relations as the medium parameters vary. This behavior signals strong coupling between the corresponding resonant states, leading to a restructuring of the eigenmode spectrum.

The authors acknowledge the help of RSF Grant №23-72-10005.

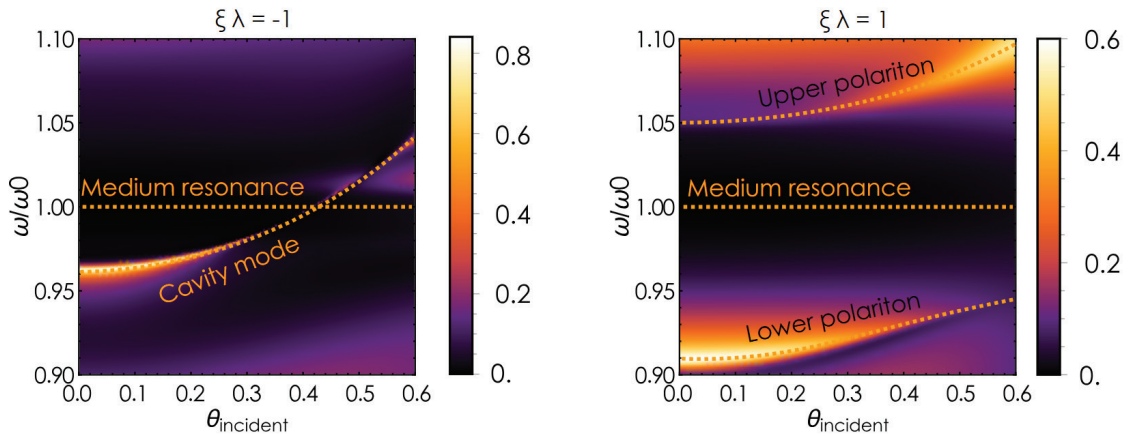

[1] D. G. Baranov et al., "Towards Molecular Chiral Polaritonics" ACS Photonics, 10, 8, 2440–2455 (2023).
[2] K. Voronin, Single-Handedness Chiral Optical Cavities, ACS Photonics, 9, 8, 2652–2659 (2022).
[3] C. Schäfer, Chiral Polaritonics: Analytical Solutions, Intuition, and Use, J. Phys. Chem. Lett., 14, 15, 3777–3784 (2023).

Nanowire heterostructures: nanophotonics and bioimaging

A. Bolshakov[1,2]

1- Centre for Photonics and Two-Dimensional Materials, Moscow Institute of Physics and Technology, Dolgoprudny, 141701 Russia
2- Alferov University, St. Petersburg, 194021 Russia

e-mail: bolshakov@live.com

Semiconductor nanowire (NW) heterostructures have emerged as a versatile platform for nanophotonic and bioimaging applications due to their unique geometry, tunable optical properties, and biocompatibility. As quasi-one-dimensional nanostructures, NWs exhibit exceptional waveguiding, light confinement, and emission characteristics, making them ideal for nanoscale photonic devices, including lasers, sensors, and waveguides. Concurrently, their ability to interact with biological systems enables novel approaches to intracellular imaging, transfection, and cellular mechanics studies. This work explores the functionality of NW heterostructures, highlighting their potential in next-generation optoelectronic devices and biomedical applications.

The optical properties of semiconductor NWs can be precisely engineered through heterostructuring, enabling tailored light-matter interactions. For instance, GaP/GaPAs NWs exhibit direct bandgap transitions, facilitating efficient luminescence for nanophotonic applications. By controlling NW diameter and length, Fabry-Pérot resonances and waveguide modes can be optimized, enhancing light emission and lasing performance. Recent advances demonstrate that NW-based nanolasers operate at ultralow thresholds due to their high-quality optical cavities and strong gain confinement. Additionally, NW heterostructures support subwavelength light manipulation, enabling on-chip photonic circuits and integrated optical sensors. The ability to grow vertical NW arrays on silicon substrates further facilitates their integration with existing semiconductor technologies, paving the way for scalable nanophotonic devices.

Beyond photonics, NW heterostructures offer unprecedented opportunities in bioimaging and intracellular studies. Vertical NW arrays interact dynamically with live cells, penetrating membranes without external stimuli and enabling efficient transfection. Studies show that cells cultivated on GaP NWs remain viable for extended periods (up to 7 days), even after internalizing and fragmenting the NWs. Remarkably, intracellular NWs undergo chemical modifications, detectable via luminescence red-shifts, providing real-time insights into cellular processes. Furthermore, NWs are redistributed within cells – aligned along the nuclear periphery or extruded into pseudopodia – revealing complex intracellular mechanics. These interactions suggest that NWs can serve as both mechanical probes and optical labels, enabling high-resolution imaging and force sensing at the single-cell level.

Future research may focus on optimizing NW biocompatibility, enhancing emission properties for in vivo imaging, and developing hybrid NW-based devices that combine sensing, actuation, and optical readout. By bridging nanophotonics and biotechnology, NW heterostructures are poised to enable breakthroughs in both fundamental research and clinical applications.

The author acknowledges the Russian Science Foundation (Grant 24-12-00225).

Photonic crystal properties of a wax layer: from morphology to biological functions

E. R. Bukhanov[1,2], A. D. Shefer[2], A. V. Shabanov[1], Yu. L. Gurevich[2], M. N. Krakhalev[1]

1- L. V. Kirensky Institute of Physics, Siberian Branch, Russian Academy of Science, Akademgorodok 50/38, Krasnoyarsk, 660036 Russia
2- Federal Research Center Krasnoyarsk Scientific Center, Russian Academy of Sciences, Siberian Branch, Akademgorodok 50, Krasnoyarsk, 660036 Russia

e-mail: eugene.bukhanov@iph.krasn.ru

In recent decades, nanophotonics has been actively progressing as an interdisciplinary field that studies how the light interacts with nanostructures which dimensions are comparable to the radiation wavelength. Some biological systems attract special attention of scientists. Among them are butterfly wings, opals and plant tissues that were evolutionarily optimized for efficient control of light fluxes, as evidenced by numerous studies of photonic crystals in them [1]. Epicuticular wax, which forms complex surface structures with characteristic sizes of 100–500 nm [2], can possibly show unique optical properties [3], although its role as a biological photonic crystal has not been studied enough yet. In the context of modern "green" photonics trends, the study of such biological systems can become particularly important as it offers new principles for the creation of environmentally friendly optical materials. Due to the growing interest in biomimetic approaches in nanotechnology, where natural systems serve as prototypes for the development of artificial metamaterials, these studies are seen as even more relevant.

We have performed comprehensive research of the optical and spectral properties of blue spruce epicuticular wax. The studies focused on the structural features that determine its unique characteristics. The main finding is that optical effects observed are caused by the complex morphology of the wax layer and not by its chemical composition. Electron microscopy revealed quasi-ordered structures formed from hollow tubes with a diameter of ~150 nm and a length of a few μm. Periodic layers of wax and air, which are formed in these structures, significantly affect light propagation. Optical observations confirmed that blue colour of spruce needles is due to diffraction and not the pigments containing in it. It was later confirmed by spectral analysis of the wax extracts, which showed no significant absorption in the visible area. The wax particles show optical anisotropy and structural coloration that is similar to cholesteric liquid crystals. These properties become vivid as the colour changes when observed in reflected and transmitted light.

Numerical modeling of photonic crystals based on wax parameters has revealed the presence of band gaps in the blue area of the spectrum corresponding to the observed plant coloration. Spectrofluorimetric research has shown that the wax can fluoresce under UV excitation. An essential result is how the wax layer influences photosynthetic efficiency: the width of the fluorescence peak of PC II (680 nm) decreases in the presence of wax, therefore indicating an acceleration of energy transfer between photosystems. The study demonstrates the key role of structural features of epicuticular wax in its optical properties formation and adaptation to environmental conditions.

The results obtained are not only significant for fundamental understanding of how the light interacts with biological systems but also can be applied for producing new biomimetic materials with specified optical characteristics.

[1] D. Lee, Nature's palette: the science of plant color (University of Chicago Press), 2019.
[2] S. Jacquemoud and S. Ustin, Leaf optical properties (Cambridge University Press), 2019.
[3] E.R. Bukhanov, A.D. Shefer, A.V. Shabanov, Yu.L. Gurevich, M.N. Krakhalev, Optical and spectral characteristics of epicuticular wax of blue spruce needles, Sibirskij Lesnoj Zurnal, pp. 97–106 (2024).

Role of cross-relaxation in the formation of the luminescent response of $NaYF_4$:Yb/Tm nanoluminophores at high excitation intensities

S. Burikov, A. Fedyanina, T. Dolenko

Department of Physics, Lomonosov Moscow State University, Leninskiye Gory 1/2, Moscow, 119991 Russia

e-mail: sergey.burikov@gmail.com

Recently, nanocomplexes based on lanthanide ions have been of great interest due to the possibility of implementing upconversion luminescence under infrared excitation [1]. This opens up wide opportunities for their use in various, primarily biomedical, applications, since in this case there is no need to separate the photoluminescence signal of nanoparticles from the background of autoluminescence of biological medium. Such complexes consist of the inert matrix doped with two types of lanthanide ions, one of which (sensitizer) absorbs exciting radiation in the IR range, transmits it to the other (activator), which, in turn, emits luminescence in the visible range of the spectrum. The key parameters determining luminescence response of these complexes are intensity of excitation radiation and concentrations of activators and sensitizers.

The paper presents results of the study of the dependences of the intensity of upconversion luminescence of $NaYF_4:Yb^{3+}/Tm^{3+}$ nanoluminophores in dimethyl sulfoxide on the intensity of powerful pulsed laser excitation at different concentrations of activators and sensitizers. The luminescence spectrum of such nanoparticles consists of a set of bands in the visible and near-infrared regions of the spectrum. Bands near 450 nm and 475 nm are of great interest because ratio of their intensities is sensitive to ambient temperature. This opens up the possibility of creating a temperature nanosensor [2].

It was found that at low concentrations of activators, the ratio of the intensities of the luminescence bands in the region of 450 and 475 nm does not depend on the intensity of optical excitation. An explanation of the obtained results is proposed, in which the process of cross-relaxation between thulium ions plays a key role.

The obtained results allow to conclude that elaboration of the versatile temperature nanosensor based on $NaYF_4:Yb^{3+}/Tm^{3+}$ nanoluminophores assumes sensing by short, intense laser pulses, and use of nanoparticles with low thulium concentration.

The study was supported by the Russian Science Foundation grant No. 25-22-00411, https://rscf.ru/en/project/25-22-00411.

[1] Auzel, F. Upconversion and Anti-Stokes Processes with f and d Ions in Solids. Chemical Reviews, 104(1), 139–174, (2003).
[2] Burikov, S. A., Sarmanova, O. E., Fedyanina, A. A., Plastinin, I. V., & Dolenko, T. A. A step towards versatile temperature luminescent nanosensor: Combination of luminescent and time-resolved spectroscopy of $NaYF_4:Yb^{3+}/Tm^{3+}$ nanoparticles. Spectrochimica Acta Part A: Molecular and Biomolecular Spectroscopy, 334, 125902, (2025).

1D and 2D materials for applications in photonics

A. Chernov[1,2]

1- Russian Quantum Center, Skolkovo Innovation City, Moscow, 121205 Russia
2- Center for Photonics and 2D Materials, Moscow Institute of Physics and Technology (National Research University), Dolgoprudny, 141700 Russia

e-mail: ach@rqc.ru

We demonstrate two examples of applications of low-dimensional materials in photonics. In the case of 1D materials – single-walled carbon nanotubes (SWCNTs), we developed a novel approach to efficiently increase a photoluminescence (PL) signal from individual SWCNTs by their surface protection with SiO_2 nanolayer synthesized by a modified Stöber method. The aryl functionalized (6,5)-SWCNTs covered with silicon dioxide layer demonstrate emission peaks from individual defect sites in the spectral range of 1100–1300 nm. Since the PL signal strongly depends on the local dielectric environment, the silicon dioxide shell and its formation condition create favorable conditions for the configurations with red-shifted emission (E11**, ortho+) at ~1260 nm [1]. This approach offers strong potential for sp^3 defects on larger diameter nanotubes in the development of room temperature quantum light sources capable of operating at telecommunication wavelengths.

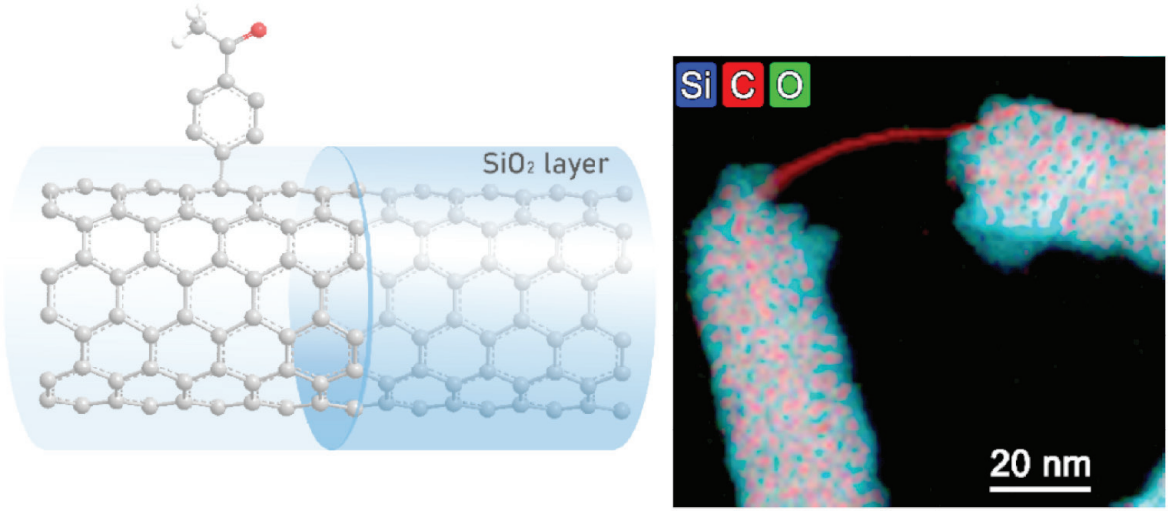

Fig. 1. Sp^3-modified SWCNT protected by SiO_2 layer (left) and color-coded STEM-EELS elemental map demonstrating a uniform coating by amorphous silica.

Two-dimensional materials have attracted much attention due to various opportunities for applications. Enhanced infrared photodetection in graphene-based heterostructures due to tunneling barriers has been recently demonstrated [2]. Stacking of van der Waals materials enables various degrees of freedom for properties control. We study several types of devices based on graphene for enhanced infrared photodetection. One of them is the small-angle twisted bilayer graphene (tBLG). It attracts much attention due to appearance of low-energy flat bands. We demonstrate the gate-tunable photoresponse and find the peculiarities at integer band fillings upon linear and circular excitation [3]. The origin of the photodetection may stem from the bulk photovoltaic effect.

[1] Sergey A. Dozmorov, Polina M. Kalachikova, Anastasia E. Goldt, Yuriy G. Gladush, Aliya R. Vildanova, Fedor M. Maksimov, Alexander I. Chernov, Albert G. Nasibulin, Photoluminescene from pristine and functionalized SWCNTs coated by silica, Surfaces and Interfaces, 68, 106674, (2025).
[2] D.A. Mylnikov, M.A. Kashchenko, K.N. Kapralov, D.A. Ghazaryan, E.E. Vdovin, S.V. Morozov, K.S. Novoselov, D.A. Bandurin, A.I. Chernov, and D.A. Svintsov, Infrared photodetection in graphene-based heterostructures: bolometric and thermoelectric effects at the tunneling barrier. npj 2D Materials and Applications, 8(1), p.34, (2024).
[3] Alexei V. Shupletsov, Dmitry A. Mylnikov, Dmitry A. Svintsov et al., Infrared responsivity signatures of valley degeneracy in twisted bilayer graphene at filling factors ±1. (submitted)

Nonlinear response of one-dimensional photonic crystal with cavity polaritons

O. A. Dmitrieva[1,2], S. G. Tikhodeev[1–3]

1- Lomonosov Moscow State University, GSP-1, Leninskie Gory, Moscow, 119991 Russia
2- Skolkovo Institute of Science and Technology, Bolshoy Boulevard 30, bld. 1, Moscow, 121205 Russia
3- Prokhorov General Physics Institute of the RAS, GSP-1, Vavilova str. 38, Moscow, 119991 Russia

e-mail: dmitrieva.oa16@physics.msu.ru

Recently optical structures with cavity polaritons are attracting interest [1–5]. In such structures, due to nonlinearity, a shift of the resonant frequency is observed with a change in pumping intensity, which can lead to bi- and multi-stability of the response. Various designs of such systems are being considered in literature, manufactured on the basis of microcavities, plasmon gratings, photonic crystalline layers, etc. [4].

It is known that with an increase in the pumping intensity and a corresponding increase in exciton density, the interaction between excitons leads to a blue shift in the resonant frequency. In the case of chiral systems, the asymmetry between the states of light with right and left circular polarization leads to sharp changes in the intensity and degree of circular polarization of the response when the intensity of external pumping increases at a frequency close to the resonant frequency of the system in the linear case [5].

In this paper, we study the optical response of a structure similar to the one proposed in [4]. It is a layer of a one-dimensional photonic crystal on a substrate interacting with exciton polaritons in a homogeneous layer deposited on its surface. Fourier modal decomposition and the optical scattering matrix method were used to analyze the optical properties of the system [6, 7]. This approach makes it possible to analyze the linear response of layered structures.

To account for the nonlinear effects associated with the interaction between excitons, a self-consistent calculation method was developed, in which the nonlinearity appeared in altered values of the dielectric susceptibility in a layer containing cavity polaritons. Namely, for these pumping parameters, a certain initial value of this dielectric susceptibility was selected. For this value, the electric field distribution was calculated using the scattering matrix method, then the corresponding dielectric susceptibility of the exciton layer was calculated using known field distribution, taking into account the blue shift of the resonant frequency. The deviation of the resulting dielectric susceptibility from the initial one was minimized by the Newton's method.

As a result of the calculation, the dependences of the intensity of the exciton density in the system on the frequency and intensity of pumping, as well as the distribution of the electric field in the exciton layer, were obtained.

In the structure under consideration, resonances are associated with a standing wave, leading to a strong field inhomogeneity in the plane of the system. Therefore, unlike the microcavity, which we discussed earlier [5], in this case, the electric field cannot be considered to depend only on the coordinate, which varies along the normal to the structure. Therefore, the calculation also took into account the inhomogeneity of the electric field and exciton density in the plane of the structure. In the future, it is planned to use the developed approach to analyze similar chiral systems with the ability to control the degree of circular polarization of the response.

[1] N. A. Gippius, S. G. Tikhodeev, V. D. Kulakovskii et al., Nonlinear dynamics of polariton scattering in semiconductor microcavity: Bistability vs. stimulated scattering, Europhys. Lett., 67, 997–1003 (2004).
[2] N.A. Gippius, I.A. Shelykh, D.D. Solnyshkov et al., Polarization Multistability of Cavity Polaritons, Phys. Rev. Lett., 98, 236401–236404 (2007).
[3] S. S. Gavrilov "Nonequilibrium transitions, chaos, and chimera states in exciton–polariton systems" Phys. Usp. 63 123–144 (2020).
[4] Kravtsov et al., Nonlinear polaritons in a monolayer semiconductor coupled to optical bound states in the continuum, Light: Science & Applications, 9, 56 (2020).
[5] O. A. Dmitrieva, N. A. Gippius, and S. G. Tikhodeev, Multistability in a chiral semiconductor microcavity, Doklady Rossijskoj akademii nauk. Fizika, tehnicheskie nauki, 510, 10–15 (2023).
[6] Whittaker D.M., Culshaw I.S., Scattering-matrix treatment of patterned multilayer photonic structures, Phys. Rev. B, 60, 15, 2610–2618 (1999).
[7] Tikhodeev S.G., Yablonskii A.L., Muljarov E.A., Gippius N.A., Ishihara T., Quasiguided modes and optical properties of photonic crystal slabs, Phys. Rev. B, 66, 4, 045102–045118 (2002).

1D-2D laser-induced periodic surface structures on titanium metal films and phase change materials produced by femtosecond laser pulses

V. Fedyaj[1,2], K. Bronnikov[3], V. Terentyev[1], V. Simonov[1], A. Simanchuk[1], S. Babin, A. Zhizhchenko[4], A. Yakubov[5], P. Lazarenko[5], A. Kuchmizhak[4,6], A. Dostovalov[1,2]

1- Institute of Automation and Electrometry SB RAS, Russia
2- Novosibirsk State University, Novosibirsk, Russia
3- ITMO University, Saint Petersburg, Russia
4- Institute of Automation and Control Processes of the FEB RAS, Radio st. 5, Vladivostok, 690041 Russia
5- National Research University of Electronic Technology, Zelenograd, 124498 Russia
6- Far Eastern Federal University, Vladivostok, 690041 Russia

e-mail: dostovalov@iae.nsk.su

Laser-induced periodic surface structures (LIPSS) formed via ablation-free mechanisms have attracted significant attention in recent years due to outstanding regularity of the structures obtained either as a result of thermally stimulated chemical reaction of oxidation in case of metals [1], sublimation or phase transition from amorphous to crystalline one in case a-Ge [2] and a-Si thin films [3], respectively. In addition, owing to single step, vacuum-free and low-cost approach, surface nanostructuring based on LIPSS provides opportunities for the widespread applications in photonics, biomedicine, and sensing [4]. Moreover, 2D LIPSS, which exhibit periodicity along orthogonal directions, enables additional capabilities for applications demanding spatially uniform properties [5, 6].

In this study, we report the formation of highly regular 1D and 2D LIPSS including square and hexagonal lattice geometries on Ti and phase-change materials ($Ge_2Sb_2Te_5$) (GST) thin films under impact of femtosecond laser radiation. The optimal regimes for laser induced oxidation in case of Ti and local crystallization of a-GST thin film were reviled.

The diversity applications in fiber optics of proposed highly regular 1D LIPSS induced on the optical fiber tip and polished D-shaped fiber were demonstrated. In particular, TLIPSS on fiber tip facilitates light out- and in-coupling at extremely large angle (>50 degree). In the second case, the extremely high regular TLIPSS formed on fiber polished area enables resonant reflection for fundamental mode propagating in the fiber core at both cases of Ti and GST thin films deposited on D-shape fiber, which is promising for tunable, rewritable spectral filters in integrated photonic systems.

The work was supported by the Russian Science Foundation grant (No. 21-72-20162-P). In the research, we used the equipment of the following Multiple-Access Centres (MAC): MAC of the Far Eastern Federal University (FEFU), MAC "High-resolution spectroscopy of gases and condensed matters" at IAE SB RAS, MAC of the Novosibirsk State University (NSU).

[1] K. Bronnikov et al, Regulating Morphology and Composition of Laser-Induced Periodic Structures on Titanium Films with Femtosecond Laser Wavelength and Ambient Environment, Nanomaterials 12, 306 (2022).
[2] K. Bronnikov et al, Highly regular nanogratings on amorphous Ge films via laser-induced periodic surface sublimation, Optics & Laser Technology 169, 110049 (2024).
[3] A. Dostovalov et al, Hierarchical anti-reflective laser-induced periodic surface structures (LIPSSs) on amorphous Si films for sensing applications, Nanoscale 12, 13431–13441 (2020).
[4] Bonse et al, Handbook of Laser Micro- and Nano-Engineering (Springer International Publishing), Laser-Induced Periodic Surface Structures (LIPSS), (2020).
[5] S. Durbach et al., Laser-driven self-organized evolution of 1D- and 2D-Nanostructures from metal thin-films on silicon: Influence of alloying and oxidation, Applied Surface Science, 622 (2023).
[6] Q. Ibrahim et al., Laser fabrication of 1D and 2D periodic subwavelength gratings on titanium films, Optics & Laser Technology, 174 (2024),
[7] K. Bronnikov et al, Highly Regular Laser-Induced Periodic Surface Structures on Titanium Thin Films for Photonics and Fiber Optics, ACS Applied Materials & Interfaces 16 (50), 70047–70056 (2024).

Flexible diffraction microgratings fabricated from photopolymer with magnetic nanoparticles

A. Yu. Frolov, A. V. Buldakova, K. K. Kaver, V. V. Tolmacheva, M. I. Sharipova, A. A. Fedyanin

Lomonosov Moscow State University

e-mail: frolovay@my.msu.ru

The two-photon photopolymerization has found many applications in the fabrication of photonic devices, such as microlenses, metasurfaces photonic crystals, SNOM cantilevers, among others [1]. The incorporation of magnetic nanoparticles into photopolymers results in the flexibility of the microstructures when an external magnetic field is applied. The magnetic field tunable microlenses [2], magnetic field fiber-based sensors [3], and optical choppers [4] have been fabricated by using the magnetic photopolymer composites.

In this work we demonstrate the fabrication of diffraction microgratings by two photon photopolymerization technique. These gratings are made from a magnetic photopolymer composite, consisting of commercially available SZ-2080 photopolymer and superparamagnetic nanoparticles (Fe_3O_4), with concentrations ranging from 1% to 5%. The average diameter of Fe_3O_4 nanoparticles is 16 nm. The grating shapes are shown in Fig. 1 (a and b). The first grating has a periodic pattern that resembles a "snake". The second grating has a pattern that is similar to an "accordion". The period of both gratings is 3 μm. The periodic part of the grating is fixed between two stages. One stage is attached to the glass substrate while the other has a gap between it and the glass substrate. Under external magnetic field, these diffraction microgratings can shrink, stretch, and bend. This ability is also confirmed by simulations using the Comsol Multiphysics software. Due to this tunabilty, the diffraction order is deflected when an external magnetic field is applied.

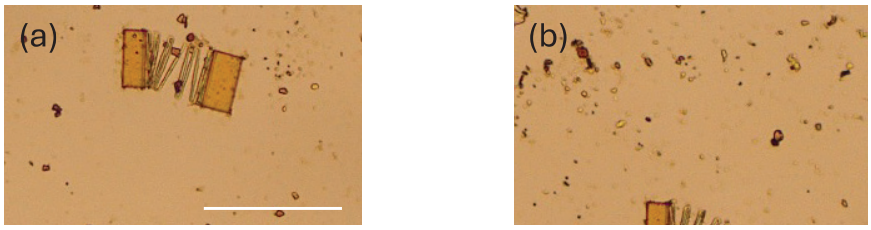

Fig. 1. Diffraction micrograting fabricated from magnetic photopolymer composite. The scale bar is 200 μm.

[1] H. Yu, Q. Du, C. R. Mendonca, L. Ranno, J. Hu, T. Gu, J. Hu, Two-photon lithography for integrated photonic packaging, Light: Advanced Manufacturing, vol. 4, (2023)
[2] V. Vieille, R. Pétrot, O. Stéphan, G. Delattre, F. Marchi, M. Verdier, O. Cugat, T. Devillers, Fabrication and magnetic actuation of 3D-microprinted multifunctional hybrid microstructures, Advanced Materials Technologies, vol. 5, (2020).
[3] H. Huang, C. Liao, M. Zou, D. Liu, S. Liu, Y. Wang, Z. Bai, D. Liu, B. Li, J. Huang, F. Wang, J. Zhou, C. Zhao, X. Weng, L. Liu, J. Qu, Y. Wang, Four-dimensional printing of a fiber-tip multimaterial microcantilever as a magnetic field sensor, vol. 10, pp. 1916-1924, (2023).
[4] X. Lei, S. Peng, Y. Niu, S. Sun, Y. Zhu, J. Qiu, Magnetically driven micro-optical choppers fabricated by two-photon polymerization, Optics Letters, vol. 48, pp. 835-838, (2023).

Near- and mid-infrared optoelectronics with nanostructured silicides

V. Il'yaschenko[1], Yu. Borodaenko[1], A. Cherepakhin[1], D. Pavlov[1], D. Banniy[1,2], A. Bozhok[1,2], H. Zhou[3], Sh. Dou[3], Y. Li[3], A. Shevlyagin[1], A. Kuchmizhak[1,2]

1- Institute of Automation and Control Processes, FEB RAS, Vladivostok, Russia
2- Far Eastern Federal University, Vladivostok, Russia
3- Center for Composite Material and Structures, Harbin Institute of Technology, Harbin, P. R. China

e-mail: shevlyagin@iacp.dvo.ru

The modern landscape of optoelectronics and photonics is dominated by emerging materials such as perovskites and two-dimensional transition metal chalcogenides. This is because silicon (Si) technology has drawbacks such as an indirect band gap, low optical absorption in the near-infrared, and isotropic optical properties due to crystal symmetry. Fortunately, there is a class of materials called silicides that could provide solutions for almost any optoelectronic application. The diversity of their semiconducting and semimetallic phases enables the creation of structures with different functionalities, such as transparent conducting electrodes [1], optical absorbers [2], and polarisation-sensitive media, to name a few. In this regard, laser-induced nanostructuring, as a low-cost, scalable and highly precise technology, could breathe new life into the Si-silicide hybrid approach, resulting in the fabrication of diverse optoelectronic and nanophotonic devices, including advanced photodetectors, third-generation solar cells and dynamic optical filters. Here, we review the recent progress of laser processing technology applied to a Si platform [3, 4], the chemical-based route for producing nanostructured silicides [5, 6], and the hybrid bottom-up approach, in which laser-induced Si surface structures are used as templates for silicidation to create functional layers with unique modalities. For example, we have demonstrated a mesh-type transparent electrode made of calcium disilicide using laser projection lithography [7]. It can be used as the top electrode in a Si photodetector and as a highly efficient microheater. It can also be used as part of a dynamic mid-infrared (MIR) optical limiter. When integrated with phase-changing vanadium dioxide [8], it enables electrothermal switching of the metal-insulator transition. Another example is a Si polarisation-sensitive photodetector with magnesium silicide coating, which demonstrates expanded operation spectral region down to 2000 nm and preserved both high photoresponse and polarization sensitivity.

This work was supported by the Russian Science Foundation under the Grant № 24-72-10078 (https://rscf.ru/project/24-72-10078).

[1] A. Shevlyagin et. al, Semimetal hR6-$CaSi_2$ thin film: a transparent contact for Si optoelectronics, J. Alloy. Compd. Vol. 910, 164893 (2022).
[2] A. Shevlyagin et. al, Probing the Mg_2Si/Si (111) heterojunction for photovoltaic applications, Sol. Energy, Vol. 211, pp. 383–395 (2020).
[3] Yu. Borodaenko, et. al, Liquid-Assisted Laser Nanotexturing of Silicon: Onset of Hydrodynamic Processes Regulated by Laser-Induced Periodic Surface Structures, Adv. Mater. Tech. Vol. 9(8), 2301567 (2024).
[4] Yu. Borodaenko, et. al, Polarized p–n junction Si photodetector enabled by direct laser-induced periodic surface structuring, Surf. Inter. Vol. 56, 105568 (2025).
[5] A. Shevlyagin et. al, Mg_2Si is the new black: Introducing a black silicide with >95% average absorption at 200–1800 nm wavelengths, Appl. Surf. Sci. Vol. 602, 154321 (2022).
[6] A. Shevlyagin et. al, Textured Stainless Steel as a Platform for Black Mg_2Si/Si Heterojunction Solar Cells with Advanced Photovoltaic Performance, Materials Vol. 15(19), 6637 (2022).
[7] D. Pavlov et. al, Transparent Microheater Enabled by Laser Perforation of the Thin $CaSi_2$ Film, Bull. Russ. Acad. Sci. Phys. Vol. 88, pp. S418–S422 (2024).
[8] D. Pavlov et. al, Anisotropic Vanadium Dioxide Nanogratings by Direct Laser-Induced Periodic Surface Structuring (LIPSS), J. Phys. Chem. Lett. Vol. 16, pp. 4969–4974 (2025).

Erbium waveguide amplifier based on new nanocomposite materials for telecommunication C-band 1530–1565 nm

K. V. Khaydukov, P. A. Demina, I. O. Goriachuk, V. I. Sokolov

National Research Centre «Kurchatov Institute», Akademika Kurchatova sq. 1, Moscow, 123182 Russia

e-mail: haidukov_11@mail.ru

The development of modern high-speed integrated optics requires the creating compact waveguide amplifiers for the telecommunication C-wavelength range (1530–1565 nm), which can be integrated into various photonic devices [1]. The formation of such amplifiers based on nanocomposites consisting of polymer matrix with embedded lanthanide doped nanoparticles (NPs), possessing intense down-conversion photoluminescence (PL) around 1530 nm, is attracting increasing interest.

In this work, we show the new technical methods for fabricating compact high-efficiency single mode waveguide amplifiers with high optical gain. For that, nanoparticles with the host matrix $NaYbF_4$ co-doped with Er^{3+} and Ce^{3+} ions were synthesized. The embedding of Ce^{3+} ions into crystalline NP matrix leads to the suppression of Er^{3+} upconversion PL, boosting NPs photoluminescence intensity near 1530 nm, while its coating with the inert $NaYF_4$ shell significantly increases the overall PL intensity of the nanoparticles. Single-mode waveguides made from SU-8 polymer with embedded α-$NaYbF_4$:Er^{3+}, Ce^{3+}@$NaYF_4$ nanoparticles were fabricated by photolithography technique. The combination of optically transparent SU-8 polymer, optimal concentration of $NaYbF_4$:Er^{3+}, Ce^{3+}@$NaYF_4$ nanoparticles with an average size of 30 nm in the polymer matrix, as well as theoretically calculated cross section of the waveguide ensure minimum losses in the C-band due to absorption and scattering. A relative gain of 28 dB/cm was demonstrated for the 1.5 cm long waveguide amplifier when pumped with 975 nm laser at 280 mW power. The results demonstrate that α-$NaYbF_4$:Er^{3+}, Ce^{3+}@$NaYF_4$ nanoparticles embedded in the SU-8 polymer matrix are promising for fabricating compact C-band waveguide amplifiers in integrated optical interconnects on the printed circuit board.

The work was carried out within the state assignment of NRC «Kurchatov Institute».

[1] X. Zhai etc. Enhancement of 1.53 μm emission band in $NaYF_4$:Er^{3+},Tb^{3+},Ce^{3+} nanocrystals for polymer-based optical waveguide amplifiers. Optical Materials Express, Vol. 3, No. 2, p. 270, (2013).

All-optical image classification using Fourier-space diffractive neural network

A. Konovalova[1], A. Popkova[1,2], D. Pechkurova[1], T. Baluian[1,2], A. Fedyanin[1]

1- Lomonosov Moscow State University, Department of Physics, Leninskie gory 1, Moscow, 119991 Russia
2- AMSU-BIT University Shenzhen, Department of Materials Science, Shenzhen, 517182 P.R.C

e-mail: konovalova.av18@physics.msu.ru

Neuromorphic photonics is gaining traction as a prospective alternative to electronic processors in machine learning applications. Photonics offers several advantages over electronics. These include low heat loss, high speed and throughput, and the ability to implement parallel computing through the use of various degrees of freedom inherent in light signals (wavelength, polarization, and mode). The use of photonic technologies to construct optical neural networks has the potential to enhance the speed and energy efficiency of computations. Furthermore, it can facilitate the development of neuromorphic architectures that differ fundamentally from the von Neumann architecture.

Among the various optical neuromorphic architectures, diffractive neural networks (DNNs) are particularly notable for their suitability for matrix computations and all-optical image processing [1]. In these networks, amplitude or phase masks function as layers. The parameters of the masks serve as trainable synaptic weights. These weights are determined during computer-based model optimization.

In this work, we investigate a Fourier diffraction neural network [2] for the classification of hand-written digits (MNIST dataset) in the visible spectral range. Signal modulation in the network is achieved through phase masks fabricated via two-photon laser lithography – a technique well-established for manufacturing photonic devices, including optical linear perceptrons [3]. We investigate the optimization of the diffraction network's macroparameters and explore modeling techniques to enhance performance, while accounting for the constraints imposed by the phase mask fabrication process.

The work was supported by the Foundation for the Development of Science and Education "Intellect".

[1] X. Lin, Y. Rivenson, N.T. Yardimci, M. Veli, et.al., All-optical machine learning using diffractive deep neural networks, Science, vol. 361 (6406), pp. 1004–1008, (2018).
[2] T. Yan, J. Wu, T. Zhou, H. Xie, et.al., Fourier-space diffractive deep neural network, Phys. Rev. Lett., vol. 123 (2), p. 023901, (2019).
[3] E. Goi, X. Chen, Q. Zhang, et.al., Nanoprinted high-neuron-density optical linear perceptrons performing near-infrared inference on a CMOS chip, Light Sci. Appl., vol. 10 (1), p. 40, (2021).

Using single upconversion $NaYF_4$:Yb,Er nanoparticle as multifunctional luminescent sensor

A. Leontyev, L. Nurtdinova, E. Mityushnkin, A. Shmelev, D. Zharkov, A. Chuklanov, N. Nurgazizov, V. Nikiforov

Zavoisky Physical-Technical Institute, FRC Kazan Scientific Center of RAS, Sibirsky tract 10/7, Kazan, 420029 Russia

e-mail: vgnik@mail.ru

Rare earth doped micro/nano crystals have become a topic of interest due to their potential use as probes for monitoring environmental parameters, super-resolution imaging, and precision tracking, especially for biological applications. This report discusses the possibility of fabricating a single multi-functional sensor based on $NaYF_4$:Yb,Er nanocrystals. These luminophores are known to have efficient luminescence in the visible spectrum when irradiated with a wavelength of 980 nm, allowing them to be used as biosensors that operate within the "transparency window" of biological tissue. The choice of a fluoride matrix for the luminophores is based on their high chemical stability and low crystal lattice phonon energy (~300 cm^{-1}), which contributes to their high quantum yield of luminescence by minimizing nonradiative multi-phonon relaxation. The synthesis of $NaYF_4$:Yb,Er nanocrystals was carried out using a proven hydrothermal method with oleic acid as a stabilizer. This method allows for the control of the size and shape of the nanoparticles. The selection and positioning of individual nanoparticles on a substrate was performed using atomic force microscopy. The luminescence properties of a single phosphor were investigated using a confocal microscope in a photon counting regime. Studies showed that the spectral characteristics of $NaYF_4$:Yb,Er upconversion phosphors are sensitive to temperature and intensity of exciting radiation. Additionally, a strong polarization dependence of luminescence was observed depending on the orientation of the crystal axis of the $NaYF_4$:Yb,Er nanoparticles. We propose a method for calibrating the luminescence characteristics of the upconversion phosphor $NaYF_4$:Yb,Er, making it a single multifunctional sensor capable of measuring local temperature, sensor orientation, and exciting radiation intensity.

This work was performed at Zavoisky Physical-Technical Institute with support from the Russian Science Foundation's grant No. 23-42-10012 (https://rscf.ru/en/project/23-42-10012).

Photo- and electroluminescence of color centers in CVD diamond nanostructures

M. A. Lobaev, A. L. Vikharev, D. B. Radishev, A. M. Gorbachev, S. A. Bogdanov, V. A. Isaev, M. N. Drozdov

Institute of Applied Physics RAS, Ul'yanov Street 46, Nizhny Novgorod, 603950 Russia

e-mail: val@ipfran.ru

Currently, research on quantum technologies is actively developing, including the use of color centers in diamond. Color centers in diamond are defects of the crystal lattice, usually in the form of an impurity atom and a vacancy. Nitrogen NV, silicon SiV and germanium GeV centers in diamond are widely studied. They are created by the ion implantation method, as well as by the CVD method directly during the process of diamond growth in microwave plasma assisted CVD reactors. To localize the centers, 3-D structures (nanopillars, nanopyramids) are formed on the surface of the crystal.

The report presents an overview of the results of studies conducted at the IAP RAS and devoted to various aspects of studying color centers in CVD diamond [1–10]. The incorporation of nitrogen and silicon into CVD diamond to form NV and SiV centers was studied depending on the conditions of diamond synthesis. The photoluminescence of color centers was studied using a continuous laser at a wavelength of 514 nm. Various methods for controlling color centers in diamond were investigated. Combined doping with donor (phosphorus) or acceptor (boron) impurities affected the charge states of NV and SiV centers. The design features of the CVD reactor used made it possible to form thin, nanometer-thick, doped layers in diamond. Depending on the amount of dopant, delta doping was used to obtain ensembles with a high concentration of NV and SiV centers, as well as single fluorescent NV centers, the position of which relative to the crystal surface was determined with nanometer accuracy. To localize the color centers along the crystal surface, methods of selective etching of diamond through a mask and activation by an electron beam were tested.

A series of works devoted to the study of electroluminescence of color centers created in the internal region of a diamond p-i-n diode has also been conducted. (1) When the internal region of the diode is doped with nitrogen, a study of the luminescence of the line at a wavelength of 533 nm, associated with the presence of nitrogen in diamond, has been conducted for the first time with combined photo- and electrical excitation. A comparison has been made of the change in the intensity of this line with the change in the intensities of the zero-phonon lines of the NV-center in the neutral and negative charge states with varying the current through the diode and the power of the exciting laser. (2) By doping the internal region of the diode with silicon, the intensity of electroluminescence of SiV centers is achieved comparable to the intensity of photoluminescence due to the high current density in the diode. (3) Also, the electroluminescence of germanium-vacancy color centers (GeV centers) in a diamond p-i-n diode was demonstrated for the first time. To create color centers in the internal region of the diode, a layer implanted with germanium ions was created in this experiment. The presented results can be used to create color centers with different parameters required for various applications (magnetometers, single photon sources).

[1] A.L. Vikharev, A.M.Gorbachev, M.A. Lobaev et al., Novel microwave plasma-assisted CVD reactor for diamond delta doping, Phys. Status Solidi RRL, vol. 10, pp. 324–327.(2016).
[2] M.A. Lobaev, A.M. Gorbachev, S. A. Bogdanov et al., NV-Center Formation in Single Crystal Diamond at Different CVD Growth Conditions, Phys. Status Solidi A, 1800205 (2018).
[3] S.A. Bogdanov, S.V. Bolshedvorskii, A.I. Zeleneev et al., Optical investigation of as-grown NV centers in heavily nitrogen doped delta layers in CVD diamond, Materials Today Communications, vol. 24, 101019 (2020).
[4] M.A. Lobaev, D.B. Radishev, S.A. Bogdanov et al, Diamond p-i-n Diode with Nitrogen Containing Intrinsic Region for the Study of Nitrogen-Vacancy Center Electroluminescence, Phys. Status Solidi RRL, vol. 14, 2000347 (2020).
[5] D.B. Radishev, M.A. Lobaev, S.A. Bogdanov et al., Investigation of NV centers charge states in CVD diamond layers doped by nitrogen and phosphorous, J. Luminescence vol. 239, 118404 (2021).
[6] M.A. Lobaev, A.M. Gorbachev, D.B. Radishev et al., Investigation of silicon-vacancy center formation during the CVD diamond growth of thin and delta doped layers, J. Mater. Chem. C, vol. 9, pp. 9229–9235 (2021).
[7] M.A. Lobaev, D.B. Radishev, A.L. Vikharev et al., SiV centers electroluminescence in diamond merged diode, Phys. Status Solidi RRL, 2200432 (2022).
[8] M.A. Lobaev, D.B. Radishev, A.L. Vikharev et al., SiV center electroluminescence in high current density diamond p-i-n diode, Appl. Phys. Lett., vol. 123, 251116 (2023).
[9] M.A. Lobaev, D.B. Radishev, A.L. Vikharev et al., Technical Physics Letters, vol. 51, no. 8, p. 3 (2025) (in Russian)
[10] M.A. Lobaev, D.B. Radishev, A.L. Vikharev et al., Technical Physics Letters, vol. 51, no. 10, p. 48 (2025) (in Russian)

Laser fabrication of optical and electrochemical nanosensors

A. A. Manshina, A. A. Vasileva, A. S. Levshakova, E. M. Khayrullina, G. I. Bikbaeva

Institute of Chemistry, St. Petersburg State University, St. Petersburg, 198504 Russia

e-mail: a.manshina@spbu.ru

The detection and identification of diverse analytes is an urgent priority in fields ranging from healthcare and ecology to food safety and security. Contemporary optical and electrochemical sensor platforms, which leverage the properties of nanostructured materials, offer significant potential to address this need. The critical step in developing these sensors is the controlled fabrication of substrates decorated with metal nanoparticles that exhibit either plasmonic (for SERS) or electrochemical activity.

Herein, we present laser-induced deposition (LID) as a universal fabrication strategy for such sensors. The LID process involves illuminating the substrate-solution interface with a laser to trigger a heterogeneous redox reaction, resulting in the deposition of metal nanoparticles from precursor solutions. This method offers exceptional tunability; the composition, morphology, and functionality of the deposits are controlled by varying the precursor type, concentration, solvent, and laser parameters. LID is compatible with a vast array of substrates, including amorphous, crystalline, and flexible materials, as well as intricate 3D structures like nanowires and porous membranes. The functionality of LID-fabricated substrates has been validated through their application as SERS sensors for toxins and bioanalytes and as electrochemical sensors for compounds such as glucose, paracetamol, and dopamine [1–4].

This work was supported by RSF project 23-49-10044. Authors are grateful to "Centre for Optical and Laser materials research" and ''Interdisciplinary Resource Centre for Nanotechnology'' Research Park of Saint Petersburg State University for technical support.

[1] O.Eremina, Silver nanoparticle-based SERS sensors for sensitive detection of amyloid-β aggregates in biological fluids, Talanta 266, (2024).
[2] A. Levshakova, A. et al., Simultaneous Catechol and Hydroquinone Detection with Laser Fabricated MOF-Derived Cu-CuO@C Composite Electrochemical Sensor. Materials,16, 7225 (2023).
[3] A. Vasileva, et al., 3D Nanocomposite with High Aspect Ratio Based on Polyaniline Decorated with Silver NPs: Synthesis and Application as Electrochemical Glucose Sensos, Nanomaterials, 13, 1002 (2023).
[4] A. Vasileva, et al., Laser-Induced Synthesis of Electrocatalytically Active Ag, Pt, and AgPt/Polyaniline Nanocomposites for Hydrogen Evolution Reactions. Nanomaterials, 13, 88 (2023).

Singular optics for biosensing: From zero reflection to shot noise modeling

V. A. Maslova, D. G. Baranov

Moscow Institute of Physics and Technology, Dolgoprudny, 141700 Russia

e-mail: lera.maslova00@gmail.com

The growing interest in studying phase singularities in various optical systems is driven by their diverse practical applications, including ultrafast analog computing [1], holography [2], and the potential for creating highly sensitive sensor platforms for molecular detection [3–5]. However, most of the existing approaches to implementing phase singularities remain technologically complex and cumbersome. The robustness of singularity-based sensors to imperfections in physical systems also remains an open question.

The first part of our work is devoted to the investigation of the possibility of realizing phase singularities in reflection from a uniaxial absorbing material, which represents a new platform for realizing singularities in the response function. Using the analytical condition of zero reflection, we demonstrated the emergence, evolution, and annihilation of the singularities in the space of incidence angle and wavelength depending on system parameters. We also noted the possibility of implementing a phase singularity in the space of tangential components of the wave vectors by violating the axial symmetry.

In the remaining part of the work, we investigated the effect of shot noise on the performance of the refractometric sensor based on the proposed platform. We developed a theoretical model for a spectroscopic ellipsometry scheme with an integrated shot noise model [6] operating near the phase singularity. We introduced noise into the model by assuming that the number of photons registered by the detector is a random quantity and obeys a Poisson distribution with a mean value described by the expression for the ellipsometric scheme. We noted two mechanisms which influence sensor resolution associated with theoretical sensitivity and the influence of shot noise. The results of numerical simulations demonstrated that the incidence angle serves as an effective parameter for achieving a balance between these contributions for measuring the analyte refractive index changes. This capability allows topological darkness sensors to function efficiently even at low light source power, making them suitable for use in compact devices.

The work was supported by BASIS Foundation (grant No. 24-1-5-136-1) and Russian Science Foundation (grant No. 23-72-10005).

[1] Zhu T., et al, Topological optical differentiator, Nature Communications, vol. 12(1): 680, (2021).
[2] Yingwei Wang, et al, Atomically Thin Noble Metal Dichalcogenides for Phase-Regulated Meta-optics, Nano Letters, vol. 20(11), (2020).
[3] Kravets V. G., et al, Singular phase nano-optics in plasmonic metamaterials for label-free single-molecule detection, Nature materials, vol. 12(4): 304–309, (2013).
[4] Ermolaev G., et al, Topological phase singularities in atomically thin high-refractive-index materials, Nature Communications, vol. 13(1): 2049, (2022).
[5] Tselikov, Gleb I., et al, Topological darkness: how to design a metamaterial for optical biosensing with ultrahigh sensitivity, ACS nano, vol. 17(19): 19338–19348, (2023).
[6] Carmichael Howard, An open systems approach to quantum optics: lectures presented at the Université Libre de Bruxelles, October 28 to November 4, 1991. vol. 18. Springer Science & Business Media (2009).

Improving the efficiency of solar cells by converting high-energy photons

E. Mityushkin, A. Solodov, A. Shmelev, A. Leontiev, L. Nurtdinova, D. Zharkov, V. Nikiforov

Zavoisky Physical-Technical Institute, FRC Kazan Scientific Center of RAS, Kazan, Russia

e-mail: m1tyushck1n@yandex.ru

The spectral distribution of sunlight at Air Mass 1.5 global (AM 1.5G) consists of photons with wavelength range from 300 to 2500 nm, but silicon photovoltaic cells only utilize a relatively small fraction of the solar photons (900–1100 nm). As a result, a significant part of the energy of incident short-wave solar radiation is lost during thermalization in the semiconductor material during the formation of electron-hole pairs [1]. This limits the theoretical maximal level of efficiency for silicon solar cells, known as the Shockley-Queisser limit, to 33.7% [2]. However, the conversion efficiency of most silicon solar panels is only 16–22%. To increase the efficiency of single-junction solar cells, a down-conversion coating consisting of a polymer and down-conversion nanoparticles can be used [3]. Down-conversion is a process in which one incident high-energy photon is converted into two or more lower-energy photons [4]. The quantum efficiency of this process is higher than 100%, which can be used to minimize non-radiative losses According to the calculation, the efficiency of silicon solar sells modified with a down-conversion layer on the front surface can reach 38.6% [5]. The practical use of the down-conversion coating assumes that it has a wide absorption band in the wavelength range of 300–500 nm and transparency in the rest of the visible range, a luminescence spectrum matching the characteristic bandgap of the silicon solar panel, and photostability. The optical properties of the coating are based on the characteristics of down-conversion nanoparticles, which are its functional filler. In turn, the properties of down-conversion nanoparticles are determined by the nature of the crystalline matrix and the type of luminescent centers – ions of rare earth metals. The transparency of the coating depends on the nature of the polymer, its thickness, size and content of nanoparticles in the polymer. The photostability of the down-conversion film is determined by the type of phosphor used. An example of combining all these requirements in one composite material represents a complex scientific and technical problem, the solution of which is the subject of this report.

The research was carried out with the financial support of Agreement with the Ministry of Science and Higher Education of the Russian Federation No. 075-15-2024-624 dated 12.07.2024.

[1] X. Huang, Enhancing solar cell efficiency: the search for luminescent materials as spectral converters, Chem. Soc. Rev., 42, 173 (2013).
[2] W. Shockley, H. Queisser, Detailed balance limit of efficiency of p-n junction solar cells, J. Appl. Phys., 32, 510–519 (1961).
[3] S.M. Ferro, M. Wobben, B. Ehrler, Rare-earth quantum cutting in metal halide perovskites – a review, Mater. Horiz., 8. 1072–1083 (2021).
[4] Wegh R.T., Donker H., van Loef E.V.D., et al., Quantum cutting through downconversion in rare-earth compounds, A. J. Lumin., 87–89, 1017–1019 (2000).
[5] T. Trupke, M. Green, P. Wurfel, Improving solar cell efficiencies by down-conversion of high-energy photons, J. Appl. Phys., 92, 1668–1674 (2002).

Magnetic field modulation of optical spatial differentiation in magnetoplasmonic crystals

A. A. Nerovnaya, A. Yu. Frolov, A. A. Fedyanin

Lomonosov Moscow State University, Leninskie gory 1, Moscow, 119991 Russia

e-mail: nerovnayaaa@my.msu.ru

In recent years, analog optical computing has attracted significant attention due to its high performance and low energy consumption [1]. Recent advances in metasurfaces have enabled the miniaturization of such systems to subwavelength scales. Previously, it was demonstrated that spatial differentiation of an input signal can be realized in thin plasmonic films [2]. However, most of metasurfaces operate in a static regime that limits their performance. Active modulation of their optical response – such as switching between differentiation modes is critical for enhanced functionality [3]. In this work, we experimentally investigate the optical spatial differentiation using magnetoplasmonic crystals (MPC), which allows for modulation of the optical response under an external magnetic field.

The key condition for optical spatial differentiation is achieving a near-zero reflectance that is proportional to the value of the in-plane wavevector of the incident light in the vicinity of resonance incident angles. A nickel plasmonic crystal with a period of 575 nm and a corrugation depth of 116 nm was used. Fig. 1 presents the image of a slit's edges captured with a CMOS camera at a resonance incidence angle of 22°, where the reflection coefficient is almost zero. As the incidence angle deviates from the resonance, the visibility of the edges diminishes until it disappears. Fig. 2 shows that the edges of the slit exhibit higher intensity compared to the surrounding areas, confirming the realization of optical spatial differentiation. Moreover, we demonstrate magnetic-field-induced modulation of the spatial intensity profile of the differentiated image under application of magnetic field in transversal field. It corresponds to $\Delta(x) = \pm 3\%$ in the slit area. The modulation values align with the transverse magneto-optical Kerr effect in this MPC.

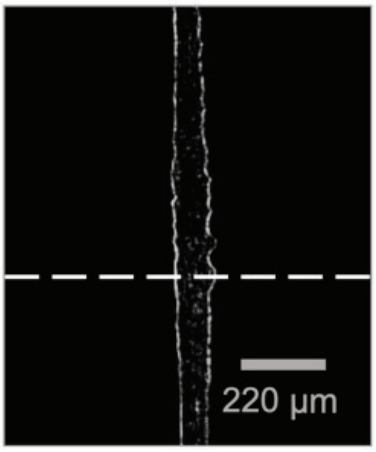

Fig. 1. Image of slit edges on the CMOS camera.

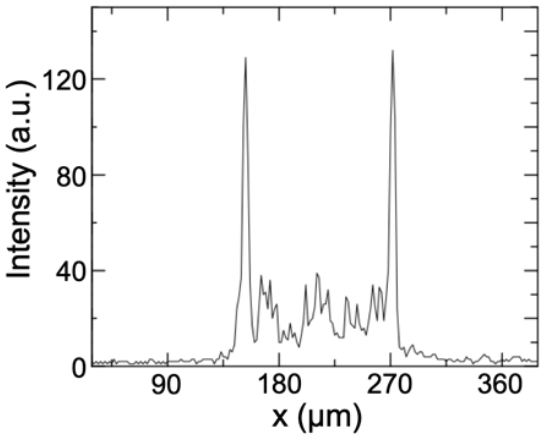

Fig. 2. The spatial cross-section of the image corresponding to the white dashed line in Fig. 1

The demonstrated capabilities of magnetoplasmonic crystals pave the way for the development of a new generation of ultrafast, compact, and energy-efficient computing devices based on magnetic-field-induced tunability.

[1] J. Touch, et al., Optical computing, Nanophotonics, vol. 6, p. 503–505, (2017).
[2] T. Zhu, et al., Plasmonic computing of spatial differentiation, Nat. Commun., vol. 8, p. 15391, (2017).
[3] M. Cotrufo, et al., Reconfigurable image processing metasurfaces with phase-change materials, Nat. Commun., vol. 15, p. 4483, (2024).

Strain-induced photoluminescence enhancement in WSe_2 monolayers on Au-nanobumps

A. V. Nikolaeva[1,2], M. A. Anikina[1,2], V. M. Kondratev[1,2], V. A. Sharov[1,4], E. Y. Barulina[5,6], A. A. Kuchmizhak[3], A. D. Bolshakov[1,2,7]

1- Alferov University, Saint Petersburg, Russia
2- Moscow Institute of Physics and Technology, Moscow, Russia
3- Far Eastern Federal University, Vladivostok, Russia
4- Ioffe Institute, Saint Petersburg, Russia
5- Russian Quantum Center, Moscow, Russia
6- Moscow Center for Advanced Studies, Moscow, Russia
7- Laboratory of Advanced Functional Materials, Yerevan State University, Armenia

e-mail: nikalex2000@bk.ru

Two-dimensional materials, particularly transition metal dichalcogenides (TMDs) like MoS_2, WS_2, $MoSe_2$, and WSe_2, exhibit exceptional optical and electronic properties, including direct bandgaps in monolayer form, strong light-matter interactions, and tunable exciton behavior [1–3]. Among them, WSe_2 stands out for its superior luminescence, making it promising for optoelectronic applications. This work explores a hybrid system combining WSe_2 with plasmonic nanostructures to enhance optical properties through exciton-plasmon coupling. Additionally, strain induced by transferring WSe_2 onto nanostructured surfaces modifies its bandgap and exciton transitions, further boosting photoluminescence efficiency.

In our work, WSe_2 monolayers were obtained using a mechanical exfoliation method and transferred to a target substrate with Au-nanobumps of various heights. The Au-nanobumps metasurface was fabricated by combination of an inexpensive and scalable magnetron sputtering of thin Au films with a direct fs-laser printing technique.

Optical properties of such a structure were characterized using Raman and photoluminescence microspectroscopy.. The PL spectra shown that the intensity of the response from the WSe_2 monolayer lying on the nanobumps in the wavelength range 720–780 nm with a peak at 750 nm exceeded the signal intensity from the WSe_2 monolayer lying on the flat gold substrate surface by a factor of 3, which can be explained by the effective interaction of the WSe_2 monolayer with plasmonic surface nanostructures.

The innovation and practical significance of the presented work is attributed to the use of nanobumps, the formation of which is carried out by a simple and effective method alternative to the traditional processes of lithography and etching. The laser radiation parameters allow controlling the geometry of the nanobumps and the lattice period, which provides the possibility of precise control over the optical characteristics of the hybrid structure. Furthermore, the ability to transfer two-dimensional WSe_2 layers onto such structures with good adhesion provides an avenue for the fabrication of efficient hybrid emitters and heterostructures based on this platform.

A.D.B. and A.V.N. acknowledges Russian Science Foundation (Grant 24-12-00225) for support of the experiments. M.A.A. thanks The Ministry of Science and Higher Education of the Russian Federation (FSMG-2025-0005) for support of Raman and photoluminescence microspectroscopy analysis.

[1] A. Kuznetsov, M. A. Anikina, A. N. Toksumakov, A. N. Abramov, V. V. Dremov, E. Zavyalova, V. M. Kondratev, V. V. Fedorov, I. S. Mukhin, V. Kravtsov, K. S. Novoselov, A. V. Arsenin, V. S. Volkov, D. A. Ghazaryan, A. D. Bolshakov, In-Plane Directional MoS_2 Emitter Employing Dielectric Nanowire Cavity, Small Structures, vol. 6, p. 2400476, (2025).
[2] G. A. Ermolaev, Y. V. Stebunov, A. A. Vyshnevyy, D. E. Tatarkin, D. I. Yakubovsky, S. M. Novikov, D. G. Baranov, T. Shegai, A. Y. Nikitin, A. V. Arsenin, V. S. Volkov, G. A. Ermolaev, Broadband optical properties of monolayer and bulk MoS_2, npj 2D Materials and Applications, vol. 4, p. 21, (2020).
[3] A. Splendiani A, L. Sun, Y. Zhang, T. Li, J. Kim, C.-Y. Chim, G. Galli, F. Wang, Emerging Photoluminescence in Monolayer MoS_2, Nano Lett, vol. 10, pp. 1271–1275, (2010).

Optical Pendellösung effect in anodic alumina 2D photonic crystals

V. B. Novikov[1], K. A. Smirnov[1], A. A. Dotsenko[1], I. V. Roslyakov[2], E. O. Sotnichuk[2], K. S. Napolskii[2,3], A. I. Maydykovskiy[1], T. V. Murzina[1]

1- Department of Physics, M. V. Lomonosov Moscow State University, Leninskie Gory, Moscow, 119991 Russia
2- Department of Materials Science, M. V. Lomonosov Moscow State University, Leninskie Gory, Moscow, 119991 Russia
3- Department of Chemistry, M. V. Lomonosov Moscow State University, Leninskie Gory, Moscow, 119991 Russia

e-mail: vb.novikov@physics.msu.ru

Multimode interference is a powerful tool in photonics for routing light. In periodic structures, it allows for the angular redistribution of the radiation that can be attained by the Pendellösung effect. This phenomenon initially discovered for the x-ray Bragg diffraction in crystals, consists in oscillations of the radiation power in diffracted beams under the variation of the crystal length or the incident angle. Special attention is attracted to photonic crystals (PhCs) possessing great spatial modulation of the refractive index and comprehensive feasibility in the dispersion design of light modes. These provided extra opportunities to tame Pendellösung effect for light control, e.g., polarizing beam splitting or optical switching [1]. In optics, the Pendellösung fringes were observed in 1D PhCs and holographic gratings [1, 2], whereas they have not been studied in 2D PhCs in the Laue diffraction geometry. In this work, we experimentally and numerically investigate the Pendellösung effect under light propagation through 2D hexagonal PhCs. Spectral, angular, and polarization properties of the effect are investigated. The experimental structure was a 2D PhC with a thickness of 30 μm. It consisted of air cylindrical pores packed in a hexagonal array in anodic alumina with the lattice constant of 400±16 nm; the pore diameter was 182±4 nm. The structure was obtained by anodizing of aluminum foil with prepatterned periodic seeds formed using a focused ion beam [3].

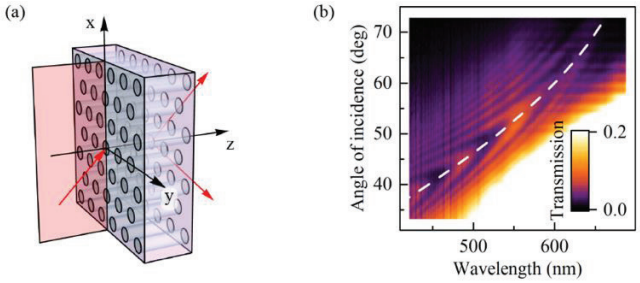

Fig. 1. (a) Scheme of the Laue diffraction of light in 2D PhC, (b) measured spectral-angular dependence of the PhC transmission coefficient for s-polarized light incident in the XZ plane. The dashed curve corresponds to the Bragg diffraction condition.

We revealed pronounced oscillations (Fig. 1b) in the measured spectral-angular dependence of the PhC transmission coefficient in the zero-order diffraction beam for the s-polarized light incident in the XZ plane, i.e., along the ΓM direction in the reciprocal space (Fig. 1a). These oscillations are centered around the Bragg diffraction curve. This finding is the manifestation of the Pendellösung effect. It was corroborated by the extra observations of π-phase-shifted oscillations of the diffraction efficiency of the first-order diffraction peak, which sustain the energy exchange between the two output diffraction beams. Numerical analysis confirmed our finding about the most pronounced broadband Pendellösung fringes for the ΓM direction of light incidence for the s-polarized radiation compared to the case of ppolarization or the incidence plane oriented along the ΓK direction.

Summing up, we revealed the Pendellösung effect in high-quality 2D anodic alumina PhC. This finding can be applied for optical sensing, beam splitting and switching.

[1] V.B. Novikov, S.E. Svyakhovskiy, A.I. Maydykovskiy, T.V. Murzina, B.I. Mantsyzov, Optical pendulum effect in one-dimensional diffraction-thick porous silicon based photonic crystals, J. Appl. Phys., vol. 118, p. 193101, (2015).
[2] M.L. Calvo, P. Cheben, O. Martinez-Matos, F. del Monte, J.A. Rodrigo, Experimental detection of the optical Pendellösung effect, Phys. Rev. Lett., vol. 97 (8), p. 084801, (2006).
[3] I.V. Roslyakov, S.E. Kushnir, V.B. Novikov, A.A. Dotsenko, D.M. Tsymbarenko, N.A. Sapoletova, T.V. Murzina, V.S. Stolyarov, K.S. Napolskii, Three-dimensional photonic crystals based on porous anodic aluminum oxide, J. Phys. Chem., vol. 15 (16), pp. 4319–4326, (2024).

Controlled formation of fluorescent centers in diamond particles smaller than 50 nm

D. G. Pasternak[1], R. H. Bagramov[2], A. M. Romshin[1], I. P. Zibrov[2], V. P. Filonenko[2], I. I. Vlasov[1]

1- Prokhorov General Physics Institute of the Russian Academy of Sciences, Vavilov str. 38, Moscow, 119991 Russia
2- Vereshchagin Institute of High-Pressure Physics of the Russian Academy of Sciences, Kaluzhskoe shoss 14, Troitsk, 108840 Russia

e-mail: vlasov@nsc.gpi.ru

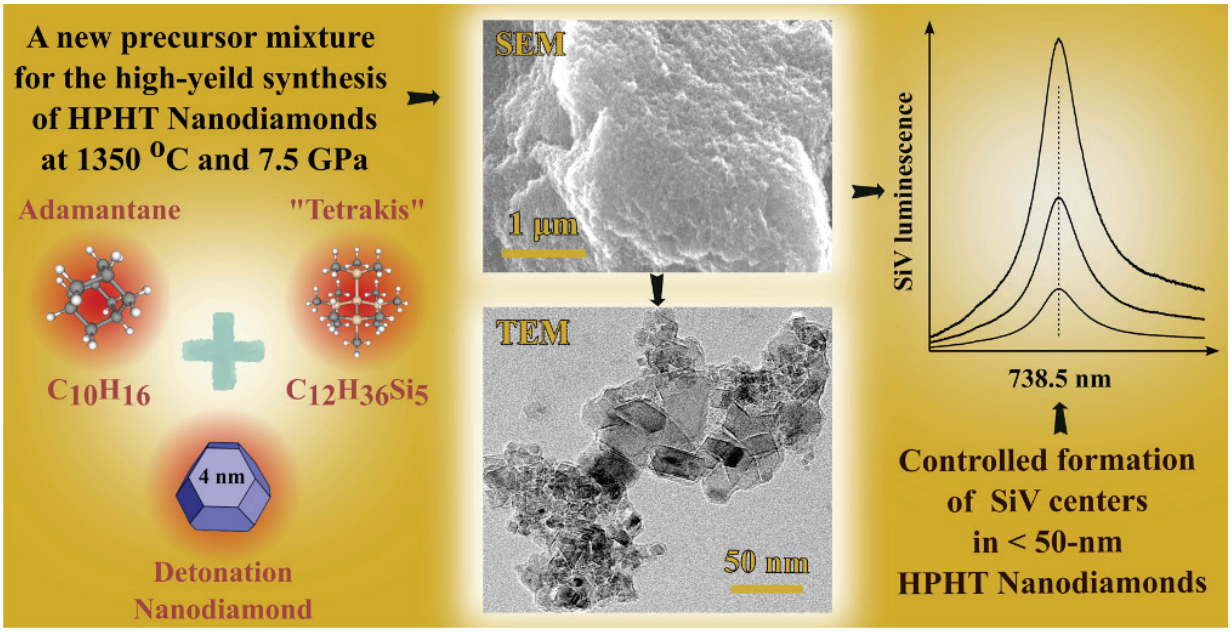

Despite progress in the high-pressure synthesis of nanodiamonds from hydrocarbons, the problem of controlled formation of fluorescent impurity centers in them still remains unresolved. In our work, we explore the potential of a new precursor composition, a mixture of adamantane with detonation nanodiamond, both in the synthesis of nanodiamonds and in the controlled formation of negatively charged silicon-vacancy centers in such nanodiamonds. Using different adamantane/detonation nanodiamond weight ratios, a series of samples was synthesized at a pressure of 7.5 GPa in the temperature range of 1200–1500 °C. It was found that temperature around 1350 °C, is optimal for the high-yield synthesis of nanodiamonds <50 nm in size. For the first time, controlled formation of negatively charged silicon-vacancy centers (SiV) in such small nanodiamonds was demonstrated by varying the atomic ratios of silicon/carbon in the precursor in the range of 0.01–1%. This allows the use of such SiV-containing nanodiamonds both as sources of single photons in quantum technologies and as nanosensors of ultra-local temperature fields [1].

This work was supported by Russian Science Foundation, grant No 23-14-00129 (https://rscf.ru/project/23-14-00129).

[1] D.G. Pasternak, R.H. Bagramov, A.M. Romshin, I.P. Zibrov, V.P. Filonenko, I.I. Vlasov, Controlled Formation of Silicon-Vacancy Centers in High-Pressure Nanodiamonds Produced from an "Adamantane + Detonation Nanodiamond" Mixture, Nanomaterials 14, 1843 (2024)

Ultrafast dynamics of semiconductor metasurfaces and space-time metastructures

M. Petrov

School of Physics and Engineering, ITMO University, Saint Petersburg, 191002 Russia

e-mail: trisha.petrov@gmail.com

The all-optical and ultrafast control of resonant nanophotonic structures has emerged as one of the most dynamic and promising directions in modern optics. With recent advances in the development of dielectric and semiconductor metasurfaces, achieving ultrafast modulation of their optical properties has become a particularly topical challenge.

In this talk, I will present theoretical studies introducing novel methods for ultrafast, all-optical modulation of semiconductor metasurfaces. The generation of non-equilibrium carriers in semiconductors leads to rapid and reversible changes in their optical response. These transient effects can be exploited to create spatio-temporal optical metasurfaces – even within homogeneous semiconductor films.

I will propose a new mechanism for the excitation of surface plasmon polaritons (SPPs) via transient grating formation in thin semiconductor layers. Our analysis predicts that such transient gratings can enable the generation of ultrashort surface plasmon polariton pulses, significantly shorter than the duration of the excitation pulse itself.

Additionally, I will introduce an approach for ultrafast modulation of metasurfaces supporting bound states in the continuum (BICs). By illuminating the metasurface with an obliquely incident pump pulse, we induce an asymmetric spatial distribution of non-equilibrium carriers, effectively breaking the symmetry of the BIC. This temporal symmetry breaking opens a radiative channel, drastically reducing the Q-factor on sub-picosecond timescales.

We believe that the proposed theoretical frameworks, along with the developed computational tools, will provide valuable insights and contribute to the advancement of ultrafast all-optical control in nanophotonic metastructures.

[1] O. Pashina, A. Seredin, G. Crotti, G. D. Valle, A. Bogdanov, M. Petrov, C. De Angelis, Excitation of surface plasmon-polaritons through optically-induced ultrafast transient gratings. arXiv arXiv:2411.17314 [Preprint] (2024). http://arxiv.org/abs/2411.17314.
[2] G. Crotti, A. Schirato, O. Pashina, O. Sergaeva, M. Petrov, C. De Angelis, G. Della Valle, Ultrafast switching of a metasurface quasi-bound state in the continuum via transient optical symmetry breaking, Accepted to Light: Science and Applications Journal, 2025.

Spin-preserving reflection from low-symmetry metasurfaces

A. Pozharkova, D. G. Baranov

Moscow Institute of Physics and Technology

e-mail: pozharkova.ao@phystech.edu

Currently, research is actively underway in the field of nanophotonics, considering electromagnetic radiation with a given circular polarization. This direction is of interest because it allows us to approach the creation of a resonator that supports the propagation of a wave with a certain circular polarization – a chiral resonator, which will make it possible to enhance the circular dichroism of the medium placed in it [2, 4]. One of the problems for a chiral resonator is related to the circular polarization of the wave reflected from the resonator wall. A classical mirror reflects light with a right circular polarization into light with a left circular polarization, and vice versa, however, for low-symmetry metasurfaces, for example, with a vertical axis of rotation of the order of no more than 2 orders, reflection while maintaining chirality is possible [1].

This work is dedicated to investigating the dependence of scattering matrix coefficients for two-dimensional periodic dielectric structures, specifically rhombic and monoclinic arrays. To determine the target characteristics, simulations were performed using the Fourier Modal Method (FMM). Geometric parameters – including the angle between the basis vectors (for monoclinic systems also the ratios of the lattice constants), the element radius and height – were optimized to maximize the reflection coefficient preserving RH polarization (RRR). For monoclinic systems, the effect of selective reflection was also analyzed. The influence of geometric parameters on the target functions within these systems was thoroughly examined. Additionally, the maximum achievable effects for various complex dielectric permittivities were studied. For some systems, the scattering matrix coefficients were fitted within the framework of coupled mode theory [3, 4].

[1] Semnani, B., Flannery, J., Al Maruf, R. et al. Spin-preserving chiral photonic crystal mirror // Light Sci Appl. – 2020. – Vol. 9, 23.
[2] Feis, J. et al. Helicity-Preserving Optical Cavity Modes for Enhanced Sensing of Chiral Molecules // Physical Review Letters. – 2020. – Vol. 124.
[3] Shanhui Fan, Wonjoo Suh, and J. D. Joannopoulos / Temporal coupled-mode theory for the Fano resonance in optical resonators // J. Opt. Soc. Am. A. – 2003. – Vol. 20. – P. 569–572.
[4] Voronin, K., Taradin, A. S., Gorkunov, M. V. & Baranov, D. G. / Single-Handedness Chiral Optical Cavities // ACS Photonics. – 2022. – Vol. 9. – P. 2652–2659.

Strong coupling between optical dielectric voids and resonant media

E. Ryabkov, D. G. Baranov

Center for Photonics and 2D Materials, Moscow Institute of Physics and Technology, Dolgoprudny, 141700 Russia

e-mail: ryabkov.research@gmail.com

Optical and material excitations in the strong coupling regime – a distinct regime of electromagnetic interaction – host stationary hybridized states known as polaritons [1]. Realizing light-matter coupling and boosting its strength relies on various cavities to confine electromagnetic radiation. In this context, the systems with better fabrication robustness and less demanding fabrication process are of considerable interest [2]. Within this landscape, spherical cavities formed within a dielectric medium have emerged as a compelling area of investigation. In this study, we present a comprehensive theoretical analysis of the resonant characteristics and polaritonic spectra exhibited by spherical void cavities that are saturated with a resonant medium. Furthermore, we analyze the inverse scenario, wherein a spherical void is formed inside a resonant dispersive medium. Our investigation reveals crucial parameter ranges for spherical voids that dictate the emergence of both weak and strong coupling regimes. We observe and explain the resonant Q-factor improvement in such systems [3] from polaritonic point of view. Finally, we develop and utilize the criterion for spatial field localization in spherical voids embedded in resonant dispersive media. The results presented in this work hold significant value for the design and optimization of new polaritonic systems.

[1] D. L. Mills and E. Burstein, Polaritons: The electromagnetic modes of media, Rep. Prog. Phys 37, 817 (1974).
[2] D. G. Baranov, M. Wers¨all, J. Cuadra, T. J. Antosiewicz, and T. Shegai, Novel Nanostructures and Materials for Strong Light-Matter Interactions, ACS Photonics 5, 24 (2018).
[3] Hentschel, M., Koshelev, K., Sterl, F. et al., Dielectric Mie voids: confining light in air, Light Sci Appl 12, 3 (2023).

Hybrid Ni-Ag magnetoplasmonic crystals

D. A. Safiullin, M. A. Kiryanov, M. O. Sivkov, M. M. Grechukhina, V. V. Popov, T. V. Dolgova, A. A. Fedyanin

Faculty of Physics, Lomonosov Moscow State University, Moscow, 119991 Russia

e-mail: safiullinda@my.msu.ru

Magneto-plasmonic crystals (MPCs) supporting surface plasmon polaritons (SPPs) provide a platform for enhancing magneto-optical effects via strong subwavelength electromagnetic field localization. The magneto-optical enhancement is governed by the Q-factor of SPP resonances in these nanostructures. Metallic ferromagnetic systems [1] exhibit high optical losses, while composites of noble metals and magnetic dielectrics [2] show less magneto-optical activity. The most efficient approach involves hybrid structures that combine a noble metal to support high-Q SPP resonances and a ferromagnetic metal as a magnetically active component [3]. In plasmonic systems there are two main energy loss pathways: radiative losses caused by scattering at inhomogeneities and non-radiative absorption. The balance between these loss mechanisms governs the light-to-SPP coupling efficiency, with optimal energy transfer achieved when the losses are matched. This condition manifests spectrally as a near-zero reflectance minimum at the plasmon resonance wavelength.

In this work, the studied sample is a silver grating coated with a thin layer of nickel. We have studied how the geometrical parameters of the hybrid MPC (the groove depth and the nickel thickness) influence the SPP excitation to enhance the transverse magneto-optical Kerr effect (TMOKE). The grating profile depth serves as the primary control parameter for radiative losses, while the nickel layer thickness governs the absorption losses. We have identified specific parameter combinations of grating depth and nickel thickness that satisfy the optimal coupling condition by numerical simulations. These predicted patterns were subsequently verified experimentally for two distinct nickel layer thickness values. For quantitative characterization of plasmon-enhanced TMOKE, we calculated the figure-of-merit (FOM), defined as the difference in reflectance for opposite magnetization states. Calculations of the dependence of FOM on the thickness of the nickel layer with the optimal lattice depth have been carried out. While one might initially assume that the magneto-optical response would increase monotonically with nickel content until reaching saturation, numerical simulations reveal a more complex relationship. The maximum FOM of 0.36% was achieved for a specific nickel thickness of 3.5 nm combined with an optimal grating depth of 54 nm, demonstrating the existence of an optimal configuration rather than simple saturation behavior. Experimental measurements performed at a near-optimal nickel thickness of 4.5 nm demonstrated significant TMOKE enhancement reaching 0.84% with an associated FOM of 0.15%.

[1] M. Kiryanov et. all, APL Photon., vol. 7, 026104, (2022).
[2] V. Belotelov et. all, Nat. Nanotechnol., vol. 6, 370-376, (2011).
[3] A.R. Pomozov et. all, Appl. Phys. Lett., vol. 116, 013106, (2020).

Nanothermometry: nanoparticles or Cu(I) complexes based composites?

A. G. Shmelev[1], I. D. Strelnik[2], A. V. Leontyev[1], L. A. Nurtdinova[1], E. O. Mityushkin[1], R. M. Gataullina[1], A. N. Solodov[1], V. G. Nikiforov[1], A. A. Karasik[2]

1- Zavoisky Physical-Technical Institute, FRC Kazan Scientific Center of RAS, Sibirsky tract str. 10/7, Kazan, 420029 Russia
2- Arbuzov Institute of Organic and Physical Chemistry of FRC Kazan Scientific Center of RAS, Arbuzov str. 8, Kazan, 420088 Russia

e-mail: sgartjom@gmail.com

Modern micro- and nano-devices require local temperature monitoring with nanometer spatial resolution, which is crucial for their reliability and efficiency. This is especially important for promising photonics, spintronics, and quantum information technology applications. Remote monitoring of local temperatures is becoming increasingly relevant for critical components in aerospace, automotive, and military equipment as well as satellite communication systems. This ensures the reliability and safety of these devices under high-stress conditions. The development of nanosensors with high sensitivity and spatial resolution is a significant step forward in nanotechnology and sensing systems. In this study, we aim to compare two approaches for creating nanothermosensors: upconversion nanoparticles (UCNPs) and copper(I) complexes.

We synthesized and calibrated two types of nanomaterials: classical UCNPs (based on fluorides and vanadates) doped with rare earth ions (such as Yb, Eu, and Er), and new Cu(I) complexes. The luminescent properties of these materials were characterized both at the bulk and microscopic levels. To do this, we used a standard spectrofluorometer and a confocal microscope.

To compare the performance of the two materials, we selected several key characteristics, including total measurement time, calibration time, accuracy, and stability of the temperature sensors. We conducted comparative measurements on a confocal microscope with a controlled substrate temperature, using a heated micro-object (a copper micro-wire embedded in epoxy resin) as a test material.

Our goal was to provide researchers with comparative data that can help them choose the most suitable nanothermosensor type for their specific needs. The strengths and weaknesses of the studied nanothermosensors will be discussed in the report.

UCNPs synthesis and bulk spectroscopic measurements were performed with the financial support from the government assignment for FRC Kazan Scientific Center of RAS. Cu(I) complexes synthesis and microscopic measuremenst were performed with support by the Russian Science Foundation (project No. 25-63-00021 https://rscf.ru/project/19-43-04119).

Photon sources for quantum communications: achievements and challenges

S. V. Sorokin, N. A. Maleev, M. M. Kulagina, A. I. Galimov, G. V. Klimko, Yu. M. Serov, M. V. Rakhlin, Yu. M. Zadiranov, I. V. Sedova, M. A. Bobrov, A. R. Vasiliev, S. I. Troshkov, Yu. A. Saliy, D. S. Berezina, A. I. Veretennikov, A. A. Toropov

Ioffe Institute, Polytekhnicheskaya str. 26, St. Petersburg, 194021 Russia

e-mail: toropov@beam.ioffe.ru

Single photon sources emitting photons "on demand" at telecommunication wavelengths are the basic building blocks for creating fiber-optic quantum networks [1]. Such photons can serve as "flying qubits", transferring quantum information along an optical fiber over relatively large distance. Self-organizing InAs/GaAs quantum dots (QDs) in microcavities, which are most widely used to create single-photon sources, provide close-to-ideal indistinguishability and purity of single photons, as well as record-high efficiency of their generation under pulsed optical pumping (57% [2]). However, such QDs emit efficiently only at wavelengths of 900–1000 nm, outside the standard telecommunication ranges. Mastering other wavelengths, including those corresponding to telecommunication frequencies, remains unresolvedWe present an original solution to the problem of creating efficient single-photon sources for the telecom C-band (around 1.55 μm), using molecular beam epitaxy (MBE) in combination with photolithography, ion-plasma etching and precision deposition of dielectric layers. The developed design of the columnar hybrid optical microcavity is based on the use of a metamorphic buffer, which made it possible to match the parameters of the crystal lattice of the GaAs (001) substrate and the In-GaAs active region, in which InAs/InGaAs QDs are formed (Fig. 1a). The lower mirror of the microcavity, a distributed Bragg reflector (DBR) $Al_{0.9}Ga_{0.1}As$/GaAs, is formed during the MBE growth of the initial heterostructure, while the upper DBR consists of several pairs of layers of deposited dielectric materials Si/SiO_2. The structures allowed implementation of a resonant coherent mode of pulsed excitation of a single QD, providing, at a pump power corresponding to the first Rabi oscillation (π-pulses), record-high parameters of single-photon emission at a wavelength of 1.554 μm: single-photon emission purity of ~97.5% ($g^{(2)}(0) \sim 0.025$) (Fig. 1b) and an average photon emission frequency of 5.35 MHz (in a single-mode optical fiber at a pump frequency of 78.3 MHz) that corresponds to the "first-lens" efficiency as high as 22.8%.

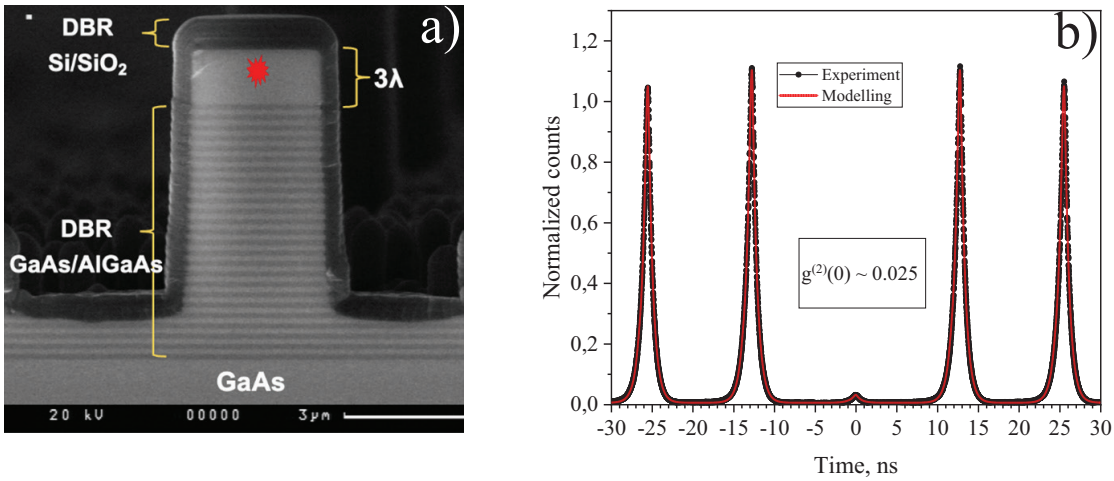

Fig. 1. a) Cross-sectional image of a hybrid microcavity obtained in a scanning electron microscope. b) Second-order correlation function $g^{(2)}$ measured under excitation conditions with π-pulses.

[1] T. Heindel, J.-H. Kim, N. Gregersen et al., Adv. Opt. Photon., 613–738, (2023).
[2] X. Ding, Y.-P. Guo, M.-C. Xu et al. Nat. Nanotechnol. 16, 399–403, (2021).

Photonic NanoJets and Optical tweezer for laser processing and additive micro-structuring

S. V. Starinskiy[1,2]

1- S. S. Kutateladze Institute of Thermophysics SB RAS, Lavrentyev ave. 1, Novosibirsk, 630090 Russia
2- Novosibirsk State University, Pirogova str. 2, Novosibirsk, 630090 Russia

e-mail: starikhbz@mail.ru

Light, as a fundamental physical phenomenon, has been extensively studied and utilized in scientific and engineering applications. The development of laser technology has enabled the generation of coherent, monochromatic, and high-intensity photon beams, revolutionizing multiple fields from industrial manufacturing to biophysical research. Among its most notable applications are optical trapping techniques and precision laser-based material processing, which have been recognized with several Nobel Prizes in Physics for their groundbreaking contributions. Optical tweezers, first demonstrated by Arthur Ashkin, represent a powerful non-invasive method for manipulating microscopic objects, including living cells and nanoparticles, with remarkable precision. This technology relies on the momentum transfer of photons to create gradient forces capable of trapping dielectric particles at the focus of a highly focused laser beam. In parallel, advances in laser processing have enabled unprecedented control over material modification at micro- and nanoscales. Techniques such as two-photon polymerization allow for the fabrication of complex three-dimensional structures with submicron resolution, while direct laser writing facilitates the nanofunctionalization of two-dimensional materials. A critical challenge in these applications involves overcoming the diffraction limit to achieve even greater spatial resolution. Current research explores various approaches, including the use of plasmonic effects and near-field enhancement, to push beyond this fundamental barrier. The choice of processing medium – whether liquid or gaseous environment – presents another important consideration, as it significantly influences heat dissipation, chemical reactions, and ultimately the quality of processing. Particularly intriguing is the phenomenon of liquid boiling during laser irradiation, which can either enhance processing through cavitation effects or degrade precision through uncontrolled bubble formation. Understanding these thermophysical and hydrodynamic phenomena is essential for optimizing laser-based technologies. Recent developments have also focused on integrating optical trapping with other techniques, such as optical nanojets, to create hybrid systems for advanced material manipulation. These interdisciplinary efforts bridge fundamental physics with practical engineering, offering new possibilities for nanotechnology, biophysics, and materials science. The continued refinement of laser technologies promises to unlock further capabilities in precision manufacturing, single-molecule studies, and quantum control, making this field one of the most dynamic and impactful areas of modern physical research.

The work was supported by the Russian Science Foundation (Grant No. № 24-79-10070, https://rscf.ru/project/24-79-10070).

Light absorption in disordered cholesteric doped with plant photosynthetic pigment extract

L. E. Tyryshkina, E. R. Bukhanov, A. V. Shabanov, N. V. Rudakova, D. P. Fedchenko, I. V. Timofeev

Kirensky Institute of Physics, Krasnoyarsk Scientific Center, Siberian Branch, Russian Academy of Sciences, Akademgorodok 50, building 38, Krasnoyarsk, 660036 Russia

e-mail: letyryshkina@iph.krasn.ru

Chiral structures are often found in nature [1]. They play a significant role in biological systems: chiral structures of beetle chitin, cellulose in the leaves of young plants. Plants thus increase the efficiency of photosynthesis. Self-organization of solid structures of chitin and cellulose is like the formation of chiral liquid crystal structures. Chiral liquid crystals include cholesteric liquid crystals (cholesterics).

Cholesterics are a special type of liquid crystals in which the molecules are oriented in a spiral with a preferred direction. This leads to the formation of a helicoidal structure. The structure of a cholesteric determines its unique optical properties. Such materials can be considered photonic crystals.

In this paper, we numerically simulated the effect of disorder in the helicoidal structure of cholesteric doped with an extract of photosynthetic pigments on the magnitude of resonance absorption of the edge mode for the long-wavelength boundary of the selective reflection region. Earlier, in [2], the change in the magnitude of resonance absorption for a photonic crystal structure consisting of alternating dielectric layers with a defect was experimentally and numerically shown. The defect layer was also filled with an extract of plant pigments. This allows us to imitate a real biological photonic crystal structure.

To calculate the spectral characteristics of the helical structure model, the basic parameters were used from [3]. The cholesteric parameters were taken close to 5CB, twisted with a chiral dopant. The position of the edge mode was selected in accordance with the absorption maxima of chlorophylls. Disordering of the structure was carried out by changing the polar angle of each helicoid step from the basic value by a random number. Figure 1a shows the dependence of the permittivity on the coordinate for the structure under study.

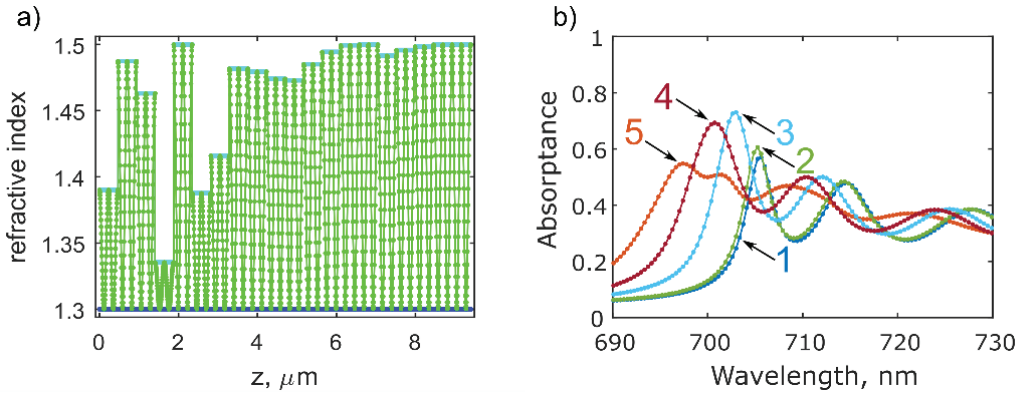

Fig. 1. a) Dependence of the permittivity on the coordinate for the studied structure of cholesteric doped with an extract of photosynthetic pigments. b) Absorption spectra of this structure at different degrees of disorder.

It is evident from Fig. 1b that a certain level of light absorption is observed in an ordered system. As disorder in the system increases light absorption exhibits interesting behavior. At first, absorption increases (spectra 2 and 3), and then, with further increase in disorder, it begins to decrease (spectra 4 and 5).

[1] V. Tuchin, Tissue Optics: Light Scattering Methods and Instruments for Medical Diagnostics, Third Edition, 2015.
[2] L.E. Tyryshkina, A.V. Shabanov, A.V. Katkova, A.I. Krasnov, N.V. Rudakova, P.S. Pankin, T.A. Zotina, I.V. Timofeev. Effect of asymmetry of the periodic structure imitating the biological periodic structure of chloroplast on resonant absorption of light, Physical Bases of Instrumentation, vol. 13, No. 4(54), (2024).
[3] A. Lakhtakia, Resilience of circular-polarization-state-sensitive reflection against morphological disorder in chiral structures, J. Nanophotonics, vol. 18, No. 22, pp. 036005-1–036005-17, (2024).

Is nanoimprint lithography applicable for creating 2.5D optics elements?

A. G. Vitukhnovsky[1,2], A. V. Gritsienko[1,2], D. A. Kolymagin[1], A. D. Patolyatov[1]

1- Moscow Institute of Physics and Technology (National Research University), Dolgoprudny, 141701 Russia
2- P. N. Lebedev Physical Institute, Russian Academy of Sciences, Moscow, 119991 Russia

e-mail: vitukhnovsky@mail.ru

The creation of micro-optical and optoelectronic structures (such as microlens arrays, optical connectors, diffraction photonic elements and waveguides) is an important problem for the production of photonic devices. However, at the moment, approaches to the mass production of such elements with adjustable parameters are under development.

One of the ways to create micro-optical elements, as well as 3D microstructures that do not require vacuum technology with submicron resolution is direct laser printing technology (Direct Laser Writing – DLW). However, this technology has low performance and is poorly scalable. On the other hand, nanoimprint lithography (NIL) is a promising method for creating high-precision micro- and nanostructures, which has recently found application in microelectronics, optoelectronics and biomedicine.

The main advantages of NIL are low cost, simplicity and the potential to achieve high resolution (element width < 10 nm). But despite all the advantages, the implementation of this lithography requires the presence of complex stamps and the possibility of precision control of the distance between the stamp and the substrate on which the lithography is performed.

It is planned to create prototypes of templates for creating 2.5D micro-optics and optoelectronics elements (an array of microlenses and diffraction elements) and testing them for nanoimprint lithography.

The work was supported by the grant of the Russian Science Foundation No. 25-79-20031.

Giant enhancement of second harmonic generation at metasurface optical resonances

E. S. Vyatkin, S. A. Tarasenko

Ioffe institute, Polytechnicheskaya 26, St. Petersburg, 194021 Russia

e-mail: vyatkin.egor@mail.ioffe.ru

The increase of the local electromagnetic field near the metasurface at optical resonances facilitates the enhancement of nonlinear optical effects such as second harmonic generation (SHG). These effects are currently being actively studied both experimentally and theoretically [1, 2]. Theoretical works are typicaly focused on modeling the electric field distribution and determining the parameters of optical Fano resonances from numerical calculations.

Here, we present a microscopic analytical theory of the SHG enhancement on optical resonances of metasurfaces. The theory takes into account both the conventional SHG mechanism related to the lack of the inversion center in the medium as well as the recently uncovered mechanism originating from the spatial inhomogeneity of the electromagnetic field [3]. We show that the interference of the microscopic mechanisms leads to elliptical polarization of SHG emission. Moreover, the selective excitation of metasurface resonances enables the control of the emission direction.

We consider a metasurface being a thin dielectric layer with lateral modulation of dielectric permittivity, Fig. 1a. In such a system, the incident electromagnetic wave can excite waveguide modes confined in the dielectric slab [4]. At normal incidence of light, the resonant excitation of the waveguide standing wave leads to the enhancement of SHG in the nonlinear layer near the metasurface. The magnitude of the amplification $Q \sim \omega_0^2\Gamma_0^2/(\Gamma_0+\Gamma)^4$ is determined by the resonant frequency ω_0, the radiative $1/\Gamma_0$ and non-radiative $1/\Gamma$ lifetimes of the waveguide mode. The spectral position and the radiative lifetimes are analytically described in terms of the metasurface parameters. A small deviation of the angle of incidence of light from the normal enables also the excitation of the BIC (bound state in continuum) weakly interacting with light. This leads to a further enhancement of the SHG signal, Fig. 1b.

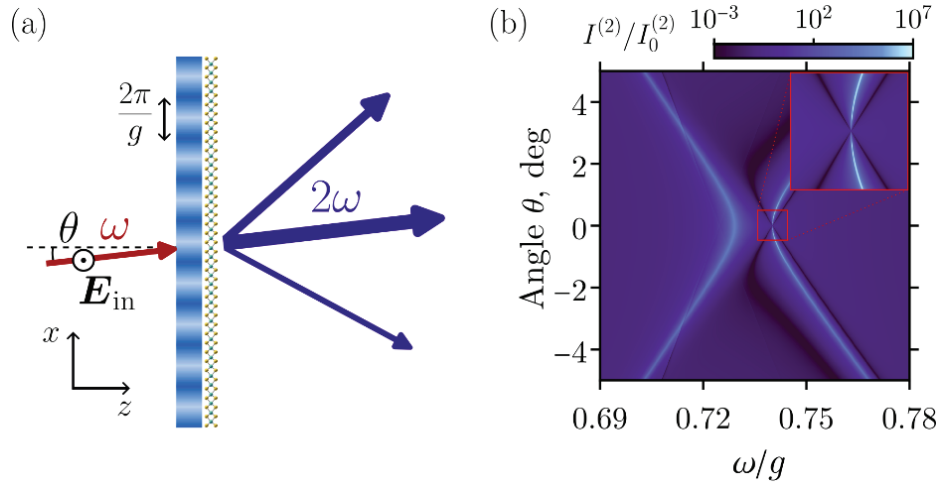

Fig. 1. (a) SHG in 2D material with nonlinear permittivity near the metasurface. (b) SHG enhancement as a function of the light frequency and the angle of incidence.

This work was supported by the Russian Science Foundation, grant No. 22-12-00211-П.

[1] T. Ning et al., Giant enhancement of second harmonic generation from monolayer 2D materials placed on photonic moiré superlattice, Nanophotonics 12, 4009 (2023).
[2] K. L. Koshelev et al., Subwavelength dielectric resonators for nonlinear nanophotonics, Science 367, 288 (2020).
[3] A.A. Gunyaga, M.V. Durnev, and S.A. Tarasenko, Second Harmonic Generation due to the Spatial Structure of a Radiation Beam Phys. Rev. Lett. 134, 156901 (2025).
[4] E.S. Vyatkin, A.V. Poshakinskiy, and S.A. Tarasenko, Emergent spin and orbital angular momentum of light in twisted photonic bilayer, Phys. Rev. B 111, 125303 (2025).

Wafer-scale graphene-inspired ultrathin gold films for flexible and transparent optoelectronics

D. I. Yakubovsky[1], M. S. Mironov[2], G. A. Ermolaev[1,2], A. S. Slavich[2], A. V. Arsenin[1,2], V. S. Volkov[2]

1- Center for Photonics and 2D Materials, Moscow Institute of Physics and Technology, Dolgoprudny, Russia
2- Emerging Technologies Research Center, XPANCEO, Dubai Investment Park First, Dubai, United Arab Emirates

e-mail: dmitrii-y@mail.ru

Ultrathin metal films are utilizing as components for next-generation optoelectronics from flexible transparent electrodes to subwavelength plasmonic interconnects. Sub-10-nm films can possess high optical transparency with mechanical flexibility, outperforming indium tin oxide (ITO) electrodes. The conventional fabrication of high-quality continuous ultrathin films typically requires seed or adhesion layers and specialized substrates to enable 2D metallic growth. For example, molybdenum disulfide underlayers have been shown to facilitate the growth of continuous ultrathin gold films with enhanced plasmonic and electronic properties [1, 2]. However, the introduction of ultrathin metal films in variety of applications remains limited by the presence of additional layer or substrate choice, thus transfer of ultrathin film onto arbitrary surface via graphene-like transfer techniques is desirable.

Currently, the emerging field of transparent conductive materials focuses on developing fabrication techniques for 2D metallic layers of varying dimensions and characterizing their properties [3]. For the first time, we proposed the adaptation of CVD-graphene synthesis technology to produce transferrable wafer-scale adhesion-free ultrathin and quasi-2D gold films [4]. We demonstrate the fabrication of atomically smooth and continuous ultrathin gold films (<8 nm thickness) exhibiting highest optoelectronic performance: optical transparency-conductance trade-off and flexibility. We have performed comprehensive study of ultrathin gold films using atomic-force, transmission electron and scanning electron microscopy, spectroscopic ellipsometry, broadband optical transmission and sheet resistance measurements, scanning near-field optical microscopy. Also, by theoretical simulation and experiments we showed that the developed graphene-inspired technique approaches the fundamental limits in achieving of 2D metal. Finally, the functionality of the films was demonstrated through multiple applications, including flexible OLED electrodes and transferrable electronic tattoo devices.

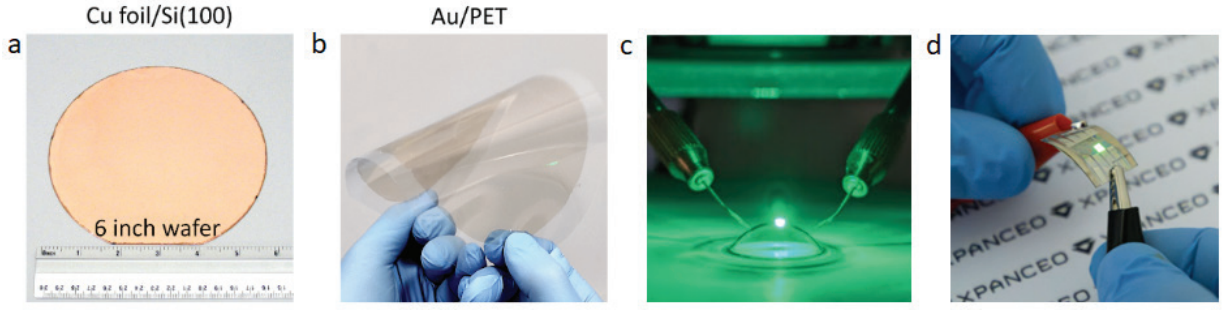

Fig. 1. Photographs demonstrating 6 inch-scale wafer of Cu foil (a) for the graphene-inspired transfer of a 5 nm-thick ultrathin gold film (b) onto a flexible polyethylene terephthalate (PET) substrate. Images of a smart contact lens showing an operating LED connected by an ultrathin transparent electrode (c) and photograph of an illuminated flexible OLED (d) with an 8 nm ultrathin gold film using as the transparent electrode.

[1] D. I. Yakubovsky, Yu. V. Stebunov, R. V. Kirtaev, G. A. Ermolaev, M. S. Mironov, S. M. Novikov, A. V. Arsenin, V. S. Volkov. Adv. Mater. Interfaces, vol. 6, p. 1900196 (2019).
[2] D. I. Yakubovsky, et al. Nano Lett., vol. 23, 20, pp. 9461–9467 (2023) https://doi.org/10.1021/acs.nanolett.3c02947
[3] C. Pan, Y. Tong, H. Qian, et al. Nat. Commun., vol. 15, p. 2840 (2024) https://doi.org/10.1038/s41467-024-47133-7
[4] M. S. Mironov, D. I. Yakubovsky, et al. Nano Lett., vol. 24, 51, pp. 16270–16275 (2024) https://doi.org/10.1021/acs.nanolett.4c04311

Perovskite structures integrated with polymer resonance systems for on-chip light control

S. Yurovskaya, A. Popkova, T. Baluian, A. Fedyanin

Faculty of Physics, Lomonosov Moscow State University, Moscow, 119991 Russia

e-mail: sonya12k34@mail.ru

The light source is a fundamental component of photonic integrated circuits (PICs). Integrating a laser directly into the chip minimizes losses occurred typically when coupling light from an external source to the PIC, therefore enhancing the efficiency of optical signal transmission. Additionally, incorporating optical sources on the PIC reduces assembly costs and improves production scalability.

A major obstacle to silicon-based PICs' commercialization is the lack of efficient electrically pumped light sources made from silicon. Bulk silicon is an indirect-bandgap semiconductor, the presence of which results in extremely low laser efficiency for practical applications. Halide perovskites are especially notable among other materials for photonic implementations. These materials exhibit a direct bandgap, relatively high refractive index, and significant optical gain, exceeding 10^3 cm^{-1} at room temperature [2]. Furthermore, their emission spectrum can be tuned from 400 nm to 1000 nm by varying the anion in the compound [3]. These electronic and photonic properties have enabled laser generation in perovskite-based structures [3–4]. A key drawback of such microlasers is the lack of control over positioning of resonant structures on the substrate due to chemical growth methods. An alternative approach involves chemically grown perovskite films that are subsequently structured to provide optical feedback [5].

This work explores a new approach to perovskite microlasers fabrication – structuring perovskite films using two-photon laser lithography (TPL). By printing polymer structures on a $CsPbBr_3$ film that resonantly interact with its luminescence, conditions for optical feedback and laser generation are achieved. This work focuses on modeling polymer structures supporting high-quality modes within the $CsPbBr_3$ emission range. Through this optimization, controlled structuring of perovskite films for laser generation becomes feasible.

[1] A. Lamichhane and N.M. Ravindra, Energy gap-refractive index relations in perovskites, Materials (Basel), vol. 13, no. 8., p. 1917 (2020).
[2] B.R. Sutherland, et al. Perovskite thin films via atomic layer deposition, Adv. Mat., vol. 27, no. 1, pp. 53–58 (2015).
[3] H. Zhu, et al. Lead Halide Perovskite Nanowire Lasers with Low Lasing Thresholds and High Quality Factors, Nat. Mater, vol. 14, no. 6, p. 636 (2015).
[4] Q. Zhang, et al. Room-temperature near-infrared high-Q perovskite whispering-gallery planar nanolasers, Nano Lett, vol. 14, no. 10. pp. 5995–6001 (2014).
[5] Tatarinov DA, et al. High-Quality $CsPbBr_3$ Perovskite Films with Modal Gain above 10 000 cm^{-1} at Room Temperature, Adv. Opt. Mater., vol. 11, no. 7, pp. 2202407 (2023).

Bright non-blinking quantum emission of SiV-centers in nitrogen-rich nanodiamonds with dual-color optical excitation

A. A. Zhivopistsev[1], A. M. Romshin[1], D. G. Pasternak[1], R. K. Bagramov[2], V. P. Filonenko[2], F. M. Maksimov[3,4], A. I. Chernov[3,4], I. I. Vlasov[1]

1- Prokhorov General Physics Institute of the Russian Academy of Sciences, Moscow, Russia
2- Vereshchagin Institute of High-Pressure Physics RAS, Troitsk, Moscow Region, Russia
3- Center for Photonics and 2D Materials, Moscow Institute of Physics and Technology (MIPT), Dolgoprudny, Russia
4- Russian Quantum Center, Bolshoy Bulvar 30, Building 1, Skolkovo Innovation Center, Moscow, Russia

e-mail: azh253@gmail.com

Silicon-vacancy (SiV) centres in nanodiamonds are of particular interest as photonic emitters due to their exceptional optical properties, including narrow zero-phonon line (ZPL) at 738 nm and high photostability, even at room temperature [1]. These properties render them promising candidates for quantum photonics applications, including single-photon sources [2] and quantum sensing [3]. At the same time, the practical application of SiV centers is significantly limited by the instability of their charge state [4, 5].

In this work, the luminescence of SiV^- centers in nanodiamonds synthesized by the high pressure and temperature (HPHT) method from adamantane with a controlled N_S content is studied in detail. It was found that simultaneous exposure to two lasers – the primary red (660 nm, 10 mW) and an auxiliary green (532 nm, <100 mW) – leads to an increase in the photoluminescence of SiV^- centers from 2 to 10 times compared with excitation with only a red laser.

We conducted a systematic study of the dependence of luminescence increase on the concentration of N_S in nanodiamonds (from 1 to 1000 ppm). The maximum raise (up to 10 times compared with only red laser excitation) was observed at a concentration of about 4 ppm, which indicates the presence of an optimal range for efficient electron transition between nitrogen and SiV^- centers. The photophysical features of the intensity fluctuations of individual SiV centers under different excitation modes was studied. When excited only by a red laser, a pronounced grouping is observed in a time interval of about 40 ns, indicating the presence of trapping states in the process of SiV^- radiation. The addition of weak green light leads to a gradual suppression of the amplitude of the bunching peak, the effect disappears completely when the 532 nm laser power reaches 500 μW. The observed effect is explained by the ionization of substitution nitrogen into the conduction band ($N_S \rightarrow N^+$), which reduces the number of available donors, converting SiV^- to the SiV^{2-} dark state, in presence of weak green excitation. The revealed mechanisms open up new possibilities for creating reliable and controllable quantum radiation sources based on SiV centers.

This work was supported by Russian Science Foundation, grant No 23-14-00129 (https://rscf.ru/project/23-14-00129).

[1] C. Bradac, W. Gao, J. Forneris, M. E. Trusheim, I. Aharonovich, Quantum nanophotonics with group IV defects in diamond, Nature communications, 10.1 (2019).
[2] S. A. Castelletto, R. E. Scholten, Heralded single photon sources: a route towards quantum communication technology and photon standard, The European Physical Journal-Applied Physics, 41.3 (2008).
[3] C. Chen, B. Jiang, X. Hu, Research progress on silicon vacancy color centers in diamond, Functional Diamond, 4.1, (2024).
[4] A. Gardill, I. Kemeny, M. C. Cambria, Y. Li, H. T. Dinani, A. Norambuena, J. R. Maze, V. Lordi, and S. Kolkowitz, Probing charge dynamics in diamond with an individual color center, Nano Letters 21.16 (2021).
[5] G. Garcia-Arellano, G. I. López-Morales, N. B. Manson, J. Flick, A. A. Wood, and C. A. Meriles, Photo-Induced Charge State Dynamics of the Neutral and Negatively Charged Silicon Vacancy Centers in Room-Temperature Diamond, Advanced Science, 11.22 (2024).

Edge mode behavior under partial disordering in helicoidal structure

E. R. Bukhanov[1,2], A. V. Shabanov[1], L. E. Tyryshkina[1], N. V. Rudakova[1], D. P. Fedchenko[1], I. V. Timofeev[1]

1- L. V. Kirensky Institute of Physics, Siberian Branch, Russian Academy of Science, Akademgorodok 50/38, Krasnoyarsk, 660036 Russia
2- Federal Research Center Krasnoyarsk Scientific Center, Russian Academy of Sciences, Siberian Branch, Akademgorodok 50, Krasnoyarsk, 660036 Russia

e-mail: eugene.bukhanov@iph.krasn.ru

The study focuses on the resistance of helical photonic structure band gap to partial disordering. Helical structures with helical symmetry demonstrate Bragg's reflection at the wavelengths that are close to the screw (helicoid) pitch, for circular polarization of light [1, 2]. Influence of the optical axis tilt at the boundaries of the band gap has been studied more closely. The study has discovered that a band gap short-wave boundary is resistant to the optical axis tilt towards the helicoid axis while the long-wave boundary is more sensitive to such changes. For a conical helical structure with a cone angle of 30 degrees, the long-wavelength boundary changes more than for a structure with a normal cone opening (90 degrees).

Still, the edge mode wavelength at the short-wave boundary is strictly constant under arbitrary distortions. The difference in the long-wavelength edge position between cone orientations is due to different extraordinary refractive indices. Anisotropy is often a special feature of a crystalline solid but it can be also discovered in natural objects [3]. Fig. 1a demonstrates the calculations of 121 averaged charts with deviations from 0 to 100 percent. For the data shown in Fig. 1a, the slope of the band gap for the shortwave and longwave edges (Fig. 1b) was calculated depending on the degree of disordering.

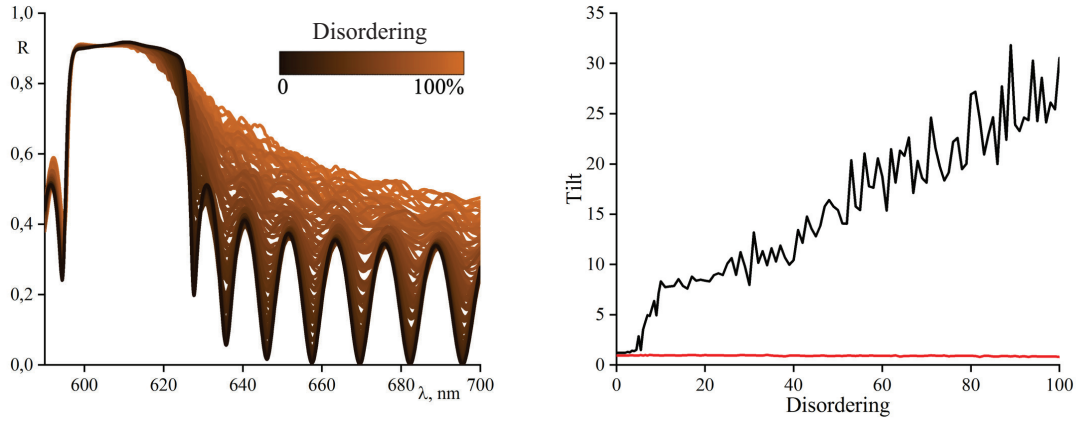

Fig. 1. (a) Averaged reflectance spectra of the helicoidal structure with varying deviation of the optical axis from the helicoidal axis. (b) Dependence of the effect of disordering on the slope of the band gap edge. The black line indicates the long-wavelength edge, the red line is for the short-wavelength edge.

Numerical simulations performed with the application of the anisotropic transfer matrix and the Berreman matrix has confirmed the analytical findings described in [2]. The results demonstrate the resistance of the short wavelength boundary of the reflection band under strong distortions of the helicoid, which is explained by the preservation of the ordinary refractive index. This characteristics is important for understanding the optical properties of partially disordered helicoidal biophotonic structures.

[1] V.A. Belyakov, Diffraction Optics of Complex-Structured Periodic Media: Localized Optical Modes of Spiral Media, (Springer International Publishing), 2019.
[2] S.Y. Vetrov, I.V. Timofeev, V.F. Shabanov, Localized modes in chiral photonic structures, Physics-Uspekhi, vol. 63, No. 1, pp. 33–56, (2020).
[3] E.R. Bukhanov, A. V. Shabanov, M.N. Krakhalev, M.N. Volochaev,Yu.L. Gurevich, The effect of the structure on the optical properties of epicular blue spruce wax (Picea pungens), Memoirs of the Faculty of Physics, vol. 5, pp. 1950502-1, (2019).

Diffraction characteristics of multiplexed multilayer inhomogeneous PDLC diffraction structures

D. M. Chubarov, Y. A. Altuhov, D. S. Rastrygin, V. O. Dolgirev, S. N. Sharangovich

Tomsk State University of Control System and Radioelectronics, Lenin avenue 40, Tomsk, 634050 Russia

e-mail: chudarovtt20@gmail.com

Currently, the field of optics is being actively researched by many scientists, leading to advancements in light control technologies for applications such as optical data transmission and information processing. One of the key research areas involves diffractive optical elements, particularly multilayer inhomogeneous holographic diffractive structures (MIHDS) based on polymer-encapsulated nematic liquid crystals (PDLC). These structures can be used as components for generating sequences of femtosecond laser pulses or for spectral light filtering [1, 2].

In previous studies [1], it was demonstrated that when an external electric field was applied to the diffractive layers of a multiplexed MIHDS with PPM-LC (liquid crystal concentration exceeding 90%), angular selectivity exhibited a shift and a reduction in diffraction efficiency (DE). However, the influence of an external electric field on the diffractive layers of a multiplexed MIHDS with PDLC was not investigated.

Thus, the aim of this work is to study the diffractive characteristics of multiplexed MIHDS based on PDLC when probed with linearly polarized light and subjected to an external electric field.

Figure 1 shows the dependence of the DE of a two-layer holographic structure on the probing angle and the magnitude of the electric field strength applied to one diffractive layer.

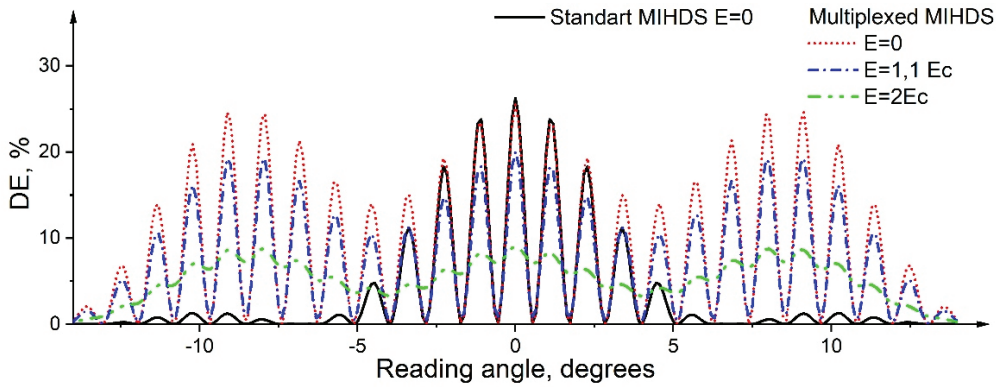

Fig. 1. Dependence of DE when reading a linear polarization light wave.

As can be seen from Fig. 1, as the strength of the external electric field applied to one diffractive layer increases, the DE decreases, and the angular selectivity transforms to resemble that of a single-layer HDS.

The study revealed that multiplexing can increase the number of local maxima by nearly three times compared to a conventional MIHDS. At the same time, for MIHDS with PDLC, the DE decreases in magnitude under increasing electric field strength but does not exhibit the angular shift characteristic of MIHDS with PPM-LC, which possess a smooth optical inhomogeneity along the material depth.

[1] Dolgirev V.O. Studying the diffraction of light on electrically controlled multiplexed multilayer inhomogeneous holographic diffraction structures based on photopolymerizing compositions with nematic liquid crystals / V.O Dolgirev, D.S. Rastrygin, S.N. Sharangovich // Bull. Russ. Acad. Sci.: Phys. – 2024. – Vol. 88, No. 1. – P. 6–12.
[2] Yan, A. Bragg diffraction of multilayer volume holographic gratings under ultrashort laser pulse readout / A. Yan, A Liu, Y. Zhi, D. Liu, J. Sun // J. Opt. Soc. A. – 2009. – Vol. 26, No. 1. – P. 135–141.

Intensity and angular control of photoluminescence in Eu-based complexes combined with plasmonic crystals

A. Yu. Frolov, M. P. Belov, A. Yu. Gladkikh, V. V. Popov, V. V. Utochnikova, A. A. Fedyanin

Lomonosov Moscow State University

e-mail: frolovay@my.msu.ru

Photoluminescence of lanthanide complexes attracted a lot of attention in the creation of LEDs, biomarkers, and thermosensors [1]. To improve the functionality of devices based on lanthanide complexes, it is necessary to enhance the photoluminescence output. One of the promising approaches to enhance the photoluminescence of quantum dots and dyes is the use of photonic structures with optical resonances [2, 3]. Such resonances include surface plasmons, which are coupled oscillations of electrons and light propagating at the interface between a metal and a dielectric [4]. They can be used to increase the density of optical states, which makes them promising for enhancing photoluminescence.

In this work, the spectral and angular dependences of the photoluminescence of the europium $Eu(dbm)_3(TDZP)$ (dbm = dibenzoylmethanate and TDZP = thiadiazolophenanthroline), with a thickness of 70 nm deposited on the surface of a one-dimensional plasmonic crystal are experimentally studied. Plasmonic crystals (PCs) are a periodically structured aluminum surface with periods of d = 385 nm and d = 480 nm. According to the phase matching condition of surface plasmon excitation at the wavelength of main europium emission line (612 nm), resonance is observed in the vicinity of angles of 27° for the PC with d = 380 nm and 7° for the PC with d = 480 nm, relative to the normal of the samples. The results of measurements of the angular dependence of the photoluminescence spectra are shown in Fig. 1 (for PC with d = 480 nm). The increase in photoluminescence at angle of 7° is associated with an increase in the density of optical states due to the surface plasmon. There is a fourfold increase in the photoluminescence intensity compared to the nonresonant angles of detection.

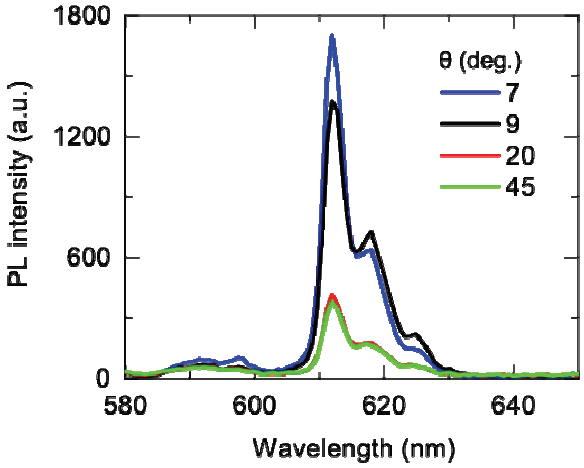

Fig. 1. Photoluminescence spectra at several detection angle for the PC with a period f of 480 nm.

This research was performed according to the Development Program of the Interdisciplinary Scientific and Educational School of Lomonosov Moscow State University "Photonic and Quantum Technologies. Digital Medicine".

[1] V. V. Utochnikova, Handbook on the Physics and Chemistry of Rare Earths, vol. 59, pp. 1–91, (2021).
[2] W. L. Barnes, A. Dereux, T. W. Ebbesen, Surface plasmon subwavelength optics, Nature, vol. 424, pp. 824–830, (2003).
[3] A. Bashiri, A. Vaskin, K. Tanaka, M. Steinert, T. Pertsch, I. Staude, Color routing of the emission from magnetic and electric dipole transitions of Eu^{3+} by broken-symmetry TiO_2 metasurfaces, ASC Nano, vol. 18, pp. 506–514, (2023).
[4] H. Sugimoto, M. Fujii, ACS Photonics, vol. 8, pp. 1794–1800, (2021).

Analysis of up-converting fluoride nanocrystals using ultra-high resolution luminescent UV microscopy

I. O. Goriachuk, V. N. Glebov, A. M. Malutin, V. I. Sokolov

NRC «Kurchatov Institute», Academician Kurchatov square 1, Moscow, Russia

e-mail: ivolgor@yandex.ru

Ultra-high resolution optical microscopes with UV illumination are typically employed in semiconductor industry for nano-scale objects inspection [1]. These microscopes are characterized by half-pitch Rayleigh resolution $R_{hp} = 0.5 \cdot 0.61 \cdot \lambda/NA$, where NA is the numerical aperture of the objective. Decreasing the wavelength λ of UV illumination leads to the increase in the resolution up to the level of $R_{hp} = 60$ nm. They could be engaged for the investigation of mixed fluoride nanocrystals doped with rare-earth elements. These nanocrystals emit visible and UV light under IR laser irradiation due to up-conversion phenomenon [2]. Ultra-high resolution microscopy enables observing them both in transmitted UV radiation and in their own up-conversion photo-luminescence light. The technique admits size, shape and spatial distribution analysis of individual particles within the sample under examination [3].

In the present work optical microscope LUMAM IUF-1 has been equipped with digital UV camera, DKsSh-120 lamp, monochromator, IR laser and UV-transparent IR-reflecting beam-splitter. Hexagonal shape and spatial orientation of individual β-$NaYF_4$:Yb^{3+},Tm^{3+} crystals with the average size of 0.74 μm have been clearly resolved in transmitted light with $\lambda = 343$ nm. Fig. 1a illustrates simultaneous observation of the crystal particles in transmitted light at $\lambda = 343$ nm and their own luminescence corresponding to $^1I_6 > {}^3F_4$ transition in Tm^{3+} ions. IR laser excitation of photo-luminescence allows distinguishing the particles among other nanoscale objects. The spectra of the lamp at use and crystal photo-luminescence are presented in Fig. 1b. Spatial resolution of the microscope can be further enhanced by using of $^1I_6 > {}^3H_6$ transition line (see Fig. 1b).

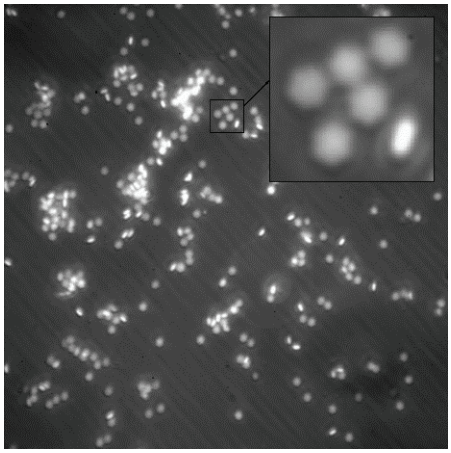

(a)

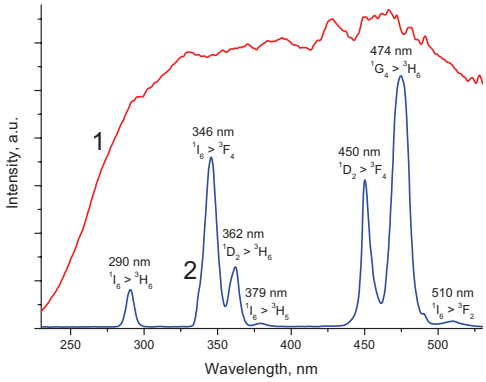

(b)

Fig. 1. (a) The image of β-$NaYF_4$:Yb^{3+},Tm^{3+} particles. The inset demonstrates 5x magnified region. (b) The spectra of DKsSh-120 lamp (curve 1) and the crystal luminescence (curve 2).

The work was carried out within the state assignment of NRC "Kurchatov Institute".

[1] W. Vollrath, Ultra-high-resolution DUV microscope optics for semiconductor applications, Proc. SPIE, vol. 5865, pp. 1–9, (2005).
[2] D.N. Karimov, P.A. Demina, A.V. Koshelev, V.V. Rocheva, A.V. Sokovikov, A.N. Generalova, V.P. Zubov, E.V. Khaydukov, M.V. Koval'chuk, V. Ya. Panchenko, Upconversion nanoparticles: synthesis, photoluminescence properties, and applications, Nanotechnologies in Russia, vol. 15, pp. 655–678, (2020).
[3] V.I. Sokolov, V.N. Glebov, I.O. Goriachuk, A.M. Malutin, Attachment to optical luminescent microscope LUMAM IUF-1 for observation of nanoparticles in deep UV-range, Pribory i Tekhnika Experimenta, vol. 67, pp. 152–155, (2024).

Integrated metasurface based on antimony selenide for waveguide mode conversion

G. A. Kolosov[1], E. V. Kabak[1,2], A. S. Shorokhov[1], A. A. Fedyanin[1]

1- Faculty of physics, Lomonosov Moscow State University, Moscow, 119991 Russia
2- Sarov branch, Lomonosov Moscow State University, Sarov, 607182 Russia

e-mail: kolosovga@my.msu.ru

Phase-change materials (PCMs) based on germanium (Ge), antimony (Sb), and tellurium (Te) alloys enable the development of compact devices capable of performing machine learning algorithms and artificial intelligence tasks at the speed of light [1]. The materials under discussion are ideal for constructing photonic tensor cores, i.e. optical devices that perform matrix-vector multiplication, due to their ability to maintain many distinct phase states without energy consumption.. In this context, PCM cells act as weight coefficients, where a value of "0" corresponds to full radiation absorption and "1" to full transmission. However, a key limitation of this approach is the implementation of only positive weights, as well as scalability issues caused by the high absorption of PCM cells in the crystalline state [2].

An alternative method for obtaining weight coefficients involves spatial conversion of radiation in a multimode waveguide [3]. This design includes a programmable array of PCM-based nanostructures. Each nanostructure scatters the fundamental input mode (TE_0), inducing a phase shift and transforming it into a higher-order mode (TE_1). This approach enables the representation of both positive and negative values by using differential detected signals of the resulting modes. Nevertheless, previous implementations relied on chalcogenide glasses, which suffer from high absorption in their crystalline state – thus limiting the scalability of the photonic tensor core matrix.

In this work, we propose an analogous device using antimony selenide as the PCM. The geometric design of the metasurface nanostructures was optimized using the SHGO algorithm to maximize modal contrast upon phase transitions of the material. Numerical simulations were conducted to analyze the output distribution as a function of the nanostructure array state and to determine the achievable value range for weight implementation. The results demonstrate the potential of this approach for future development of scalable photonic tensor cores.

[1] F. Brückerhoff-Plückelmann, J. Feldmann, C. David Wright; H. Bhaskaran, W. H. P. Pernice, Chalcogenide phase-change devices for neuromorphic photonic computing, J. Appl. Phys.,. 129, pp. 1–8, (2019).
[2] J. Feldmann, N. Youngblood, M. Karpov, H. Gehring, X. Li, M. Stappers, M. Le Gallo, X. Fu, A. Lukashchuk, A. S. Raja, J. Liu, C. D. Wright, A. Sebastian, T. J. Kippenberg, W. H. P. Pernice, H. Bhaskaran, Convolutional processing using an integrated photonic tensor core, Nature 589, 52–58 (2021).
[3] C. Wu, H. Yu, S. Lee, R. Peng, I. Takeuchi, M. Li, Programmable Phase-change Metasurfaces on Waveguides for Multimode Photonic Convolutional Neural Network, Nat. Commun. 12, 1–8 (2020).

Spectrally Resolved White Light Interferometry for magnetostriction measurement

I. G. Likhachev, V. I. Pustovoy

A. M. Prokhorov General Physics Institute, RAS, Moscow, Russia

e-mail: iglikhachev@gmail.com

The magnetostrictive effect is widely used in modern technologies such as sensors and actuators, ultrasound devices, energy industry and others. So the study of the magnetostrictive characteristic of different materials represents an actual problem. In this paper, high-precision fiber-optic displacement measurement technique was used to demonstrate the magnetostriction of the sample. The method is based on processing the spectrum of broadband radiation reflected from a Fabry-Perot fiber-optic interferometer (FPI) used as a mechanical displacement sensor. Specially developed software was utilized to calculate the FPI length up to nanometer accuracy. The pure (99.99%) nickel Ni rod was used as a sample to illustrate the capabilities of the technique. The dependence of the sample strain on the strength of the applied magnetic field was measured by means of Spectrally Resolved White Light Interferometry (SRWLI). The technique can be applied to any other magnetostrictive materials.

Determination of microresonator thermal parameters for the case of complex time dependence of pump power

V. Pavlov

Russian Metrological Institute of Technical Physics and Radio Engineering, Mendeleevo, Russia

e-mail: pvi044@gmail.com

The absorption of optical power in microresonators leads to thermal effects, which significantly affect nonlinear processes, including the solitons and platicons formation and noise level [1]. To take into account thermal effects, rate equations with effective thermal parameters are used [2]. Despite the convenience and simplicity of this approach, its applicability for a certain range of microresonator parameters may not be accurate enough. This is due to the fact that the real temperature dynamics in microresonators can be quite complex and differ from the exponential dependence [2]. In this work, we compared various methods for determining the effective parameters in a wide range pump pulse duration for integrated miroresonator. For this purpose, we simulated the temperature dynamics during pulsed power in the region of propagation of optical mode.

As result, it was shown that for region of standard parameters of microresonators, the accuracy of approximation by one rate equation can be rather low, but the addition of several rate equations corresponding to different thermal modes can significantly improve the accuracy of the approximation (see Fig. 1). We investigated the dependence of the approximation accuracy on the number of rate equations in a wide range of parameters and found the optimal one. As a result, we propose a new method for determining the effective thermal parameters of microresonators that takes into account various thermal relaxation processes. The proposed method agrees better with both direct numerical simulation and theoretical formulas over the entire range of microresonator parameters, in contrast to the classical approach.

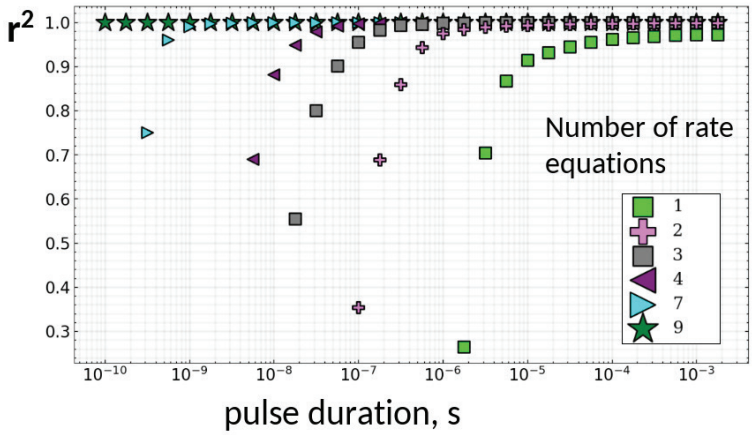

Fig. 1. Dependence of the approximation accuracy on the duration of the pump power pulse for a different number of rate equations.

[1] V. I. Pavlov et al., Almanac of Modern Metrology, 4(32), 18–26 (2022).
[2] Pavlov, et all. Microresonator Effective Thermal Parameters Definition via Thermal Modes Decom-position. Photonics, 10, 1131 (2023).

Ответственный редактор Т. П. Гаврилова, редактор Н. П. Хакамова,
технический редактор С. М. Ахмин
Издательство ФИЦ КазНЦ РАН,
420029, Казань, ул. Сибирский тракт, 10/7, лицензия № 0325 от 07.12.2000